



National Aeronautics and
Space Administration

P-494
304581

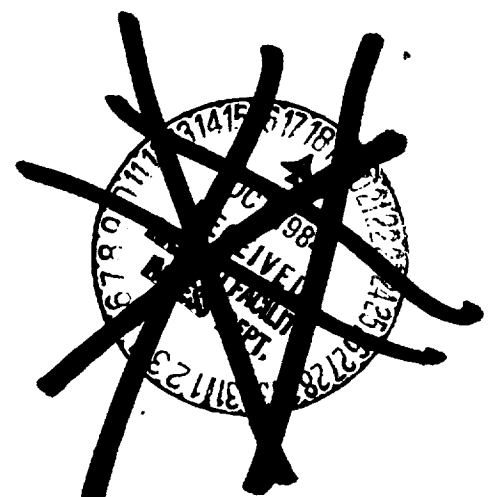
ENERGY EFFICIENT ENGINE

**Combustion System Component Technology
Performance Report**

By

D.L. Burrus, C.A. Chahrour, H.L. Foltz
P.E. Sabla, S.P. Seto, and J.R. Taylor

Aircraft Engine Business Group
Advanced Technology Programs Dept.
Cincinnati, Ohio 45215



Prepared for

NATIONAL AERONAUTICS AND SPACE ADMINISTRATION

(NASA-CR-168274) ENERGY EFFICIENT ENGINE
(F3) COMBUSTION SYSTEM COMPONENT TECHNOLOGY
PERFORMANCE REPORT Draft Report (GP) 494 p
CSCL 21E

N90-23550

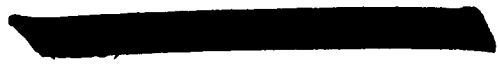
Unclass

33/07 0304581

These limitations shall be considered void after two (2) years after date of
such data.

NASA-Lewis Research Center
Contract NAS3-20643



1. Report No. CR-168274	2. Government Accession No.	3. Recipient's Catalog No.	
4. Title and Subtitle Energy Efficient Engine (E ³) Combustion System Component Technology Performance Report		5. Report Date July 1984	
		6. Performing Organization Code	
7. Author(s) D.L. Burrus, C.A. Chahrour, H.L. Foltz, P.E. Sabla, S.P. Seto, and J.R. Taylor		8. Performing Organization Report No. R82AEB401	
		10. Work Unit No.	
9. Performing Organization Name and Address General Electric Company Aircraft Engine Business Group Cincinnati, Ohio 45215		11. Contract or Grant No. NAS3-20643	
		13. Type of Report and Period Covered Draft	
12. Sponsoring Agency Name and Address National Aeronautics and Space Administration Washington, D.C. 20546		14. Sponsoring Agency Code	
15. Supplementary Notes NASA Project Manager, C.C. Ciepluch, E ³ Project Office NASA Project Engineer, D. Sokolowski NASA-Lewis Research Center, Cleveland, Ohio 44135			
16. Abstract <p>The Energy Efficient Engine (E³) combustor effort was conducted as part of the overall NASA/GE E³ Program. This effort included the selection of an advanced double-annular combustion system design based on technology derived from the NASA/GE Experimental Clean Combustor and QCSEE Clean Combustor Development Programs. The primary intent of this effort was to evolve a design that meets the stringent emissions and life goals of the E³, as well as all of the usual performance requirements of combustion systems for modern turbofan engines.</p> <p>Numerous detailed design studies were conducted to define the features of the combustion system design. Development test hardware was fabricated, and an extensive testing effort was undertaken to evaluate the combustion system subcomponents in order to verify and refine the design. Technology derived from this effort was incorporated into the engine combustion system hardware design. The advanced engine combustion system was then evaluated in component testing to verify the design intent.</p> <p>What evolved from this effort was an advanced combustion system capable of satisfying all of the combustion system design objectives and requirements of the E³.</p>			
17. Key Words (Suggested by Author(s)) Combustion Emissions Ignition Pattern Factor Double-Annular Combustion Split Duct Diffuser		18. Distribution Statement 	
19. Security Classif. (of this report) Unclassified	20. Security Classif. (of this page) Unclassified	21. No. of Pages 475	22. Price*

[REDACTED]

[REDACTED]

TABLE OF CONTENTS

<u>Section</u>		<u>Page</u>
1.0	INTRODUCTION	1
2.0	SUMMARY	3
3.0	DESIGN SELECTION	4
	3.1 Objectives and Goals	4
	3.2 Design Approach	6
4.0	AERO DESIGN	12
	4.1 Requirements	12
	4.2 Key Studies	14
	4.3 Combustor Design Features	37
5.0	MECHANICAL DESIGN	47
	5.1 Requirements	47
	5.2 General Design Features	47
	5.3 Liner	51
	5.4 Casing	74
	5.5 Dome	81
	5.6 Centerbody	85
	5.7 Fuel Delivery System	85
6.0	COMBUSTOR SUBCOMPONENT DEVELOPMENT TESTING	95
	6.1 Combustion System Diffuser Test	95
	6.2 Sector Combustor Subcomponent Test	132
	6.3 Fuel Nozzle Calibration Testing	215
7.0	FULL-ANNULAR COMBUSTOR COMPONENT DEVELOPMENT TESTING	219
	7.1 Test Hardware Description	219
	7.2 Test Methods	231
	7.3 Baseline Development Combustor Test Results	241
	7.4 Mod I Development Combustor Test Results	284
	7.5 Mod II and Mod III Development Combustor Test Results	328
	7.6 Mod IV and Mod V Development Combustor Test Results	338
	7.7 Mod VI and Mod VII Development Combustor Test Results	349
	7.8 Engine Combustor Test Results	372
	7.9 Conclusion and Summary	428
8.0	CONCLUDING REMARKS	431

PRECEDING PAGE BLANK NOT FILMED

PRECEDING PAGE BLANK NOT FILMED

TABLE OF CONTENTS (Concluded)

<u>Section</u>		<u>Page</u>
APPENDIX A	LOCATION AND NUMBERING OF E ³ ANNULAR RIG INSTRUMENTATION	433
APPENDIX B	COMBUSTOR SPLIT DUCT DIFFUSER PERFORMANCE DATA	437
APPENDIX C	SUMMARY AND DESCRIPTION OF COMPONENT SECTOR RIG TEST CONFIGURATIONS AND RESULTS	453
APPENDIX D	EMISSIONS CORRECTION AND CORRELATION EQUATIONS	461
APPENDIX E	ESTIMATED AIRFLOW DISTRIBUTION OF FULL-ANNULAR COMBUSTOR CONFIGURATIONS	462
APPENDIX F	DEVELOPMENT ANNULAR COMBUSTOR TEST SUMMARY	463
REFERENCES		475

LIST OF ILLUSTRATIONS

<u>Figure</u>		<u>Page</u>
1.	E ³ Combustor Cross Section.	7
2.	NASA/GE Double-Annular Combustors.	8
3.	Comparison of QCSEE and E ³ Double-Annular Combustors.	9
4.	E ³ Combustor Film/Impingement Liner Design.	11
5.	Performance Requirements.	12
6.	Turbine Inlet Radial Temperature Profile Requirements.	13
7.	Effect of Pilot Dome Airflow on CO Emissions.	15
8.	Comparison of E ³ Combustor Design Airflow Distribution.	16
9.	Split Duct Diffuser Design.	19
10.	E ³ Double-Annular Combustor Fuel Nozzle Design.	21
11.	Effect of Fuel Inlet Temperature on Fuel Nozzle Temperature.	23
12.	Combustor Fuel-Air Ratio Versus Core Compressor Flow.	26
13.	Combustor Exit Temperature Profile.	27
14.	Double-Annular Combustor Dome Velocity Comparison.	29
15.	Comparison of Combustor Fuel Staging Sequence.	30
16.	Comparison of Core Engine Start Models.	33
17.	Swirl Cup Design.	38
18.	Recirculation Flow Compared to Sleeve "Included Angle."	40
19.	Venturi Anticarboning Design Criteria.	41
20.	E ³ Dilution Thimble Designs.	42
21.	Comparison of E ³ Dilution Jet Penetration.	43
22.	E ³ Fuel Nozzle Flow Characteristics.	44
23.	Fuel Nozzle Staging - Pilot to Main Stage.	46

LIST OF ILLUSTRATIONS (Continued)

<u>Figure</u>		<u>Page</u>
24.	Combustor Mechanical Design Objectives.	47
25.	Assembled E ³ Combustor.	48
26.	Combustor Materials Selection.	50
27.	Combustor Inner Support Liner.	52
28.	Assembled Combustor Inner Liner.	53
29.	E ³ /GE23 Shingle Support Foot Design Comparison.	55
30.	E ³ /GE23 Shingle Edge Seal Configurations.	56
31.	Effect of Edge Seal Leakage on Shingle Temperature.	57
32.	Dilution Eyelet Design.	59
33.	Liner Cooling Flow Distributions.	60
34.	Liner Cooling Flow Distributions.	61
35.	Predicted Peak Liner Temperatures.	63
36.	Predicted Axial Temperature Distribution for a Shingle.	64
37.	Recommended Mission Mix for E ³ .	66
38.	Shingle Structural Model.	67
39.	Analytically Predicted Pressure Stresses for Shingle.	68
40.	Shingle Foot Size Versus Rupture Life Capability.	69
41.	Shingle Low Cycle Fatigue Model Temperature Distribution.	70
42.	Analytically Predicted Shingle Stress in Hot Streak.	72
43.	E ³ Combustor Shingle Predicted LCF Life.	73
44.	Predicted Stress for Combustor Support Liners.	75
45.	Predicted Stress for Combustor Support Liners.	76
46.	Support Liner Buckling Analysis Model.	77

LIST OF ILLUSTRATIONS (Continued)

<u>Figure</u>		<u>Page</u>
47.	Outer Support Liner Critical Buckling Pressures.	78
48.	Effect of Out-of-Roundness on Buckling Characteristics.	79
49.	Combustor Casing.	80
50.	Predicted Axial Stress Distribution for Casing.	82
51.	Combustor Support Pin Design.	83
52.	E ³ Combustor Dome.	84
53.	E ³ Combustor Centerbody Structure.	86
54.	Detailed View of Centerbody Structure and Domes.	87
55.	Predicted Centerbody Structure Life Levels.	88
56.	E ³ Fuel Delivery System.	89
57.	E ³ Fuel Nozzle Mechanical Features.	91
58.	E ³ Fuel Nozzle Assembly.	92
59.	Fuel Nozzle Vibration Model.	93
60.	Fuel Nozzle Campbell Diagram.	94
61.	E ³ Prediffuser Wall Contours.	97
62.	Inlet Diffuser CAFD Analysis.	99
63.	Inlet Diffuser Wall Velocities.	100
64.	Split Duct Diffuser Flow Regimes.	102
65.	Diffuser Water Table Model.	105
66.	Water Table Model Test.	106
67.	Combustor Cowling Modifications.	107
68.	E ³ Annular Diffuser Model.	109
69.	E ³ Annular Diffuser Model.	110

LIST OF ILLUSTRATIONS (Continued)

<u>Figure</u>		<u>Page</u>
70.	E ³ Annular Diffuser Model.	111
71.	Annular Diffuser Model Instrumentation Layout.	112
72.	Keil Pressure Probe.	114
73.	Schematics of Diffuser Inlet Profilers for Model.	119
74.	Diffuser Inlet Velocity Profiles.	120
75.	Static Pressure Recovery Levels.	122
76.	Static Pressure Recovery Levels.	123
77.	Static Pressure Recovery Levels.	124
78.	Static Pressure Rise Coefficients.	126
79.	Static Pressure Rise Coefficients.	127
80.	Static Pressure Rise Coefficients.	128
81.	Total Pressure Loss Coefficients.	129
82.	Effect of Airflow Levels of Passage Losses.	133
83.	Dome Assembly Cross Section Used in Fuel Spray Testing.	137
84.	Fuel Spray Visual Test Setup.	138
85.	Swirl Cup Recirculation Test Stand.	140
86.	Fuel Spray Patternation Results.	144
87.	Fuel Spray Patternation Results.	145
88.	Swirl Cup Axial Velocity Profiles.	146
89.	Swirl Cup Axial Velocity Profiles.	147
90.	Dome Metal Temperature Test Hardware.	149
91.	Dome Metal Temperature Test Instrumentation.	151
92.	Dome Metal Temperature Test Rig.	152

LIST OF ILLUSTRATIONS (Continued)

<u>Figure</u>		<u>Page</u>
93.	Dome Metal Temperature Test Results.	156
94.	E ³ Sector Combustor.	160
95.	Sector Combustor Hardware.	161
96.	E ³ Sector Combustor Test Rig.	163
97.	Sector Test Rig Inlet Diffuser.	164
98.	Sector Test Rig Gas Sampling Rake.	167
99.	Schematic of Typical Rake Sampling Element.	168
100.	Sector Combustor Baseline Ignition Results, Pilot Stage.	180
101.	Sector Combustor Mod I Ignition Results, Pilot Stage.	181
102.	Sector Combustor Mod I Ignition Results, Main Stage.	182
103.	Sector Combustor Mod I Ignition Results Versus Cycle Requirement.	184
104.	Sector Combustor Mod III Ignition Results.	185
105.	Sector Combustor Mod II and III Main Stage Ignition Results.	187
106.	Sector Combustor Mod III Ignition Results at Atmospheric Condition.	188
107.	Sector Combustor Mod III Ignition Results at Actual Inlet Pressure.	189
108.	Sector Combustor Mod V Ignition Results at Actual Inlet Pressure.	190
109.	Sector Combustor Mod VI Ignition Results.	192
110.	E ³ Sector Combustor Subidle Exhaust Gas Temperature (EGT) Profiles (Pilot Only).	193
111.	E ³ Sector Combustor Subidle EGT Profiles (Staged).	194

LIST OF ILLUSTRATIONS (Continued)

<u>Figure</u>		<u>Page</u>
112.	E ³ Sector Combustor EGT Profiles at Simulated SLTO.	195
113.	Sector Combustor Pressure Drop Versus Flow Function Parameter.	197
114.	E ³ Sector Combustor Emissions Results.	198
115.	E ³ Sector Combustor Emissions Results.	199
116.	E ³ Sector Combustor Emissions Results.	200
117.	E ³ Sector Combustor Emissions Results.	202
118.	E ³ Sector Combustor Emissions Results.	203
119.	E ³ Sector Combustor Emissions Results.	204
120.	E ³ Sector Combustor Emissions Results.	205
121.	E ³ Sector Combustor Emissions Results.	207
122.	E ³ Sector Combustor Emissions Results.	208
123.	E ³ Sector Combustor Emissions Results.	210
124.	E ³ Sector Combustor Altitude Relight Test Results.	211
125.	Engine Fuel Nozzle Assemblies Flow Calibration Results.	217
126.	E ³ Full-Annular Development Combustor.	220
127.	E ³ Test Rig Fuel Nozzle Assembly.	222
128.	E ³ Full-Annular Combustor Component Test Rig.	224
129.	Test Rig Bleed Simulation System.	226
130.	Test Rig Instrumentation Spool.	228
131.	ACTS Traverse System.	230
132.	E ³ Full-Annular Combustor EGT Thermocouple Rakes.	233
133.	Thermocouple Rake Modifications.	234

LIST OF ILLUSTRATIONS (Continued)

<u>Figure</u>		<u>Page</u>
134.	E ³ Full-Annular Combustor Gas Sampling Rakes.	237
135.	Gas Sampling Rake Instrumentation for Ignition Testing.	238
136.	Effect of Gas Rake Cooling Medium on CO and HC Emissions.	239
137.	Development Combustor Baseline Atmospheric Ignition Test Results.	244
138.	Development Combustor Baseline EGT Performance Test Results.	248
139.	Development Combustor Baseline EGT Performance Test Results.	249
140.	Development Combustor Baseline EGT Performance Test Results.	250
141.	Development Combustor Baseline EGT Performance Test Results.	251
142.	Development Combustor Baseline EGT Performance Test Results.	252
143.	Baseline Combustor Instrumentation Layout.	255
144.	Baseline Combustor Instrumentation Layout.	256
145.	Baseline Combustor Instrumentation Layout.	257
146.	Baseline Combustor Instrumentation Layout.	258
147.	Combustor Test Rig Instrumentation.	260
148.	Baseline Combustor Emissions Results.	261
149.	Baseline Combustor Emissions Results.	262
150.	Baseline Combustor Emissions Results, 30% Power Approach Operating Condition.	264
151.	Baseline Combustor Emissions Results.	265
152.	Baseline Combustor Emissions Results.	266

LIST OF ILLUSTRATIONS (Continued)

<u>Figure</u>		<u>Page</u>
153.	Diffuser Inlet Mach Number Profile (Baseline Test).	270
154.	Measured Combustor Pressure Losses for Baseline.	273
155.	Measured Combustor Metal Temperatures for Baseline Test.	274
156.	Measured Combustor Metal Temperatures for Baseline Test.	275
157.	Measured Combustor Metal Temperatures for Baseline Test.	276
158.	Measured Combustor Metal Temperatures for Baseline Test.	277
159.	Measured Combustor Metal Temperatures for Baseline Test.	278
160.	Measured Combustor Metal Temperatures for Baseline Test.	279
161.	Measured Combustor Metal Temperatures for Baseline Test.	280
162.	Measured Combustor Metal Temperatures for Baseline Test.	281
163.	Measured Combustor Metal Temperatures for Baseline Test.	282
164.	Mod I Combustor Hardware Modifications.	286
165.	Mod I Atmospheric Ignition Test Results.	288
166.	Mod I Atmospheric Ignition Test Results.	289
167.	EGT Thermocouple Correction.	293
168.	Mod I EGT Performance Test Results.	294
169.	Mod I EGT Performance Test Results.	296
170.	Mod I EGT Performance Test Results.	297
171.	Mod I EGT Performance Test Results.	298
172.	Mod I Ignition Results at True Cycle Conditions.	300
173.	Mod I Combustor Instrumentation Layout.	303
174.	Mod I Combustor Instrumentation Layout.	304

LIST OF ILLUSTRATIONS (Continued)

<u>Figure</u>		<u>Page</u>
175.	Mod I Combustor Instrumentation Layout.	305
176.	Mod I Combustor Instrumentation Layout.	306
177.	Mod I Emissions Test Results.	307
178.	Mod I Emissions Test Results.	308
179.	Mod I Emissions Test Results.	309
180.	Mod I Emissions Test Results.	310
181.	Diffuser Inlet Mach Number Profile (Mod I Test).	314
182.	Measured Pressure Losses for Mod I Combustor.	316
183.	Measured Combustor Metal Temperatures for Mod I Test.	317
184.	Measured Combustor Metal Temperatures for Mod I Test.	318
185.	Measured Combustor Metal Temperatures for Mod I Test.	319
186.	Measured Combustor Metal Temperatures for Mod I Test.	320
187.	Measured Combustor Metal Temperatures for Mod I Test.	321
188.	Measured Combustor Metal Temperatures for Mod I Test.	322
189.	Measured Combustor Metal Temperatures for Mod I Test.	323
190.	Measured Combustor Metal Temperatures for Mod I Test.	324
191.	Measured Combustor Metal Temperatures for Mod I Test.	325
192.	Measured Combustor Metal Temperatures for Mod I Test.	326
193.	Mod II and Mod III Combustor Hardware Modifications.	331
194.	Mod II and Mod III Combustor Hardware Modifications.	332
195.	Mod III-A Atmospheric Ignition Test Results.	335
196.	Mod III-B Atmospheric Ignition Test Results.	337
197.	Mod IV Combustor Hardware Modifications.	339

LIST OF ILLUSTRATIONS (Continued)

<u>Figure</u>		<u>Page</u>
198.	Mod V Combustor Hardware Modifications.	340
199.	Mod IV Atmospheric Ignition Test Results.	342
200.	Mod V Atmospheric Ignition Test Results.	343
201.	Mod V EGT Performance Test Results.	347
202.	Mod V EGT Performance Test Results.	348
203.	Mod VI Atmospheric Ignition Test Results.	353
204.	Mod VI EGT Performance Test Results.	357
205.	Mod VI EGT Performance Test Results.	358
206.	Mod VII EGT Performance Test Results.	362
207.	Mod VII EGT Performance Test Results.	364
208.	Mod VII Ignition Results at True Cycle Conditions.	367
209.	Mod VII Emissions Test Results.	368
210.	Mod VII Emissions Test Results.	370
211.	Engine Combustor Atmospheric Ignition Test Results.	375
212.	Engine Combustor EGT Performance Test Results.	380
213.	Engine Combustor EGT Performance Test Results.	381
214.	Engine Combustor EGT Performance Test Results.	382
215.	Engine Combustor EGT Performance Test Results.	384
216.	Engine Combustor EGT Performance Test Results.	385
217.	Engine Combustor Hardware Modifications.	388
218.	Comparison of Test Rig and Prototype Fuel Nozzle Tips.	389
219.	Engine Combustor Instrumentation Layout.	390

LIST OF ILLUSTRATIONS (Continued)

<u>Figure</u>		<u>Page</u>
220.	Engine Combustor Instrumentation Layout.	391
221.	Engine Combustor Instrumentation Layout.	392
222.	Engine Combustor Instrumentation Layout.	393
223.	Engine Combustor Instrumentation Layout.	394
224.	Engine Combustor Instrumentation Layout.	395
225.	Engine Combustor Instrumentation Layout.	396
226.	Engine Combustor Instrumentation Layout.	397
227.	Engine Combustor Instrumentation Layout.	398
228.	Engine Combustor Instrumentation Layout.	399
229.	Engine Combustor Instrumentation Layout.	400
230.	Engine Combustor Ignition Results at True Cycle Conditions.	402
231.	Engine Combustor Emissions Results.	403
232.	Engine Combustor Emissions Results.	406
233.	Engine Combustor Emissions Results.	408
234.	Engine Combustor Emissions Results.	409
235.	Engine Combustor Emissions Results.	410
236.	Measured Engine Combustor Pressure Losses.	414
237.	Estimated Versus Design Intent Flow Distribution for Engine Combustor.	416
238.	Measured Engine Combustor Metal Temperatures.	417
239.	Measured Engine Combustor Metal Temperatures.	418
240.	Measured Engine Combustor Metal Temperatures.	419
241.	Measured Engine Combustor Metal Temperatures.	420

LIST OF ILLUSTRATIONS (Concluded)

<u>Figure</u>		<u>Page</u>
242.	Measured Engine Combustor Metal Temperatures.	421
243.	Measured Engine Combustor Metal Temperatures.	422
244.	Measured Engine Combustor Metal Temperatures.	423
245.	Measured Engine Combustor Metal Temperatures.	424
246.	Measured Engine Combustor Metal Temperatures.	425
247.	Measured Engine Combustor Metal Temperatures.	426
248.	Comparison of Predicted and Measured Peak Metal Temperatures.	427

LIST OF TABLES

<u>Table</u>	<u>Page</u>
I. E ³ Program Emissions Goals.	4
II. E ³ Combustor Performance Goals.	5
III. E ³ Combustor Life Goals.	5
IV. E ³ FPS Design Cycles.	17
V. Chronology of E ³ Starting Studies.	25
VI. Starting Background.	25
VII. Adverse Impacts of Pilot and Main Stage Ground Start Ignition.	31
VIII. Revised Engine Start Analysis.	31
IX. Ignition Study Results.	32
X. Ground Idle Cycle Comparison.	34
XI. E ³ Emissions Adjustment Relationships.	36
XII. E ³ Combustor Estimated Emissions.	35
XIII. E ³ /GE23 Shingle Design Comparison.	54
XIV. Predicted Shingle Maximum Operating Temperature in the FPS Application.	62
XV. E ³ Combustor Shingle Predicted Life Levels.	71
XVI. Diffuser Pressure Loss Goals.	103
XVII. Diffuser Model Measured Performance.	131
XVIII. Diffuser Model Performance Comparison.	131
XIX. Test Conditions for Fuel Spray Visualization Testing.	139
XX. Fuel Spray Visualization Test Results.	142
XXI. Dome Metal Temperature Test Point Schedule.	153
XXII. Estimated Dome Metal Temperatures for Full Annular Combustor Testing.	157

LIST OF TABLES (Continued)

<u>Table</u>		<u>Page</u>
XXIII.	Flow Area Distribution for Baseline Sector Combustor Configuration.	162
XXIV.	Sector Combustor Ignition Test Point Schedule.	171
XXV.	Sector Combustor Emissions Test Point Schedule.	173
XXVI.	Altitude Ignition Testing Summary.	213
XXVII.	Altitude Ignition Testing Summary.	213
XXVIII.	Altitude Ignition Testing Summary.	214
XXIX.	Altitude Ignition Testing Summary.	214
XXX.	CAROL Calibration Gases.	240
XXXI.	Development Combustor Baseline Atmospheric Ignition Test Point Schedule.	242
XXXII.	Development Combustor Baseline Atmospheric EGT Performance Test Point Schedule.	246
XXXIII.	Development Combustor Baseline Emissions Test Point Schedule.	254
XXXIV.	Baseline Combustor EPAP Results.	268
XXXV.	Baseline Combustor Smoke Results.	269
XXXVI.	Calculated Diffuser Performance for Baseline Test.	271
XXXVII.	Development Combustor Mod I Atmospheric Ignition Test Point Schedule.	285
XXXVIII.	Development Combustor Mod I Atmospheric EGT Performance Test Point Schedule.	292
XXXIX.	Development Combustor Mod I Emissions Test Point Schedule.	302
XL.	Mod I Combustor EPAP Results.	313

LIST OF TABLES (Concluded)

<u>Table</u>		<u>Page</u>
XL I.	Calculated Diffuser Performance For Mod I Test.	315
XL II.	Mod II and III Atmospheric Ignition Test Point Schedule.	333
XL III.	Mod V Atmospheric EGT Performance Test Point Schedule.	345
XL IV.	Mod VI and VII Atmospheric Ignition Test Point Schedule.	352
XL V.	Mod VI Atmospheric EGT Performance Test Point Schedule.	355
XL VI.	Mod VII Atmospheric EGT Performance Test Point Schedule.	360
XL VII.	Mod VII Emissions Test Performance.	365
XL VIII.	Mod VII Emissions Results at Approach Power.	369
XL IX.	Mod VII EPAP Results.	371
L.	Engine Combustor Atmospheric Ignition Test Point Schedule.	374
LI.	Engine Combustor Atmospheric EGT Performance Test Point Schedule.	378
LII.	Engine Combustor Emissions Test Point Schedule.	386
LIII.	Emissions Results at 30% Approach Power Operation.	405
LIV.	Engine Combustor EPAP Results.	411
LV.	Engine Combustor Smoke Results.	413
LVI.	Summary of Full-Annular Combustor Configurations and Test Results.	429
LVII.	Summary of Full-Annular Combustor Configurations and Test Results.	430
LVIII.	Estimated EPAP Numbers for E ³ FPS Combustion System.	432

1.0 INTRODUCTION

The General Electric Co. is currently engaged in the Energy Efficient Engine (E³) Program under Contract NAS3-20643 to the NASA-Lewis Research Center. The purpose of the E³ Program is to develop and demonstrate the technology for obtaining higher thermodynamic and propulsive efficiencies in advanced, environmentally acceptable turbofan engines for possible use in future commercial transport aircraft. The Program involves technology development for engine components, including the design of an advanced low-emissions combustor.

The purpose of the E³ combustor effort relative to the overall E³ program is to develop an advanced combustion system capable of meeting both the stringent emissions and the long-life goals of the E³, as well as meeting all of the usual performance requirements of combustion systems for modern turbofan engines. Aerothermo and mechanical analyses were conducted to define a design of this advanced combustor. To meet the emissions and performance requirements an advanced, short-length, double-annular dome combustor design concept was adopted. To meet the long-life goals an advanced, double-walled, segmented liner concept using impingement and film cooling was selected. This design approach was chosen based on the low-emissions combustor design technology developed in the NASA Experimental Clean Combustor Program (ECCP) (Reference 2) and the NASA Quiet Clean Short-Haul Experimental Engine (QSCEE) Program (Reference 3). In these programs it was demonstrated that with the double-annular combustor design concept, low emissions levels could be obtained in addition to obtaining the other combustor performance capabilities required for satisfactory operation of a turbofan like the E³.

This report summarizes the results of the detailed design and analysis efforts on the combustion system for General Electric's Energy Efficient Engine. It includes a general description of the combustion system and represents the current status of the design.

This report also includes a presentation of the results for technology development tests carried out during the detail design and hardware procurement phase of the combustor program. These tests included subcomponent as

well as full-annular tests of prototype designs to evolve the current core engine combustor configuration.

2.0 SUMMARY

The Energy Efficient Engine (E³) combustor effort was conducted as part of the overall NASA/GE E³ Program. The key elements of this five-year effort included the selection of an advanced double-annular combustion system design based on technology derived from the NASA/GE Experimental Clean Combustor and QCSEE Clean Combustor Development Programs. Numerous preliminary and detailed design studies were conducted in order to define the features of the combustion system design. Test hardware was fabricated, and an extensive testing effort was undertaken to evaluate the combustion system subcomponents in order to verify and refine the design. This testing effort included full-scale diffuser model testing to develop diffuser performance, sector combustor testing to develop acceptable ignition and emissions characteristics, and full-annular combustor development testing to further develop ignition and emissions characteristics, as well as develop acceptable exit temperature performance. The technology derived from this component testing effort was incorporated into the engine combustion system hardware design. This advanced engine combustion system was then evaluated in component testing to verify that it satisfied the design intent. What evolved was an advanced combustion system capable of satisfying all E³ combustion system design objectives and requirements.

Following completion of this successful component effort, the engine combustion system hardware was delivered to E³ Evaluation Engineering for incorporation into the buildup of the E³ Combustor Diffuser Nozzle (CDN) assembly as part of the preparation for core engine testing. As part of this testing effort, the combustion system will undergo further evaluation of its overall performance as an integral part of the E³.

3.0 DESIGN SELECTION

3.1 OBJECTIVES AND GOALS

The key objective of this program is to design and develop an advanced combustion system capable of meeting both the stringent emissions and the long-life goals of the E³, as well as meeting all of the usual performance requirements of combustion systems for modern turbofan engines.

As presented in Table I, the E³ program goals for carbon monoxide (CO), unburned hydrocarbons (HC), and oxides of nitrogen (NO_x) emissions are equivalent to the current requirements specified by the Environmental Protection Agency (EPA) for Class T2 (rated thrust greater or equal to 89 kN [20,000 lb thrust] subsonic application) aircraft engines newly certified after 1981 (Reference 4).

Table I. E³ Program Emissions Goals.

EPA 1981 Standards for Newly Certified Engines

● Carbon Monoxide (CO)	}	lb pollutant	3.0
● Hydrocarbons (HC)		per 1000 lbf	0.4
● Nitrogen Oxides (NO _x)		- hrs per cycle	3.0
● Smoke		SAE Smoke Number	20.0

Revisions to EPA standards have been finalized. These revised standards impose a reasonable emission requirement for HC's effective after 1984. However, the CO and NO_x requirements are obviated by the revised standards. Therefore, the E³ program emissions goals are much more challenging than the goals imposed by the final EPA standards. The E³ combustion system also must produce an invisible exhaust plume which corresponds to an SAE smoke number of 20 or lower.

The key combustor performance goals for the E³ program are presented in Table II. Most of the current conventional combustor designs developed by General Electric already provide performance levels generally equal to or better than the goals established for the E³ combustor.

Table II. E³ Combustor Performance Goals.

● Combustion Efficiency at SLTO (%)	99.5 (Min.)
● Total Pressure Drop at SLTO (%)	5.0 (Max.)
● Exit Temperature Pattern Factor at SLTO	0.250 (Max.)
● Exit Temperature Profile Factor at SLTO	0.125 (Max.)
● Altitude Relight Capability (ft)	30,000 (Min.)
● Ground Idle Thrust (% of SLTO)	6.0 (Max.)

The E³ combustor life requirements are summarized in Table III. General Electric design standards require that all combustor designs meet twice the technical life goals in order to assure an adequate design margin. Thus, for technical life goals of 9,000 cycles to repair, the GE design standard requires a design with 18,000 cycles predicted capability. It is observed from Table III that E³ combustor life goals represent a significant advancement over current GE combustor life goals.

Table III. E³ Combustor Life Goals.

	<u>Hours</u>	<u>Flight Cycles</u>
● Hot Parts		
- First Repair	18,000	9,000
- Total	36,000	18,000
● Cold Parts		
- Total	36,000	36,000
● Current Goal for CF6-50 Rolled Ring Combustor, 3000 Cycles Before First Repair		

3.2 DESIGN APPROACH

To meet the emissions goals and other performance requirements of the E³, an advanced short-length, double-annular dome combustor design concept was chosen for the E³ combustion system. A cross section of the E³ combustor design and some of its key features are shown in Figure 1. This combustor concept is based on the technology developed in two NASA/GE combustor programs conducted prior to the start of the E³ program.

The NASA/GE Experimental Clean Combustor Program (ECCP) involved the design and development of a CF6-50-sized double-annular dome combustor. This program was directed toward developing a large-size combustor design with very low CO, HC, and NO_x emissions (compared to a conventional CF6-50 combustor design) over the range of operating conditions of a modern high pressure ratio turbofan engine.

The NASA/GE QCSEE Clean Combustor Program involved the design and development of a double-annular dome combustor as part of the Quiet Clean Short Haul Experimental Engine (QCSEE) Program. This program was similar to the NASA/GE ECCP except that the QCSEE combustor is much smaller and more compact than the CF6-50 combustor design in Figure 2. But in order to meet the challenging NO_x emissions goals of the E³ program, the combustor design was made shorter and more compact than the design evolved in the QCSEE program. This comparison is presented in Figure 3.

To obtain extremely low CO and HC emission levels at ground idle and low NO_x emission levels at high power conditions requires a staged combustion process. Only the outer dome is fueled at low power settings, providing a rich combustion zone for rapid consumption of the CO and HC emissions, while at high power settings both domes are fueled and designed for very lean combustion zone operation. This lean combustion is accomplished for the most part by introducing large quantities of airflow into the inner dome annulus. The introduction of these large quantities of airflow into the combustion zone severely limits the availability of air to perform the other aerodynamic functions.

ORIGINAL PAGE IS
OF POOR QUALITY

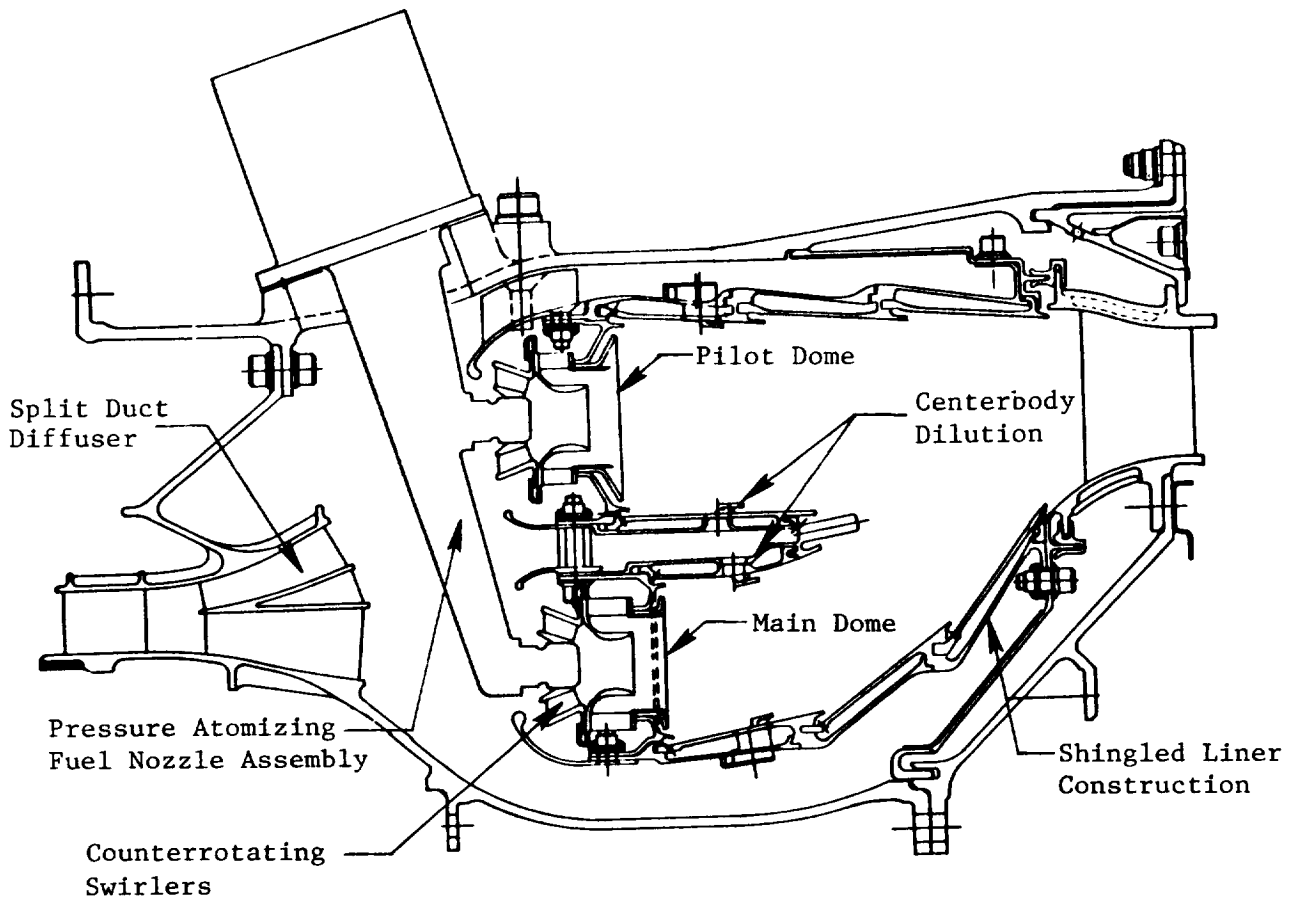
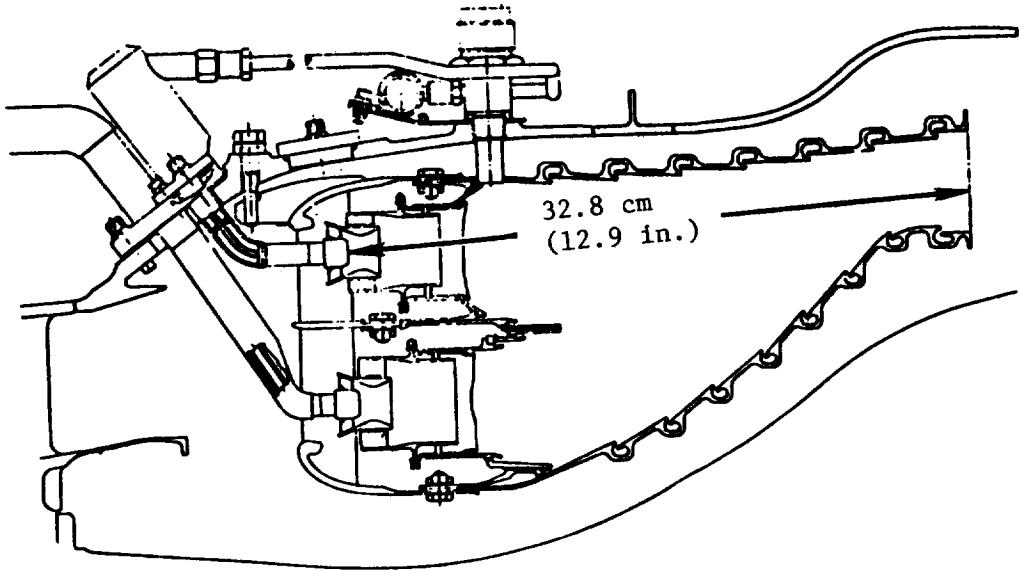


Figure 1. E³ Combustor Cross Section.

ORIGINAL PAGE IS
OF POOR QUALITY

NASA/GE
ECCP
(CF6-50)



NASA/GE QCSEE

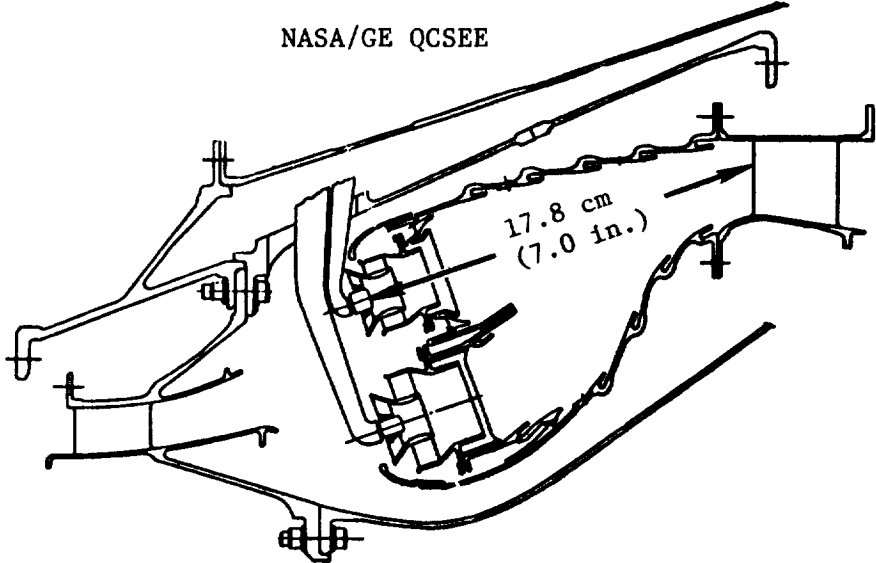


Figure 2. NASA/GE Double Annular Combustors.

ORIGINAL PAGE IS
OF POOR QUALITY

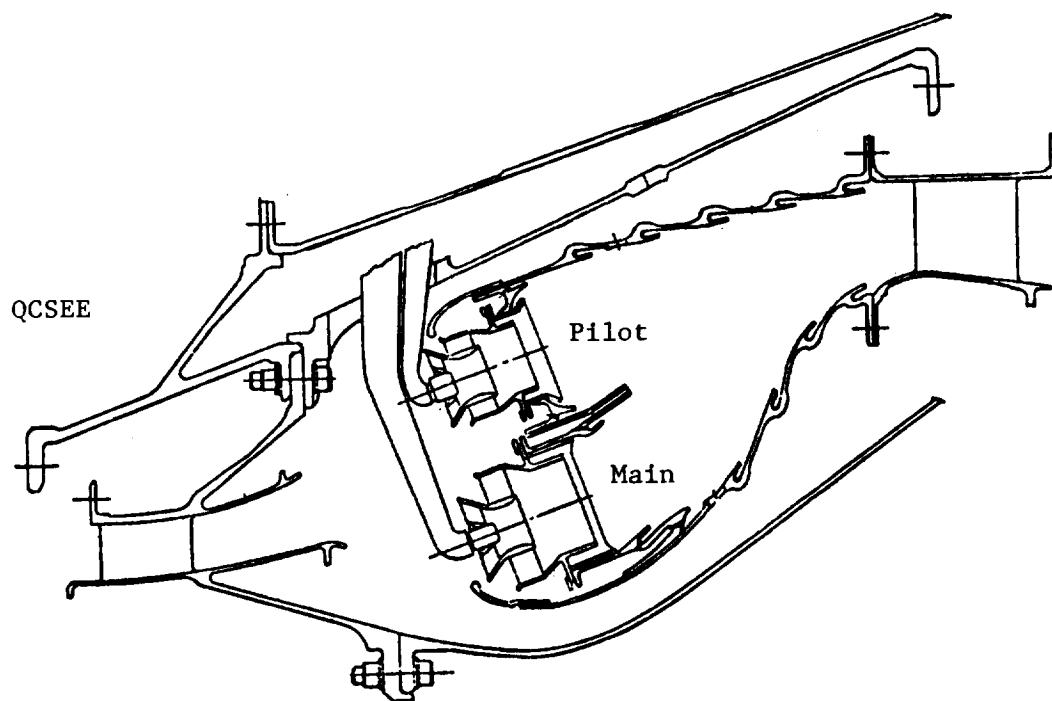
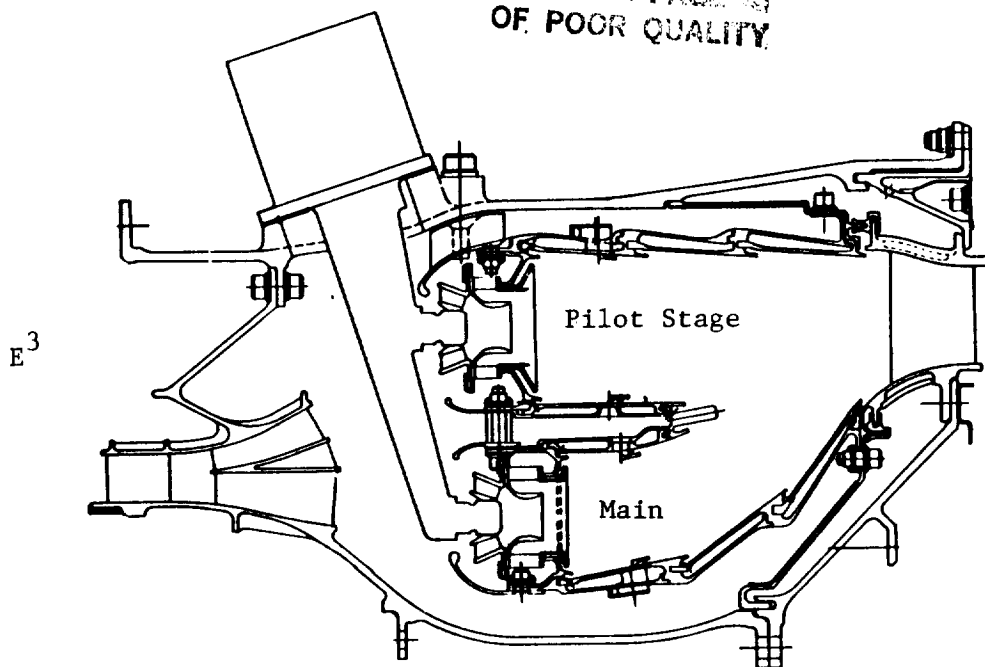


Figure 3. Comparison of QCSEE and E³ Double-Annular Combustors.

To meet the life goals of the E³ combustor program, studies of various liner configurations were conducted to identify a design that would provide the required long-life characteristics. These studies were devoted to the analysis of advanced film plus impingement-cooled liner designs. Such a design concept features a two-piece liner construction (a film liner) and an impingement liner. An illustration of this advanced liner design is shown in Figure 4. A preliminary analysis of an advanced machined ring film plus an impingement-cooled liner design strongly indicated it would not satisfy the E³ technical life goal of 9,000 flight cycles to first repair. Because of the uncertainty of meeting E³ life goals with this liner design concept, a segmented version of the liner design approach (the shingle liner) was evaluated. This even more advanced liner design concept has been developed especially for applications with unusually high-peak combustor liner metal temperatures, as well as for long life.

The desirable features of using a shingle liner approach are summarized as follows:

- Segmented axially and circumferentially
- Reduced stress
- A 360° support structure carries the mechanical loads
- Maintainability
- Life >10⁵ cycles
- Cooling levels consistent with NO_x requirement
- Required for growth engine cycle.

This liner design approach will reduce the thermal stresses in the liner material because the hot-film liner is segmented, thus producing longer life through both the low stress design and the ability to use higher temperature alloys. This advanced "shingled" cooling liner design concept, in conjunction with the drastic short length of the combustor design, is projected to result in the requisite long-life objectives of the E³ program, but within the cooling flow limitations necessary for the E³ NO_x emission level goals.

ORIGINAL DESIGN
OF POOR QUALITY

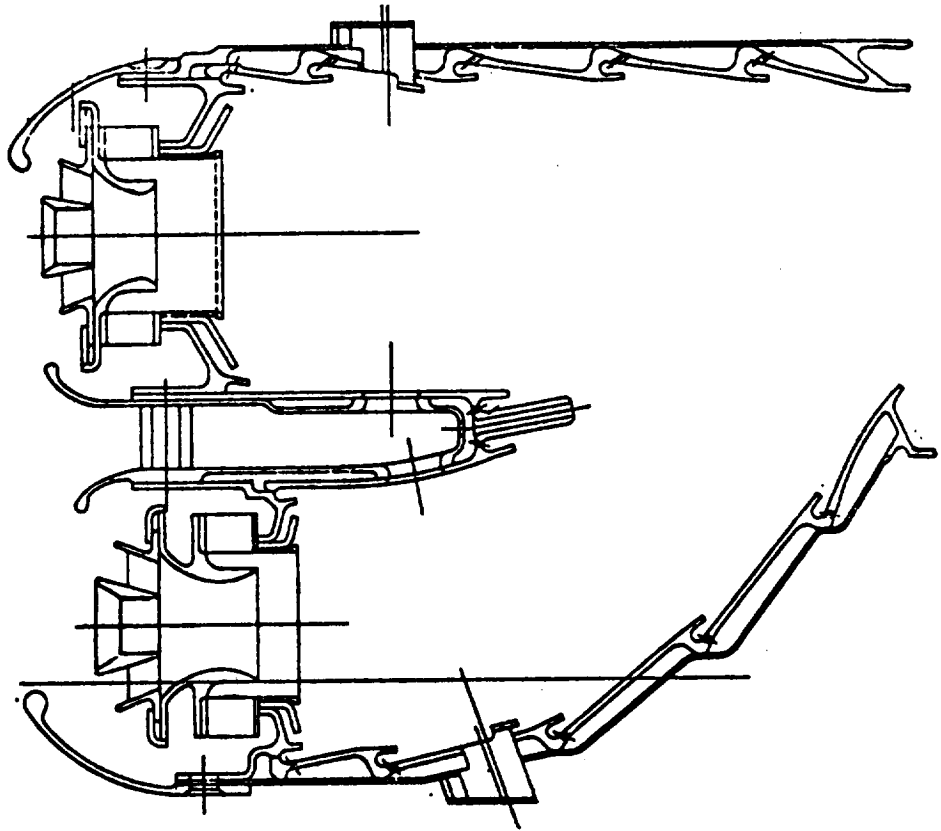


Figure 4. E³ Combustor Film/Impingement Liner Design.

4.0 AERO DESIGN

4.1 REQUIREMENTS

The major emphasis in the combustion system design is directed toward meeting the technically challenging emissions and life goals of the program. In addition, the combustion system must provide the performance characteristics required for operation of a typical modern turbofan engine.

The performance parameters generally considered most important in a combustion system are shown in Figures 5 and 6. It should be noted that not only is high combustion efficiency required at sea level takeoff (SLTO) conditions for this design, but such efficiency must be maintained at a level greater than 99.0% at idle in order to meet the CO and HC emissions goals of the program.

In order to satisfy the combustion system performance requirements and to meet the stringent emissions goals specified for the E³, the selection of an advanced combustor design approach was required.

● Combustion Efficiency (Minimum)	99.5%
● Total Pressure Drop (Maximum)	5.0%
● Exit Temperature Pattern Factor (Maximum)	0.250
● Exit Temperature Profile Factor (Maximum)	0.125
● Ground Start Ignition to Ground Idle Within 60 Seconds	
● Stable Combustion Within the Flight Envelope	
● Altitude Relight Capability up to 9.15 km (30,000 ft)	
● Carbon-Free Operation	
● No Resonance or Starting Growl Within the Flight Envelope.	

Figure 5. Performance Requirements.

• SLTO SLS Standard Day

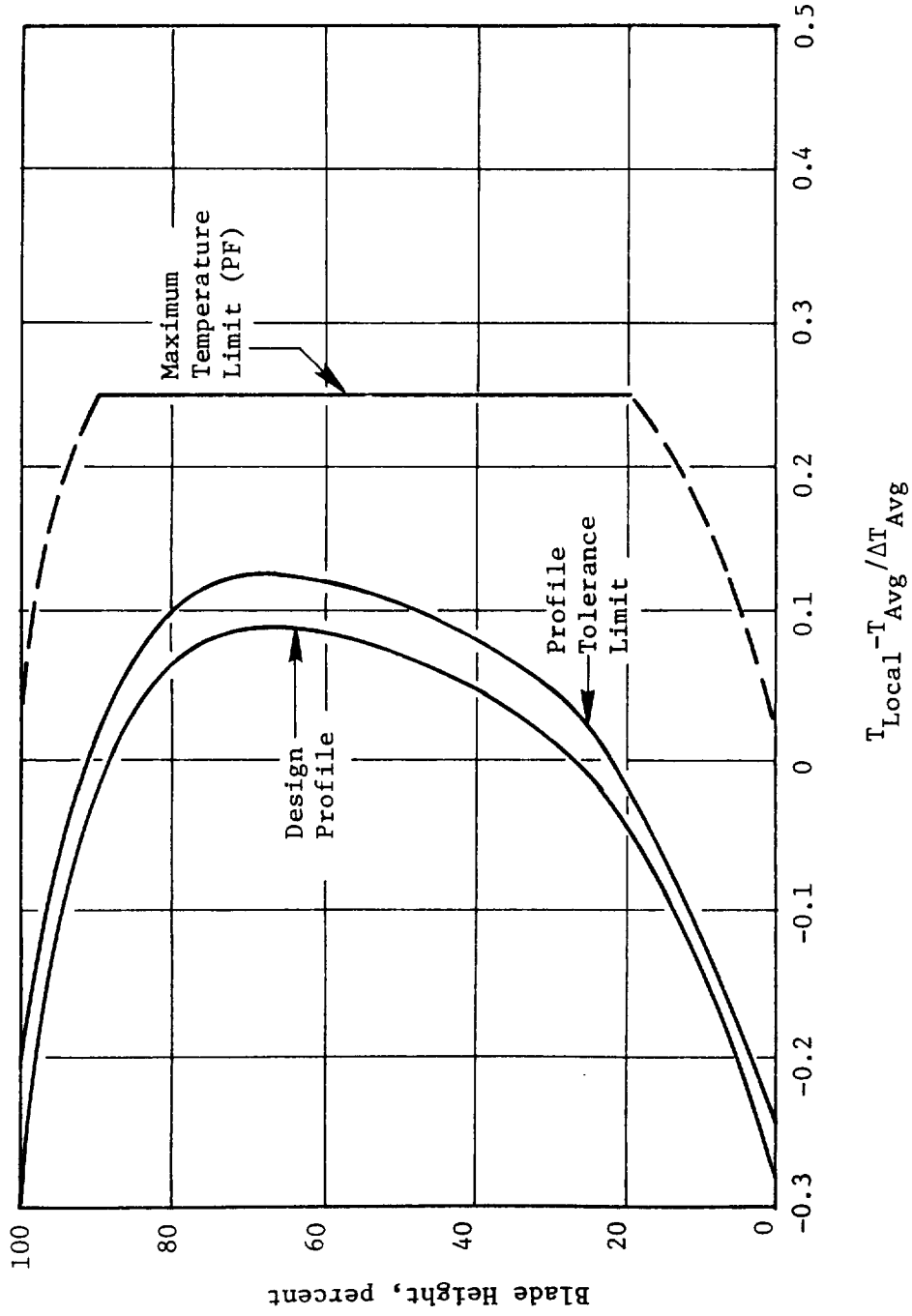


Figure 6. Turbine Inlet Radial Temperature Profile Requirements.

4.2 KEY STUDIES

A large number of design studies were conducted during the process of evolving the preliminary design of the combustor and refining the design features into the detailed core engine design.

The four major study areas were related to detail component and systems design which included aerodynamic analysis, ground start sequence, fuel staging modes, and estimates of the emissions levels to be expected from the core, ICLS, and FPS engine designs.

The major objectives of the aerodynamic analysis were to define a desirable combustor flowpath within the constraints of the engine envelope and to develop the required distribution of airflow within the flowpath to meet all of the combustor performance, emissions, and life objectives.

4.2.1 Cycle Studies

One of the key inputs in evolving the airflow distribution was the engine operating cycle. Two of the most important operating modes are ground idle and sea level takeoff (SLTO). Both of these cycle conditions are utilized in the EPA landing/takeoff (EPA-LTO) cycle to calculate emissions performance; sea level takeoff is generally selected as the combustor design point for combustor sizing and analysis. Of the four EPA-LTO conditions, ground idle is extremely important for a staged combustor design like the double annular, since the pilot stage dome design is based primarily on this operating condition. The CO emissions levels are highly sensitive to the pilot dome equivalence ratio at this condition (see Figure 7). However, ground idle combustor inlet conditions may vary as the engine cycle is refined, as shown in Table IV. For this reason, several iterations on airflow distribution may be required to satisfy the requirements of the emissions goals, establish cooling airflows in order to maintain metal temperatures, and select combustion zone airflows to meet performance. The airflow distribution evolved for the baseline design is compared to airflow distributions finally evolved for the core engine (Figure 8). This comparison illustrates how significantly the aerodynamics can change.

ORIGINAL PAGE IS
OF POOR QUALITY

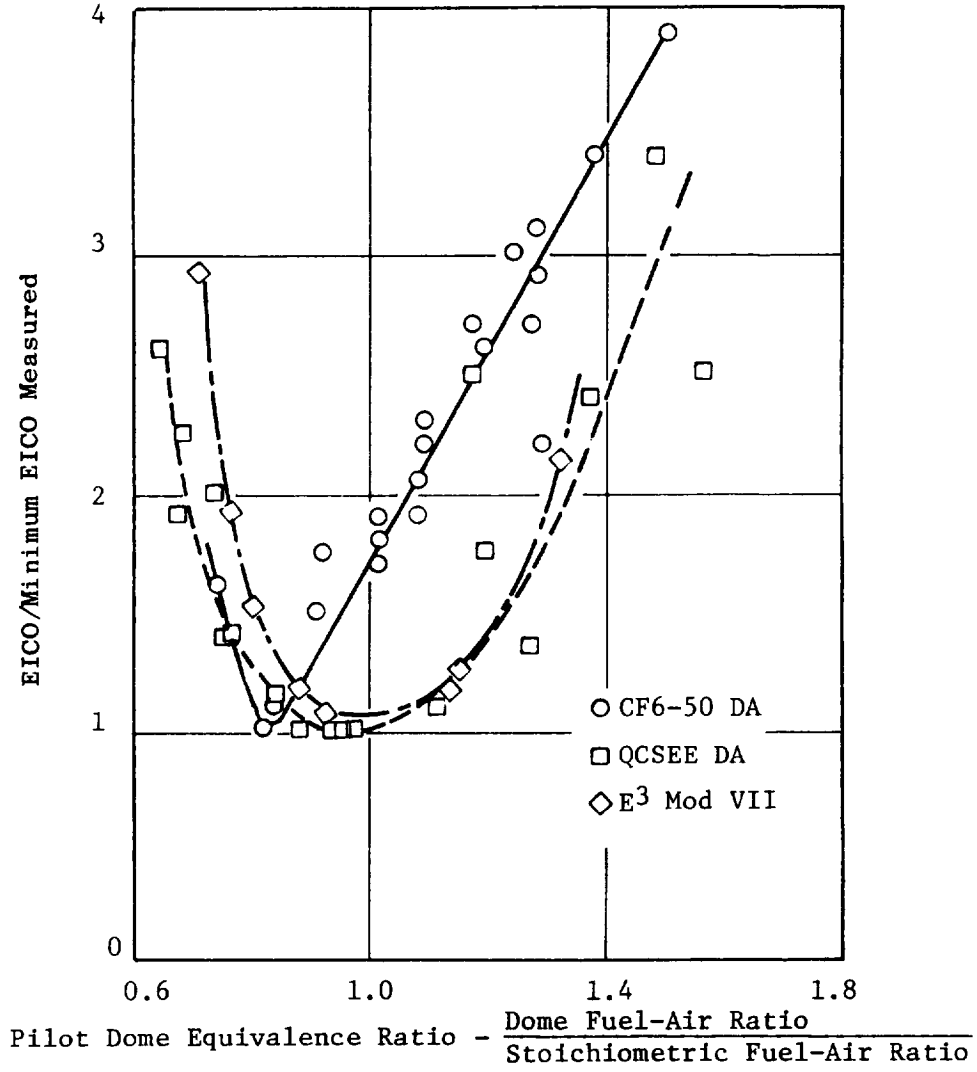


Figure 7. Effect of Pilot Dome Airflow on CO Emissions.

ORIGINAL PAGE IS
OF POOR QUALITY

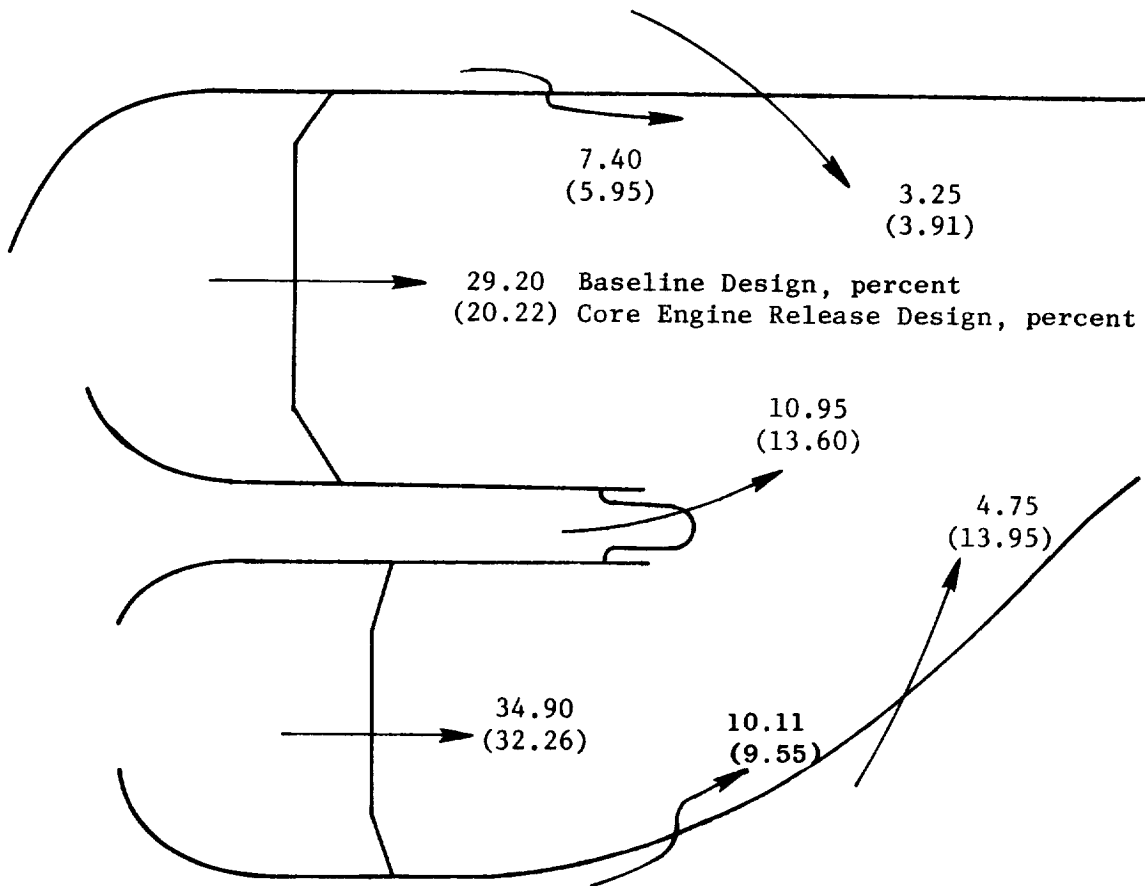


Figure 8. Comparison of E³ Combustor Design Airflow Distribution.

Table IV. E³ FPS Design Cycles.

<u>Ground Idle (6% F_N)</u>	<u>Proposed Idle Cycle (Data)</u>		
	<u>PDR (7/78)</u>	<u>IDR (4/79)</u>	<u>DDR (8/81)</u>
T ₃ - K (° R)	485 (873)	517 (931)	497 (894)
P ₃ - MPa (psia)	0.40 (58)	0.43 (62)	0.43 (63)
FAR 4	0.012	0.0141	0.0123
<u>SLTO (100% F_N)</u>			
T ₃ - K (° R)	814 (1465)	815 (1467)	815 (1467)
P ₃ - MPa (psia)	3.01 (438)	3.02 (439)	3.02 (439)
FAR 4	0.0244	0.0244	0.0245

4.2.2 Diffuser

One of the key components in the combustion system that directly affects combustor as well as engine performance is the diffuser. The diffuser accepts air from the compressor discharge and directs it to the combustor. The key design requirements for the diffuser are as follows:

- Positive flow distribution
- Stable flow, separation-free
- Short length
- Low pressure losses
- Bleed airflow capability

The design of the combustor diffuser depended on the selection of a turbine cooling air extraction configuration, definition of the diffuser wall contours, and modeling of the diffuser system aerodynamics. The design approach selected was a dual-passage step-diffuser system which provides for the large area change between the compressor discharge and the double-dome height of the combustor. This diffuser design is defined as a split duct.

Two approaches for extracting turbine cooling air from the compressor airstream were considered for the split-duct diffuser design. The configurations investigated were leading edge and trailing edge designs. The leading edge approach, which extracts turbine cooling air from the centerline location of the compressor flowpath, offers the advantage of positive total pressure feed and lower air temperature. The airflow is metered through a circumferential slot located at the leading edge of the splitter vane. The airflow is then diffused into the strut cavity and routed through the hollow strut passage into the cooling circuit. Since the flowmetering is done at the leading edge slot, extremely accurate dimensional control is required. The leading edge design also has higher frontal blockage which results in a higher OGV Mach number that requires longer diffuser passages.

The trailing edge approach has positive design features such as dirt separation, enhanced diffuser stability, and good mechanical strength. However, the trailing edge design depends on static pressure feed and has slightly higher cooling air temperatures due to mixing in the prediffuser passages. In this design the airflow is metered through circular orifices in the discharge base of the splitter vane and dumps into the strut cavity. Such an approach permits accurate metering and easy modification of bleed flow quantity.

Although the leading edge design does offer the advantage of slightly improved sfc due to the lower cooling air temperature and higher combustor inlet temperature, the disadvantages of increased hardware cost, cooling air metering dimensional sensitivity, and rework difficulty were considered critical risks and led to selection of the trailing edge approach shown in Figure 9. Additional design studies using conventional design practices (such as the Stanford Diffuser Separation Correlations) and analyses using the General Electric Compressor Axisymmetric Flow Determination (CAFD) computer program were conducted on the prediffuser design to determine the passage Mach numbers and pressure distribution. The configuration analyzed included the effects of blockage from the 30 prediffuser struts and an estimated compressor discharge airflow radial profile. These analyses provided information concerning the velocity characteristics and permitted selection of the prediffuser wall coordinates. After the coordinates were defined, the system was analyzed to determine the expected performance for comparison to the design requirements.

ORIGINAL DESIGN
OF POOR QUALITY

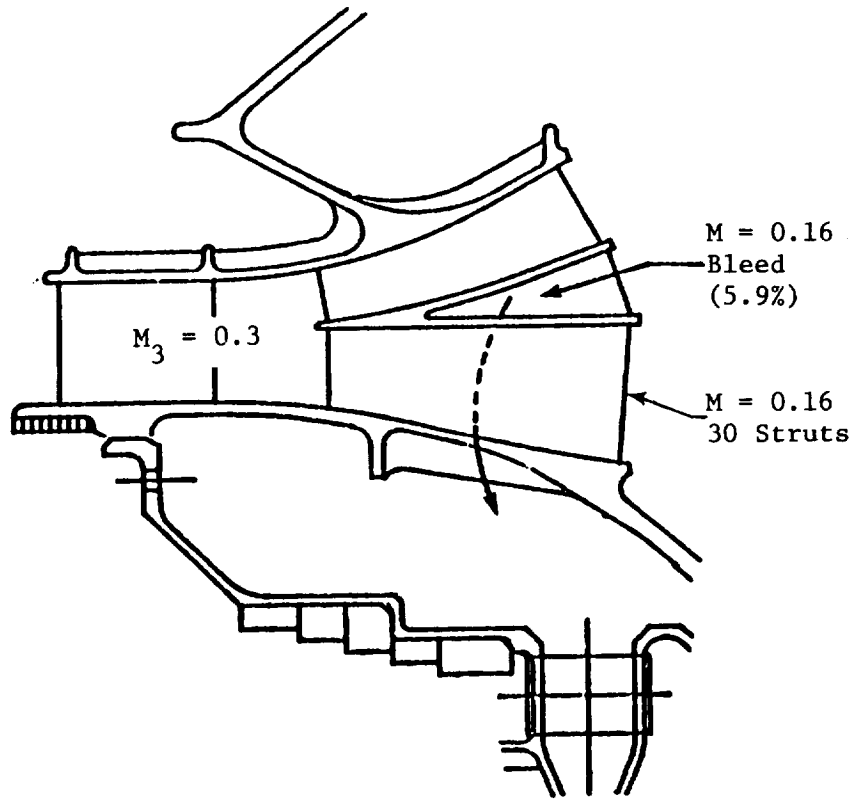


Figure 9. Split Duct Diffuser Design.

The results predicted a mass-weighted total pressure loss of 1.5 percent. No major problem areas were identified for the diffuser; therefore, the identified design was transmitted to General Electric's Corporate Research and Development Center for fabrication of a water table model and a full-annular, full-scale aerodynamic model.

4.2.3 Fuel Nozzle

Several studies dealing with fuel nozzle hydraulic and heat transfer characteristics were carried out. The fuel nozzle design features and design requirements are shown in Figure 10. The nozzle hydraulic system features a primary and secondary duplex fuel nozzle system in both the pilot and main stage systems. The primary system provides excellent fuel atomization at low-power operating conditions where the combustor inlet environment is less favorable for combustion. At high power, where combustor inlet conditions are favorable, the secondary system provides excellent fuel atomization and the desired flow capacity to achieve full engine power. The valve mechanism mounted above the flange provides the fuel metering schedule between primary and secondary nozzle flow and is cooled by fan air to reduce thermal problems.

A major design effort was directed toward heat transfer analyses of the fuel nozzle designs for the core and ICLS systems. These design studies were conducted to assure that no fuel gumming or carboning would occur during the demonstrator program to be conducted with ambient fuel temperatures at sea level conditions. Additional studies were conducted on the FPS system where fuel inlet temperatures as high as 408 K (734° R) would be expected and where the nozzles would be exposed to high heat loads with low fuel flows that exist during high altitude operation.

The heat loading conditions selected for the design of the annular test rig fuel nozzles were simulated SLTO conditions. The estimated critical temperature range for incipient carbon formulation is 422 K (760° R) to 450 K (810° R). Without any insulating features, the fuel wetted wall temperatures of the test rig nozzle assemblies were expected to exceed 478 K (860° R). This could result in a marginal design. The wall temperatures are reduced markedly to levels well below the critical limit with the addition of insulating tubes

ORIGINAL PAGE IS
OF POOR QUALITY

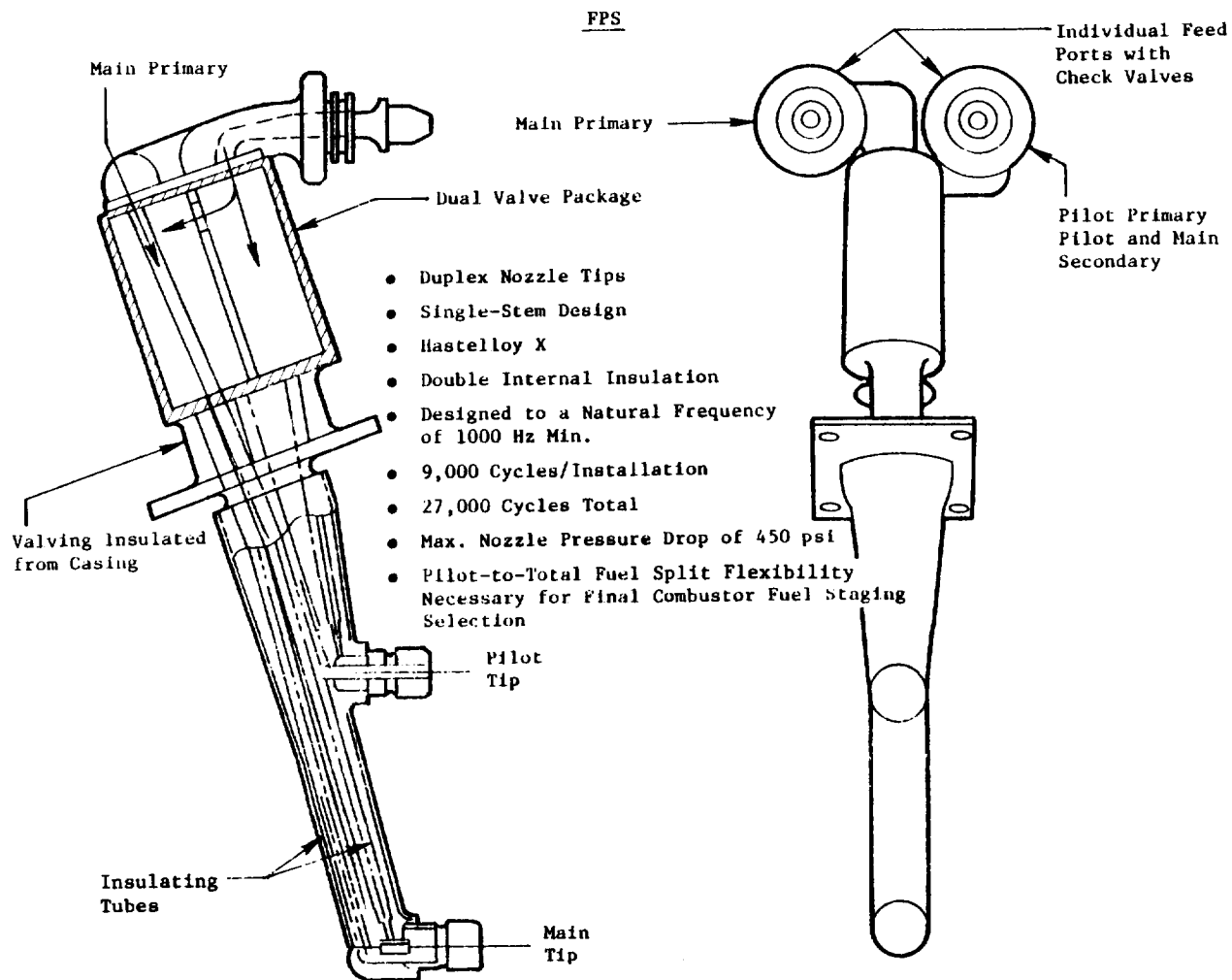


Figure 10. E³ Double-Annular Combustor Fuel Nozzle Design.

in the fuel passages. This design feature was incorporated into the annular test rig fuel nozzle assemblies.

The core engine and ICLS fuel nozzle design was analyzed in a similar fashion. However, the core and ICLS design featured an external heat shield as well as fuel passage insulating tubes. The heat load conditions selected for this design study were the ICLS SLTO conditions. As expected with ambient inlet fuel temperatures, the wall temperatures were notably low. But as shown in Figure 11, at higher fuel inlet temperatures the wall temperatures approached the critical limit. Based on these results, a more rigorous analysis was conducted on the FPS design where more severe operating conditions might exist. The analysis indicates that the worst heating condition is near the flange where the heat shield is in contact with the stem and forms a heat conduction path. The analysis showed that the tube-wall temperature can be reduced significantly if the original fuel tube insulating gap is increased from 0.020 to 0.051 cm (0.008 to 0.020 inch). As long as the duration of exposure to the maximum inlet fuel temperature of 408 K (734° R) is short, carbon buildup or fuel gumming is expected to be negligible.

Because the combustor was in a stage of development where the optimum proportion of fuel between the pilot dome and main dome had not yet been determined, it was necessary to provide a degree of flexibility in the amount of fuel that could be scheduled to each system without exceeding the flow capacity of the engine fuel system. The fuel system was oversized to incorporate this flexibility. By installing a fixed orifice in the main stage fuel system, the fuel flow split between the pilot stage and main stage could be adjusted to provide the desired flow split. Following completion of the core engine combustor component test program, the hydraulic characteristics for the two fuel systems will be selected and the appropriate orifice size will be installed.

4.2.4 Ignition System

One additional design study conducted was related to the ICLS ignition system. The mounting provisions for the ICLS ignition system require that the igniter lead be routed underneath the core cowl to connect the spark igniter

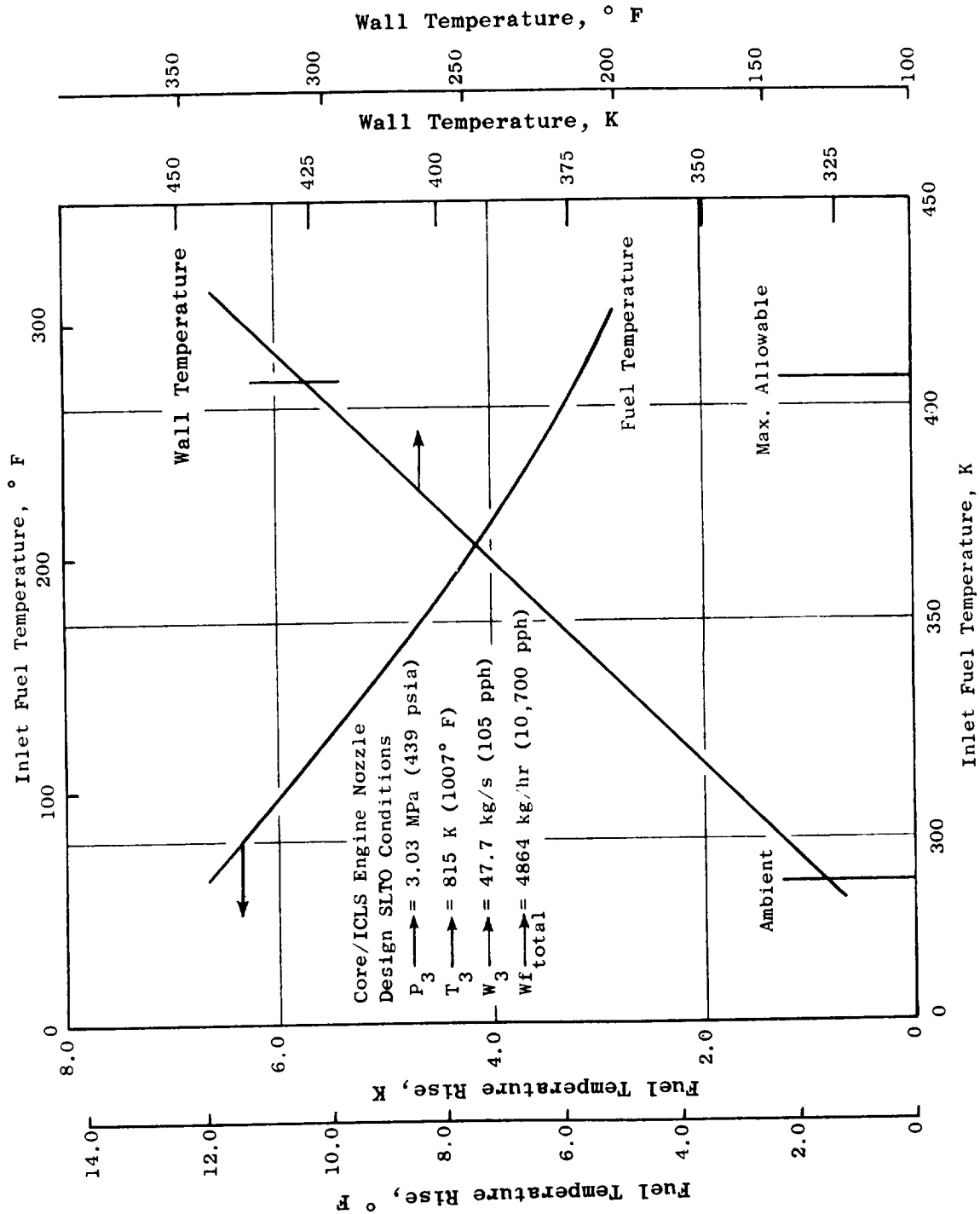


Figure 11. Effect of Fuel Inlet Temperature on Fuel Nozzle Temperature.

to the ignition exciter box. The core cowl region is generally purged with fan air at about 478 K (860° R). But a more severe condition is expected to exist on a shutdown from maximum power where casing temperatures heat the core cavity air to higher levels than the fan purge air. A transient heat transfer analysis was conducted based on measured core cavity temperature responses in a CF6-50 on shutdown from maximum power. Based on these analyses, using the E³ core cavity geometry, a peak air temperature of 606 K (1109° R) would be expected during soak back. The Teflon lining of the ignition lead will withstand 700 K (1260° R) without material damage; thus, it was concluded that a standard lead design without auxiliary cooling would be adequate.

4.2.5 Starting

One of the major, most intensive studies conducted on the combustor system dealt with obtaining an acceptable ground start ignition sequence for the E³ engine equipped with the parallel-staged combustor design. The key highlights of this effort are presented in Table V. E³ ignition requirements are typical of those used in conventional commercial aircraft engine applications. These requirements were (1) stable ignition and propagation, (2) 60-second accel to idle, and (3) start free of stall and noise. A substantial amount of experience in starting engines equipped with a parallel-staged combustor, such as the E³, had been obtained in the NASA/GE Experimental Clean Combustor Program (ECCP) conducted earlier. As shown in Table VI, the CF6-50-sized parallel-staged design tested in the ECCP demonstrated highly satisfactory experience for engine ground starts.

The key difference between the previously successful ECCP design and the E³ design centered around the ground-start compressor bleed flows required to prevent compressor stall and the associated combustor fuel-air ratios and their impact on turbine metal temperatures. Figure 12 shows that the initial estimates of the required starting compressor bleed resulted in very high combustor fuel-air ratios. These high overall fuel-air ratios, coupled with the tip peaked exit temperature profiles (Figure 13) associated with fueling only the pilot-stage dome during ground start, resulted in unacceptable turbine metal temperatures - particularly in the uncooled low pressure turbine hardware. In order to attenuate the temperature profiles associated with operation of

Table V. Chronology of E³ Starting Studies.

January 1978 - October 1978	Combustor Design - Original Concept - Pilot-Only Ignition Through Ground Idle
December 1978 - September 1979	Engine Start Studies Initiated, Model Predicts High T _{4.1} Max. with Pilot Only Fueled
February 1978 - March 1980	Combustor Ignition Studies Conducted to Develop Capability to Start Engine with Both Domes Fueled
January 1980 - May 1981	Dev. Comb. Activity Directed at Evolving Satisfactory Ignition with Both Domes Fueled from Light Off Through Ground Idle
May 1981 - Present	Start Studies Resumed with New Component Data Input That Indicate Pilot-Only Start Will Be Satisfactory

Table VI. Starting Background.

- CF6-50 Double-Annular (ECCP)
 - Staged Combustor
 - Extensive Component Test
 - Engine Tested
- Staging Procedure
 - Ground Start to Approach Power (Pilot Only)
 - Above Approach (Pilot and Main)
- Starting History
 - Satisfactory Main Stage Ignition in Component Tests
 - 56 Successful Engine Starts

One Unsuccessful Start (Aborted, Exceeded T_{4.9} Limit)

ORIGINAL PAGE IS
OF POOR QUALITY

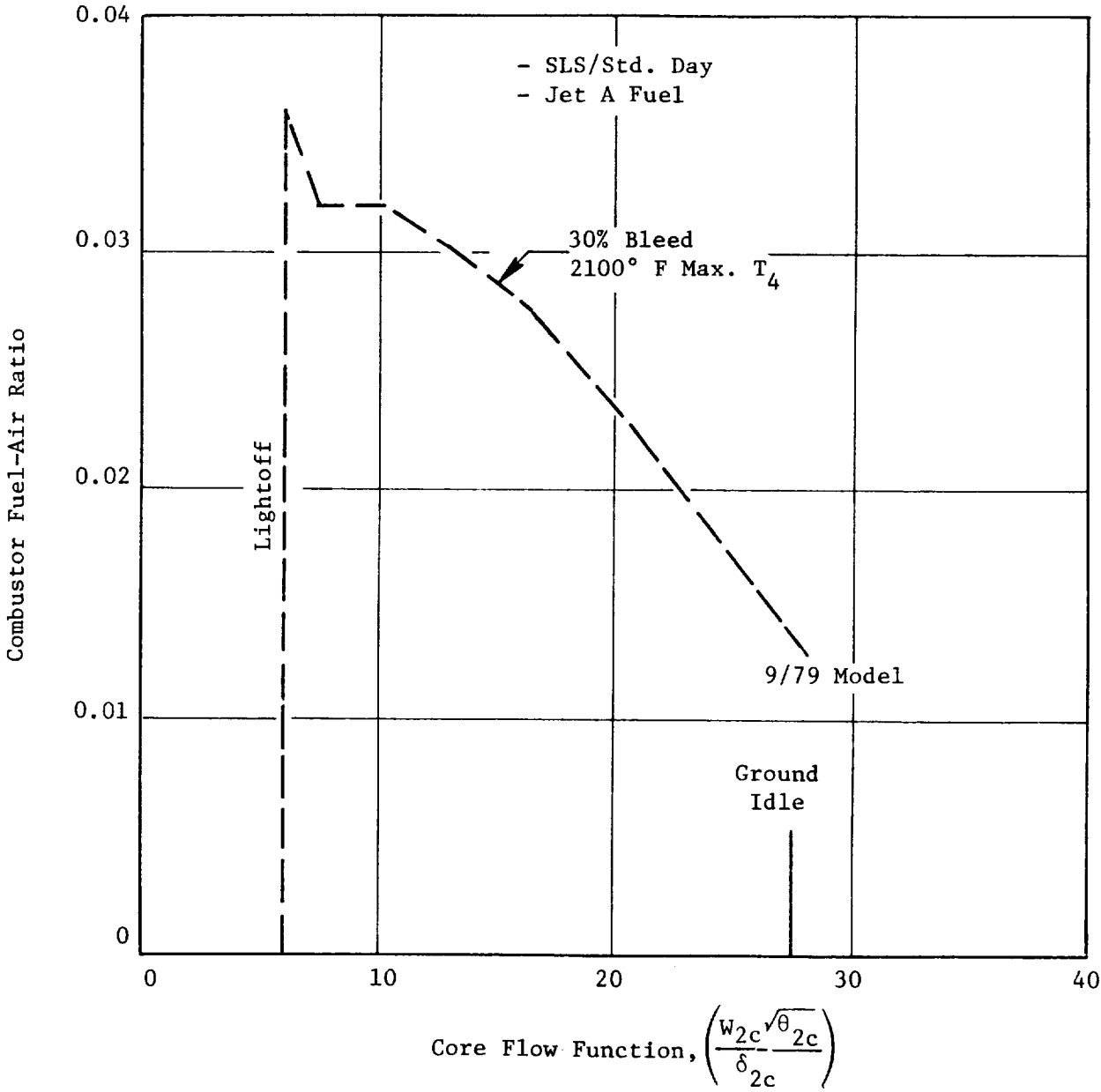


Figure 12. Combustor Fuel-Air Ratio Versus Core Compressor Flow.

ORIGINAL PAGE IS
OF POOR QUALITY

- 46% Core Speed Operating Condition
- 9/79 Start Cycle

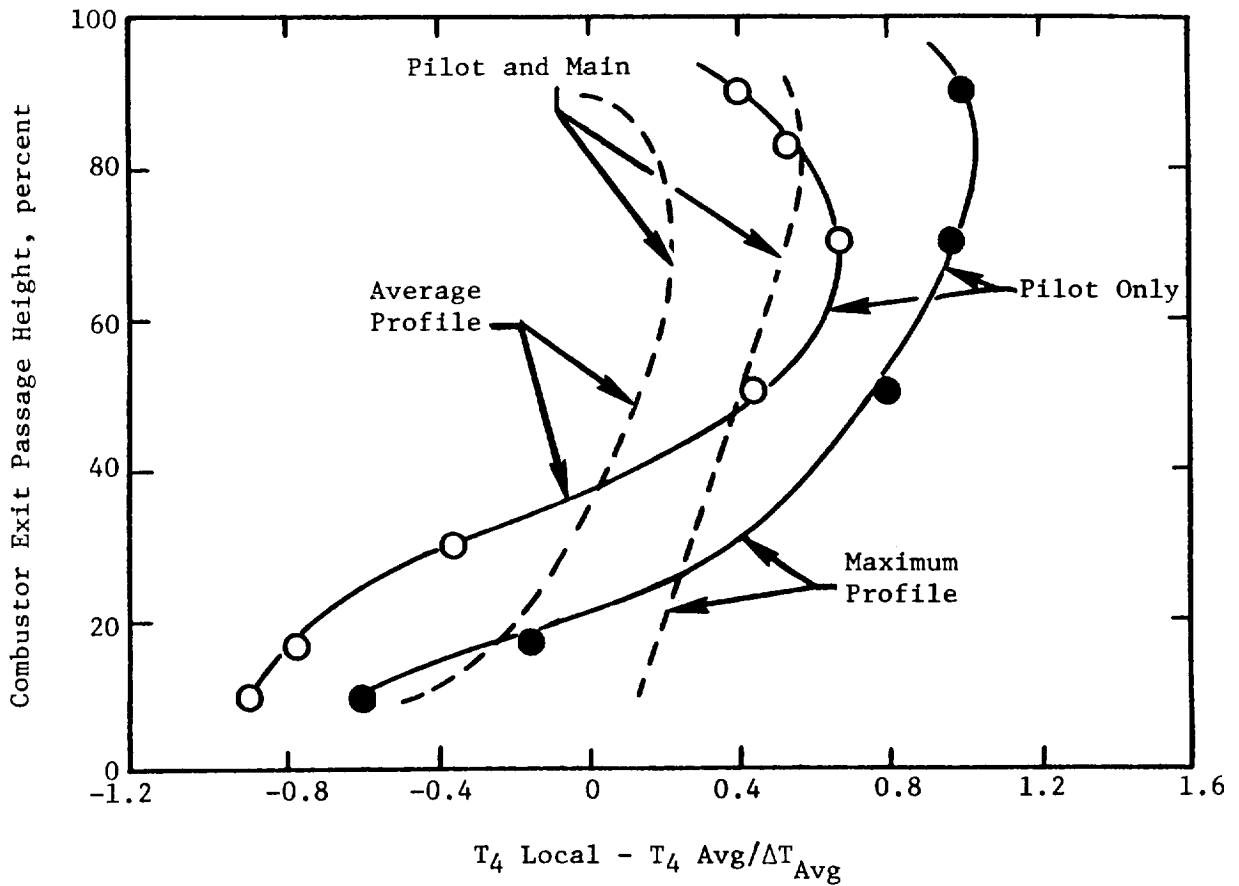


Figure 13. Combustor Exit Temperature Profile.

the pilot stage only during ground start, an alternative fueling mode was evolved. This alternate approach involved staging the combustor from the pilot-only mode to pilot and main during the ground start sequence in order to divide the fuel between both pilot and main stages, thereby providing a flatter exit temperature profile similar to that shown in Figure 13. Since the main stage was originally intended only for operation at high power operating modes where combustor inlet conditions are more favorable for ignition, several approaches were considered: (1) primary-secondary fuel nozzle, (2) alternate fuel nozzles fueled (subidle), and (3) rich domes (reduced main dome airflow). This redirection in operating requirements for the combustor and, in particular, the main stage combustion system resulted in major changes to the design. These design changes are outlined below.

- Duplex fuel nozzles in pilot and main dome
- Complex control staging at ignition
- Reduced main dome airflow
- Crossfire tube improvements

As shown in Figure 14, with the lean main stage dome evolved as the baseline design, the main stage dome velocities are considerably higher than in the pilot stage dome. Even with major reductions in airflow designed to obtain a rich main stage dome configuration, the dome velocities remain high due to the smaller annulus area of the main dome. Figure 15 shows that fuel staging becomes much more complex, requiring significantly more manipulation of the pilot and main stage fuel flows during the start sequence. The undesirable features of the rich dome design approach are outlined in Table VII. Of particular concern were the higher NO_x emission levels expected with the rich main stage dome design. However, the greatest concern was centered around the capability to start the engine satisfactorily without sustaining any damage to the engine components. Therefore, combustor development activity was redirected toward evolving a rich main dome configuration. During the first quarter of 1981, key component test results were obtained relative to the E³ compressor and turbine low speed performance. Utilizing this most recent component test data, the engine starting analysis was updated. The key points of this study are presented in Table VIII. The results of the study were:

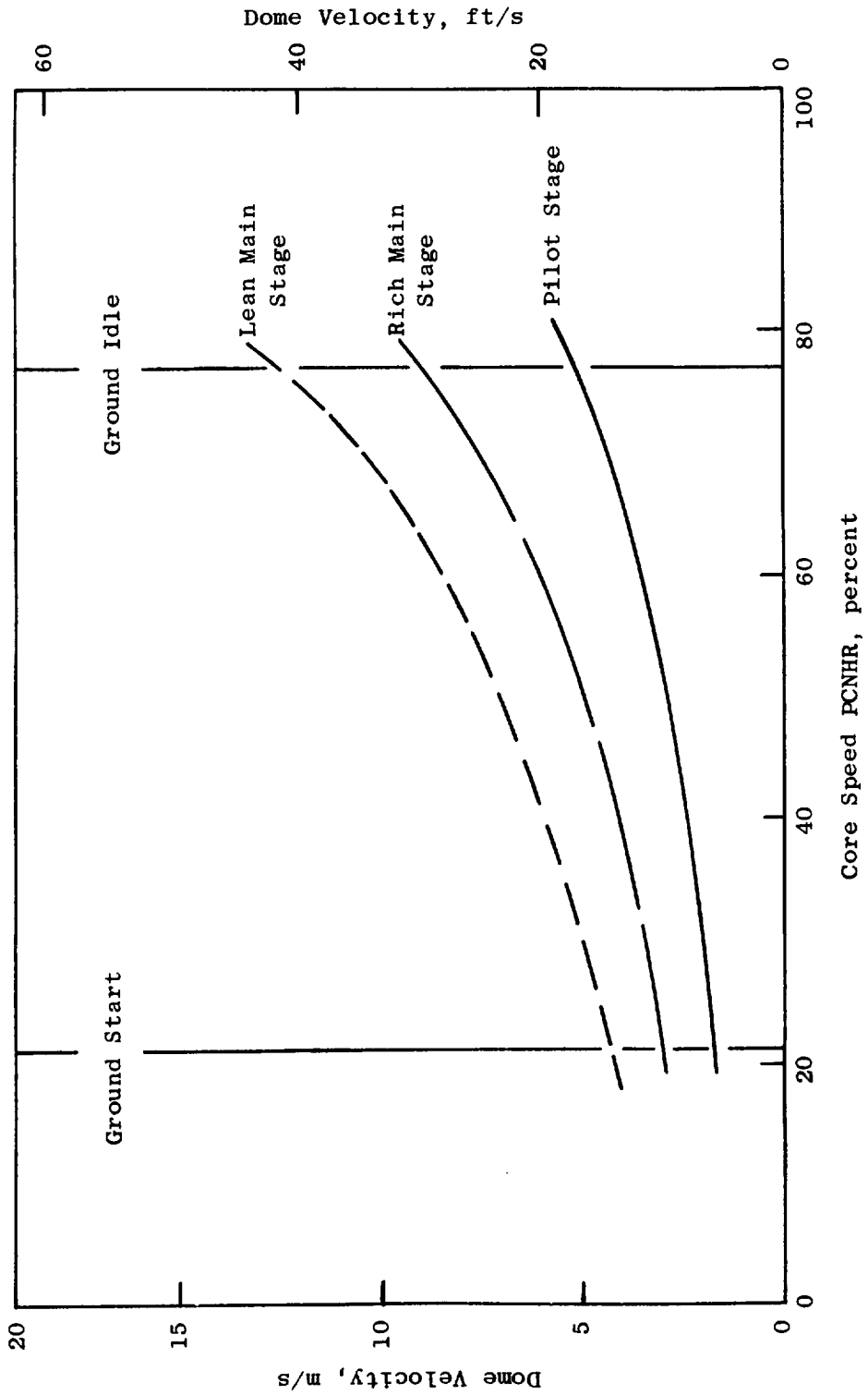


Figure 14. Double-Annular Combustor Dome Velocity Comparison.

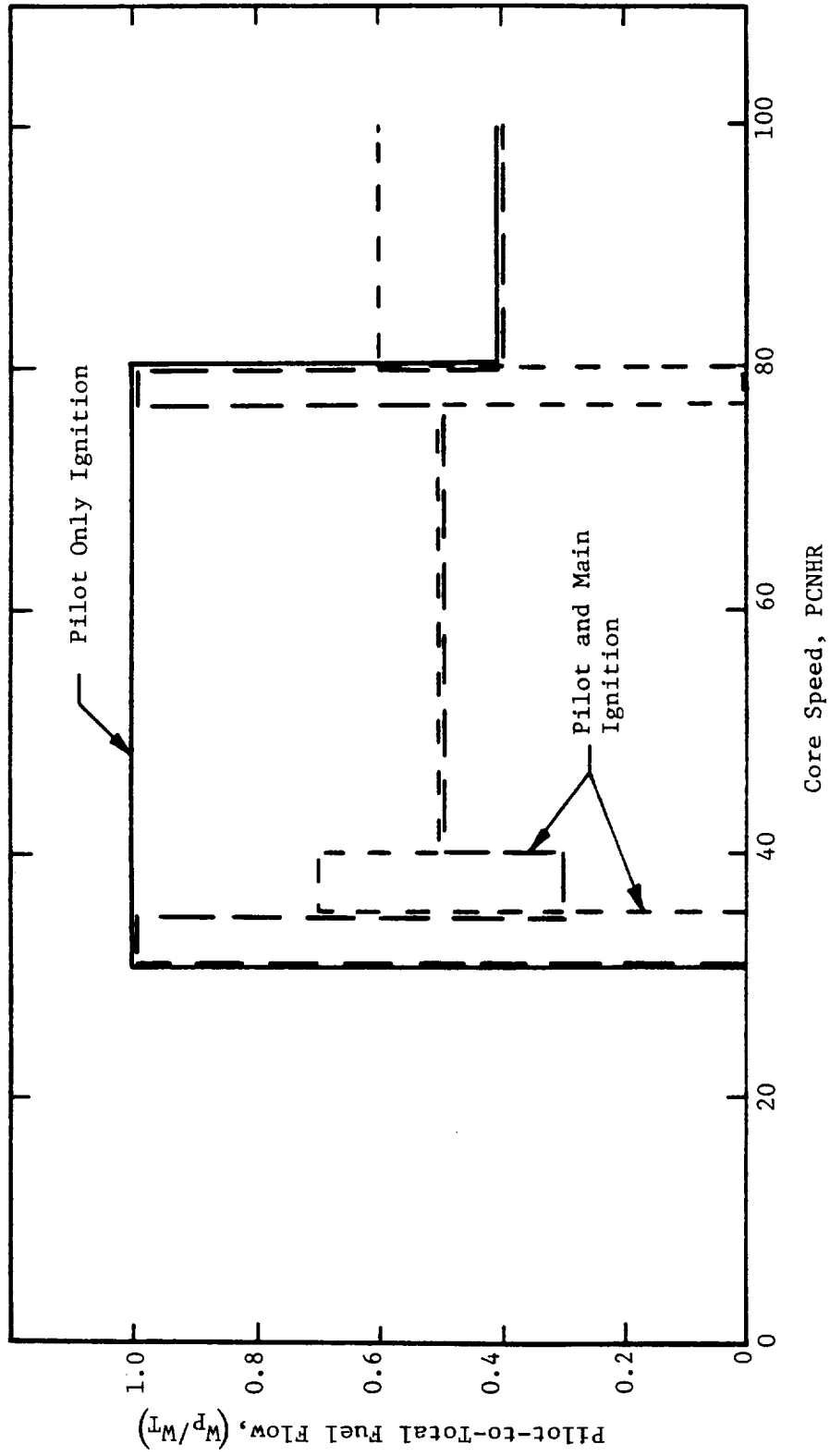


Figure 15. Comparison of Combustor Fuel Staging Sequence.

Table VII. Adverse Impacts of Pilot and Main Stage Ground Start Ignition.

- Increased Fuel Staging Complexity
- Additional Control Logic Required
- More Complex Main Stage Fuel Nozzle
 - Added Hydraulic Features (Primary Orifice)
 - Additional Fuel Tube Insulation
 - Larger Envelope (Heavier)
 - More Expensive
- Richer Main Dome Operation at High Power
 - Increased NO_x Emissions
 - Increased Liner Temperatures

Table VIII. Revised Engine Start Analysis.

- Start Model Updated 5/81
 - New Compressor Subidle Representation Based on 1 to 10 Test Results
 - Improved Low Speed Turbine Efficiency Levels Based on E³ Turbine Component Tests
 - Lower Bleed Flows Required
- Improved Profile Mixing Through High Pressure Turbine

- Satisfactory 60-second ground start
- 10% stall margin below 65% N_c
- Maximum average $T_{4.1}$ at 1228 K (1750° F) as compared to previous 1422 K (2100° F)
- Satisfactory ground start obtained operating on pilot only

The key finding of this updated study was that considerably less compressor bleed was required during start than had originally been determined. As a result, the combustor overall fuel-air ratios encountered during start were greatly reduced (Figure 16).

A comparison of the study results for the two operating modes for the combustor during ground start is summarized in Table IX. Based on these results, it was concluded that engine ground start with the pilot-stage-only fueled was the preferred mode of operation due to the very favorable ignition characteristics of the pilot dome and the significantly reduced complexity required for the control system. These conclusions obtained from the starting studies led to another redirection in the combustor development effort back to the original lean main stage dome design, but considerable development effort had been expended in designing a rich main stage dome.

Table IX. Ignition Study Results.

(Pilot Stage Only Versus Both Stages Fueled)

- Light-Off to Ground Idle in 60 Seconds
 - Both Approaches Meet Objective
 - Both Domes Fueled Require More Complex/Heavier Fuel System and Control Logic
- Stable Ignition and Flame Propagation
 - Pilot Stage Design Most Amenable to Good Ignition and Flame Propagation
 - Both Domes Require Crossfire to Main Stage
- Stall and Growl-Free Operation in Subidle Range
 - Pilot-Stage Only Provides Most Potential for Growl-Free Operations
 - Both Domes Fueled Provide Most Potential for Stall-Free Operation Due to Lower/More Uniform Combustor Exit Temperature

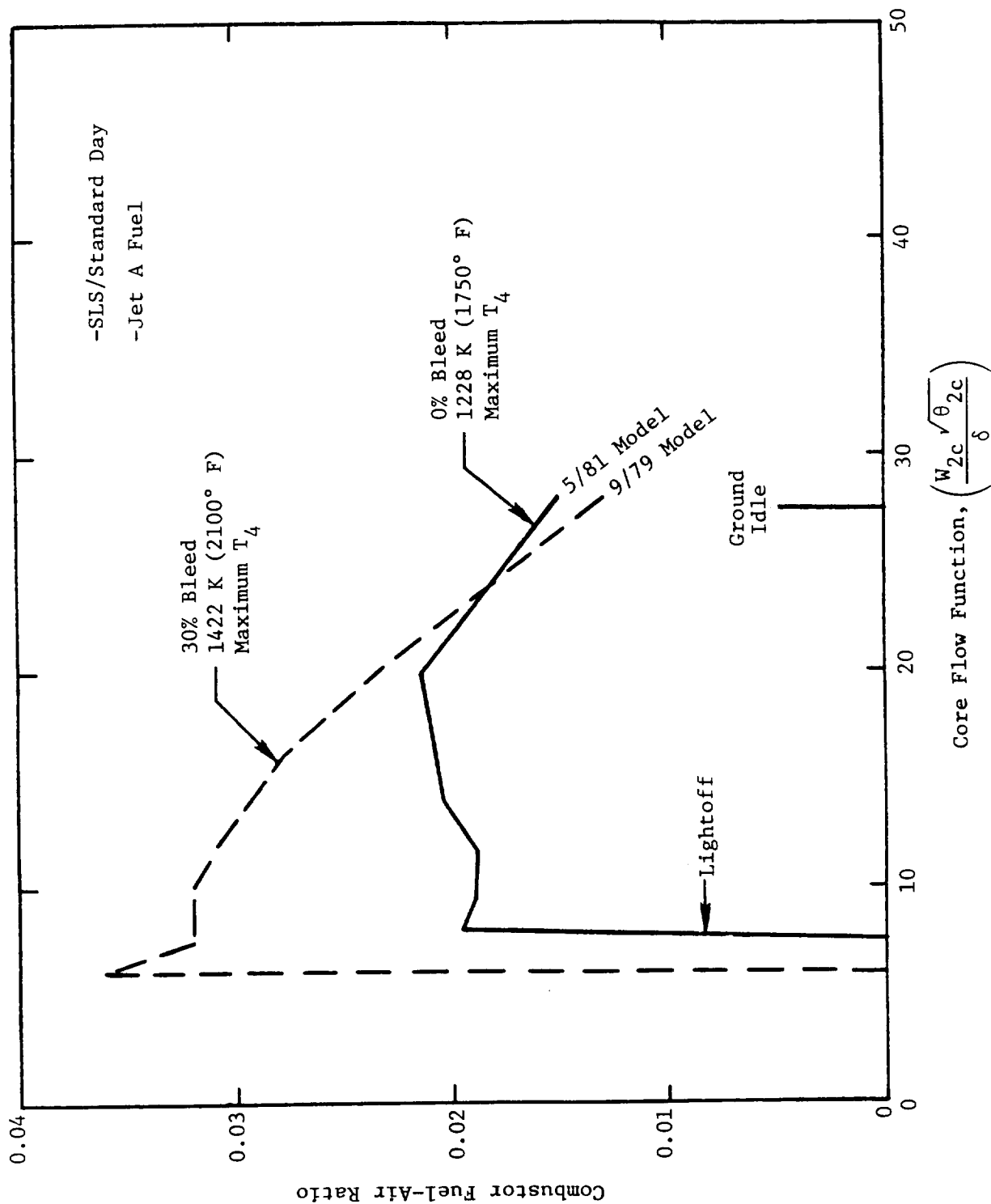


Figure 16. Comparison of Core Engine Start Models.

4.2.6 Emissions

One of the key concerns during the preliminary and detail design phases was the predicted emissions levels of the E³ combustor design and how these would compare with the program goals. The key considerations affecting the results of the E³ combustor emissions study effort were: (1) previous development experience on CF6 ECCP, QCSEE, and LOPER; (2) E³ cycle conditions; (3) E³ emissions adjustment relationships. GE has acquired considerable experience in designing advanced low emissions combustors. The NASA/GE ECCP involved development of an advanced parallel-staged full-annular combustor sized to fit a CF6-50 engine. The NASA/GE QCSEE Program also involved an advanced parallel-staged combustor similar in size to an F101/CFM56 combustor which was developed in sector combustor tests. The NASA/GE LOPER Program was directed toward obtaining ultralow CO and HC emissions at low power operating conditions in a single-annular design. These single-annular designs utilized such advanced concepts as recuperative cooled liners, hot wall liners, and catalytic combustion.

The ground-idle combustor inlet conditions for these development combustors are compared to the E³ combustor ground-idle conditions in Table X. As observed, the E³ combustor inlet conditions are more favorable for reduced levels of CO and HC emissions than the previously tested ECCP, QCSEE, and LOPER development combustors which have already demonstrated low CO and HC emissions in their respective programs. For that reason, it was expected that the E³ combustor design would have the potential for low CO and HC emissions at low power operating conditions.

Table X. Ground Idle Cycle Comparison.

	<u>T₃</u> K (° R)	<u>P₃</u> MPa (psia)	<u>f/a</u>	<u>V_{Ref}</u> m/s (fps)
QCSEE	414 (715)	0.25 (36)	0.016	15 (49)
CF6 ECCP	429 (772)	0.30 (43)	0.0110	18 (69)
LOPER	422 (760)	0.30 (44)	N/A	23 (75)
E ³	197 (894)	0.43 (63)	0.0123	15 (48)

Table XI. E³ Emissions Adjustment Relationships.

$$EI_{CO} = EI_{CO} \text{ Meas} * \left(\frac{P_3}{P_{3Cyc}} \right)^a \left(\frac{V_{Ref}}{V} \right) \text{Exp} \left(\frac{T_3 - T_{3Cyc}}{b} \right); a = 1.5, b = \infty$$

$$EI_{HC} = EI_{HC} \text{ Meas} * \left(\frac{P_3}{P_{3Cyc}} \right)^A \left(\frac{V_{Ref}}{V} \right) \text{Exp} \left(\frac{T_3 - T_{3Cyc}}{B} \right); a = 2.5, B = \infty$$

$$EI_{NO} = EI_{NO} \text{ Meas} * \left(\frac{P_{3Cyc}}{P_3} \right)^M \left(\frac{V}{V_{Ref}} \right)^N \left(\frac{F_P}{F_{PCyc}} \right)^P \left(\frac{F_M}{F_{MCyc}} \right)^P \text{Exp} \left(\frac{T_{3Cyc} - T_3}{R} + \frac{H_{Std} - H}{S} \right);$$

M = -0.37,
 N = 1.00,
 P = 0.65,
 R = -345,
 S = 53.19

$$SN = SN \text{ Meas} * \left(\frac{P_3 \text{ ER Dome}}{T_3} \right)^Z \left(\frac{W_c}{P_3 N_F} \right)^Z * \left(\frac{W_c}{W_c/P_3 N_F} \right)^Z \text{Cycle}; Z = 0$$

ORIGINAL DOCUMENT
 OF POOR QUALITY

In order to estimate the expected emissions levels for the E³ combustor, adjustments were made to an existing data base to determine the impact of combustor inlet parameters and combustor aero design features on emissions. The relationship used in making the E³ combustor estimates are shown in Table XI. These key parameters affecting CO and HC emissions at low power are inlet pressure, bulk residence time, and inlet temperature. The key parameters affecting emissions at high power, where NO_x emissions are of primary concern, are inlet pressure, inlet temperature, bulk residence time, inlet air humidity, and fuel split between pilot and main stage domes. Applying these relationships to the data base for the ECCP, QCSEE, and LOPER, the CO, HC, and NO_x emissions estimates were generated for the E³ combustor (see Table XII). With the more favorable combustor inlet parameters of the E³ cycle, the expected CO and HC emissions levels of the E³ were estimated to be below the target level with margin. The NO_x emissions were expected to closely approach the goal for both designs when the adjustment to residence time is made for the short length of the E³ combustor. The similarity of design features and airflow distributions in the ECCP and QCSEE combustors cause their emissions characteristics to closely approach those anticipated for the E³ combustor. However, LOPER incorporates more advanced state-of-the-art and unique emissions reduction concepts which result in ultralow levels of CO and HC emissions.

Table XII. E³ Combustor Estimated Emissions.

- Pilot and Main at Approach
- Pilot Only at Ground Idle

	<u>6% Idle</u>	<u>Target Level</u>	<u>Goal</u>
EPAP CO	1.9	2.5	3.0
HC	0.05	0.30	0.4
NO _x	2.7	2.7	3.0
Smoke - SN	15	16	20

1b/1000 1b Thrust-hour/Cycle

Based on these predicted levels, it was expected that the E³ combustor would meet the CO and HC emissions goals for the program with both the pilot and main stages fueled at the approach (30% F_N) operating condition. With the favorable cycle conditions at low power and the short residence time associated with the short combustor length, the E³ combustor was expected to meet all of the program goals with considerable margin, even taking into account engine-to-engine variability.

4.3 COMBUSTOR DESIGN FEATURES

The key combustor component areas where the design features were expected to significantly impact performance were the dome swirl cups, fuel nozzles, and liner dilution holes.

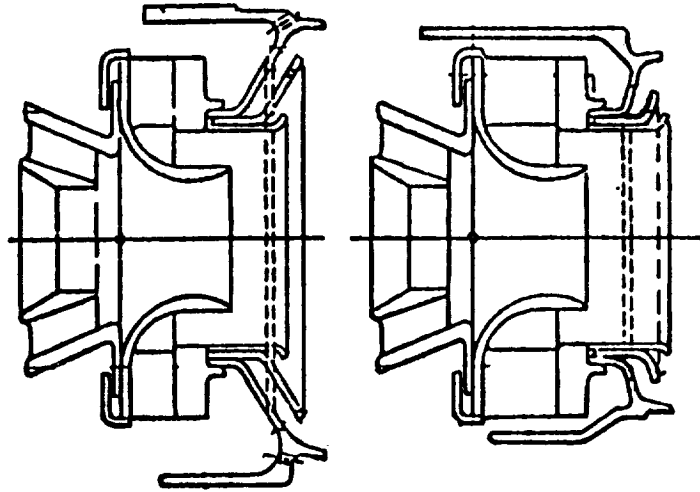
The airblast swirl cup is one of the most important components of the combustor because it atomizes, mixes the fuel and air, and prepares the fuel for burning in the combustion zone. The design features of the swirl cups for the E³ combustor were:

- Axial flow primary swirler
- Counterrotating radial inflow secondary swirler
- Venturi for carbon prevention
- Slip joint between primary-secondary for thermal growth
- Simple mechanical design

The aero features are shown in Figure 17. The key design properties for the swirl cup are: (1) fuel spray quality, (2) recirculation strength, (3) velocity through venturi, (4) primary-to-secondary swirler airflow ratio, and (5) fuel nozzle eccentricity and immersion.

These properties are important because they control combustion zone performance and durability. The swirl cup must provide a stable spray at the proper ejection angle and the fuel must be well atomized and properly distributed. The combustor flame is stabilized and seated in the dome by the recirculation zone formed by the vortex action of the fuel-air mixture exiting the swirl cup. The recirculation zone pulls hot exhaust products from the

ORIGINAL PAGE IS
OF POOR QUALITY



		<u>Pilot</u>	<u>Main</u>
Primary	Vane Angle	60°	60°
	Inlet Angle	23°	23°
	Effective Area, cm ² (in ²)	0.92 (0.143)	0.92 (0.143)
	Venturi Throat Diameter, cm (in)	1.58 (0.623)	1.58 (0.623)
Secondary	Vane Angle	80°	80°
	Vane Height, cm (in)	0.70 (0.275)	1.02 (0.400)
	Effective Area, cm ² (in ²)	1.38 (0.214)	1.87 (0.290)

Figure 17. Swirl Cup Design.

primary combustion zone upstream into the unburned mixture which helps vaporization and initiation of the combustion process. Because of this, the recirculation zone must be well controlled to prevent possible combustion instability, carboning of the swirl cup components, and/or possible damage to combustor dome components due to excessive heating. One of the swirl cup features that controls recirculation in the E³ design is the emissions reduction sleeve. As seen in Figure 18, the exit angle of the sleeve controls the amount of recirculation flow. The sleeve exit angle selected for the E³ swirl cup is 90°. Another important design feature of the swirl cup is the venturi. The venturi prevents hot combustion gases from reaching the fuel nozzle face and creating carbon deposits. A parametric development study was conducted earlier as part of the ECCP in order to determine the key design values of the venturi which would prevent carbon buildup. The results of this study are shown in Figure 19. Using this design criteria, the E³ swirl cup venturi parameters were selected to assure that carboning of the fuel nozzle or venturi surfaces would not occur.

A unique feature of the advanced film-impingement liner construction selected for the E³ combustor is that dilution air can be introduced either at full liner pressure drop or at a lower pressure drop level. These two dilution designs are illustrated in Figure 20. Figure 21 illustrates that these concepts provide different jet penetration characteristics. This provides additional design flexibility when trying to control the exit temperature profile characteristics of the combustor.

The E³ combustor fuel nozzle is similar in design to the type used in conventional combustion systems, except that it provides fuel for the pilot and main stage systems. The hydraulic flow schedule is shown in Figure 22. The combustor operates on the small-size primary system to assure high nozzle pressure drop and good atomization in the low engine speed region where combustion conditions are most severe. The primary systems of the pilot and main stage nozzles are identical. Therefore, when both primary systems are operating, the fuel flow is split equally between the pilot and main stage domes. At engine speeds above ground idle, the metering valve opens and permits fuel into the high-flowing secondary system. At these more favorable inlet conditions, where combustor inlet pressures and temperatures are higher, the larger

ORIGINAL PAGE IS
OF POOR QUALITY

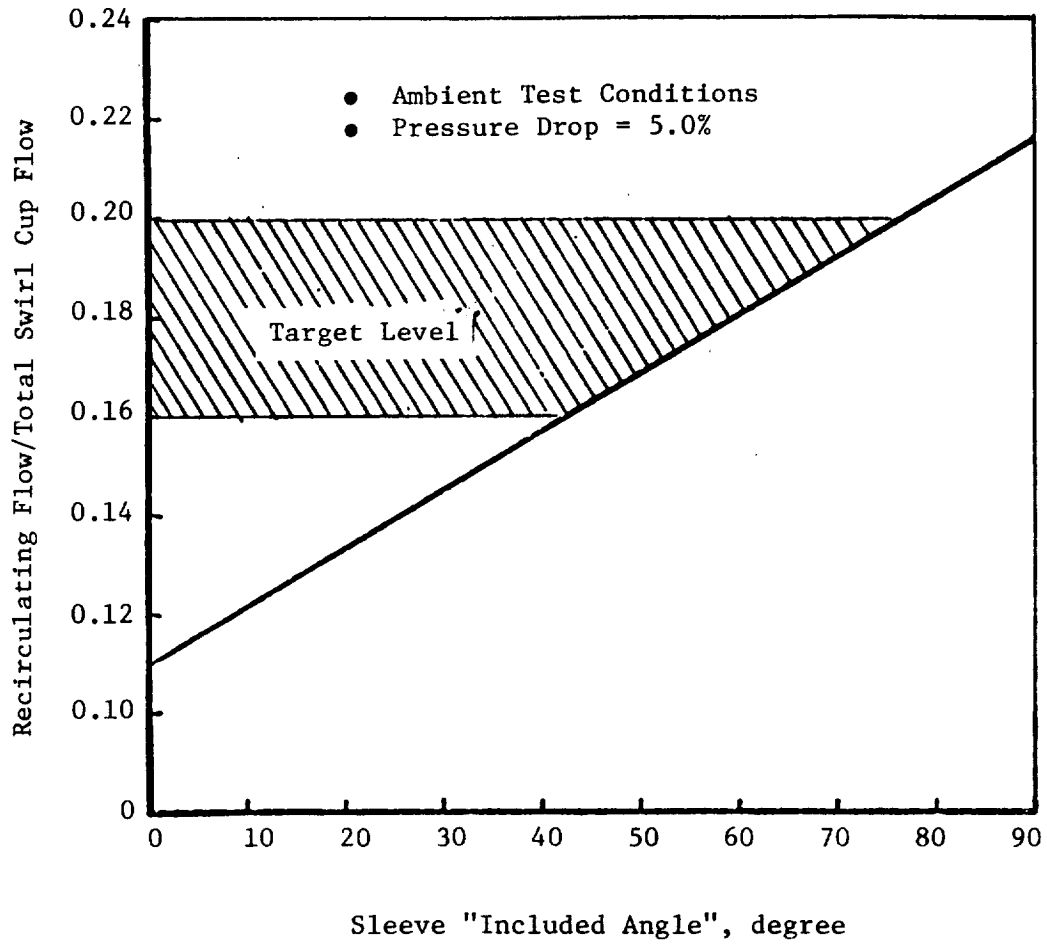


Figure 18. Recirculation Flow Compared to Sleeve "Included Angle".

ORIGINAL DESIGN
OF POOR QUALITY

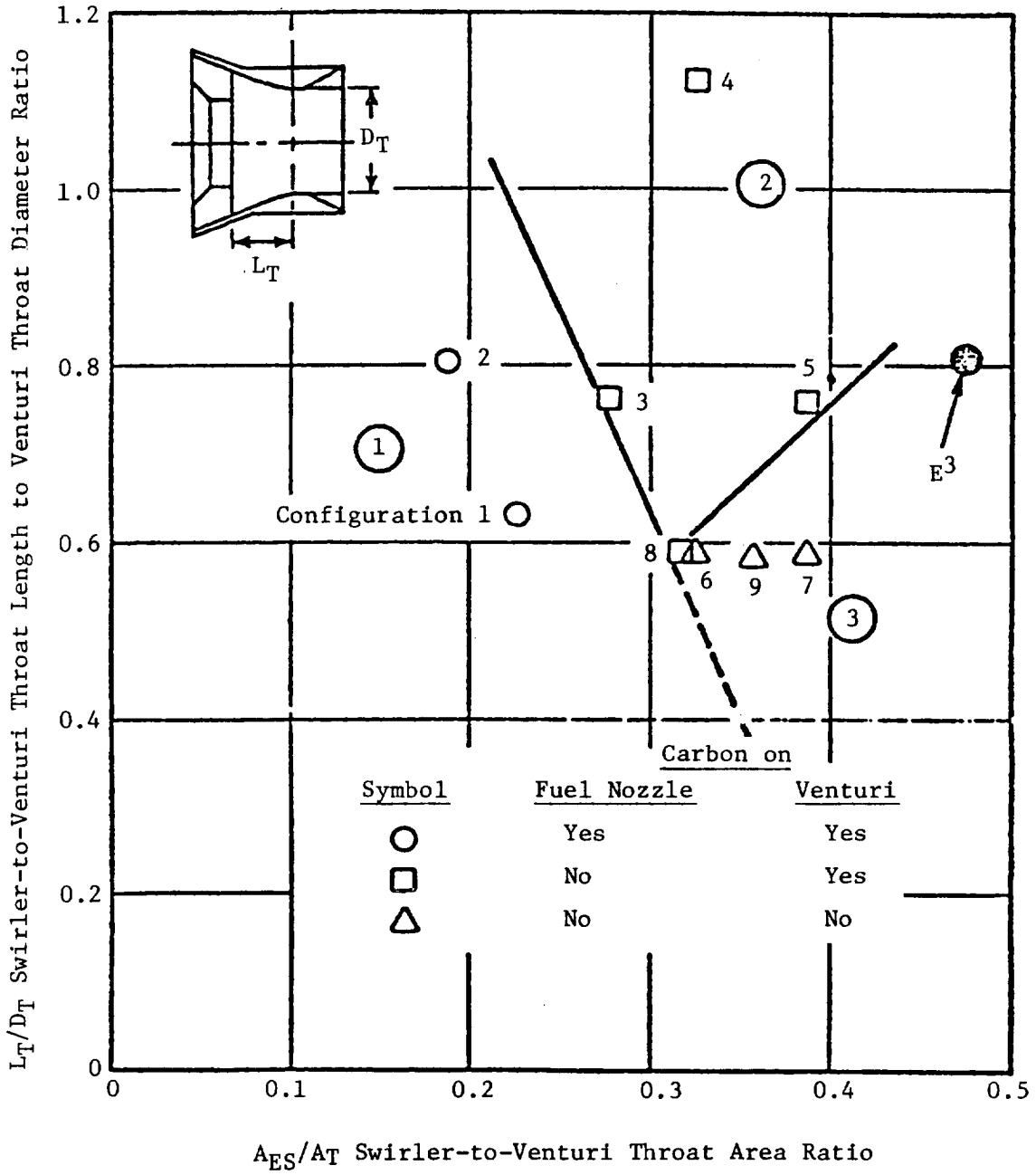
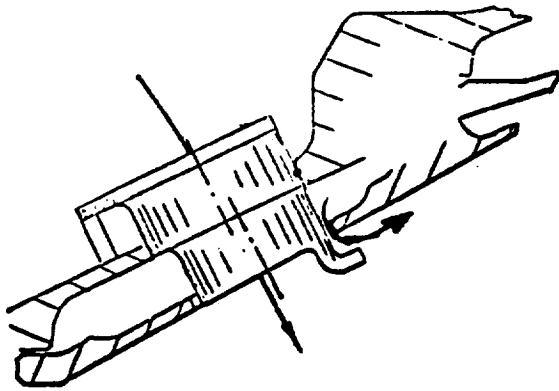
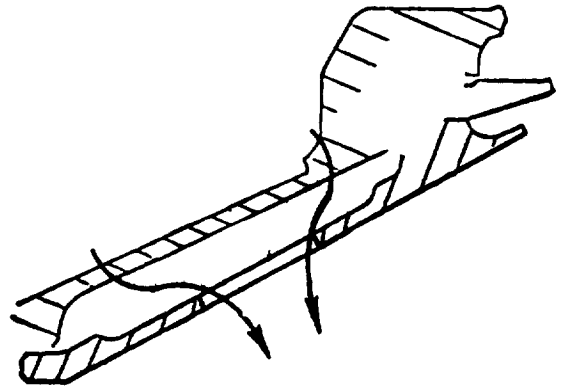


Figure 19. Venturi Anticarboning Design Criteria.

ORIGINAL PAGE IS
OF POOR QUALITY



Full Pressure Drop



Spent Impingement Dilution

Figure 20. E^3 Dilution Thimble Designs.

ORIGINAL COPY
OF POOR QUALITY

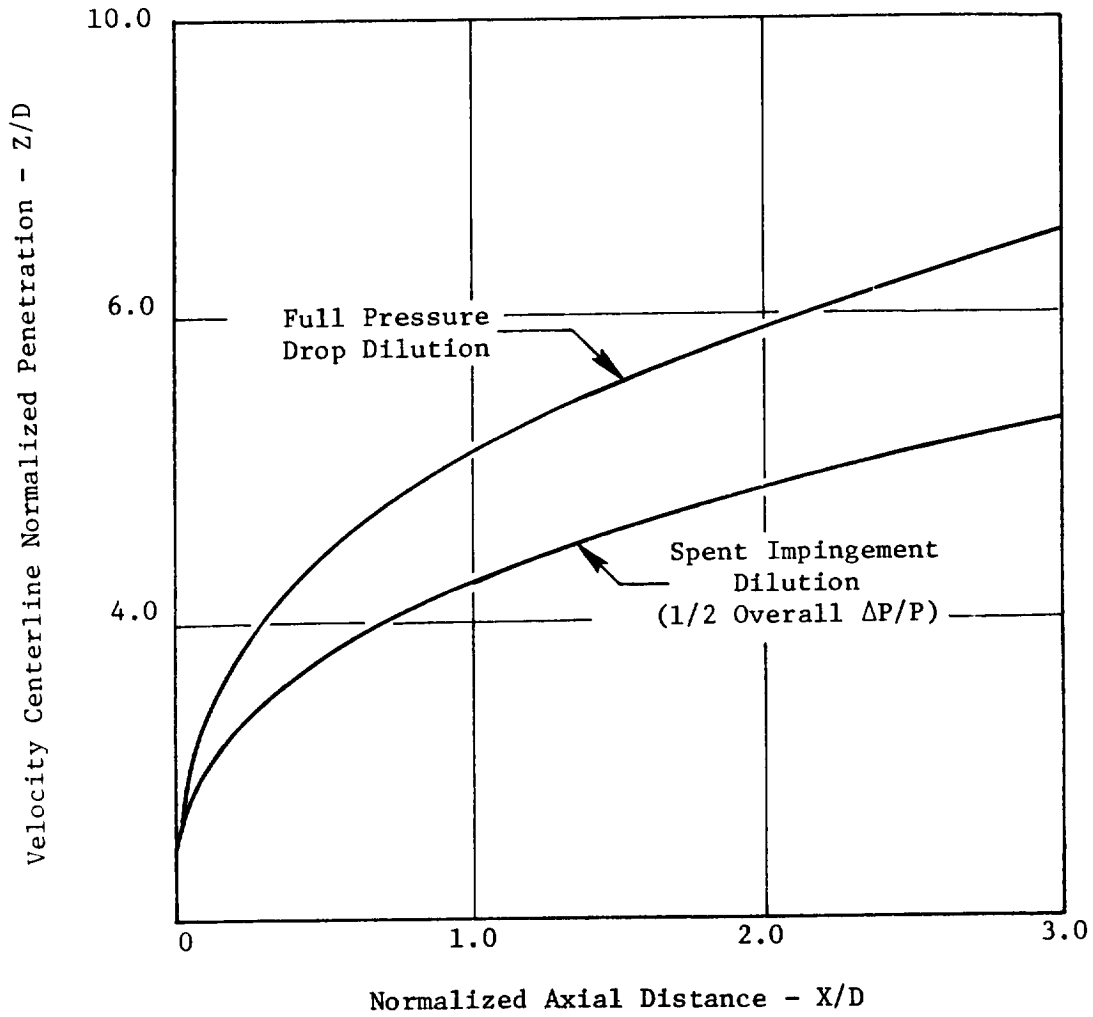


Figure 21. Comparison of E³ Dilution Jet Penetration.

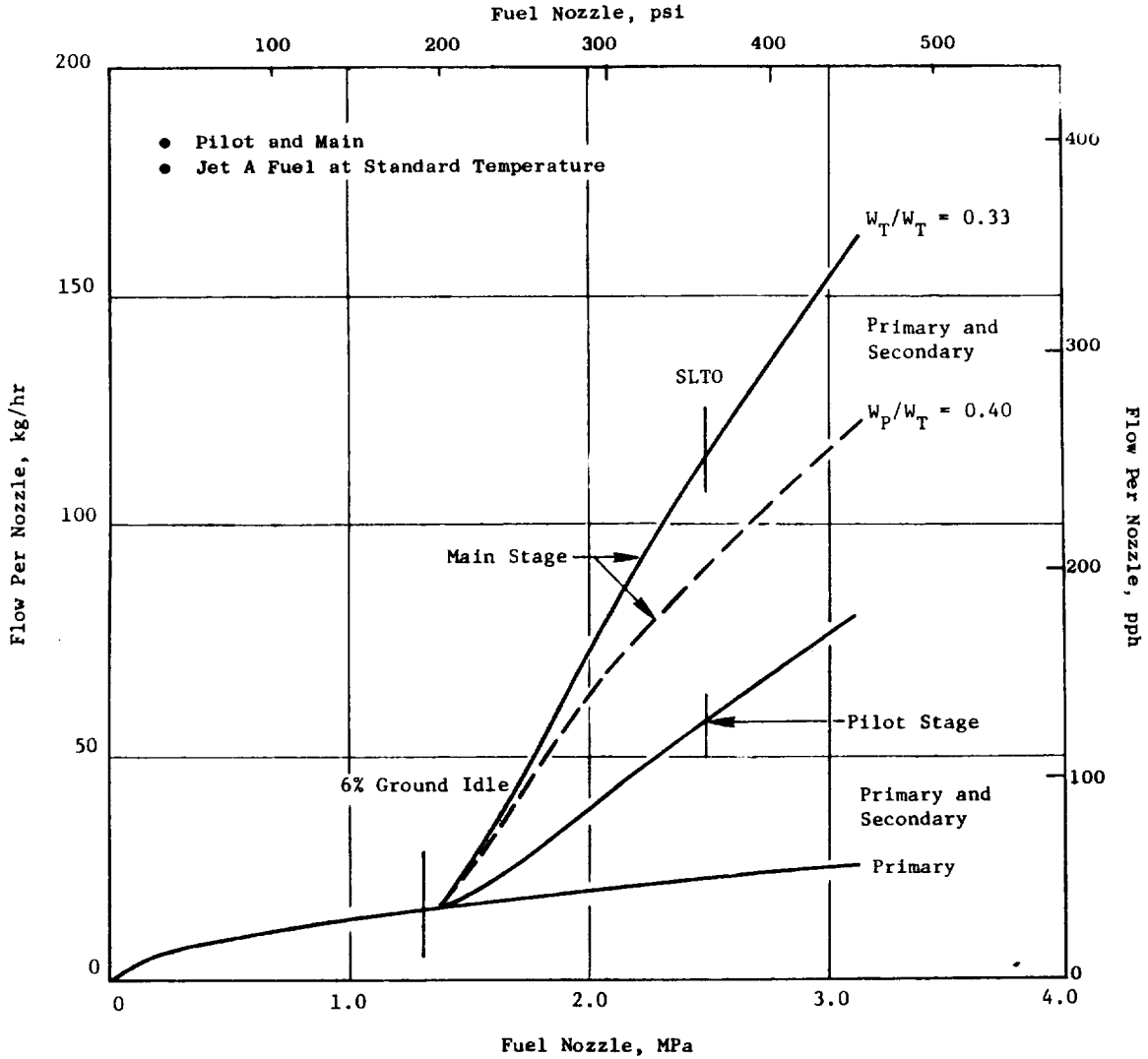


Figure 22. E³ Fuel Nozzle Flow Characteristics.

spray droplets from the secondary system are more easily vaporized. The main stage total flow is about twice that of the pilot above the secondary cut-in in order to bias the fuel flow to the lean main stage dome at high-power operating conditions for NO_x emissions control. However, the exact flow split has not been selected. As a result, the fuel systems were oversized to provide some flow split flexibility. The pilot and main fuel systems are supplied from a common line; consequently, they operate from a common fuel flow and pressure source. By installing a restriction in the main or pilot-stage fuel inlet line, the flow split can be shifted by inducing additional pressure drop into that system. As an example, if the pilot stage fuel system were operating at 2.41 MPa (350 psi), and if a restriction were added to the main supply line to provide an additional pressure drop of 0.35 MPa (50 psi), the resulting flow curve would look like the one shown in Figure 22 for the 40% pilot-to-total flow split. The operating characteristics of the pilot and main stage fuel systems across the E^3 FPS standard day operating line are presented in Figure 23.

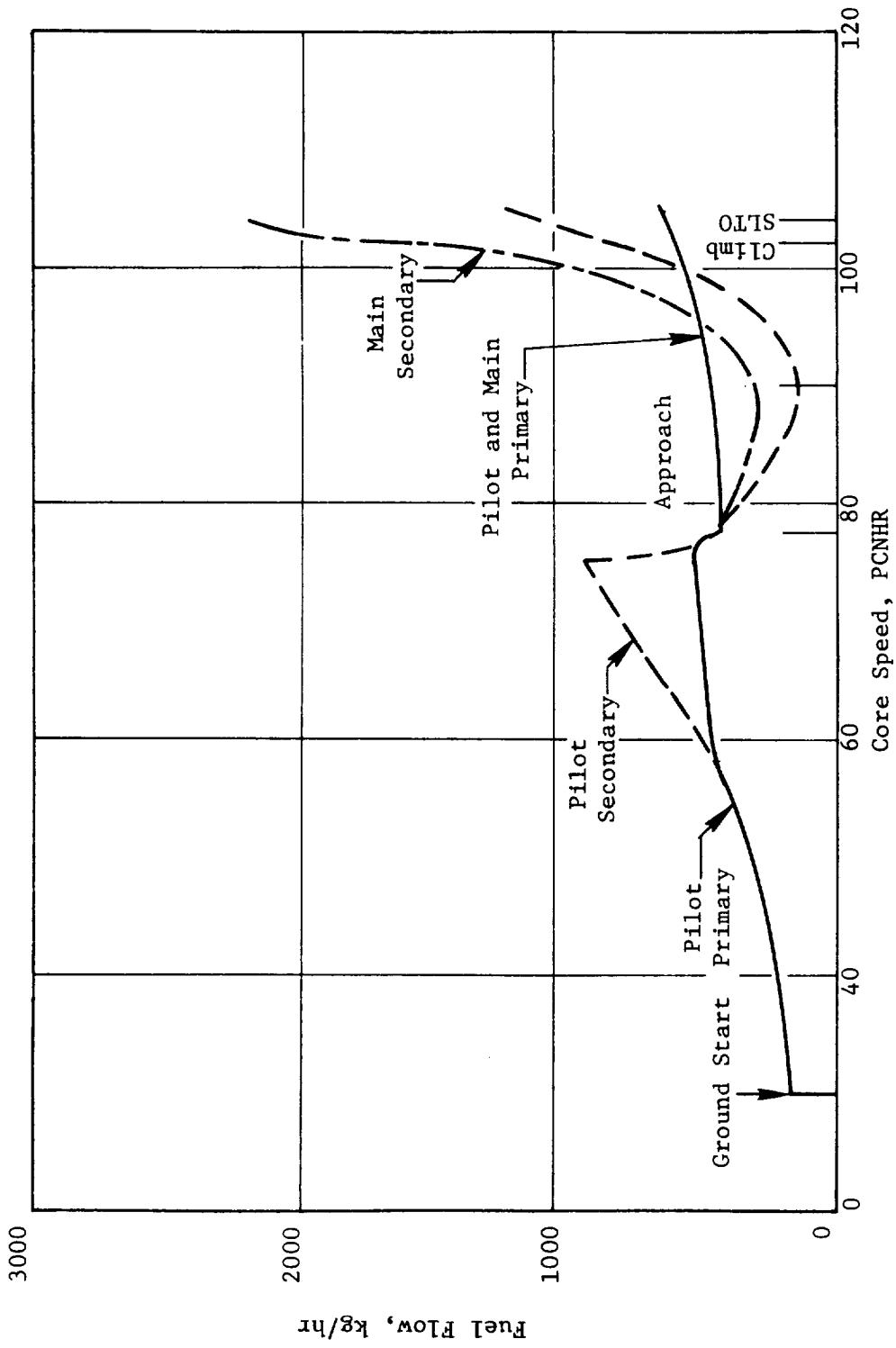


Figure 23. Fuel Nozzle Staging - Pilot to Main Stage.

5.0 MECHANICAL DESIGN

5.1 REQUIREMENTS

The E³ combustor mechanical design life goals (Figure 24) are consistent with the engine technical requirements. The combustion system hot parts were designed to a cyclic life capability of 9,000 cycles to first repair, with an ultimate life of 18,000 cycles for these parts. Based on the typical engine mission of two-hour duration, the cyclic life requirement translates to 18,000 hours to first repair with an ultimate life of 36,000 hours.

	<u>Operating Time</u>	
	<u>Hours</u>	<u>Cycles</u>
● Life Goals		
To First Repair	18,000	9,000
Total Life	36,000	18,000
● Maximum Operating Conditions - (Growth Engine)		
Inlet Temperature	927 K (1669° R)	
Inlet Pressure	3.91 MPa (567 psia)	
Fuel-to-Air Ratio	0.025	

Figure 24. Combustor Mechanical Design Objectives.

5.2 GENERAL DESIGN FEATURES

Figure 25 shows the assembled E³ combustor. A cross section of the combustor design was previously shown in Figure 1. The E³ combustor design features a double-annular dome with a common swirl cup design used in each dome. A centerbody structure separates the outer pilot dome from the inner main stage dome. Fuel is introduced to the combustor through 30 dual-tip fuel nozzles.

ORIGINAL PAGE IS
OF POOR QUALITY



Figure 25. Assembled E³ Combustor.

Each fuel nozzle features completely independent fuel metering for each dome. The combustor liners utilize a double-walled shingled liner concept to provide long life. The combustor is supported at the upstream end by 30 support pins. These support pins transmit all the mechanical force loads from the liners and dome to the outer combustor case. The combustor-turbine interface is sealed with machined fishmouth seals which accommodate the relative growth and mechanical stackups between the two components.

The outer casing supports the combustor, fuel nozzles, fuel delivery system, ignition system, and engine firewall. Ports are provided in the casing for borescope inspection, compressor discharge bleed, and instrumentation leadout.

Several design changes were incorporated into the combustor mechanical design since the preliminary design review. Liner shingle geometry was optimized to a shingle array which featured three axial rows. The shingle edges were designed with circumferential overlap seals, thereby eliminating 105 leaf seals in the combustor assembly. The selected shingle alloy was X-40. This high-temperature, cobalt-based alloy provides excellent durability for the E³ application. The turbine cooling air filtration screens located at the combustor aft end were removed in order to be consistent with current commercial engine design philosophy and to reduce system weight complexity and cost.

The combustor centerbody was shortened from the original configuration to provide a more rigid, more readily cooled design. In addition, centerbody thermal relief slots were incorporated to reduce thermal stress and provide adequate component life capability.

The materials selected for the combustion system are shown in Figure 26. Conventional combustor high-temperature alloys, such as Hastelloy-X and X-40, were chosen for the components that are exposed to hot combustion gases: the dome, centerbody, shingles and dilution eyelets. Supporting structures, such as the outer casing and the impingement liners, are made of nickel-based alloys. The fuel system was fabricated from stainless steel alloys.

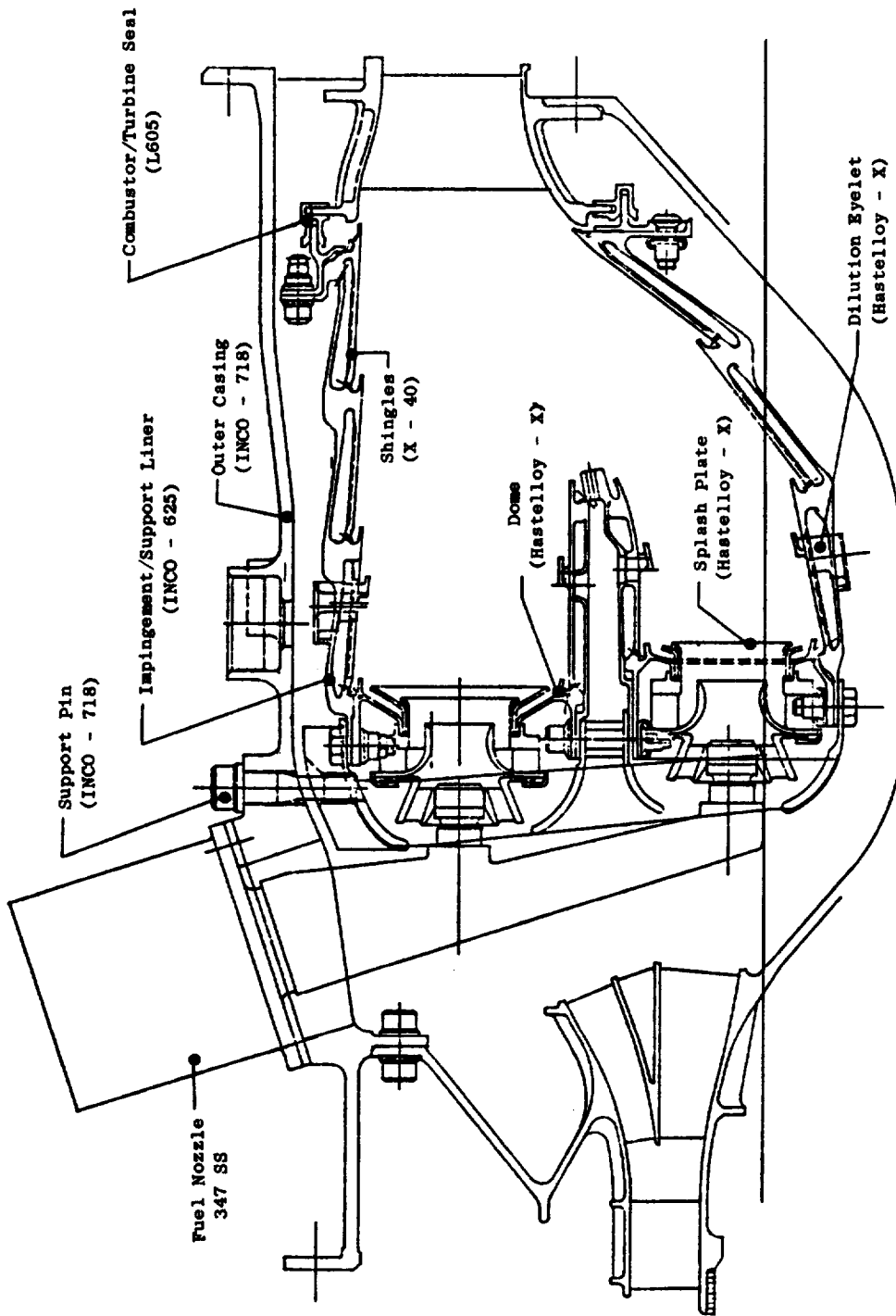


Figure 26. Combustor Materials Selection.

5.3 LINER

Combustor liners utilize a double-walled shingled liner concept similar to the liners developed in the GE23/ATEGG engine program. The liners consist of a load carrying 360° turning which supports individual heat shields or shingles. The shingles are segmented axially and circumferentially to reduce stress and provide long life. The support liner, in addition to supporting the shingles, provides impingement cooling to the shingle. Figure 27 shows the inner support liner. All of the cooling and dilution holes in both support liners were laser drilled. Laser hole drilling of combustors is a new application of this technology, with savings in both time and cost over conventional hole drilling methods such as EDM (electrodischarge machining). Figure 28 shows the assembled inner liner.

The E³ shingle design is similar to the ATEGG/GE23 shingle design. The GE23 combustor features a cast shingle design. This design background provided the basis for the E³ combustor liner design. A comparison between the GE23 shingle geometry and the E³ shingle geometry is shown in Table XIII. One significant difference in the design configuration between E³ and GE23 combustor shingles is the support foot configuration. A comparison of the two support foot designs is provided in Figure 29. The E³ design was optimized to allow the maximum coolant flow introduction between feet while maintaining sufficient foot width for mechanical strength. The optimization consisted of trading off cyclic fatigue life against rupture life capability for the shingle design.

Another significant difference in shingle design is the method of controlling leakage between adjacent shingles. Figure 30 illustrates the GE23 and E³ edge seal configuration. The GE23 shingle utilizes individual sheet metal leaf seals which fit into slots along the edges of the shingle. The E³ shingle introduces a novel concept for between-shingle leakage control. This shingle design has overlapping edges which eliminates the need for individual edge seals. The edge leakage flow is controlled by closely dimensioning the gap between the overlapping shingle edges. The elimination of the shingle edge seal does introduce a controlled leakage and a slight penalty in loss of shingle coolant and slightly increased operating temperature. Figure 31 shows the effect of shingle edge leakage on shingle operating temperature.

ORIGINAL SOURCE
OF POOR QUALITY

ORIGINAL PAGE
BLACK AND WHITE PHOTOGRAPH

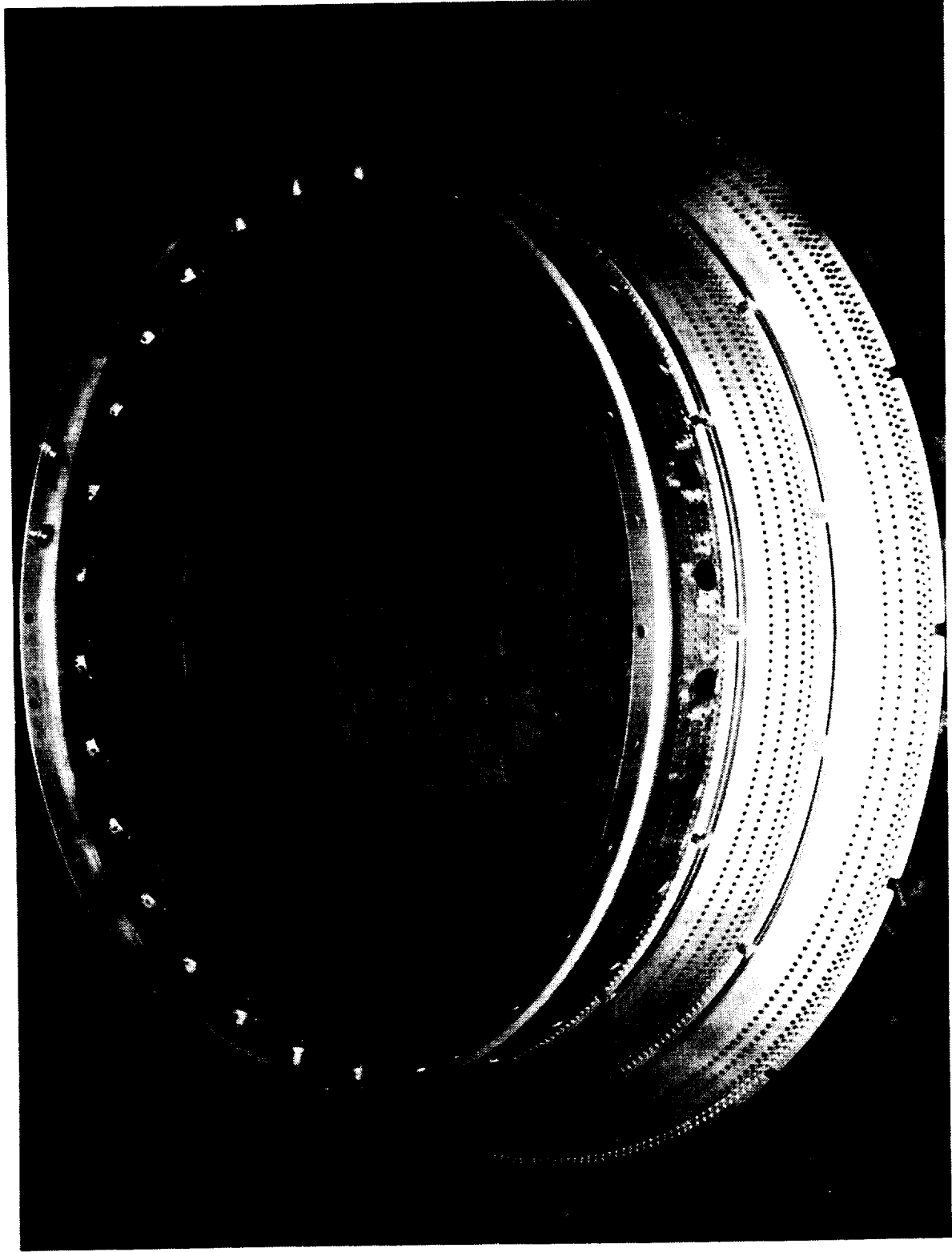


Figure 27. Combustor Inner Support Liner.

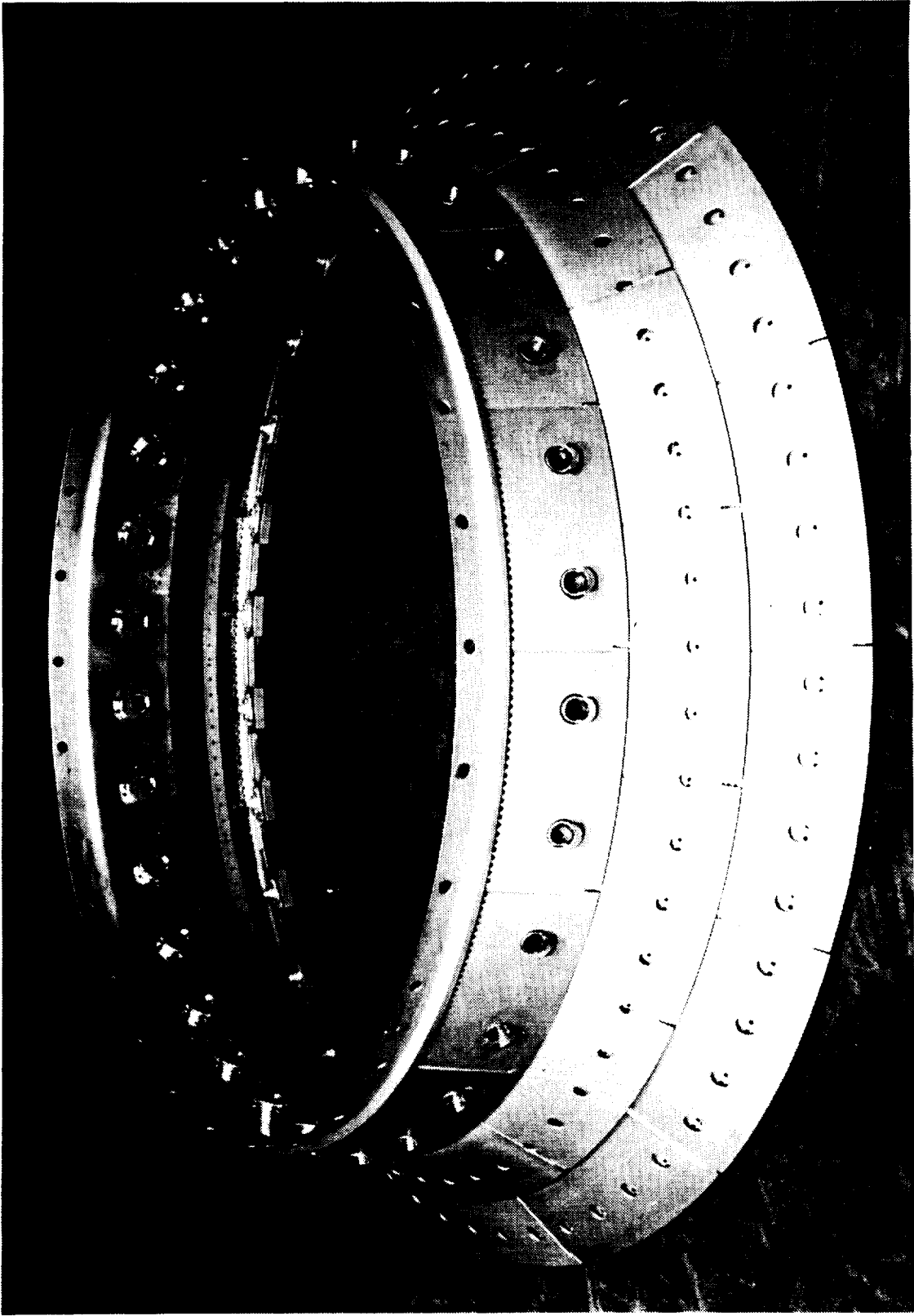


Figure 28. Assembled Combustor Inner Liner.

Table XIII. E3/GE23 Shingle Design Comparison

<u>Design</u>	<u>No. of Axial Panels</u>	<u>No. of Circumferential Segments</u>	<u>Panel Length, cm (in.)</u>	<u>No. of Feet</u>	<u>Shingle Thickness, cm (in.)</u>	<u>Shingle Arc Width, cm (in.) max.</u>
E3	3	20	4.47 (1.76)	11	0.127 (0.050)	11.76 (4.63)
	3	15	4.78 (1.88)	11		12.24 (4.82)
GE23	4	20	4.62 (1.82) Max.	11		11.41 (4.49)
	4	20	3.56 (1.40) Max.	9		9.68 (3.81)

100-1000
 100-1000
 100-1000

<u>GE23</u>	<u>W,</u> <u>cm (in.)</u>	<u>S,</u> <u>cm (in.)</u>	<u>W/S</u>
Outer Liner	0.58 → 0.66 (0.23) → (0.26)	0.33 → 0.38 (0.13) → (0.13)	1.8
Inner Liner	0.51 → 0.66 (0.20) → (0.26)	0.31 → 0.38 (0.12) → (0.15)	1.9
 <u>E³</u>			
Outer Liner	0.51 (0.20)	0.51 (0.20)	1.0
Inner Liner	0.46 → 0.56 (0.18) → (0.22)	0.46 → 0.56 (0.18) → (0.22)	1.0

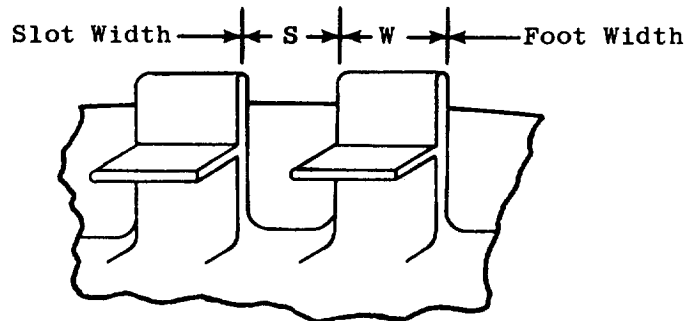
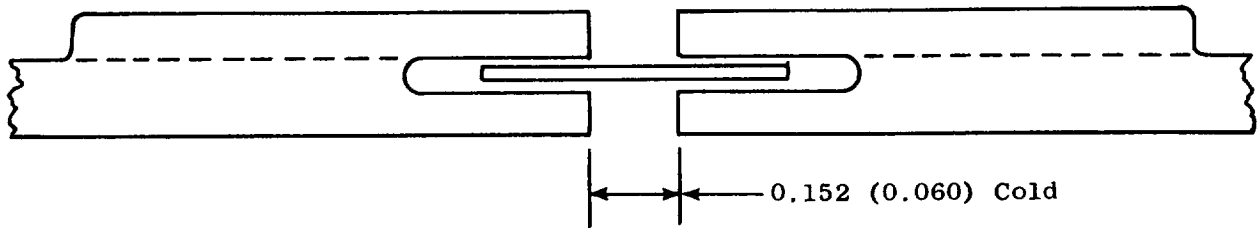


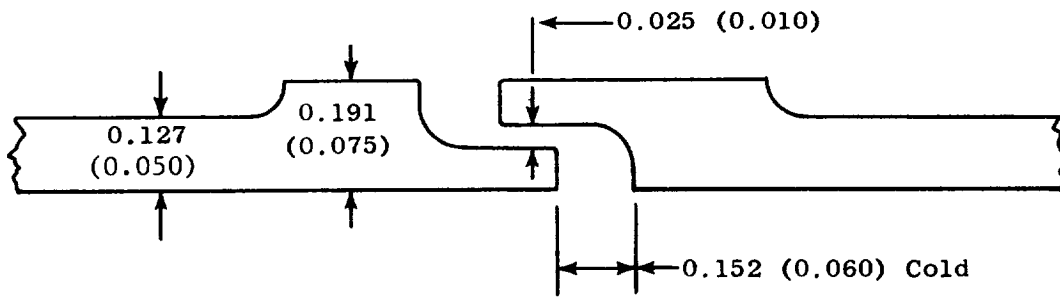
Figure 29. E³/GE23 Shingle Support Foot Design Comparison.

ORIGINAL PAGE IS
OF POOR QUALITY



GE23 Shingle

• All Dimensions Are in cm and (in.)



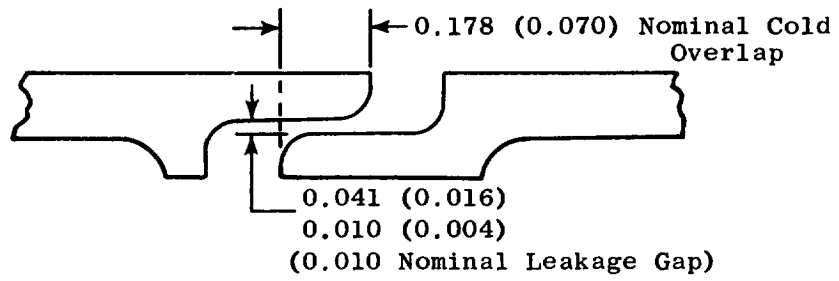
E³ Shingle

Advantage: Elimination of 105 Parts

Figure 30. E³/GE23 Shingle Edge Seal Configurations.

ORIGINAL DESIGN
OF POOR QUALITY

• Dimensions Are in cm and (in.)



E³ Combustor Shingle Overlap Detail

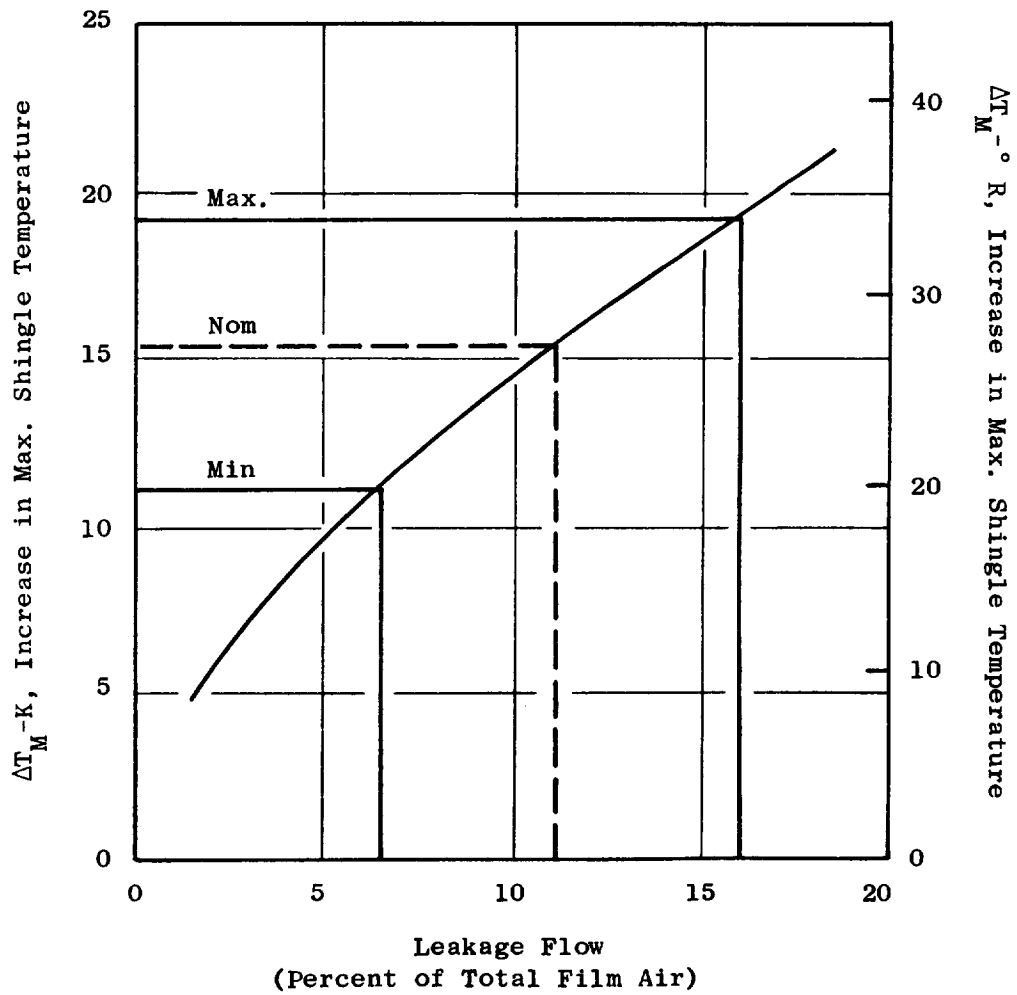


Figure 31. Effect of Edge Seal Leakage on Shingle Temperature.

The maximum increase in metal temperature due to this leakage is on the order of 19 K (34° F). The E³ design can accommodate this metal temperature increase penalty in light of the significant reduction in component pieces and the easier liner assembly achieved with the overlapping shingle design.

Another combustor liner feature similar to the GE23 combustor design is the liner dilution eyelet. The liner dilution eyelet is supported by the support liner. As shown in Figure 32, a coannular gap is utilized at the shingle interface to avoid interference between the "hot" shingle and the "cold" eyelet during engine operation. The aft portion of the annular gap flow is directed onto the shingle with a film restarter lip in order to restore the dilution jet stripped cooling film. This technique was developed on the ATEGG combustors and has demonstrated significant shingle temperature reduction in the areas downstream of the dilution holes.

The combustor liner design is supported with extensive heat transfer and stress analysis. Good heat transfer data are essential to ensure reliable stress and life predictions. The shingle heat transfer analysis utilized the two-dimensional heat transfer model of the inner liner Panel 1 shingle. The shingle stress analysis was carried out by using a three-dimensional finite-element computer analysis.

The combustion liner heat transfer analysis techniques employed in the E³ liner analysis are consistent with standard GE liner heat transfer design guidelines. Both average and hot-streak liner temperature predictions were made for the E³ combustor. Similar predictions have been generated for the ATEGG engine combustor family with good agreement obtained with measured engine data.

Figures 33 and 34 show the E³ inner and outer liner cooling flow distributions compared to the GE23 combustor and CF6-50 (ECCP) double-annular combustor. The GE23 represents prior shingle liner design experience, and the CF6-50 is the only prior GE double-annular engine combustor design. As shown, the E³ inner liner cooling rate is comparable to the other combustors, except at the forward end of the CF6-50 combustor where higher coolant flow was required to cool a hot panel. The outer liner cooling rates are very similar in all three designs.

ORIGINAL PAGE IS
OF POOR QUALITY

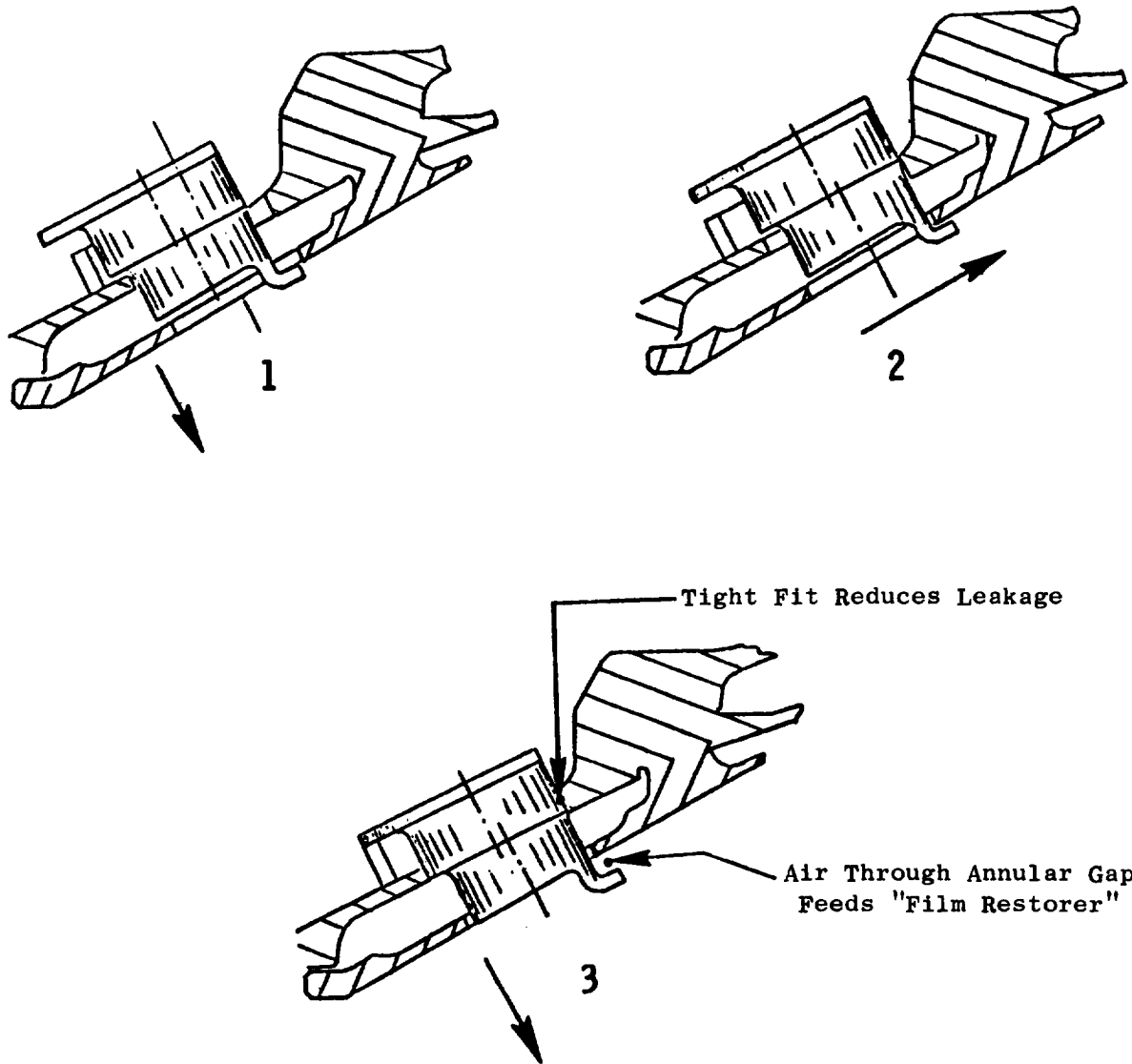


Figure 32. Dilution Eyelet Design.

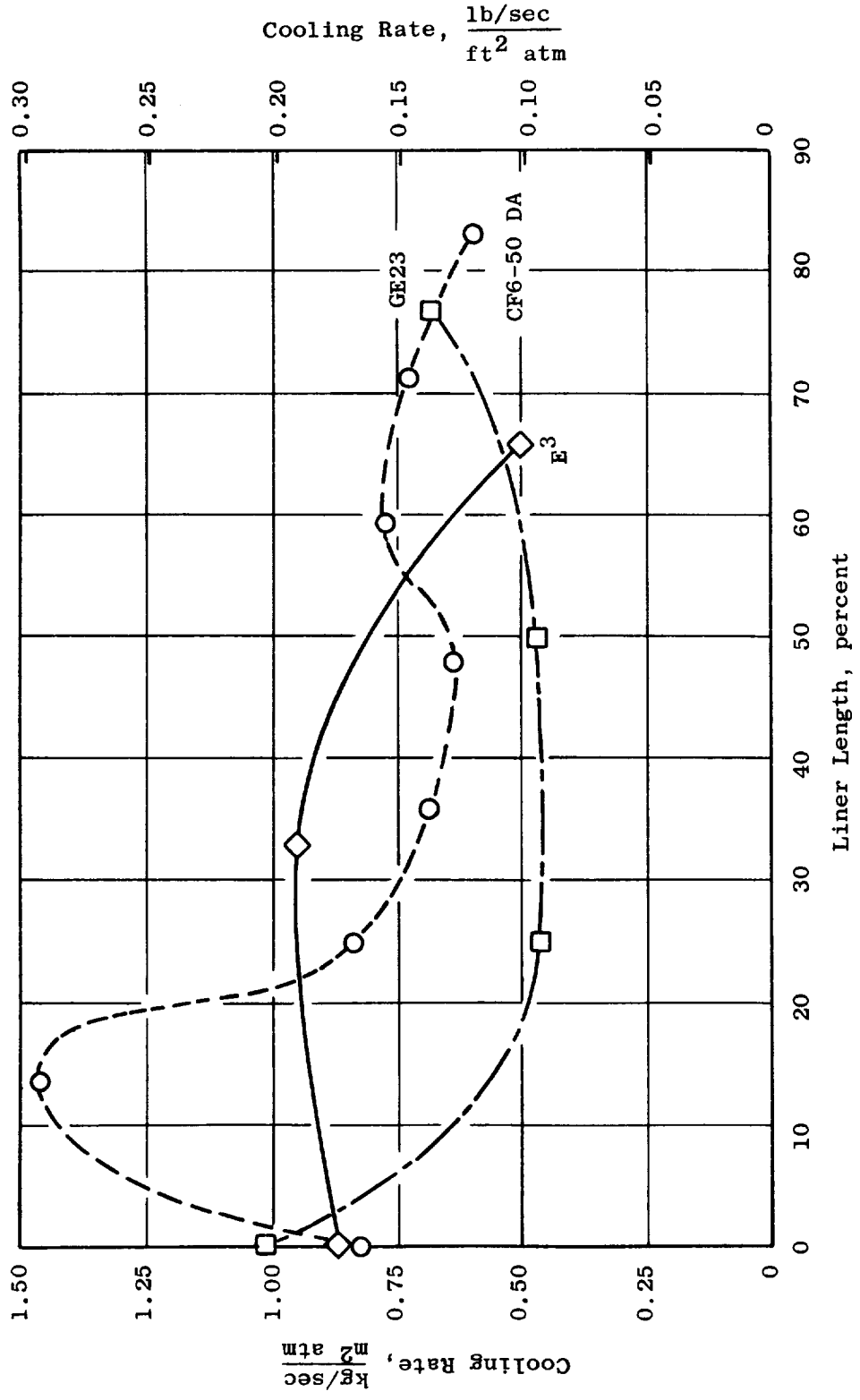


Figure 33. Liner Cooling Flow Distributions.

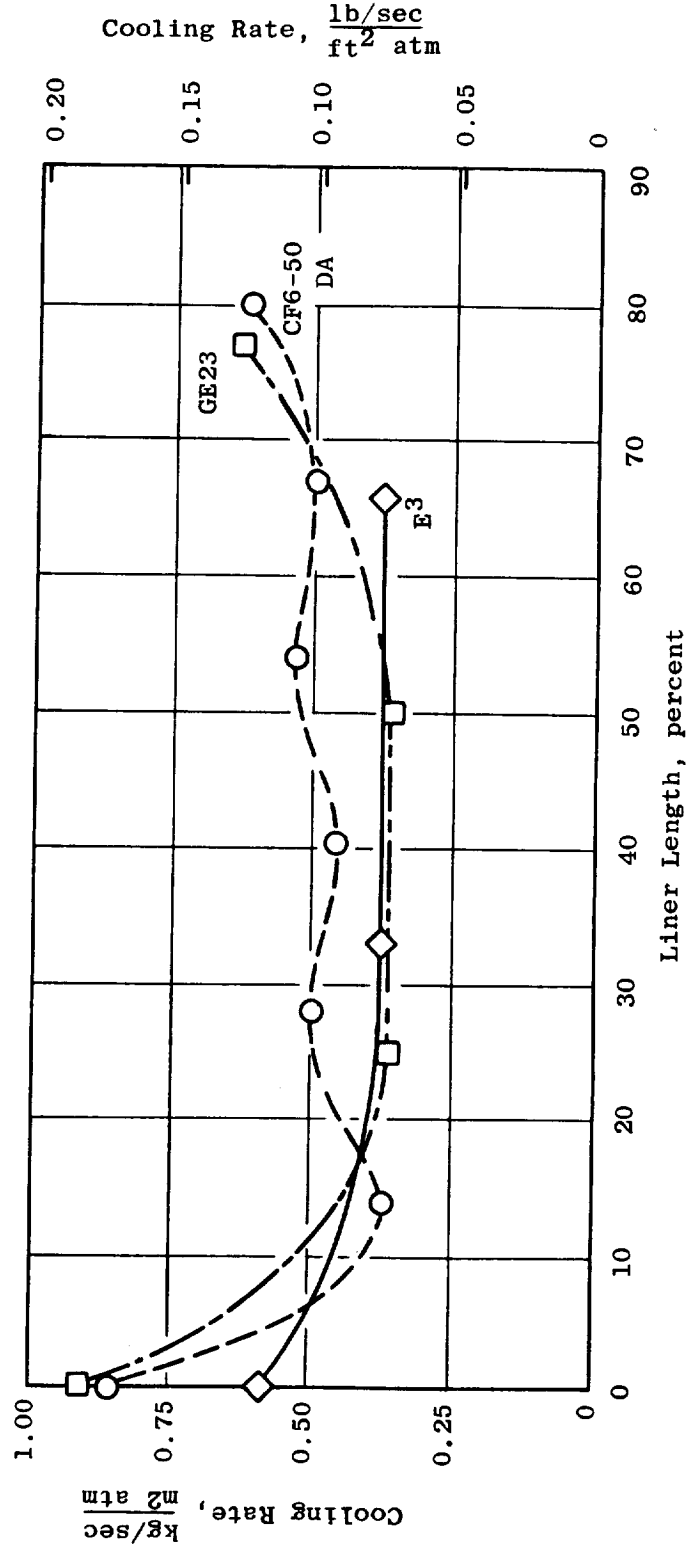


Figure 34. Liner Cooling Flow Distributions.

Based on the chosen liner cooling rates, a prediction of operating temperature was made for each panel. Figure 35 shows the predicted baseline and growth overhang temperature levels for each panel. These results are based on a one-dimensional hot streak calculation which was conducted to identify the life-limited shingle. The inner liner forward panel was identified as the hottest liner region and, therefore, the life-limited shingle. This shingle location was selected to model for further detailed heat transfer, stress, and life analyses.

Two-dimensional heat transfer studies were conducted to identify the maximum operating temperatures at shingle locations other than the overhang. Figure 36 shows the temperatures along the life-limited shingle at growth engine hot-day takeoff conditions. Both average and hot-streak temperature distributions were predicted. As shown, the peak shingle temperature distributions were predicted. Also shown, the peak shingle temperatures occur in the region of the support foot with the coolest temperature at the forward end where the coolant film is introduced. These studies indicated a maximum shingle temperature of 1283 K (1850° F) for growth engine operation. The growth engine takeoff roll condition exhibits a higher combustor inlet temperature. However, the reduced pressure levels result in lower liner heat loads and subsequently lower metal temperatures than the growth engine takeoff condition. Similar heat transfer studies were conducted at the baseline engine and growth engine takeoff conditions. The results of these studies are summarized in Table XIV.

Table XIV. Predicted Shingle Maximum Operating Temperature in the FPS Application.

<u>Takeoff</u>	<u>T₃, K (° F)</u>	<u>P₃, MPa (psia)</u>	<u>T_{Overhang}, K (° F)</u>	<u>T_{Max.}, K (° F)</u>	<u>Location</u>
Baseline Engine	814(1006)	3.020(438)	1083(1490)	1111(1540)	Inner Panel 1
Growth Engine	910(1178)	3.751(544)	1233(1760)	1283(1850)	Panel 1
Growth Engine (Takeoff Roll)	927(1209)	3.296(478)	1224(1744)	1272(1830)	Panel 1

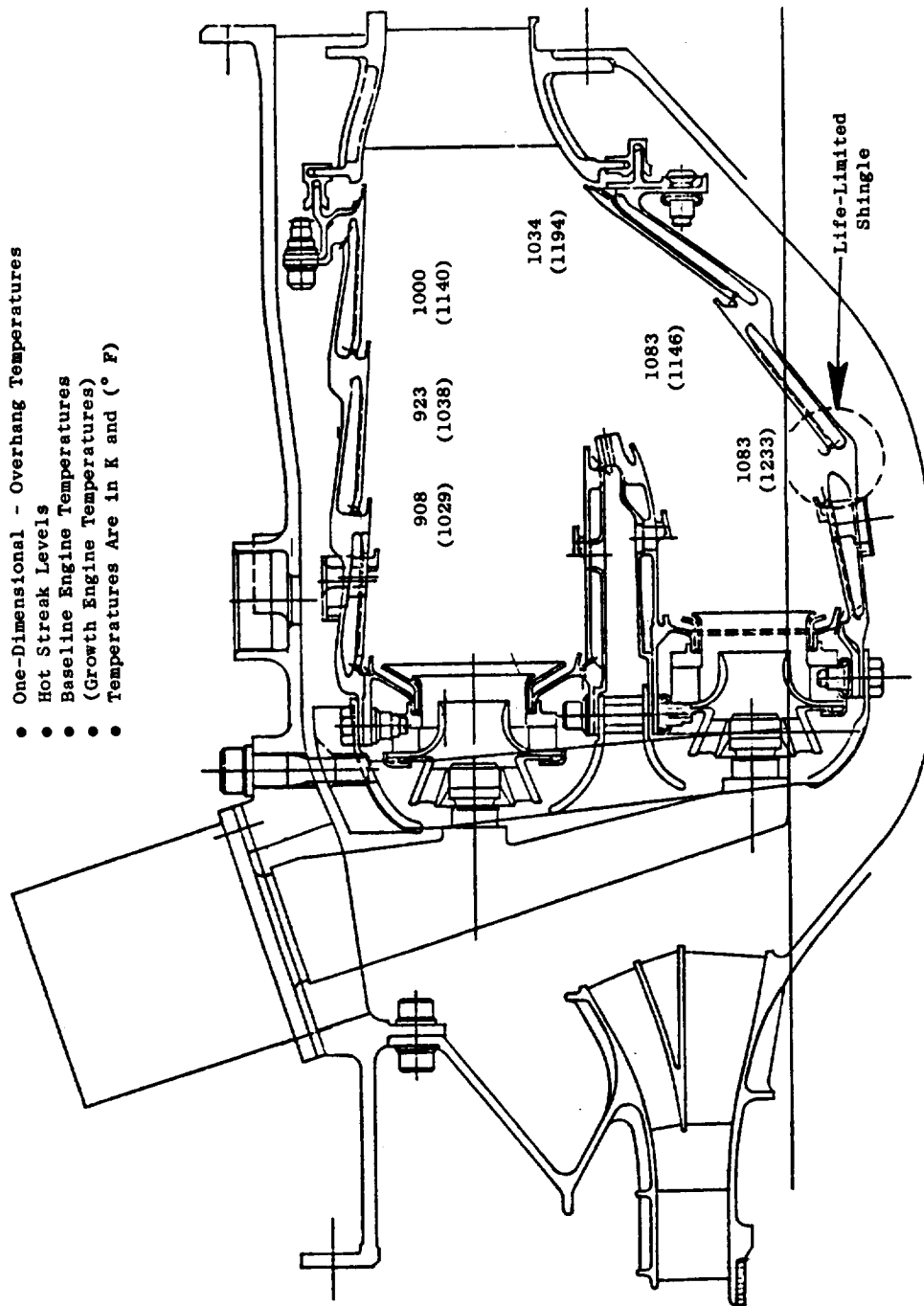


Figure 35. Predicted Peak Liner Temperatures.

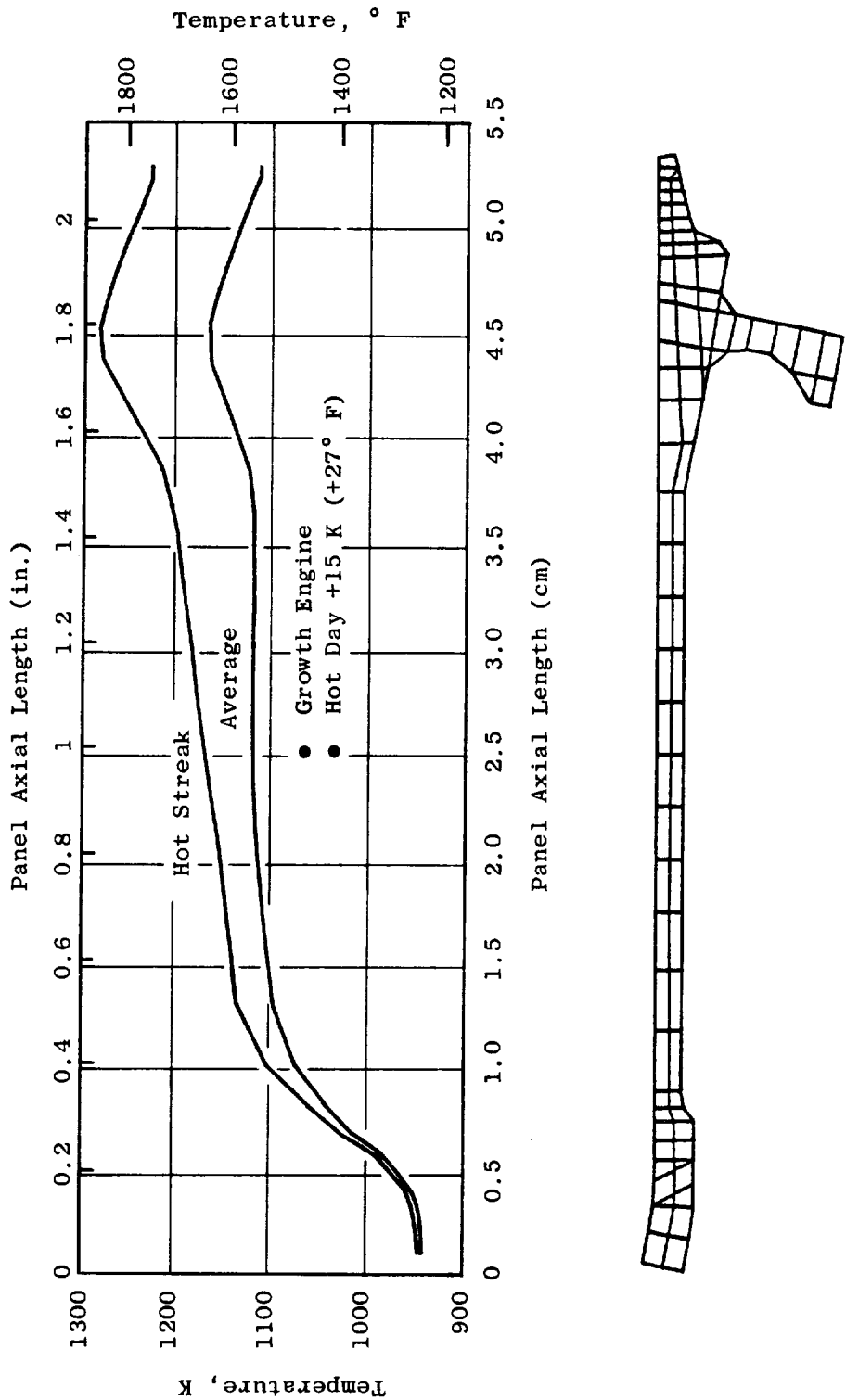


Figure 36. Predicted Axial Temperature Distribution for a Shingle.

A recommended mission mix provided in the E³ engine technical requirements is shown in Figure 37. This mission indicates engine operation at the most severe condition (hot day) on only 20% of the total flights. However, in order to provide a conservative approach to the shingle liner durability assessment, life studies evaluated cyclic life by assuming constant hot-day engine operation. A comparison of liner heat loads for the growth engine tropical day 15 K (+27° F) and hot day 35 K (+63° F) indicates that the tropical day condition is life-limiting due to higher metal temperature gradients.

In order to assess shingle operating stresses, a finite-element model of the shingle was constructed. The computer program, MASS (Mechanical Analysis of Space Structures), was employed. Figure 38 shows the MASS model of the shingle. The model consisted of a series of curved plates and beams and accurately modeled the actual shingle casting. Only half the shingle was modeled because it is symmetric about the axial centerline. Boundary conditions on the model accurately simulate the combustor environment and structural attachment. The MASS program is capable of calculating stress levels due to pressure, mechanical, and temperature loading.

The shingle MASS model was employed in order to determine shingle pressure stresses. The maximum anticipated combustor liner pressure drop was imposed across the panel. A safety factor of 1.5 was applied to account for engine surges during transient operation. As shown in Figure 39, the maximum pressure stress occurred in the support foot region of the shingle; this stress determines the ultimate rupture life of the liner.

A shingle support foot rupture life was estimated based on the foot operating stress and temperature. Increased rupture life can be obtained by increasing the shingle foot width relative to the slot between feet (that is, by increasing the foot cross-sectional area). Figure 40 shows that the chosen E³ design meets the engine life goal with margin.

The low cycle fatigue life of the shingle was assessed at the hot-day growth takeoff condition with a hot streak located at the quarter shingle position (Figure 41). The hot streak was modeled as a narrow axial band. Various locations were evaluated and the quarter shingle position produced

ORIGINAL PAGE IS
OF POOR QUALITY

Life Assessment Approach
Evaluate Life at Constant
Hot Day +15 K (27° F)
Operation

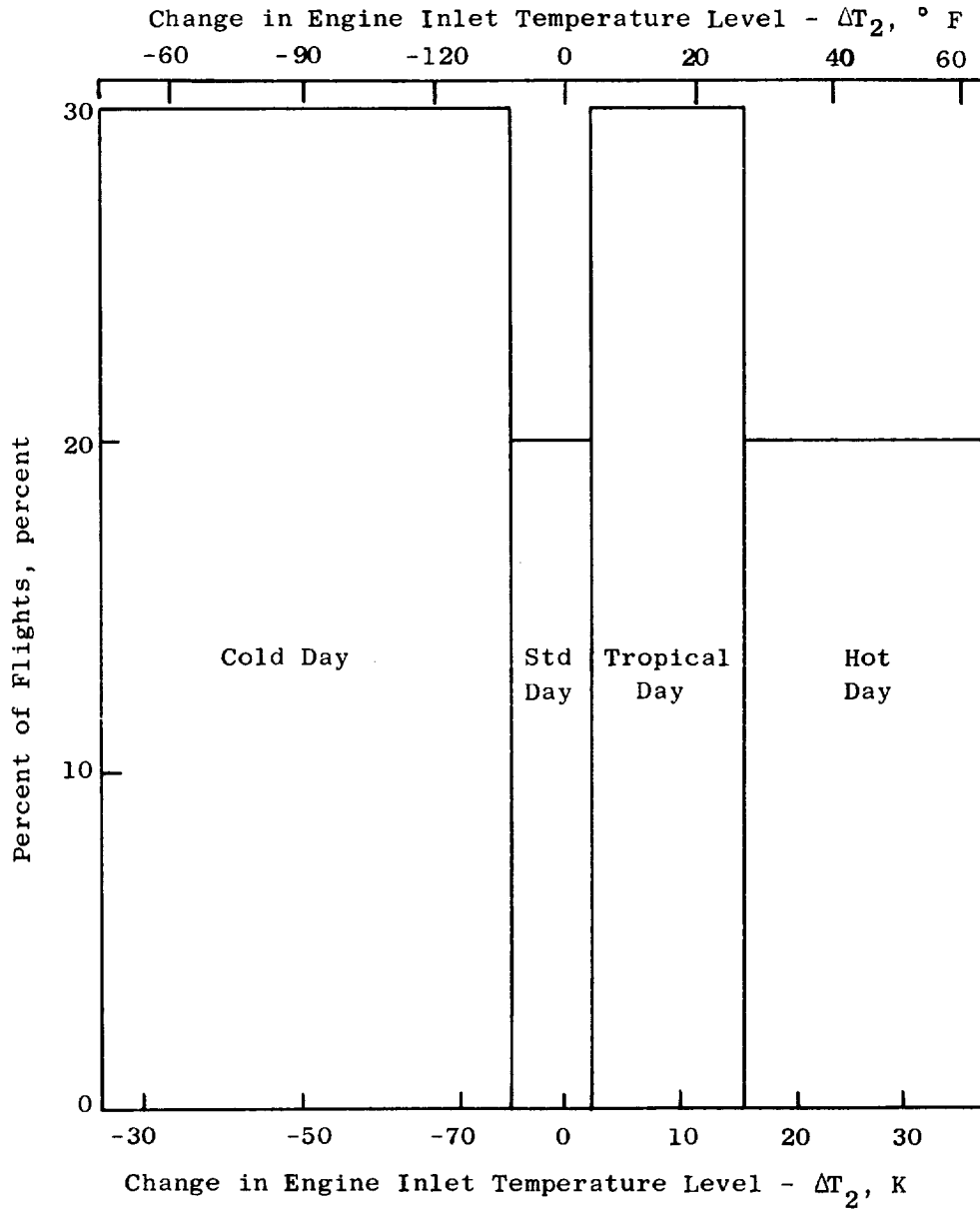


Figure 37. Recommended Mission Mix for E^3 .

ORIGINAL PAGE IS
OF POOR QUALITY

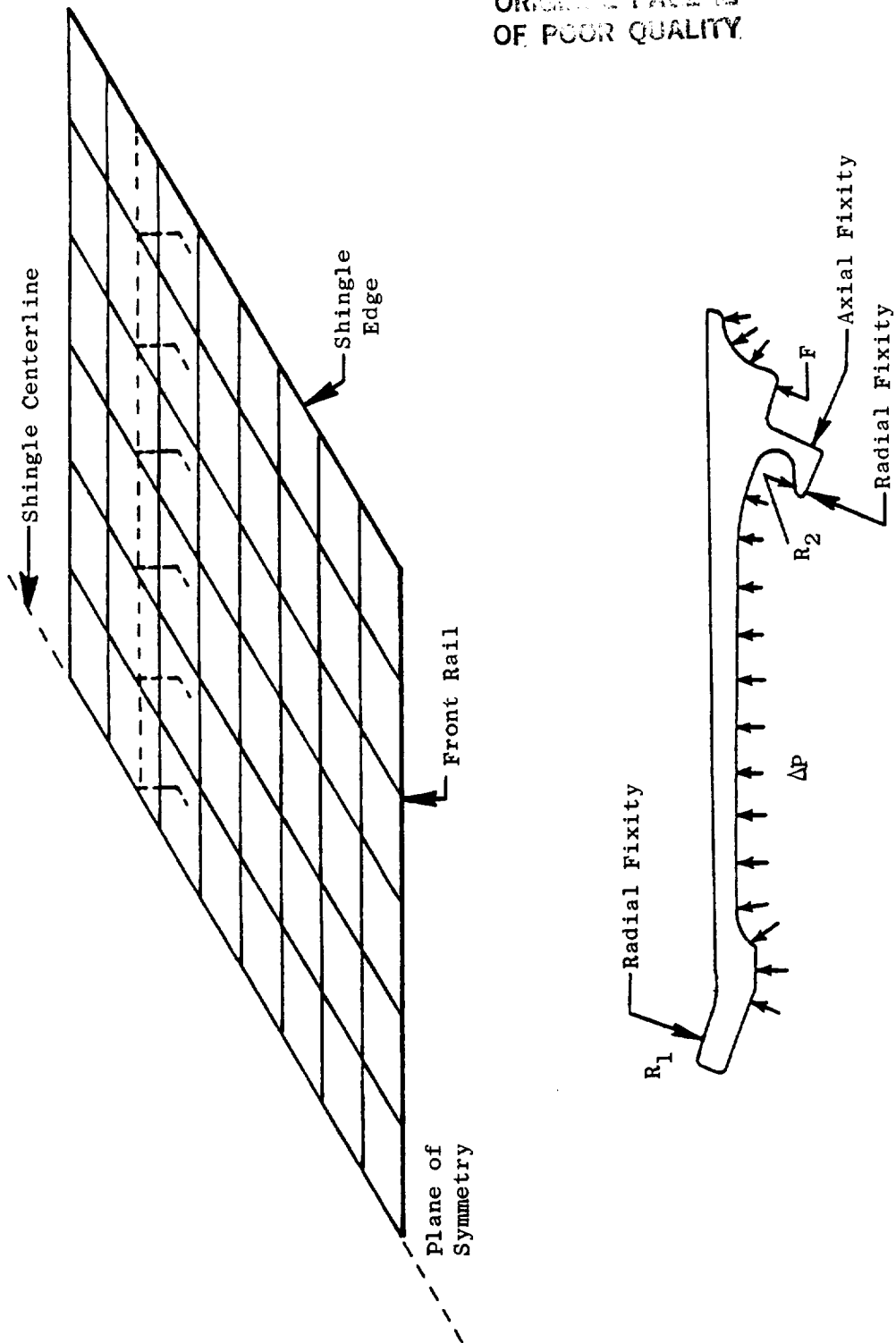


Figure 38. Shingle Structural Model.

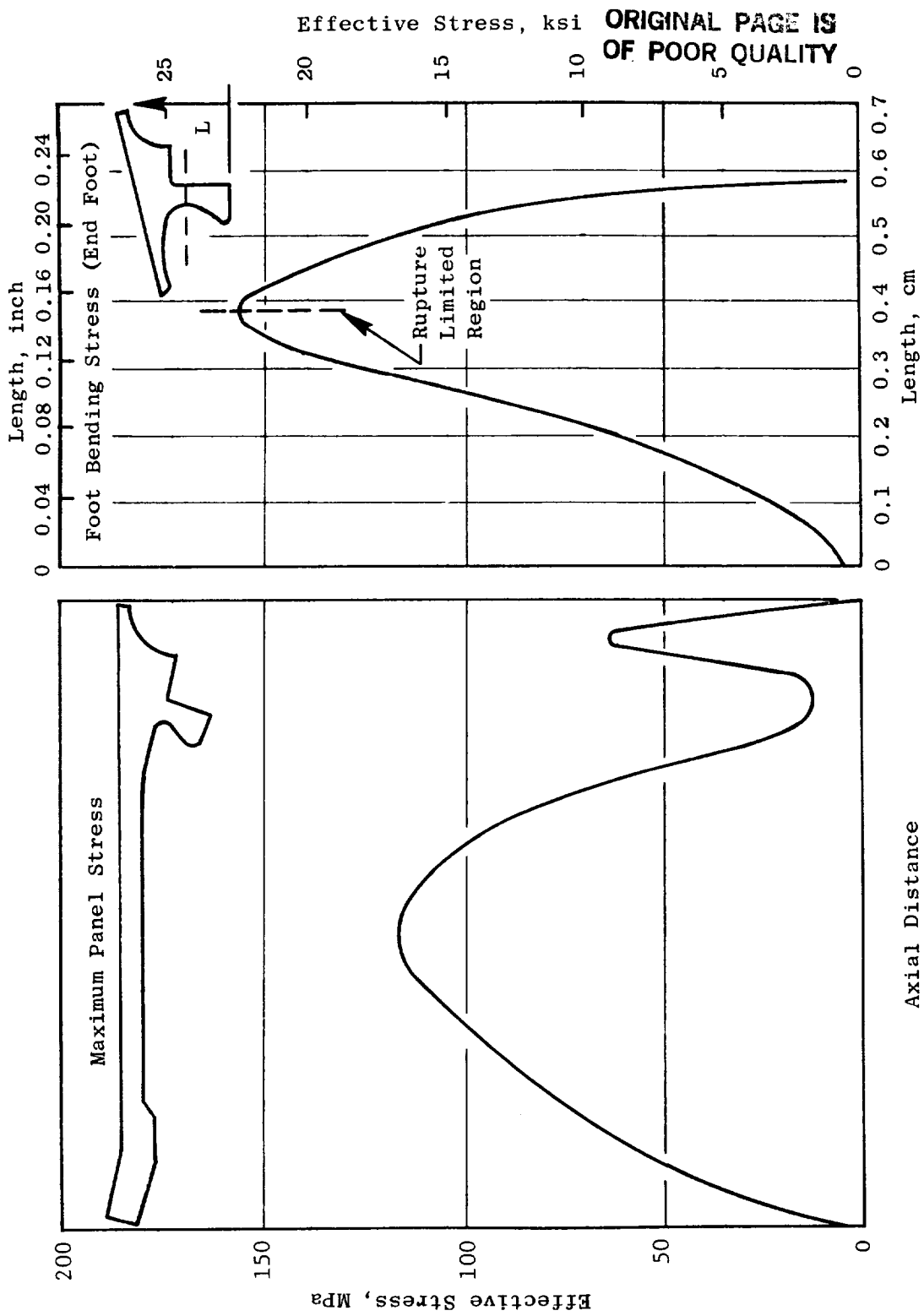


Figure 39. Analytically predicted Pressure Stresses for Shingle.

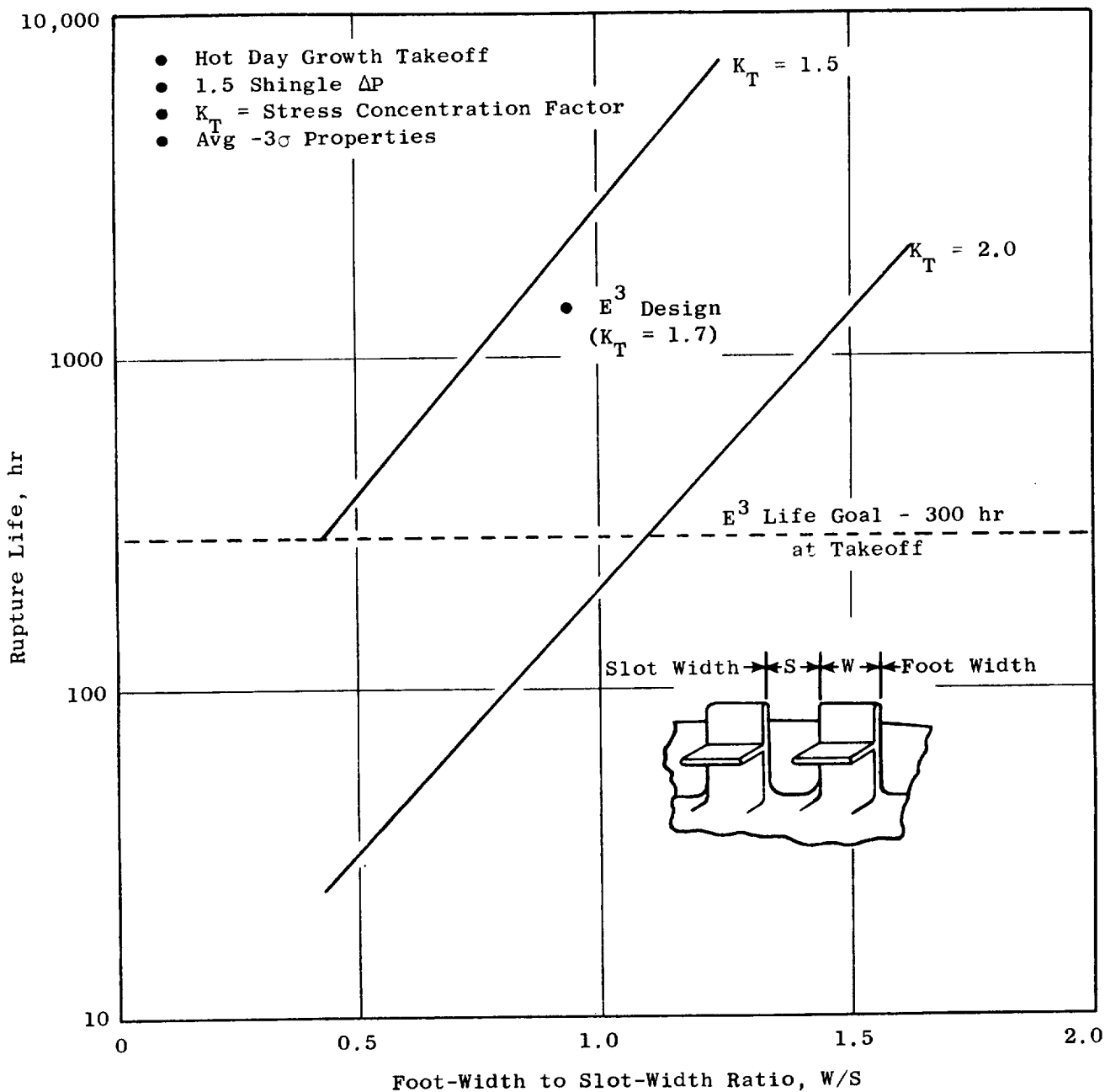


Figure 40. Shingle Foot Size Versus Rupture Life Capability.

ORIGINAL PAGE IS
OF POOR QUALITY

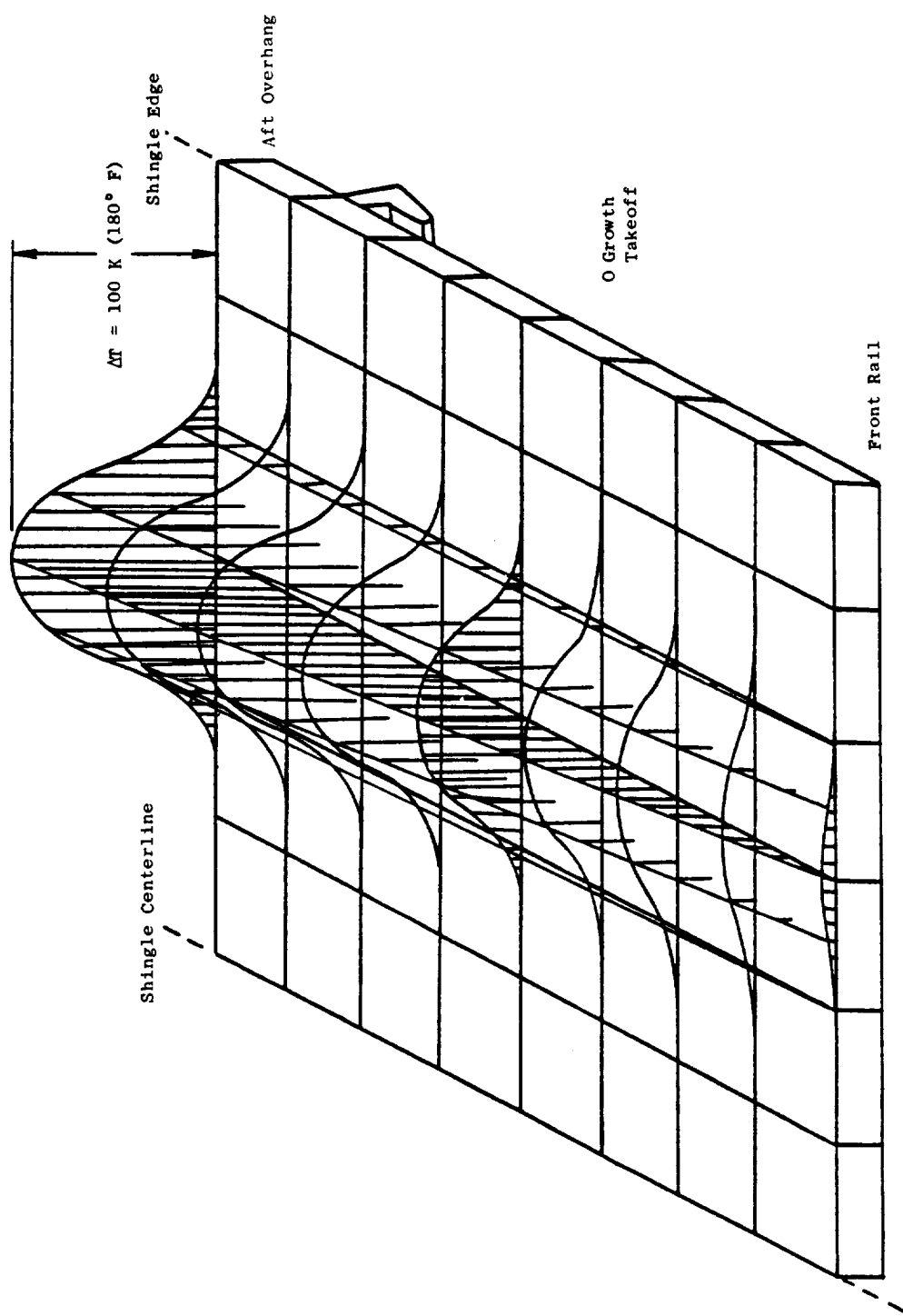


Figure 41. Shingle Low Cycle Fatigue Model Temperature Distribution.

the highest shingle stress level. Figure 42 shows the stress distribution at the hot streak location. The life-limited region of the shingle was the aft support foot region.

An estimate of cycle life was made by utilizing the shingle thermal stress and operating temperature predictions. The cyclic life was estimated based on the effects of foot-width to slot-width ratio and operating temperature. Cyclic life capability can be increased by opening the slot width, thereby allowing increased coolant flow introduction. However, this slot-width size is limited by rupture life considerations. Adequate foot width must be maintained to provide sufficient rupture life as shown in the prior rupture analysis. As shown in Figure 43, the chosen shingle configuration provides adequate fatigue life. For constant hot day operation, degraded material properties, and hold-time effects included, the shingle design meets the life goal with margin.

The shingle cyclic life capability is very sensitive to operating temperature. A moderate increase in shingle temperature results in a significant loss in cyclic life capability. If shingle temperature predictions are exceeded during actual engine operation, then liner cooling distributions would be adjusted to ensure adequate component life.

Table XV shows a comparison of the predicted shingle life capability to the program design goals. Adequate rupture and fatigue life are provided with the chosen design. The growth engine combustor would utilize Mar-M-509 as the cast shingle alloy to meet the cyclic life requirements.

Table XV. E³ Combustor Shingle Predicted Life Levels.

	<u>Fatigue Life, Cycles (Hold-Time Effects Included)</u>	<u>Rupture Life, Hours (Stress Concentration Effects Included)</u>
E ³ Goal	9,000	300 hr
Baseline Engine, X-40 Shingle (T _{Max.} = 1111 K (1540° F))	10 ⁵	5,000
Growth Engine, Mar-M-509 Shingle (T _{Max.} = 1283 K (1850° F))	26,000	1,000

ORIGINAL PAGE IS
OF POOR QUALITY

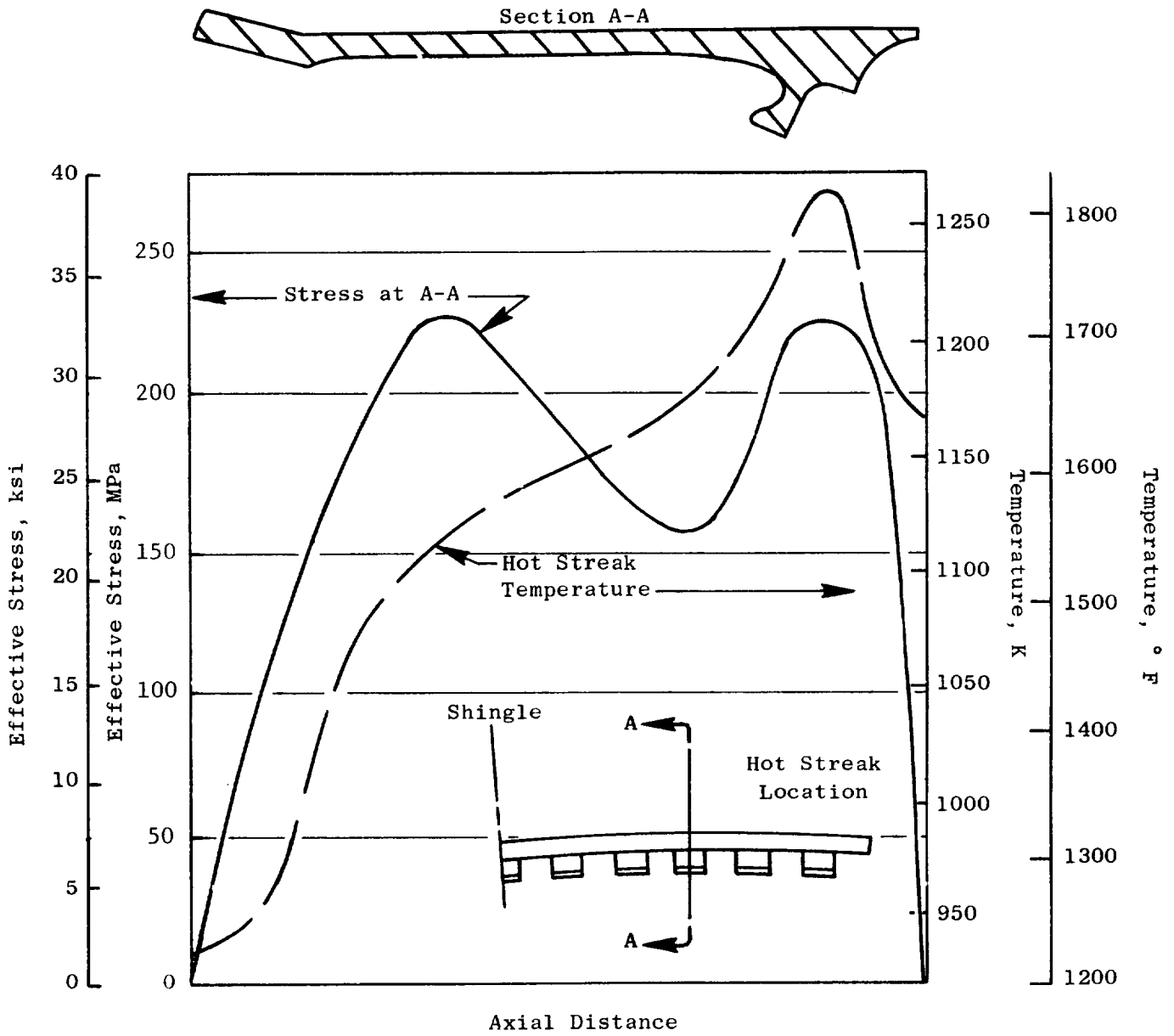


Figure 42. Analytically Predicted Shingle Stress in Hot Streak.

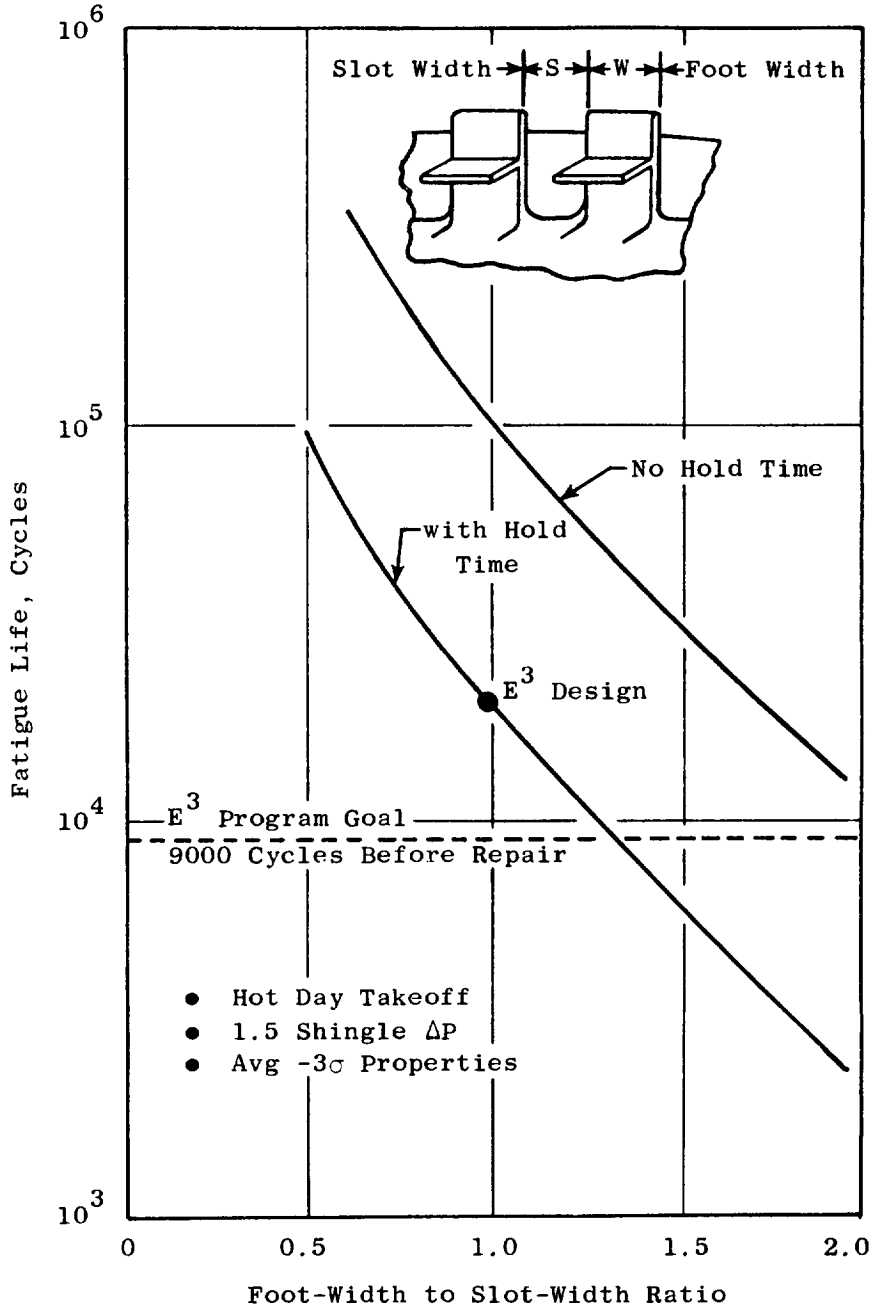


Figure 43. E³ Combustor Shingle Predicted LCF Life.

The combustor support liners were analyzed using CLASS-MASS and BOSOR (Buckling of Shells of Revolution) computer programs. The CLASS-MASS model was used to produce the stress levels due to pressure, mechanical, and temperature loadings. The BOSOR model was used to identify the critical buckling pressures and mode shapes of the outer liner. Adjustments were made to the critical buckling pressure level to allow for out-of-roundness effects.

The CLASS-MASS analysis of the shingle support liners was conducted to assess the operating stress levels at the most adverse operating conditions. The models simulated the growth engine maximum pressure conditions and the actual structural attachment boundary conditions. The effective stress distributions for the outer and inner support liners are shown in Figures 44 and 45, respectively.

An important design consideration in the liner design is the buckling capability of the outer liner. The liner shell is subjected to the buckling loads resulting from the combustor pressure drop. The E³ design was analyzed using the model shown in Figure 46. Various liner thicknesses were evaluated over a range of 0.76 to 1.27 mm (0.03 to 0.05 in.). The buckling analysis utilized the maximum growth engine pressure drop condition.

The critical pressure drop across the outer liner that produces buckling of the shell is dependent on several factors: the end fixity of the shell, thickness of the shell, number of nodes of the deflected structure, and the roundness of the initial structure. Figure 47 shows that for a round structure with a thickness of 1.02 mm (0.040 in.), a minimum critical pressure of approximately 1.24 MPa (180 psi) is indicated. This pressure is well above the anticipated operating pressure drop of the liner. However, when the liner out-of-roundness effects are considered, the margin of safety is reduced. Figure 48 shows the effect of out-of-roundness on the buckling characteristics. The chosen E³ liner thickness and radial concentricity requirements provide a 2X safety margin at maximum growth engine operation.

5.4 CASING

The primary function of the combustor casing (Figure 49) is to support the combustor and its fuel delivery and ignition systems. The casing features

ORIGINAL SOURCE
OF POOR QUALITY

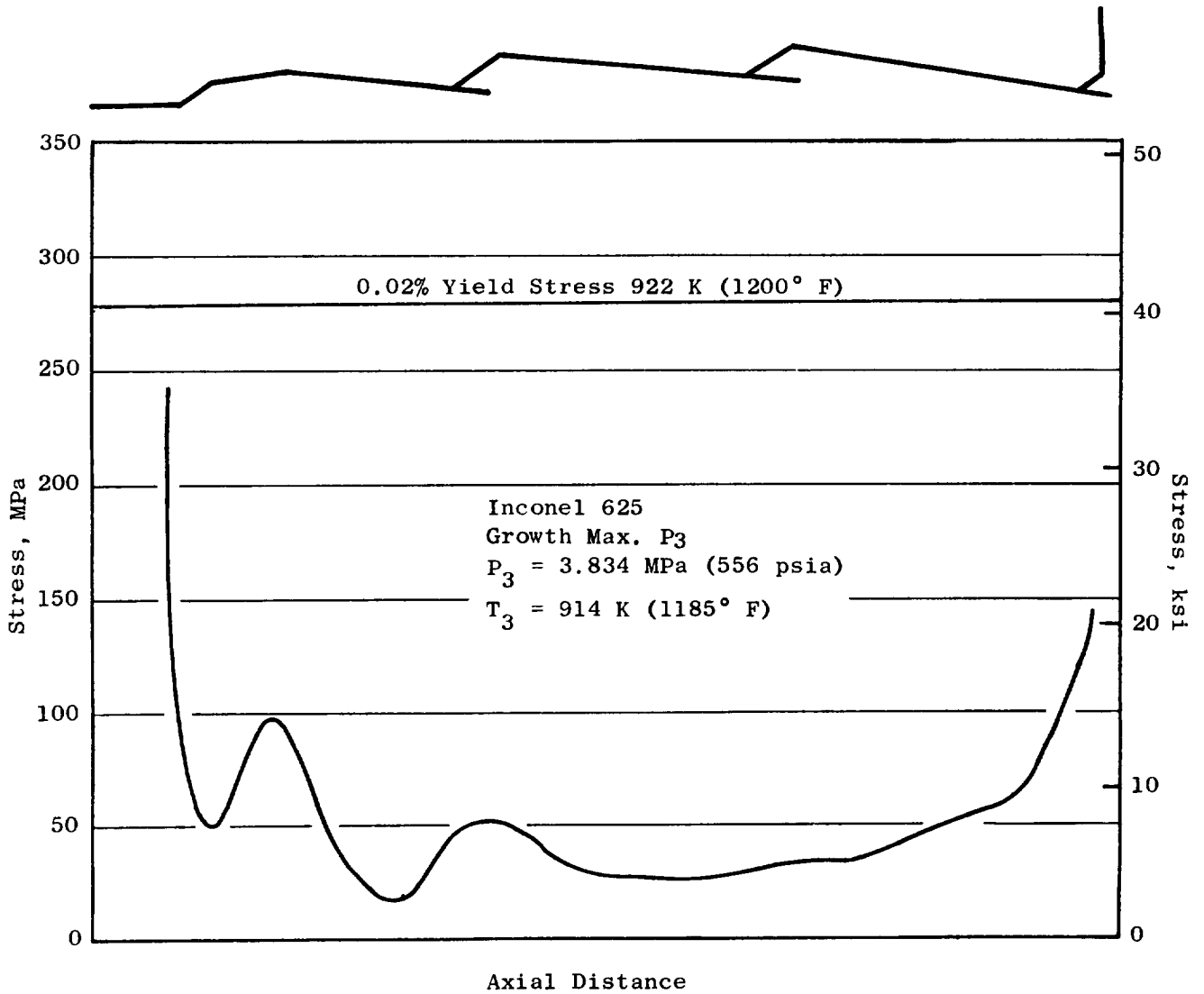


Figure 44. Predicted Stress for Combustor Support Liners.

ORIGINAL PAGE IS
OF POOR QUALITY

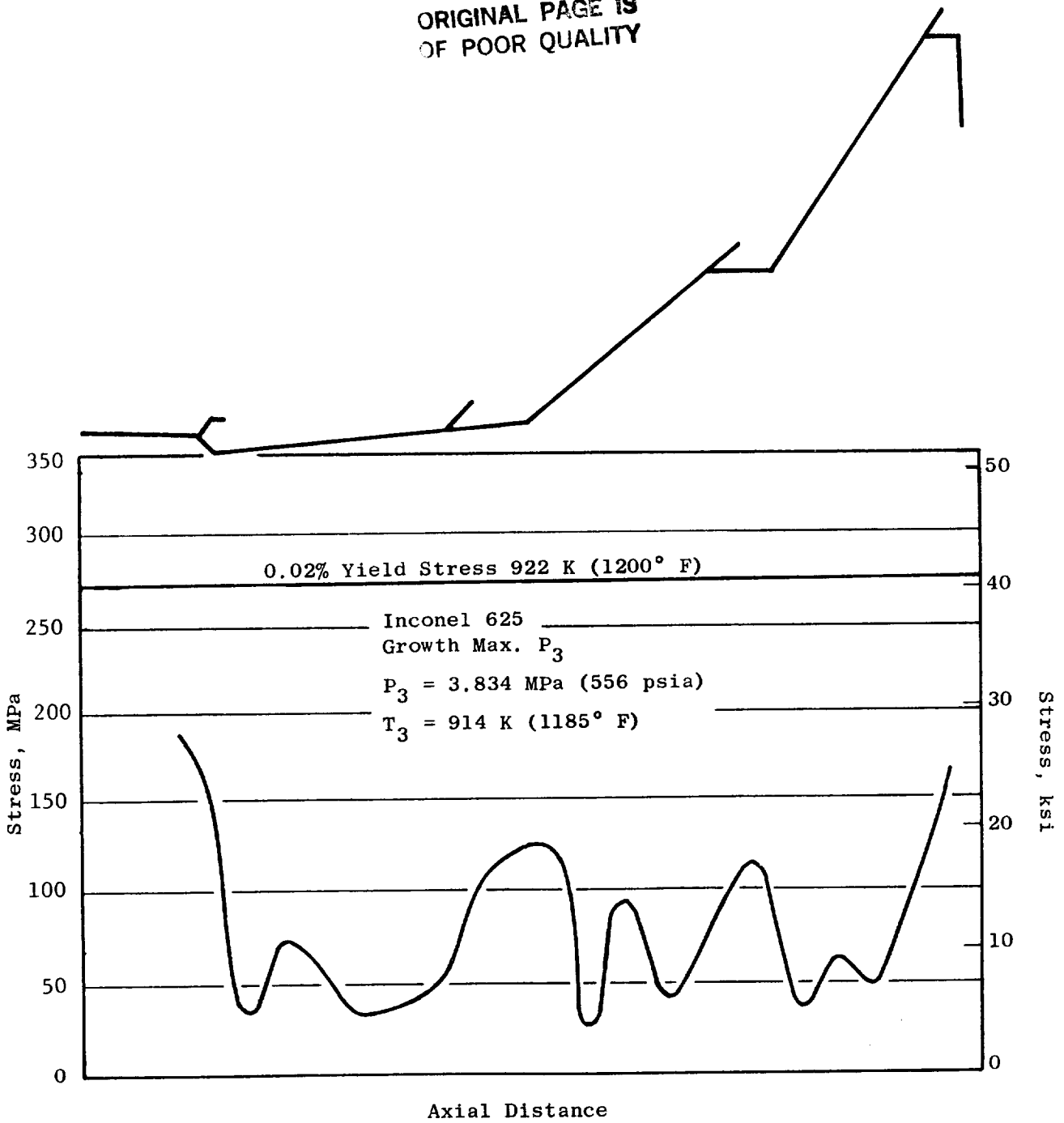
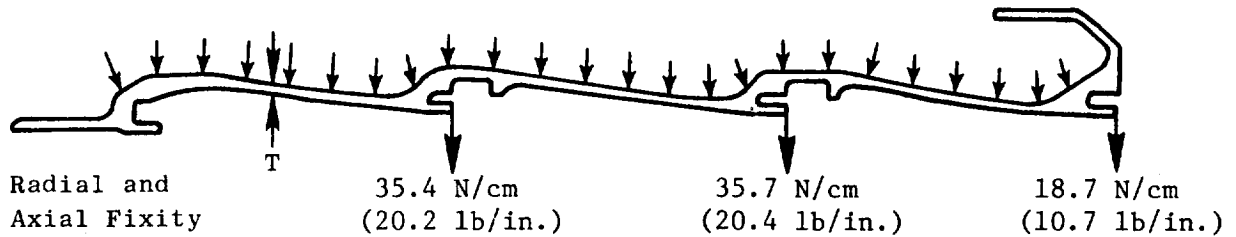


Figure 45. Predicted Stress for Combustor Support Liners.

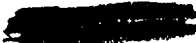
ORIGINAL PAGE IS
OF POOR QUALITY

$$\Delta P = 0.193 \text{ MPa (28 psia)}$$



- Growth, Max. P_3 Condition
- $P_3 = 3.91 \text{ MPa (567 psia)}$
- $T_3 = 94 \text{ K (1185}^\circ \text{ F)}$
- Inconel 625
- BOSOR Program
- Liner Thickness, $T = 0.26\text{--}1.27 \text{ mm (0.03\text{--}0.05 \text{ in.})}$

Figure 46. Support Liner Buckling Analysis Model.



ORIGINAL PAGE IS
OF POOR QUALITY

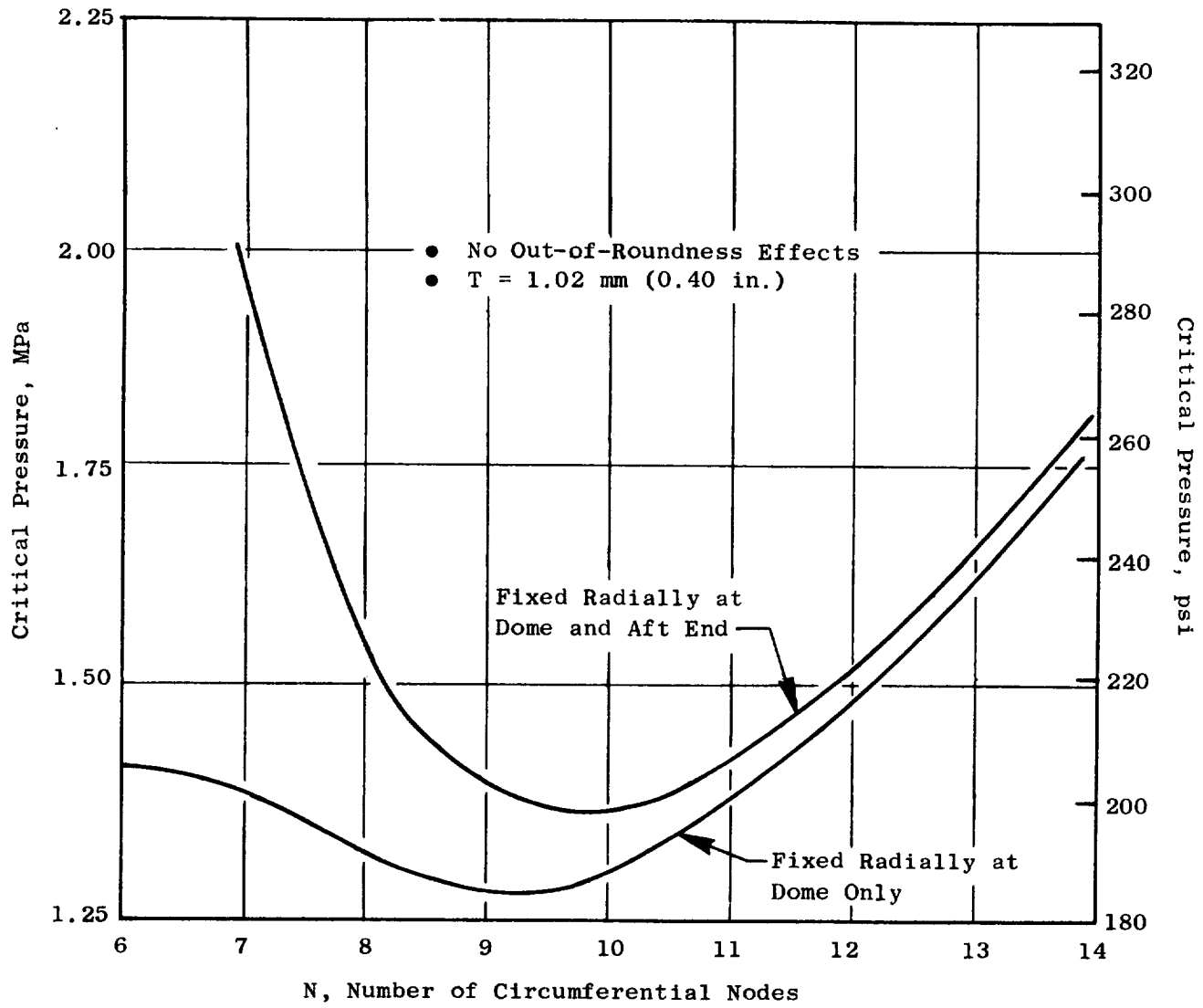


Figure 47. Outer Support Liner Critical Buckling Pressures.

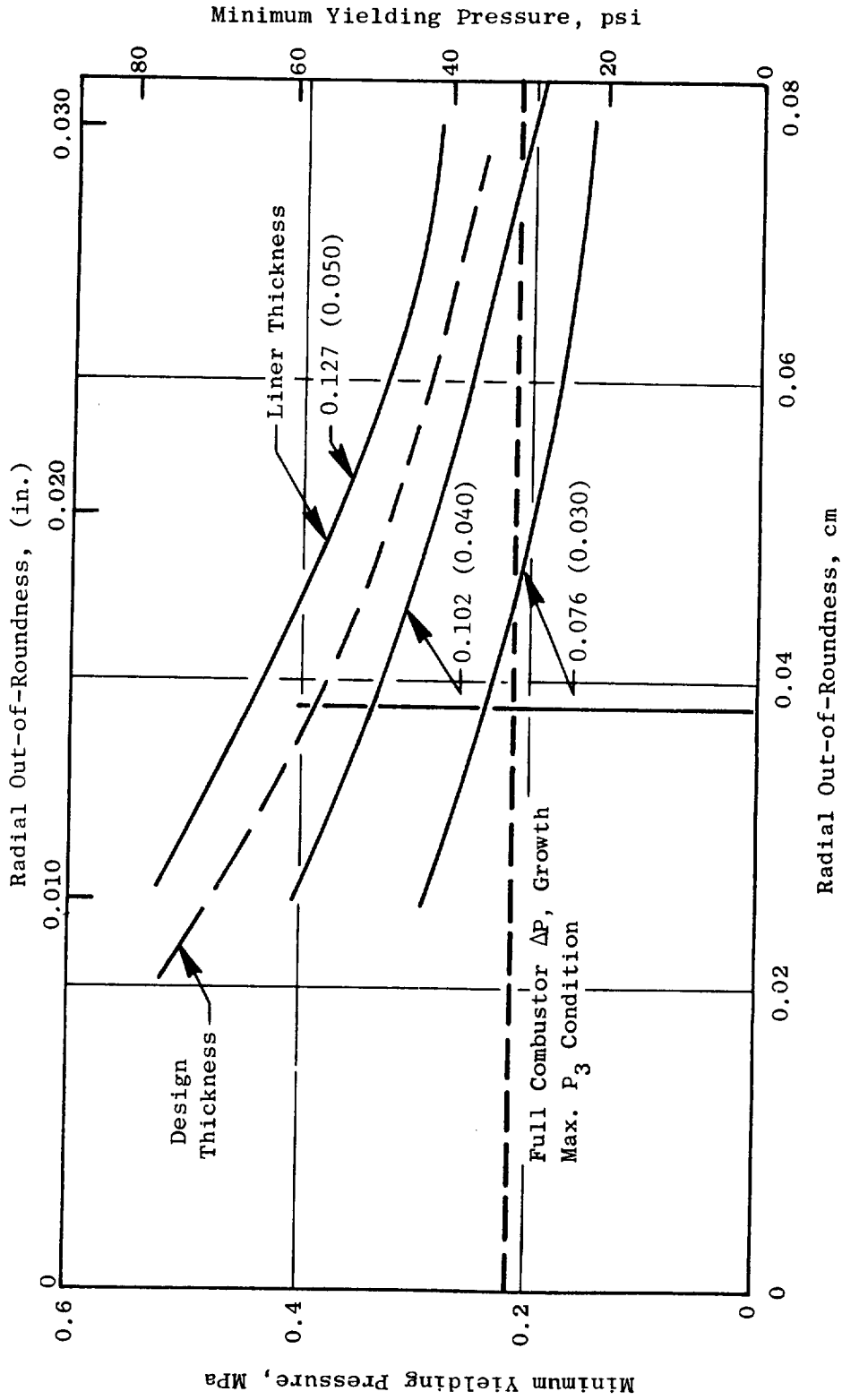
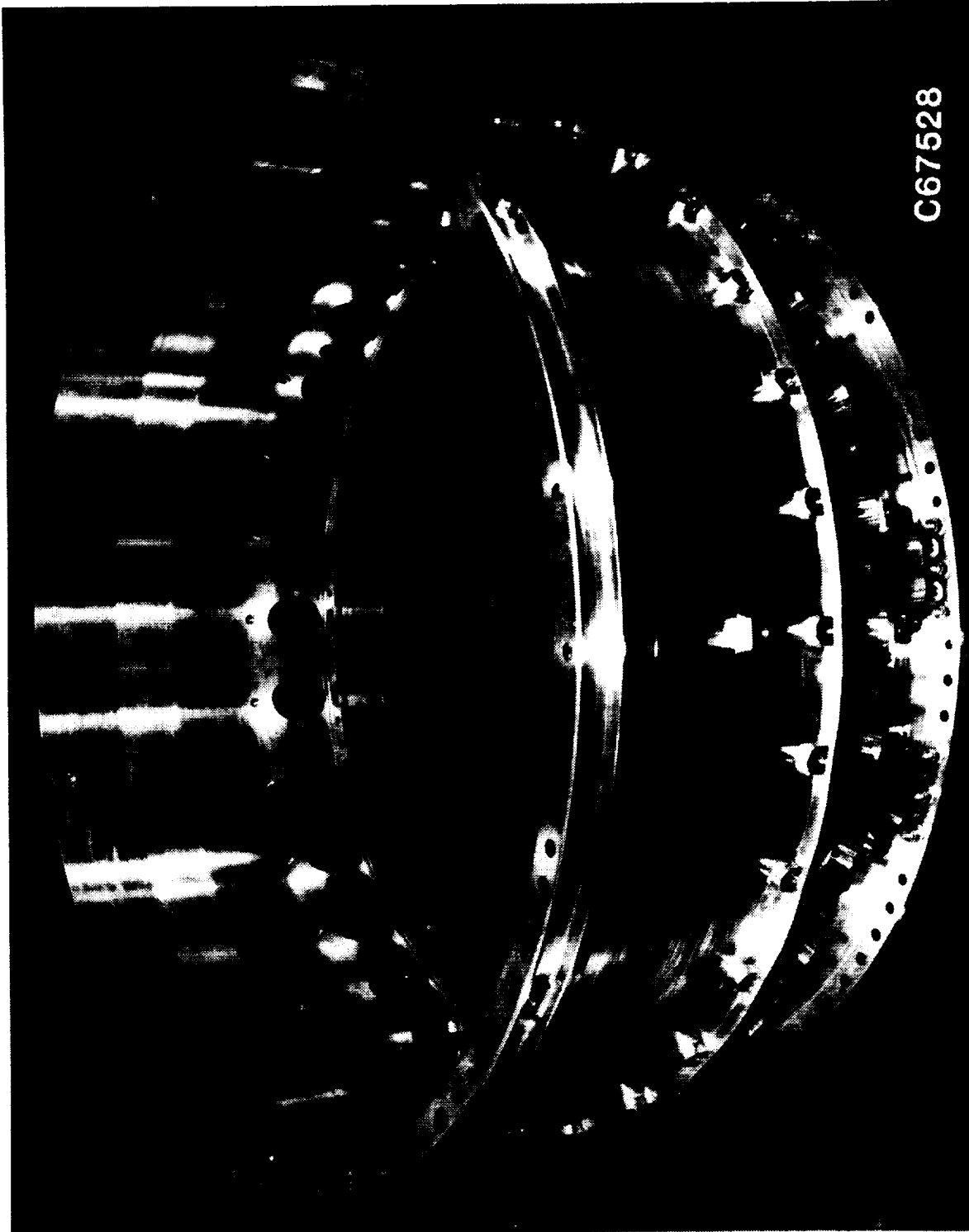


Figure 48. Effect of Out-of-Roundness on Buckling Characteristics.

ORIGINAL PAGE
OF POOR QUALITY

ORIGINAL PAGE
BLACK AND WHITE PHOTOGRAPH



C67528

Figure 49. Combustor Casing.

mounting pads for the fuel nozzles, igniters, and combustor mounting pins. In addition, the casing has compressor discharge bleed ports, instrumentation ports, and borescope inspection ports.

The combustor casing was analyzed using the CLASS-MASS computer program. Figure 50 shows the stress levels of the casing at the growth engine maximum pressure loading conditions. In this analysis the casing temperature is assumed to be fairly uniform and slightly less than the compressor discharge temperature. The casing thickness was chosen so that the maximum stress levels would have a 50% yield strength of the casing material.

Figure 51 shows the combustor support pin design. This design is similar to the CF6 support pin design. The 30 support pins are bolted to the outer case and establish the axial location of the combustor through mating holes in the cowl struts. The combustor loads are transmitted to the combustor case through the aerodynamic support pins. A wear-resistant surface is provided at the support pin/cowl interface with a triballoy coating on the support pin and a Stellite 6 bushing in the cowl.

5.5 DOME

Figure 52 shows a forward-looking-aft view of the combustor dome assembly. Each of the domes consists of 30 swirl cups supported by a 360° spectacle plate. The spectacle plate is the main structural member of the dome and is protected from the hot gases by individual splash plates at each swirl cup location. The swirl cups are comprised of counterrotating primary and secondary swirlers. The swirlers are machined from adjustable area swirler castings which allow flexibility in flow sizing.

The primary swirler features a slip joint attachment to the swirler cup which allows the primary vane assembly to "float" within certain limits. This floating vane arrangement allows for assembly stackup plus thermal expansion between the dome and fuel nozzle.

The domes are bolted to the cowl assembly. The cowl struts transmit the aerodynamic loads from the domes and liners through the support pins to the

- Design Intent - 50% Yield
- Growth Engine - Max. P_3

$P_3 = 3.91 \text{ MPa (567 psia)}$
 $T_3 = 914 \text{ K (1185}^\circ \text{ F)}$

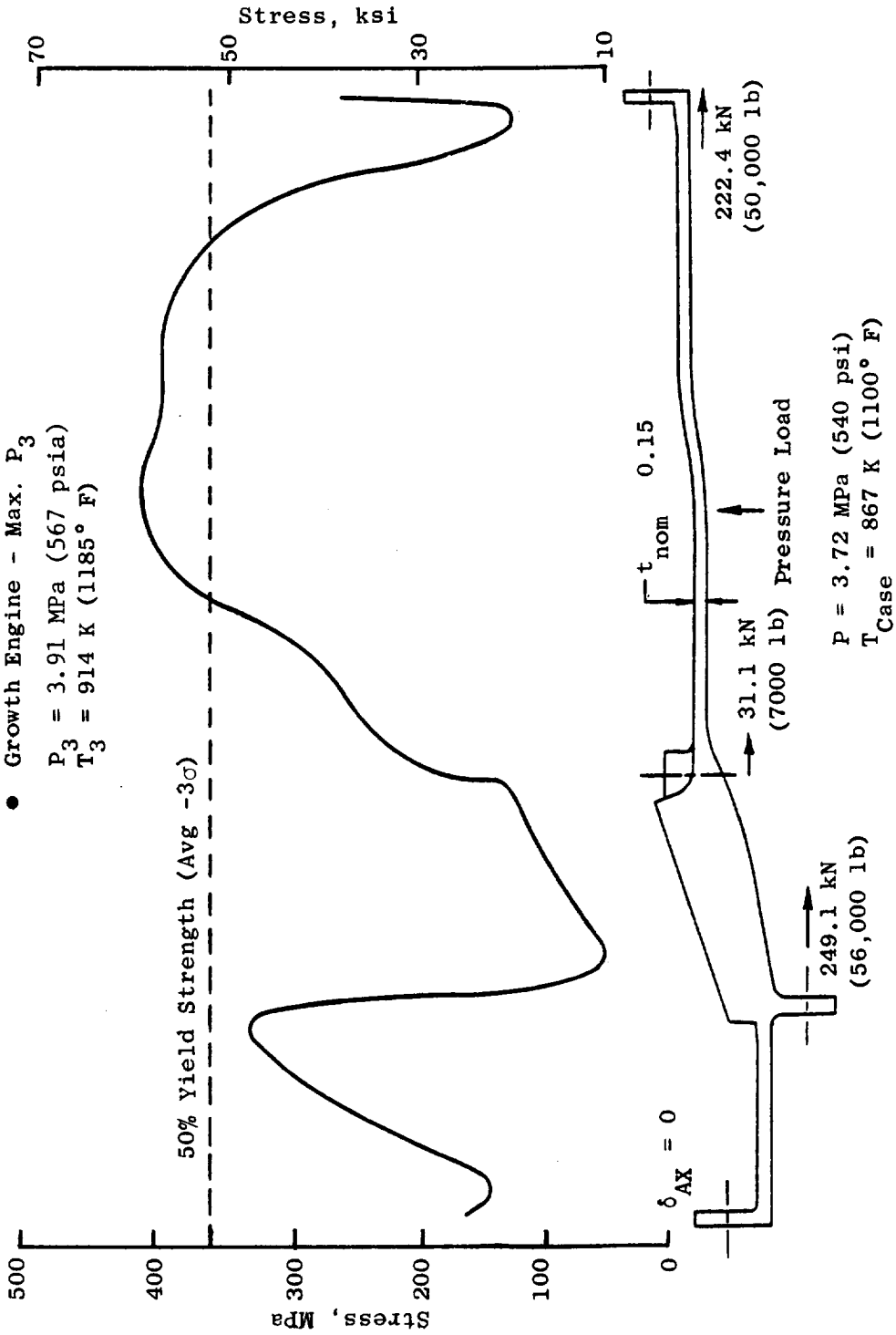


Figure 50. Predicted Axial Stress Distribution for Casing.

CRITICAL PARTS
OF POOR QUALITY

30 Total
Max. Load = 805 N (181 lb) Each Pin
Max. Stress = 345 MPa (50 ksi) Bending
(Yield = 793 MPa (115 ksi) Avg -3σ)

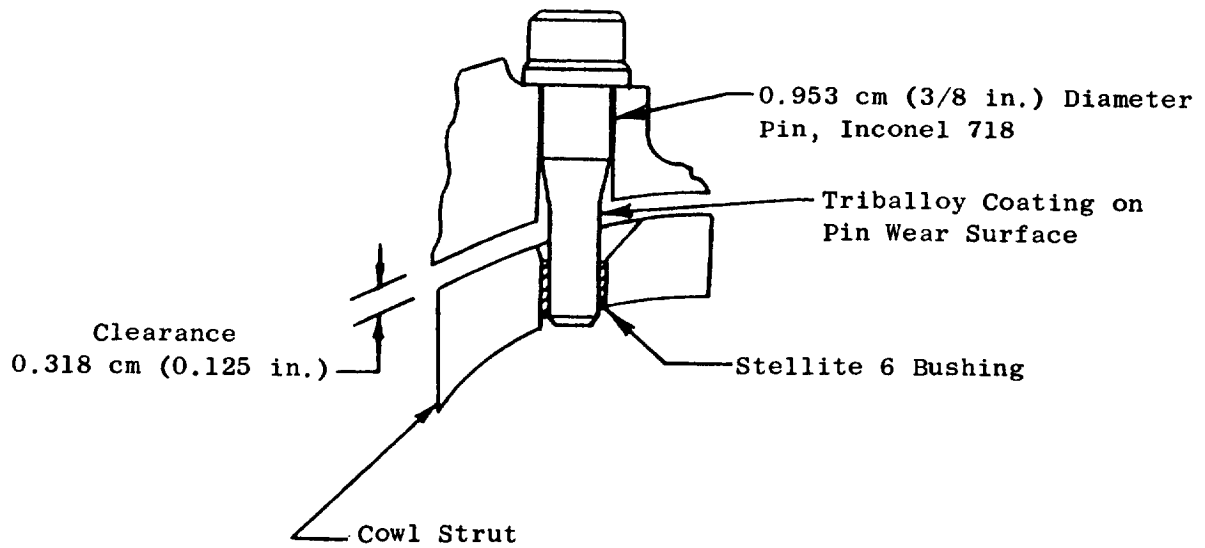


Figure 51. Combustor Support Pin Design.

ORIGINAL PAGE IS
OF POOR QUALITY

ORIGINAL PAGE
BLACK AND WHITE PHOTOGRAPH

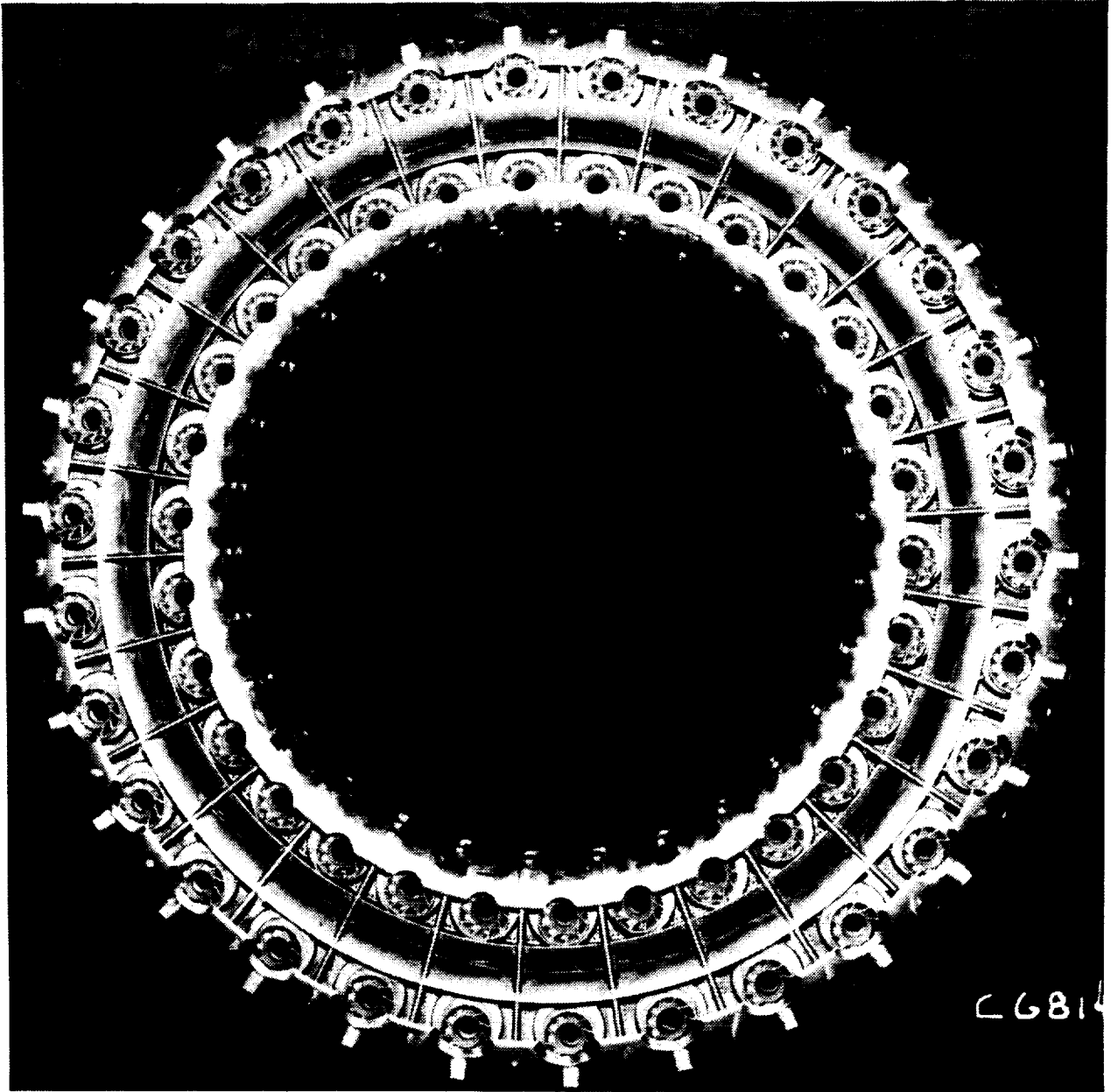


Figure 52. E³ Combustor Dome.

combustor casing. Scallops are provided on the inner and outer cowls to allow installation and removal of the fuel nozzles without major engine disassembly.

5.6 CENTERBODY

Figure 53 shows the centerbody structure. Its primary function is to separate the primary burning zones of the pilot and main stage domes. The main structure of the centerbody consists of a 360° machined piece with both film and impingement cooling. A sheet metal impingement baffle is brazed inside the centerbody cavity. Each dome has dilution air introduced through 30 dilution eyelets which are brazed to the main structure. Two crossfire tubes, in line with the two igniters, provide flame propagation across the centerbody to the main stage dome. Figure 54 shows a closeup view of the combustor, illustrating the centerbody region near a crossfire tube. Other features shown in the figure are pilot side dilution holes and tip cooling holes.

Several design changes to the centerbody were incorporated since the preliminary design review. The centerbody tip was shortened to add rigidity and to eliminate a difficult tip hole drilling operation. This tip was also slotted to reduce thermal stress. A stable thermal barrier coating material was applied to reduce the metal temperature. "Gill" cooling holes were provided downstream of each crossfire tube in order to increase the film cooling in that region.

Figure 55 shows the results of the centerbody life analysis. A comparison was made between different centerbody configurations to determine the effect that the design changes have on cyclic life. As shown, the baseline configuration with tip slots and thermal barrier coating provides a life level in excess of the required 9,000 cycles.

5.7 FUEL DELIVERY SYSTEM

The fuel delivery system (Figure 56) consists of two completely independent systems which feed each dome through a single-stem fuel nozzle. The fuel manifolds and pigtail assemblies are fabricated from stainless steel. The

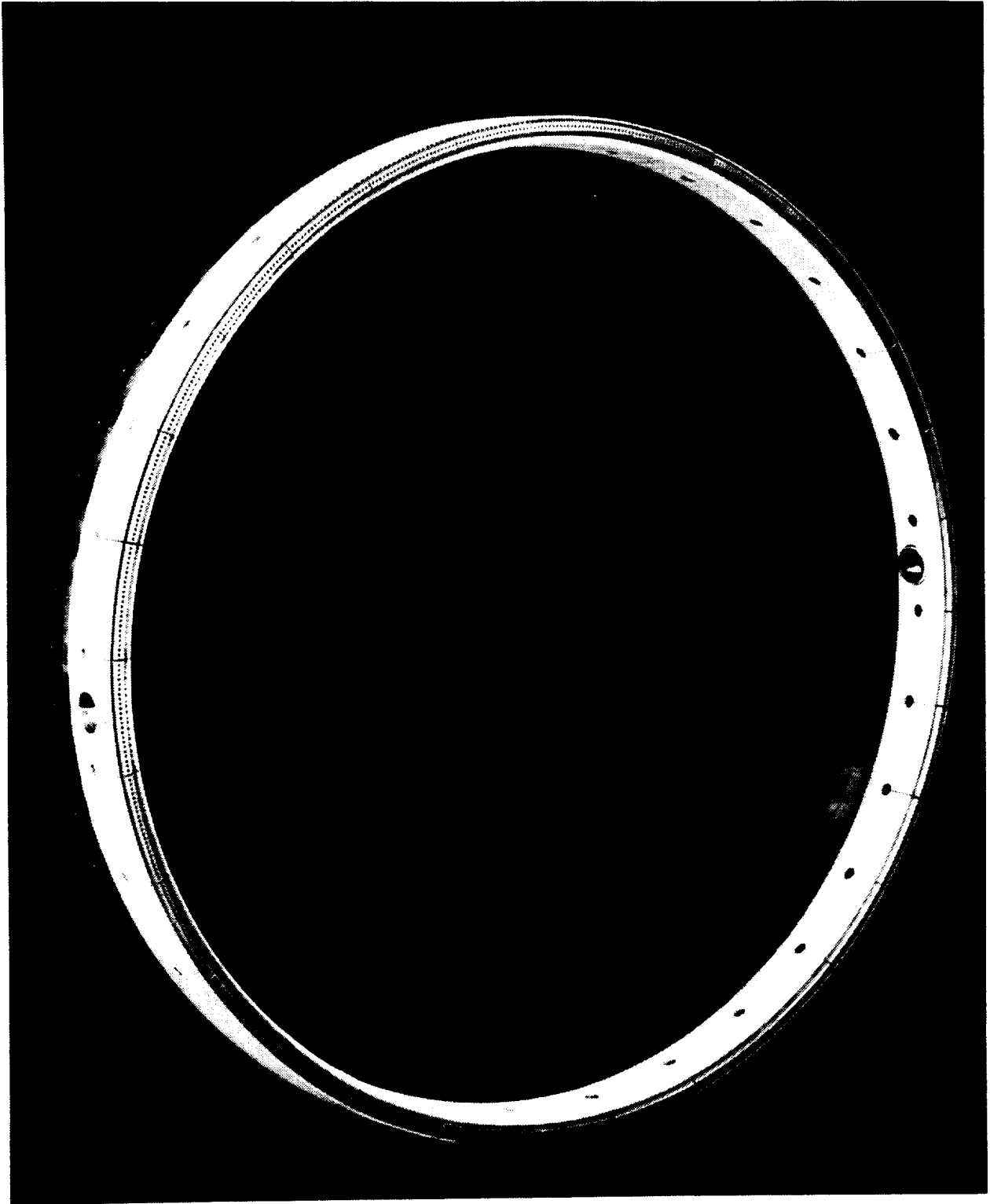


Figure 53. E³ Combustor Centerbody Structure.

ORIGINAL PAGE 19
OF POOR QUALITY.



8110252

Figure 54. Detailed View of Centerbody Structure and Domes.

ORIGINAL PAGE
BLACK AND WHITE PHOTOGRAPH

ORIGINAL PAGE IS
OF POOR QUALITY

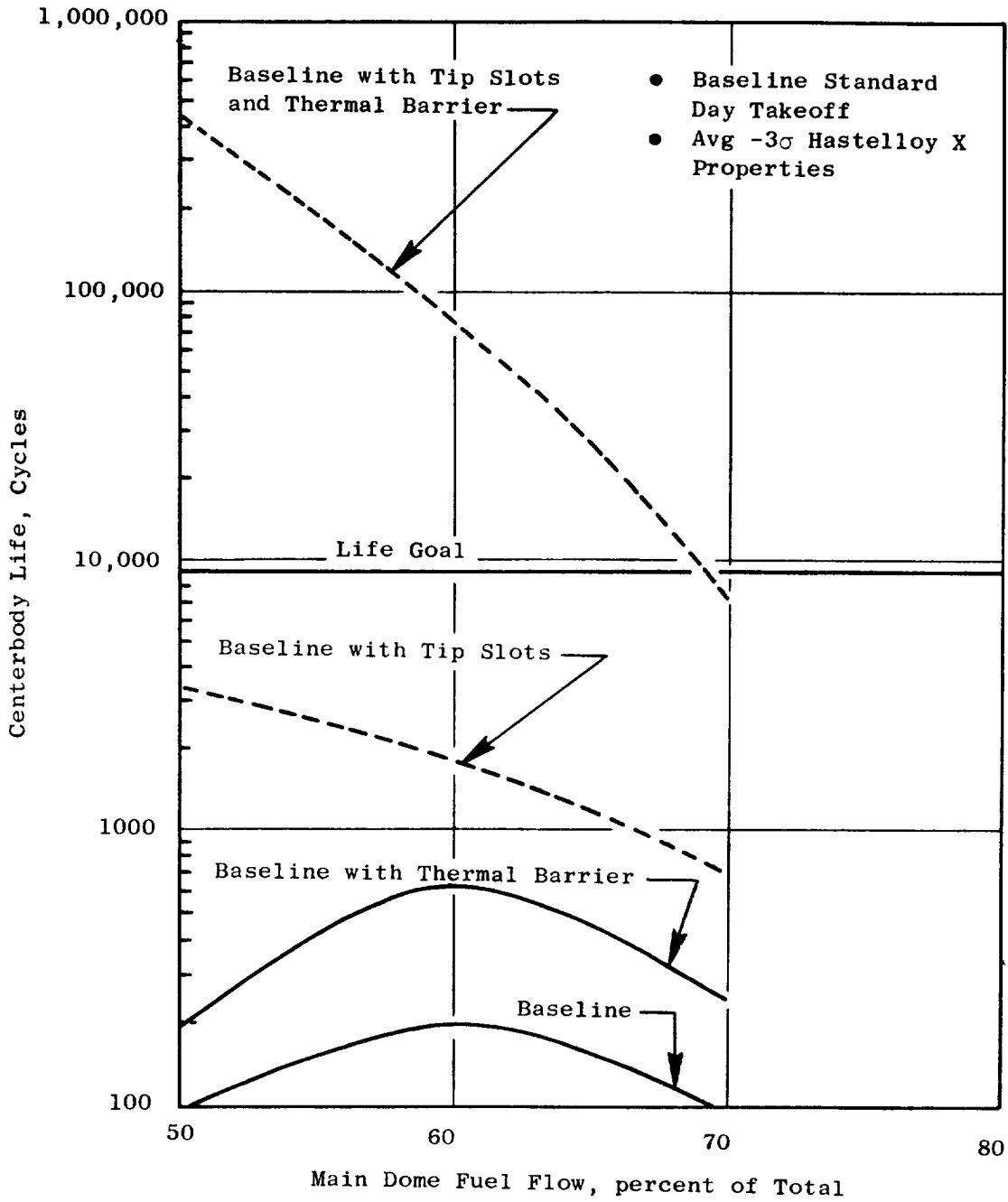


Figure 55. Predicted Centerbody Structure Life Levels.

CONFIDENTIAL

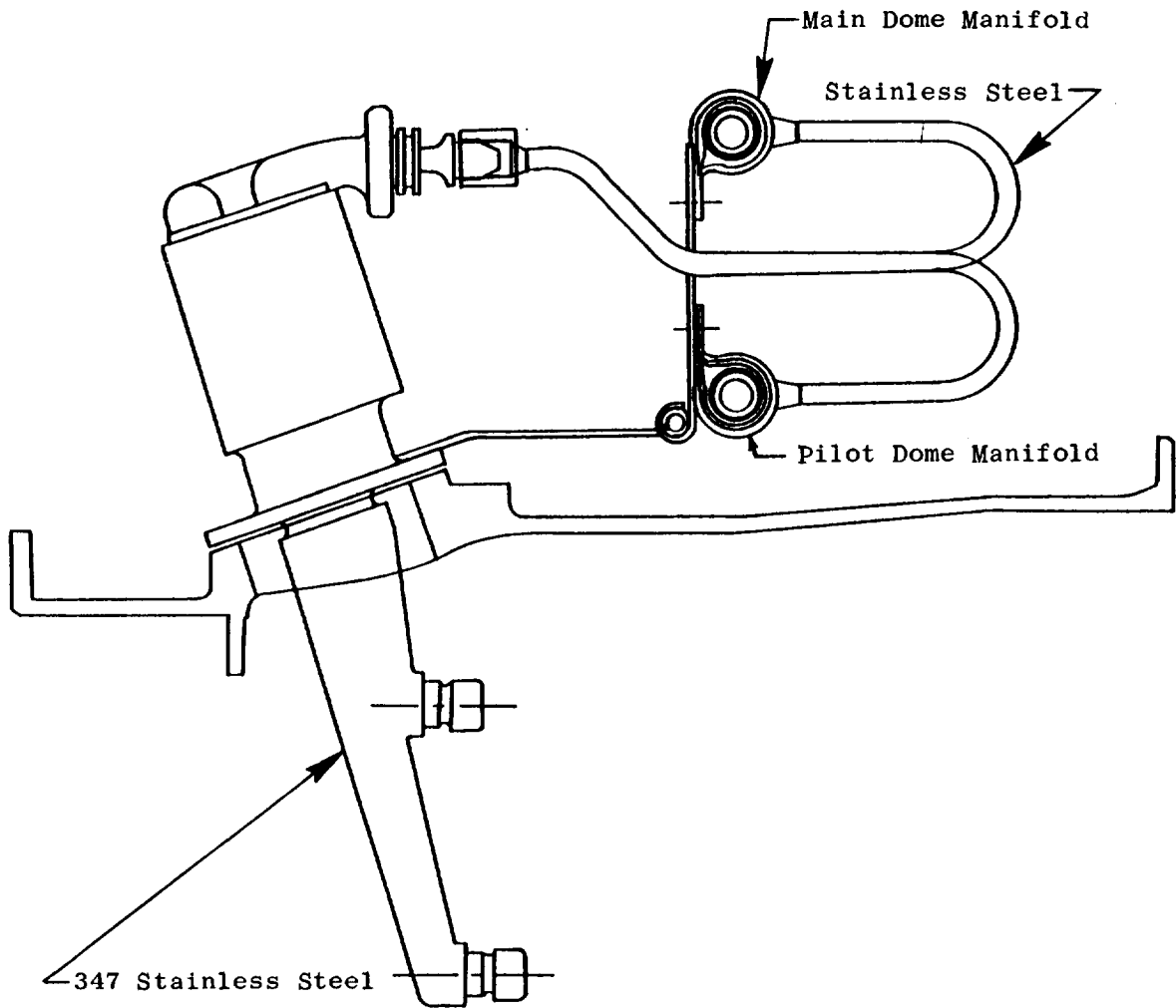


Figure 56. E³ Fuel Delivery System.

fuel nozzle is made from a stainless steel forging. The materials selection is based on extensive demonstrated commercial engine experience and reduced fabrication costs.

The fuel nozzle mechanical design features are shown in Figure 57. Each circuit has its own positive check valve to maintain fuel in the manifolds and to reduce system fill time. Double heat insulation is provided by a stem heat shield and a coking gap around each fuel passage to prevent fuel boiling. Each nozzle tip is fed through individual primary and secondary fuel tubes to accommodate off-design conditions. An extended valve standoff is provided to isolate the metering valve from the engine casing and its associated heat loads, which might cause fuel gumming or varnishing of the valve components. Figure 58 illustrates the fuel nozzle assembly.

Extensive vibration and geometric studies were conducted to ensure that the fuel nozzle design would avoid critical frequencies on the high-power operating range, meet geometric constraints, and minimize aerodynamic losses.

Vibration analysis was conducted by using the MASS computer program. The nozzle stem was modeled as a series of constant area beams and included the effects of the fuel passages. Figure 59 shows the model used to determine the first flex frequencies of the fuel nozzle. The results of the vibration study are shown in Figure 60. The Campbell diagram shows the first flex frequencies of two nozzle stem designs versus engine speed. The stiffened configuration represents the initial design intent to have a minimum natural frequency of 1000 Hz at takeoff power. But the chosen design has a frequency of 750 Hz at takeoff. The 750-Hz configuration was chosen on considerations of lower associated aerodynamic losses due to stem blockage, combustor/fuel nozzle assembly envelope, and lower fuel nozzle weight. The calculated stem vibration characteristics were verified by a laboratory bench analysis. This test indicated that the E³ fuel nozzle stem has adequate rigidity for engine application.

ORIGINAL FIGURE
OF POOR QUALITY

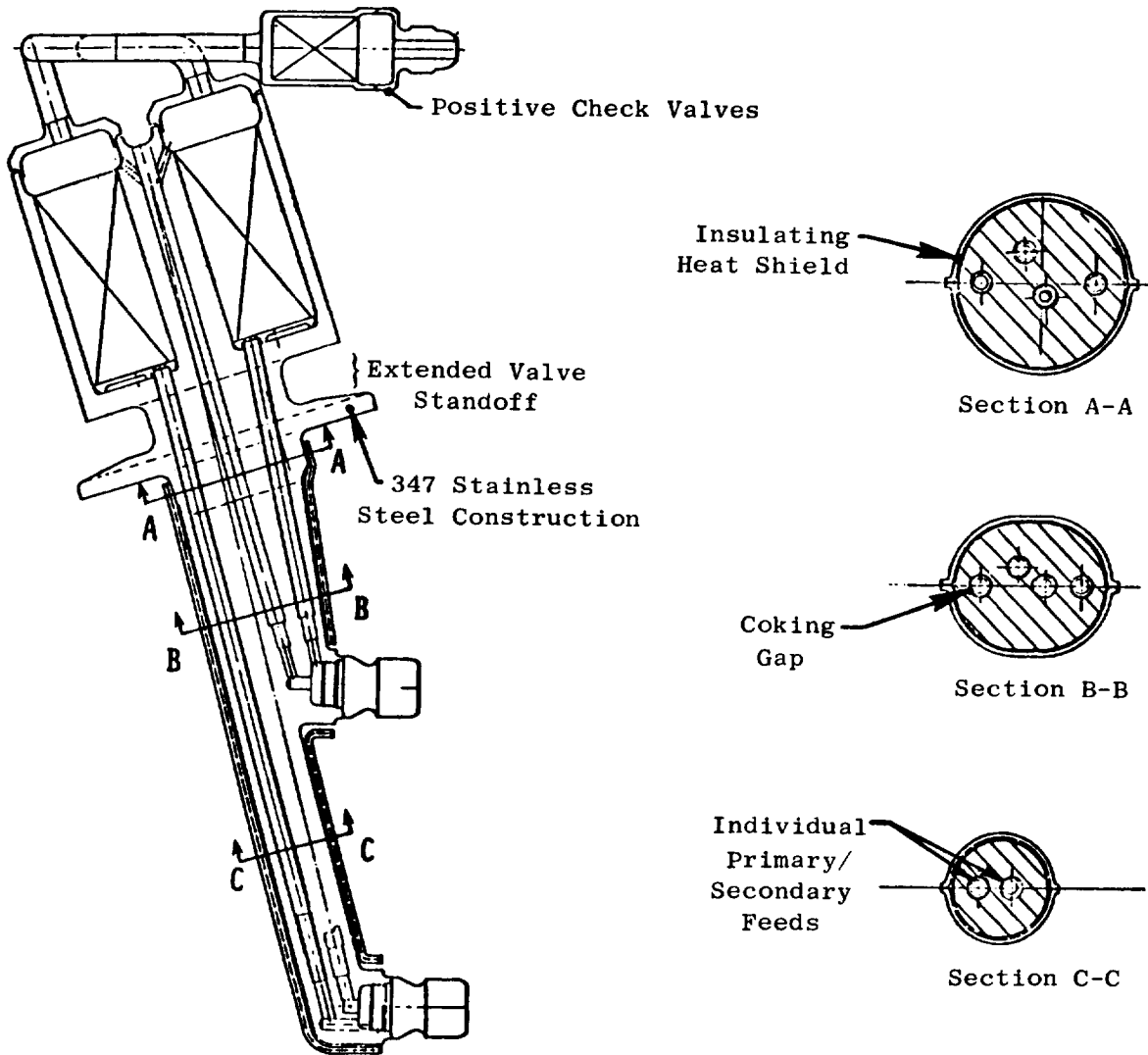


Figure 57. E³ Fuel Nozzle Mechanical Features.

ORIGINAL PAGE IS
OF POOR QUALITY

ORIGINAL PAGE
BLACK AND WHITE PHOTOGRAPH

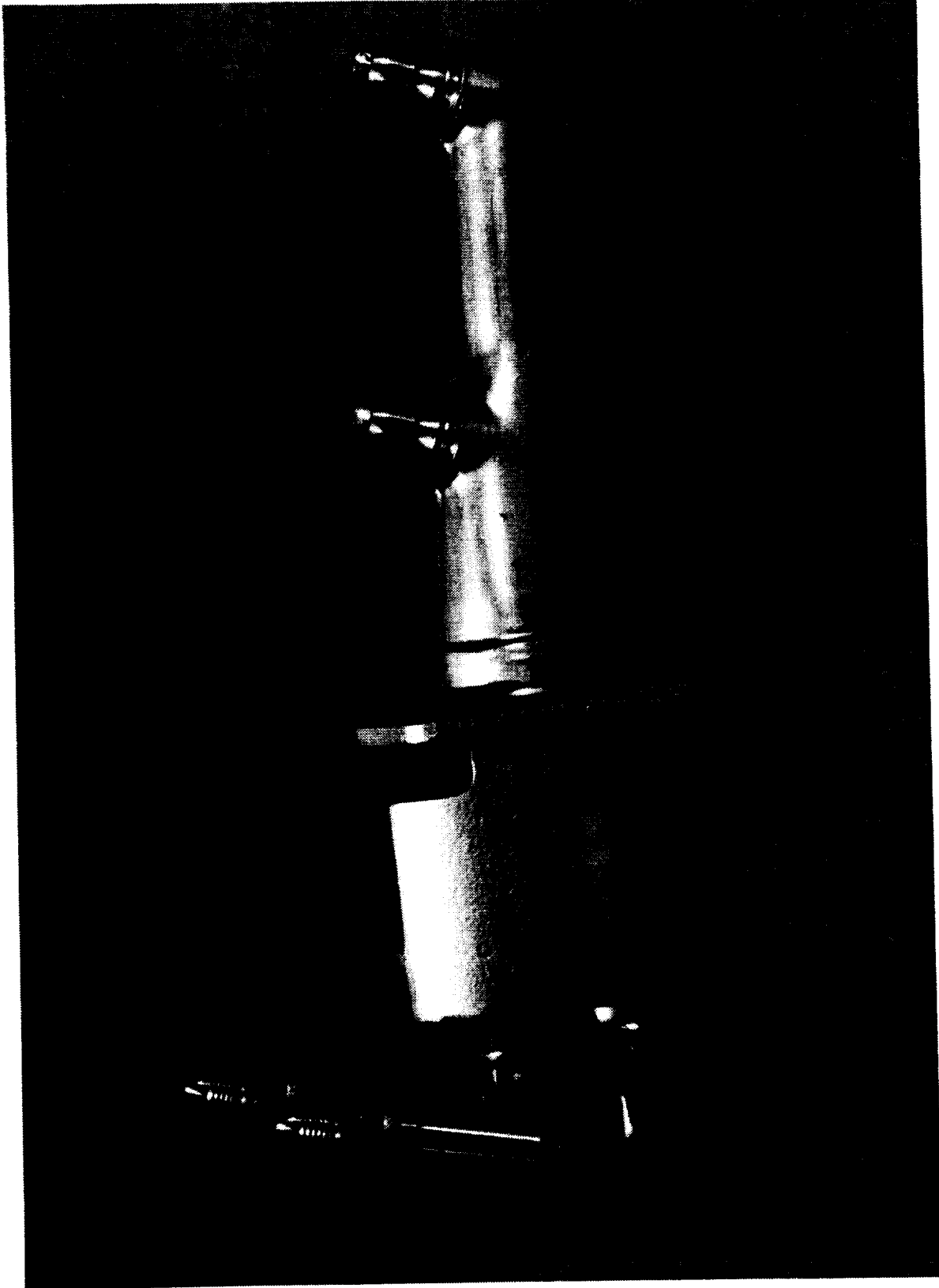
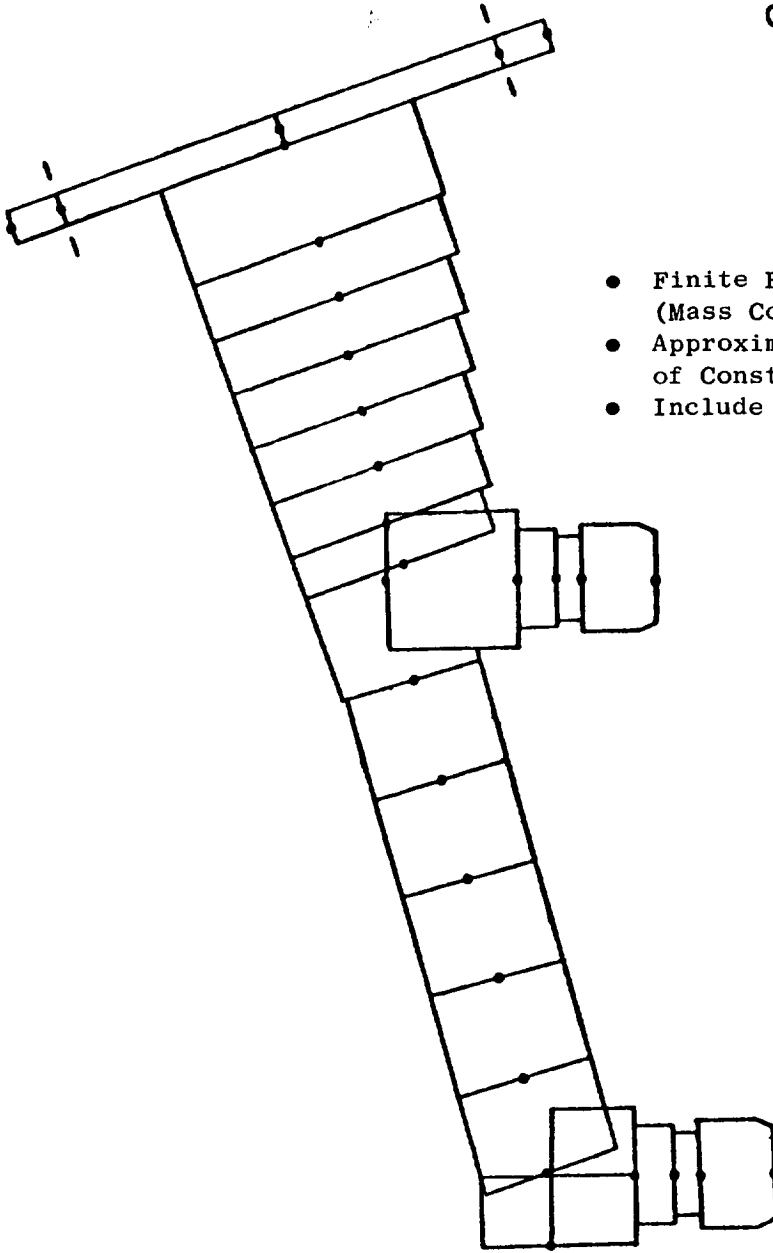


Figure 58. E³ Fuel Nozzle Assembly.

ORIGINAL PAGE IS
OF POOR QUALITY



Method

- Finite Element Model
(Mass Computer Program)
- Approximate Stem with a Series
of Constant Area Beams
- Include Effect of Fuel Passages

Figure 59. Fuel Nozzle Vibration Model.

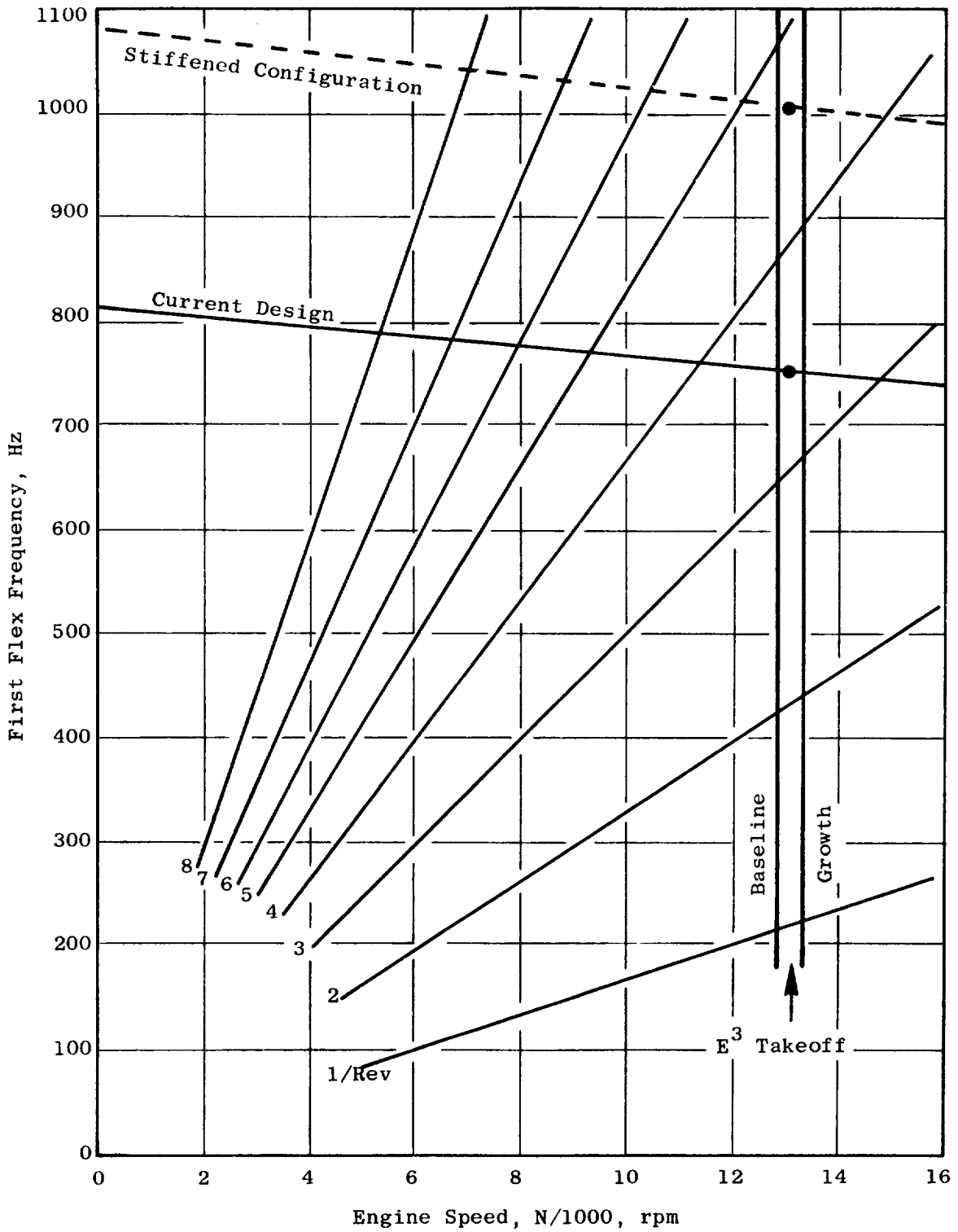


Figure 60. Fuel Nozzle Campbell Diagram.

6.0 COMBUSTOR SUBCOMPONENT DEVELOPMENT TESTING

PREFACE

This section describes the subcomponent test programs that were used to assist in the development of the E³ combustor system. Subcomponent testing was used to verify analytical aerodynamic designs for the combustor diffuser system and the combustor dome. Performance development was then continued in annular sector test vehicles in parallel to and in advance of the full-annular combustor development program to ensure that performance goals were attainable and to quickly solve annular performance problems relating to aerodynamics, thermodynamic performance, and emissions.

Use of subcomponent testing for these purposes greatly facilitates the overall development of the full-annular combustor, and provides an inexpensive and rapid means for problem solving during the development cycle. In addition, hardware changes can be evaluated separately from the annular effort to provide necessary alternative approaches for changes in design philosophy or engine system modifications.

6.1 COMBUSTION SYSTEM DIFFUSER TEST

6.1.1 Introduction

The purpose of this test program was to develop and characterize the aerodynamic performance of the Energy Efficient Engine (E³) combustor inlet diffuser (as a supporting effort to the E³ combustor development program). This diffuser is an advanced, short-length design that is closely integrated with the low emissions double-annular E³ combustor system. For this program, a full-scale annular model of the E³ diffuser was built and tested at the General Electric Corporate Research and Development Center (CRDC) in Schenectady, New York. This model was constructed of wood and aluminum and was designed to accurately duplicate the E³ diffuser flow passages from the compressor outlet guide vanes (OGV's) to the five coaxial combustor annular flow passages downstream of the combustor dome region. A metering plate at the exit end of the model was used to independently vary the flow in each passage.

Static pressure recovery characteristics and total pressure loss coefficients were measured for a wide range of flow splits in each of the five flow passages. These measurements were made for three different inlet velocity profiles with the final modified version of the E³ flowpath contours.

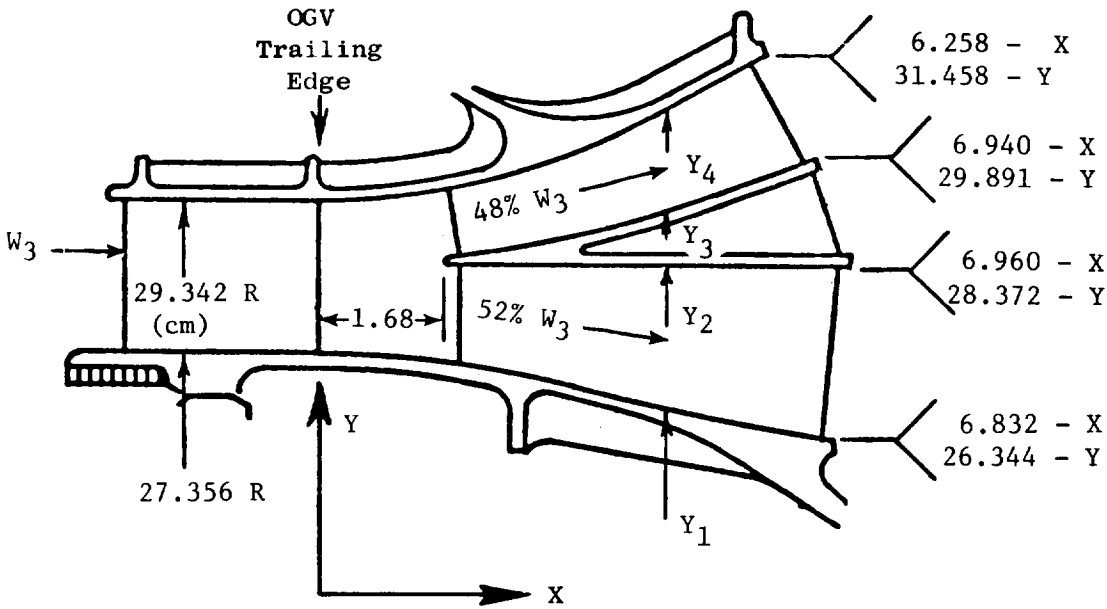
Diagnostic tests with a two-dimensional water table were conducted earlier in the test program and revealed excessive flow spillage from the combustor dome cowlings with the original flowpath contours. Several cowling contours were tested on the water table, and a design was selected for the airflow model that had significantly reduced flow spillage from the dome region.

Test results for the final version of this diffuser design show that the pressure losses in the outer flow passage are about 0.5% higher than expected. Pressure losses in the remaining four passages are nearly the same or somewhat less than anticipated. The test results also show that all of the individual passage static pressure recovery characteristic curves have negative slopes at the design flow conditions, which indicates that this diffuser design has a high degree of flow stability. High turbulence levels generated by the inlet velocity profilers for the peaked-out and peaked-in profiles resulted in significantly lower diffuser pressure losses when tested with these profilers.

6.1.2 Design Features

An advanced, short-length, low-emissions, double-annular combustion system was selected for the NASA/GE Energy Efficient Engine. This combustion system design has many new technology features, including a high performance, split-duct inlet diffuser. The design configuration was selected to achieve a short-length prediffuser, positive flow direction to the combustor domes, reduced air temperature extraction for turbine rotor cooling, and low pressure losses.

As illustrated in Figure 61, the E³ combustor inlet diffuser accepts core engine airflow from the compressor OGV's and divides this flow into two parallel prediffuser passages. The outer passage curves outward and directs



X	Y ₁	Y ₂	Y ₃	Y ₄
0	27.356	-	-	29.342
0.508	27.347	-	-	29.356
1.016	27.319	-	-	29.398
1.524	27.272	-	-	29.468
1.676	27.255	28.430	28.430	29.494
1.778	27.242	28.372	28.504	29.514
2.032	27.207	↓	28.536	29.557
2.540	27.123	↓	28.613	29.696
3.048	27.019	↓	29.708	29.856
3.556	26.906	↓	28.820	30.049
4.064	26.799	↓	28.952	30.278
4.572	26.700	↓	29.102	30.542
5.080	26.608	↓	29.269	30.818
5.588	26.523	↓	29.439	31.094
6.084	26.446	↓	29.605	31.363
6.096	26.445	↓	29.609	-
6.604	26.374	↓	29.779	-
6.613	26.373	↓	29.782	-
6.832	26.344	↓	-	-
6.960	-	28.372	-	-

Figure 61. E³ Prediffuser Wall Contours.

about 48% of the airflow toward the outer dome annulus of the combustor. The inner passage directs the remaining 52% of the airflow toward the inner dome annulus of the combustor. Each of these two passages has a diffusion area ratio of 1.8.

Flow leaving this short prediffuser is dumped into the combustor liner passages and into the plenum region upstream of the combustor domes. The dumping area ratio in the liner passages is 2.5. The resulting dumping pressure loss is small because the compressor exit velocity head is reduced from 5.8% of the total pressure at takeoff conditions to 1.7% by the prediffuser. Nearly all of the prediffuser exit velocity head is recovered in a "free stream" diffusion region entering each of the plenums ahead of the two combustor domes. With this configuration, total pressure losses from the compressor OGV's to the combustor domes are very small.

A short, constant-area section is provided in the diffuser passage immediately downstream of the OGV's to permit the wakes from the OGV's to mix and decay before the flow is diffused. Downstream of this section, the outer and inner walls of the prediffuser begin to diverge and a single-annular splitter vane is positioned in the passage to divide the prediffuser into two parallel annular passages. The splitter contours, along with the outer and inner wall surfaces of the prediffuser, are designed to provide the desired rate of diffusion through these passages. Each passage is designed to fall below the line of no appreciable stall on the Stanford diffuser flow-regime correlation (Reference 5). The splitter vane reduces the length required for the prediffuser and also directs the airflow leaving the prediffuser into the combustor dome regions.

A compressible, axisymmetric potential flow computer program (CAFD) was used to analyze several configurations for the E³ prediffuser contours. A streamline plot of the final selected version is presented in Figure 62. The CAFD Program accounts for the flow blockage of the support struts by introducing a distributed blockage as a function of radial position at each axial station. Velocity distributions on the outer and inner prediffuser wall surfaces from the CAFD analysis are presented in Figure 63. These wall velocity distributions show the effects of the prediffuser wall curvature and the

ORIGINAL PAGE IS
OF POOR QUALITY

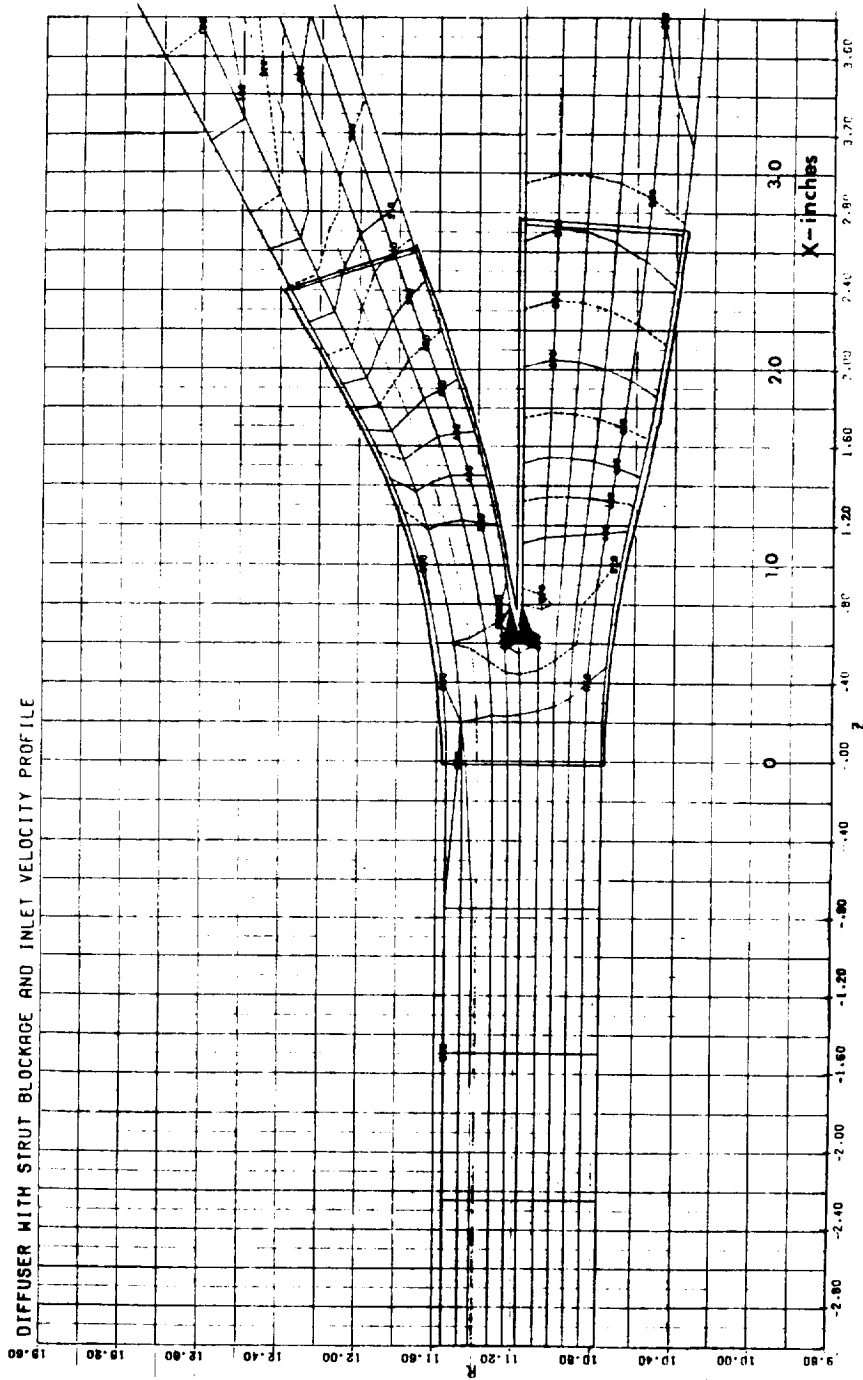


Figure 62. Inlet Diffuser CFD Analysis.

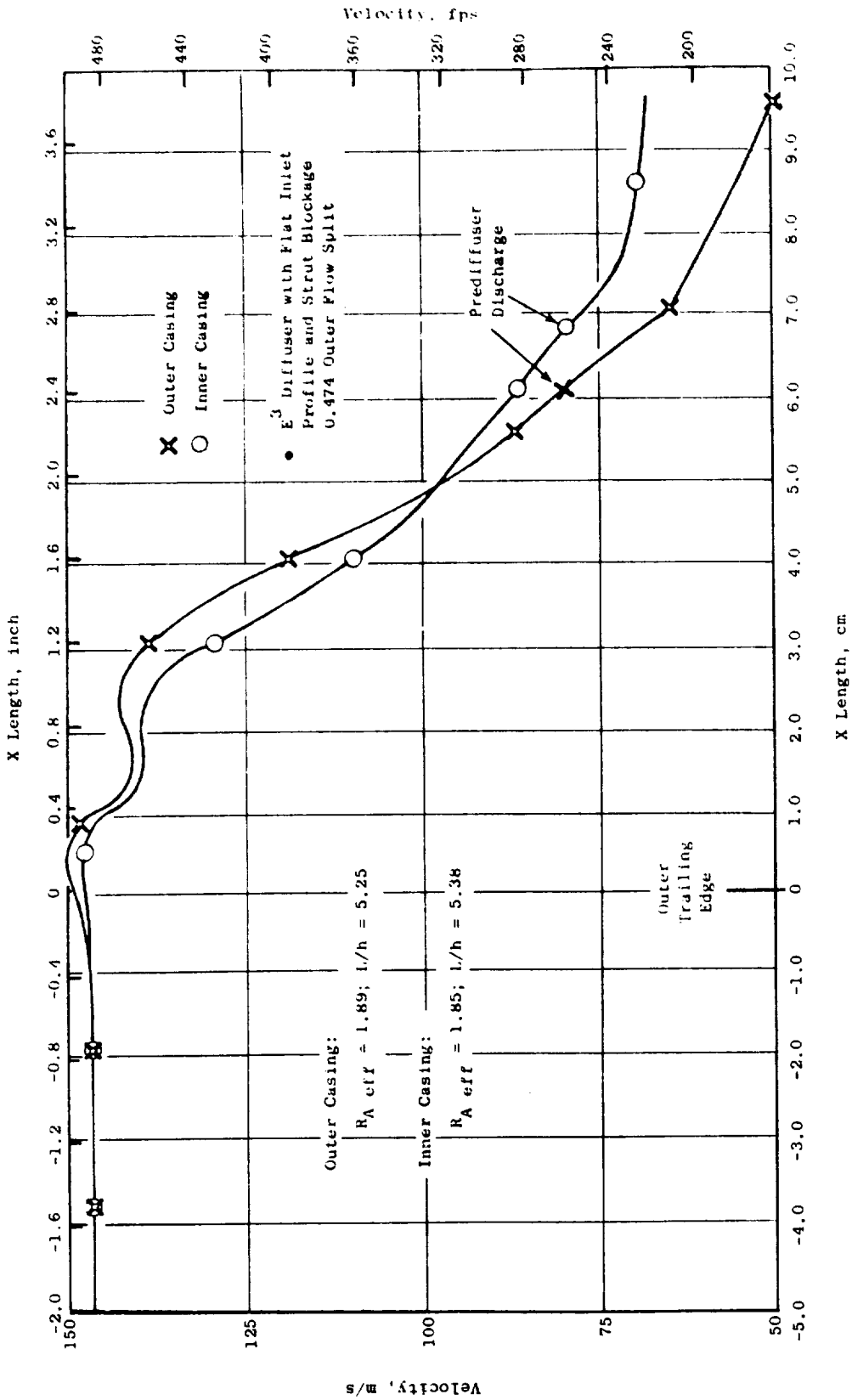


Figure 63. Inlet Diffuser Wall Velocities.

effects of the splitter vane and support strut blockages. The effective area ratio and length-to-inlet-height ratio of equivalent straight diffusers were determined directly from these velocity distributions and plotted on the Stanford diffuser flow regime correlations (Figure 64). The design level values for the equivalent straight diffusers fall below the line of no appreciable stall on the Stanford correlations.

As a result of this analysis, the selected E³ diffuser design can be expected to have stable flow patterns with no regions of flow separation for a broad range of engine operating conditions.

Bleed airflow for turbine rotor cooling (about 6% of the total flow) is supplied through holes in the base region of the splitter vane. This airflow enters the hollow splitter vane structure, which serves as a plenum chamber for this flow, and passes through the 30 splitter vane support struts to the inner cavity of the engine to the first-stage turbine rotor. This bleed-flow arrangement provides the turbine with cooling air that is taken from the center of the compressor exit flow. Such core flow is considerably cooler than the flow near the casing walls of the compressor. Also, bleed flow from the base region of the splitter vane helps to stabilize the flow pattern in the dumping region downstream of the prediffuser.

6.1.3 Design Goals

The purpose of the combustor diffuser system is to deliver the high velocity airflow supplied by the compressor to the combustor and cooling flow to the turbine nozzle vanes with the smallest possible pressure loss.

The overall pressure loss goal for the E³ combustion system is 5% of the inlet total pressure to the combustor and is measured from the OGV exit to the Stage 1 turbine nozzle inlet. This overall pressure loss is distributed throughout the combustion system.

A portion of the pressure loss is attributed to the prediffuser and the dumping loss due to the sudden expansion of the airflow streams as they discharge from the prediffuser. The remaining pressure loss is associated with

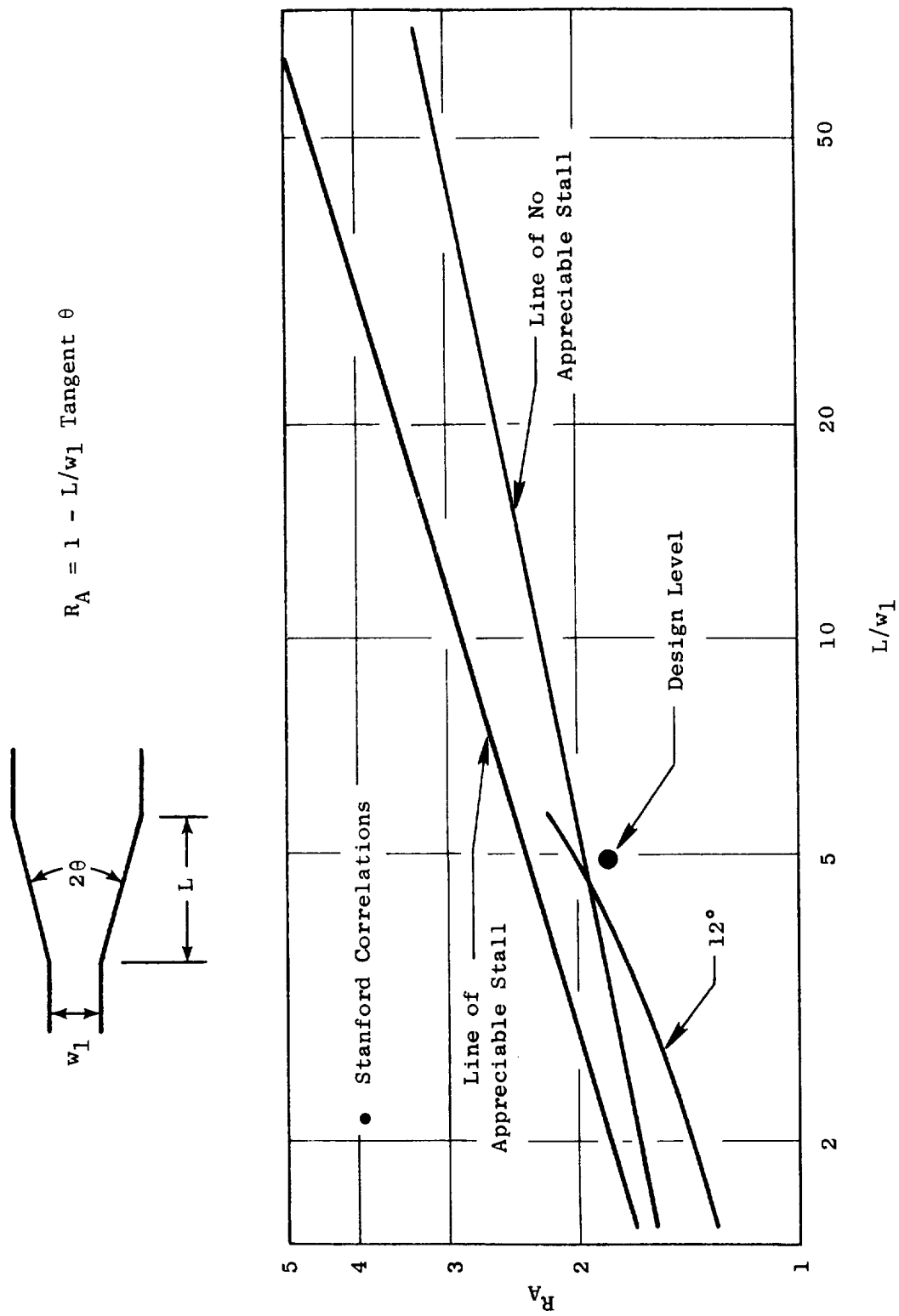


Figure 64. Split Duct Diffuser Flow Regimes.

the pressure drop required to flow the airflow through the fixed orifices of the combustor surfaces. The sum of these pressure losses when mass weighted for the airflow in each of the combustor passages comprises the overall combustion system pressure loss. Therefore, low diffuser pressure losses are important to provide the maximum available pressure loss to the combustor passages. The available pressure energy is a key parameter with respect to combustor and turbine performance. Therefore, keeping the losses in available pressure energy small is necessary to provide the desired combustor fuel-air mixing and gas temperature dilution to obtain the required combustor exit temperature distribution into the turbine. In addition, adequate pressure must be maintained in the passages which supply cooling air to the turbine nozzle to prevent hot combustion gases from being ingested into the turbine nozzle cooling circuits. This minimum level of pressure drop required is referred to as the turbine nozzle backflow margin. The goals for the diffuser system are shown in Table XVI in terms of pressure loss relative to the total pressure at the diffuser system inlet.

Table XVI. Diffuser Pressure Loss Goals.

	<u>Outer Passage</u>	<u>Outer Dome</u>	<u>Center Passage</u>	<u>Inner Dome</u>	<u>Inner Passage</u>	<u>Mass-Weighted Average</u>
Prediffuser $\Delta P/P$	1.1	-	-	-	1.1	-
Overall $\Delta P/P$	2.49	0.75	2.95	0.75	2.16	1.5
Turbine Backflow $\Delta P/P$	2.00	-	-	-	2.00	-

6.1.4 Water-Table Model Tests

Preliminary diagnostic tests were conducted early in the program on a two-dimensional model of the diffuser using a water table. The test configuration was a three-times scale model of the full-annular configuration which simulated all of the key system features including prediffuser strut blockage

and turbine cooling airflow extraction. The purpose of these tests was to identify any locations within the diffuser passages where regions of flow separation or instability might exist. These tests were conducted at very low Reynolds numbers compared to the engine. Therefore, the water table tests were used to obtain early diagnostic information as opposed to performance data.

The two-dimensional model of the E³ combustor passages tested on the water table is shown in Figure 65. The flow behavior around the cowl of the outer dome shows flow spillage from the dome region and flow entering the outer dome, center, and inner dome passages as visualized with dye injections and shown in Figure 66. The flow split in each of the channels was simulated by adjusting holes in a perforated plate that was inserted at the discharge of the channel. The flow rate in each channel was measured by observing the rate of movement of the injected dye with a stopwatch. The bleed flow was simulated with a plastic suction tube inserted into the hollow splitter vane. The total circulated flow was 120.7 l/min (31.9 gpm) and the bleed flow was 7.2 l/min (1.92 gpm) or 6% of the total flow.

For the initial test series on the water table, there was no evidence of flow separation or flow instability. However, considerable flow spillage from the combustor dome regions around the cowling leading edges was observed. Subsequent tests of the full-annular airflow model of the diffuser with the original cowling design indicated lower than expected static pressure recoveries in the outer and inner liner passages which were probably caused by the flow spillage from the cowlings. Therefore, modified versions of the cowling leading edges were tested on the water table. The outer and inner cowlings were extended to reduce the capture area of the openings. These modifications were made in two stages as illustrated in Figure 67. On the water table, the Mod I design eliminated the cowling flow spillage. Consequently, the airflow model cowling contours were changed to the Mod I design and all of the following airflow testing was conducted with this design.

6.1.5 Annular Model Airflow Tests

The test facility used for airflow testing is located in the Gas Dynamics Building at the K-1 site of the GE/CRDC. The air supply for this facility

ORIGINAL PAGE IS
OF POOR QUALITY

ORIGINAL PAGE
BLACK AND WHITE PHOTOGRAPH



Figure 65. Diffuser Water Table Model.

ORIGINAL PAGE IS
OF POOR QUALITY



Figure 66. Water Table Model Test.

ORIGINAL PAGE
BLACK AND WHITE PHOTOGRAPH

ORIGINAL PAGE IS
OF POOR QUALITY.

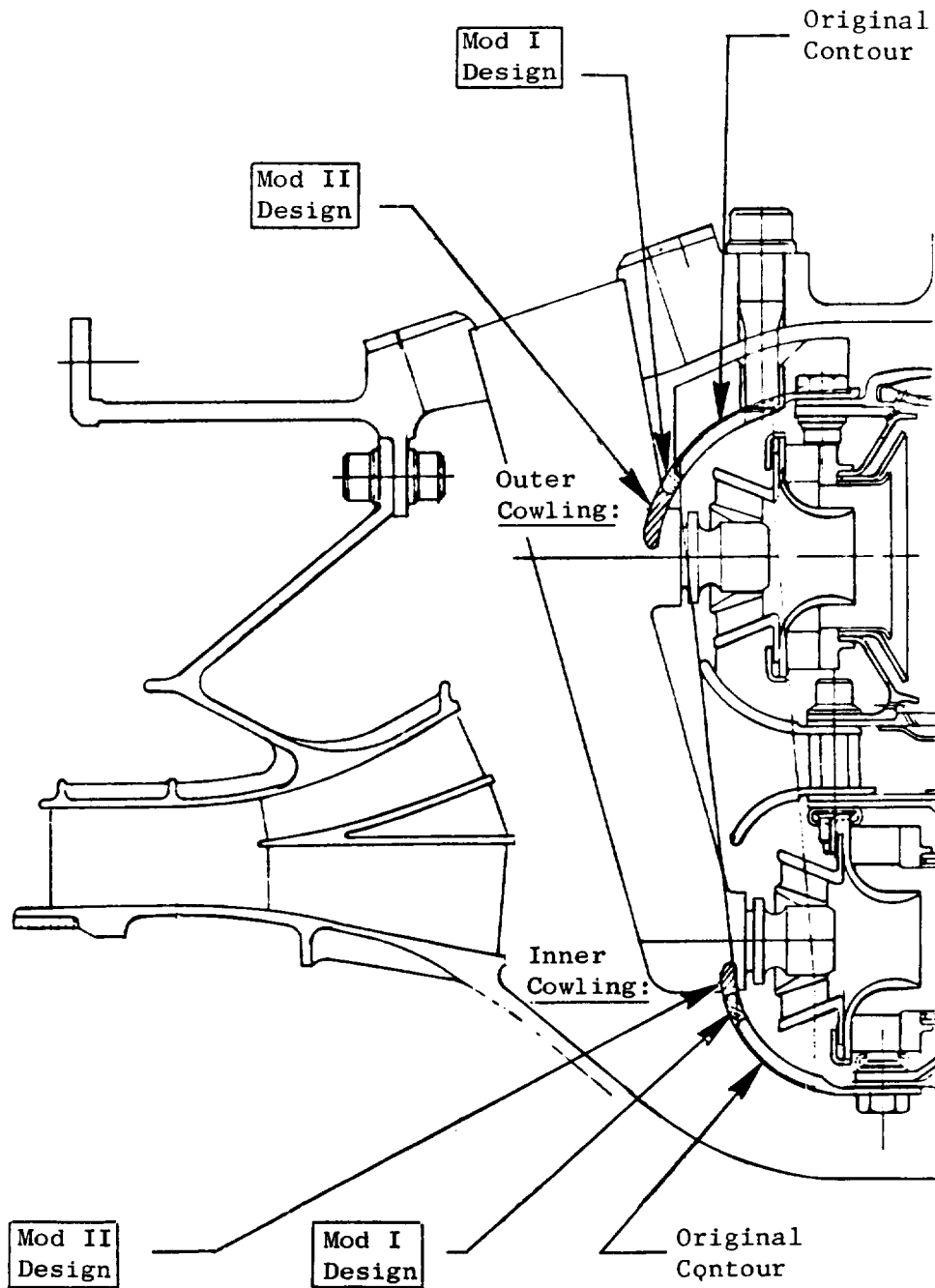


Figure 67. Combustor Cowling Modifications.

consists of four Fuller rotary vane-type air compressors. From the compressors, the air is ducted by means of 30.5-cm (12-in.) piping to a 116.8 cm (46-in.) diameter plenum chamber to which the model was attached. This chamber is equipped with screens and honeycomb to provide smooth, uniform flow to the model. The piping between the compressors and the plenum chamber is equipped with a metering section in which various-sized sharp-edge orifices can be installed. This facility is capable of delivering approximately 5.23 kg/sec (11.5 lb/sec) of air at pressures up to 0.13 MPa (4.0 psi). At reduced flow rates, higher pressures are available.

For this test program, pressure measurements were made using a Scanivalve system and data logger. By automatic stepping of the Scanivalve pressure switches, the pressure from the various taps on the model were ducted to a single pressure transducer. The output of the transducer was fed to a digital voltmeter. At steady-state conditions the data logger was automatically triggered. The output of the data logger was transmitted to a teletype readout and punched on paper tape. The paper tape was then fed to a computer for data reduction.

The E³ model assembled on its test pedestal is shown in Figure 68 and component sections of the model are shown in Figures 69 and 70.

Figure 69 shows the prediffuser discharge and strut assembly; Figure 70 shows the fuel nozzles, the combustion chamber outer passage, outer dome, center passage, inner dome, and the inner passage throttling plate with its perforated holes. This throttle plate provides the flexibility to independently vary the flow in each passage and thus determine the performance of each passage as a function of airflow quantity.

A total of 132 static pressure taps were installed in the model. The location of these taps is shown in Figure 71, and the exact axial and circumferential positions are shown in Appendix A. The pressure tap located on the inner and outer surfaces of each of the passages was used to determine the static pressure recovery of each passage. The pressure taps located at the exit of each passage, when used in conjunction with the pressure taps located on the downstream side of the throttling plate, were used to determine passage airflow splits.

ORIGINAL PAGE IS
OF POOR QUALITY

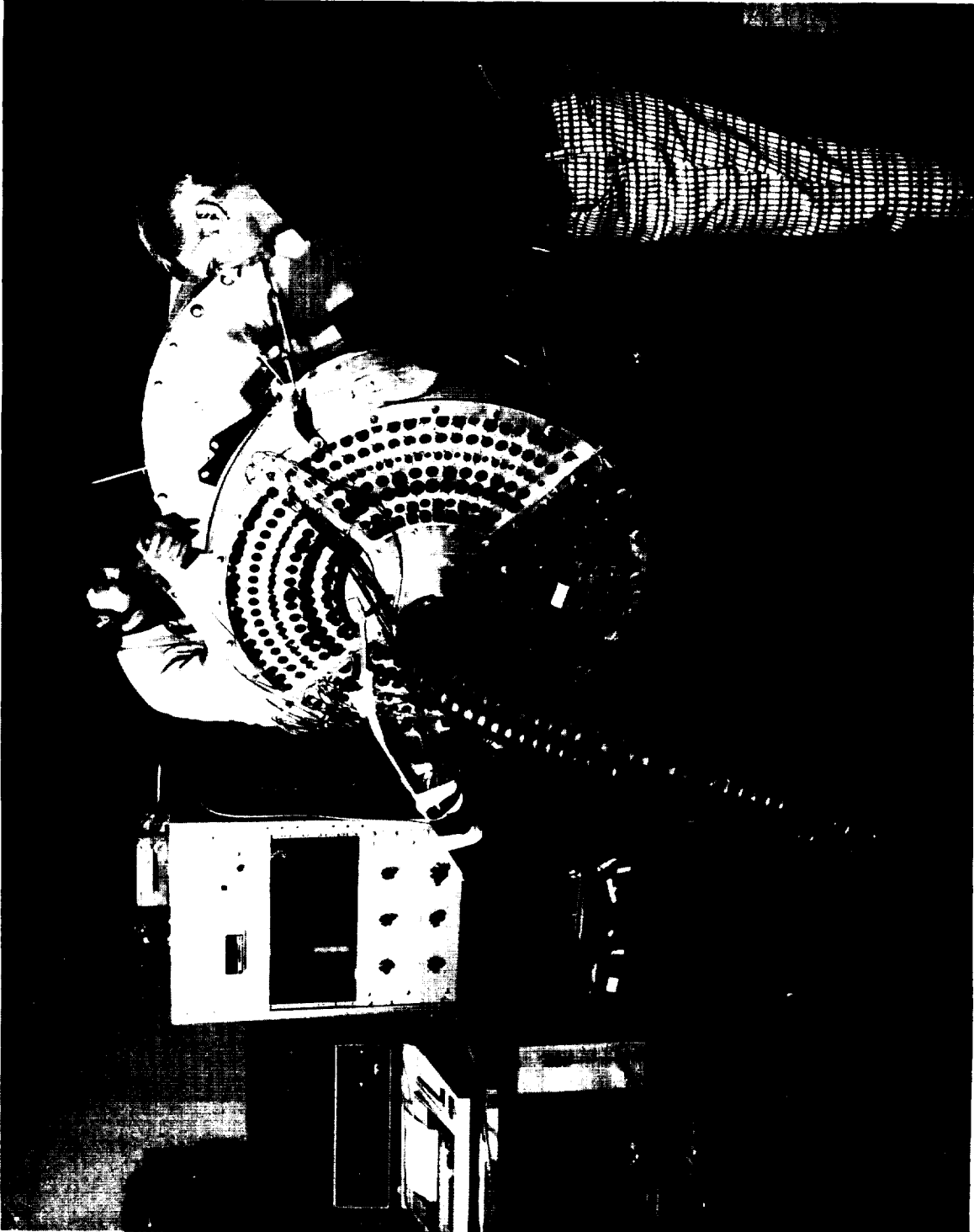
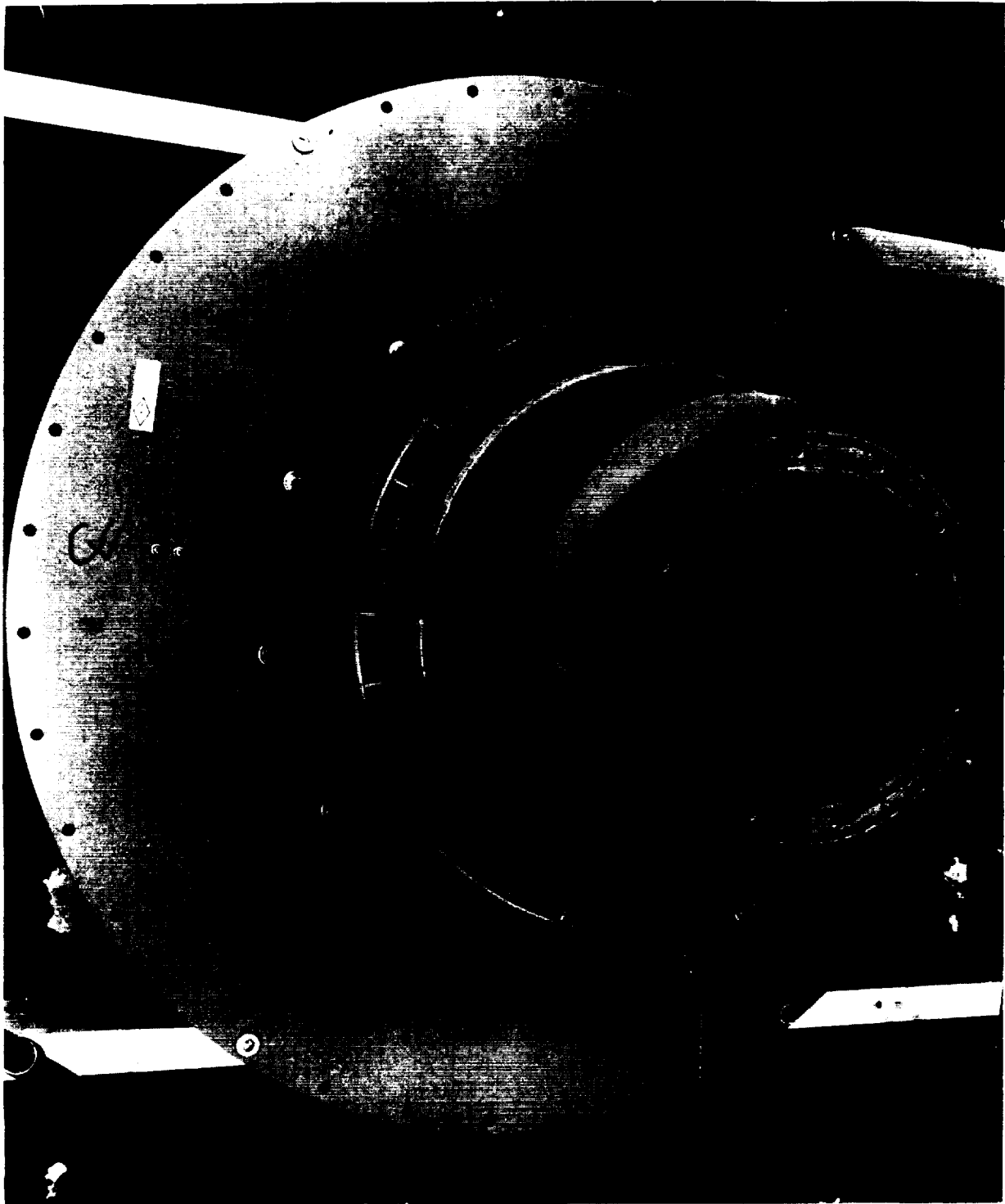


Figure 68. E^3 Annular Diffuser Model.

ORIGINAL PAGE
BLACK AND WHITE PHOTOGRAPH



ORIGINAL PAGE
BLACK AND WHITE PHOTOGRAPH

Figure 69. E^3 Annular Diffuser Model.

ORIGINAL PAGE IS
OF POOR QUALITY



Figure 70. E^3 Annular Diffuser Model.

ORIGINAL PAGE
BLACK AND WHITE PHOTOGRAPH

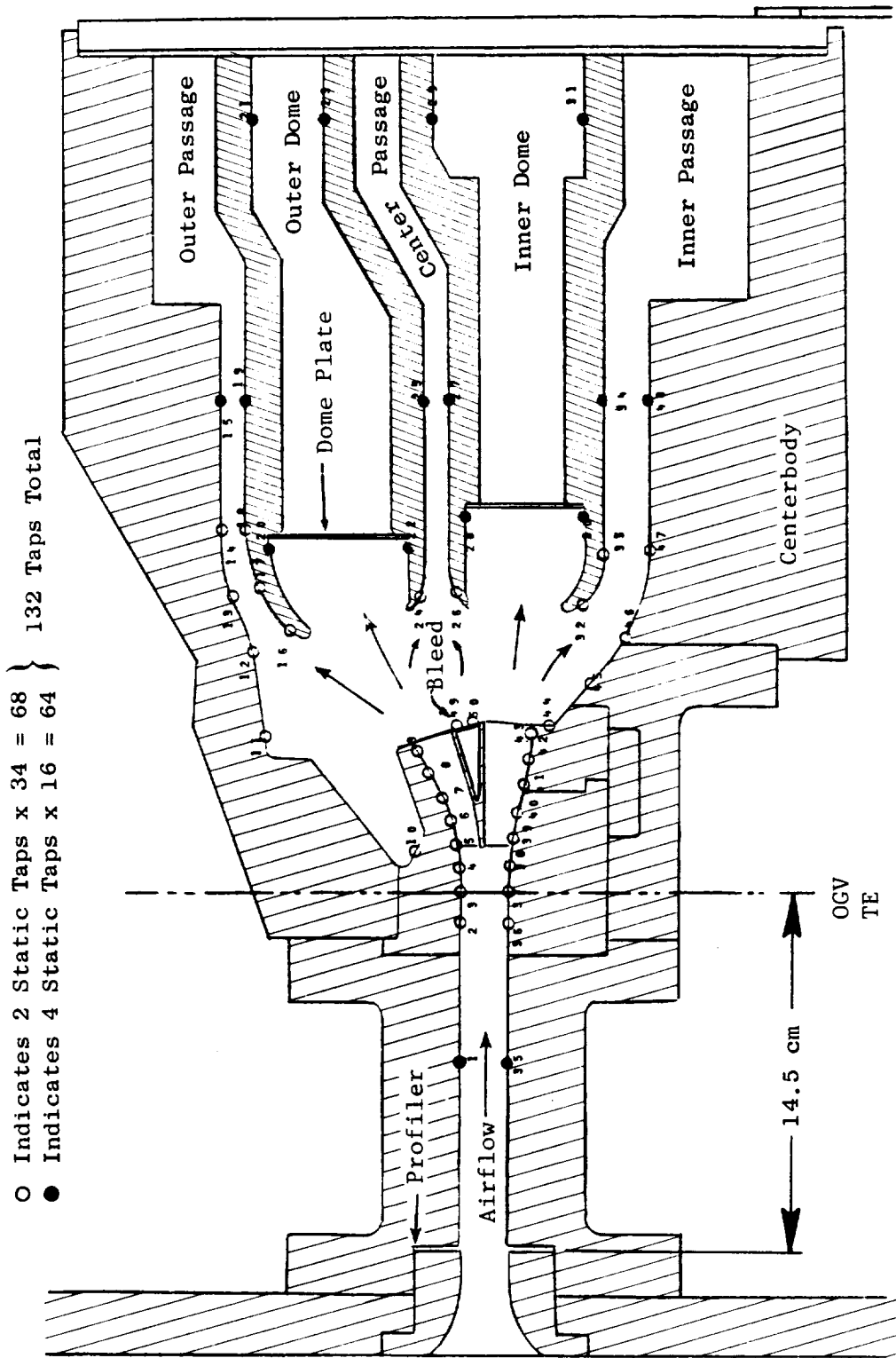


Figure 71. Annular Diffuser Model Instrumentation Layout.

ORIGINAL PAGE IS
 OF POOR QUALITY

Kiel probes and hot film probes were employed to obtain the velocity profiles at the diffuser inlet plane and at the prediffuser discharge. The Kiel probe is a specially designed probe similar to that shown in Figure 72. This probe accurately measures the total pressure with minimum interference effects due to probe structure. The local velocity was calculated based on the measured total pressure and a measured wall static pressure. For the diffuser inlet profiler, a Kiel probe radial traverse was made at four equally spaced circumferential locations. The Kiel probe was traversed at nine radial stations to describe the radial velocity profile at these four circumferential locations. The hot film probe provides an indication of velocity directly based on calibration of the hot wire. The hot wire is less sensitive to flow direction than the Kiel probe, since it operates on an electrical resistance principle and essentially measures absolute velocity. However, it is sensitive to contamination from foreign substances which might be entrained in the air. Therefore, it was used only for the prediffuser discharge where measurement normal to the airflow would be difficult.

A series of calibration runs was made to calibrate each of the five passage exits to determine the variation of airflow with pressure drop across the orifice plate for several discharge orifice plate openings as represented by the different corking arrangements (that is, number of exit holes corked). The procedure used to perform these calibrations was to seal off four passage exits while calibrating the fifth. For each exit orifice plate flow area, a discharge coefficient was computed as a function of airflow rate. These discharge coefficients were then plotted on a curve fit of the form

$$C_D = \alpha_1 \sqrt{\Delta P} + \alpha_0$$

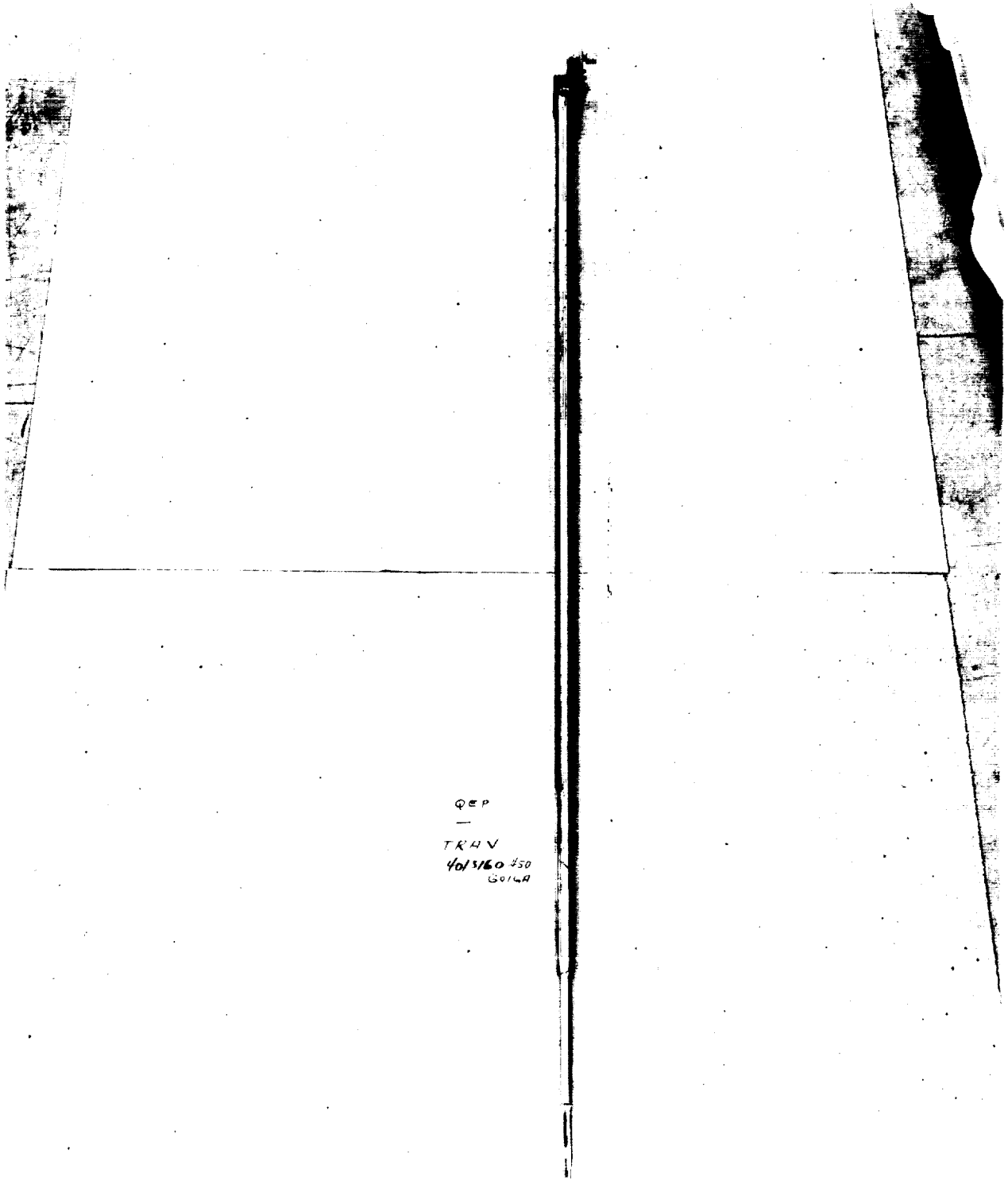
was obtained, where

C_D is discharge coefficient

ΔP is pressure drop across orifice plate

α_1, α_0 are coefficients which best correlated the data.

ORIGINAL PAGE IS
OF POOR QUALITY



ORIGINAL PAGE
BLACK AND WHITE PHOTOGRAPH

Figure 72. Keil Pressure Probe.

Finally, the coefficients, α_1 and α_0 were plotted as a function of flow area and were fitted by a least-squares polynomial curve fit. This procedure was followed for each of the five passages. The values obtained are shown below.

	<u>Outer Liner</u>	<u>Outer Dome</u>	<u>Centerbody</u>	<u>Inner Dome</u>	<u>Inner Liner</u>
α_0	0.0136	0.0176	0.00523	0.0208	0.0137
α_1	-0.0007	-0.000112	-0.0000485	-0.00015	-0.00006

The static pressure recovery of each of the five passages was based on the differential pressure between the average of the inner and outer surface of each of the passages and the prediffuser upstream static pressure. The flow split in the five passages was evaluated from the static pressure instrumentation located at each of the passage discharge stations and static pressure taps located just downstream of the orifice plate.

The pressure data recorded during the test of the E³ model was fed into a computerized data reduction program to obtain the performance characteristics. The computed performance characteristics fall into a number of basic categories as discussed below.

Based on the measured airflow to the model and the average inlet pressure, the average inlet velocity and Reynolds number were calculated. The Reynolds number was based on the hydraulic diameter of the passage; that is, two annular passage heights. The amount of bleed flow was calculated from the air temperature and the measured pressures upstream and downstream of the 10.2 cm (4.0 in.) bleed-flow orifice.

Flow split runs were made for each of the five passages of the E³ combustor diffuser mode. The nominal flow splits selected for evaluation in the tests were evolved during the preliminary design phase of the combustor. These flow splits were selected based on design considerations including emissions,

performance, and flowpath requirements. The design percentage flow split level for each passage is shown below:

Outer Channel	16.2% W_3
Outer Dome	24.4% W_3
Center Dome	9.15% W_3
Inner Dome	29.18% W_3
Inner Channel	15.25% W_3
Bleed Flow	5.82% W_3

The flow split level percentage was first obtained by varying the number of corks in the discharge orifice plate of each passage. The off-nominal flow setting of the outer channel was then varied while the flow areas at the discharge orifice plate of the other four channels were held fixed. This procedure was followed to obtain four off-nominal flow settings for the outer passage. In a similar manner, off-nominal settings for the other four passages were made. The sum of the five passage flows was added to the bleed flow, and the total airflow was then compared to that measured with the airflow supply upstream orifice plate to give an indication of the accuracy of the results. The airflow error for each test generally ranged from 2% to 3%.

One measure of the performance of the diffuser is provided by the surface static pressure coefficient distribution within the diffuser. This coefficient was determined for all pertinent wall static measurements and was defined as:

$$C_{PW} = \frac{P - P_{s_{inlet}}}{(1/2)\rho\bar{V}_{inlet}^2} = \frac{P - P_{s_{inlet}}}{\bar{q}_{inlet}}$$

where $P_{s_{inlet}}$ is the average of the inlet static pressures, P is the measured wall static pressure, and \bar{q} is the dynamic head based on the area-averaged inlet velocity.

An important measure of the performance of a diffuser passage is the degree of passage static pressure recovery. For this purpose, a passage static pressure recovery coefficient, C_{pp} was defined by using the same expression as used for the wall static pressure recovery:

$$C_{pp} = \frac{P - P_{s_{inlet}}}{(1/2)\rho\bar{v}_{inlet}^2} = \frac{P - P_s}{\bar{q}_{inlet}}$$

where in this definition P is the average of the static pressures measured at the point in the passage where the recovery is to be determined.

A measurement of the performance of the complete combustor-diffuser is given by the mean total pressure loss coefficient, C_{p_T} , defined as follows:

$$\begin{aligned} C_{p_T} &= \frac{P_{T_{inlet}} - P_T}{\bar{q}_{inlet}} = \bar{\omega} \\ &= \frac{\left(P_{T_{inlet}} - P_{s_{inlet}} \right) - \left(P_s - P_{s_{inlet}} \right) - \left(P_T - P_s \right)}{\bar{q}_{inlet}} \\ &= \left(1 - C_p \right) - \frac{q}{\bar{q}_{inlet}} \end{aligned}$$

where P_T and P_s are the total and static pressures, respectively, in the passage where the pressure recovery was determined, q is the dynamic pressure at the same point, and C_p is the static pressure recovery.

Since there are five passages (outer passages, outer dome, center passage, inner dome, and inner passage), the mean total pressure loss coefficient was calculated using the mass weighted average

$$C_{P_{Tmean}} = \frac{\sum_{n=1}^5 W_n C_{P_{Tn}}}{\sum_{n=1}^5 W_n}$$

where W_n is the flow rate in passage n and C_{P_T} is the corresponding total pressure loss coefficient.

The full annular airflow tests were conducted with three different inlet velocity profiles. These inlet velocity profiles were generated by profilers installed in the inlet passage. Schematics of the profilers used are shown in Figure 73. The velocity profiles (Figure 74) had peak velocities near the outer wall, in the center, and near the inner wall of the inlet section of the diffuser. Velocity profiles at the E³ engine compressor exit station are expected to be similar to the center peaked profile.

During initial testing of the diffuser model, some very unexpected and disappointing results were obtained for the measured inlet velocity profiles and the diffuser performance. A posttest inspection of the diffuser model revealed a separation of the 30 struts from the outer flowpath (pilot stage) of the diffuser model. Further investigation revealed the source of the strut failure and unexpected poor diffuser performance levels. The airloading on the test rig centerbody was of sufficient magnitude to deform the inlet plenum support struts and permit the test rig centerbody to move aft approximately 0.25 cm (0.10 in.). Not only did this result in prediffuser strut failure at the wall, it also resulted in an off-design prediffuser area ratio. The diffuser model was repaired and a method to strengthen the test rig to prevent deflection of the inlet struts and retain the axial location of the centerbody was incorporated. Testing with the refurbished diffuser model and reinforced test rig was then resumed.

Static pressure recovery levels in each of the five E³ diffuser passages are presented in Figure 75 as a function of the flow level in the passage with the center peaked inlet velocity profile. Recovery levels with

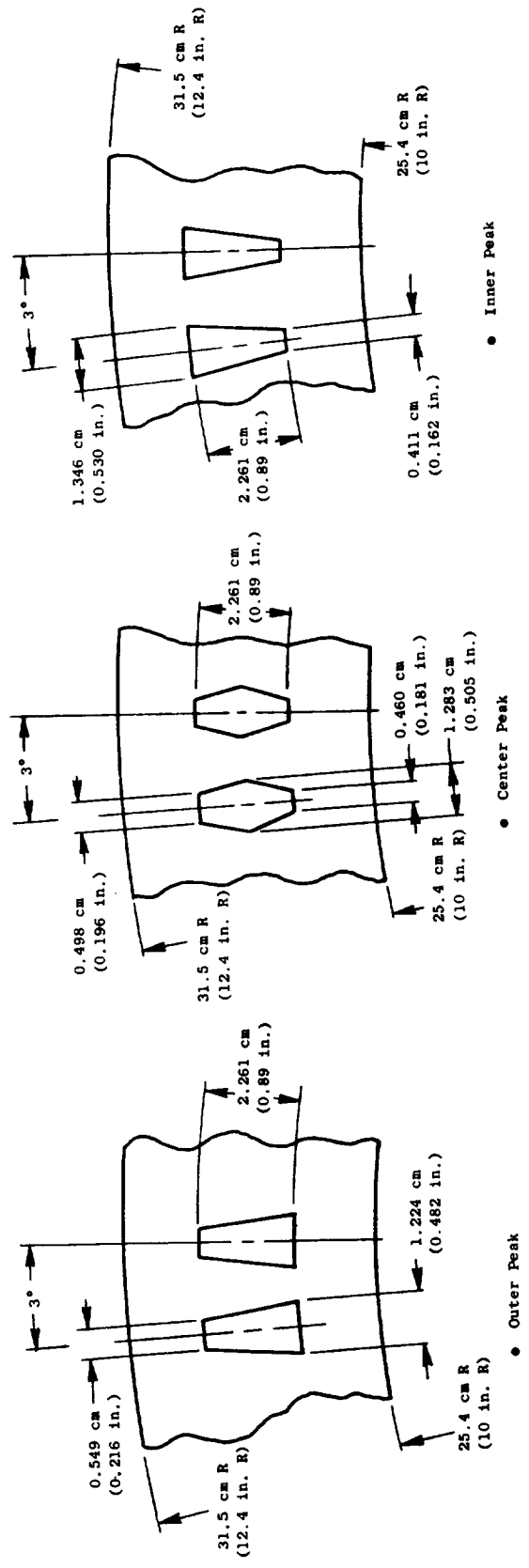


Figure 73. Schematics of Diffuser Inlet Profilers for Model.

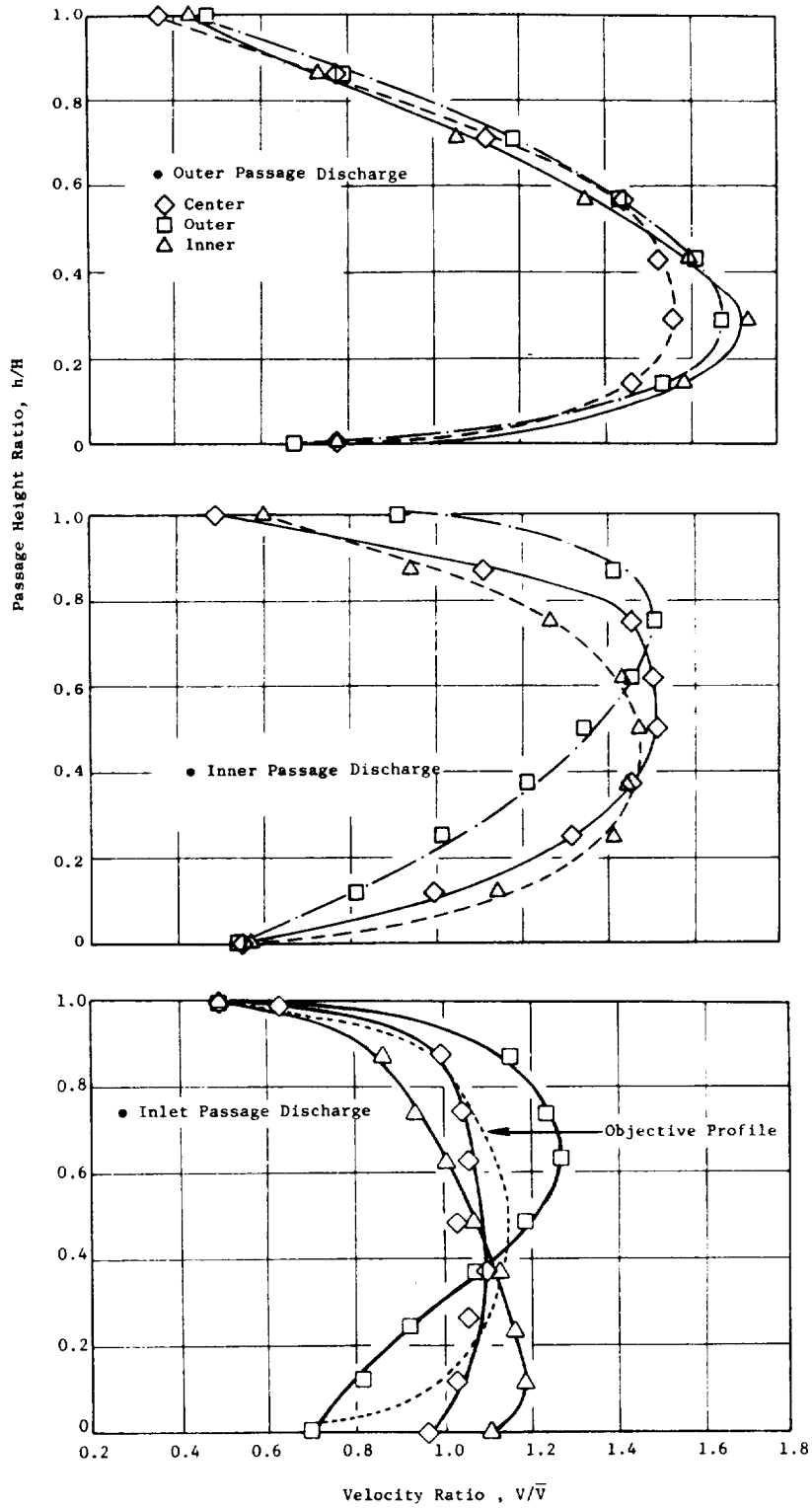


Figure 74. Diffuser Inlet Velocity Profiles.

the outer peaked inlet velocity profile are presented in Figure 76, and recovery levels with the inner peaked inlet velocity profile are presented in Figure 77. Each of these sets of static pressure recovery curves represents a summary of all of the individual passage test runs. Static pressure recovery curves for each one of the individual passage test runs are included as Figures 1B through 15B in Appendix B.

As illustrated in Figure 75, for the center peaked profile, the static pressure recovery levels in all of the passages are unusually high at the design level flow conditions, although the outer passage recovery and the dome flow recoveries are not quite as high as anticipated. The dome recoveries were expected to be about 0.85 and the outer passage recovery was expected to be about 0.50. The inner passage recovery is very close to the expected value, and the center passage recovery is higher than the expected value. These results are similar to those of several previous diffuser test programs. The consistent results and the high recovery levels indicate that the flow in this diffuser is extremely stable and that the prediffuser does not have regions of flow separation.

With the outer peaked and inner peaked inlet velocity profiles, the recovery levels are higher than those with the center peaked profile. Recovery levels in the outer passage and outer dome region were considerably higher with the outer peaked profile, as anticipated. However, recovery levels were higher in the inner passage, the inner dome region, and in the center passage, also. With the inner peaked profile, recovery levels were much higher in the inner passage and inner dome region as may be expected, but they also were higher in the outer passage and in the center passage. The most probable reason for these high recovery levels is the high turbulence levels generated by the blockage elements of the inlet velocity profilers. Higher turbulence levels usually improve diffuser performance (References 6 and 7). The blockage elements of the outer and inner peaked profilers were larger than those for the center peaked profile and would generate larger scale turbulence.

All of the static pressure recovery curves have negative slopes at the design point flow conditions. This is an indication of a high degree of flow stability in the passages and low sensitivity to combustion system resonance effects.

● Center Peaked Profile

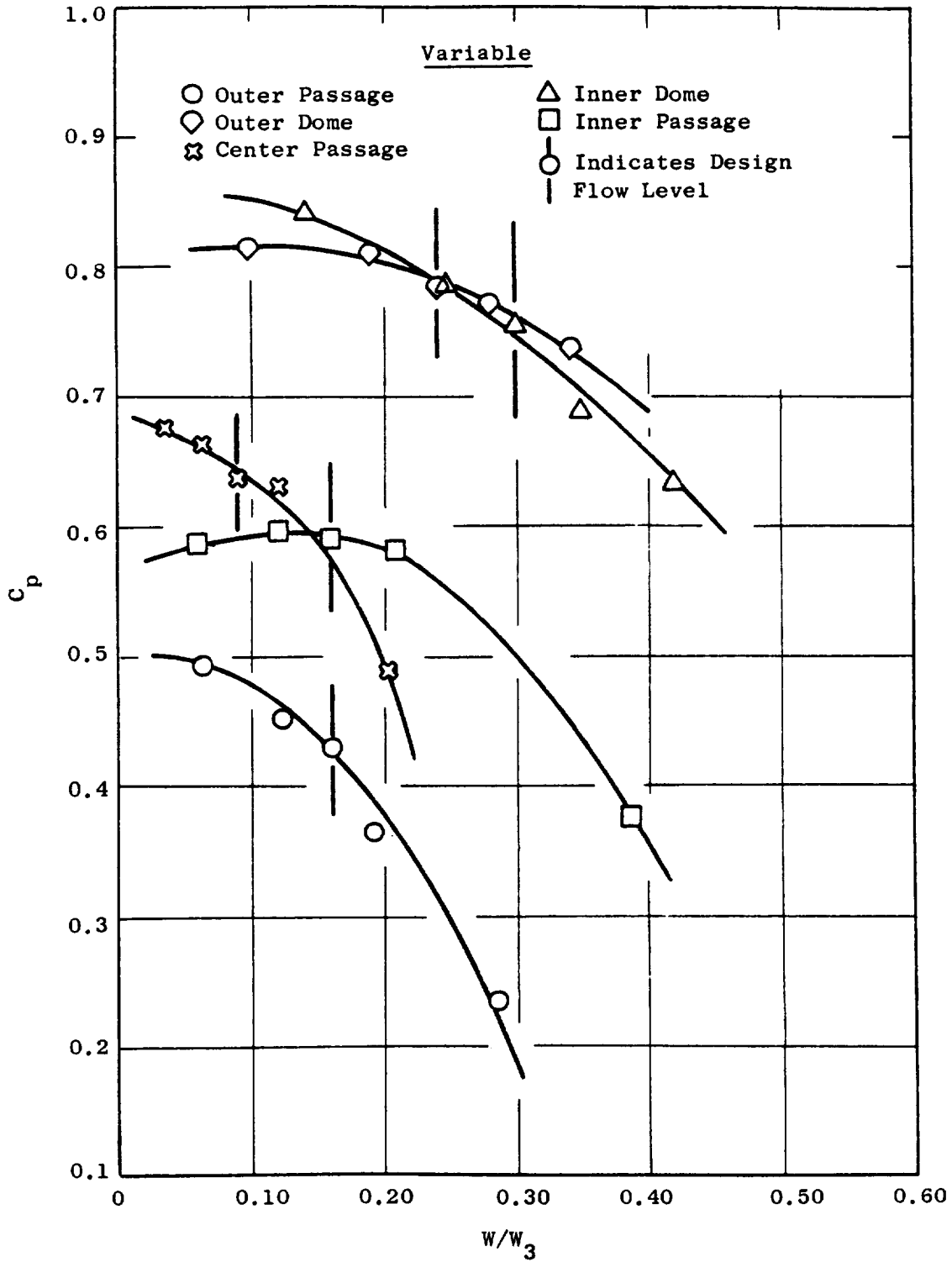


Figure 75. Static Pressure Recovery Levels.

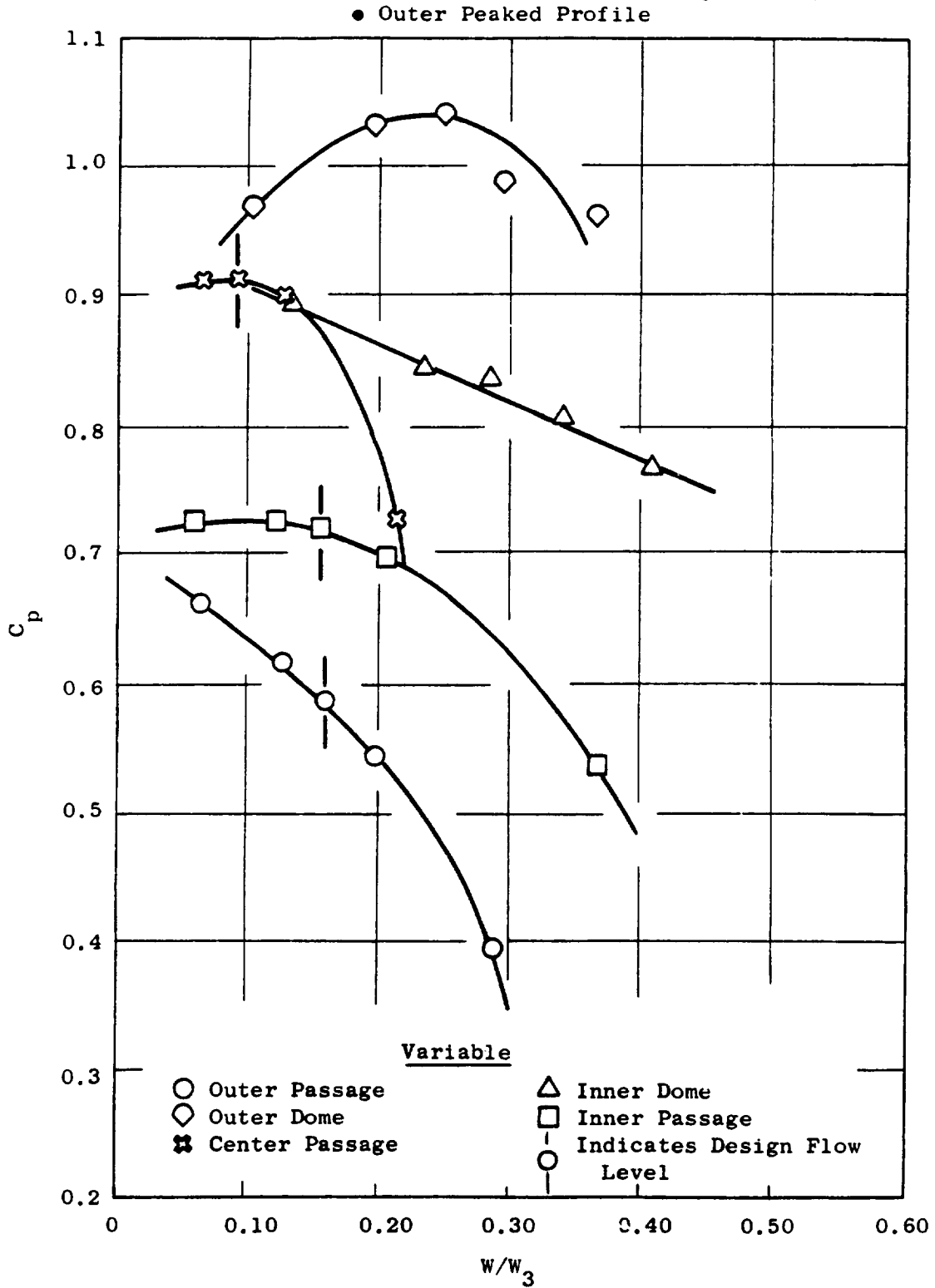


Figure 76. Static Pressure Recovery Levels.

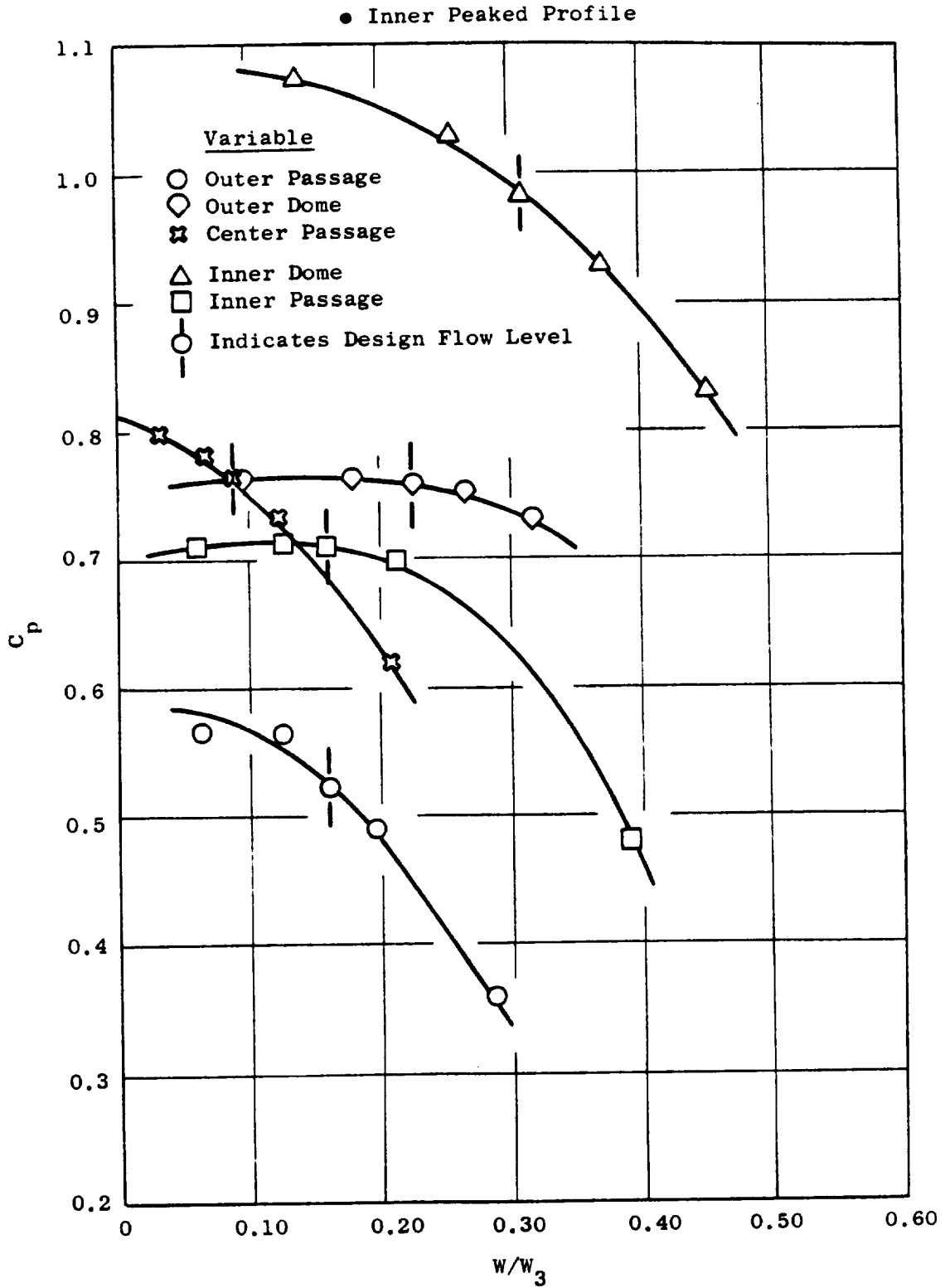


Figure 77. Static Pressure Recovery Levels.

Static pressure rise coefficients, measured with the pressure taps located along the outer and inner prediffuser and combustor casing walls, are presented in Figure 78 for design flow conditions with the center peaked inlet velocity profile. Similar curves for the outer peaked profile and for the inner peaked profile are presented in Figures 79 and 80, respectively. The initial reduction in static pressure, immediately downstream of the diffuser inlet, shows the effects of the diffuser wall curvature and the blockage of the strut and splitter vane leading edges. The static pressure increases strongly along the prediffuser walls to the end of the prediffuser. The pressure in the bluff base region of the splitter vane is somewhat higher than in the other base regions which may account for the higher-than-expected recovery levels in the center passage.

In the inner diffuser passage adjacent to the inner cowling, the static pressure continues to rise due to passage velocity profile mixing. In the outer passage, however, the static pressure drops sharply behind the fuel nozzle which is an indication of parasitic drag losses in this passage. The drag loss is probably caused by the fuel nozzle stems and the combustor mounting struts.

Total pressure loss coefficients for each of the five diffuser passages are presented in Figure 81 as a function of the flow levels in the passages. These curves are plotted for the center peaked velocity profile. The total pressure loss of any particular passage is the product of the total pressure loss coefficient for that passage and the diffuser inlet velocity head which, for the E³ engine at sea level static conditions, is 5.78% of the compressor exit total pressure.

These curves further show the effects of parasitic drag losses in the outer diffuser passage. In the inner passage, as flow is increased, the total pressure loss coefficient decreases because the effective dumping area ratio is reduced. But in the outer passage the pressure loss coefficient increases with increased flow, which is an indication of increased drag losses.

Such total pressure loss coefficient curves were used to calculate the diffuser passage total pressure losses for the E³ engine at sea level static

ORIGINAL PAGE IS
OF POOR QUALITY

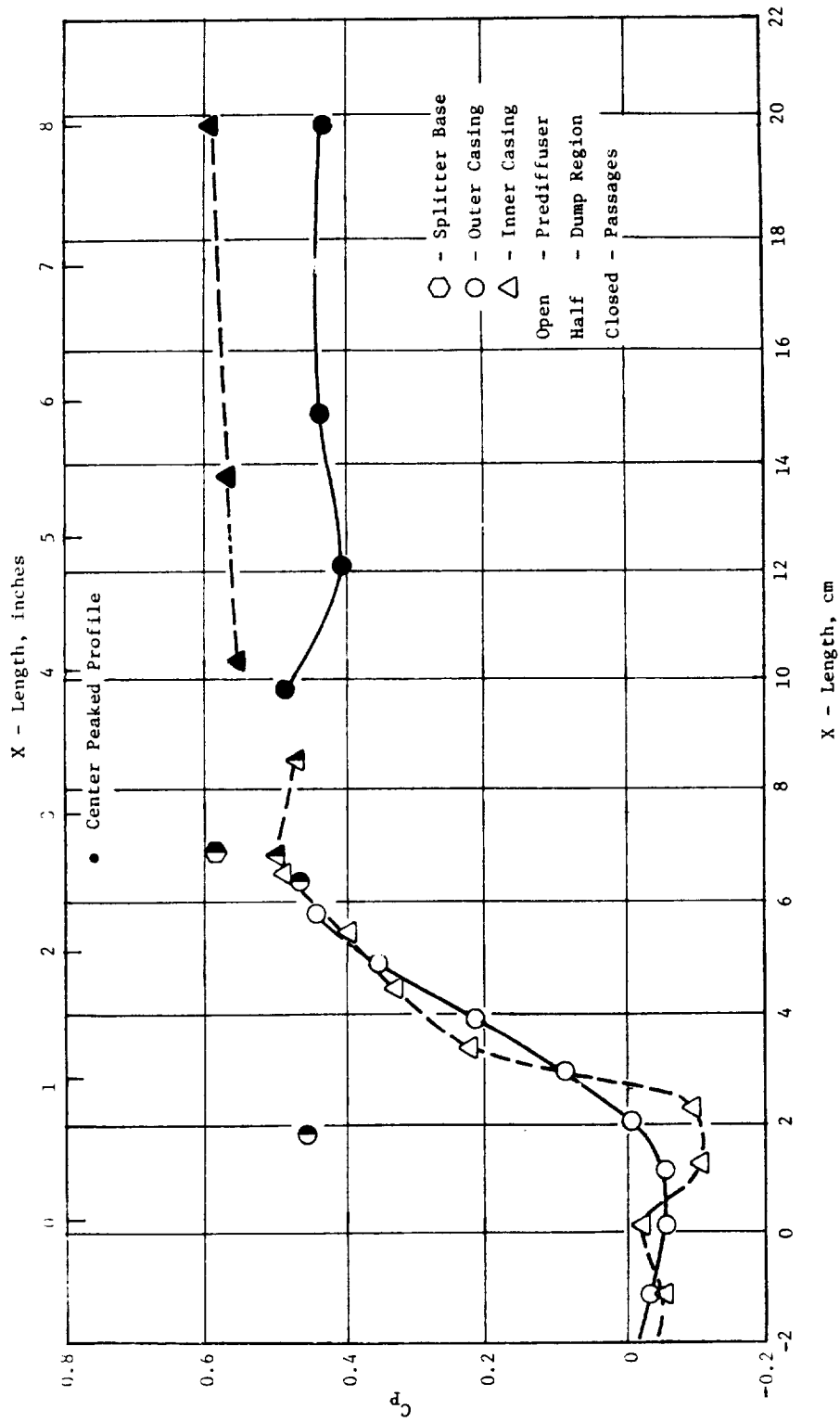


Figure 78. Static Pressure Rise Coefficients.

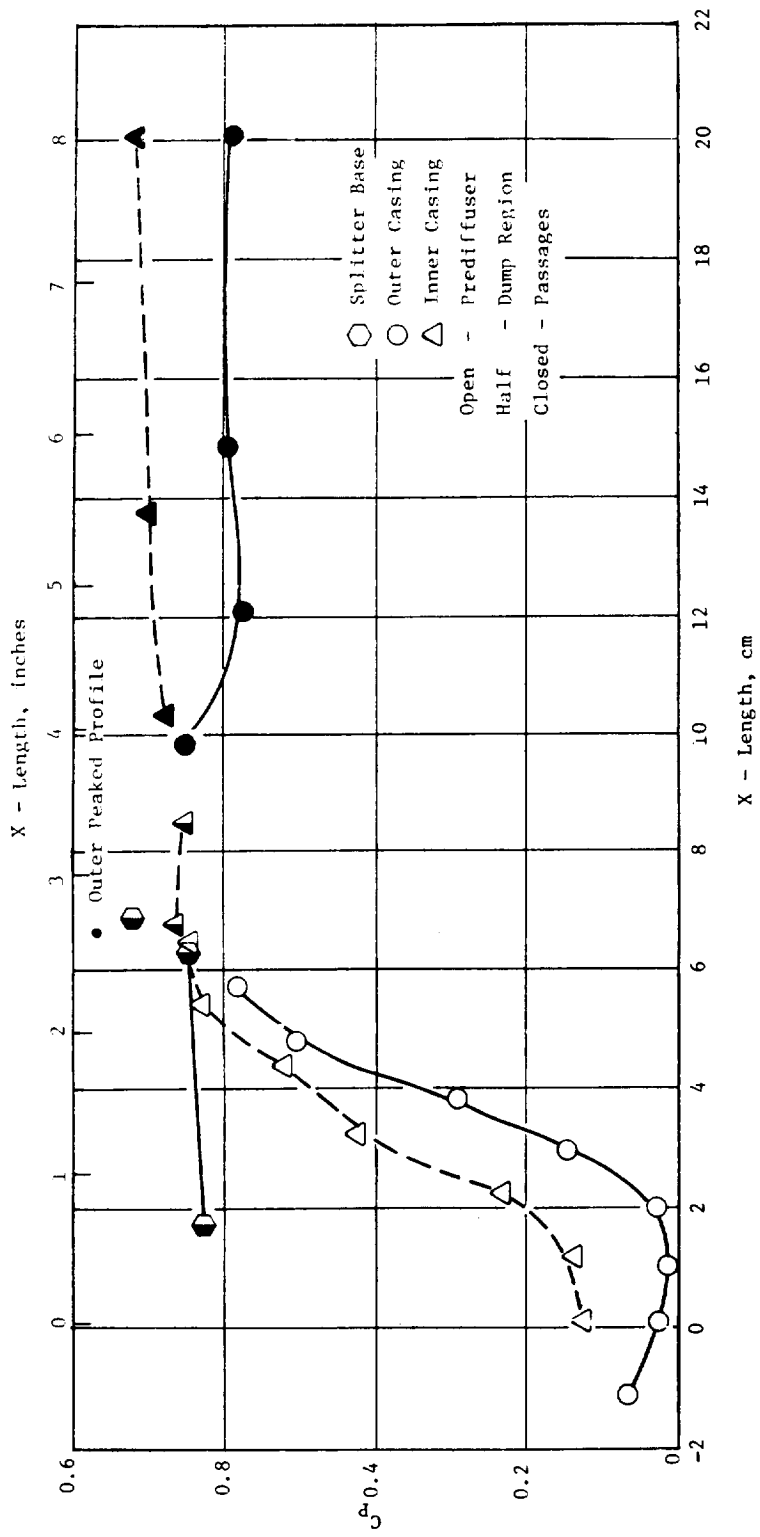


Figure 79. Static Pressure Rise Coefficients.

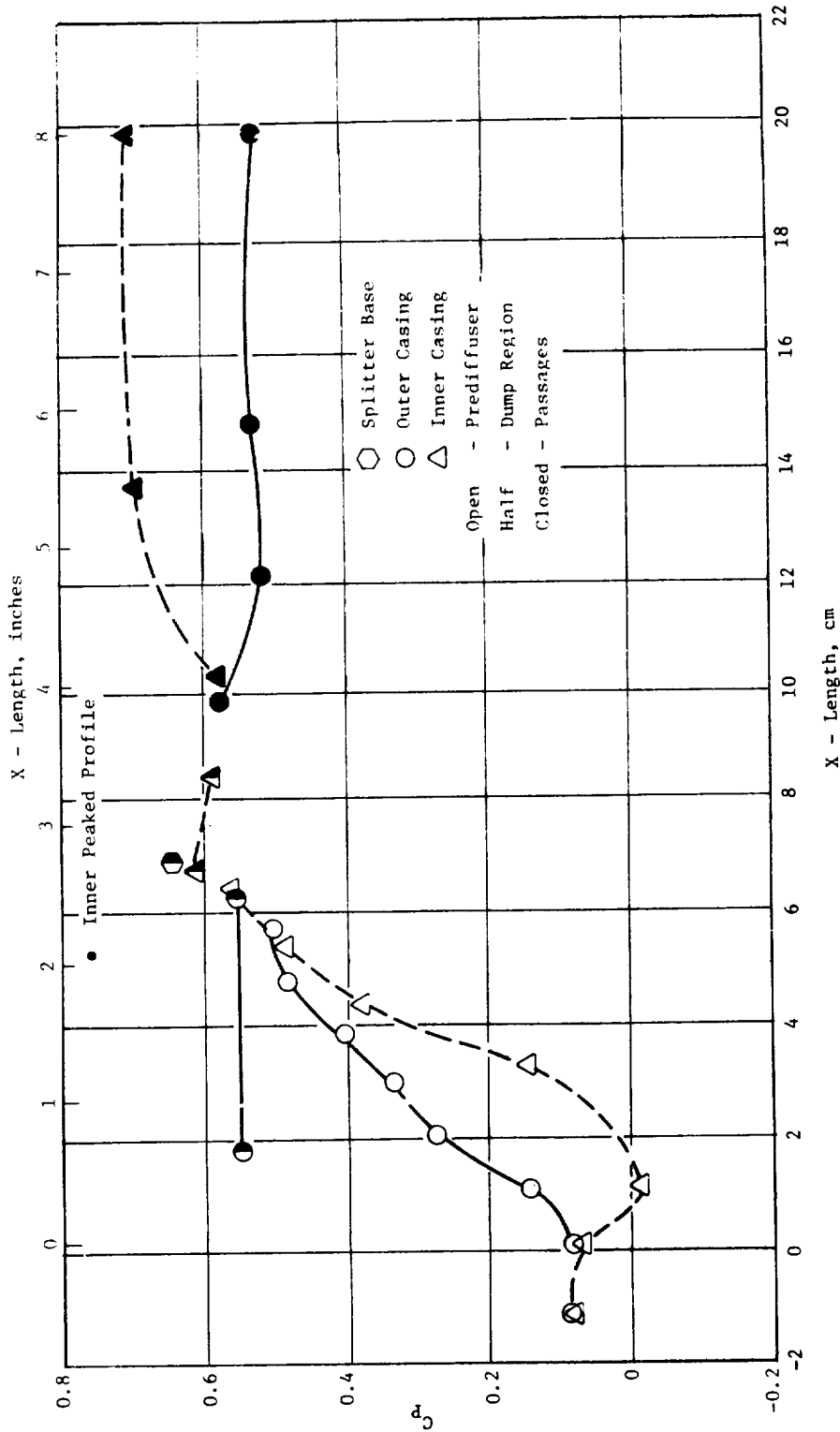


Figure 80. Static Pressure Rise Coefficients.

ORIGINAL PAGE IS
OF POOR QUALITY

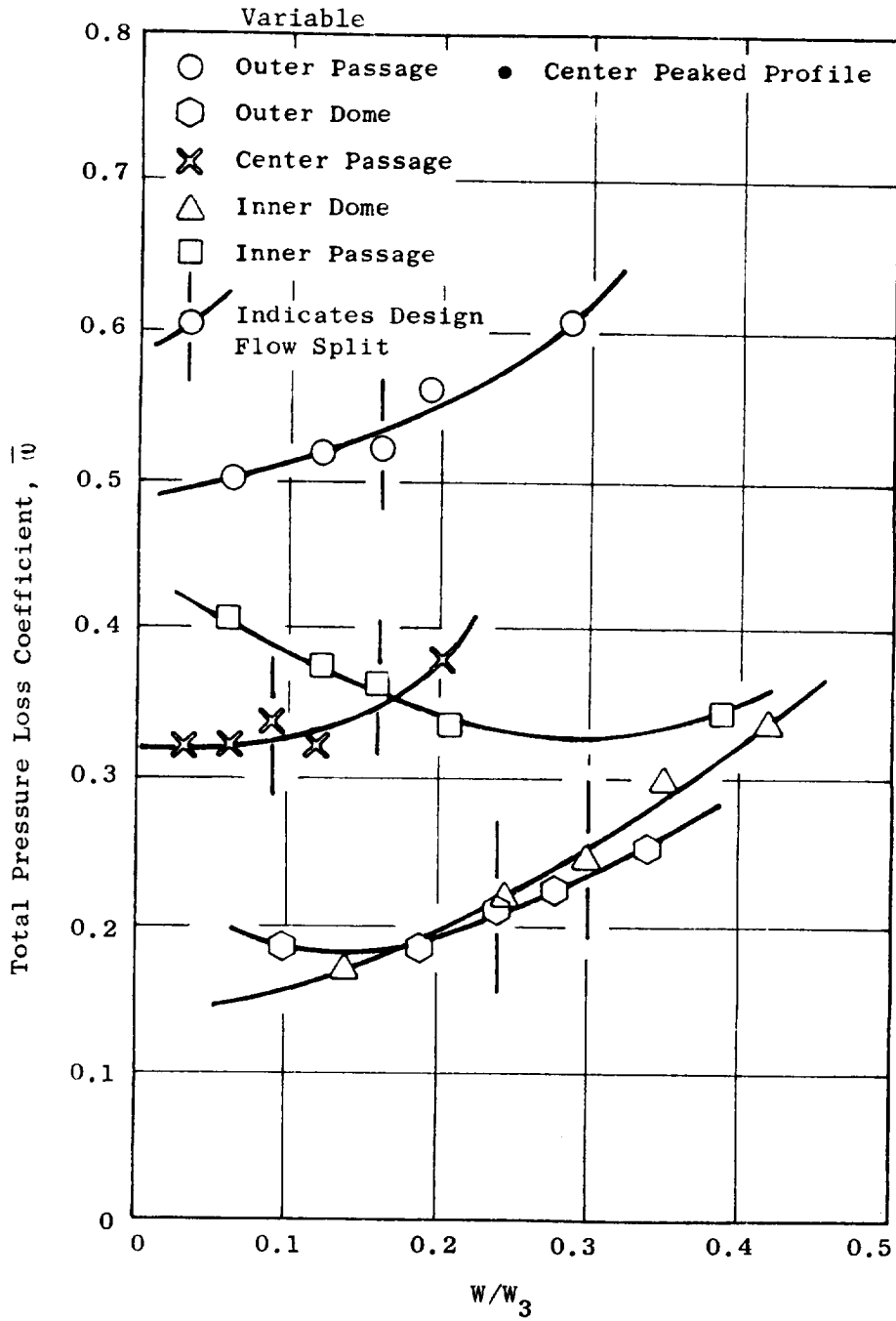


Figure 81. Total Pressure Loss Coefficients.

conditions. The values are presented in Table XVII where the measured diffuser pressure losses are compared to the values that were predicted prior to the test program. The overall mass-weighted loss is notably close to the predicted value, but the measured outer passage pressure loss is about 0.5% higher than the predicted value. This increment in total pressure loss is most likely associated with the higher than expected parasitic dray losses associated with the fuel nozzle bodies.

In addition, two other aspects of the diffuser performance were investigated which related to off-design performance of the baseline diffuser configuration. First, the impact of the absence of diffuser bleed at the base of the splitter was evaluated. Second, the effect of a uniform, low level turbulent inlet velocity was investigated by removing the profiler located upstream of the splitter vane. As expected, the absence of prediffuser bleed had hardly any effect on the diffuser performance. However, as shown in Table XVIII, the uniform inlet velocity produced significantly poorer results than obtained with the nominal flow split design with a center peaked profiler in place. This performance deficiency is attributed to the very long undisturbed inlet passage which exists without the profiler. An exceptionally thick low-energy laminar boundary layer builds up in this passage which is easily separated from the walls as the passages diffuse. However, in the engine installation the turbulence levels are expected to be much higher than experienced in the test rig due to the rotating machinery. Therefore, turbulence levels in the rig with the profilers in place are similar to those expected in the engine application.

6.1.6 Conclusions

Based on the results of the E³ diffuser model test program, it was concluded that:

1. The performance of the E³ combustor inlet diffuser design is satisfactory and meets the requirements of the E³ engine.
2. The annular splitter vane used to design a short-length, high area ratio combustor inlet diffuser has good performance with stable, stall-free operation.

Table XVII. Diffuser Model Measured Performance.

- Diffuser Bleed
- Ambient Test Conditions
- Nominal Flow Split

	Outer Passage	Outer Dome	Center Passage	Inner Dome	Inner Passage	Mass Weighted Average	Inlet Velocity Profile
Passage $\Delta P/P$	3.06	1.21	1.88	1.44	2.08	1.81	Center Peaked
	2.47	1.43	1.21	0.08	1.44	1.17	Inner Peaked
	2.07	0.03	1.22	1.00	1.32	1.31	Outer Peaked
Goal	2.49	0.75	2.95	0.75	2.16	1.50	Center Peaked
Turbine $\Delta P/P^*$	1.60				2.55		Center Peaked
	2.10				3.20		Inner Peaked
	2.50				3.32		Outer Peaked
Goal	2.00				2.00		Center Peaked
*Backflow Margin							

Table XVIII. Diffuser Model Performance Comparison.

- Nominal Flow Split
- Ambient Test Conditions
- Center Peaked Profile

	Outer Passage	Outer Dome	Center Passage	Inner Dome	Inner Passage	Mass Weighted Average
Baseline Configuration ($\Delta P/P$)						
- Bleed	2.97	1.19	1.90	1.27	2.09	1.74
- No Bleed	2.98	1.11	2.01	1.38	2.11	1.66
- No Profiler	3.98	1.16	2.75	1.47	3.03	2.07
Goal	2.49	0.75	2.95	0.75	2.16	1.50

3. Combustor dome cowling designs must be carefully executed to provide high pressure recoveries with minimum flow spillage from the high pressure regions.
4. Lower than expected pressure recoveries in the outer liner passage of the E³ diffuser are probably due to higher than expected parasitic drag losses around the fuel nozzle stems and combustor liner support struts.
5. High inlet turbulence levels result in improved diffuser performance.
6. Elimination of diffuser bleed has no major impact on diffuser performance.

6.1.7 Recommendations

Based on the results of the E³ diffuser model test program, the following is recommended:

1. Modify the Stage 1 leading edge turbine bleed to supply as much of the turbine cooling flow as possible from the inner passage. Figure 82 shows that increasing the flow to the inner passage and decreasing the flow to the outer passage results in reduced pressure losses in both passages.
2. Redesign the fuel nozzle stems to reduce parasitic drag losses in the outer passage and retest.
3. Retest the E³ combustor inlet diffuser model with various levels of inlet turbulence. Measure the inlet turbulence scale and intensity levels and correlate the improved diffuser pressure recovery performance with the inlet turbulence levels.

6.2 SECTOR COMBUSTOR SUBCOMPONENT TEST

6.2.1 Introduction

The E³ combustor subcomponent test program was a part of the overall effort to develop a combustion system for the NASA/GE Energy Efficient Engine Program. This subcomponent test program was designed for the purpose of evaluating and refining the significant aerothermodynamic characteristics of the combustion system necessary to produce low pollutant emissions and acceptable ignition performance.

ORIGINAL VALUE IS
OF POOR QUALITY

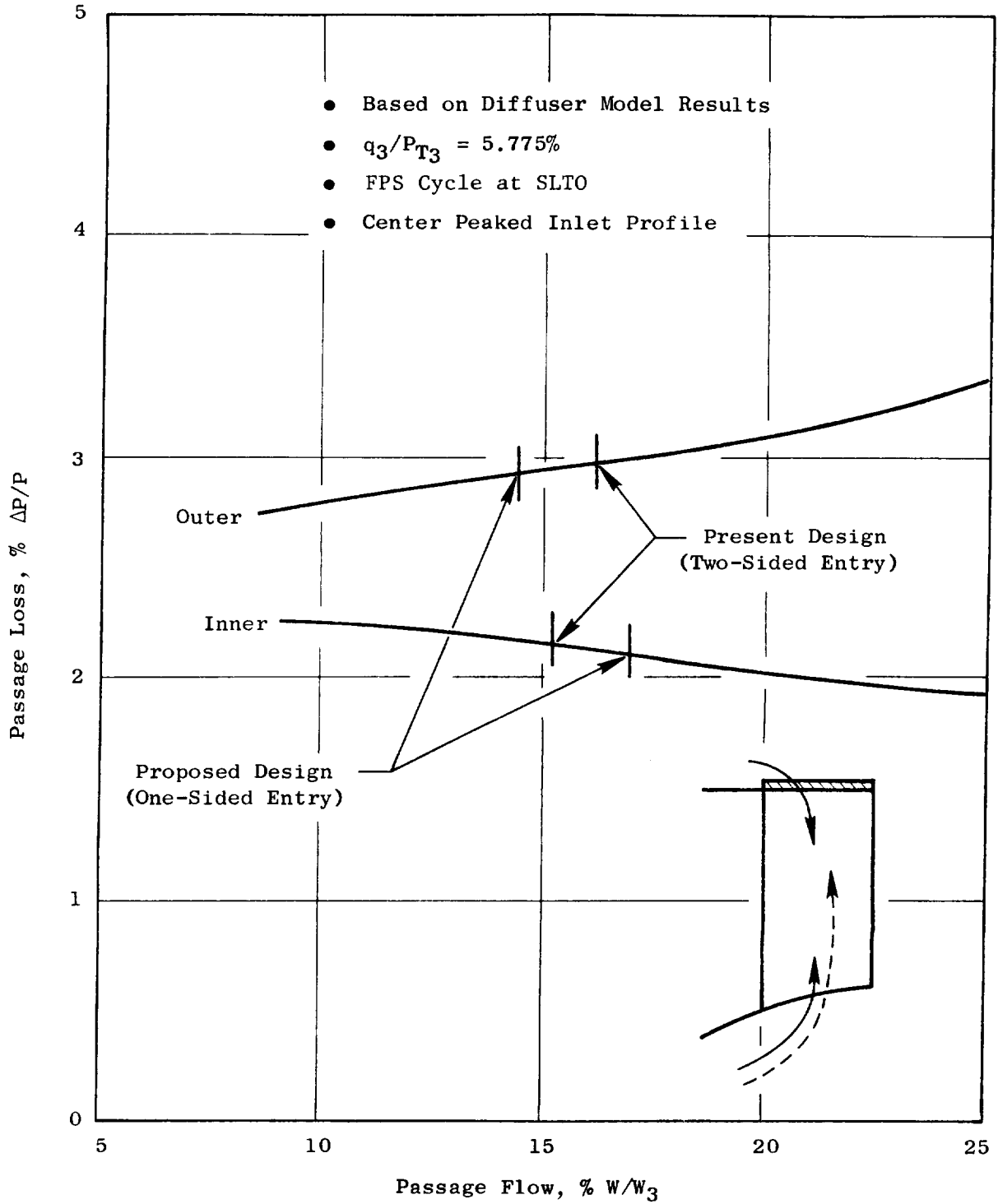


Figure 82. Effect of Airflow Levels on Passage Losses.

The program consisted of three separate test categories which included swirl cup fuel spray investigation tests, dome metal temperature tests, and sector combustor tests. These tests were conducted over a 30-month period spanning the time prior to and during the full-annular combustor development test effort.

The swirl cup fuel spray investigation tests were conducted to refine the fuel spray characteristics of the E³ swirl cup design and to identify an effective emission reduction sleeve configuration for the design. The swirl cup was tested for fuel spray quality and distribution with several sleeve designs. A 45° included-angle sleeve was shown to produce the most desirable fuel spray and, hence, was selected for the baseline configuration of the E³ five-cup sector combustor.

The dome metal temperature tests were conducted to determine the effectiveness of the E³ combustor pilot stage splash plate cooling and to investigate the effects of burning broader specification fuels on dome metal temperatures.

The results of the dome metal temperature tests indicated that adequate splash-plate cooling airflow levels were selected for both combustor stages with metal temperatures remaining below 1100 K (1520° F), even under the most severe combustor operating conditions. Furthermore, the use of broad specification fuels such as marine diesel and ERBS (Experimental Referee Broad Specification) fuels had only a minor effect on dome metal temperatures.

The sector combustor tests constituted the major part of the E³ sub-component testing program. These tests were conducted in a five-cup sector combustor and were devoted to developing the combustor main performance characteristics including ignition, emissions, exit temperature profiles, and altitude relight.

A total of seven basic sector combustor configurations were tested. Some of these configurations were subjected to more than one test with one or more of their features somewhat varied to investigate specific performance aspects. The sector combustor ignition performance was improved throughout

the sector combustor testing effort to meet the E³ start cycle fuel flow schedule. CO idle emissions also met the E³ target level for two of the test configurations. However, for one of these configurations the HC emissions target level was exceeded, while for the other the ignition performance deteriorated. NO_x emissions exceeded the target level for all configurations. However, experience with the full-annular combustor demonstrated that generally higher NO_x emissions are produced in the sector combustor than the full-annular combustor for similar configurations.

6.2.2 Swirl Cup Investigation Tests

6.2.2.1 Design and Development Approaches

The spray quality of fuel introduced into the combustion zone has a major impact on the pollutant emissions levels, on ignition capabilities, and on combustor life. Fuel spray characteristics, such as mass distribution, spray angle, and droplet size, are of significant importance to the overall combustor performance; all are directly influenced by the swirl cup design characteristics - mainly its recirculation zone. The spray angle has a direct effect on flame stability. Wide fuel sprays tend to produce bimodal fuel spray; hence, an unstable flame, while too narrow fuel sprays concentrate the fuel in the center region of the swirl cup producing an extended flame front inside the combustion chamber. The droplet size directly influences both ignition performance and emissions, and fuel mass distribution affects emissions as well as the life of the combustor liner.

The swirl cup and fuel spray visualization tests were conducted to determine the fuel spray characteristics of the pilot and main stage swirl cup design of the E³ double-annular combustor. The tests were also intended to identify an emission reduction sleeve configuration that will produce the desired spray quality and spray distribution. The effects of varying the fuel nozzle tip immersion and the primary swirler radial location relative to the assembly centerline (eccentricity) were investigated, as well.

The E³ swirl cup design featured an axial flow primary swirler coupled with a counterrotating radial inflow secondary swirler for both pilot and main

stage domes. Other swirl cup design features included an emissions reduction sleeve, a carbon-preventing venturi, a primary-secondary swirler slip joint, and an overall simple mechanical design.

All of the swirl cup components tested were E³ sector combustor test hardware installed in an F101 engine dome plate and splash plate, modified to simulate the E³ dome. The cooling hole pattern for the dome plate was modified to provide 4.3% W_{comb} cooling air for the splash plate as specified for the E³ pilot dome design. Dome ring cooling was added to the dome to better approximate the E³ dome aerodynamic and mechanical design. The fuel nozzle used in the tests was a simplex tip with 85° included spray angle rated at 20.5 kg/hr (45.2 lb/hr). The pilot dome and main dome swirl cup configurations for the E³ double-annular sector combustor were sized during these tests by selecting the appropriately sized secondary swirler to be used in the cup assembly and matching the primary to the secondary. A schematic of the test swirl cup dome assembly used is shown in Figure 83.

Three different categories of tests were conducted on the E³ swirl cup assembly:

1. Fuel spray visualization tests
2. Fuel spray patternation tests
3. Recirculation zone survey tests

The spray visualization tests were conducted in GE-Evendale Building 302 Fuel Nozzle Laboratory. The apparatus used consisted of a box used as a plenum. Fuel and air supplies were piped into the box. The dome swirl cup assembly was mounted on one side of the box in such a way that it discharged to the outside of the box into a collector. A schematic of the test setup is shown in Figure 84.

For the patternation tests a similar apparatus to that of the visualization tests was used except that the discharged fuel was collected into an array of graduated tubes positioned in a semicircular arrangement. Each tube represented one radial location of a spray plane. The tubes were rotated to different plane locations and the fuel spray pattern was then determined.

ORIGINAL PAGE IS
OF POOR QUALITY

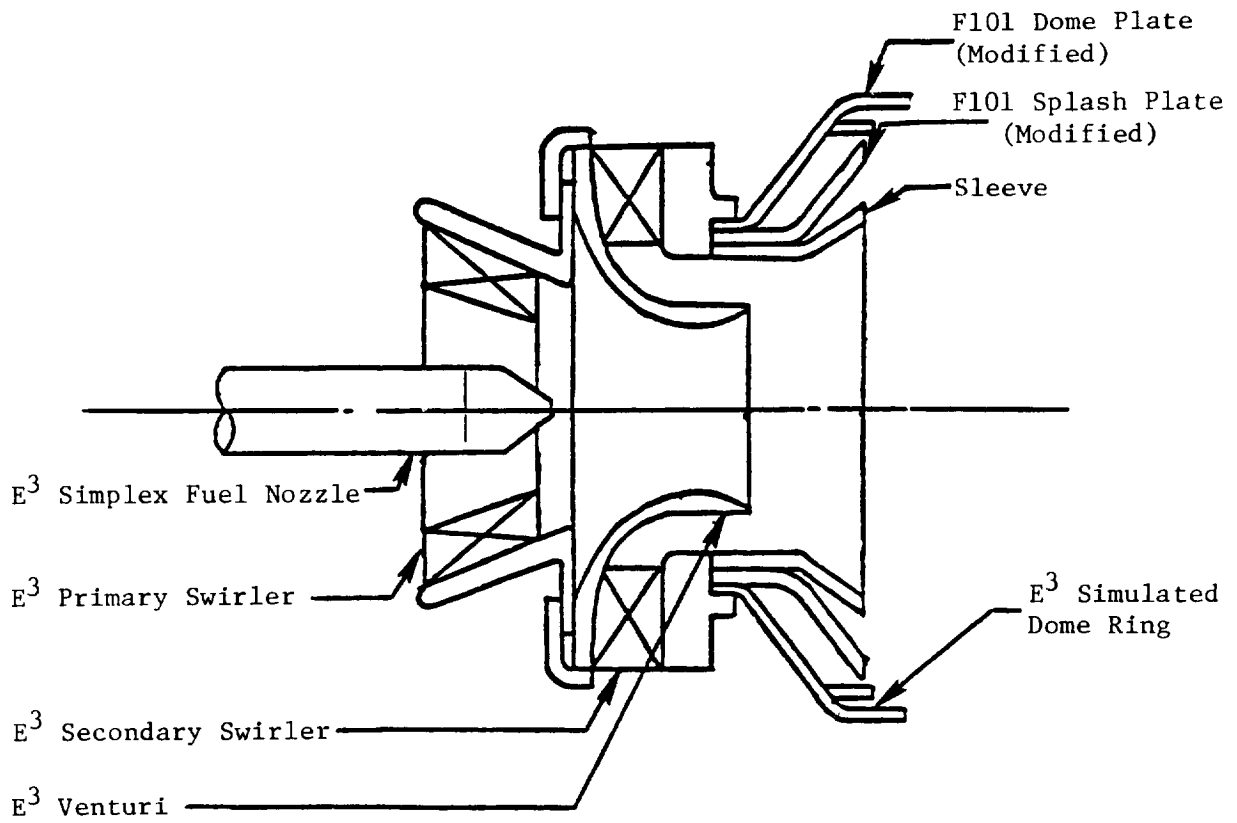


Figure 83. Dome Assembly Cross Section Used in Fuel Spray Testing.

ORIGINAL PAGE IS
OF POOR QUALITY

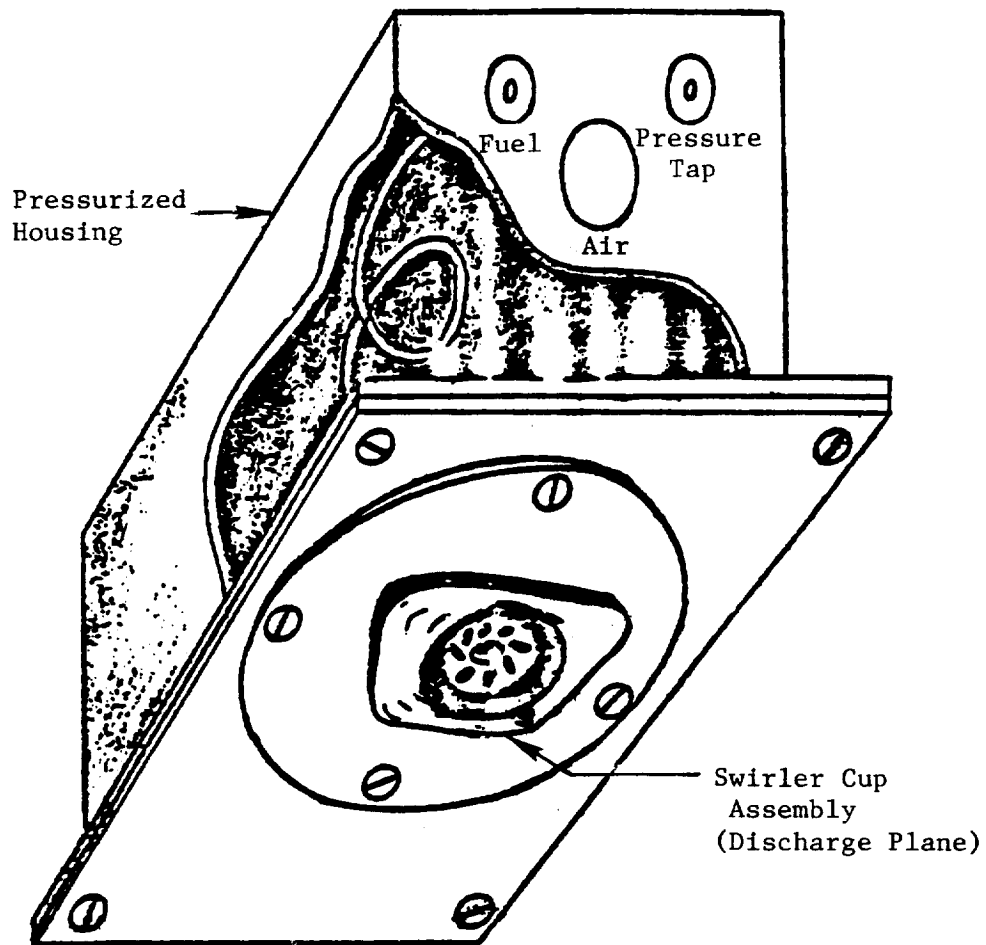


Figure 84. Fuel Spray Visual Test Setup.

The swirl cup recirculation zone tests were conducted in GE-Evendale Building 304 Laboratory using the test stand shown schematically in Figure 85. The strength of the recirculation zone was determined by using a three-element aerodynamic probe to measure static and total pressures at the exit plane. The depth of the recirculation zone was obtained by the aid of a halogen detection device that was used to measure how far upstream halogen was able to recirculate when sprayed at the exit plane of the swirl cup.

The test conditions set for the visualization tests were those required to simulate the E³ key cycle conditions at the combustor inlet (Table XIX). These conditions included ground start, ground idle, and sea level takeoff. For each of these test conditions, three critical swirl cup parameters were simulated: dome pressure drop, swirl cup velocity, and fuel-to-air momentum ratio.

Table XIX. Test Conditions for Fuel Spray Visualization Testing.

<u>Cycle Condition</u>	<u>Swirl Cup Parameter Simulated</u>	<u>ΔP Dome-H₂O, cm (in.)</u>	<u>Fuel Flow, kg/hr (pph)</u>	<u>Fuel-Air Ratio</u>
Ground Start	ΔP Dome	6.1 (2.4)	11.34 (25)	5 x f/a (SS)
	Swirl Cup Velocity	7.1 (2.8)	11.80 (26)	5 x f/a (SS)
	Momentum Ratio	76.2 (30.0)	5.44 (12)	f/a (SS)
Ground Idle	ΔP Dome	40.6 (16.0)	26.76 (59)	5 x f/a (SS)
	Swirl Cup Velocity	68.1 (26.8)	27.67 (61)	4 x f/a (SS)
	Momentum Ratio	40.6 (16.0)	7.71 (17)	f/a (SS)
Sea Level Takeoff	ΔP Dome	44.4 (17.5)	14.97 (33)	5 x f/a (SS)
	Swirl Cup Velocity	127.0 (50.0)	12.25 (27)	2 x f/a (SS)
	Momentum Ratio	44.4 (17.5)	10.43 (23)	f/a (SS)

The visualization test procedure simply requires setting the dome pressure drop and fuel flows, then visually inspecting the resulting fuel spray for its critical characteristics. A stable spray was defined as a single

ORIGINAL PAGE IS
OF POOR QUALITY

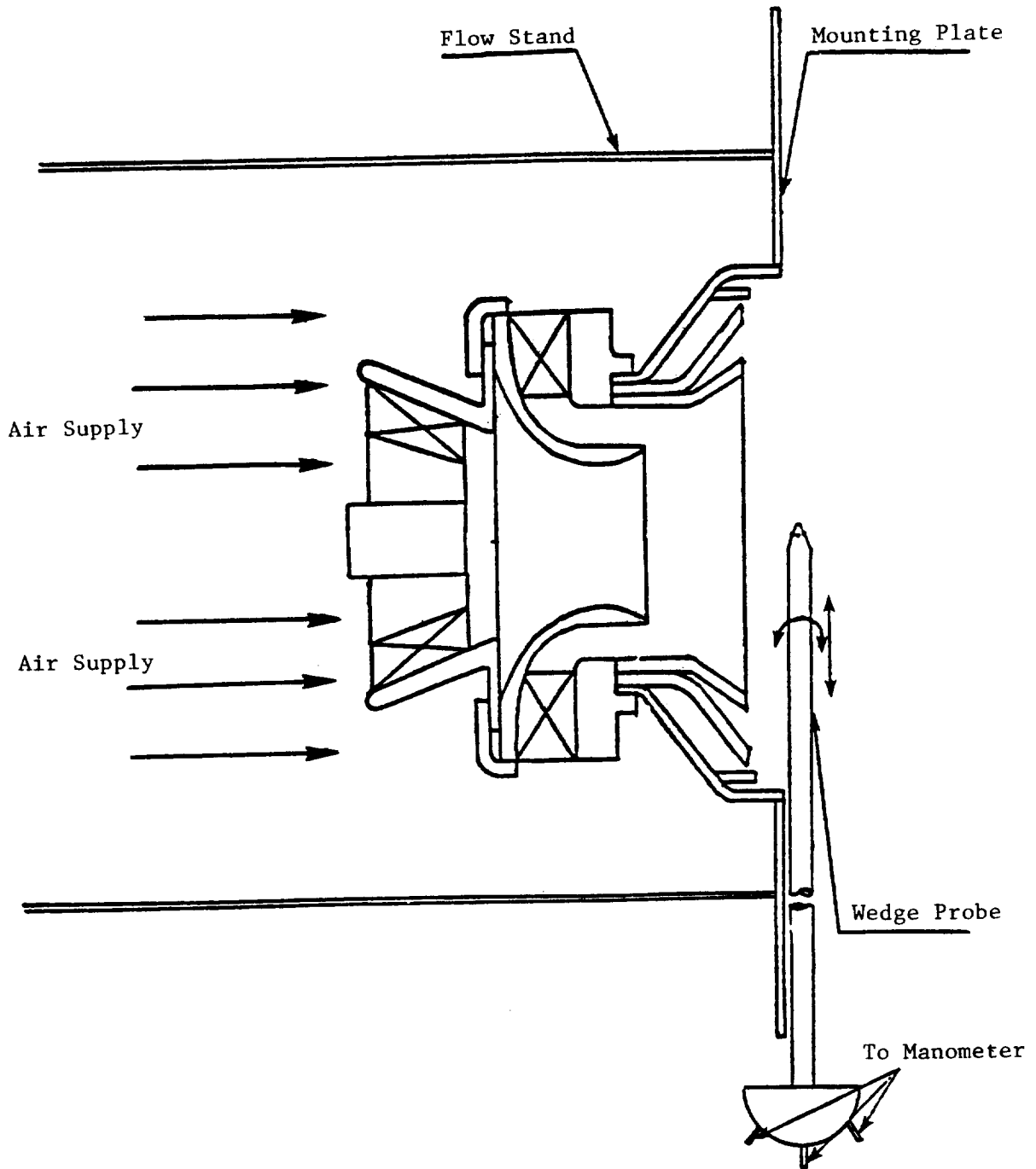


Figure 85. Swirl Cup Recirculation Test Stand.

angle spray which could not be altered by any aerodynamic or mechanical disturbance. Photographs were taken at each point-setting and were used to compare the spray angle. The spray angle measurements were made to include the outermost boundary of the spray envelope and are considered to be only qualitative.

The same conditions used in the visualization tests were also used in the patternation tests. The discharged fuel was allowed to accumulate in the collecting tubes for 20 minutes at each test point. The volume of fuel collected in each tube was measured and used to establish the fuel flow mass distribution. Due to the length of time involved in these tests, only promising configurations from the visualization tests were tested on the patternation stand.

For the swirl cup recirculation zone tests, representative pressure drops across the dome were set to simulate the swirl cup aero conditions at ground idle and SLTO operation. Static and total pressure measurements were made along the horizontal cup centerline axis of the swirler assembly. The three-element probe used for the pressure measurement also had the capability of determining the direction of flow at each point by balancing the two static pressure elements in the probe tip.

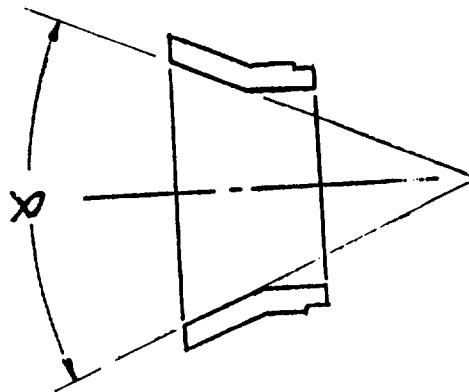
For the halogen detector testing, a small tube was inserted through a rubber plug inserted into the hole in the swirl cup which would normally house the fuel nozzle. The tube had a degree of freedom along the swirl cup axis. The upstream end of the tube was connected to a detector that transmitted an audible signal when halogen was present. Freon gas was sprayed at the swirl cup exit with the detection tube tip in one position, and when a signal was recorded it was considered an indication that the recirculation zone extended at least to that particular tip location. The procedure was repeated with the tube moved to a new upstream position until no further signal was transmitted by the detector. That location was then identified as the limit of the recirculation zone.

6.2.2.2 Experimental Test Results

Each of the simulated pilot and main stage domes of the E³ combustor were tested on the visual stand with several sleeve inserts varying in included angle

between 0° (cylindrical) and 90°. Although the quality of the fuel spray atomization and the spray angle for most sleeve configurations was acceptable, stable spray (single angle) was obtained only with 45° or less included-angle sleeves. The estimated spray angle obtained with the 45° sleeve was approximately 59° at inlet conditions simulating ground start conditions. Sleeves with an included angle larger than 70° had extremely wide fuel sprays which tended to attach to the splash plate. This type of fuel spray was judged as unsatisfactory, for it tends to locate much of the fuel along the combustor liner wall, often resulting in high idle emissions and hot streaks on the combustor liners. Sleeves with angles between 50° and 70° initially produced stable fuel sprays, but when perturbed by an outside mechanical disturbance, the spray became attached to the splash plate. Table XX gives a summary of spray stability results for the various sleeve configurations tested.

Table XX. Fuel Spray Visualization Test Results.



<u>Emissions Sleeve- Included Angle (α), degrees</u>	<u>Results</u>
0 (Cylindrical)	Stable - Very Narrow Spray Angle
15	Stable - Very Narrow Spray Angle
45	Stable - Wider Spray Angle
50	Semistable - External Disturbance
60	Unstable - No Disturbance
70	Unstable - No Disturbance
90	Unstable - No Disturbance

ORIGINAL FILE
OF POOR QUALITY

Patterning tests were concentrated on the 45° sleeve because it produced the most desirable fuel spray stability and spray angle. Configurations featuring this type of sleeve produced desirable symmetrically double-peaked fuel mass distribution (see Figure 86). As shown in Figure 87, the 70° sleeve configuration further produced the double-peaked distribution. However, the bulk of the fuel was concentrated at a big, wide angle.

Varying the fuel nozzle tip immersion and/or eccentricity relative to the swirl cup centerline axis had no significant effect on the fuel spray stability. But some slight effect on fuel distribution symmetry was observed.

The wedge probe surveys were conducted on the configuration with a 45° included-angle sleeve to identify the velocity profile at the exit plane of the dome and to estimate the size and intensity of the recirculation zone. Similar surveys were conducted on the pilot and main stage swirl cups. The results of the surveys are presented as plots of axial velocity versus the radial distance from the centerline in Figures 88 and 89. The plots indicate that the diameter of the recirculation zone is approximately 2.3 cm (0.9 in.) for the pilot stage cup and 2.0 cm (0.8 in.) for the main stage cup at a plane flush with the mounting plate. The halogen detector tests indicated that the depth of the recirculation zone upstream of the mounting plate was found to equal 1.63 cm (0.64 in.) for the pilot stage and 1.55 cm (0.61 in.) for the main stage.

6.2.2.3 Concluding Remarks

The swirl cup test results indicated that the geometry of the emissions reduction sleeve has a significant effect on the spray stability and fuel distribution. Using a sleeve with a 45° included angle in either the pilot stage or main stage swirl cup designs of the E³ sector combustor produced the most desirable fuel spray characteristics necessary for reducing emissions levels. The baseline configuration pilot and main stage swirl cup recirculation zones were determined to be satisfactory in terms of strength and penetration. Based on these results, it was decided to use the 45° angle sleeves for the baseline configuration of the sector combustor.

ORIGINAL PAGE IS
OF POOR QUALITY

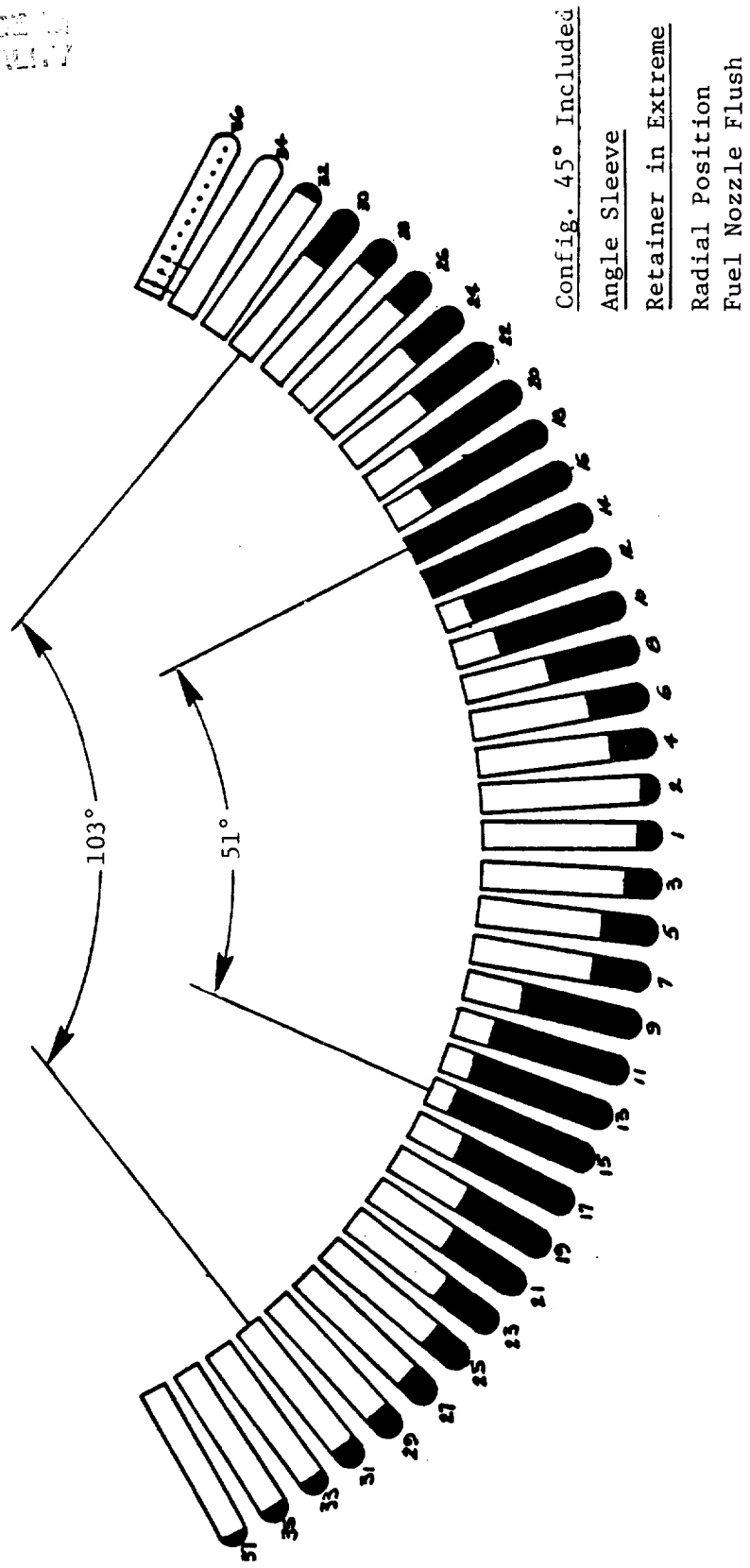


Figure 86. Fuel Spray Patternation Results.

CONFIDENTIAL
OF FUEL QUALITY

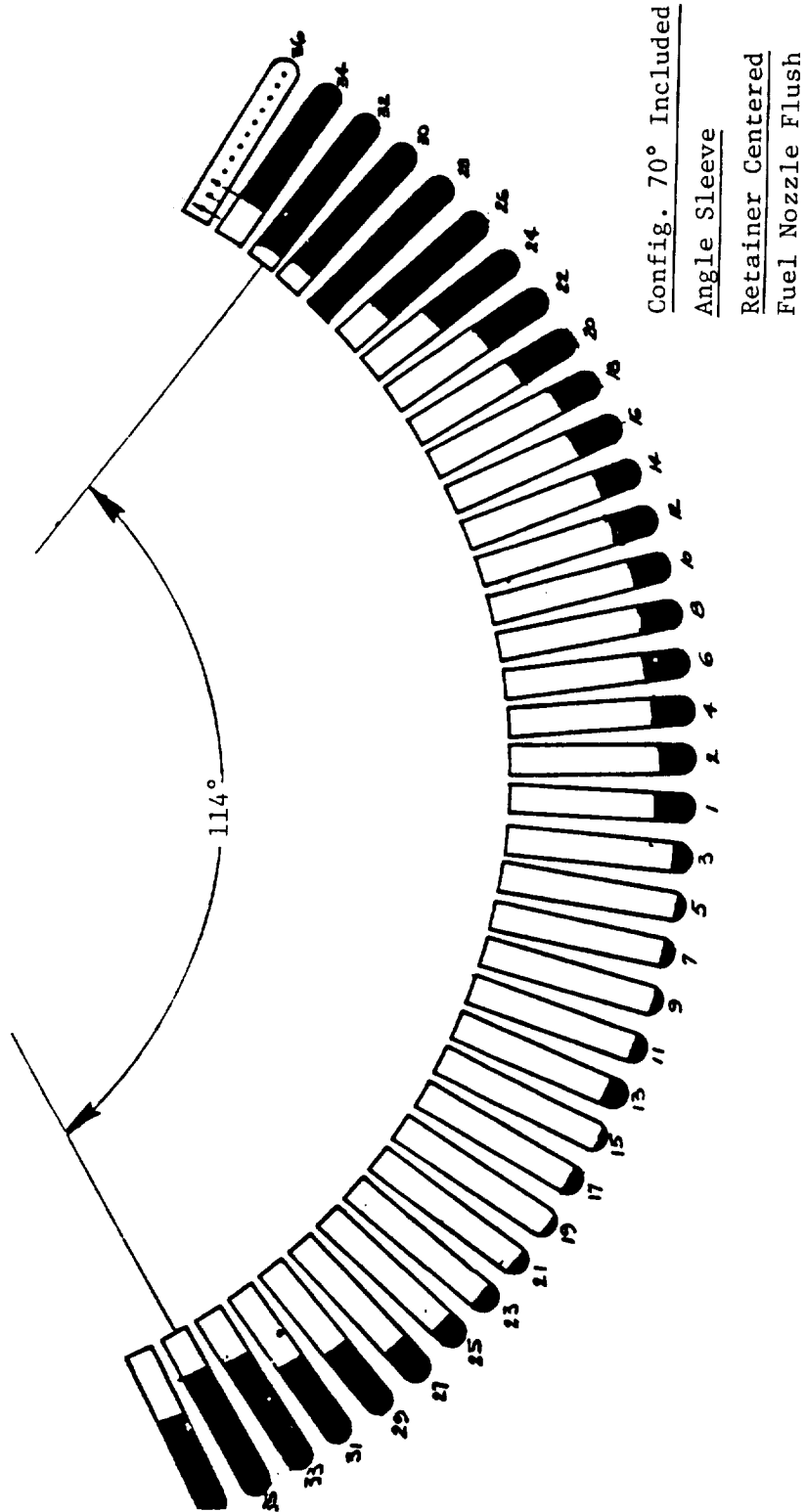


Figure 87. Fuel Spray Patternation Results.

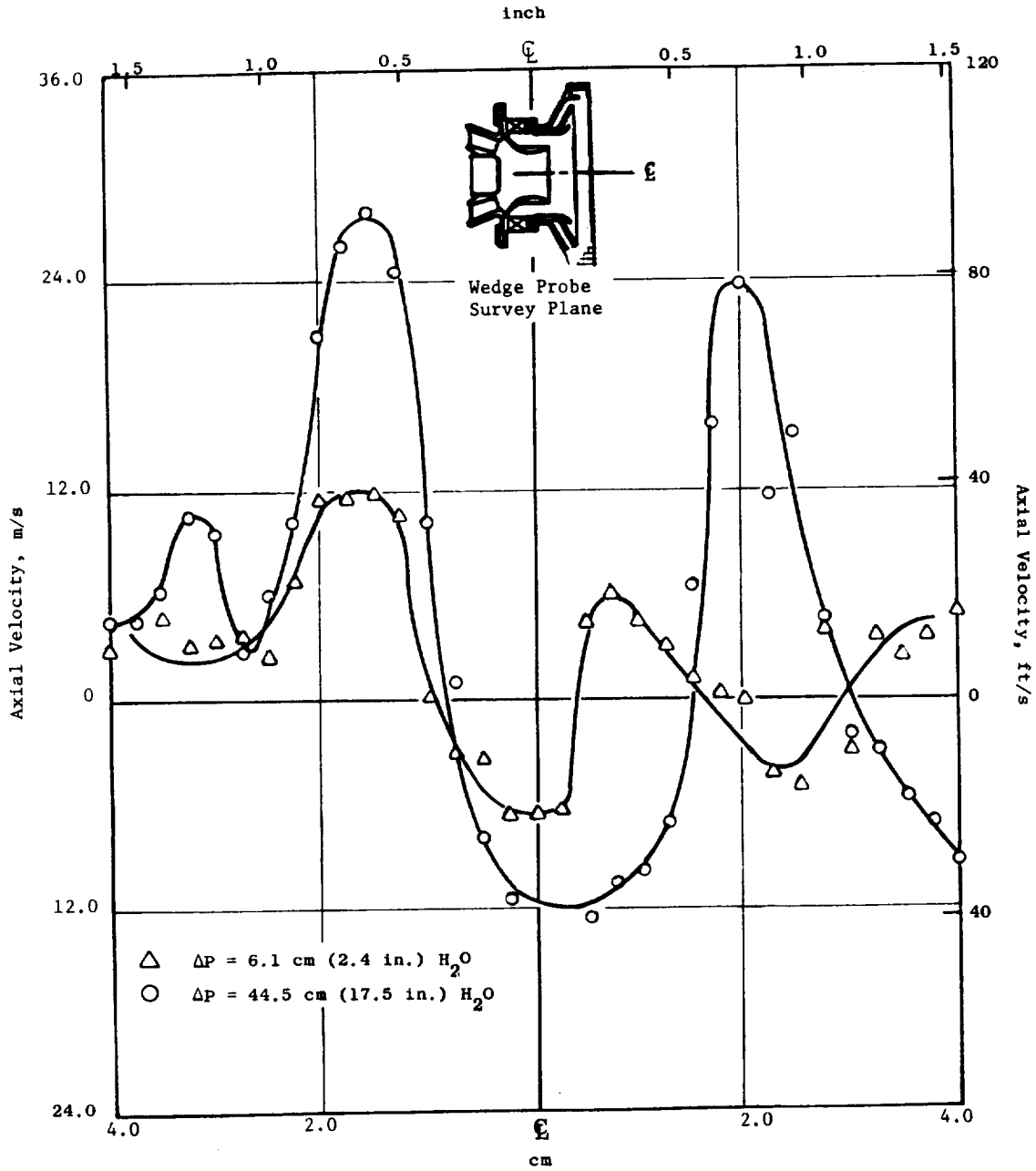


Figure 88. Swirl Cup Axial Velocity Profiles.

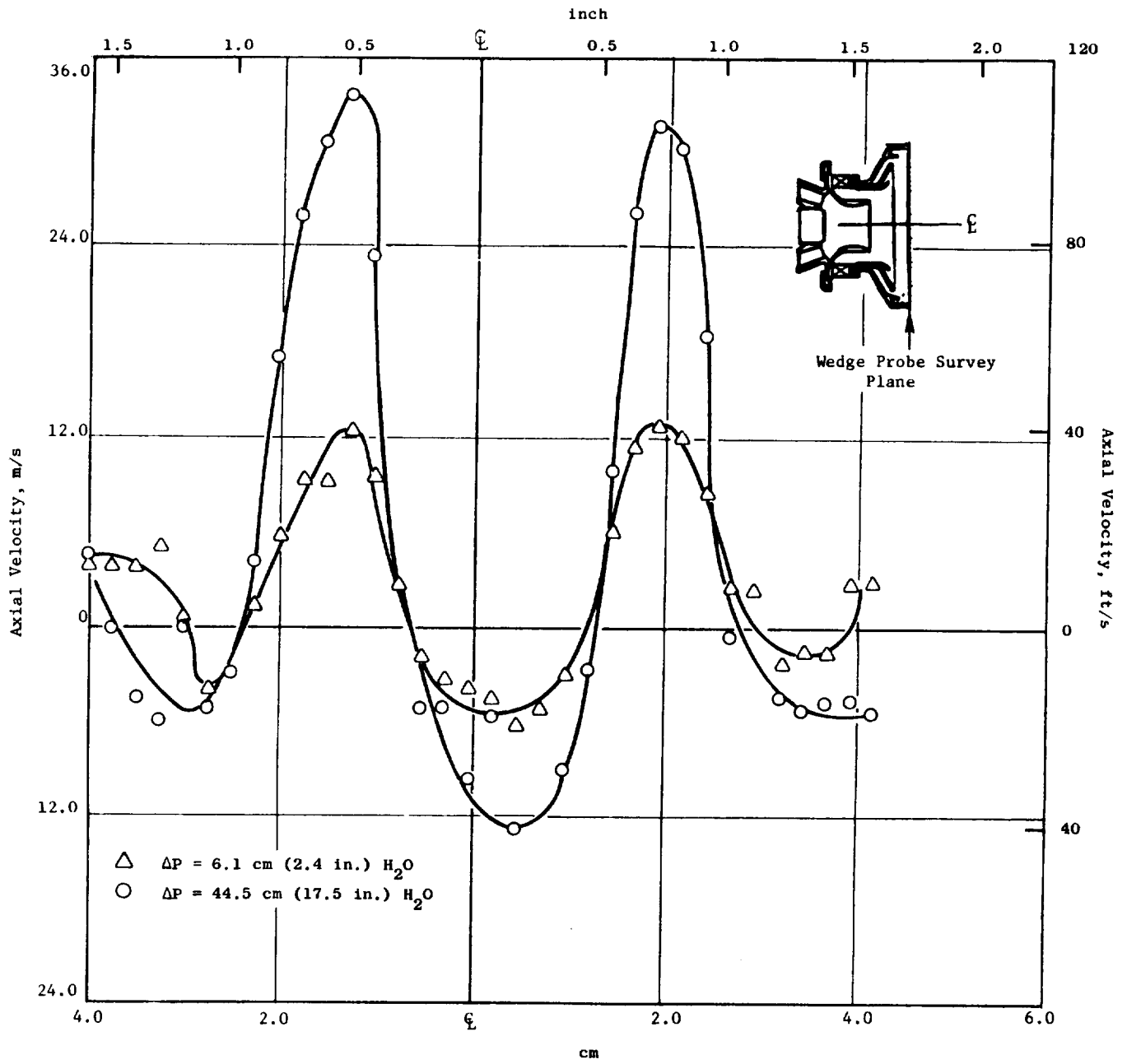


Figure 89. Swirl Cup Axial Velocity Profiles.

6.2.3 Dome Metal Temperature Tests

6.2.3.1 Introduction

The initial E³ double-annular combustor design specified 4.3% of the combustor airflow for the pilot dome splash-plate cooling. This level of cooling airflow was predicated on the expectation that low dome cooling flows result in lower carbon monoxide (CO) and unburned hydrocarbons (HC) emissions levels at ground idle operating conditions. Also, the surface area of the E³ pilot dome is smaller than for a conventional single-annular configuration. Although splash plate cooling is strongly dependent on dome geometry, the selected airflow level for the E³ pilot dome is relatively low when compared to those of existing GE combustors. Therefore, the adequacy of the splash plate cooling airflow selected for the E³ pilot dome design was questioned, in light of past design practices.

The dome metal temperature tests were designed to determine the effectiveness of the pilot stage dome cooling and the impact of this unconventional low dome cooling airflow level on the life of the combustor hardware. The test rig availability also provided a good opportunity to investigate the effects of burning broad specification fuels on the dome metal temperatures in back-to-back tests.

6.2.3.2 Dome Design and Evaluation Approach

The approach chosen to conduct the dome metal tests was that of using a single-cup setup to simulate the E³ dome design. Similar test configurations have been used extensively for this purpose in other programs. The simulated E³ pilot stage dome was constructed from a combination of available E³ sector combustor swirl cup hardware and modified hardware from previous development programs. The dome assembly (see Figure 90 for hardware items) as tested consisted of the following hardware:

- F101-type dome plate modified in size, cooling hole pattern, and area to approximate the E³ pilot stage dome
- F101-type splash plate also modified to simulate the E³ pilot stage dome plate in size and shape

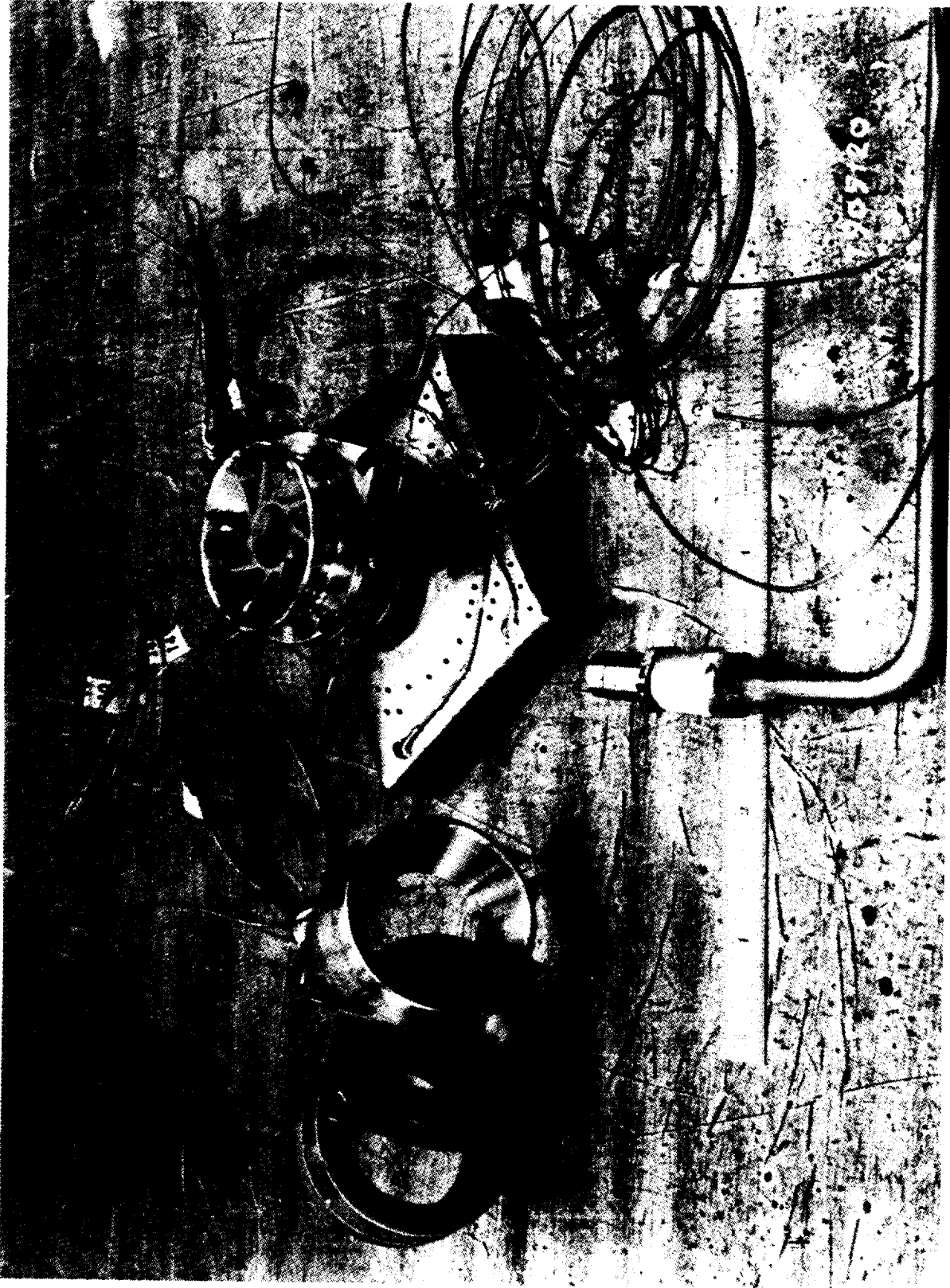


Figure 90. Dome Metal Temperature Test Hardware.

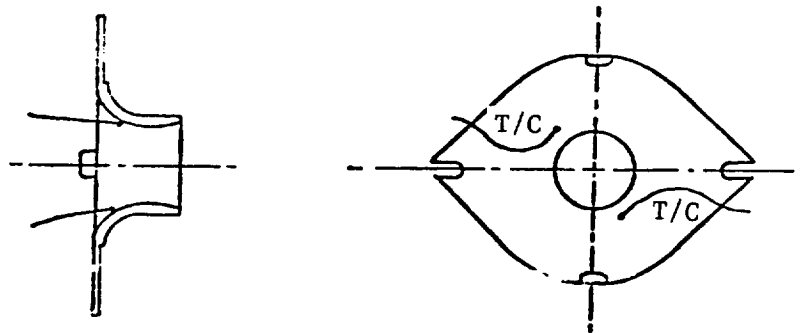
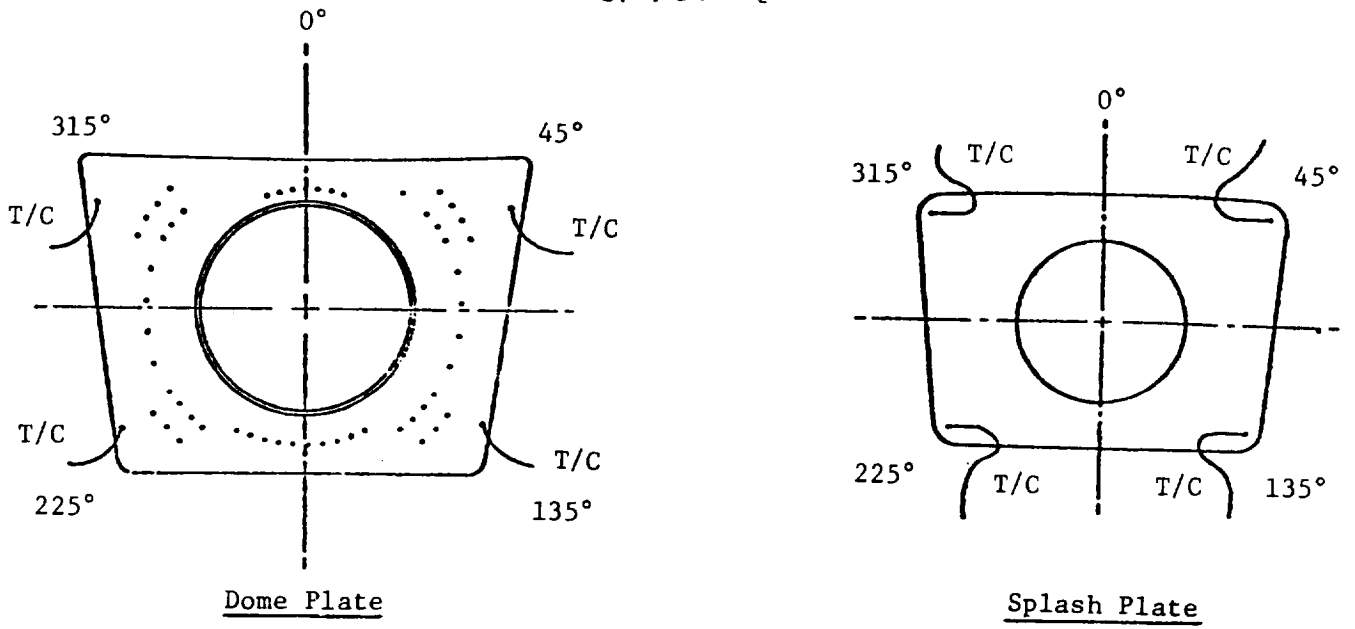
- NASA/Experimental Clean Combustor Program (ECCP)-type primary swirler with an effective flow area approximately equal to the E³ primary swirler area
- F101-type emissions reduction sleeve with a 70° included angle
- E³ sector combustor pilot stage secondary swirler
- E³ sector combustor carbon-preventing venturi
- F101-type simplex fuel nozzle tip.

The dome plate, splash plate, venturi, and sleeve were instrumented with thermocouples at critical locations (Figure 91). To obtain accurate metal temperatures of the hardware close to the combustion gas, the splash plate thermocouples, venturi thermocouples, and sleeve thermocouples were embedded in the metal surface.

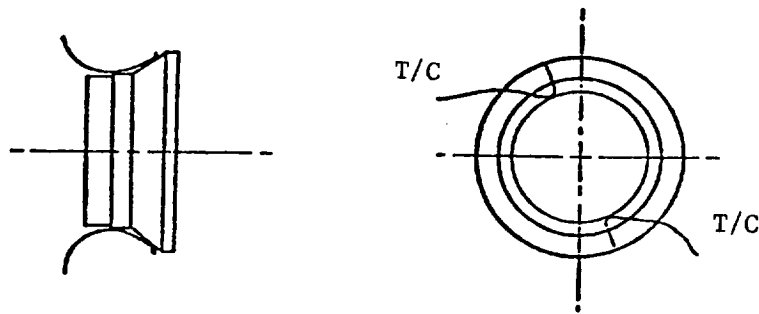
The assembled dome hardware was welded to a can-type liner and mounted inside a plenum in the test facility as shown schematically in Figure 92. The tests were conducted at the General Electric-Evendale ACL Cell A5E test facility. This facility has capabilities for testing components at high pressure, high temperature conditions. An indirect gas-fired heater is utilized to heat the inlet air supplied to the test piece. Nominal facility limits are 840 K (1052° F), 18 atmospheres, and 5.5 kg/sec (12.1 lb/sec).

The test point schedule for the dome metal temperature tests is shown in Table XXI. The test parameters shown in the table simulate actual E³ combustor inlet conditions at the key cycle operating points indicated. The air-flow levels were approximated by setting similar pressure drops to those calculated in the cycle conditions. Fuel flows were selected to cover a wide range of fuel-air ratios including the design levels.

ORIGINAL PAGE IS
OF POOR QUALITY



Venturi



Sleeve

Figure 91. Dome Metal Temperature Test Instrumentation.

ORIGINAL PAGE IS
OF POOR QUALITY

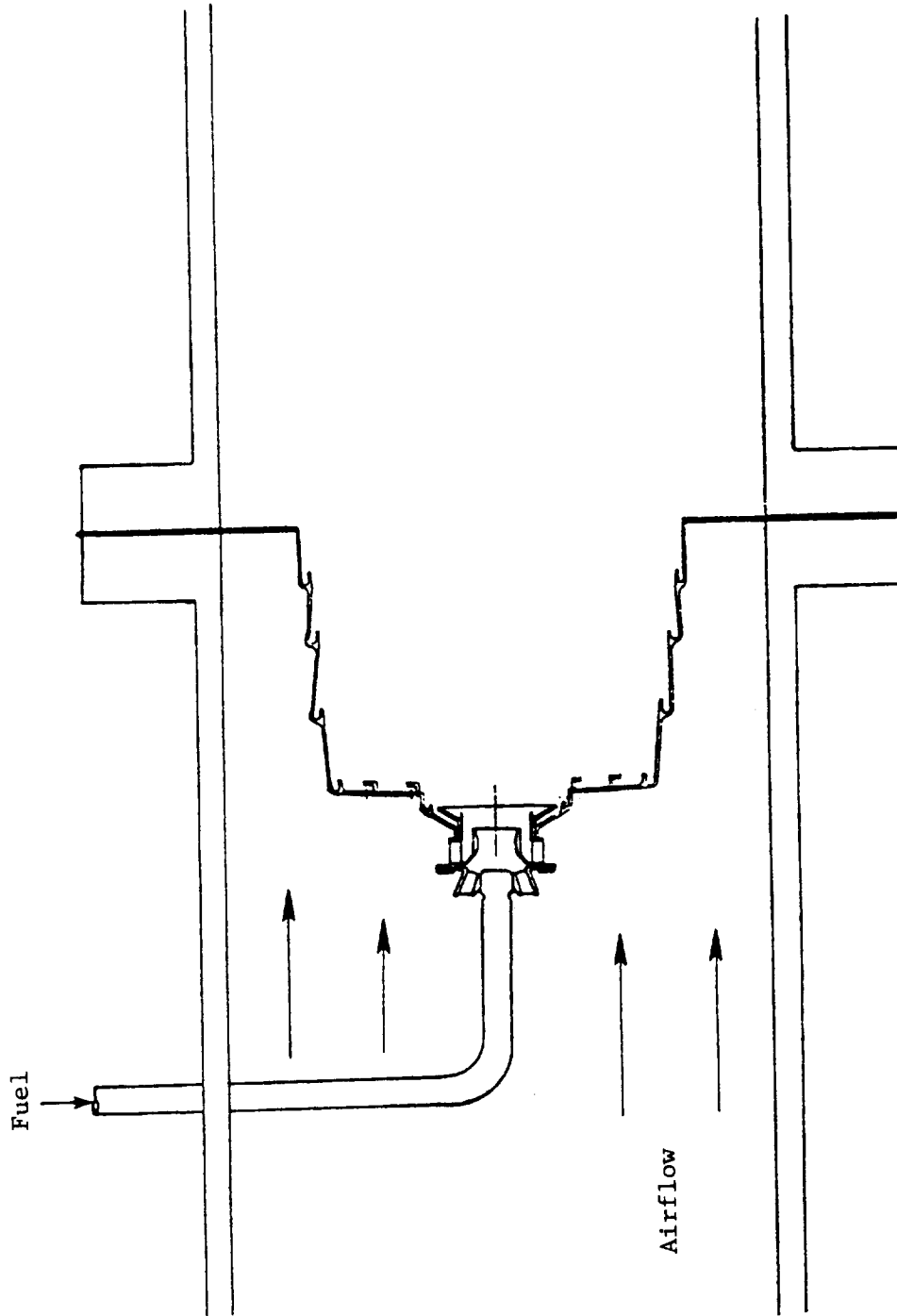


Figure 92. Dome Metal Temperature Test Rig.

Table XXI. Dome Metal Temperature Test Point Schedule.

Point	Engine Condition Simulated	P_{T3} atm	T_{T3} K (°F)	W_f kg/hr (lb/hr)	ΔP atm	$\Delta P/P$ %
1	Approach ↓	11.84	667 (740)	45.8 (20.8)	0.592	5.0
2				76.7 (34.8)		
3				107.5 (48.8)		
4				45.4 (20.6)		
5				57.2 (25.9)		
6	Cruise ↓	12.86	782 (948)	46.3 (21.0)	0.643	5.0
7				76.7 (34.8)		
8				107.5 (48.8)		
9				45.4 (20.6)		
10				57.2 (25.9)		
11	SLTO (Derated) ↓	19.05	814 (1005)	67.1 (30.4)	0.952	5.0
12				111.6 (50.6)		
13				136.1 (61.7)		
14				74.8 (33.9)		
15				83.0 (37.6)		

The test procedure consisted of setting the combustor inlet pressure, inlet temperature, combustor pressure drop, and combustor fuel flow for each test point in the test point schedule. Steady-state readings of all instrumentation were then recorded. Three complete test runs through the point schedule were made. The first run was conducted with Jet A fuel, the second with ERBS-type fuel, and the third with marine diesel fuel. During the tests a 1255 K (1800° F) limit was imposed on all thermocouple-indicated temperatures to reduce instrumentation attrition and prevent hardware damage.

At the end of each test run a flashback test was conducted to determine if burning could be detected upstream of the swirl cup venturi throat during a fuel flow chop. A flashback test consisted of resetting the combustor inlet conditions specified for Test Point 12. These aero operating conditions were held constant while the fuel flow was rapidly decreased from 112 to 44 kg/hour. When a fuel flow of 44 kg/hr (20 lb/hr) was reached, the fuel flow was rapidly increased back to 112 kg/hour (50.8 lb/hr).

After completion of each test run, the test rig was opened at the aft end for visual inspection of the swirl cup and dome hardware.

6.2.3.3 Experimental Test Results

To stay within the 1255 K (1800° F) limit on all of the thermocouple readings, the overall fuel-air ratio was limited to 0.021 corresponding to a dome fuel-air ratio of 0.101. This fuel-air ratio is significantly higher than that which either the pilot dome or the main dome would experience during normal operation of the engine.

For simulated sea level takeoff (SLTO) operation, peak metal temperatures recorded for the splash plate, dome plate, and sleeve were 1216, 939, and 1107 K (1730°, 1230°, and 1533° F), respectively, at a dome fuel-air ratio of 0.088. Based on these results peak metal temperatures of 989 K (1320° F) for the pilot stage and 1041 K (1414° F) for the main stage would be expected at the FPS sea level takeoff operating conditions. The estimated increase in metal temperature to account for the derated pressure conditions is approximately 60 K (108° F).

The SLTO conditions are the most severe conditions that the combustor will encounter under normal operating conditions. As expected, the recorded peak dome metal temperatures at approach and maximum cruise conditions were significantly lower than those obtained at SLTO conditions and, therefore, represent no threat to dome hardware integrity. Figure 93 presents a plot of the splash-plate metal temperatures recorded versus fuel-air ratio at all three engine operating conditions simulated. Table XXII presents a summary of the expected dome metal temperatures for each of the conditions during full-annular combustor testing.

The results of the dome metal temperature tests, when using ERBS and marine diesel fuels, were nearly identical to those obtained when using Jet A fuel. All dome metal temperatures followed a similar pattern and showed similar dependence on fuel-air ratios. When testing with marine diesel fuel at simulated SLTO conditions and high fuel-air ratio (Point 13), an unstable condition was encountered with the splash plate and sleeve metal temperatures fluctuating widely. The explanation for the fluctuating temperatures was an unstable fuel spray. Fuel spray instability was caused by the combined effect of airflow and fuel-flow momentums. However, because this condition was encountered only with diesel fuel, it is possible that the fuel properties were a contributing factor.

Hardware inspection at the conclusion of testing with marine diesel fuel revealed a thin film of carbon deposited on the splash-plate surface. Since the test rig was not inspected between the ERBS and diesel fuels tests, it is uncertain as to which fuel caused the deposits. Inspection of the hardware after the Jet A fuel tests revealed no carboning.

6.2.3.4 Concluding Remarks

The following conclusions were derived from the dome metal temperature tests:

1. Airflow levels selected for pilot stage dome splash-plate cooling will be adequate in keeping the dome hardware metal temperatures at acceptable levels during the E³ Combustor Development Test Program. Specifically, the 4.3% of total combustor airflow selected for the pilot stage splash-plate cooling is sufficient to maintain metal temperatures below 1100 K (1520° F) under the

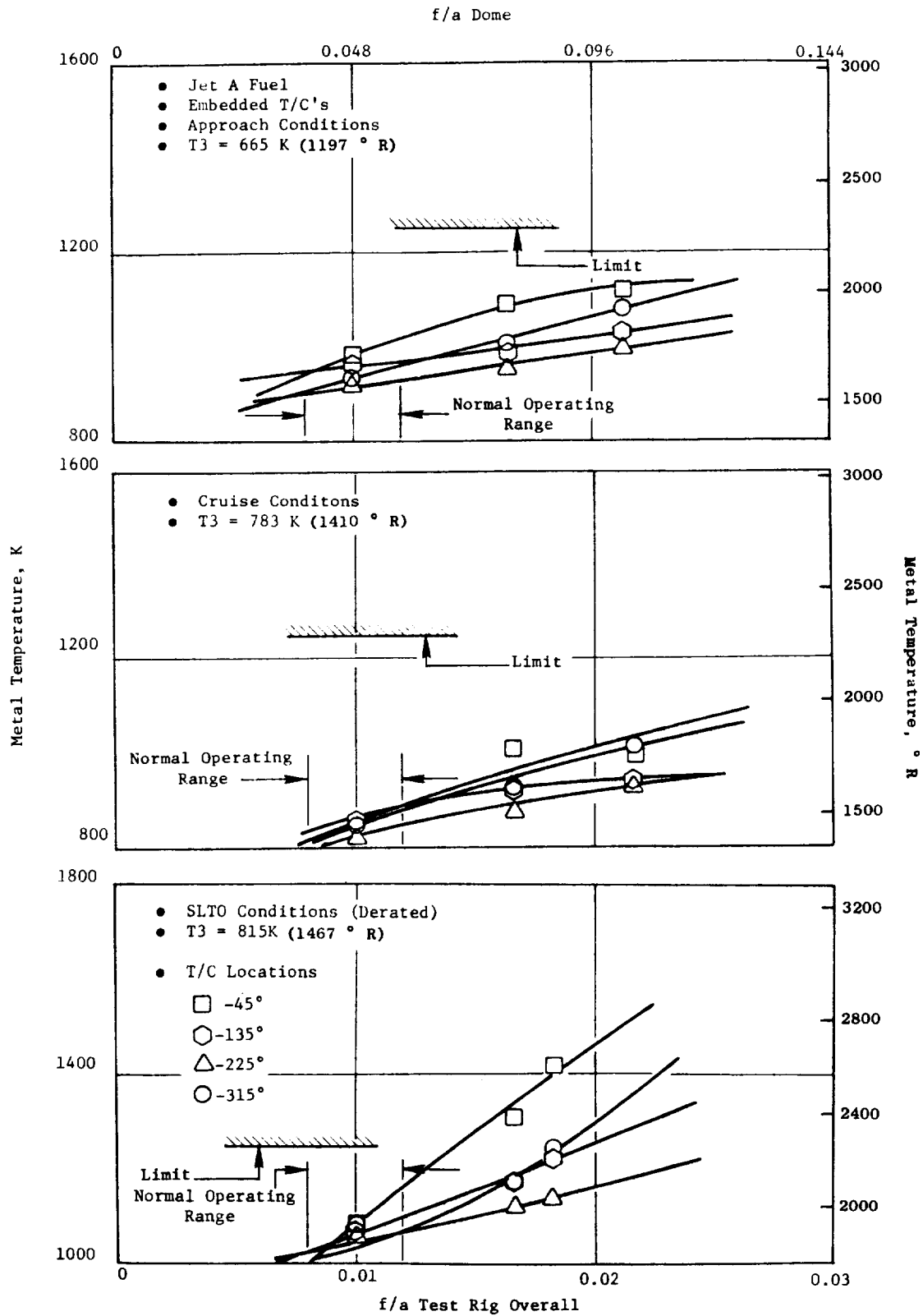


Figure 93. Dome Metal Temperature Test Results.

Table XXII. Estimated Dome Metal Temperatures for Full-Annular Combustor Testing.

	Pilot Stage		Main Stage		Sleeve Temp, K (° F)
	Splash Plate Temp, K (° F)	Dome Plate Temp, K (° F)	Splash Plate Temp, K (° F)	Dome Plate Temp, K (° F)	
Approach	722 (840)	691 (784)	---	---	---
Maximum Cruise	811 (1000)	819 (1014)	850 (1070)	825 (1025)	894 (1150)
SLTO	866 (1100)	889 (1140)	1044 (1420)	966 (1279)	1102 (1524)

most severe combustor operating conditions expected. The main stage dome splash plate has a smaller surface area than the pilot stage; hence, an equal level of splash-plate cooling airflow is expected to be at least as effective as in the pilot stage.

2. The relatively cold fuel impinging on the inside of the venturi provides excellent cooling and maintains the venturi metal temperatures at levels near the combustor inlet air temperature levels.
3. As measured from the tests, dome metal temperatures closely agree with temperatures measured during similar single cup, high pressure tests previously conducted in other development programs.
4. The burning of broad specification fuels, such as ERBS and marine diesel, had only a very minor effect on dome metal temperatures. With the exception of a slight carbon deposition on the splash-plate surface when using these fuels, results from all tests were identical in terms of peak metal temperature location on hardware.

6.2.4 Sector Combustor Tests

6.2.4.1 Introduction

The Sector combustor tests constituted the major part of the E³ sub-component testing program. They were intended to develop the E³ combustor performance characteristics including ignition, emissions, exit temperature profiles, efficiency, and altitude relight. The sector combustor tests were planned to run parallel to the full-annular development program to permit refinement and investigation of any of these performance characteristics without interrupting the full-annular testing effort.

6.2.4.2 Design Approach

A five-cup, 60° annular sector combustor was selected as the test vehicle. This sector combustor was designed to duplicate the aerodynamic flowpath and physical dimensions of the baseline design of the E³ engine combustor. It was fabricated from prototype hardware because of the shorter manufacturing cycle. The prototype swirlers used were machined parts welded together, while the development swirlers were made from castings of the complete swirler unit. The sector combustor liners were fabricated from sheet metal panels, spin formed into shape rather than brazed together, while the development combustor liners were machined from forgings. These differences in manufacture were not expected to result in any performance discrepancies.

The E³ sector combustor featured a double-annular dome design with an outer pilot stage and an inner main stage like the full-annular development combustor. Key design features of the E³ double-annular combustor included an axial primary, radial secondary counterrotating swirl cups, a carbon-preventing venturi, and an emissions reduction sleeve in pilot and main stages. The original design called for 90° included angle sleeves; however, these were modified to 45° angle sleeves in the sector combustor baseline configuration based on the results of the swirl cup investigation. The combustor stages are separated by a film-cooled centerbody structure. Each of the combustor liners consisted of three panels, also film cooled. The baseline inner and outer liner design also featured Panel 2 primary dilution holes and Panel 3 trim dilution holes located in-line with swirl cups. The primary dilution hole design was an extended dilution tube to simulate the thimble design featured on the engine combustor design. Figure 94 shows a cross section of the sector combustor and its key components. Figure 95 presents a photo of the assembled sector combustor hardware. The flow area distribution for the baseline sector combustor is presented in Table XXIII.

The sector combustor design included a split duct diffuser that also duplicated the design and flowpath of the full-annular combustor diffuser including diffuser bleed at the strut location.

6.2.4.3 Test Rig and Instrumentation

A schematic of the E³ sector combustor test rig is shown in Figure 96. The test rig was designed to house the five-cup, 60° sector combustor and to operate at up to 4 atmospheres of pressure and 750 K (890° F) of temperature at the combustor inlet. It consisted of the inlet plenum chamber and the diffuser sector combustor and combustor exit instrumentation sections.

The inlet plenum chamber section of the test rig was attached to the test facility air supply. This plenum consisted of a large-diameter pipe which served as a flow conditioner before the air entered the diffuser passage. The sector combustor diffuser was housed in another plenum just downstream of the inlet plenum. The diffuser was a single-passage inlet with a split duct exit that provided the desired flow split between the two combustor stages. A photo of the diffuser section (discharge) and housing is shown in Figure 97.

ORIGINAL PAGE IS
OF POOR QUALITY

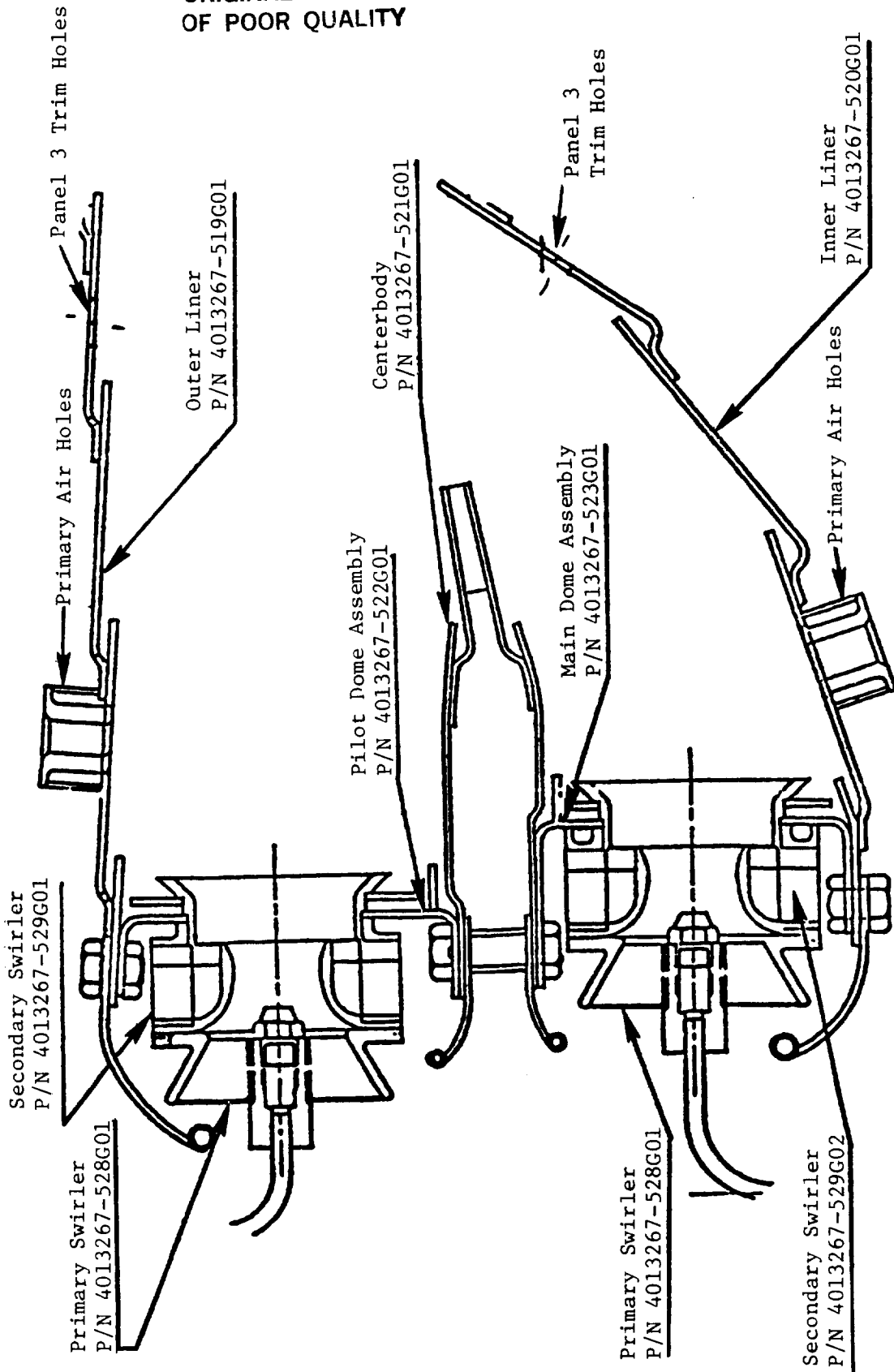


Figure 94. E³ Sector Combustor.

ORIGINAL PAGE IS
OF POOR QUALITY

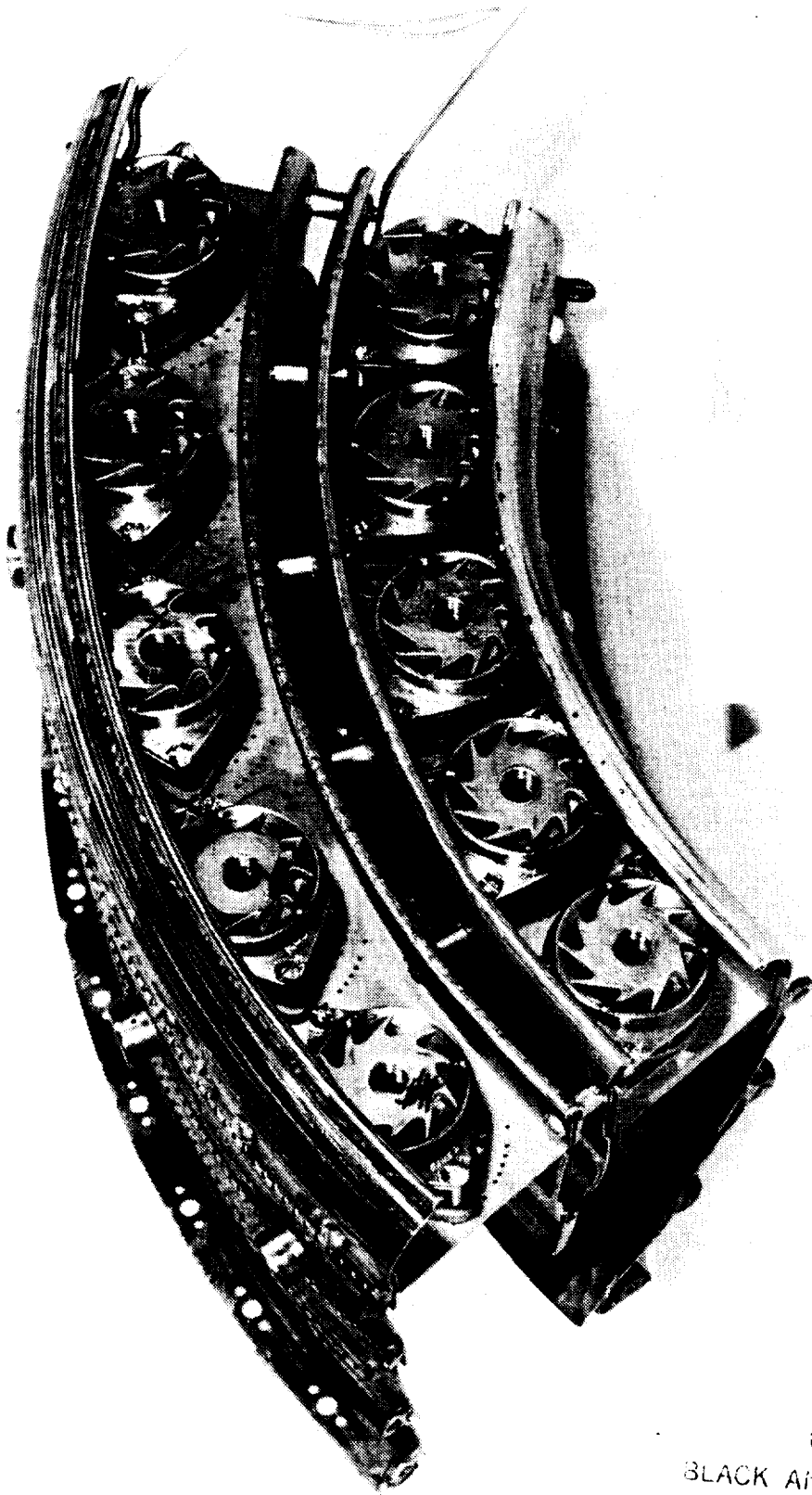


Figure 95. Sector Combustor Hardware.

ORIGINAL PAGE
BLACK AND WHITE PHOTOGRAPH

Table XXIII. Flow Area Distribution for Baseline Sector Combustor Configuration.

<u>Outer Liner</u>	<u>Area, cm² (in²)</u>	<u>Total Area, %</u>
Cooling Row 1 + Ring Cooling	1.84 (0.28)	3.55
Cooling Row 2	1.21 (0.19)	2.33
Cooling Row 3	1.07 (0.16)	2.07
Cooling Row 4	0.66 (0.10)	1.28
Primary Dilution	1.25 (0.19)	2.40
Trim Dilution	0.80 (0.12)	1.54
Total Outer Liner	6.83 (1.06)	13.18
<u>Inner Liner</u>		
Cooling Row 1 + Ring Cooling	1.86 (0.28)	3.60
Cooling Row 2	2.00 (0.31)	3.87
Cooling Row 3	1.47 (0.23)	2.84
Cooling Row 4	1.08 (0.17)	2.09
Primary Dilution	1.81 (0.28)	3.50
Trim Dilution	0.75 (0.12)	1.46
Total Inner Liner	8.03 (1.24)	15.49
<u>Centerbody</u>		
Outer Cooling Row 1 + Ring Cooling	0.72 (0.11)	1.38
Outer Dilution	1.64 (0.22)	3.16
Outer Cooling Row 2	0.37 (0.06)	0.72
Multijet	0.59 (0.09)	1.15
Inner Cooling Row 1 + Ring Cooling	1.16 (0.18)	2.24
Inner Dilution	1.82 (0.28)	3.15
Inner Cooling Row 2	0.59 (0.09)	1.15
Total Centerbody	6.90 (1.07)	13.93
<u>Pilot Dome</u>		
Swirl Cups	9.77 (1.51)	18.86
Splash-Plate Cooling	3.94 (0.61)	7.61
Total Pilot Dome	13.71 (2.13)	26.47
<u>Main Dome</u>		
Swirl Cups	13.68 (2.12)	26.40
Splash-Plate Cooling	2.66 (0.41)	5.13
Total Main Dome	16.34 (2.53)	31.53
Total Area	51.81 (8.03)	100

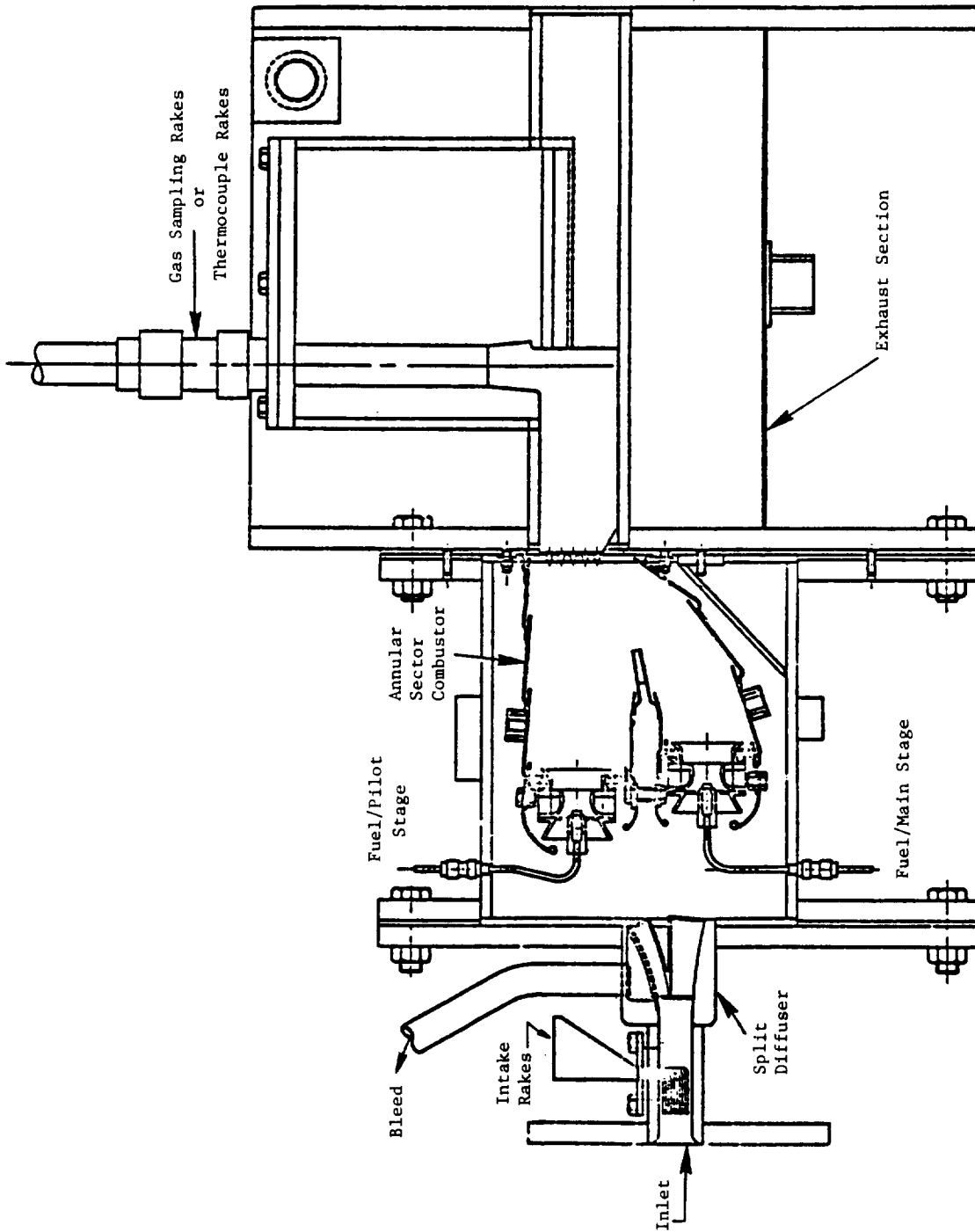


Figure 96. E³ Sector Combustor Test Rig.

ORIGINAL PAGE
BLACK AND WHITE PHOTOGRAPH

ORIGINAL PAGE IS
OF POOR QUALITY.

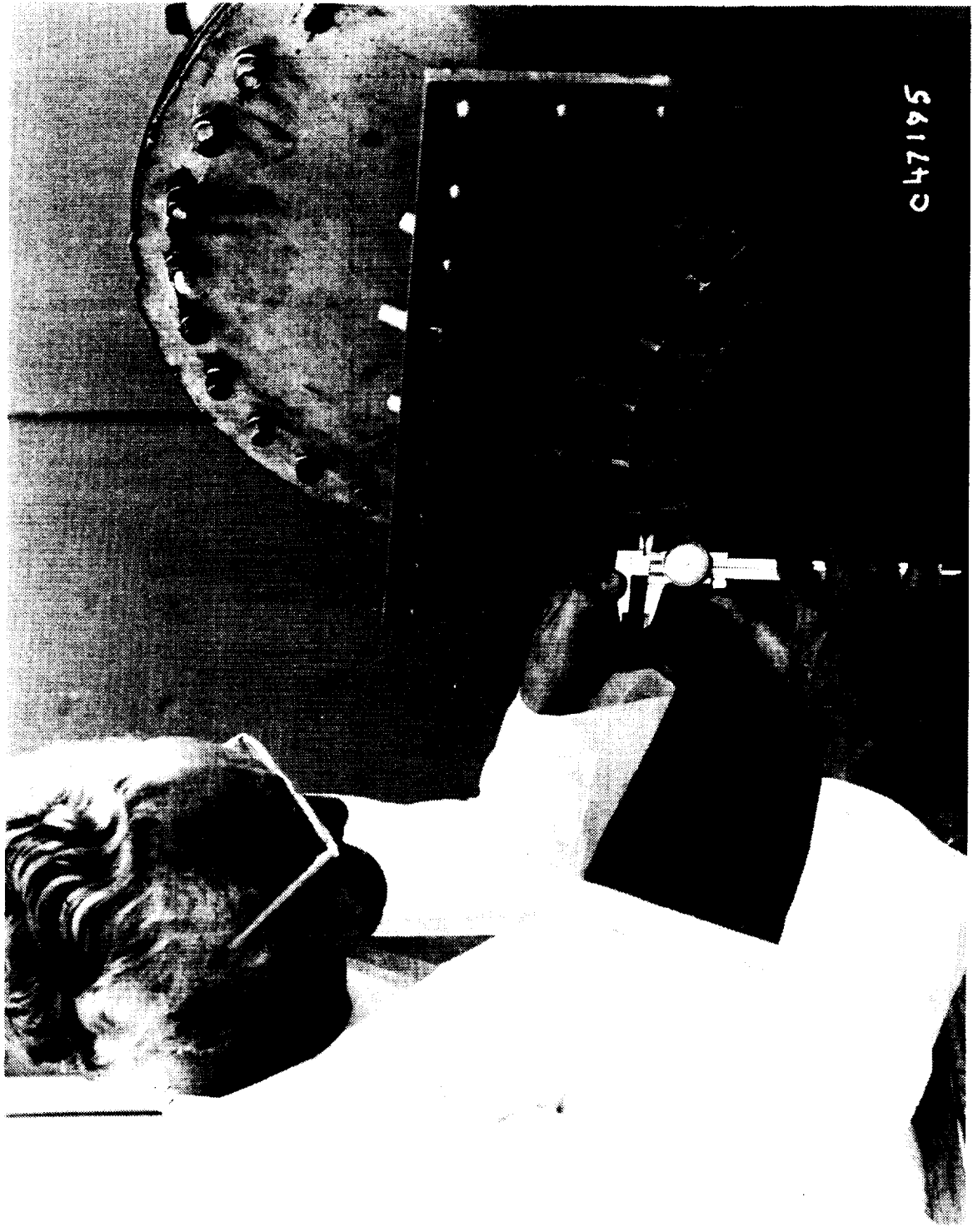


Figure 97. Sector Test Rig Inlet Diffuser.

The combustor housing section was attached to the diffuser discharge and contained the fuel delivery system and the sector combustor. The fuel was supplied to the 10 fuel nozzles through a double-manifold system. One manifold supplied the five pilot stage nozzles (outer annulus), the other supplied the five main stage (inner annulus) nozzles. The fuel manifold system could be operated independently. The instrumentation section of the test rig housed the rake assembly used to measure exhaust gas temperatures or to obtain gas samples for emissions measurements, depending on the type of rake installed.

Test rig instrumentation included various thermocouples and pressure probes in addition to the exhaust rake system. The thermocouples and pressure probes were used to obtain temperature and pressure data critical to rig operation, combustor performance, and mechanical integrity. The pressure measurements included (1) diffuser inlet total and static pressures, (2) diffuser exit total and static pressures, (3) dome upstream total and dome downstream static pressures, and (4) liners hot- and cold-side static pressures. The total pressure at the combustor exit was measured using the gas sampling rake elements. These pressure measurements were employed in calculating combustor inlet velocity, pressure drops of the domes and liners, and overall combustor pressure drop.

Temperature measurements were made of the rig inlet airflow and on inner/outer liner surfaces and on centerbody surfaces. Combustor exit temperature profiles were measured using four chromel-alumel thermocouple rakes installed in the instrumentation section of the test rig. Each of the exit rakes had seven thermocouples equally spaced on the leading edge of the rake and covered the entire sector combustor exit passage height. Several thermocouples were also located downstream of the instrumentation section in the facility exhaust system to monitor the facility operation.

The sector combustor exhaust gas samples were extracted from the exhaust flow by means of four gas sampling rakes installed, when required, in the instrumentation section of the test rig. Each of the gas sampling rakes had five sampling elements. The four rakes could be individually sampled or manifolded together to provide an average circumferential sample. Each of the five sampling elements was designed with a quick-quenching probe tip. In this

design, the chemical reaction of the gas sample is quenched as soon as the sample enters the rake. Quenching is necessary to suppress any further chemical reaction of the gas sample within the sampling lines. Both water cooling of the rake body and steam heating of the gas sample lines within the rake were incorporated into the design. Water cooling of the rake body was required to protect the rake from damage due to the high temperature environment created at the combustor exit. Steam heating of the gas sampling lines was employed to prevent condensation of hydrocarbon compounds and water vapor within the sampling lines. A photo of a gas sampling rake is shown in Figure 98 and a schematic of typical sampling element is in Figure 99.

6.2.4.4 Test Facility

All E³ sector combustor testing was conducted in the Advanced Combustion Laboratory Facility, GE-Evendale Building 306. This facility is equipped with the inlet ducting, exhaust ducting, controls and instrumentation necessary for conducting sector combustor tests. The range of operating conditions obtainable in this facility is limited because of the airflow and heater capacity currently available. Airflow levels up to 2.8 kg/sec (6.17 lb/sec) can be supplied to the facility from a large compressor, plus an additional 1.8 kg/sec (3.97 lb/sec) can be supplied by the Shop Air System. Combustor inlet air temperatures above ambient are obtained using the facility liquid fueled indirect-air preheater. The preheater has the capability to heat 1.35 kg/sec (2.98 lb/sec) airflow to 700 K (800° F). Jet A fuel was supplied to the sector combustor test rig by a pipeline from storage tanks located adjacent to the facility. Instrumentation cooling and exhaust gas quenching was accomplished using the facility domestic water supply with pressure boost where necessary.

In addition, the facility has the capability of simulating altitude conditions with the aid of a steam ejector system. This system allows the operator to reduce test rig pressure to 0.30 atmospheres. However, the facility does not have cold air or cold fuel capability. Therefore, all the altitude ignition testing was conducted at ambient air and fuel temperatures.

Test conditions were monitored using the facility instrumentation readout equipment. Airflows were monitored by manometer readings of pressure drops

ORIGINAL PAGE
OF POOR QUALITY

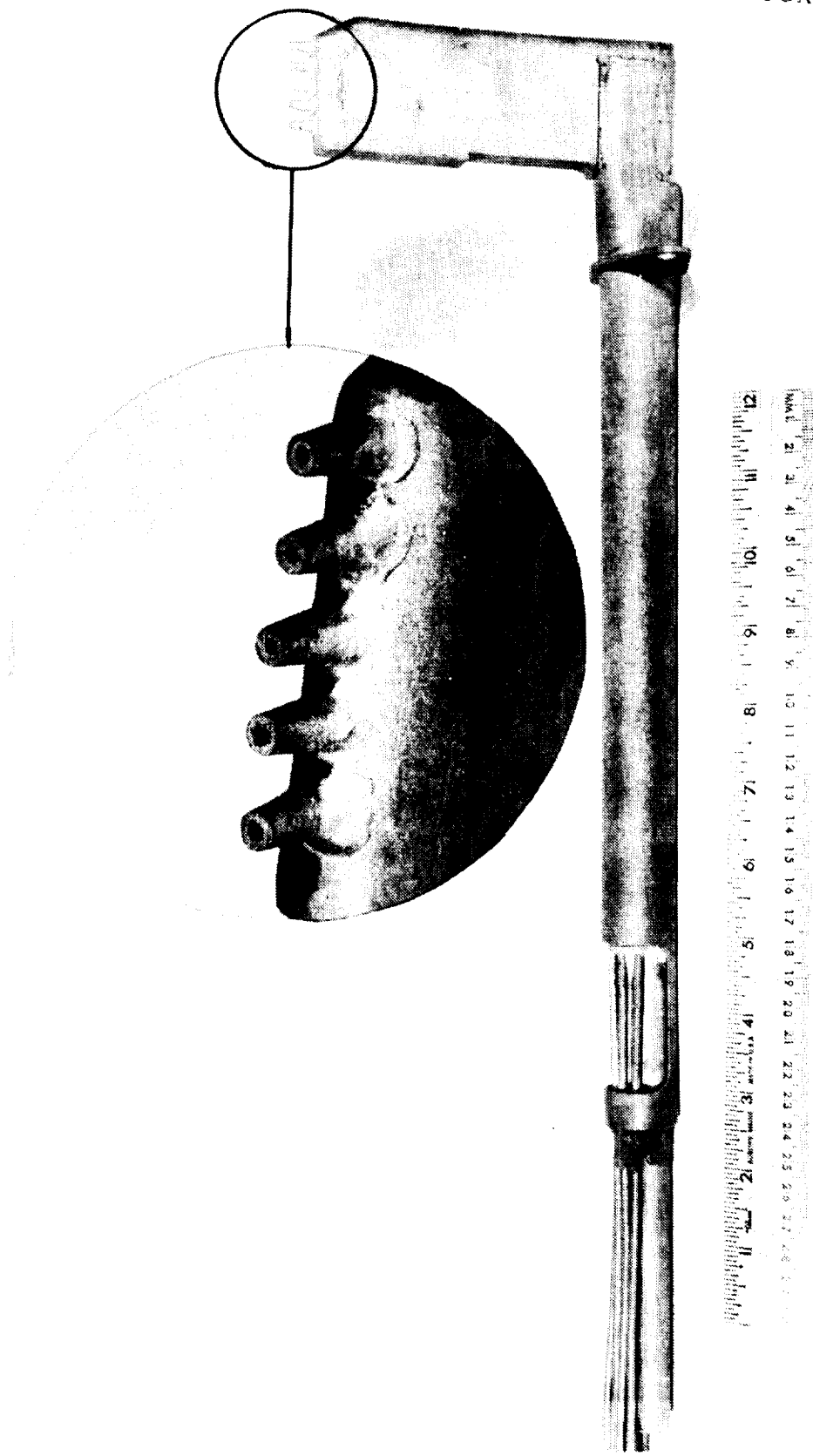


Figure 98. Sector Test Rig Gas Sampling Rake.

ORIGINAL PAGE
BLACK AND WHITE PHOTOGRAPH

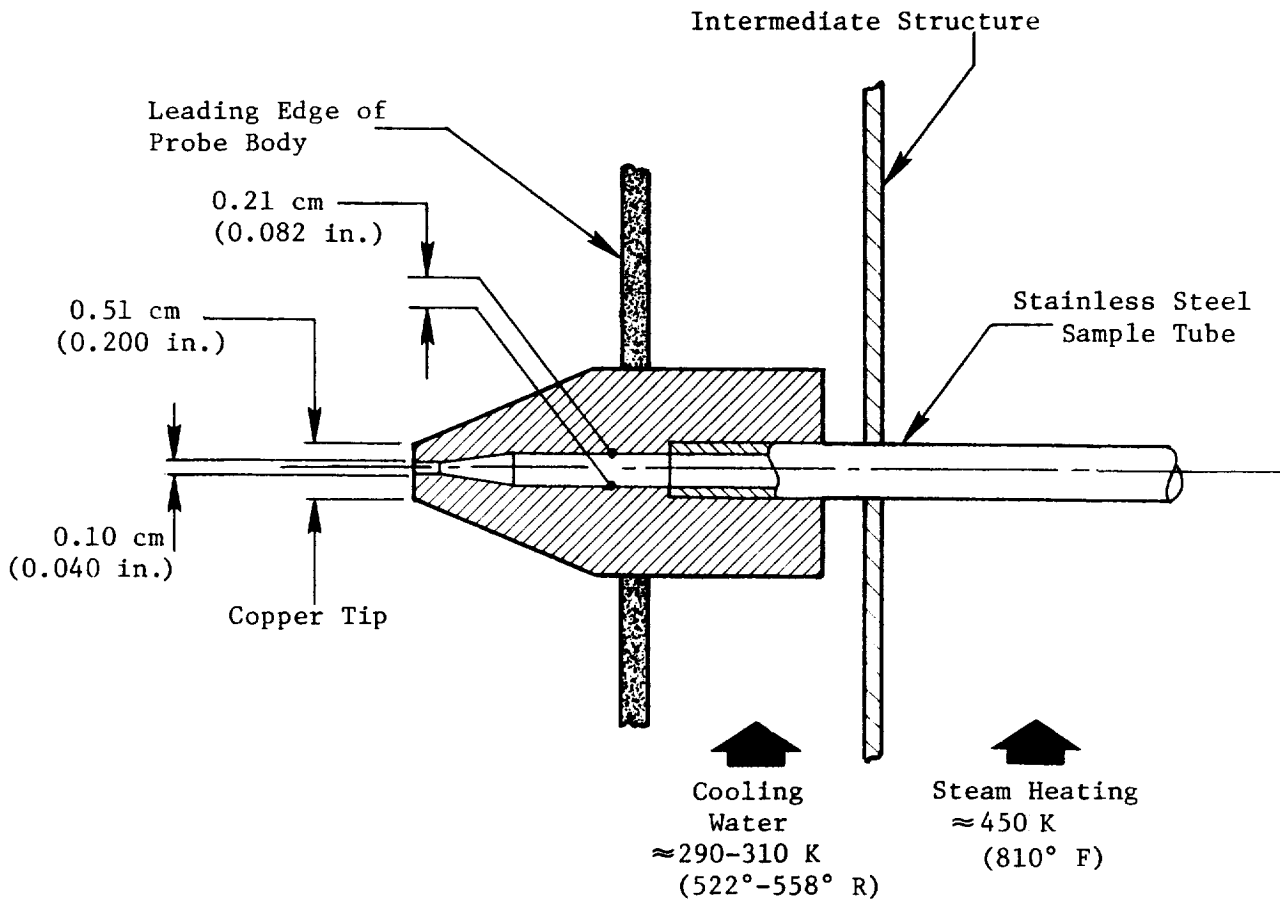


Figure 99. Schematic of Typical Rake Sampling Element.

across a standard ASME orifice in the air supply line. Fuel flows were metered by turbine-type flowmeters whose signal was input to an electronic frequency readout meter. Test rig pressures were monitored by either manometers or pressure gages, and thermocouple readings were obtained by self-balancing potentiometer recording instruments.

Sector combustor emissions were measured using the CAROL (Contaminants Are Read On Line) gas analysis system located in the test facility. This system consisted of the following instruments:

- Beckman Model 402 total hydrocarbon analyzer (flame ionization detector)
- Beckman Model 315-A carbon monoxide and carbon dioxide analyzer (NDIR)
- Beckman Model 915 No_x analyzer (chemiluminescence with converter, trap required).

Extracted exhaust gas samples were transmitted to this analysis equipment and the measured emissions levels were recorded on strip charts. An adequate supply of bottled calibration gases for the CAROL system was maintained throughout the emissions testing. A qualified technician calibrated and operated the CAROL system throughout the duration of data acquisition for each emissions test.

6.2.4.5 Test Procedures

The conditions selected for conducting the sector combustor ground start ignition tests simulated E³ combustor inlet conditions at various core speeds from the E³ sea level standard day start model. The initial tests were conducted at atmospheric conditions with the instrumentation section of the test rig removed to allow for visual observation and monitoring of the ignition performance. The procedure for these tests entailed the following: An air-flow level and temperature simulating a set of conditions from within the E³ start model were set. The ignition source was activated and the pilot stage fuel flow was slowly increased. The fuel flow was recorded when at least one

cup was lit. With the ignition source now deactivated, fuel flow was further increased and recorded where each cup was lit until full propagation (all five cups) of the pilot stage was achieved. Then the fuel flow was decreased and the level at which each cup extinguished was recorded. The procedure was repeated until sufficient data repeatability was obtained.

In 1979 the engine startup procedure was revised to require operating the combustor on both stages up to idle speed, at which point the main stage would be shut off. This required crossfiring the main stage as soon as the pilot stage was fully propagated. Hence, a major portion of the ground start ignition tests were devoted to developing crossfire performance. Once the pilot stage was fully propagated, the fuel flow was set at a level slightly above the pilot lean blowout limit, when main stage fuel flow was introduced and increased slowly until one or more main stage cups were lit. The fuel flow was recorded, then recorded again when all cups were lit. Main stage lean blowout fuel flow levels were established in a procedure similar to that followed for the pilot stage.

For promising sector combustor configurations, a pressure ignition test was conducted with the instrumentation section of the test rig attached. These tests followed a similar procedure to the atmospheric ignition tests, except in this case ignition was determined by monitoring thermocouples situated at the exit plane of the sector combustor downstream of each swirl cup. Actual pressures from the E³ start cycle were set for the pressure ignition tests. Table XXIV presents the test points and corresponding operating conditions for the ignition tests.

Sector combustor performance evaluation tests consisted of conducting exit temperature surveys at ground start conditions for the calculation of combustion efficiencies and at simulated SLTO conditions to establish exit temperature profiles. Other data obtained during these tests included pressure drops and metal temperatures. The temperature surveys were conducted using the four 7-element controls/accessories thermocouple rakes located in the instrumentation section of the test rig. During ground start efficiency tests, various core speeds, ranging from 46% to 77%, were evaluated with either pilot only or staged operation. The sea level takeoff temperature profile

test conditions were limited by the available facility pressure level (~4 atmospheres). The proper inlet temperatures, combustor fuel-air ratios, and Mach numbers were set in the test rig. Exit temperature profiles were then recorded for various pilot-to-main-stage fuel flow splits at a constant overall combustor fuel-air ratio.

Table XXIV. Sector Combustor Ignition Test Point Schedule.

- Based on E³ 9/27/79 Start Model
- Sector Combustor Flow Conditions (Annular Flow/6.0)

<u>Pressure Test</u>				
XNRH	P ₃	T ₃	W _c	$\frac{W_c \sqrt{T_3}}{P_3}$
%	atm	K (° F)	kg/sec (lb/sec)	
21	1.020	295 (71)	0.21 (0.46)	3.54
58	1.837	383 (230)	0.57 (1.26)	6.07
70	2.463	427 (309)	0.79 (1.74)	6.63

<u>Atmospheric Test</u>				
XNRH	P ₃	T ₃	W _c	$\frac{W_c \sqrt{T_3}}{P_3}$
%	atm	K (° F)	kg/sec (lb/sec)	
21	1.0	295 (71)	0.20 (0.44)	3.54
32	1.0	314 (105)	0.25 (0.55)	4.43
46	1.0	344 (160)	0.28 (0.62)	5.19
58	1.0	383 (230)	0.31 (0.68)	6.07
70	1.0	427 (309)	0.32 (0.71)	6.63

All sector combustor instrumentation readings, including static pressures, total pressures, and thermocouples, were recorded throughout these tests. The recorded data was used in calculating dome and liner pressure drops, overall combustor pressure drops, and the conditions for and locations of highest metal temperatures.

The test conditions for the sector combustor emissions tests included low power, as well as simulated high power operating conditions along the standard day sea level static E³ FPS operating cycle. The low-power conditions included ground idle at 4% and 6% of SLTO power with the pilot stage only fueled, and the EPA-defined 30% power (approach) operating condition with both pilot only and staged combustor operation. The high power conditions tested simulated the 85% power (climbout) and SLTO operating conditions in the staged combustor operating mode.

For low power emissions tests, true combustor operating conditions were duplicated in the sector combustor test rig. However, for higher power emissions tests the combustor flow function was simulated by derating the test rig inlet conditions in order to be consistent with the test facility limits. For all of the sector combustor test rig conditions, data were obtained over a range of combustor fuel-air ratios. A summary of the test point schedule for the emissions tests is presented in Table XXV.

The combustor inlet conditions and corresponding fuel-air ratio for each point were set, then the fixed combustor instrumentation readings were recorded. Exhaust gas samples were extracted by using the gas sampling rakes, and the pollutant emissions data from the gas analysis system was recorded. The normal procedure was to obtain a ganged sample from all four rakes simultaneously. However, for points of particular interest, individual samples from each rake were obtained and analyzed, as well.

The altitude windmilling characteristics for the E³ engine were not defined prior to testing, therefore, the CF6-50 engine windmilling map was used as a substitute in order to investigate the altitude relight capability of the E³ sector combustor. Actual pressures at altitude were set during these tests. However, ambient temperature inlet air and fuel were used. The tests consisted of determining the ignition and lean blowout limits over a

Table XXV. Sector Combustor Emissions Test Point Schedule.

Cycle Condition	P3 atm	T3 K(° F)	W3 kg/s (pps)	Wbleed kg/s (pps)	Wf (pilot) kg/hr (pph)	Wf (total) kg/hr (pph)	f/a Overall	$\frac{Wf(pilot)}{Wf(total)}$
4% Idle	3.40	466 (379)	1.45 (320)	0.11 (0.24)	48 (105.8)	0	0.0100	1.0
	3.40	466 (379)	1.45 (320)	0.11 (0.24)	65 (143.3)	0	0.0135	1.0
	3.40	466 (379)	1.45 (320)	0.11 (0.24)	96 (211.6)	0	0.0200	1.0
	3.40	466 (379)	1.45 (320)	0.11 (0.24)	120 (264.6)	0	0.0250	1.0
6% Idle	4.1	497 (434)	1.75 (3.86)	0.13 (0.29)	58 (127.9)	0	0.0100	1.0
	4.1	497 (434)	1.75 (3.86)	0.13 (0.29)	71 (156.5)	0	0.0122	1.0
	4.1	497 (434)	1.75 (3.86)	0.13 (0.29)	93 (205.0)	0	0.0160	1.0
	4.1	497 (434)	1.75 (3.86)	0.13 (0.29)	116 (255.7)	0	0.0200	1.0
30% Approach	4.1	497 (434)	1.75 (3.86)	0.13 (0.29)	145 (319.7)	0	0.0250	1.0
	3.40	636 (685)	1.33 (2.93)	0.10 (0.22)	63 (138.9)	0	0.0141	1.00
	3.40	636 (685)	1.33 (2.93)	0.10 (0.22)	18 (39.7)	27 (59.5)	0.0100	0.40
	3.40	636 (685)	1.33 (2.93)	0.10 (0.22)	25 (55.1)	32 (70.5)	0.0141	0.40
85% Climbout	3.40	636 (685)	1.33 (2.93)	0.10 (0.22)	36 (79.4)	54 (119.0)	0.0200	0.40
	3.40	700 (800)	1.22 (2.69)	0.09 (0.20)	37 (81.6)	54 (119.0)	0.0140	0.40
	3.40	700 (800)	1.21 (2.67)	0.09 (0.20)	23 (50.7)	34 (75.0)	0.0140	0.40
	3.40	700 (800)	1.21 (2.67)	0.09 (0.20)	29 (63.9)	44 (97.0)	0.0180	0.40
Sea Level Takeoff	3.40	700 (800)	1.21 (2.67)	0.09 (0.20)	39 (86.0)	59 (130.1)	0.0244	0.40
	3.40	700 (800)	1.21 (2.67)	0.09 (0.20)	45 (99.2)	68 (150.0)	0.0280	0.40
	3.40	700 (800)	1.21 (2.67)	0.09 (0.20)	29 (63.9)	69 (152.1)	0.0244	0.30
	3.40	700 (800)	1.21 (2.67)	0.09 (0.20)	49 (108.0)	49 (108.0)	0.0244	0.50
Sea Level Takeoff	3.40	700 (800)	1.21 (2.67)	0.09 (0.20)	44 (97.0)	65 (143.3)	0.0280	0.40
	3.40	700 (800)	1.21 (2.67)	0.09 (0.20)	34 (75.0)	51 (112.4)	0.0220	0.40
	3.40	700 (800)	1.21 (2.67)	0.09 (0.20)	22 (48.5)	34 (75.0)	0.0244	0.40
	3.40	700 (800)	1.21 (2.67)	0.09 (0.20)	29 (63.9)	44 (97.0)	0.0244	0.40

selected range of windmilling conditions. The sector combustor inlet conditions were set, fuel flow initiated, and fuel flow levels at which each cup ignited were recorded. Then fuel flow is slowly decreased, and levels at which each cup was extinguished were recorded. For some conditions where ignition was unsuccessful, inlet pressure was slowly increased while holding a constant fuel flow until ignition was obtained.

6.2.4.6 Data Reduction Procedures

The recorded data of the ground start ignition tests and the altitude relight tests were simply reduced by calculating ignition and lean blowout fuel-air ratios for each test point and presenting the results as plots of fuel-air ratios versus either core speed or combustor inlet conditions.

Exit temperature profiles were obtained from plots of the thermocouple rake data to which a radiation correction factor had been applied. Combustion efficiencies were determined from rake data by calculating the ratio between the average of the measured exit temperatures and the theoretical gas temperature for the test fuel-air ratio.

Various sector combustor pressure drops and airflow distributions were calculated from recorded test data and the known effective flow areas of the sector combustor hardware by using a computer data reduction program.

Emissions data reduction was accomplished using two data reduction computer programs. One program performed curve-fit calculations on the CAROL system calibration data obtained at the start of an emissions test. Calibration checks of the gas analysis system were performed before and after each emissions test run to prevent data drift. During a test, the measured emissions data were recorded on chart recorders contained within the CAROL system. The emissions data were additionally recorded on test log sheets. Following the completion of each test run, the emissions data, along with the sector combustor performance data, were input into the other data reduction program where the reduction of the raw emissions data to emissions indices was performed. The calculation equations used in this program were basically those contained in SAE ARP 1256. In these calculations the CO and CO₂ concentrations were corrected for the removal of water from the sample before

analysis. A fuel hydrogen-to-carbon atom ratio of 1.92, representing Jet A fuel, was used in these calculations. Calculated combustion efficiency, sample fuel-air ratio, and an overall emissions index were also obtained from the data reduction program. The overall emission index represents a weighted average of the values obtained from each individual gas sampling rake and is defined as

$$EI_j \text{ (Overall)} = \frac{\sum_{i=1}^N (EI_j)_i * (F/A \text{ Sampled})_i}{\sum_{i=1}^N (F/A \text{ Sampled})_i}$$

The j subscript refers to the identity of the gaseous pollutant (CO, HC, or NO_x), and the i subscript refers to the individual rakes where N represents the total number of gas sampling rakes. Expressing the average of the emissions in this form reduces the influence of very lean combustion zones within the combustor where the concentrations of gaseous pollutants is low, but where the calculated emissions indices are quite high. These weighted average emissions values are presented in the numerous data tables and figures of this report.

At the high-power operating conditions where the combustor inlet pressure, temperature, and airflow were derated due to facility limitations, the measured emission levels were adjusted to reflect the actual engine cycle conditions. The adjustment relations used are defined in Appendix D.

6.2.4.7 Test Configurations

A total of seven basic configurations were tested during the E³ Sector Combustor Test Program. Some of these configurations were subjected to "piggy-back" tests, with one or more of their features somewhat varied to investigate specific performance aspects. A brief description of each of the configuration's features (relative to the baseline configuration) is presented below.

The following modifications to the baseline configuration design were incorporated for the Mod I configuration:

- Primary dilution holes in the outer and inner liners were relocated to between swirl cups from in-line with cups in the baseline configuration. This modification was introduced in order to achieve a more uniform fuel-air mixture balance between the two zones.
- Ninety-degree-angle sleeves replaced the 45° angle sleeves featured in the baseline design. These wider angle sleeves were expected to produce a more dispersed fuel spray; this was desired in spite of anticipated problems with spray instability. The 45° sleeve had been selected based on swirl cup investigation results. But when installed in the sector combustor, these sleeves appeared to produce a somewhat more narrow spray angle than was desired, leading to a fuel-rich zone in between the cups. The wider angle sleeve did produce a more uniform primary zone fuel-air ratio distribution and had no observable instability problems.
- Pilot dome splash plate cooling was reduced by approximately 40% to bring it closer to the originally intended design level of 4.3% of the combustor airflow. This change was expected to help the CO emissions, particularly at idle conditions.

The Mod II configuration featured the incorporation of the E³ full-annular development combustor-type swirl cups to replace the prototype swirlers. Furthermore, this configuration had a modified airflow distribution characterized by a reduction in the pilot stage swirl cup airflow and by an increase in the main stage for the purpose of reducing NO_x emissions at high power conditions.

The Mod III configuration of the E³ sector combustor featured changes that were directed primarily at improving ignition performance. Key changes included a substantially reduced main stage swirl cup airflow and the use of full-annular development-type fuel nozzles in both stages in order to duplicate the full-annular combustor fuel system design. In addition, a crossfire tube, similar in design to that of the full-annular combustor, was incorporated into the centerbody to provide an ignition source for the main stage. Up to this point, main stage ignition had been achieved by means of an auxiliary ignition system installed through the sector combustor sidewall. The 90° angle sleeves were retained in the Mod III because none of the anticipated fuel spray instability problems had occurred. In order to determine the effects of

the fuel nozzle spray angle and the fuel nozzle shroud air on CO and HC emissions levels, several fuel nozzle configurations were tested in the Mod III configuration for emissions at the 6% ground idle conditions. There were three variations: Mod III-A differed from Mod III by blocking off the fuel nozzle shroud air, Mod III-B featured the prototype simplex peanut fuel nozzles in place of the development nozzles, and Mod III-C utilized air shrouded, development-type fuel nozzles rated at 23 kg/hr (50.7 lb/hr).

For the Mod IV configuration, the pilot stage primary dilution airflow was increased to double the Mod III configuration level in order to provide more penetration and enhance mixing of the fuel and air to reduce idle emissions. Furthermore, the centerbody multijet length was shortened by approximately 1.78 cm (0.70 in.) for mechanical considerations. These two design changes were evaluated during Mod IV configuration tests of the sector combustor, with emphasis placed on evaluating whether a shorter centerbody would adversely affect the ignition and low power emissions performance.

The Mod V configuration of the E³ sector combustor featured a substantial increase in the main stage primary dilution effective area. This increase resulted in an approximate 7% increase in total sector combustor effective flow area and caused a reduction in the pilot stage swirl cup airflow as a percentage of total airflow. This reduction in swirl cup airflow was expected to further reduce idle CO and HC emissions, while the increase in main stage primary dilution flow was expected to reduce NO_x emissions at high power combustor operating conditions.

The Mod VI configuration featured a simultaneous reduction in the swirl cup airflow level and an increase in the primary dilution airflow level of the sector combustor pilot stage. The swirl cup airflow was reduced by blocking 3 of the 12 vane passages for each of the secondary swirlers. This resulted in a reduction of approximately 20% of the pilot stage swirl cup airflow in relation to the Mod V configuration. The pilot stage dilution airflow was increased by opening up the flow area of the dilution holes in the outer liner and the pilot stage side of the centerbody. In addition, 50% of the outer liner Row 1 and corresponding centerbody cooling holes, located in-line with

swirl cups, were closed off. All of these modifications were intended to produce a more uniform fuel-air distribution within the pilot stage dome of the sector combustor.

Five variations on the Mod VI configuration were tested in an effort to identify any quick design changes that could be implemented in the full-annular combustor design for the purpose of improving the main stage crossfire performance. In Mod VI-A, every other passage in the main stage primary swirler was blocked and the main stage splash-plate cooling flow was reduced by approximately 30%. This change was intended to enrich the main stage dome and improve the crossfire performance.

For Mod VI-B, the blockage from the pilot stage secondary swirler was removed to permit a stronger recirculation zone and possibly force a larger flame through the crossfire tube into the main stage. In Mod VI-C, an extension was added to the main stage side of the crossfire tube. The purpose of the extension was to shelter the flame passing through the tube and prevent it from being swept downstream by the swirl cup flow. Another extension, added to the pilot stage side of the crossfire tube, made up the Mod VI-D configuration. The purpose of this extension was to capture the flame from the pilot stage and force it into the crossfire tube.

The crossfire tube geometry was again modified for the Mod VI-E configuration. The originally cylindrical tube was redesigned into a D-shaped cross section with an area equal to that of the circular design. The intent of this modification was to move the flow area of the crossfire tube as far forward on the centerbody as possible.

A summary of the test configurations, their features, their effectiveness, and their estimated airflow distributions are provided in Appendix E.

6.2.4.8 Ignition Test Results

The atmospheric ignition test results on the baseline configuration indicated that excessively high fuel-air ratios were required to light the pilot stage with ignition not attainable at the 21% core speed conditions.

Full propagation was not possible for any of the test conditions in the E³ engine starting schedule. For those cups that did light, the fire appeared to be concentrated in between swirl cups, rather than evenly distributed across the entire sector combustor. Figure 100 is a plot of the pilot stage light off and lean blowout fuel-air ratios versus the percent core speed for the baseline configuration.

Attempts to crossfire the main stage during baseline configuration tests were unsuccessful; however, the crossfire tube had not yet been incorporated into the centerbody design, so crossfire had to occur across the tip of the centerbody.

As was the case for the baseline configuration tests, the initial Mod I ignition tests were conducted using a hydrogen torch as the ignition source. An improvement of approximately 20% in the pilot stage ignition performance was obtained with the Mod I configuration. Furthermore, full propagation was achieved at all test points, and visual observation of the fire at the sector combustor exit indicated a more uniform flame. The pilot stage ignition test results for this configuration are shown in Figure 101. The improvement in the ignition performance was attributed to reducing the splash plate cooling airflow in the pilot stage and the wider angle sleeves. On the other hand, flame uniformity was attributed to relocating the primary dilution to between swirl cups.

Using a spark plug igniter in place of the hydrogen torch in a subsequent test on the Mod I configuration resulted in approximately the same light off and lean blowout fuel-air ratio. Because the crossfire tube was not yet incorporated into the design, no crossfire attempts were made on this configuration. However, the main stage ignition performance was investigated using a hydrogen torch igniter installed through the sector sidewall. The results are shown in Figure 102. Main stage light-off fuel-air ratios were slightly higher than those of the pilot stage due to the higher velocities in the main stage dome.

Since the proposed E³ start sequence required the obtaining of ignition in both pilot and main stages at a selected core speed, it was necessary for

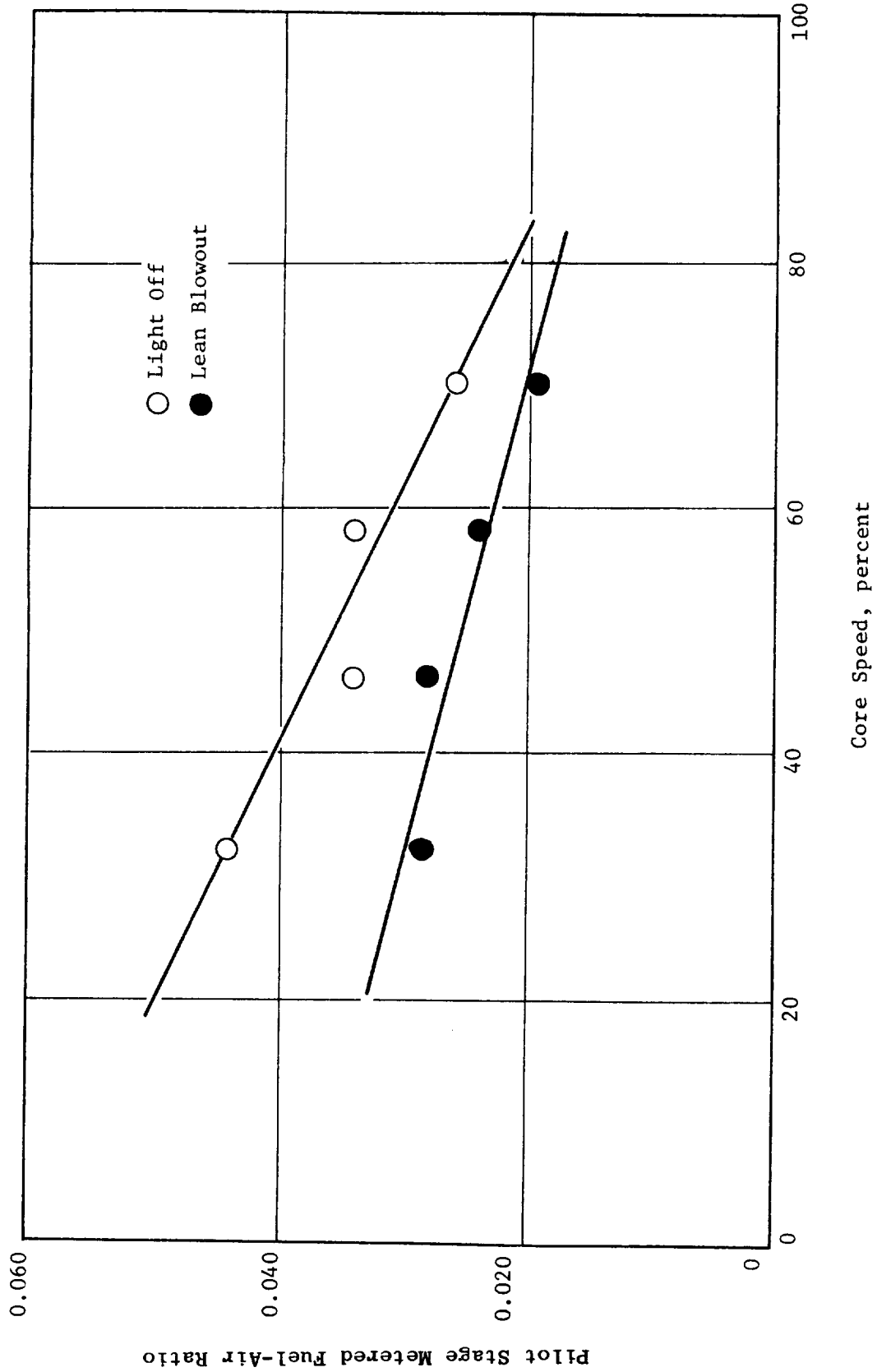


Figure 100. Sector Combustor Baseline Ignition Results, Pilot Stage.

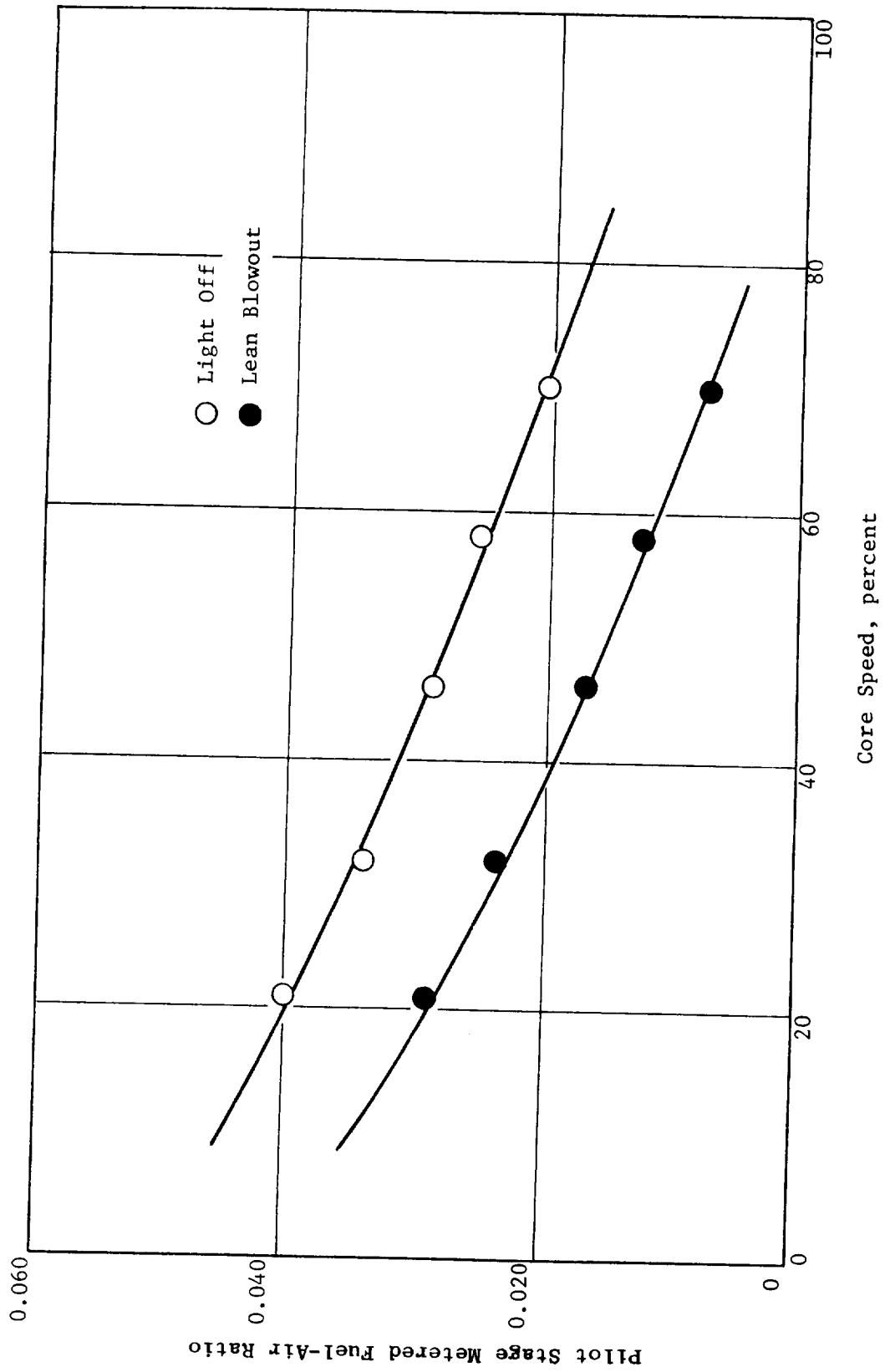
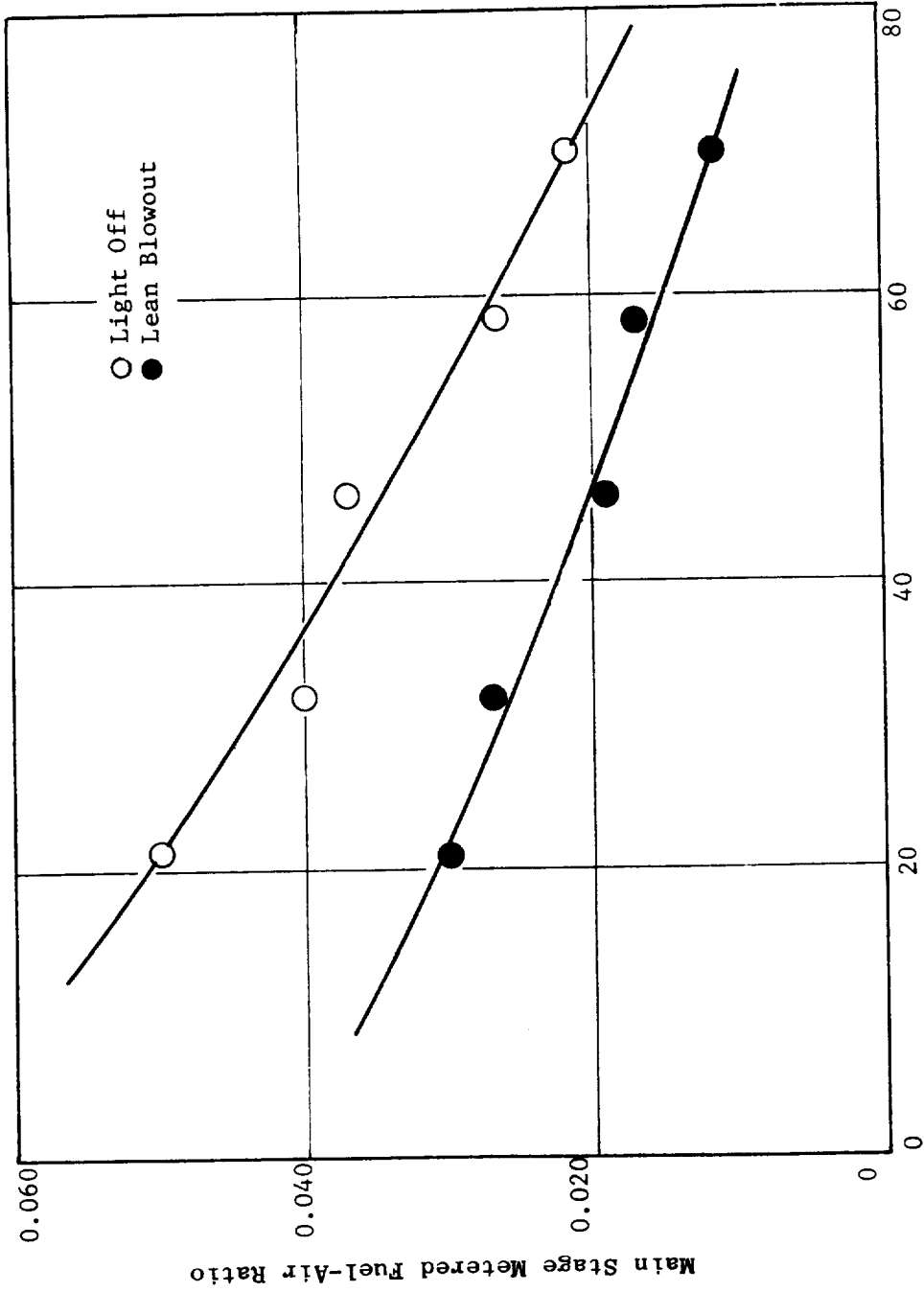


Figure 101. Sector Combustor Mod I Ignition Results, Pilot Stage.

ORIGINAL PAGE IS
OF POOR QUALITY



Core Speed, percent

Figure 102. Sector Combustor Mod I Ignition Results, Main Stage.

the sum of the pilot stage lean blowout and main stage light-off fuel-air ratios to fall within the specified operating line at that core speed. Figure 103, which plots the results for the Mod I configuration, clearly indicated that further improvement was still required to satisfy this start requirement.

The Mod II configuration, which featured development combustor-type swirl cups in both stages, produced disappointing ignition results. Light-off and lean blowout fuel-air ratios obtained for the pilot as well as the main stage were higher than those obtained with the Mod I configuration. Visual observation of the fire at the sector exit indicated no signs of nonuniformity of the fuel spray. Yet, posttest fuel spray visualization tests of the swirl cup fuel nozzle assembly revealed that the development combustor-type swirlers produced a significantly narrower fuel spray angle than that obtained with the prototype swirlers. This narrow fuel spray limited the ignition performance by causing the discharged fuel to be too far away from the ignition source.

Results of Mod III ignition tests were much more encouraging than those of the Mod II results. Figure 104 shows that a reduction of approximately 45% of the light-off and lean blowout fuel-air ratios of the pilot stage was obtained. As expected, main stage ignition performance approached the performance of the pilot stage due to the similarity in the swirl cup airflow levels. The improvement in pilot stage ignition performance was largely attributed to the use of the development-type fuel nozzles instead of the prototype nozzles used in all earlier tests.

A crossfire tube was also installed in the sector combustor centerbody for the Mod III configuration; a crossfire test was conducted according to the test plan. Successful crossfire was obtained for each of the points in the ignition test point schedule. At low core speeds the crossfire fuel-air ratios were somewhat higher than the full propagation fuel-air ratios obtained with the hydrogen torch igniter for this configuration. However, at higher core speeds the difference in the fuel-air ratio for the two ignition sources was reduced significantly. This was attributed to the fact that at low core speeds, crossfire occurred across the centerbody trailing edge rather than through the

ORIGINAL PAGE IS
OF POOR QUALITY

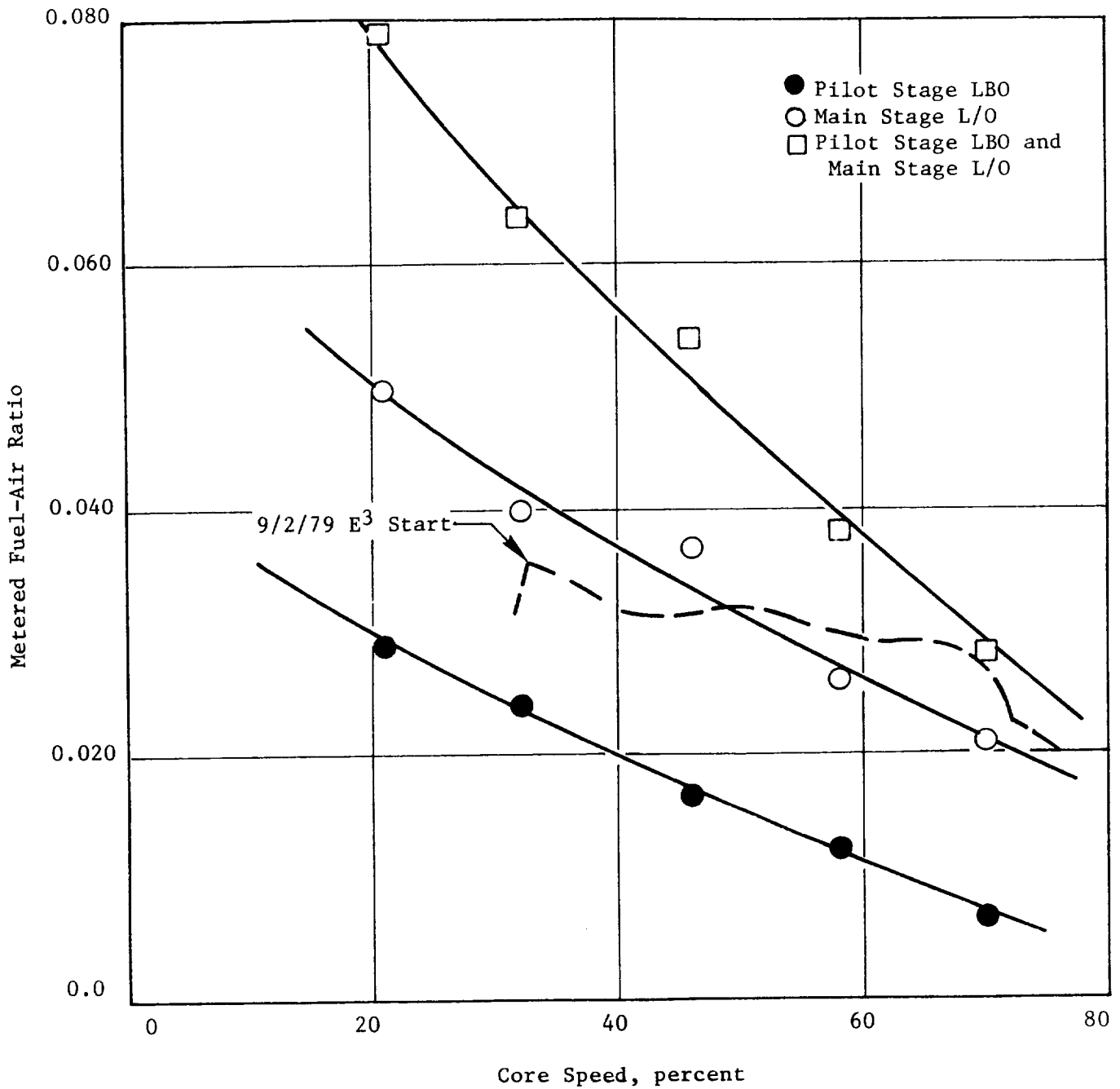


Figure 103. Sector Combustor Mod I Ignition Results Versus Cycle Requirement.

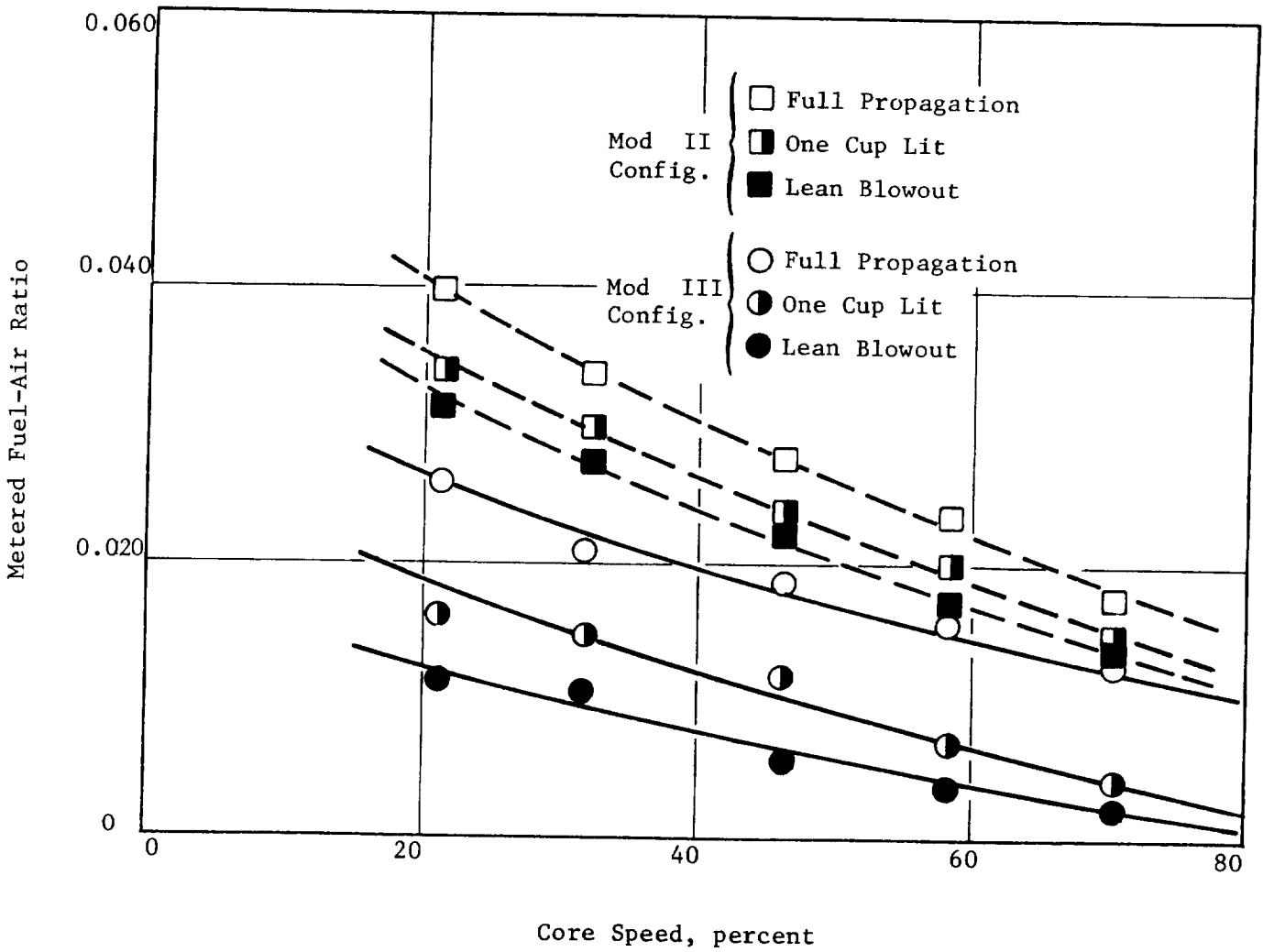


Figure 104. Sector Combustor Mod III Ignition Results.

crossfire hole at high core speeds. Figure 105 compares the crossfire fuel-air ratio to those obtained using a hydrogen torch ignition in both Mod II and III configurations.

A plot of the overall combustor fuel-air ratio, required to obtain main stage crossfire versus core speed, along with the September 1979 E³ ground start fuel schedule for the Mod III configuration is presented in Figure 106. This figure indicates that this sector combustor configuration meets the E³ start requirement at core speeds of 53% or higher.

A pressure ignition test, representing actual E³ conditions at the combustor inlet, also was conducted on the Mod III configuration. The results of this test showed a significant improvement over the atmospheric ignition test results in both pilot stage ignition and main stage crossfire performances. Figure 107 presents a plot of fuel-air ratio versus core speed for the Mod III pressure ignition results. The figure suggests that the E³ requirement will be met at core speeds of 38% or higher as compared to the 53% core speed level obtained from the atmospheric test results.

The ground start ignition test results of the Mod IV configuration were similar to those of the Mod III configuration results. A shorter centerbody design had no adverse effects on sector combustor ignition performance. The only other modification introduced into the Mod IV configuration was increased primary dilution airflow which was intended for emission reduction purposes only.

The E³ sector combustor ignition performance was further improved in the Mod V configuration. Improvement occurred primarily in the main stage crossfire performance and was attributed to a decreased swirl cup airflow and an increased dilution airflow. Figure 108 shows the results of the pressure ignition test for this configuration, indicating that the E³ engine start requirement is met at 32% and higher core speeds.

No net gain in sector combustor ignition performance was realized from the changes incorporated in the Mod VI configuration. The richer dome in the pilot stage that was expected to improve its ignition capability was offset by weaker recirculation due to a reduction in the secondary swirler airflow.

ORIGINAL TEST RESULTS
OF FUEL QUALITY

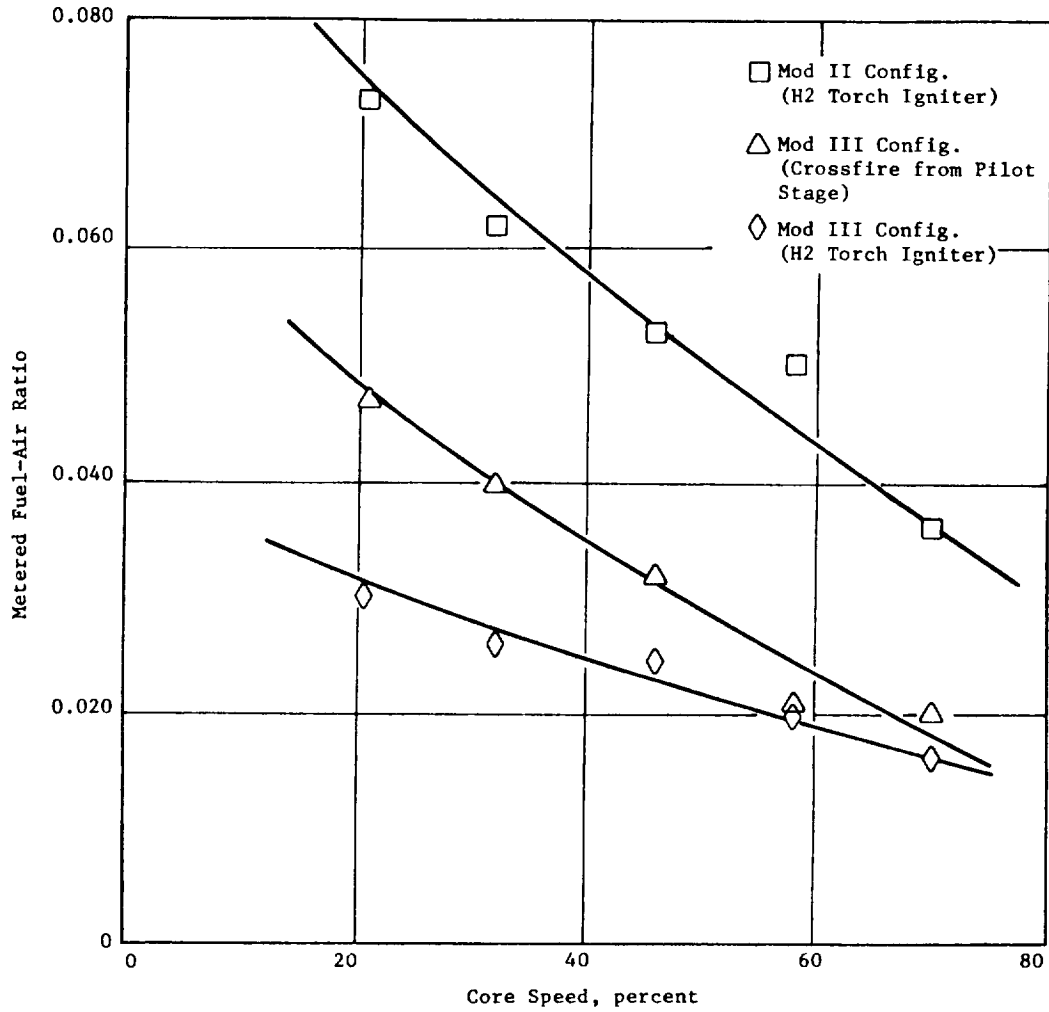


Figure 105. Sector Combustor Mod II and III Main Stage Ignition Results.

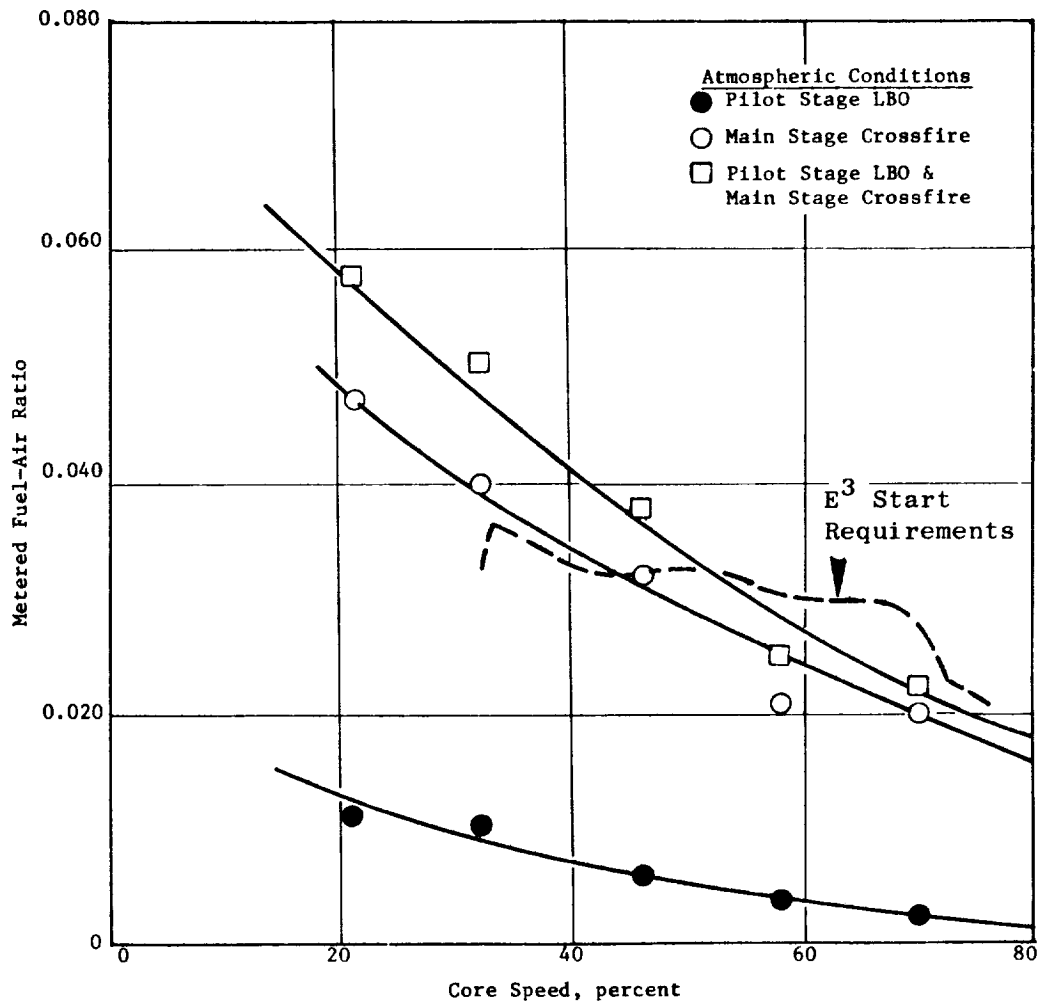


Figure 106. Sector Combustor Mod III Ignition Results at Atmospheric Condition.

ORIGINAL PAGE IS
OF POOR QUALITY

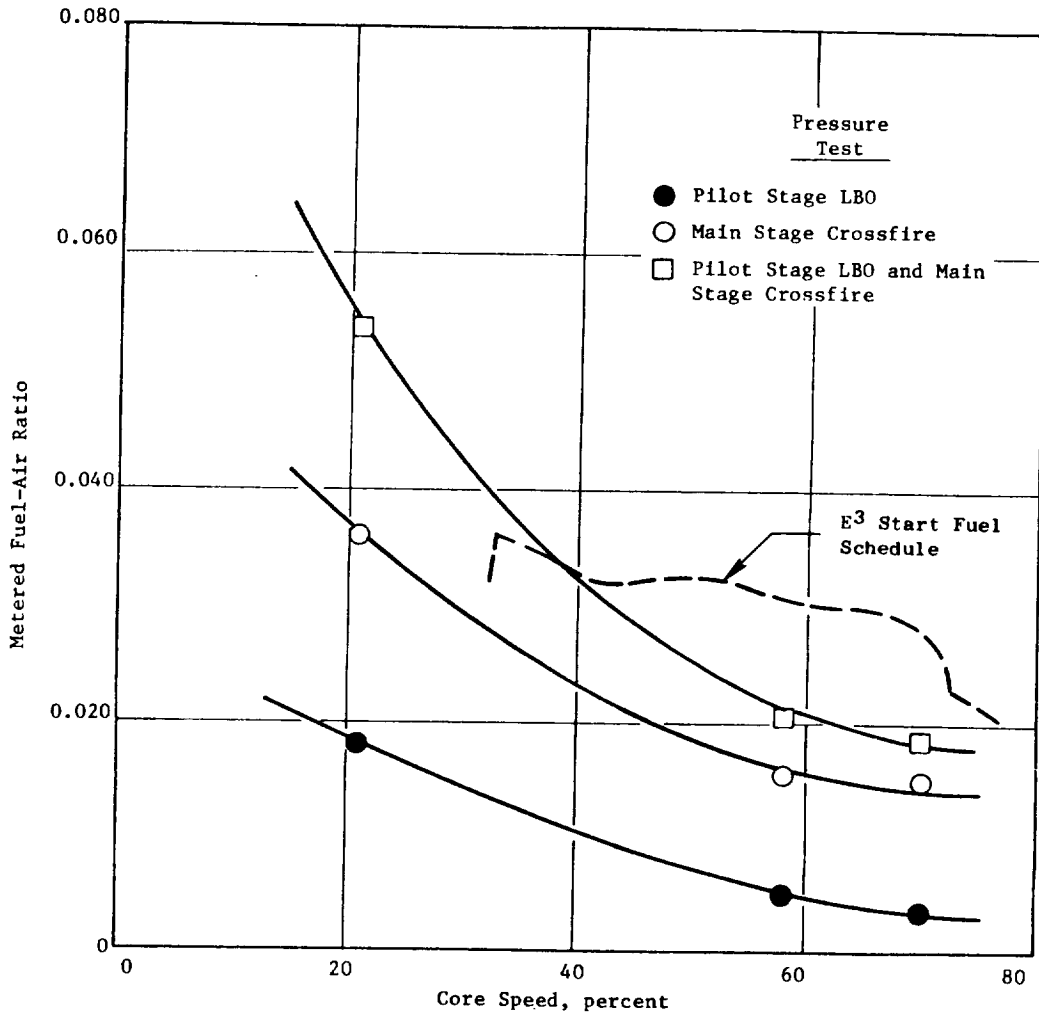


Figure 107. Sector Combustor Mod III Ignition Results at Actual Inlet Pressure.

ORIGINAL PAGE IS
OF POOR QUALITY

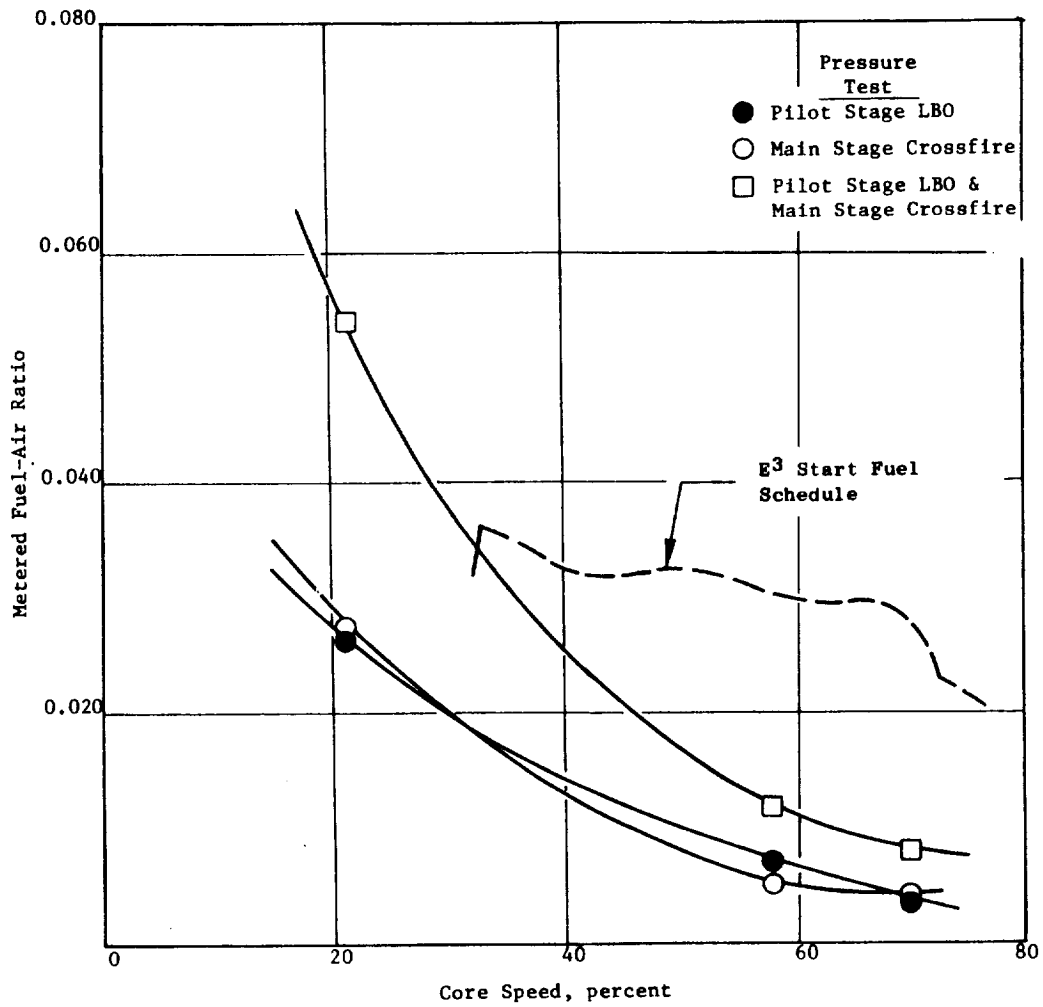


Figure 108. Sector Combustor Mod V Ignition Results at Actual Inlet Pressure.

Hardware modifications, later introduced to the Mod VI configuration (namely, reducing the main stage swirl cup airflow, adding extensions to the crossfire tube, and redesigning the crossfire hole geometry), were very effective in further improvement to the crossfire performance. However, concurrent with this stage of the sector combustor testing effort, a revised E³ SLS standard day ground start cycle was issued. This revised cycle eliminated the requirement of obtaining ignition in the main stage at subidle conditions. A pilot stage ignition test using the revised cycle conditions produced excellent results (Figure 109). At 32% core speed, at which engine start is expected, the full propagation fuel-air ratio was approximately 0.0130, which was well below the 0.020 fuel-air ratio specified by the fuel schedule. Since the main stage ignition is required only above idle, no difficulty was anticipated in obtaining crossfire from the pilot stage to the main stage.

6.2.4.9 Exit Temperature Performance Test Results

Ground start efficiency tests and exit temperature profile tests were conducted only on the baseline configuration of the E³ sector combustor. Calculated combustion efficiencies at ground start conditions with the pilot stage only fueled, ranged from 0.58 at 46% core speed to 0.98 at 77% core speeds. As expected, average exhaust gas temperature (EGT) profiles at these conditions were peaked outward (Figure 110). In the staged combustor operating model for the same core speed with equal fuel flow in each dome, the temperature profiles are relatively flat (indicated in Figure 111). As simulated SLTO conditions, the temperature profile and combustion efficiency were a function of the fuel flow split as illustrated in Figure 112. With a fifty-fifty fuel split, the temperature profile compares favorably with design limits. However, with a 30/70 pilot-to-main fuel split, the profile is peaked inboard at the design fuel-air ratio and considered unacceptable.

6.2.4.10 Pressure Drop Performance Results

Pressure measurements were obtained throughout the sector combustor test effort. Calculated pressure drops from these measurements varied slightly

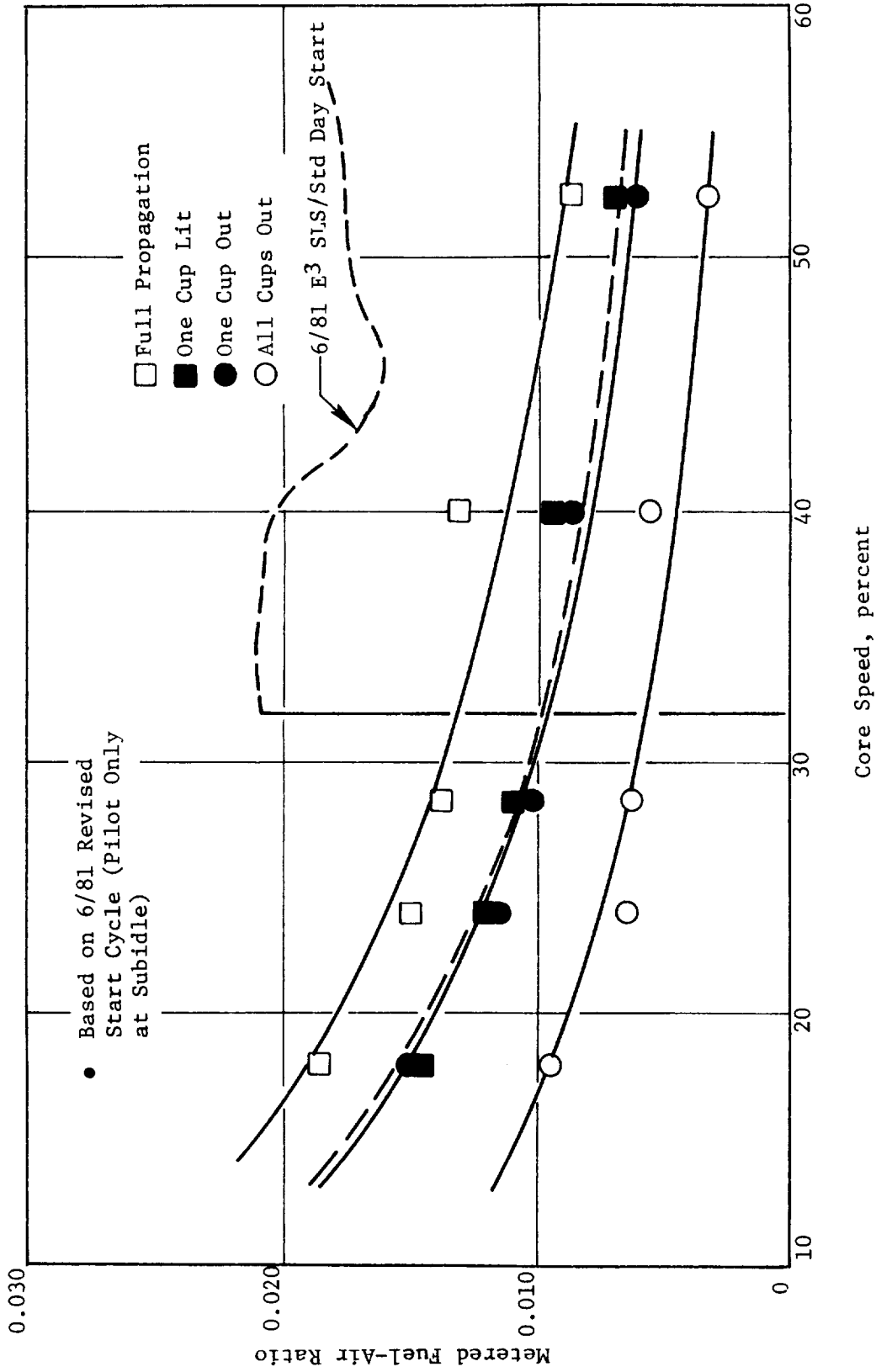


Figure 109. Sector Combustor Mod VI Ignition Results.

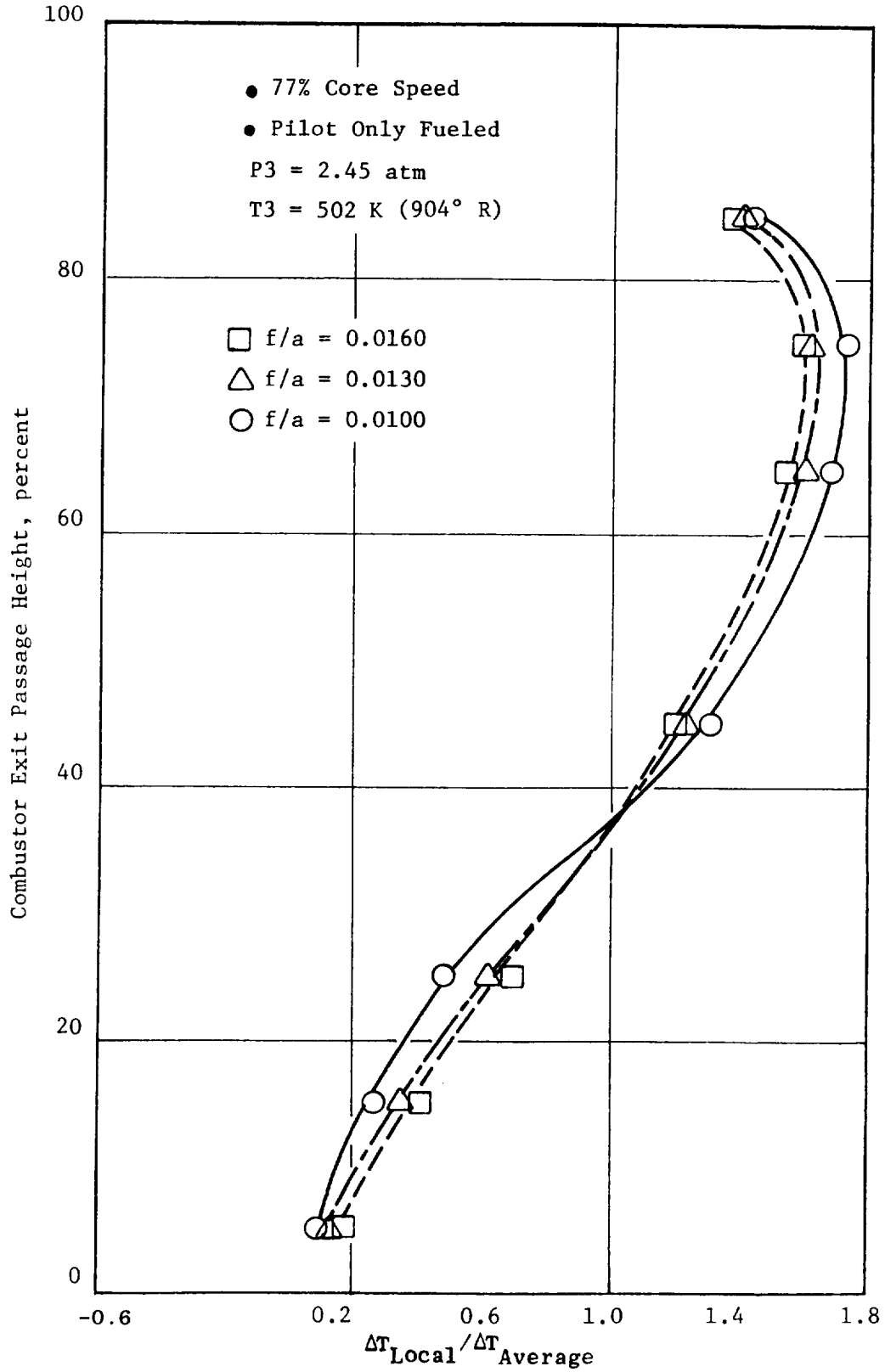


Figure 110. E³ Sector Combustor Subidle Exhaust Gas Temperature (EGT) Profiles (Pilot Only).

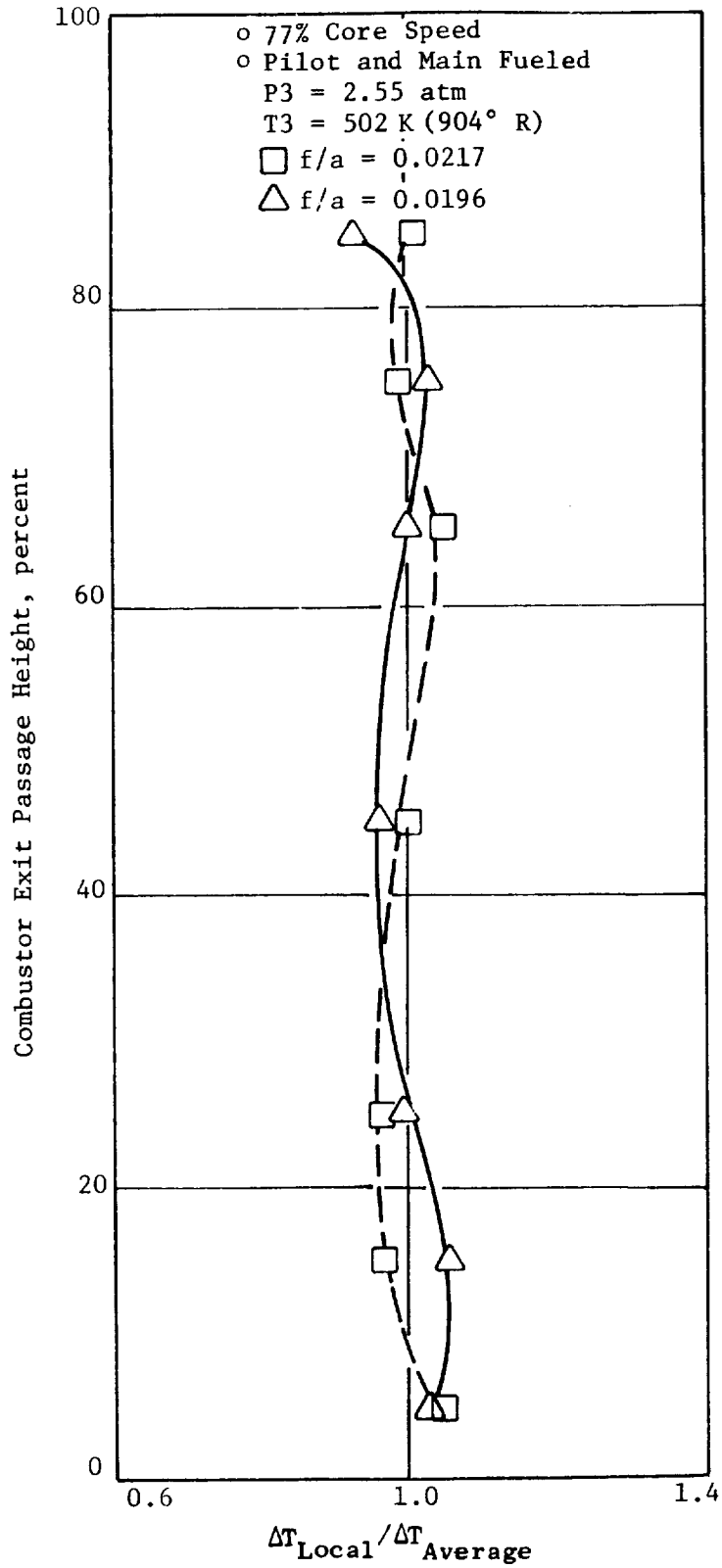


Figure 111. E³ Sector Combustor Subidle EGT Profiles (Staged).

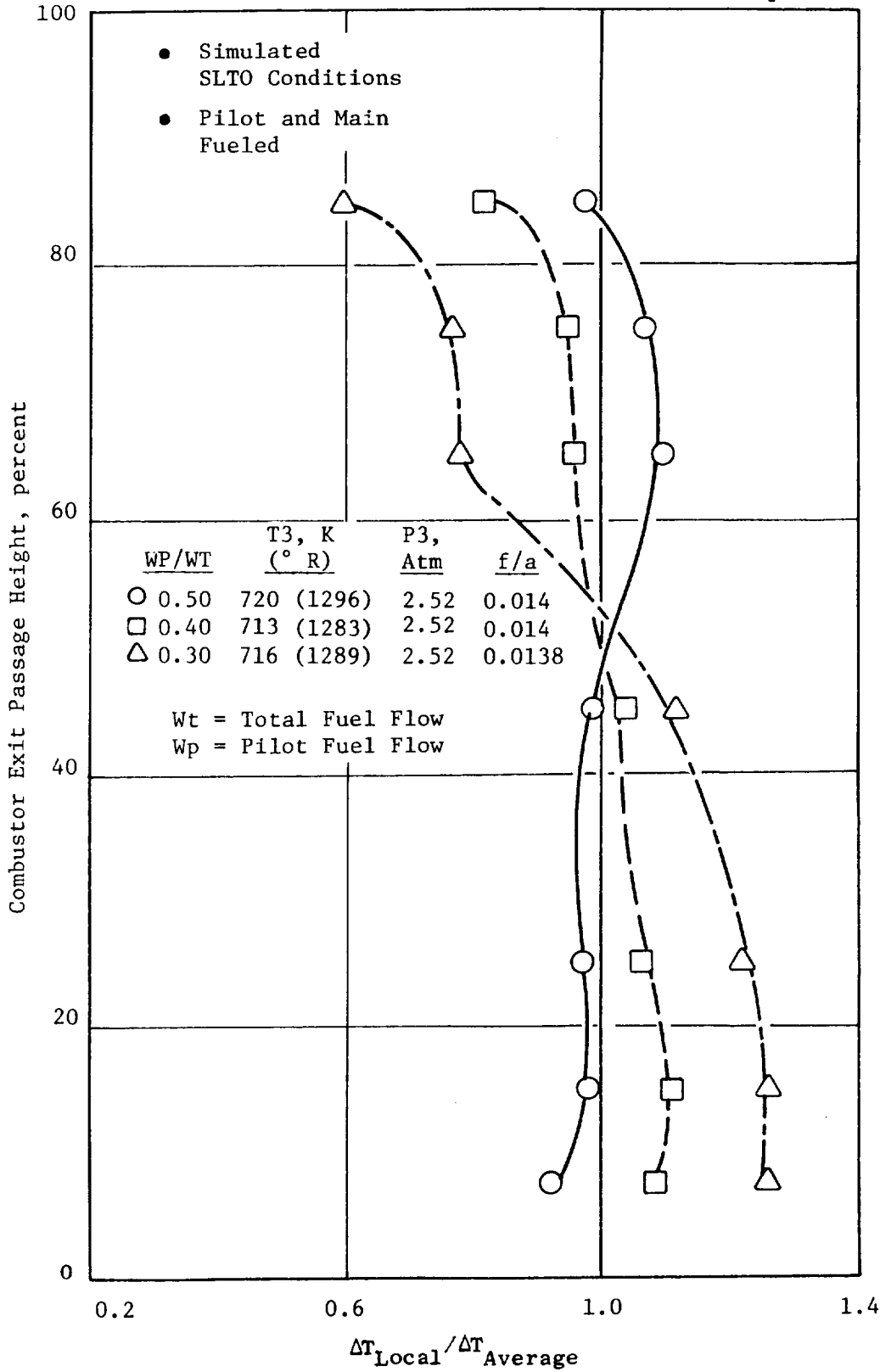


Figure 112. E3 Sector Combustor EGT Profiles at Simulated SLTO.

according to the effective areas of the configurations. But the overall combustor pressure drop generally compared well with the design pressure drop level of 5%. Figure 113 is a plot of pressure drop versus combustor flow function for one of the configurations tested.

6.2.4.11 Emissions Test Results

Idle emissions test results for the baseline configuration are presented in Figure 114. At 6% ground idle conditions, which represent the actual E³ engine idle power setting, the measured CO and HC emissions were 40.0 g/kg (40.0 lbm/1000 lb) of fuel and 4.5 g/kg (4.5 lbm/1000 lb) of fuel, respectively. These levels significantly exceeded the target levels of 20.7 g/kg (20.7 lbm/1000 lb) of fuel for CO and 2.8 g/kg (2.8 lbm/1000 lb) of fuel for HC. However, they were considered extremely encouraging for the early stage of the combustor development. Comparison of individual rake samples indicated that the between cup zones were significantly richer in fuel than the in-line cup zones. This observation led to the relocation of the primary dilution to between cups for the Mod I configuration in addition to using wider angle sleeves and reducing the pilot stage splash plate cooling. These modifications did result in a more uniform fuel-air distribution and a subsequent reduction of approximately 60% in CO and HC emissions to bring their levels very near the E³ Program target. A proportional improvement in emissions levels was also obtained at the 4% ground idle setting. The idle emissions results for Mod I are shown in Figure 115.

The Mod II configuration, which primarily features the development-type swirl cups and a reduction in the pilot stage swirl cup airflow, provided the design with the lowest idle emissions levels obtained during the entire sector combustor test effort. At 6% ground idle conditions the CO and HC emission levels obtained were 15.0 g/kg (15.0 lbm/1000 lb) of fuel and 1.8 g/kg (1.8 lbm/1000 lb) of fuel, respectively, at the design fuel-air ratio of 0.0122. With considerable margin, these levels met the E³ Program target levels for the two emissions categories. A plot of the CO and HC emissions versus the metered fuel-air ratio at 4% and 6% idle conditions for this configuration is shown in Figure 116.

ORIGINAL ENGINE IS
OF POOR QUALITY

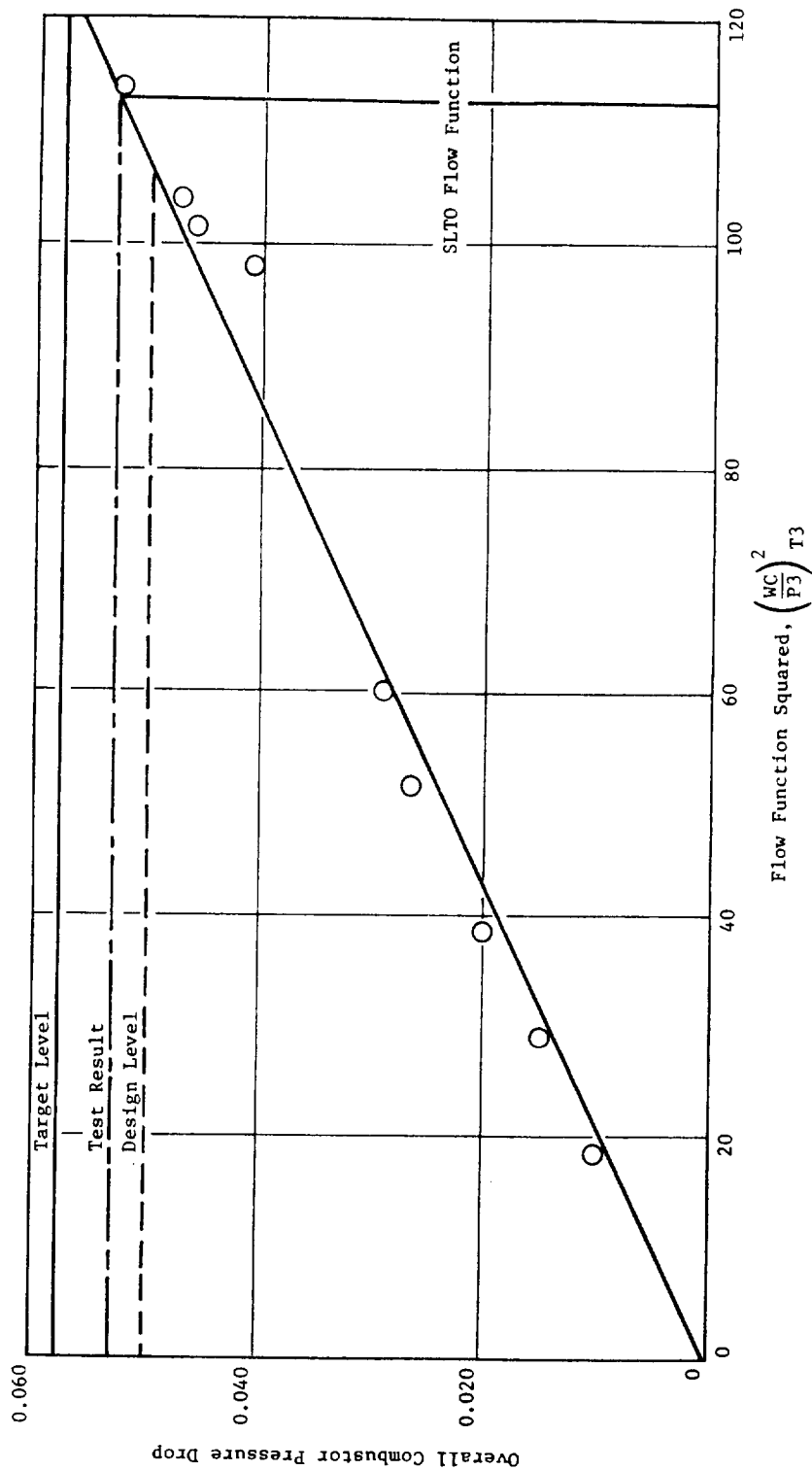


Figure 113. Sector Combustor Pressure Drop Versus Flow Function Parameter.

ORIGINAL PAGE IS
OF POOR QUALITY

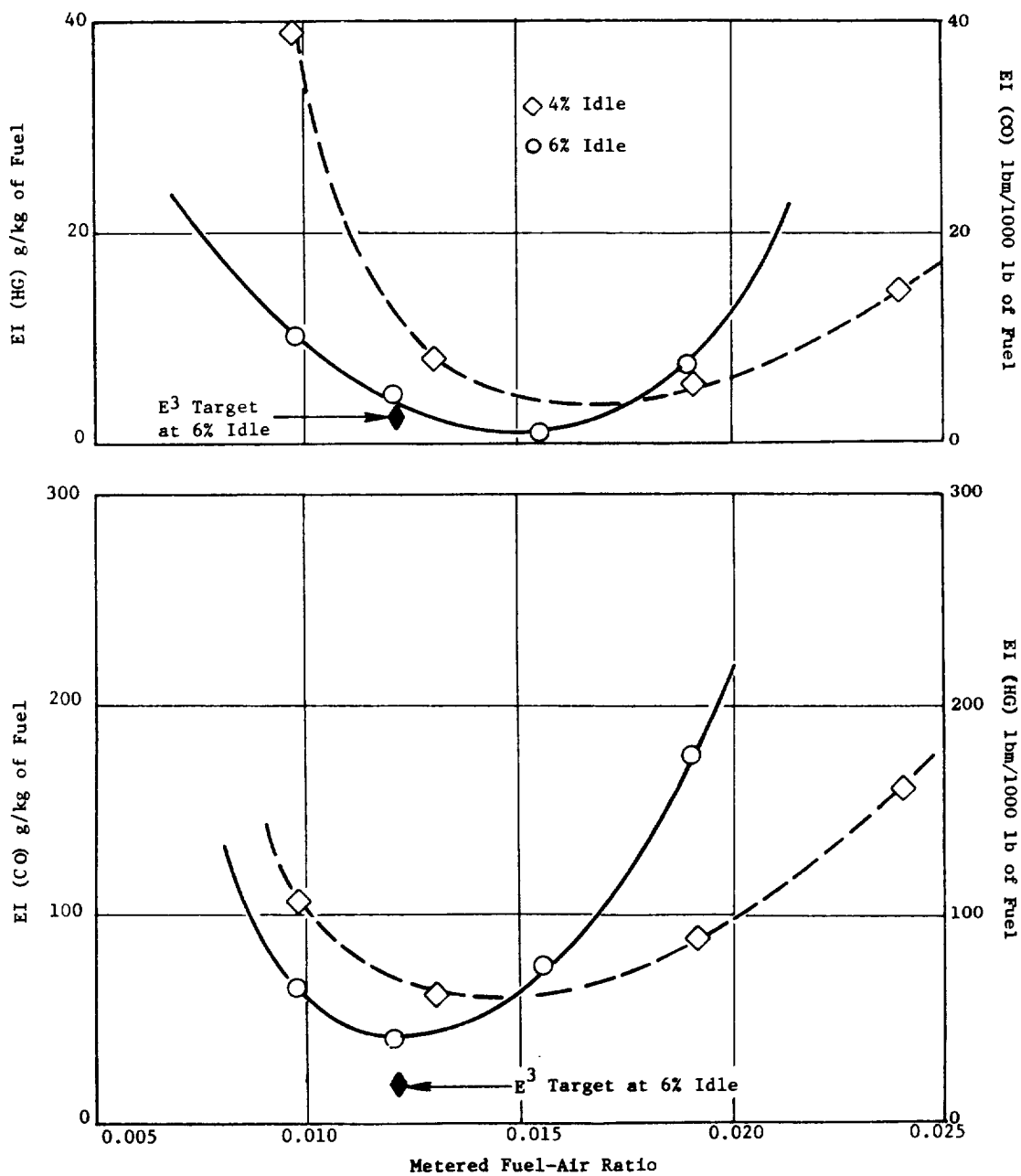


Figure 114. E³ Sector Combustor Emissions Results.

ORIGINAL PAGE IS
OF POOR QUALITY

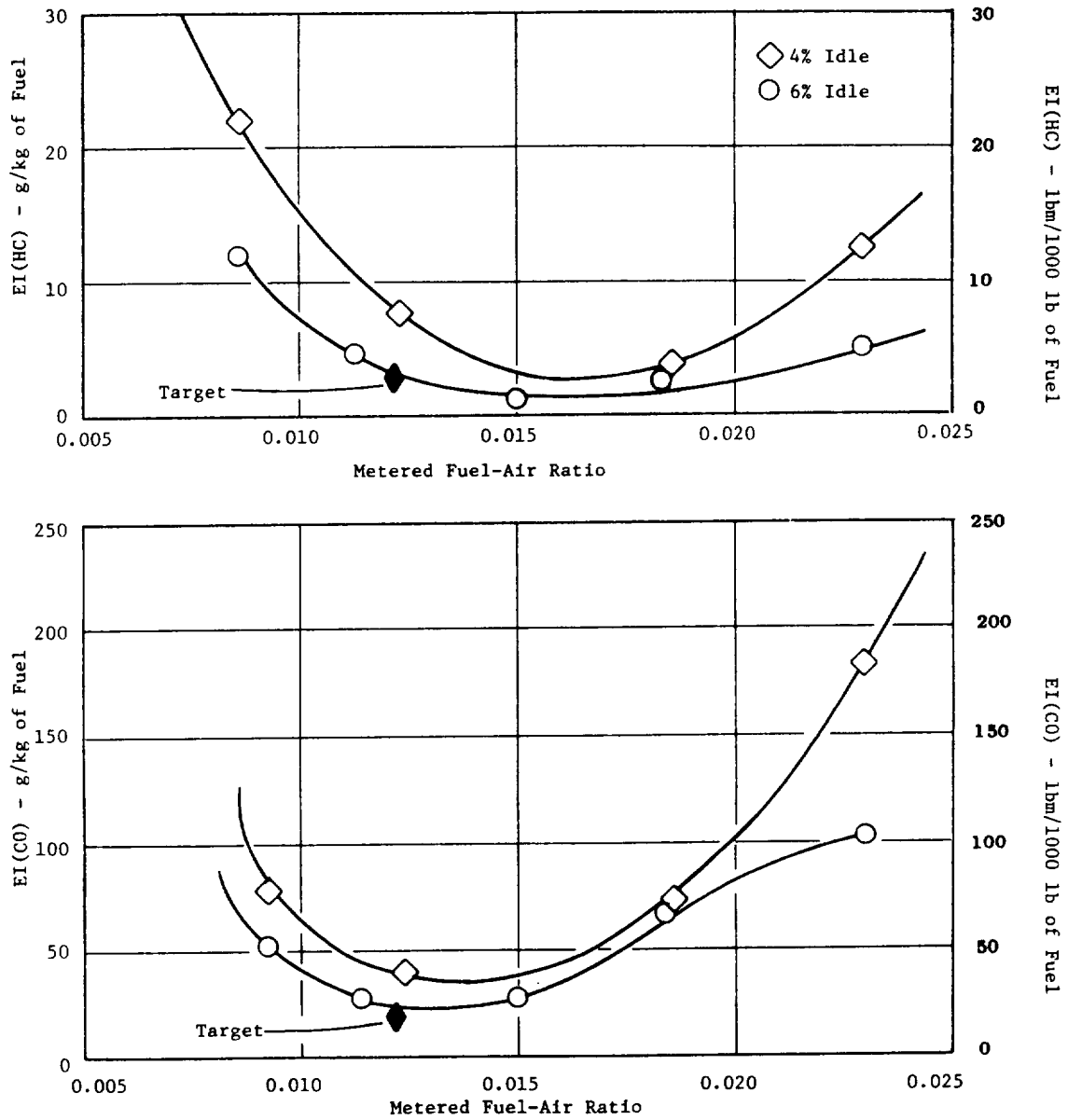


Figure 115. E³ Sector Combustor Emissions Results.

ORIGINAL PAGE IS
OF POOR QUALITY

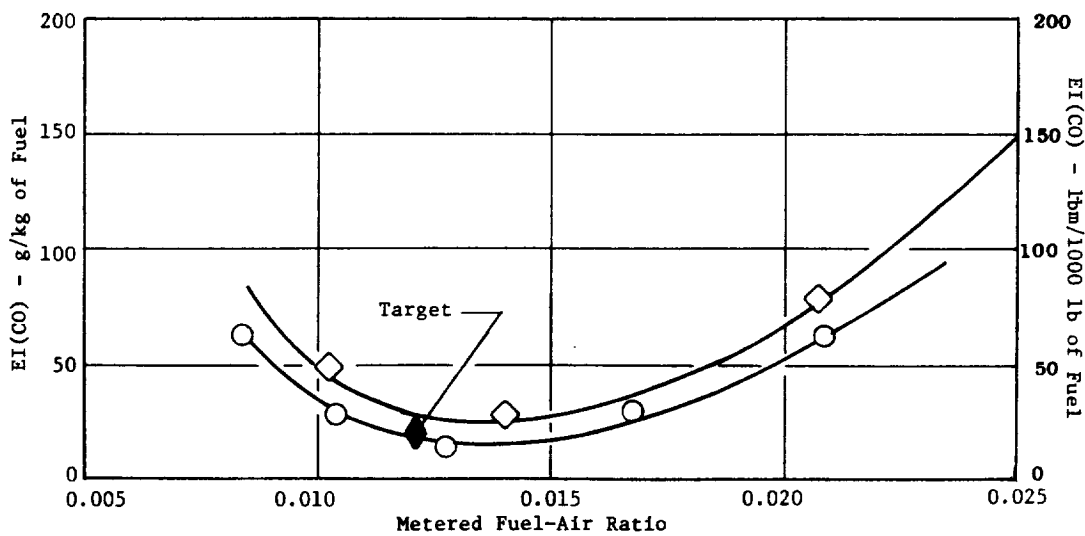
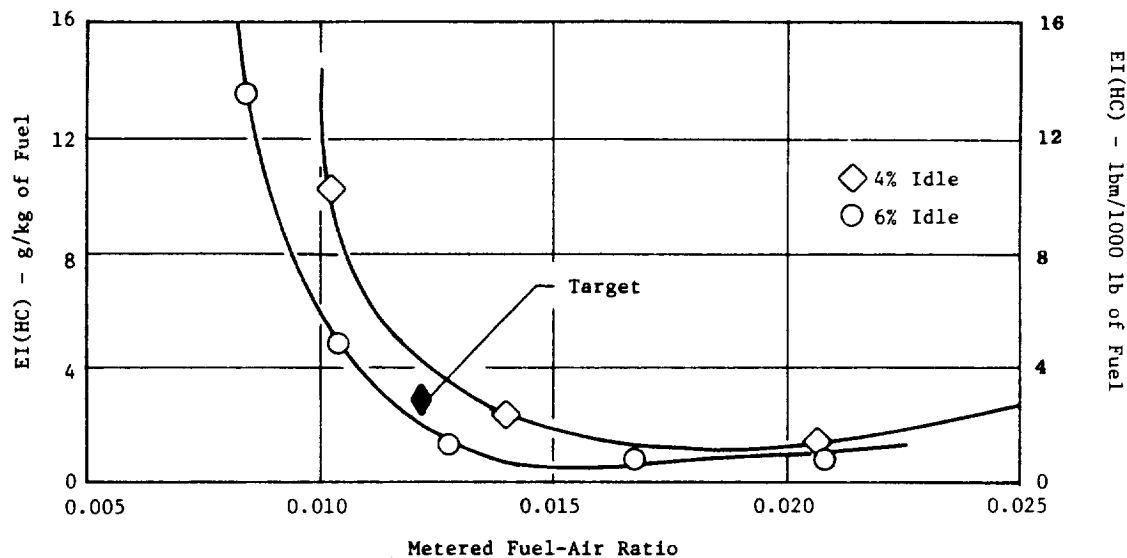


Figure 116. E³ Sector Combustor Emissions Results.

Replacing the peanut-type fuel nozzles with development-type fuel nozzles in the Mod III configuration resulted in an increase of the idle emissions to approximately double the Mod II configuration levels (Figure 117). The development-type fuel nozzles are air shrouded and are known to have a significantly more narrow spray angle than the prototype nozzles. This narrower spray angle in combination with the shroud air was the primary cause of the increased CO and HC emissions levels. Nevertheless, this same narrow spray angle was thought to be a strong contributor to the improved ignition performance for the Mod III configuration.

The effect of the fuel nozzle characteristics on idle emissions was further investigated in the Mod III configuration. Figure 118 shows a plot of the 6% idle emissions versus the fuel-air ratio for the different types of nozzles investigated. The lowest CO and HC idle emissions were again obtained with the prototype peanut nozzles. Eliminating the air shroud from the development nozzles helped to reduce the idle emissions by approximately 13%; however, shroud air prevents fuel nozzle plugging and carbon buildup on the venturi discharge surface.

Increasing the pilot stage primary dilution airflow in the Mod IV configuration resulted in only a modest reduction in the CO idle emissions as shown in Figure 119. But this resulted in a slight increase in the HC emissions. As expected, shortening the centerbody did not appear to have a significant impact on idle emissions.

The Mod V configuration featured an increased main stage dilution and, consequently, a richer pilot stage dome, thereby resulting in a significant reduction in CO and HC emissions at idle (Figure 120). The measured levels for this configuration at 6% idle and the design fuel-air ratio were 23.0 g/kg (23.0 lbm/1000 lb) of fuel for CO and 2.6 g/kg (2.6 lbm/1000 lb) of fuel for HC emissions.

CO and HC emissions increased slightly in the Mod VI configuration as a result of a simultaneous reduction in the secondary swirler airflow level and an increase in the primary dilution airflow level of the pilot stage. Increased dilution alone caused a shift of the CO and HC emissions versus

ORIGINAL PAGE IS
OF POOR QUALITY

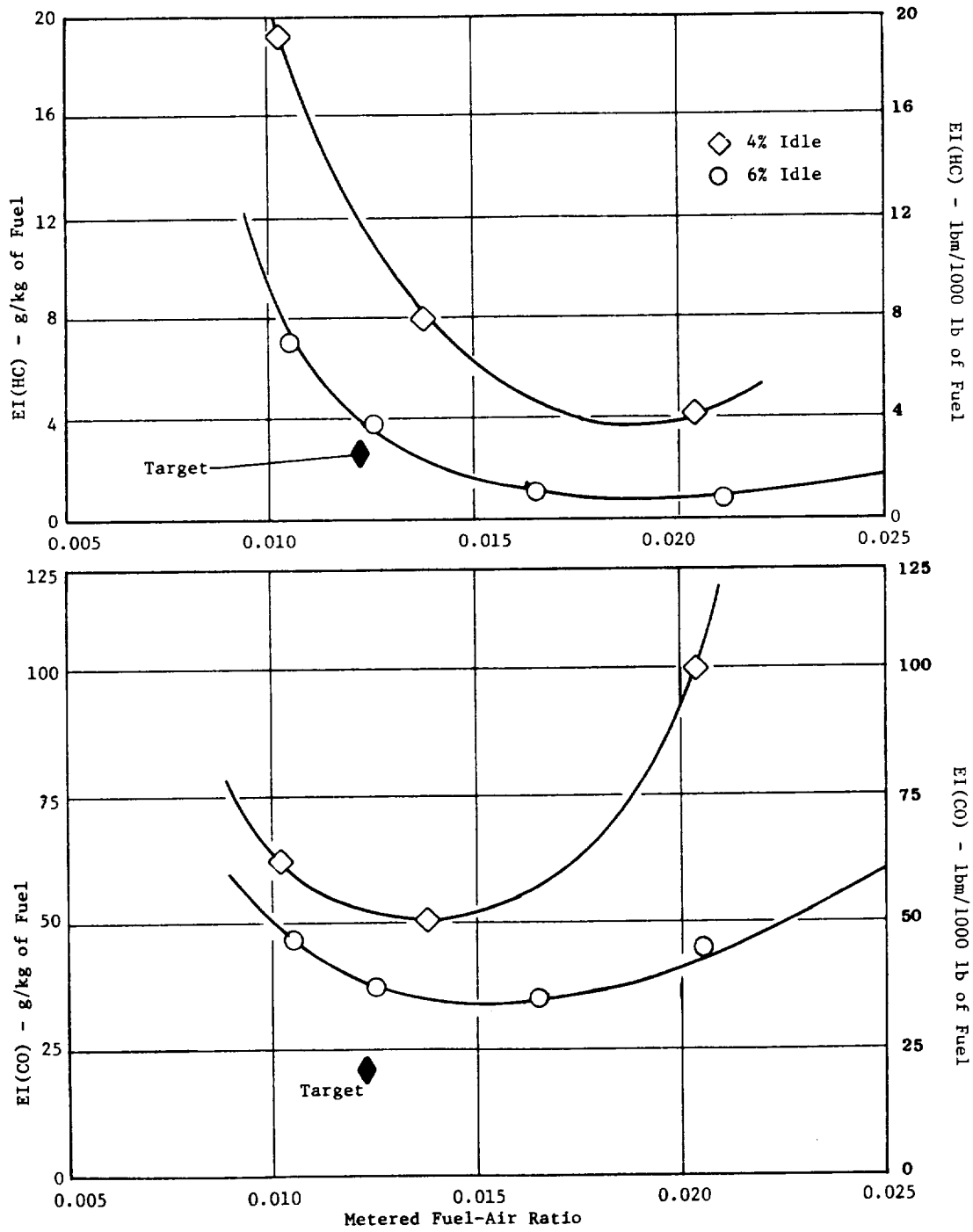


Figure 117. E³ Sector Combustor Emissions Results.

ORIGINAL PAGE 19
OF POOR QUALITY

	Fuel Type Nozzle	Shroud Air (2% W _c)	Fuel Nozzle Spray Angle
△	Development - type 26 pph at 100 psid	Yes	55°
○	Development - type 26 pph at 100 psid	No	55°
□	Prototype 25 pph at 100 psid	No	85°
◻	Development - type 50 pph at 100 psid	Yes	70°

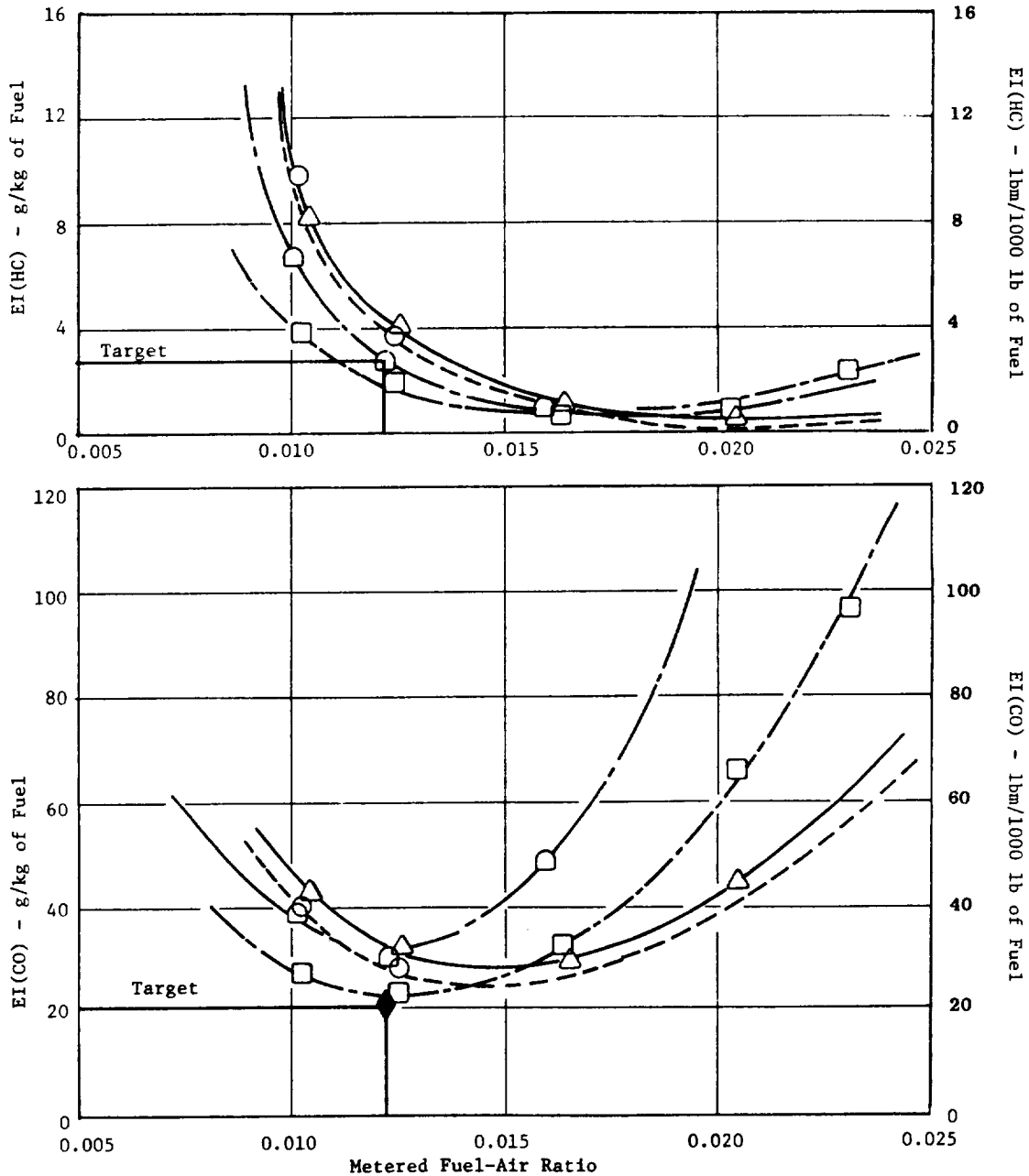


Figure 118. E³ Sector Combustor Emissions Results.

ORIGINAL PAGE IS
OF POOR QUALITY

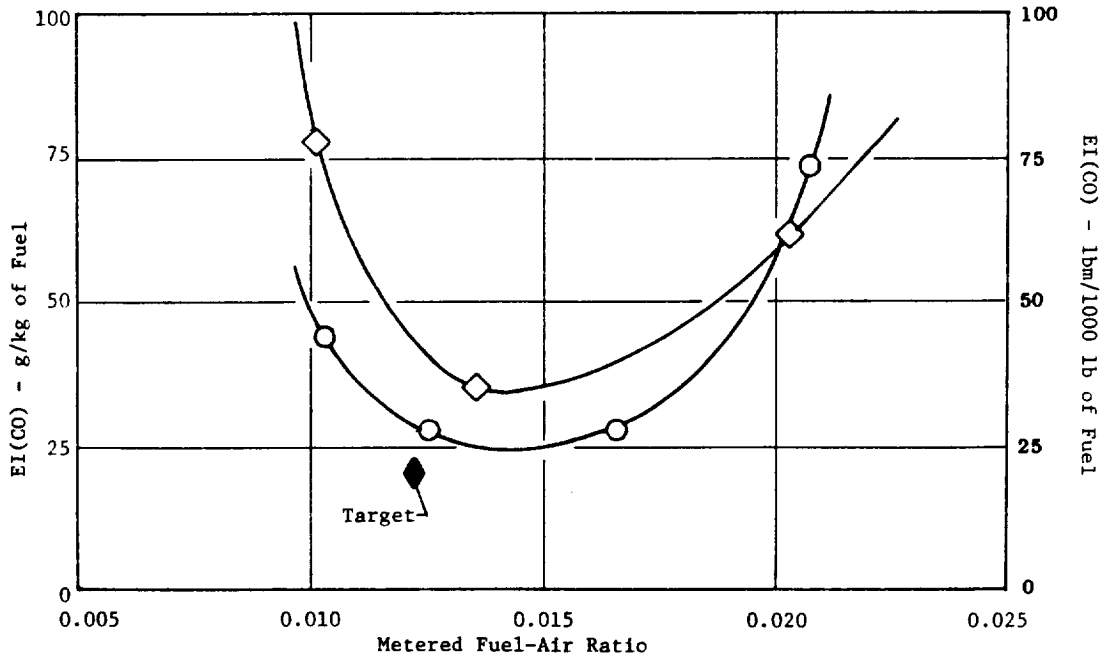
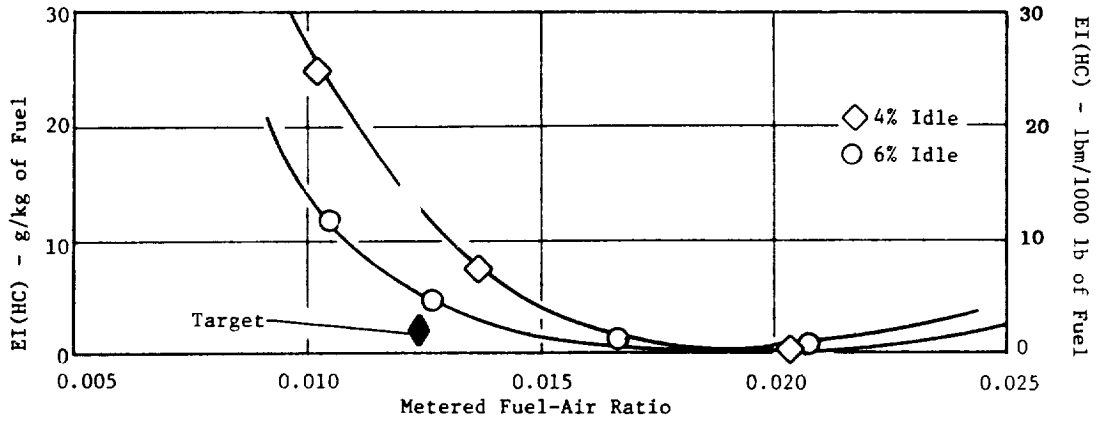


Figure 119. E³ Sector Combustor Emissions Results.

ORIGINAL PAGE IS
OF POOR QUALITY

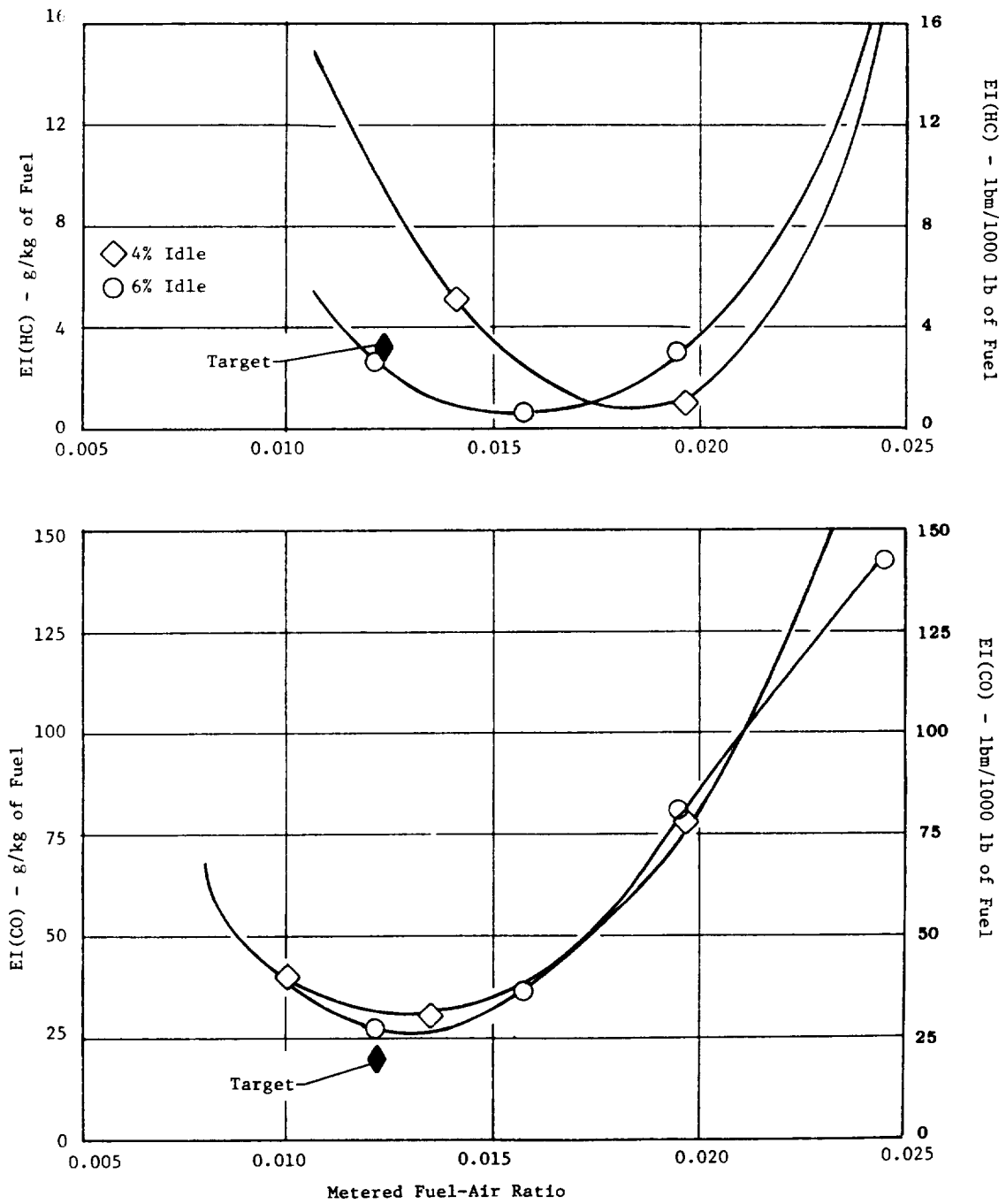


Figure 120. E³ Sector Combustor Emissions Results.

fuel-air ratio curves to the right. This resulted in a lower CO emission level and higher HC emission levels at the design fuel-air ratio for the 6% ground idle. The results for this configuration are shown in Figure 121. CO and HC emissions were also measured at simulated EPA landing-takeoff approach conditions [30% F_N (SLTO)] throughout the sector combustor tests. These emissions data were obtained with the pilot stage only operating mode and in the staged operating mode. In the pilot only mode at the approach power operating condition, CO emissions were generally low [<5 g/kg (5.0 lbm/1000 lb) of fuel], while HC emissions were practically nonexistent for all configurations tested. With both stages fueled, the CO and HC emissions varied with the configuration tested. The lowest levels, however, were obtained with the Mod V configuration which featured a significantly increased main stage dilution and somewhat richer dome regions in both stages.

The E^3 target levels for CO and HC emissions at approach power are a function of CO and HC emissions at idle conditions (Figure 122). This dependency is a result of these two operating modes being the key contributors to CO and HC emissions in the EPA landing-takeoff cycle. This figure suggests that the HC emissions for the Mod V configuration will meet the E^3 target with either pilot only or pilot and main stages lit. The CO emissions, on the other hand, fall short of meeting the target in either mode. The figure also indicates that the Mod II configuration CO and HC emissions levels, even though higher than those of the Mod V, will meet the target level due to the lower idle emissions.

NO_x emissions measurements at simulated sea level takeoff conditions were obtained only for the baseline, Mods I, II, and V configurations. NO_x emissions data was collected at idle and approach conditions for all configurations. From this low-power data, NO_x emission levels at sea level takeoff conditions were estimated with the use of a severity parameter linear correlation which takes into account the influence of pressure, temperature, humidity, fuel-air ratio, and fuel flow split between the pilot and main stages. The linear nature of this correlation allows for the extrapolation of NO_x results obtained at low-power operating conditions to high-power operating

ORIGINAL PAGE IS
OF POOR QUALITY

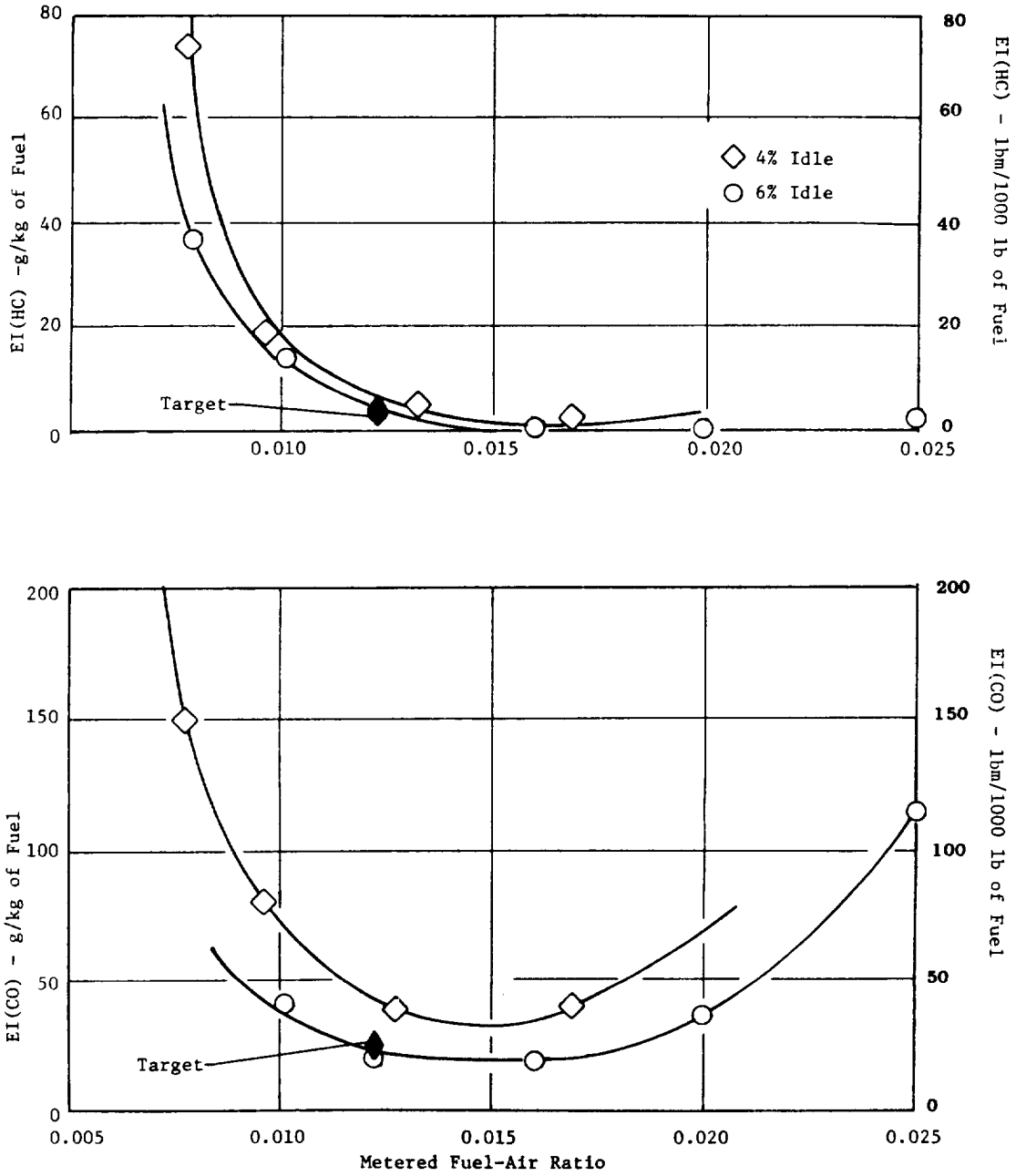


Figure 121. E³ Sector Combustor Emissions Results.

ORIGINAL PAGE IS
OF POOR QUALITY

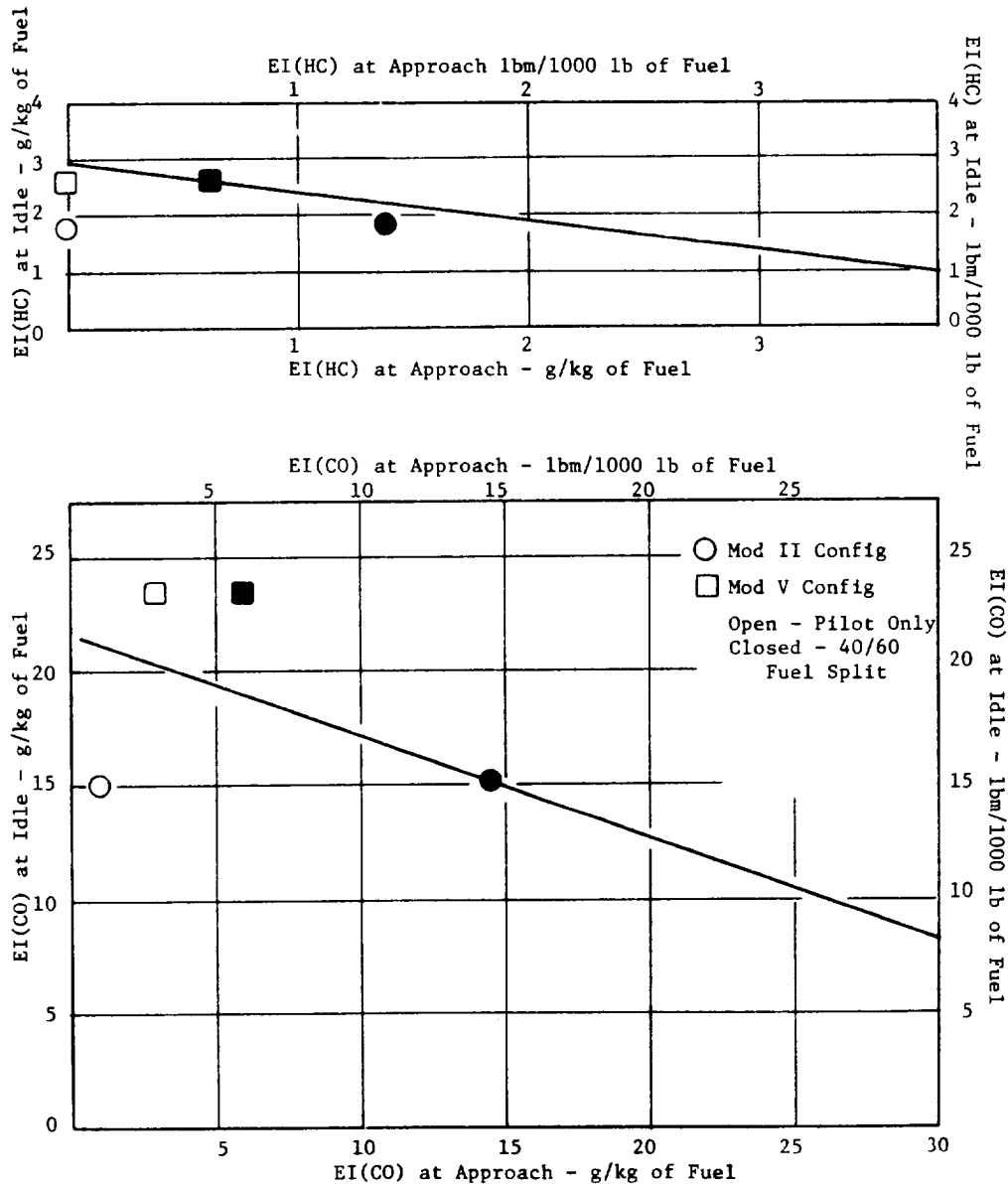


Figure 122. E³ Sector Combustor Emissions Results.

conditions. The results of the measured NO_x emissions correlation to this parameter are shown in Figure 123. The reference conditions represent the values at the actual FPS cycle sea level takeoff operating condition.

The baseline configuration produced the lowest NO_x emissions at a level of 19.2 g/kg (19.2 lbm/1000 lb) of fuel with a 40/60 pilot stage to main stage fuel flow split. The E³ target for NO_x emissions is 17.5 g/kg (17.5 lbm/1000 lb) of fuel. However, test experience indicated that the full-annular combustor generally produced lower NO_x emissions than the sector combustor with similar features.

The higher NO_x emissions obtained in all the subsequent configurations were due primarily to the higher flame temperatures resulting from higher combustion efficiencies associated with a more uniform dome stoichiometry. Furthermore, both pilot and main stage domes were enriched following the baseline configurations for ignition and idle emissions improvement purposes.

6.2.4.12 Altitude Relight Test Results

The altitude relight ignition performance of the E³ sector combustor was investigated only with the Mod VI configuration using the CF6-50 engine windmilling map. Successful relight was obtained only at test points simulating conditions in the lower left portion of the windmilling envelope as illustrated in Figure 124. This was thought to be caused by a low pressure drop across the fuel nozzle tip due to the use of relatively large-flow fuel nozzles. Low fuel nozzle pressure drop usually results in poor fuel atomization. However, a repeat test with significantly smaller fuel nozzles seemed to have little effect on the number of successful relights, even though the light-off fuel-air ratios for these successful relights dropped drastically. To verify that relight was not inhibited by a lack of fuel flow due to the small fuel nozzles, an intermediate set of nozzles was installed and the test repeated. Again, no additional points were added to the list of successful lights, and the light-off fuel-air ratios were between those of the previous runs.

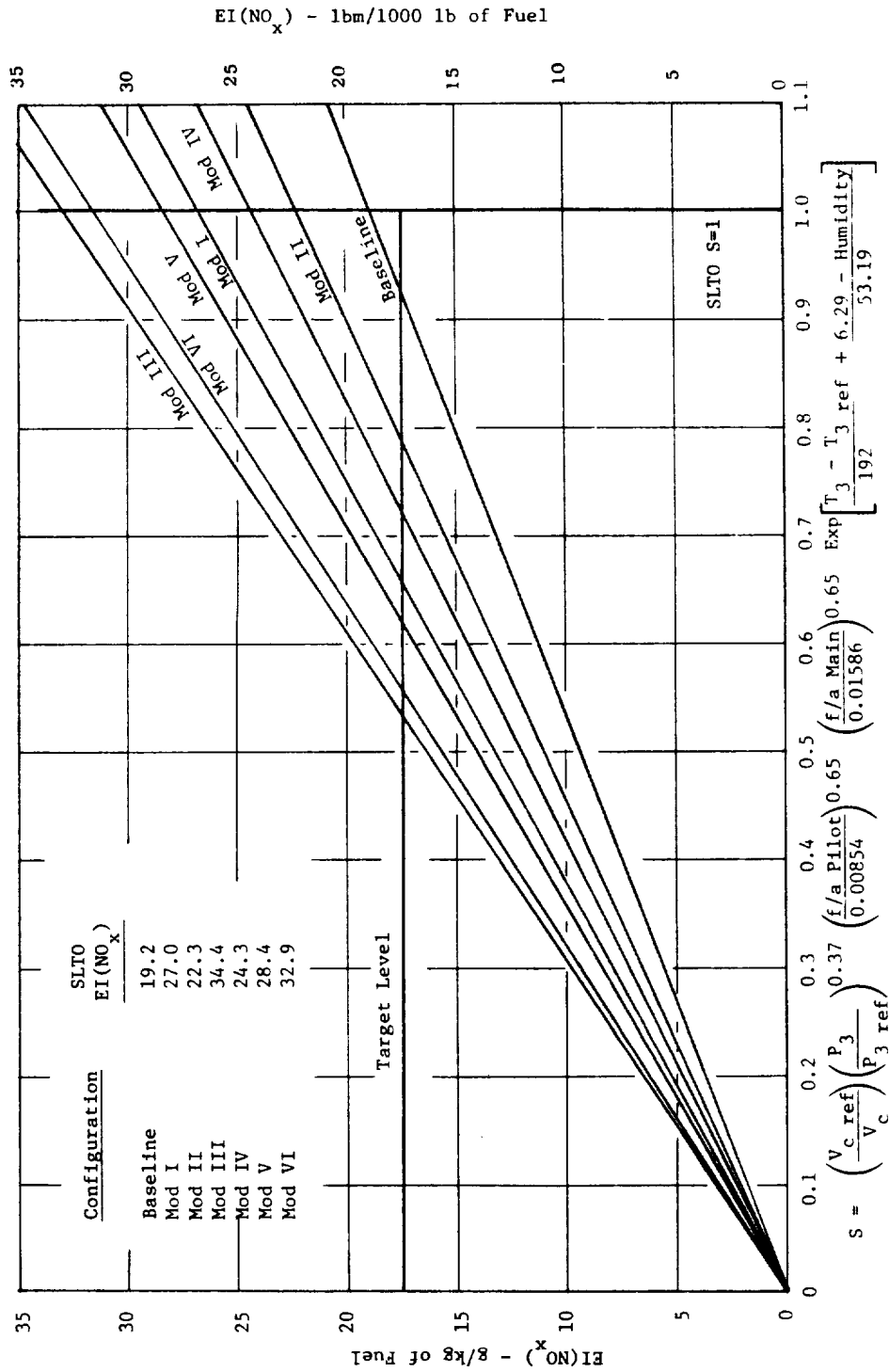


Figure 123. E³ Sector Combustor Emissions Results.

ORIGINAL PAGE IS
OF POOR QUALITY

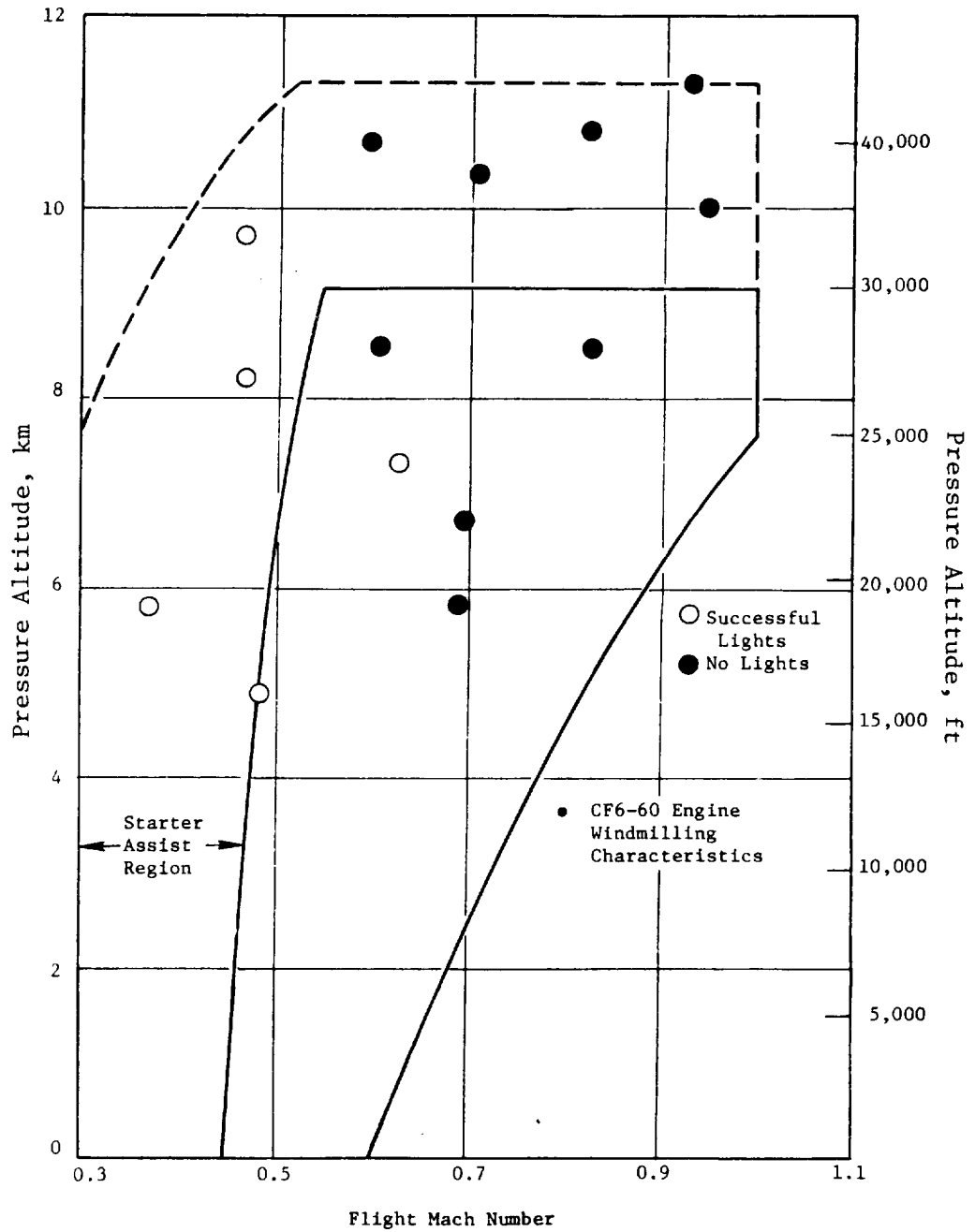


Figure 124. E³ Sector Combustor Altitude Relight Test Results.

Additional altitude relight testing, conducted with the pilot stage dilution blocked and prototype fuel nozzles, indicated that no further performance improvements were attainable with the current configurations. The detailed results of all altitude ignition testing are summarized in Tables XXVI through XXIX.

6.2.4.13 Concluding Remarks

1. Ignition Results

The sector combustor ignition performance was improved most effectively through the use of the air shrouded development-type fuel nozzles. These nozzles are known to have somewhat narrower spray angles and more effective fuel atomization than the prototype fuel nozzles. As expected, a fuel enriched dome region also enhanced the ignition performance. All the test results indicated that in order for the main stage crossfire at subidle conditions to be reasonably attainable, the main stage swirl cup airflow had to be reduced to a level near that of the pilot stage swirl cup airflow. However, the latest E³ start cycle eliminated the requirement of starting the engine on both pilot and main stages. Consequently, the pilot stage ignition performance is expected to meet the revised E³ start schedule with considerable margin. No difficulty is anticipated with main stage crossfiring at conditions above idle.

2. Performance Results

Combustion efficiency and exit temperature profile measurements were only obtained for the baseline configuration of the E³ sector combustor. However, a basic conclusion can be made and considered applicable for all configurations tested. Due to the approximately equal airflow levels in the pilot and main stages, a fuel flow split for near 50/50 is required to obtain a uniform exit temperature profile.

The sector combustor pressure drop agrees very well with the design target of 5%.

Table XXVI. Altitude Ignition Testing Summary.

11.8 kg/hr (26.0 lb/hr) Development-Type Fuel Nozzles

W_c kg/s (lb/s)	P_3 atm	T_3 K(° F)	V_{ref} m/s (ft/s)	$\frac{W_c}{P_3} 2T_3$	$\Delta P/P$	ΔP_{fuel} at L/O atm	$\frac{PT}{V_{ref}}$	$\frac{PT \Delta P}{V_{ref} P}$	f/a 1 Cup Lit	f/a All Cups Lit	φ 1 Cup Lit	φ All Cups Lit
0.19 (0.42)	0.544	304 (87)	6.4 (21.0)	37.1	0.0285	0.796	25.8	0.752	0.0292	0.0342	2.4	2.8
0.07 (0.15)	0.476	293 (67)	2.6 (8.5)	6.4	0.010	0.395	53.6	0.546	0.0556	0.0570	4.5	4.6
0.07 (0.15)	0.408	295 (71)	3.0 (9.8)	8.7	0.011	0.592	40.1	0.442		0.068	-	5.5
0.07 (0.15)	0.340	296 (73)	3.7 (12.1)	12.6	0.0135	0.551	27.9	0.377	0.0655	0.084	5.3	6.8
0.05 (0.11)	0.272	296 (73)	3.0 (9.8)	8.6	0.0110	0.673	26.9	0.297	---	0.109	---	8.8
0.06 (0.13)	0.238	297 (75)	4.8 (15.7)	21.4	0.0191	---	15.0	0.288	0.0760	---	6.1	---
0.14 (0.31)	0.272	297 (75)	9.3 (30.5)	78.7	0.0559	---	8.9	0.498		No Light		
0.22 (0.49)	0.272	298 (76)	14.4 (47.2)	188.3	0.126	---	5.8	0.724		No Light		
0.29 (0.64)	0.272	306 (91)	19.1 (62.7)	325.6	0.213	---	4.5	0.951		No Light		
0.36 (0.79)	0.361	306 (91)	18.1 (59.4)	292.4	0.192	---	6.1	1.176		No Light		
0.36 (0.79)	0.544	306 (91)	12.0 (39.4)	128.0	0.087	1.05	14.1	1.231	---	0.0180	---	1.5
0.36 (0.79)	0.408	306 (91)	16.0 (52.5)	228.1	0.151	---	8.0	1.205		No Light		
0.36 (0.79)	0.544	306 (91)	12.1 (39.7)	131.3	0.089	1.53	13.9	1.244	---	0.0210	---	1.7
0.14 (0.31)	0.340	306 (91)	10.6 (34.8)	52.5	0.039	---	10.0	0.392	0.0370	---	3.1	---
0.22 (0.48)	0.408	306 (91)	13.4 (44.0)	83.6	0.059	1.01	9.5	0.550	0.0291	0.0355	2.3	2.9
0.33 (0.73)	0.476	306 (91)	12.5 (41.0)	138.6	0.094	---	11.9	1.11		No Light		

Table XXVII. Altitude Ignition Testing Summary.

2.3 kg/hr (5.1 lb/hr) Development-Type Fuel Nozzles

W_c kg/s (lb/s)	P_3 atm	T_3 K(° F)	V_{ref} m/s (ft/s)	$\frac{W_c}{P_3} 2T_3$	$\Delta P/P$	ΔP_{fuel} at L/O atm	$\frac{PT}{V_{ref}}$	$\frac{PT \Delta P}{V_{ref} P}$	f/a 1 Cup Lit	f/a All Cups Lit	φ 1 Cup Lit	φ All Cups Lit
0.19 (0.42)	0.544	296 (73)	6.3 (20.7)	36.1	0.0290	13.40	25.6	0.742	0.0187	0.0206	1.5	1.7
0.07 (0.15)	0.476	281 (46)	2.5 (8.2)	6.1	0.0093	3.27	53.5	0.498	0.0333	0.0333	2.7	2.7
0.07 (0.15)	0.408	288 (58)	2.9 (9.5)	8.5	0.0107	3.33	40.5	0.433	0.0342	0.0342	2.8	2.8
0.07 (0.15)	0.340	294 (69)	3.6 (11.8)	12.5	0.0131	4.08	27.8	0.364	0.0370	0.0370	3.0	3.0
0.05 (0.11)	0.272	294 (69)	3.1 (10.2)	9.9	0.0111	3.47	25.8	0.286	0.0516	0.0516	4.2	4.2
0.07 (0.15)	0.245	294 (69)	4.8 (15.7)	24.0	0.0190	3.20	15.0	0.285	0.0439	---	3.5	---
0.14 (0.31)	0.286	285 (53)	8.5 (27.9)	68.3	0.0500	---	9.6	0.480		No Light		
0.22 (0.48)	0.272	277 (39)	13.0 (42.6)	181.2	0.1120	---	5.8	0.650		No Light		
0.38 (0.84)	0.408	276 (37)	15.1 (49.5)	239.4	0.1470	---	7.5	1.103		No Light		

**ORIGINAL PAGE IS
OF POOR QUALITY**

Table XXVIII. Altitude Ignition Testing Summary.

2.3 kg/hr (5.1 lb/hr) and Development-Type Fuel Nozzles
(Pilot Stage Primary Dilution Closed Off)

W_c kg/s (lb/s)	P_3 atm	T_3 K(° F)	V_{ref} m/s (ft/s)	$(\frac{W_c}{P_3})^2 T_3$	$\Delta P/P$	ΔP_{fuel} at L/O atm	$\frac{PT}{V_{ref}}$	$\frac{PT \Delta P}{V_{ref} P}$	f/a l Cup Lit	f/a All Cups Lit	ϕ l Cup Lit	ϕ All Cups Lit
0.20 (0.44)	0.574	289 (60)	6.3 (20.7)	35.1	0.032	6.19	26.3	0.842	0.0122	0.0122	0.98	0.98
0.07 (0.15)	0.476	289 (60)	2.5 (8.2)	6.3	0.0095	3.61	55.0	0.523	0.0261	0.0261	2.1	2.1
0.07 (0.15)	0.408	291 (64)	2.9 (9.5)	8.6	0.0110	3.27	40.9	0.450	0.0258	0.0258	2.1	2.1
0.07 (0.15)	0.340	294 (69)	3.5 (11.5)	12.5	0.0136	3.67	28.6	0.389	0.0272	0.0272	2.2	2.2
0.04 (0.09)	0.272	279 (42)	2.5 (8.2)	6.0	0.0098	4.83	30.4	0.298	0.0491	0.0491	4.0	4.0
0.07 (0.15)	0.245	278 (40)	4.5 (14.8)	22.7	0.0202	4.42	15.1	0.305	0.0303	0.0302	2.4	2.4
0.15 (0.33)	0.265	278 (40)	9.5 (31.2)	89.1	0.0723	---	7.8	0.564	No Light			
0.21 (0.46)	0.279	277 (39)	12.4 (40.7)	156.9	0.1206	---	6.2	0.748	No Light			
0.28 (0.62)	0.272	273 (31)	16.6 (54.5)	289.3	0.2132	---	4.5	0.594	No Light			
0.14 (0.31)	0.347	284 (51)	6.8 (22.3)	46.2	0.0388	5.85	14.5	0.563	0.0167	0.0167	1.3	1.3
0.21 (0.46)	0.408	284 (51)	8.4 (27.6)	75.2	0.0581	24.45	13.8	0.802	0.0228	0.0228	1.8	1.8
0.32 (0.70)	0.476	277 (39)	10.9 (35.8)	125.2	0.1778	22.65	12.1	2.151	0.0145	0.0188	1.2	1.5
0.15 (0.33)	0.340	277 (39)	7.4 (24.3)	53.9	0.0460	---	12.7	0.584	0.0246	0.0281	2.0	2.3
0.21 (0.46)	0.524	278 (40)	6.6 (21.7)	44.6	0.0378	---	22.1	0.835	0.0178	0.0194	1.4	1.6
0.28 (0.62)	0.766	273 (31)	5.9 (19.4)	36.5	0.0314	---	35.4	1.111	0.0145	0.0171	1.2	1.4

Table XXIX. Altitude Ignition Testing Summary.

11.3 hg/hr (24.9 lb/hr) Prototype Fuel Nozzles

W_c kg/s (lb/s)	P_3 atm	T_3 K(° F)	V_{ref} m/s (ft/s)	$(\frac{W_c}{P_3})^2 T_3$	$\Delta P/P$	ΔP_{fuel} at L/O atm	$\frac{PT}{V_{ref}}$	$\frac{PT \Delta P}{V_{ref} P}$	f/a l Cup Lit	f/a All Cups Lit	ϕ l Cup Lit	ϕ All Cups Lit
0.19 (0.42)	0.539	293 (67)	6.2 (20.3)	36.4	0.0326	1.430	25.5	0.831	0.0377	0.0377	3.0	3.0
0.07 (0.15)	0.471	294 (69)	2.6 (8.5)	6.5	0.0097	0.612	53.3	0.517	0.0683	0.0683	5.5	5.5
0.07 (0.15)	0.404	293 (67)	2.9 (9.5)	8.8	0.0111	0.748	40.8	0.453	0.0761	0.0761	6.1	6.1
0.07 (0.15)	0.337	293 (67)	3.5 (11.5)	12.6	0.0137	0.748	28.2	0.386	0.0777	0.0777	6.3	6.3
0.04 (0.09)	0.271	294 (69)	2.7 (8.8)	6.4	0.0101	1.020	29.5	0.298	0.1480	0.1480	12.0	12.0
0.07 (0.15)	0.244	294 (69)	4.8 (15.7)	24.2	0.0216	0.748	14.9	0.322	0.0777	0.0777	6.3	6.3
0.16 (0.35)	0.265	294 (69)	10.3 (33.8)	107.2	0.0788	---	7.6	0.599	No Light			
0.14 (0.31)	0.344	295 (71)	7.1 (23.3)	48.9	0.0410	1.293	14.3	0.586	0.0490	0.0490	4.0	4.0
0.21 (0.46)	0.408	295 (71)	9.0 (29.5)	78.2	0.0621	2.177	13.4	0.832	0.0429	0.0429	3.5	3.5

3. Emissions Results

CO idle emissions met the E³ target level of 20.7 g/kg (20.7 lbm/1000 lb) of fuel for only two of the configurations tested. One of these two configurations featured the prototype fuel nozzles which were found to be detrimental for the sector combustor ignition performance. The HC emissions target level of 2.8 g/kg (2.8 lbm/1000 lb) of fuel was substantially exceeded in the other configuration. The airflow distribution of the Mod V configuration resulted in the best overall idle emissions performance with the HC emissions target met and the CO emissions target exceeded by 14%.

NO_x emissions at simulated sea level takeoff conditions are estimated to have exceeded the target level of 17.5 g/kg (17.5 lbm/1000 lb) of fuel for all configurations tested for this emissions category. The NO_x emissions target was considered to be the most challenging of all the pollutant emissions targets. However, the E³ full-annular combustor test experiences have demonstrated that generally higher NO_x emissions were produced in the sector combustor than the full-annular combustor for similar configurations.

4. Altitude Relight Results

The sector combustor exhibited a limited success in altitude relight performance. Ignition was not attainable at speeds higher than Mach = 0.6 and altitudes higher than 9 km (29,500 ft). Further investigation was required for any effort to improve the altitude relight performance, but such effort was not planned in the E³ Sector Development Program scope.

6.3 FUEL NOZZLE CALIBRATION TESTING

Detailed flow testing was conducted to calibrate and measure the fuel spray angle for each of the 48 completed E³ engine fuel nozzle assemblies received. This testing was done using the Meriman flow calibration test stand located in the GE-Evendale Building 301 Fuel Nozzle Laboratory. Calibration and spray angle data obtained were checked against the design intent and the calibration data generated by the manufacturer prior to shipment.

The procedure used was to mount a nozzle assembly vertically above a catch basin. Fuel supply lines were connected to the inlet fittings of the pilot and main systems. The supplied calibration fluid closely simulates the

properties of Jet A-type aviation fuel. Nozzle tip shroud air was not used for the purposes of this calibration testing. Various fuel pressures representing points along the nozzle design curves were set, and fuel flow rates and spray angles were recorded at each pressure. Fuel spray angles were obtained by using an adjustable protractor and the human eye. Although this was a crude technique, it was considered reasonable in order to provide the desired accuracy.

The results of this in-house calibration testing revealed two problem areas which could potentially impact the overall operating performance of the combustor.

The first problem identified involved low fuel flow levels measured in the secondary system in both the pilot and main stage nozzle tips. At fuel pressures representing sea level takeoff operation, the pilot stage tips - on the average - flowed ~7% below the design intent of 80 kg/hr (176 lb/hr), $\pm 4\%$. At the same operating conditions, the main stage tips - again, on the average - flowed ~8% below the design intent of 159 kg/hr (350 lb/hr), $\pm 4\%$. The measured tip-to-tip variation in both the pilot and main systems was ~10% from the average measured flow level. Therefore, some of the nozzle tips were flowing as much as 18% below the design nominal. These results were verified by calibration data supplied by the manufacturer.

This problem was discussed with engineering representatives from the manufacturer. From these discussions it was learned that in sizing the secondary fuel metering annulus within the nozzle tip, the required secondary fuel flow level was set as a total (primary plus secondary) nozzle tip fuel flow level. Thus, the secondary systems were sized for a lower flow than specified. To achieve the correct engine fuel flow levels at the high-power operating conditions (where the secondary fuel systems are in use) will require fuel pressure increases of about 15% over the design. This is well within the engine fuel supply capacity and does not pose a problem for engine operation. The measured average fuel flow calibration data are presented with the design operating curves in Figure 125.

The other problem identified through this calibration testing involved the fuel spray cone angle of the primary fuel system for the pilot and main

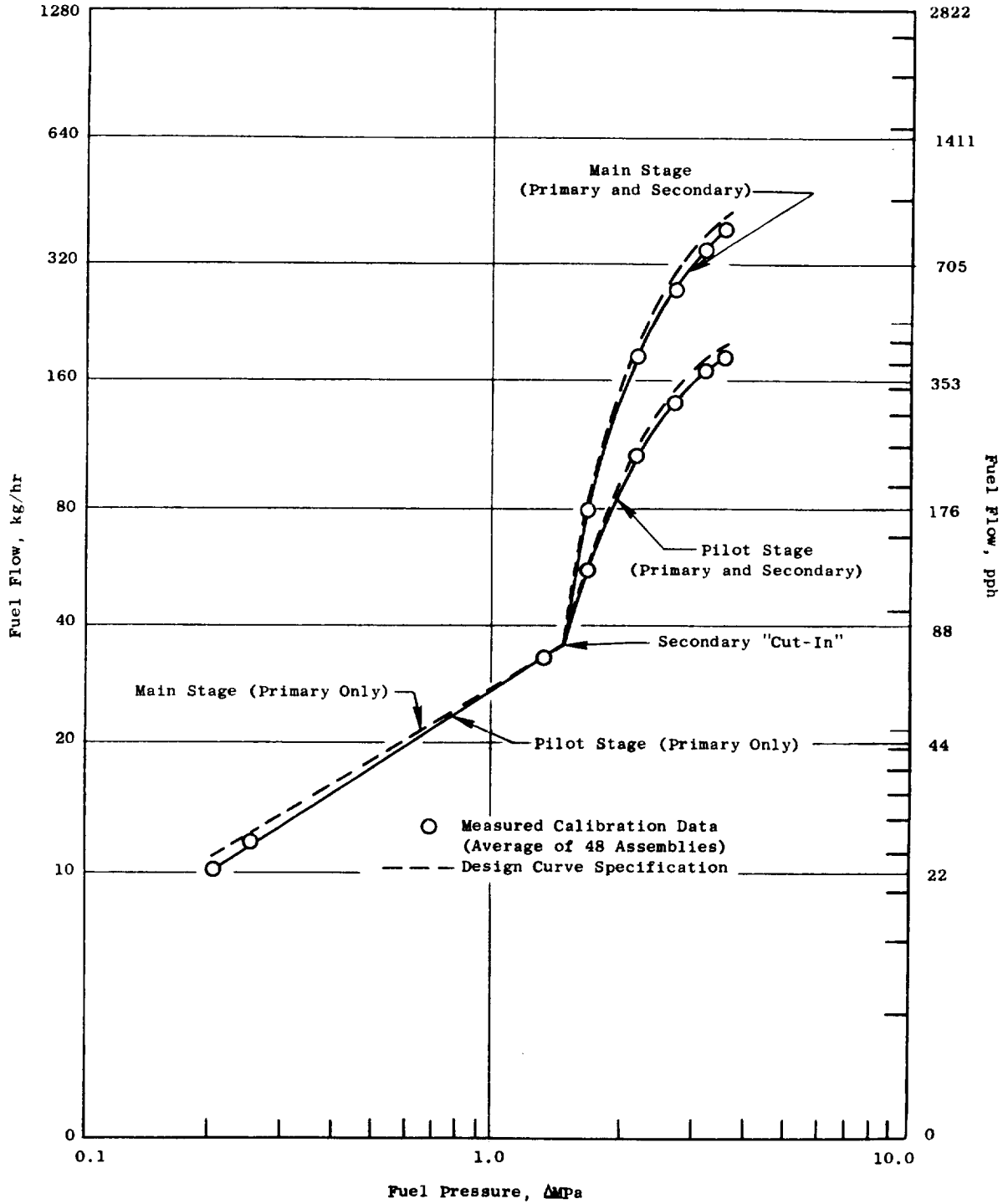


Figure 125. Engine Fuel Nozzle Assemblies Flow Calibration Results.

stage nozzle tips. The design specification requires this angle to be between 45° and 55° at a fuel pressure drop of 0.255 MPa (37 psi). Angles from 20° to over 60° were measured with considerable tip-to-tip variation. There was considerable concern over the potential negative impact on the combustor low-power performance where only the primary fuel systems would be in use.

It appears that the problem arose because during the manufacturing phase, the spray angle of the primary systems was set without the secondary system or air shroud assembled onto the tip. Apparently, the presence of these features caused a destabilizing effect on the primary spray angle. It was suggested that the fuel nozzle tips be checked for spray angle with shroud air present. The low pressure region that would form around the tip as a result of the shroud air would cause the primary fuel spray to open up. The physical boundary formed by the tip bow tail would limit this angle from providing a stabilizing effect.

To test this idea, a special box was fabricated into which the engine fuel nozzle assemblies were individually mounted. The pilot and main stage nozzle tips protruded through a wall of the box. Pressurized air was supplied to the box to energize the shroud air. Fuel was supplied to the nozzle tips. The box with nozzle assembly was set up on the fuel spray visual test stand. Observations were made of the nozzle tip operation.

The results from this testing confirmed expectations. The primary fuel spray angle opened up to the bow tail angle with just the slightest amount of shroud air. The spray angle remained opened and stable at shroud airflow levels representing combustor dome pressure drops in excess of 10%. Measured angles with the shroud air were all within the design specifications. It was also observed that the atomization quality of the primary fuel spray greatly improved with the presence of shroud air. There was no observed impact on the secondary fuel spray angle resulting from the introduction of shroud air. However, significant improvement in the fuel atomization quality was evident.

Based on the results of this testing, fears of potential combustor performance problems directly linked to the use of these nozzles were alleviated. All 48 nozzle assemblies were considered acceptable for use in combustor component testing and actual engine system testing.

7.0 FULL-ANNULAR COMBUSTOR COMPONENT DEVELOPMENT TESTING

Full-annular combustor component development testing of the E³ combustor involved two major combustor designs: lean main stage designs and rich main stage designs. The primary development effort involved the lean main stage designs, directed toward evolving a combustor design capable of satisfying all of the design objectives established in the E³ combustor development program. In this effort, the Baseline and Mods I, VI, and VII, plus the engine combustor configurations, were evaluated for ground start ignition, exit temperature performance, and emissions. The secondary development effort involved the rich main stage designs directed towards evolving a combustor design capable of staged combustion during ground start operation. The Mods II through V combustor configuration were evaluated for ground start ignition and exit temperature performance as part of this effort.

In support of each design philosophy, promising design concepts which evolved from the various subcomponent testing efforts conducted as part of the E³ combustor development program were considered for incorporation into the full-annular combustor designs. Other promising design concepts considered were identified through analysis of test results obtained from previously tested full-annular configurations. Many of these design concepts were incorporated into the full-annular combustor for detailed evaluation. This procedure resulted in a very successful full-annular test program. The engine combustor design which evolved from this development effort satisfied nearly all of the required design objectives.

7.1 TEST HARDWARE DESCRIPTION

7.1.1 Double-Annular Development Test Combustor

The E³ double-annular dome development test combustor was designed for flexibility and low cost while providing an accurate simulation of the engine combustor flowpath, key dimensions, and design features. An illustration of the E³ development combustor and key features are shown in Figure 126. The development combustor consisted of a double-annular dome assembly separated by a centerbody. Each dome has 30 equally spaced swirl-cup assemblies identical

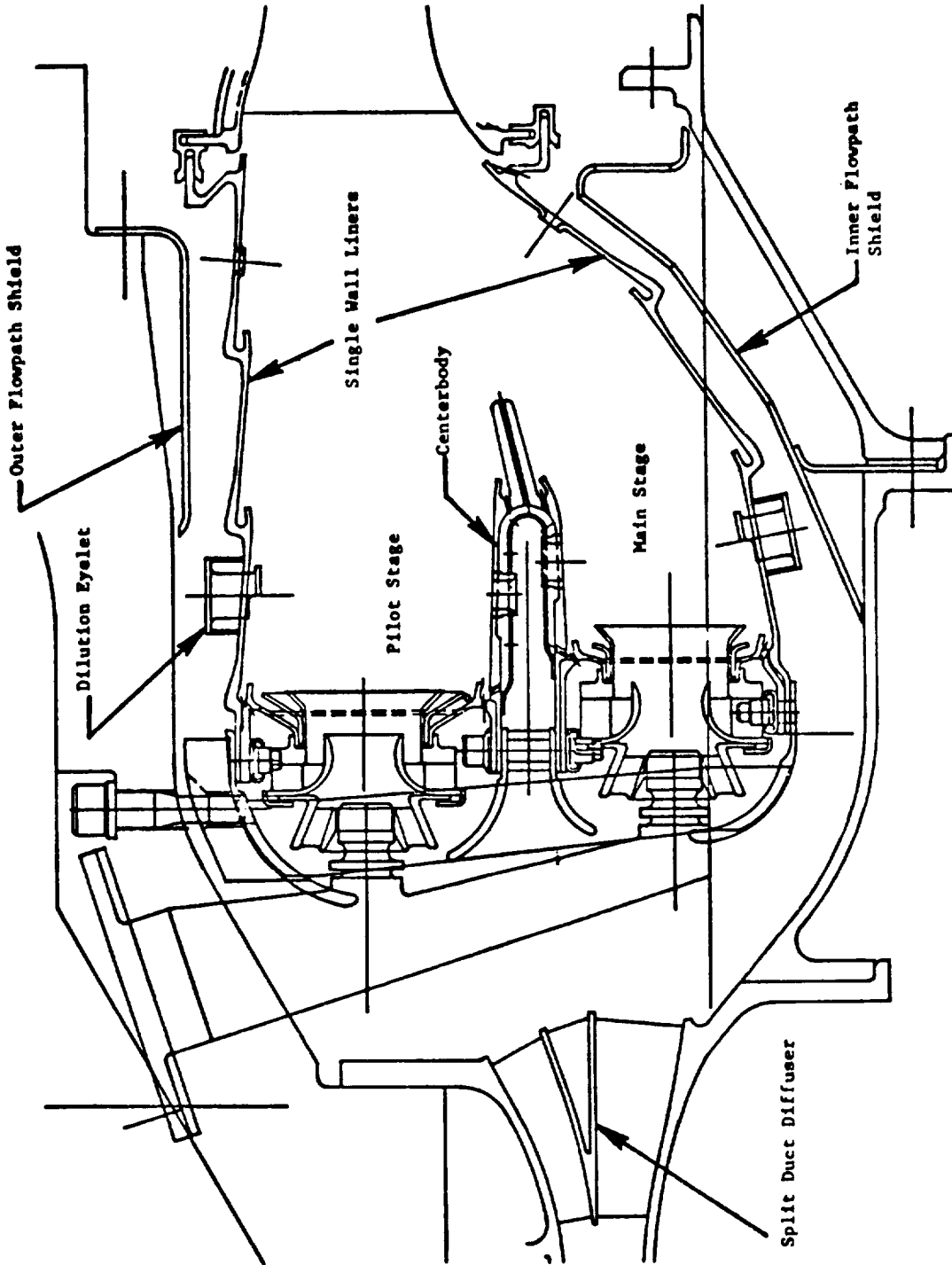


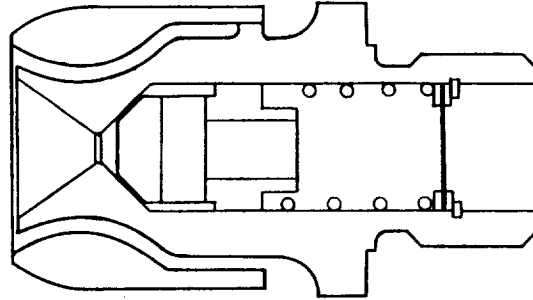
Figure 126. E³ Full-Annular Development Combustor.

in design to those of the engine combustor. The liners contain 30 equally spaced primary air holes and 60 equally spaced secondary trim air dilution holes. The primary holes are an eyelet-type design with a coannular clearance gap which provides a close simulation of the engine double-wall liner air hole aerodynamics. The liners are attached to the dome assembly by bolts which permitted assembling the liners with the primary air holes directly in-line with the swirl cups or between the swirl cups. The centerbody structure, which is also bolted to the dome assembly, provides a sheltered region between the pilot stage outer dome annulus and the main stage inner dome annulus. The centerbody structure contains two crossfire tubes to permit propagation of hot gases from one burning dome annulus into the other for the purpose of ignition. There are also 30 equally spaced primary air holes which penetrate the outer dome annulus and 30 equally spaced primary air holes which penetrate the inner dome annulus. The centerbody can also be positioned such that the primary holes are directly in-line with the swirl cups or between the swirl cups.

The development combustor liners are a conventional machined ring film cooled design as compared to the film impingement shingle liner design of the engine combustor. The inner surface of the development combustor liners match the engine combustor flowpath. However, because there is no impingement cooling liner, the outer surfaces of the liners do not match the engine combustor flowpath. In order to simulate the same inner and outer flow passage velocities and pressures, flowpath inserts were installed into the test rig combustor housing section, also shown in Figure 126. Plunged-type holes are used for the secondary trim dilution for both the inner and outer liners. Eight major configurations of the E³ development combustor were built and evaluated in this testing effort.

The development combustor fuel injector assembly, shown in Figure 127, consists of a single body with two fuel passages and two simplex-type fuel nozzle tips to supply fuel to the outer dome annulus and inner dome annulus. The envelope of the development nozzle body duplicates that of the engine nozzle but is much more simple relative to internal hydraulics. Both nozzles of each injector can be removed and replaced with simplex-type nozzle tips of different flow rates and spray characteristics. A schematic of a typical

ORIGINAL PAGE IS
OF POOR QUALITY



Typical Fuel Nozzle Tip

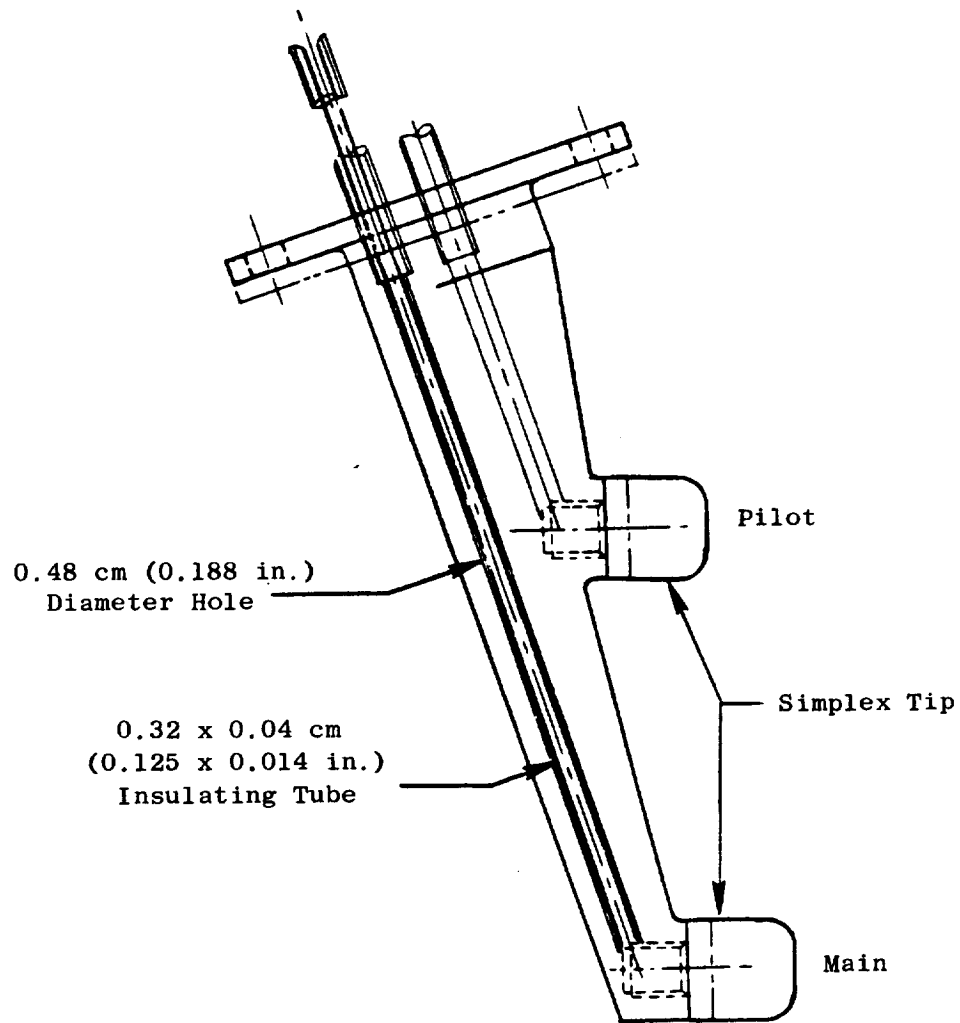


Figure 127. E³ Test Rig Fuel Nozzle Assembly.

nozzle tip is also shown in the figure. A large assortment of these tips was purchased for use in the various kinds of testing to be performed.

7.1.2 Double-Annular Engine Combustor

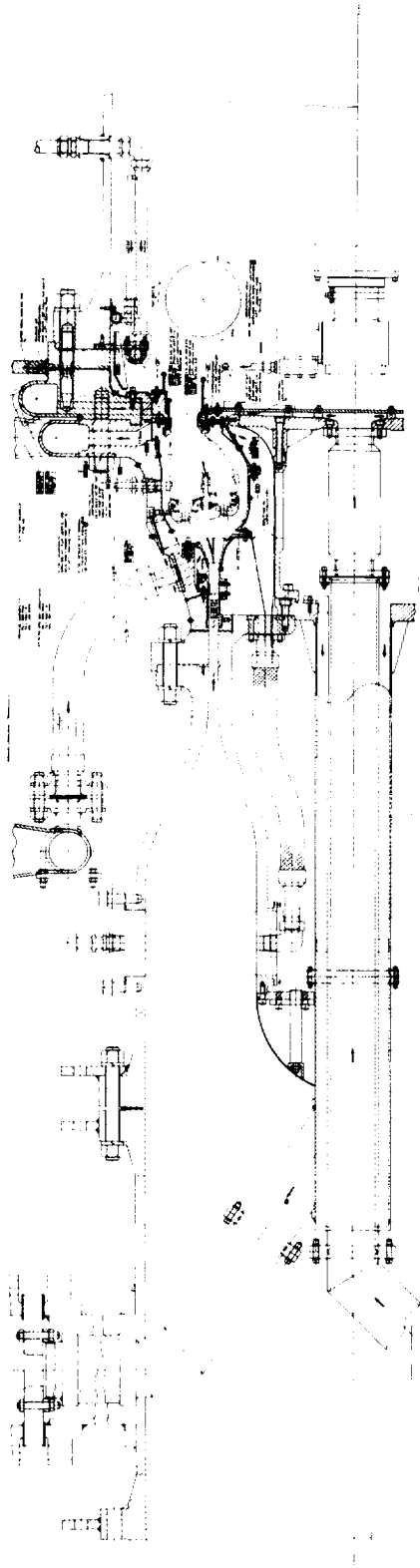
The E³ engine combustor, previously shown in Figure 1, features the same internal aerodynamic flowpath as the development combustor. The hardware featured in the domes and centerbody assembly is the same design as that used in the development combustor. However, the liners are a double wall film plus impingement cooled, segment shingle design.

The E³ engine fuel nozzle assemblies, previously shown in Figure 58, feature two pressure atomizing nozzle tips mounted onto a single stem. Each of the two nozzle tips is a duplex type featuring a low flow primary system for good fuel spray atomization at low power operating conditions, and a high flow secondary system to achieve the required fuel flow levels at high power operating conditions. Fuel is independently supplied to the pilot and main stage nozzle tips by two scheduling valves contained in the inlet of each nozzle assembly. Additional valves contained in the nozzle assembly valve housing control the fuel scheduling to the primary and secondary systems of the duplex nozzle tips. The fuel nozzle stem is encased in a heat shield to insulate the fuel from the hot compressor discharge air. Additional insulation is provided by clearance gaps surrounding each fuel passage inside the nozzle body.

7.1.3 Full-Annular Test Rig Description

The E³ double-annular dome development combustor evaluations were conducted in a full-annular, high pressure test rig specifically designed to house the E³ combustor. This full-annular combustor test rig exactly duplicates the engine combustor aerodynamic flowpath and envelope dimensions. The test rig consists of four major subassemblies, which are the inlet duct, diffuser flowpath transition section, combustor housing, and instrumentation section for gas sample data acquisition or atmospheric performance data acquisition. A detailed illustration of the test rig is presented in Figure 128.

The inlet duct assembly is attached to the test facility air supply system (not shown) at a specially designed pipe flange of 95.4-cm (37.5-in.)



ORIGINAL PAGE IS
OF POOR QUALITY

Figure 128. E³ Full-Annular Combustor Component Test Rig.

diameter. The inlet duct assembly, in addition to providing the interface with the test facility air supply, also has provisions for transferring combustor bleed air and test rig cooling air into and out of the test rig. These ancillary airflow systems are connected to test facility control and measurement systems.

The outer shell of the inlet duct attaches to the transition section, which converges to form the outer wall of the prediffuser inlet. Six radial struts support the bulletnose centerbody which transitions to the inner flow-path contour of the prediffuser inlet to duplicate the annular passage that exists at the compressor discharge plane. The centerbody provides an internal flowpath for transmitting the cooling and bleed airflows, as well as instrumentation leadouts through passages in the radial struts.

The annular passage which simulates the compressor discharge exit connects to the prediffuser assembly located within the combustor housing. This annular passage splits into two separate annular passages with inner and outer walls conforming to the exact contours of the engine split prediffuser. The split prediffuser passages are supported by streamlined struts similar to those in the engine. Airflow can be extracted at the trailing edge of the prediffuser, in the cavity formed by the splitter vane walls, through ten 2.06-cm (0.8-in.) diameter bleed ports equally spaced around the circumference. The airflow extracted through these bleed ports is routed through piping in the support struts spanning the outer prediffuser passage to a common manifold, then radially out of the rig through hoses to a bleed manifold which is connected to a standard ASME orifice run to meter the flow. A detailed schematic of this bleed system is shown in Figure 129. This prediffuser bleed system was designed to have the capability of varying the amount of bleed flow extracted from the combustor airflow to evaluate the effects of this engine flow parameter.

The combustor housing section of the test rig aerodynamically simulates the flowpath and envelope of the engine. The outer pressure vessel simulates the outer flowpath while an inner support which connects to the prediffuser provides the inner flowpath contour.

ORIGINAL PAGE IS
OF POOR QUALITY

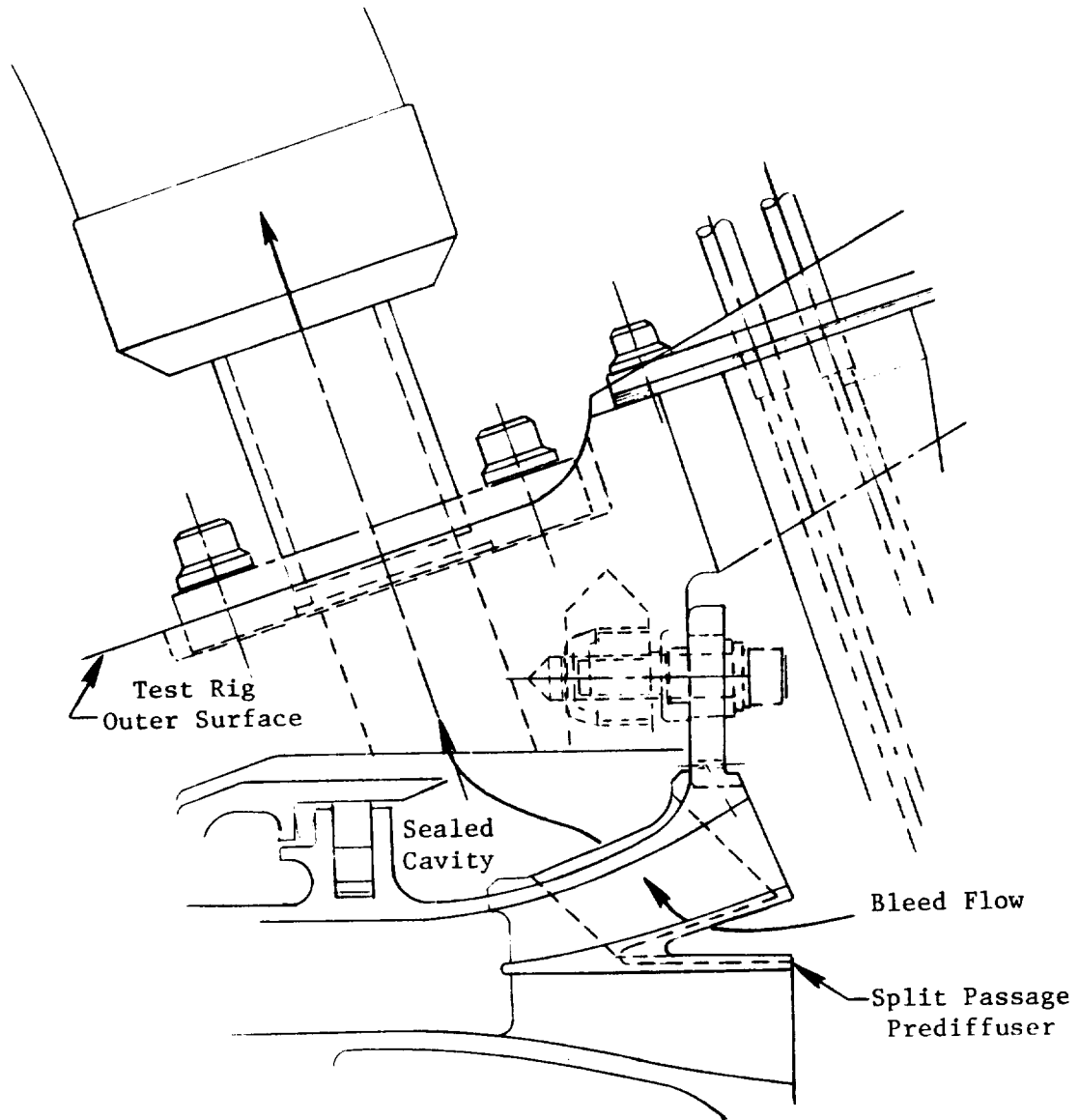


Figure 129. Test Rig Bleed Simulation System.

The outer pressure vessel housing is equipped with ports and bosses to accommodate 30 equally spaced dual-nozzle fuel injector assemblies, two igniters, and allow for borescope inspection and instrumentation leadout. Fuel is supplied to the fuel injectors through tubes which provide a connection between the dual manifold fuel supply and the pilot or main stage fuel passage in the injector body.

At the aft end of the outer flowpath, airflow can be extracted through thirty 3.0-cm (1.18-in.) diameter bleed ports, equally spaced around the circumference to simulate turbine nozzle cooling flow from the combustor outer flowpath. The flow extracted from each bleed port is routed into a collector manifold then out of the test rig. At the aft end of the inner flowpath, airflow can be extracted through nine 3.5-cm (1.18-in.) diameter bleed ports, equally spaced around the circumference, to simulated turbine nozzle cooling flow from the combustor inner flowpath. The flow extracted from each of these bleed ports is routed into a plenum cavity at the center of the test rig, then out through an annular pipe along the centerline of the centerbody assembly. Both the inner and outer passage bleed systems have standard ASME orifice runs to meter and measure the bleed flow. These bleed ports together with the prediffuser bleed ports provide the capability to accurately simulate and evaluate the effect of engine turbine cooling flows expected during engine operation.

The combustor mounting system used in the test rig is identical to that designed for the engine. The combustor is supported at the front end by engine mounting pins and is supported at the aft end by floating seals similar to those on the engine design.

The aft end of the combustor housing is connected to an adapter flange which provides cooling air to the aft outer combustor flowpath. This adapter has a single manifold cavity which feeds cooling air through twenty-two 2.5-cm (1.0-in.) radial holes to the aft tail piece. In addition, the mounting provisions for the instrument spools are located in this adapter.

The instrumentation spool features a rotating internal shaft supported by six radial struts: three forward and three aft. A cross section of the rotating spool piece is shown in Figure 130. The end of the rotating shaft,

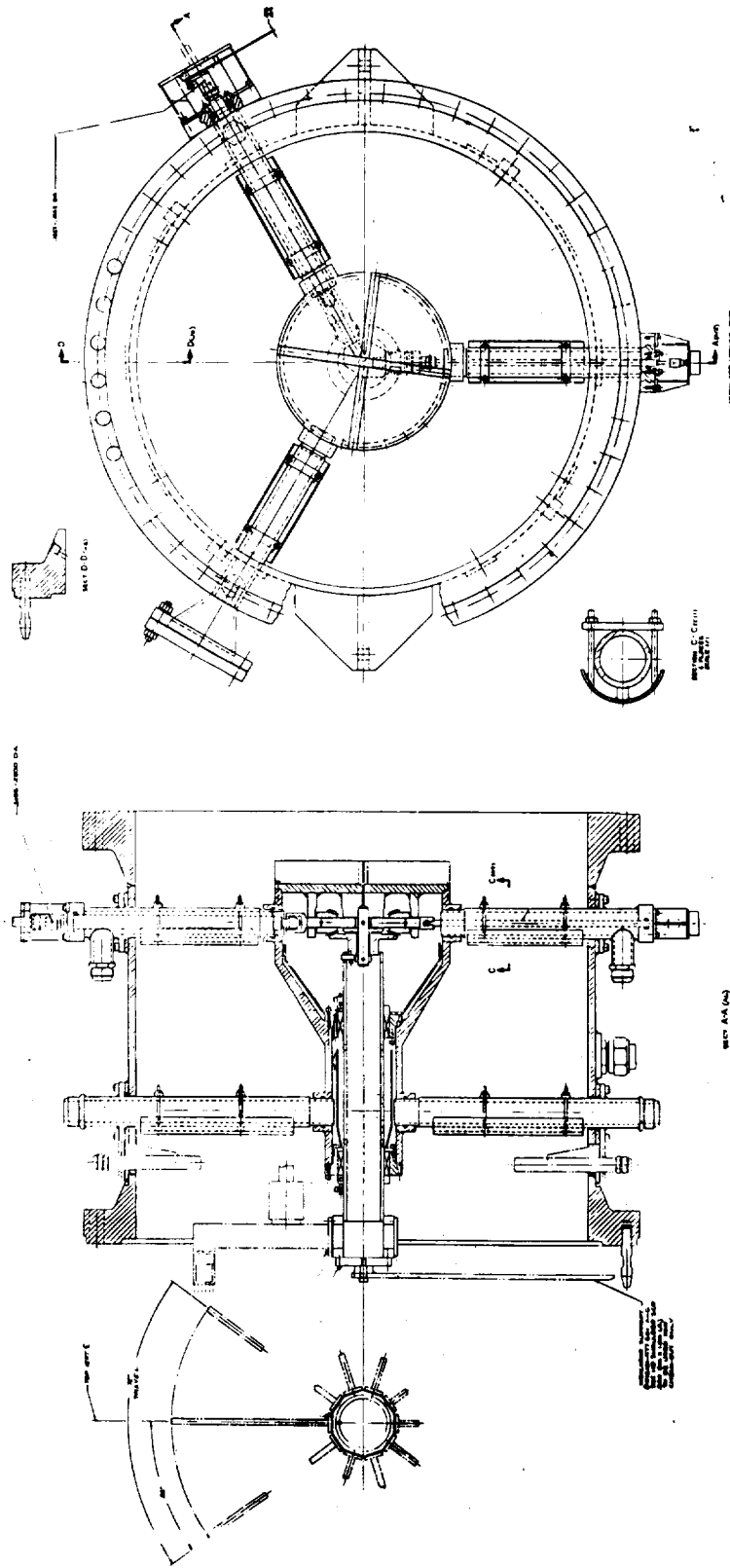


Figure 130. Test Rig Instrumentation Spool.

which is supported by two bearings, has ten mounting pads. The gas sample rakes and/or thermocouple rakes are mounted to these pads in locations and quantities as desired during test. Cooling of the shaft assembly and struts is accomplished by circulating water through the struts and along the shaft. A portion of the cooling water is directed to the rake mounting pads where it supplies an auxiliary water manifold and to the gas sample rakes for rake body cooling. The rake cooling water is discharged from the rake bodies into the duct. Additional structural cooling is accomplished by water discharged from spraybars and ring manifolds mounted near the duct walls.

Rotation of the center shaft is accomplished by a drive motor located outside the instrument spool duct wall. This motor drives a radial shaft, supported in a strut, which is connected to a helical gear set by a spherical gear coupling. The spherical gear coupling permits rotation even with some shaft misalignment. The portion of the helical gear, which is aligned with the rake mounting shaft, contains a lug. This lug engages a slot in the shaft and can rotate the shaft a total of about 36° clockwise and counterclockwise for a total of nearly 72° rotation. The input coupling has a mechanical stop to prevent excessive travel. The drive shaft is equipped with shear pins to prevent damage to the gear mechanism in the event of hangup or overtravel.

The Atmospheric Combustion Test Stand (ACTS) system is used to obtain detailed temperature measurements at the combustor exit. The system adapts to the aft end of the combustor test rig housing as shown in Figure 131. Thermocouple rakes and/or pressure rakes are attached to the traverse ring and are guided by the roller system and track. The traverse ring is motor driven and will rotate 90° clockwise or counterclockwise in increments as small as 1.5° . The thermocouple rakes are equipped with seven chromel-alumel (C/A) elements. The thermocouple elements are led to a chromel alumel thermocouple system (CATS) block which transmits the electronic signals to the data acquisition system. The exit temperature data, along with the fixed test rig and combustor instrumentation, are automatically processed by the data acquisition system and are presented in a finished format of prescribed combustor performance parameters and operating conditions.

ORIGINAL PAGE IS
OF POOR QUALITY

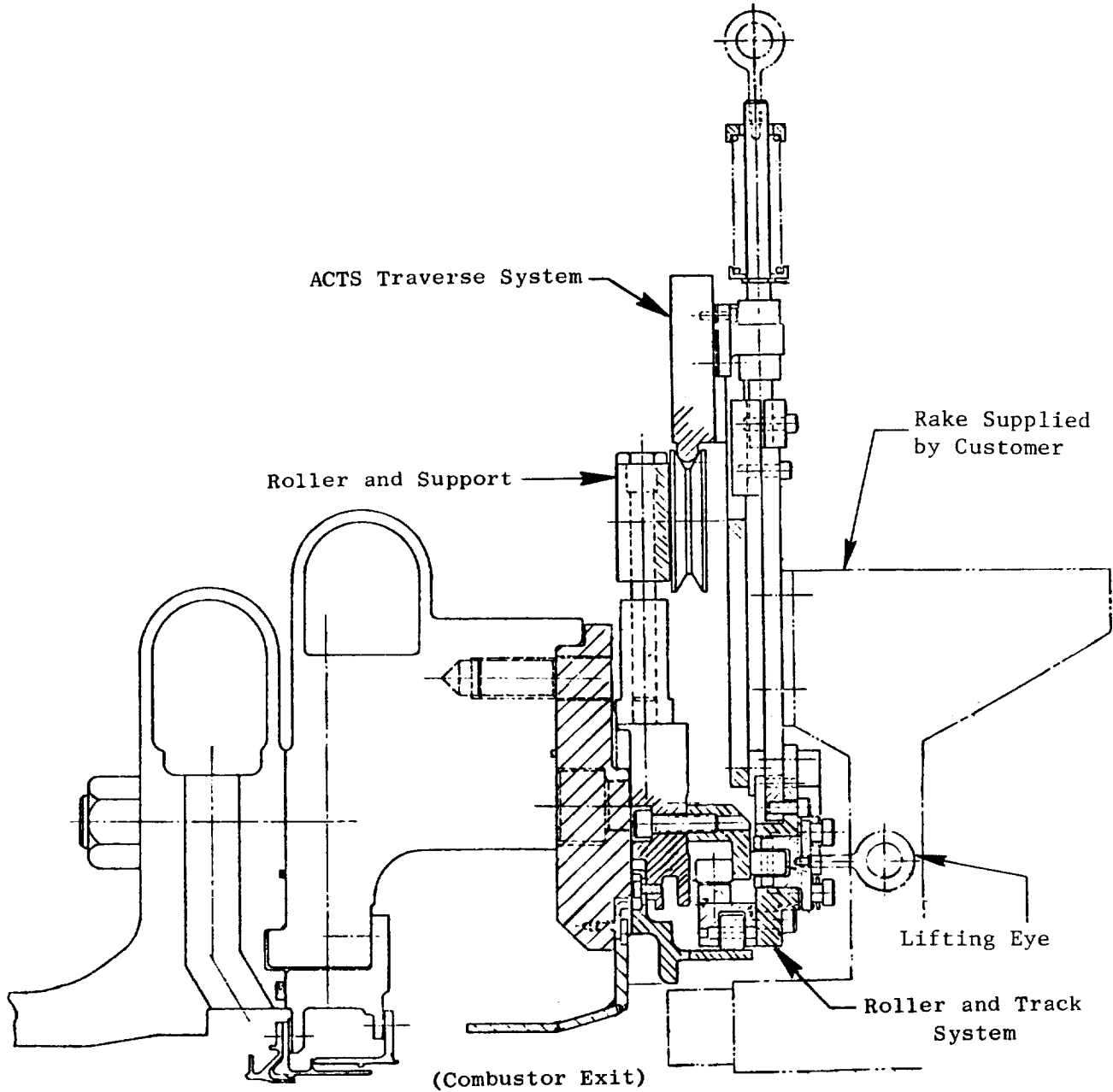


Figure 131. ACTS Traverse System.

7.2 TEST METHODS

7.2.1 Atmospheric Tests

Ground start ignition, crossfire, and exit temperature performance characteristics of the E³ development combustor were evaluated at atmospheric inlet conditions. In this testing configuration the test rig was discharged "open end" into the surrounding test cell ambient environment. This permitted useful visual observations of the combustor in operation. In these atmospheric tests, the combustor inlet temperatures duplicated the level of the desired operating cycle test point. However, the combustor airflows were scaled down to levels which simulated the combustor velocities while operating at atmospheric inlet pressure. This technique provides an inexpensive testing approach by which to develop satisfactory ground start ignition and exit temperature performance characteristics while providing accurately simulated combustor operating conditions.

Ground start ignition testing was conducted using the standard GE23 ignition system. This system consists of igniter plug (P/N 4013204-112P01), exciter unit (P/N 910M52-P11), and igniter lead (P/N 9787M47). This ignition system has an energy delivered rating of two Joules with a firing rate of two sparks per second. The igniter was positioned in outer liner panel 1° at 240° CW ALF (aft looking forward). The igniter immersion was flush with the inside surface of the liner panel wall. To further simplify this testing, no bleed flows were set during the ignition evaluations. Past experience has shown that the effects of bleed flows on the ground start ignition characteristics are insignificant. The basic testing procedure used goes as follows:

1. Set the combustor operating conditions corresponding to the selected steady-state test point.
2. Activate the ignition system.
3. Supply fuel to the pilot stage fuel nozzles. Continue to increase this fuel flow until the igniter swirl cup has ignited. Deactivate the ignition system, and record the operating conditions and fuel flow level.
4. Continue to increase the fuel flow until full pilot stage propagation is achieved. Record the operating conditions and fuel flow level.

5. Reduce the fuel flow rate slowly until one pilot stage swirl cup extinguishes. Record the operating conditions and fuel flow level.
6. Continue to decrease the fuel flow rate until total lean blowout is obtained. Record the operating conditions and fuel flow level.
7. Repeat Steps 2 through 4. Then reduce the pilot stage fuel flow to a level 10% above the level recorded at one cup extinguished.
8. Hold the pilot stage fuel flow level steady and supply fuel to the main stage fuel nozzles. Continue to increase the main stage fuel flow until the crossfire cup or cups ignite. Record the operating conditions and fuel flow levels.
9. Continue to increase the main stage fuel flow until full propagation is achieved. Record the operating conditions and fuel flow levels.
10. Reduce the main stage fuel flow slowly until total main stage lean blowout is obtained. Record the operating conditions and fuel flow levels. Then shut off the main stage fuel flow.
11. Reduce the pilot stage fuel flow slowly until total pilot stage lean blowout is obtained. Record the operating conditions and fuel flow levels.
12. Shut off all combustor fuel flow, then proceed to set the operating conditions corresponding to the next selected test point.

Throughout this procedure, visual observations were used to determine ignition, propagation, and lean blowout.

Atmospheric exit temperature performance testing was conducted using the ACTS system. Four E^3 exit temperature rakes were mounted onto the traverse ring of the ACTS system, equally spaced around the circumference. These rakes, shown in Figure 132, contained seven chromel-alumel thermocouple elements, and were especially designed for use with the E^3 combustor test rig. Throughout the duration of the E^3 combustor development testing effort, the temperature rakes underwent modifications intended to improve the quality of the data and reduce traverse problems. An illustration of these modifications is presented in Figure 133. During atmospheric performance testing only the prediffuser bleed flow was simulated. At all primary performance test points, exit temperature traverse data was obtained every 1.5° of the total 90° traverse. This provided temperature radial profile measurements at 240

ORIGINAL PAGE IS
OF POOR QUALITY

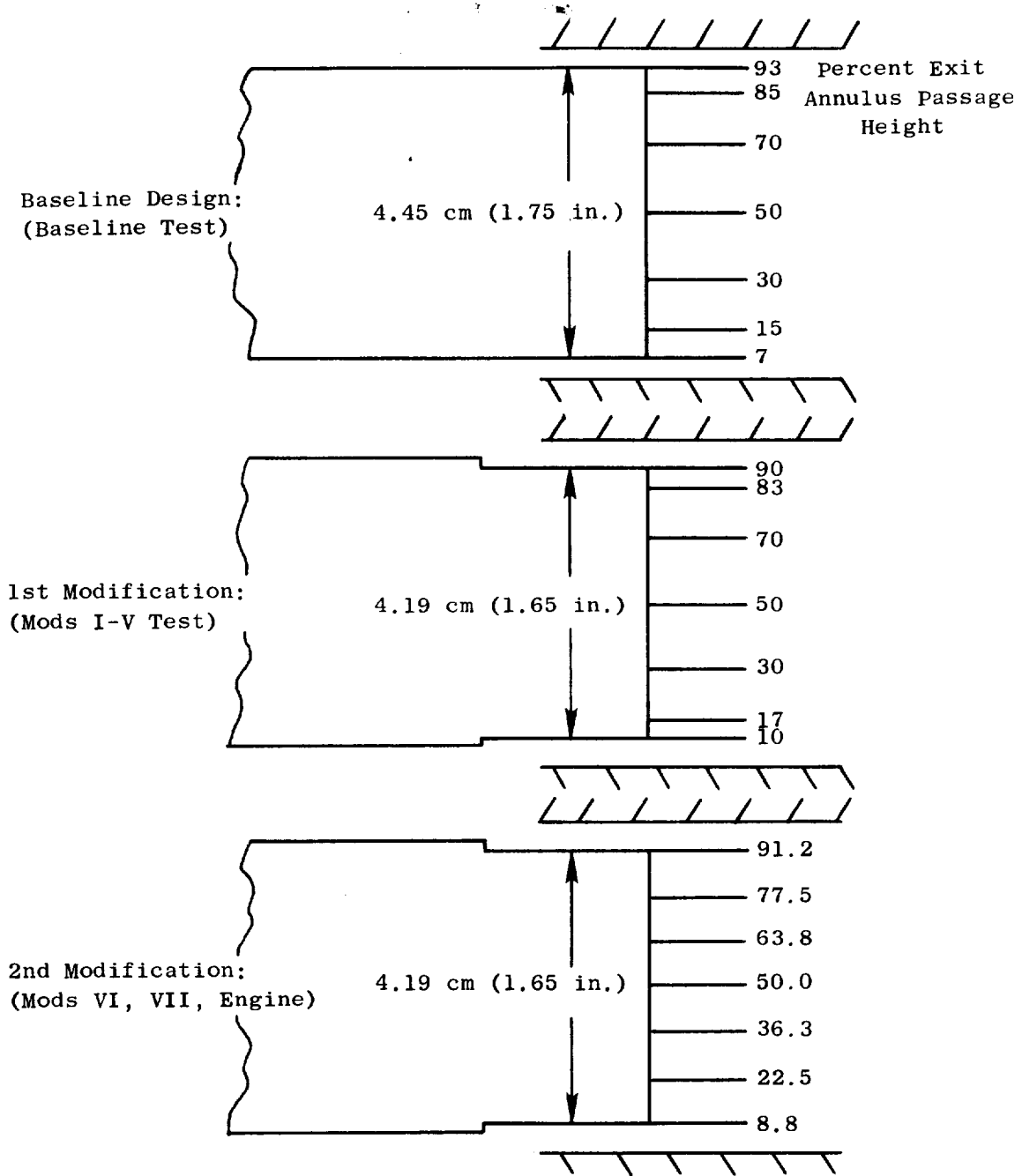


Figure 133. Thermocouple Rake Modifications.

circumferential positions for a total of 1680 individual temperature measurements. At off design or secondary test points, data was obtained every 3° around the circumference in order to save time. All combustor test rig instrumentation and exit temperature performance data were recorded on the facility data acquisition system. This information was then automatically processed through a computer data reduction program to calculate the combustor operating conditions, the average and peak radial temperature profiles, and the pattern factor and profile factor using these relations:

$$\text{Pattern Factor} = \frac{T4 (\text{max.}) - T4 (\text{avg})}{T4 (\text{avg}) - T3}$$

$$\text{Profile Factor} = \frac{T4 \text{ immersion avg (max.)} - T4 (\text{avg})}{T4 (\text{avg}) - T3}$$

7.2.2 Pressure Tests

Emissions characteristics of the E³ development combustors were evaluated at elevated inlet pressure. Several combustor configurations were also evaluated for ground start ignition and crossfire characteristics at elevated pressure as part of an emissions test. For this pressure testing, the test rig was assembled into a closed configuration. Since visual observations were not possible, monitoring the combustor operation was accomplished by using the available test rig and combustor pressure and temperature instrumentation.

Air was supplied to the test rig from the facility high pressure, high flow capacity system. With this system, combustor operating conditions in the test rig exactly duplicating the E³ FPS cycle conditions could be achieved up to 30% of sea level takeoff power. Above this power level, combustor airflow and inlet pressure were limited by the maximum capacity of the facility. At these high power operating points, test conditions were simulated. The combustor inlet temperature was set to the exact engine cycle level. The maximum available test section total pressure was approximately 1.655 MPa (240 psia). This compares to the 3.025 MPa (439 psia) level associated with the FPS sea level takeoff operating condition. Combustor test rig airflows were scaled down accordingly, such that combustor velocities simulated the velocities at true engine cycle operating conditions.

All CO, HC, and NO_x emissions levels measured at the simulated high power operating conditions were adjusted to reflect levels that would be obtained if measured under true engine cycle operating conditions. These adjustments were made using the relations presented in Appendix D.

Gas samples were extracted from the combustor discharge stream using the E³ gas sample rakes (P/N 4013100-986) shown in Figure 134. Five rakes were used, each with four sampling elements. For the purpose of ground start ignition testing, two chromel-alumel-type thermocouples were strapped onto the outermost and innermost sampling elements of each of the five gas sampling rakes. This arrangement is illustrated in Figure 135. These thermocouples were connected to a "Metroscope" visual display system within the facility control room and were used in determining ignition, crossfire, and lean extinction in the pilot stage and main stage of the combustor. A procedure similar to that used in the atmospheric ground start ignition testing was used to obtain the data.

For gas sampling purposes, all four elements of each gas rake were individually connected to the valving in the gas sampling equipment. This approach provided the flexibility to close off individual rake elements from the rake sample if problems would arise in any of the four elements. The five gas sampling rakes were equally spaced around the test rig instrumentation spool. Unheated water was used to cool the rakes during testing. The decision to use unheated water as the cooling medium was arrived at from results obtained during the emissions evaluation of the Baseline development combustor. These results, shown in Figure 136, showed that the use of unheated cooling water had only a very minor impact on idle emissions. This result plus the simplicity and lower costs of using unheated cooling water were the outstanding factors in selecting this approach.

During gas sampling, the rakes were traversed through 66° at 6° increments enabling gas samples to be obtained in-line with and between all 30 swirl cups. For ignition and blowout evaluation, the gas sampling rakes were positioned such that one rake was located at 240° CW ALF, placing that rake with its two thermocouple elements directly downstream of the pilot stage igniter cup and one of the two pilot stage-to-main stage crossfire tubes.

ORIGINAL PAGE IS
OF POOR QUALITY

ORIGINAL PAGE
BLACK AND WHITE PHOTOGRAPH

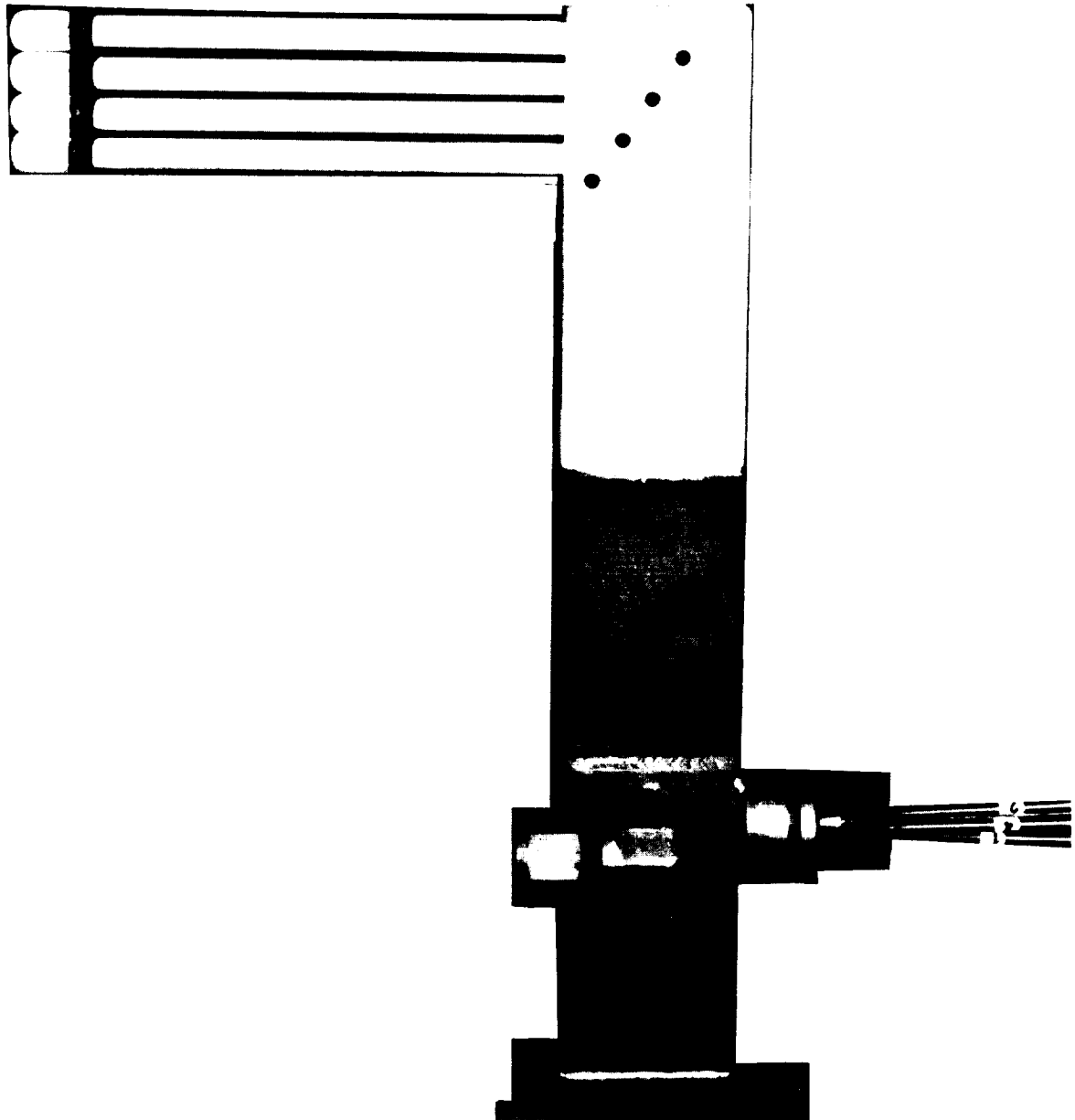


Figure 134. E³ Full-Annular Combustor Gas Sampling Rakes.

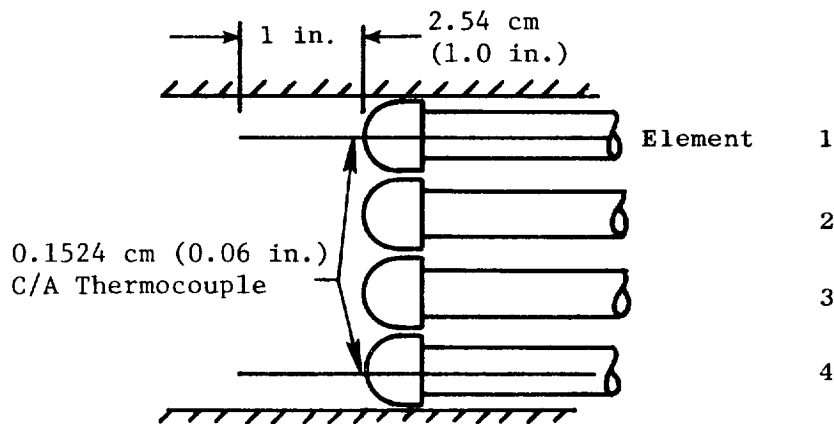
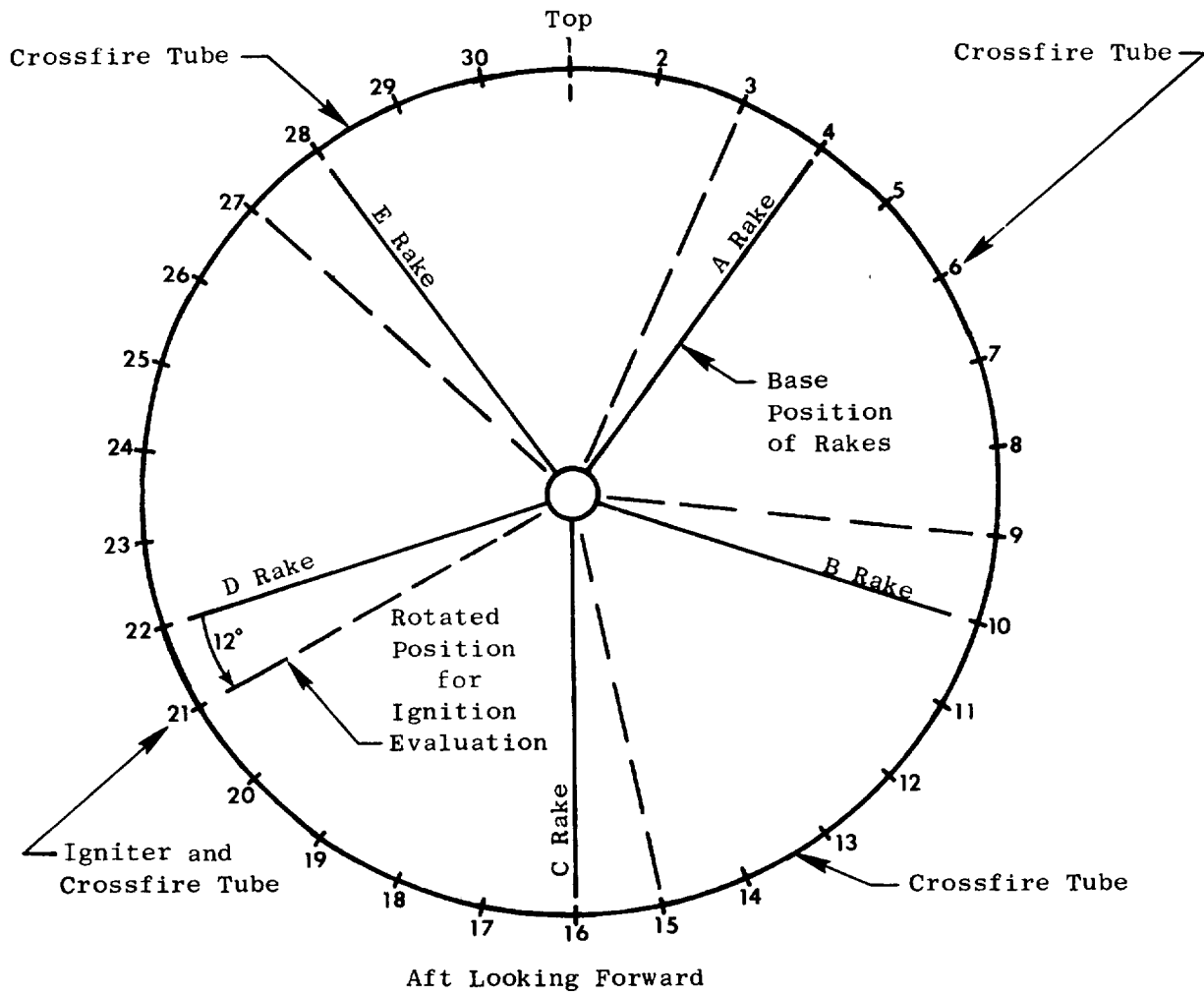


Figure 135. Gas Sampling Rake Instrumentation for Ignition Testing.

ORIGINAL PAGE IS
OF POOR QUALITY

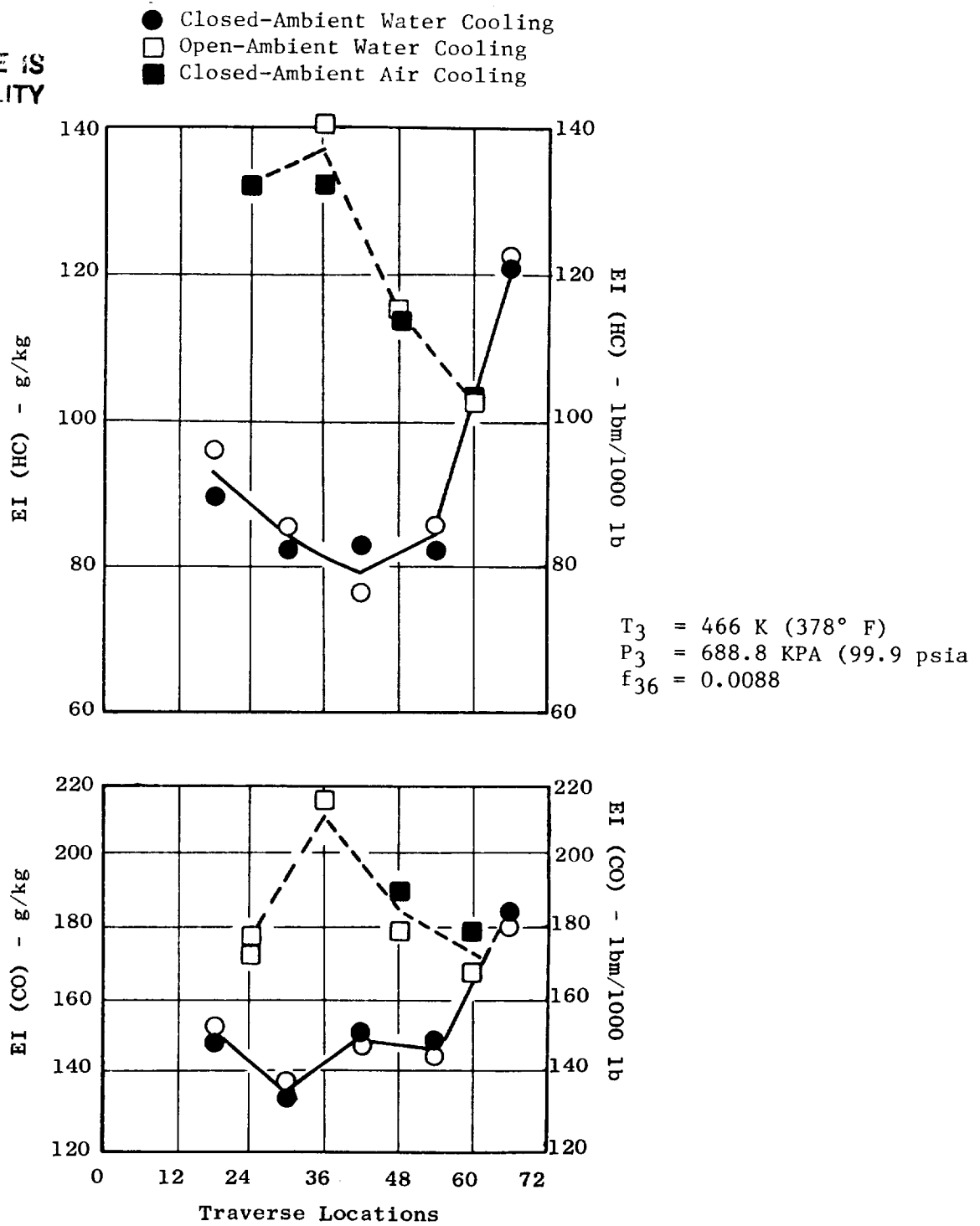


Figure 136. Effect of Gas Rake Cooling Medium on CO and HC Emissions.

Gas samples were analyzed using the CAROL II (Contaminates Are Read On Line) gas analysis system located at the test facility. Instruments featured in this system include:

- Beckman Model 402 total hydrocarbon analyzer (flame ionization detector)
- Beckman Model 315-B carbon monoxide and carbon dioxide analyzer (NIDR)
- Beckman Model 915-H NO_x analyzer (heater chemiluminescence with converter)

Sample flow was passed through a refrigerated trap to remove excess water from the sample before entering the gas analysis instruments. Prior to testing, the CAROL II system was calibrated using a set of calibration gases. These gases and their GE constituent analysis are listed in Table XXX. During testing, calibration spot checks of the instruments and any necessary adjustments were made to assure that this equipment was in good working order at all times. Inlet air humidity was measured using an EG&G Model 440 dewpoint meter.

Table XXX. CAROL Calibration Gases.

	<u>Span 1</u>	<u>Span 2</u>	<u>Span 3</u>	<u>Span 4</u>
Bottle S/N -				
CO (ppm)	261131 (227)	2960095 (468)	6742 (1085)	49244 (2350)
COa (%)	261131 (1.27)	2960095 (2.54)	6742 (4.94)	49244 (8.03)
HC (ppm)	1317746 (74.3)	49301 (143)	127885 (569)	49110 (1328)
Nox (ppm)	12553 (29.1)	12548 (69.8)	10766 (234)	3976 (543)

Smoke samples were taken only at designated key combustor operating points in the test schedule. Smoke samples were extracted from the exhaust

gases using two of the five gas sampling rakes valved in a manner which provided a single sample. At those test points where smoke samples were taken, the rakes were initially positioned in-line with the swirl cups, then rotated 6° to between swirl cups. At each of these two positions, several smoke samples, each 0.2 ft³ (0.0057 m³) in volume, were obtained using a standard GE smoke console located in the cell control room.

All emissions and instrumentation data acquisition was automatically handled by the Cell A3 medium speed digital data acquisition system. From this system, the data was processed through a computer data reduction program which performed calculations to compute the various emissions indices, combustor operating parameters, and convert digital signals from all pressure and temperature instrumentation to engineering units. All smoke samples were obtained on Wattman No. 4 filter paper. Following completion of testing, the smoke samples obtained were analyzed on a Densichron to determine the optical density used to compute the SAE smoke number.

7.3 BASELINE DEVELOPMENT COMBUSTOR TEST RESULTS

7.3.1 Atmospheric Ground Start Ignition Test

The first test of the E³ double-annular dome development combustor and test rig was conducted on 7 February 1980 in the General Electric Aero Component Lab Cell A3W test facility. The purpose of this test was to evaluate the Baseline development combustor configuration for ground start ignition, pilot to main stage crossfire, and the pilot and main stage lean blowout characteristics at atmospheric inlet pressure along the E³ (9/79) ground start operating line. Test points and corresponding operating conditions are shown in Table XXXI.

The Baseline combustor configuration featured most of the mechanical and aerothermo characteristics evolved during the design phase of the combustor development program. The only significant difference from the proposed design was in the pilot dome splash-plate cooling flow level. The combustor was designed to have approximately 4.3% of the total combustor flow for the pilot dome splash-plate cooling. However, the hardware was fabricated to have approximately 2.5 times the design flow level to provide the ability to

Table XXXI. Development Combustor Baseline Atmospheric Ignition Test Point Schedule.

<u>Point</u>	<u>Start Time, sec</u>	<u>XNRH, %</u>	<u>T₃, K (° F)</u>	<u>P₃ atm</u>	<u>W₃₆* kg/s</u>	<u>W₃₆ pps</u>
1	10	21.0	289, (60)	1.00	1.25	2.75
2	15	28.0	289, (60)	1.00	1.69	3.73
3	18	32.0	314, (105)	1.00	1.55	3.42
4	30	46.0	344, (160)	1.00	1.65	3.64
5	40	58.0	383, (230)	1.00	1.86	4.10
6	50	70.0	428, (310)	1.00	1.94	4.28
7	55	77.0	503, (445)	1.00	2.33	5.14

*If inlet air temperature cannot be set at the prescribed level, the airflow will be changed to maintain the $\frac{W_{36}\sqrt{T_3}}{P_3}$ value.

easily increase the splash-plate cooling flow level if necessary. It was intended to block off a percentage of this flow to achieve the intended design levels if baseline testing indicated sufficiently low dome metal temperatures. The estimated airflow distribution for the baseline development combustor is available in Appendix E. The fuel nozzle assemblies used featured the E³ test rig fuel nozzle bodies with simplex nozzle tips rated at 2.3 kg/hr (5 pph) at 100 psid in the inner dome, and simplex nozzle tips rated at 12.0 kg/hr (26.5 pph) at 100 psid in the outer dome. Both of these nozzle tips had fuel spray angles of approximately 50°.

It had been intended to use the GE23 ignition system to obtain the pilot stage ignition characteristics. However, problems were encountered at the onset of testing due to a failure in one of the components of the GE23 ignition system provided. As a result, a hydrogen torch ignition system was substituted and testing proceeded. Accurate pilot stage ignition data generally cannot be obtained with a hydrogen torch system due to its high specific energy

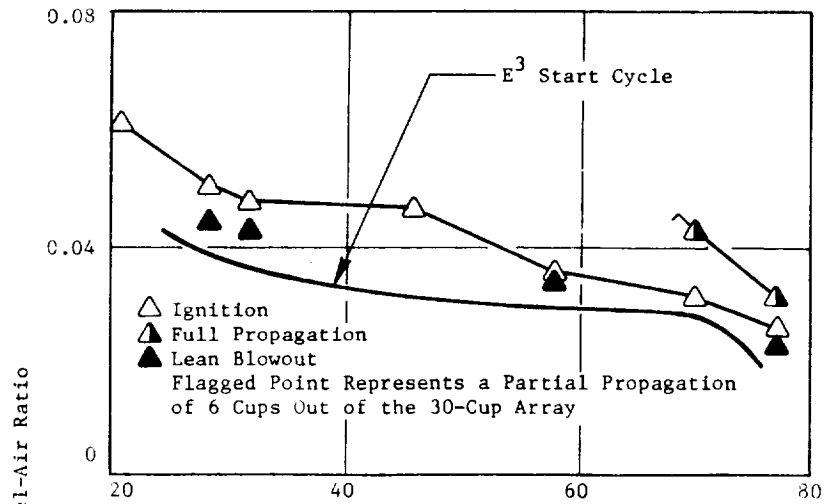
output. However, pilot stage propagation, pilot-to-main stage crossfire, and pilot and main stage lean blowout data were obtained. By the time the last test point had been set, another GE23 ignition system had been obtained. This system was installed into the test rig with the intent of obtaining pilot stage ignition data starting at the last test point and working back toward the initial test point. Following the completion of ignition at Test Points 7, 6, and 5, another failure in the electrical ignition system occurred and testing was terminated. The failures involved the igniter lead.

Test results obtained from the atmospheric ground start ignition evaluation of the E³ development combustor baseline configuration are presented in Figure 137. A detailed summary of the test data is provided in Appendix E. Ignition of the pilot stage igniter cup using the hydrogen torch proceeded without difficulty at each test point evaluated. However, once ignition occurred, a substantial increase in the pilot stage fuel flow was required to obtain a full propagation of the fire. As observed from this figure, the pilot stage ignition characteristics were within the E³ start cycle requirements.

The three test points evaluated with the GE23 ignition system show excellent agreement with the results obtained with the hydrogen torch ignition system. Past experience has generally shown that as the combustor operating conditions become more severe for ignition, greater difficulty arises in achieving ignition with electrical systems than with the hydrogen torch systems. Therefore, it was expected that pilot stage ignition results obtained with the GE23 ignition system at the simulated lower speed points would be somewhat poorer than the results obtained with the hydrogen torch system, but still within the start cycle requirements. The pilot stage demonstrated an acceptable lean blowout margin of about 30% along the entire start cycle operating line.

Ignition of the main stage was attempted at each test point. In all cases, this was accomplished by hot gases from the burning pilot stage passing through the two centerbody crossfire tubes located at 60° and 240° clockwise aft looking forward. However, propagation of the fire in the main stage was

Main Stage Crossfire Ignition Characteristics



Pilot Stage Ignition Characteristics

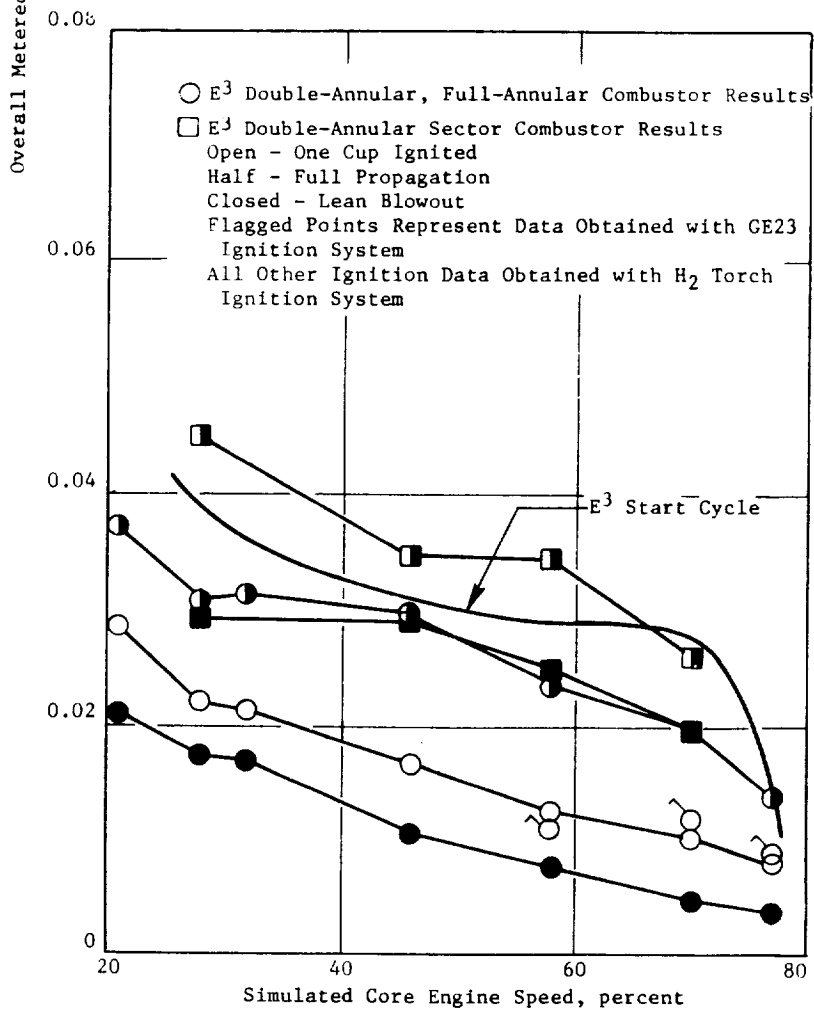


Figure 137. Development Combustor Baseline Atmospheric Ignition Test Results.

only achieved at the simulated higher speed points. The small-size fuel nozzle tips used in the main stage limited the maximum fuel flow in the main stage to approximately 160 kg/hr (350 pph) at the maximum fuel pressure that the facility could supply. A partial propagation (six cups) in the main stage was achieved at conditions representing the 70% engine speed point, while full propagation was achieved at conditions representing the 77% engine speed point. The combustor operating conditions at these points were favorable enough to offset the adverse effects of the lean main stage dome stoichiometry. Insufficient data was obtained to make a good assessment of the main stage lean blowout characteristics.

7.3.2 Atmospheric Exit Temperature Performance Test

Performance testing of the E³ double-annular dome development combustor Baseline configuration was conducted on 17 April 1980 in the Cell A3W facility. The purpose of this test was to evaluate the Baseline combustor configuration for profile and pattern factor at simulated sea level takeoff conditions with variations in the pilot and main dome fuel staging. This performance evaluation was a continuation of an earlier performance test of this combustor conducted on 20 February 1980. That test was prematurely terminated after obtaining data at the simulated 6% ground idle operating condition, when the thermocouple rakes jammed against the test rig outer aft seal, limiting the ability to traverse the rakes. All of the rakes were positioned inward from their initial positions to prevent a recurrence of the problems encountered. Some difficulty was incurred at the onset of the resumed effort. Several of the rakes were dragging along the test rig inner aft seal. Testing was interrupted and additional adjustments were made to the rake positions. When testing resumed, it was evident that some of the rakes were still dragging along the inner aft seal at several places in the test rig. However, the rakes could be traversed without great difficulty, and it was decided to proceed with testing. The test schedule and corresponding combustor operating conditions are presented in Table XXXII.

Exit temperature data were obtained at simulated sea level takeoff inlet conditions and overall fuel-air ratios of 0.020, the design level of 0.0244, and 0.0260. Fuel staging modes representing pilot-to-total fuel flow splits

Table XXXII. Development Combustor Baseline Atmospheric EGT Performance Test Point Schedule.

Test Point	T ₃ k (° F)	P ₃ atm	W ₃ kg/s (pps)	W _{Blade} kg/s (pps)	W _{Comb} kg/s (pps)	f/a	W _{Total} kg/hr (pph)	Pilot Total	W _{Pilot} kg/hr (pph)	W _{Main} kg/hr (pph)
1	495 (432)	1.00	2.67 (5.87)	0.19 (0.41)	2.48 (5.46)	0.0123	110 (242)	1.0	110 (242)	0
2	815 (1007)	1.00	2.41 (5.31)	0.15 (0.34)	2.26 (4.97)	0.0200	163 (350)	0.50	81 (179)	81 (179)
3	815 (1007)	1.00	2.41 (5.31)	0.15 (0.34)	2.26 (4.97)	0.0200	163 (350)	0.40	65 (143)	98 (215)
4	815 (1007)	1.00	2.41 (5.31)	0.15 (0.34)	2.26 (4.97)	0.0200	163 (350)	0.30	49 (107)	114 (251)
5	815 (1007)	1.00	2.41 (5.31)	0.15 (0.34)	2.26 (4.97)	0.0244	199 (437)	0.50	100 (219)	100 (219)
6	815 (1007)	1.00	2.41 (5.31)	0.15 (0.34)	2.26 (4.97)	0.0244	199 (437)	0.40	80 (175)	119 (262)
7	815 (1007)	1.00	2.41 (5.31)	0.15 (0.34)	2.26 (4.97)	0.0244	199 (437)	0.30	60 (131)	139 (306)
8	815 (1007)	1.00	2.41 (5.31)	0.15 (0.34)	2.26 (4.97)	0.0275	224 (492)	0.50	112 (246)	112 (246)
9	815 (1007)	1.00	2.41 (5.31)	0.15 (0.34)	2.26 (4.97)	0.0275	224 (492)	0.40	90 (197)	134 (295)
10	815 (1007)	1.00	2.41 (5.31)	0.15 (0.34)	2.26 (4.97)	0.0275	224 (492)	0.30	67 (148)	156 (344)

of 0.5, 0.4, and 0.3 were evaluated at the 0.020 and 0.0244 overall fuel-air ratio conditions. Pilot-to-total fuel flow splits of 0.4 and 0.3 were evaluated at the 0.0260 overall fuel-air ratio condition. All exit temperature data were reduced as uncorrected thermocouple temperatures and as corrected temperatures using the CF6 combustor family thermocouple temperature correction curve available in the test cell data reduction computer program.

Performance results obtained at simulated 6% ground idle operating conditions are presented in Figure 138. In this operating mode with only the pilot stage fueled, the exit temperature profiles are sharply peaked outward. This is typical of double annular combustor designs operating in this mode. The performance results obtained from the uncorrected temperature data at the sea level takeoff conditions are presented in Figures 139 and 140. These results illustrate the sensitivity of the exit temperature profiles to the pilot-to-main stage fuel split. Average and peak temperature profiles generally within the established limits were obtained at a 0.50 pilot-to-total fuel flow split. However, once the fuel was biased to the inner annulus main stage, the profiles became sharply peaked inward exceeding the established limits by a considerable amount. Figure 141 shows the performance results obtained at the design fuel-air ratio with corrected temperatures. While the maximum and average profiles are similar to those obtained from the uncorrected data, the pattern factor increased approximately 10%. At the 0.50 pilot-to-total fuel flow split, a pattern factor of 0.255 is obtained. This is very close to the goal of 0.250.

A plot of the average circumferential exit temperature distribution is presented in Figure 142. This temperature distribution represents corrected thermocouple data obtained at the simulated design cycle sea level takeoff operating condition, with a 0.40 pilot-to-total fuel flow split. For this combustor operating mode, the peak temperatures generally occur in line with the swirl cups while the minimum temperatures occur between swirl cups. Cooler spots in the combustor appear to exit in the vicinity of Swirl Cups 11 and 14. A posttest check of fuel nozzles revealed that the main stage nozzle tip in Cup 11 was approximately 5% below the average of all 30 main stage nozzle tips in fuel flow. The pilot stage nozzle tip in Cup 14 was approximately

ORIGINAL PAGE IS
OF POOR QUALITY

- 6% Idle (Pilot Only)
- Atmospheric Pressure
- Corrected Temperatures

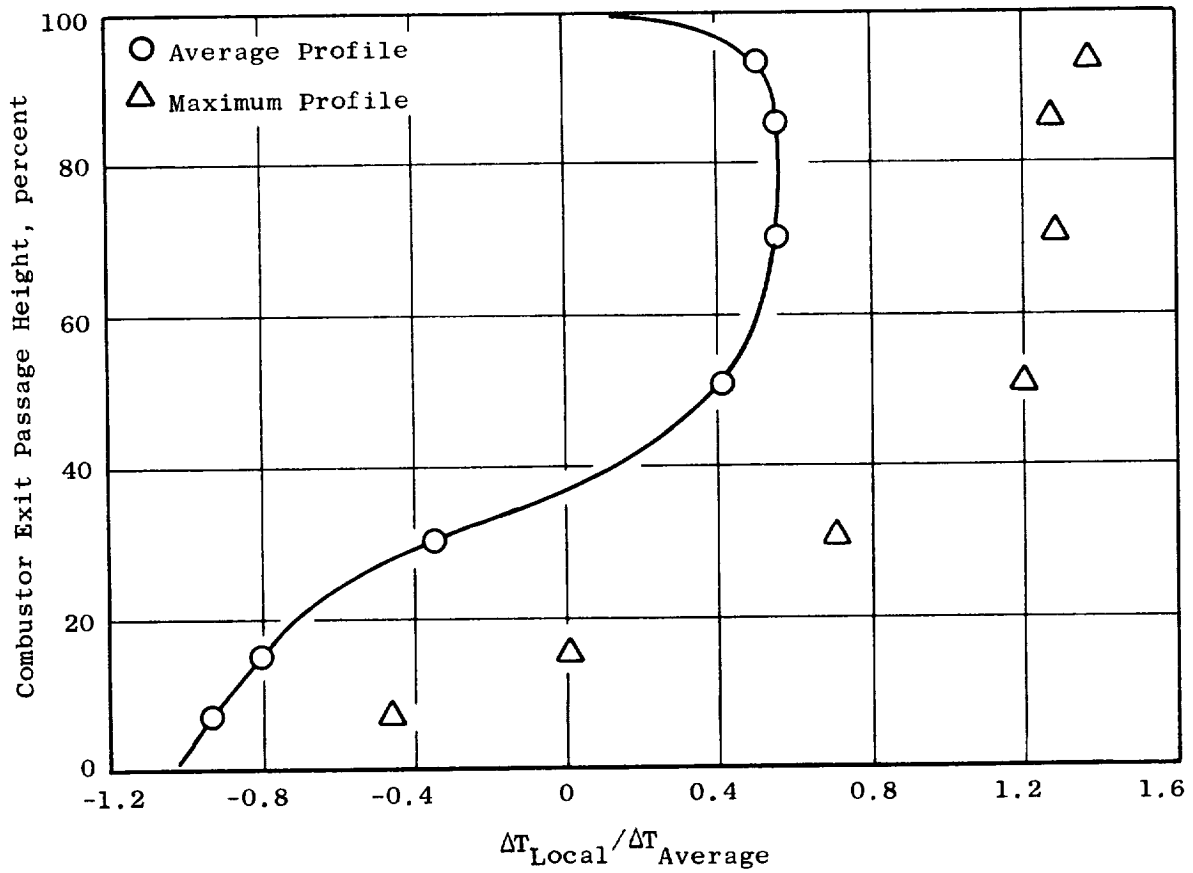


Figure 138. Development Combustor Baseline EGT Performance Test Results.

- Configuration: Baseline
- Simulated Sea Level Takeoff
- Uncorrected Thermocouples
- Run No. 6

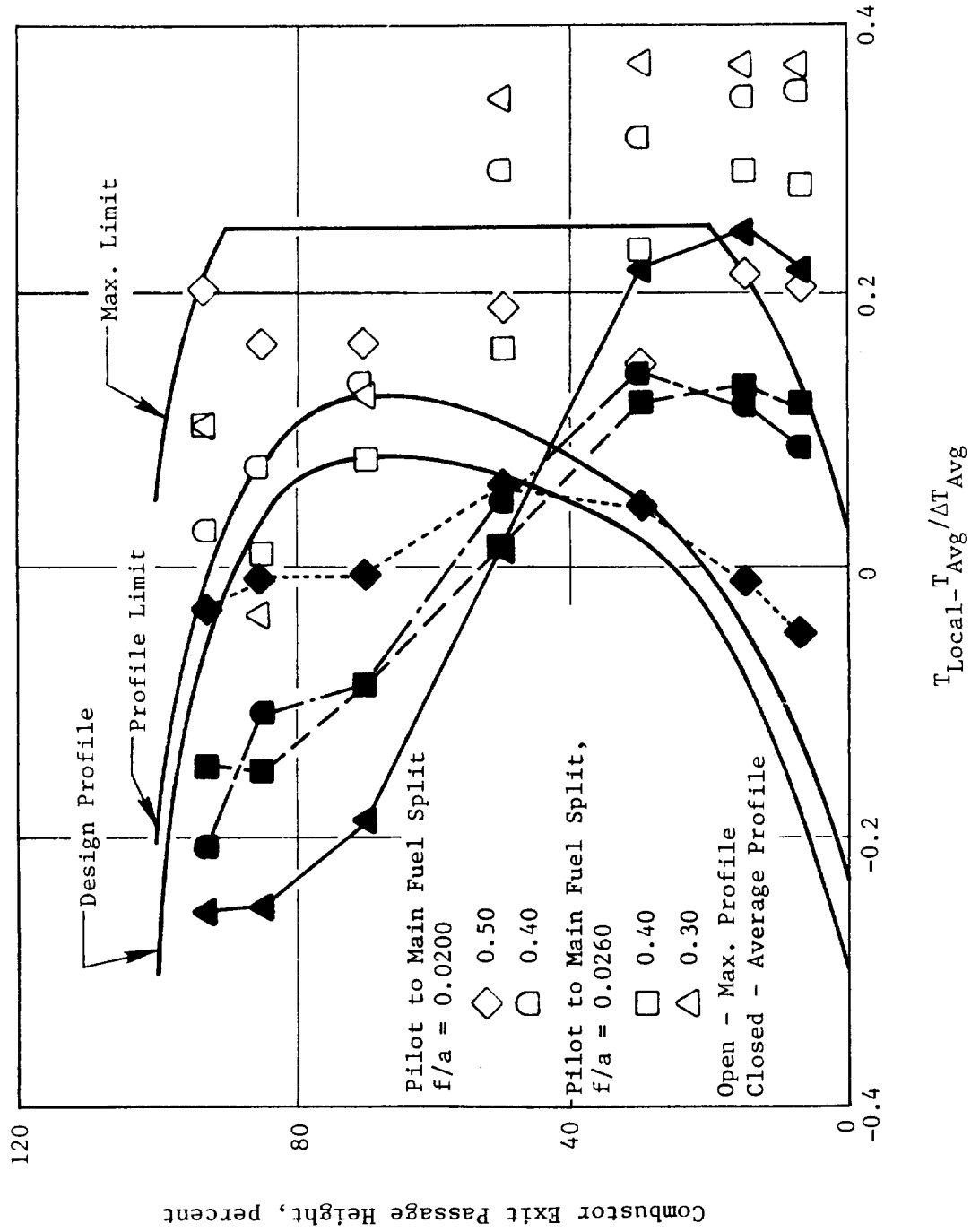


Figure 139. Development Combustor Baseline EGT Performance Test Results.

- Run No. 6
- Configuration: Baseline Simulated Sea Level Takeoff $f/a = 0.0244$ Uncorrected Thermocouples

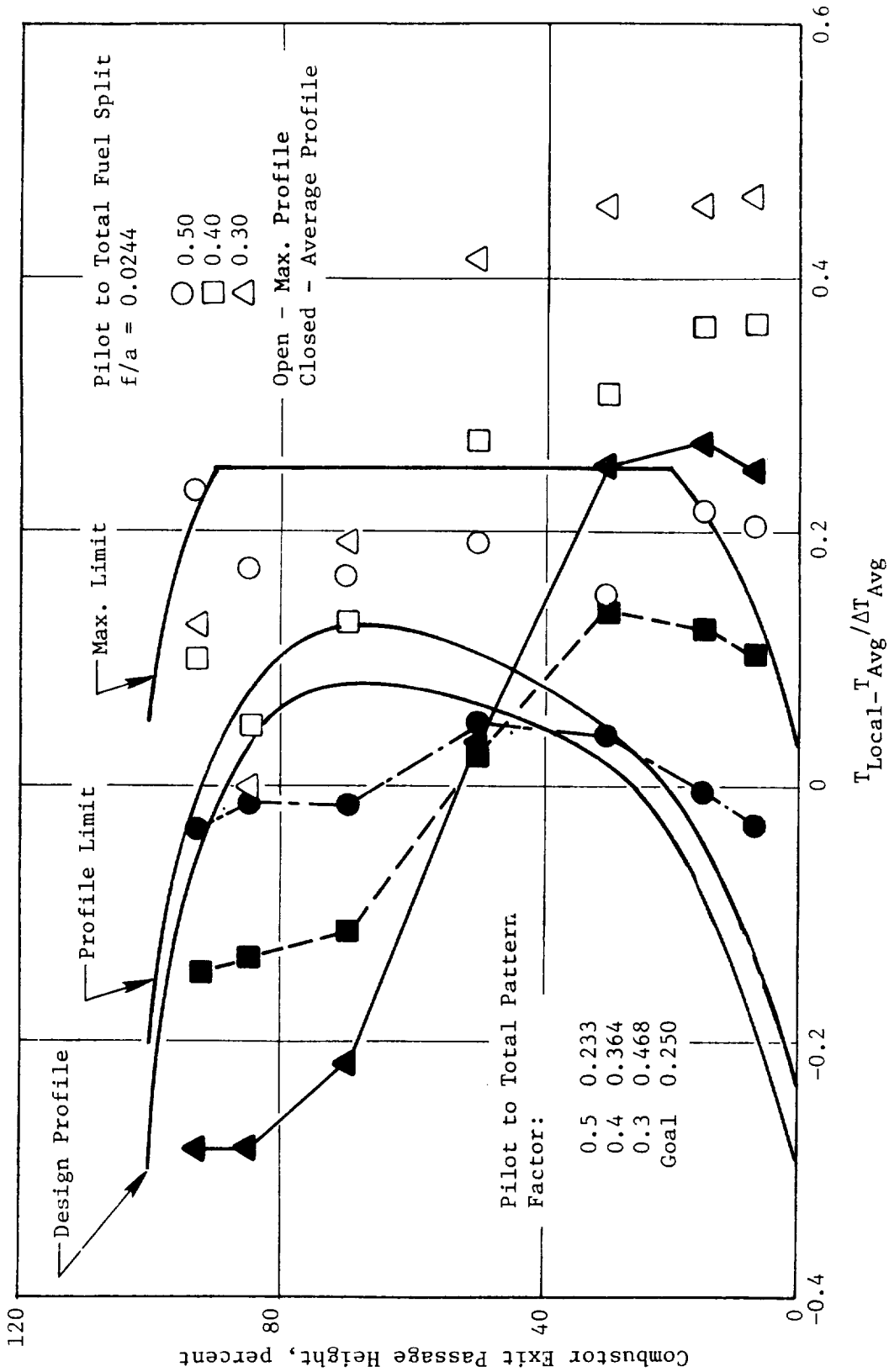


Figure 140. Development Combustor Baseline EGT Performance Test Results.

- Run No. 6
- Configuration: Baseline
- Simulated Sea Level Takeoff, $f/a = 0.0244$
- Corrected Thermocouples

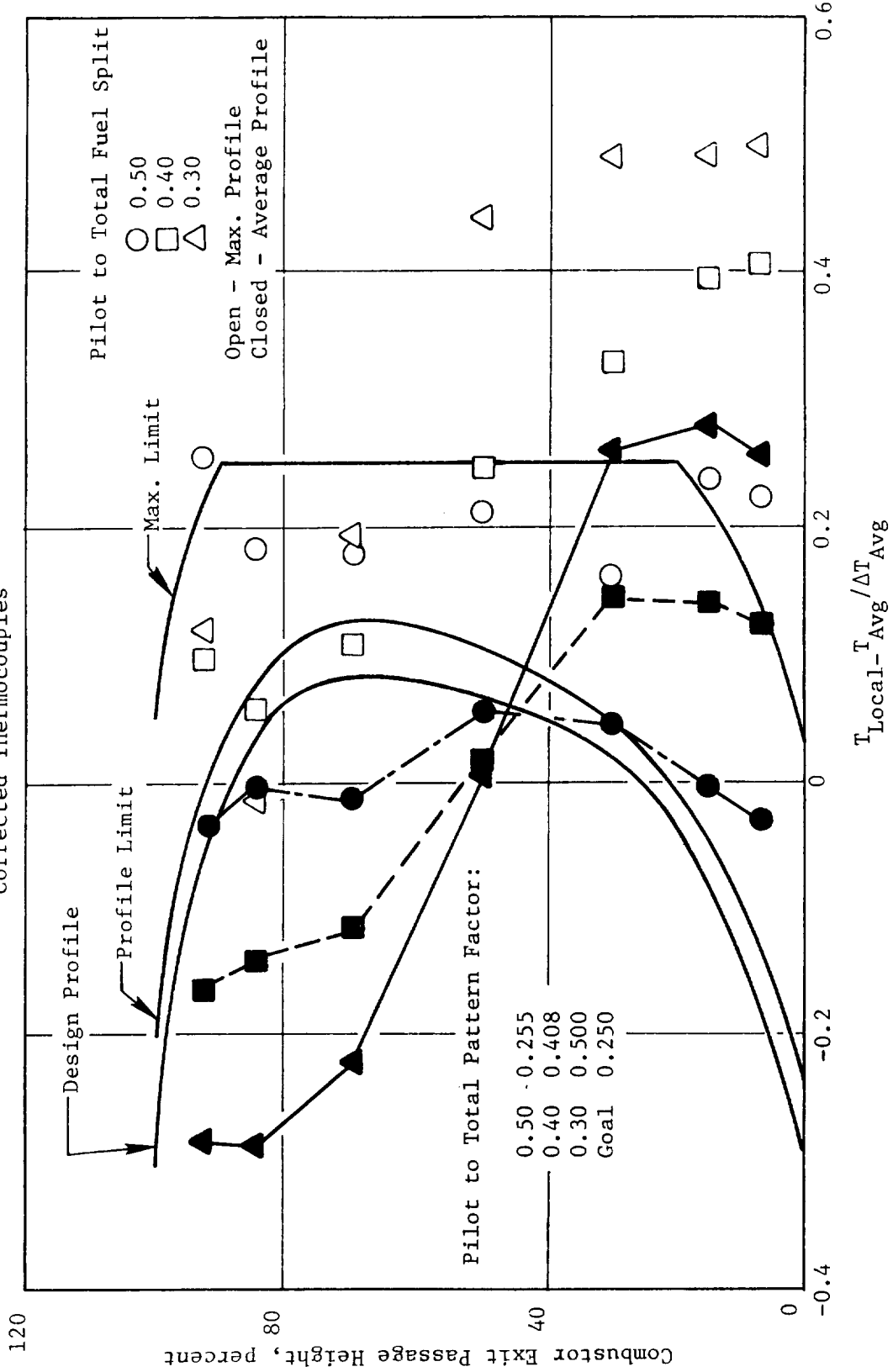


Figure 141. Development Combustor Baseline EGT Performance Test Results.

Average Circumferential Exit Temperature Distribution

- Simulated Sea Level Takeoff $f/a = 0.0244$
- 0.40 Pilot-to-Total Fuel Split
- Corrected Thermocouples

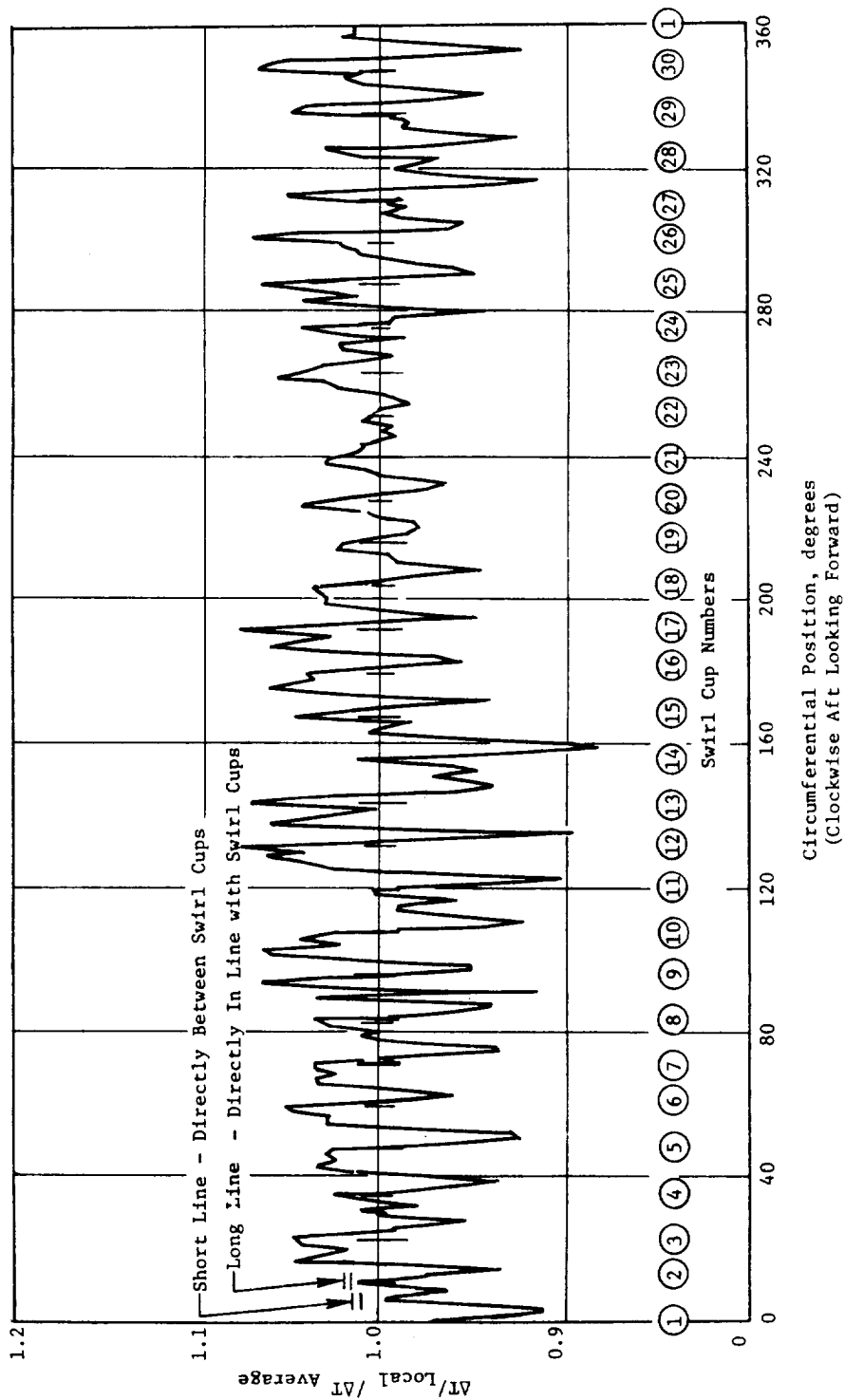


Figure 142. Development Combustor Baseline EGT Performance Test Results.

17% below the average of all 30 pilot stage nozzle tips in fuel flow. These low fuel flow levels in the two swirl cups could have produced the cooler regions observed.

7.3.3 Missions Test

Emissions testing of the E³ double-annular dome development combustor baseline configuration was conducted in the ACL Cell A3E test facility. This represented the first test in which the development combustor and test rig were operated at elevated pressure conditions. The purpose of this testing was to evaluate the Baseline combustor design for emissions, pressure drop, and metal temperature characteristics at combustor operating conditions along the E³ FPS design operating cycle. The test was conducted in two phases. The first phase involved evaluation at 4% and 6% ground idle conditions, plus 30% approach conditions with the fuel split between the pilot and main stage domes. The second phase of the test involved evaluation at 30% approach condition with only the pilot stage fueled, plus all high-power operating conditions. Bleed flows from the split duct diffuser and the outer and inner flowpaths were extracted at levels simulating the actual engine combustor operation at all test points. Test points and corresponding operating conditions evaluated in this test are presented in Table XXXVIII. During the first phase of testing, simplex-type fuel nozzles rated at 12.0 kg/hr (26.5 pph) and 23 kg/hr (50.0 pph) were used in the pilot and main stage domes respectively to simulate the fuel spray atomization quality expected from the engine duplex-type fuel nozzles at the lower power operating condition. For the higher power operating conditions, simplex-type fuel nozzles rated at 23 kg/hr (50 pph) and 55 kg/hr (120 pph) were respectively used in the pilot and main stage domes to obtain the required fuel flows within the test facility fuel pump discharge pressure capacity.

The combustor instrumentation consisted of 26 static pressures and 49 grounded and capped chromel-alumel thermocouples. This instrumentation provided important data concerning various combustor pressures and metal skin temperatures throughout the emissions test. The locations of this instrumentation on the combustor hardware are illustrated in Figures 143 through 146. The selected locations for the thermocouples were accomplished with the assistance

Table XXXIII. Development Combustor Baseline Emissions Test Point Schedule.

Test Point	Operating Condition	T ₃ K (°F)	P ₃ MPa (psia)	W ₃ kg/s (ppa)	W _{Blade Outer} kg/s (ppa)	W _{Blade Inner} kg/s (ppa)	W _{Blade} Prediff. kg/s (ppa)	W _{Comb} kg/s (ppa)	f/s Overall	Wf kg/hr (pps)	Pilot Total	W _{Pilot} kg/hr (pph)	W _{Main} kg/hr (pph)	Sampling Mode
1	4% Idle	466 (379)	0.339 (0.75)	9.55 (21.0)	0.55 (1.21)	0.50 (1.10)	0.61 (1.34)	7.86 (16.75)	0.0090	255 (562)	1.00	255 (562)	0	G
2	4% Idle	466 (379)	0.339 (0.75)	9.55 (21.0)	0.55 (1.21)	0.50 (1.10)	0.61 (1.34)	7.86 (16.75)	0.0120	340 (750)	1.00	340 (750)	0	G
3	4% Idle	466 (379)	0.339 (0.75)	9.55 (21.0)	0.55 (1.21)	0.50 (1.10)	0.61 (1.34)	7.86 (16.75)	0.0138	255 (560)	1.00	255 (560)	0	G, I, S
4	4% Idle	466 (379)	0.339 (0.75)	9.55 (21.0)	0.55 (1.21)	0.50 (1.10)	0.61 (1.34)	7.86 (16.75)	0.2000	566 (1248)	1.00	566 (1248)	0	G
5	4% Idle	466 (379)	0.339 (0.75)	9.55 (21.0)	0.55 (1.21)	0.50 (1.10)	0.61 (1.34)	7.86 (16.75)	0.0250	706 (1561)	1.00	706 (1561)	0	G
6	6% Idle	495 (431)	0.436 (0.96)	12.32 (27.2)	0.71 (1.56)	0.65 (1.43)	0.78 (1.72)	10.18 (22.44)	0.0090	330 (728)	1.00	330 (728)	0	G
7	6% Idle	495 (431)	0.436 (0.96)	12.32 (27.2)	0.71 (1.56)	0.65 (1.43)	0.78 (1.72)	10.18 (22.44)	0.0110	403 (888)	1.00	403 (888)	0	G
8	6% Idle	495 (431)	0.436 (0.96)	12.32 (27.2)	0.71 (1.56)	0.65 (1.43)	0.78 (1.72)	10.18 (22.44)	0.0123	451 (994)	1.00	451 (994)	0	G, I, S
9	6% Idle	495 (431)	0.436 (0.96)	12.32 (27.2)	0.71 (1.56)	0.65 (1.43)	0.78 (1.72)	10.18 (22.44)	0.0150	550 (1212)	1.00	550 (1212)	0	G
10	6% Idle	495 (431)	0.436 (0.96)	12.32 (27.2)	0.71 (1.56)	0.65 (1.43)	0.78 (1.72)	10.18 (22.44)	0.0200	733 (1616)	1.00	733 (1616)	0	G
11	30% Approach	637 (687)	1.206 (2.66)	31.36 (69.1)	1.80 (3.97)	1.65 (3.64)	2.00 (4.41)	25.90 (57.10)	0.0143	666 (1468)	0.5	666 (1468)	666 (1468)	G
12	30% Approach	637 (687)	1.206 (2.66)	31.36 (69.1)	1.80 (3.97)	1.65 (3.64)	2.00 (4.41)	25.90 (57.10)	0.0143	533 (1175)	0.4	799 (1761)	799 (1761)	G
13	30% Approach	637 (687)	1.206 (2.66)	31.36 (69.1)	1.80 (3.97)	1.65 (3.64)	2.00 (4.41)	25.90 (57.10)	0.0143	400 (882)	0.3	932 (2056)	932 (2056)	G
14	30% Approach	637 (687)	1.206 (2.66)	31.36 (69.1)	1.80 (3.97)	1.65 (3.64)	2.00 (4.41)	25.90 (57.10)	0.0173	1870 (4123)	0.4	748 (1649)	1122 (2474)	G
15	52% Power	700 (800)	1.524 (3.36)	36.36 (80.2)	2.09 (4.61)	1.92 (4.23)	2.31 (5.09)	30.05 (66.25)	0.0204	2284 (5035)	0.4	916 (2019)	1370 (3020)	G
16	70% Power	746 (883)	1.655 (3.65)	37.68 (83.1)	2.16 (4.76)	1.99 (4.39)	2.40 (5.29)	31.14 (68.65)	0.0225	250 (5511)	0.5	1250 (2756)	1250 (2756)	G
17	85% Climb	949 (1248)	1.655 (3.65)	37.41 (82.5)	2.15 (4.74)	1.97 (4.34)	2.38 (5.25)	30.91 (68.14)	0.0225	2504 (5511)	0.5	875 (1929)	1625 (3582)	G, I, S
18	85% Climb	949 (1248)	1.655 (3.65)	37.41 (82.5)	2.15 (4.74)	1.97 (4.34)	2.38 (5.25)	30.91 (68.14)	0.0225	2504 (5511)	0.35	500 (1102)	2000 (4409)	G
19	85% Climb	949 (1248)	1.655 (3.65)	37.41 (82.5)	2.15 (4.74)	1.97 (4.34)	2.38 (5.25)	30.91 (68.14)	0.0236	2541 (5602)	0.35	889 (1960)	1652 (3642)	G
20	93% Power	963 (1273)	1.655 (3.65)	36.27 (80.0)	2.08 (4.59)	1.91 (4.34)	2.31 (5.09)	29.95 (66.03)	0.0247	2664 (5873)	0.5	932 (2056)	1332 (2937)	G
21	100% SLTO	1007 (1353)	1.655 (3.65)	36.27 (80.0)	2.08 (4.59)	1.91 (4.34)	2.31 (5.09)	29.95 (66.03)	0.0247	2664 (5873)	0.35	932 (2056)	1732 (3818)	G, I, S
22	100% SLTO	1007 (1353)	1.655 (3.65)	36.27 (80.0)	2.08 (4.59)	1.91 (4.34)	2.31 (5.09)	29.95 (66.03)	0.0247	2664 (5873)	0.20	533 (1175)	2131 (4680)	G
23	100% SLTO	1007 (1353)	1.655 (3.65)	36.27 (80.0)	2.08 (4.59)	1.91 (4.34)	2.31 (5.09)	29.95 (66.03)	0.0247	2664 (5873)	0.20	533 (1175)	2131 (4680)	G

Sampling Modes: G - Ganged Sample
I - Individual Race Sample
S - Smoke Sample

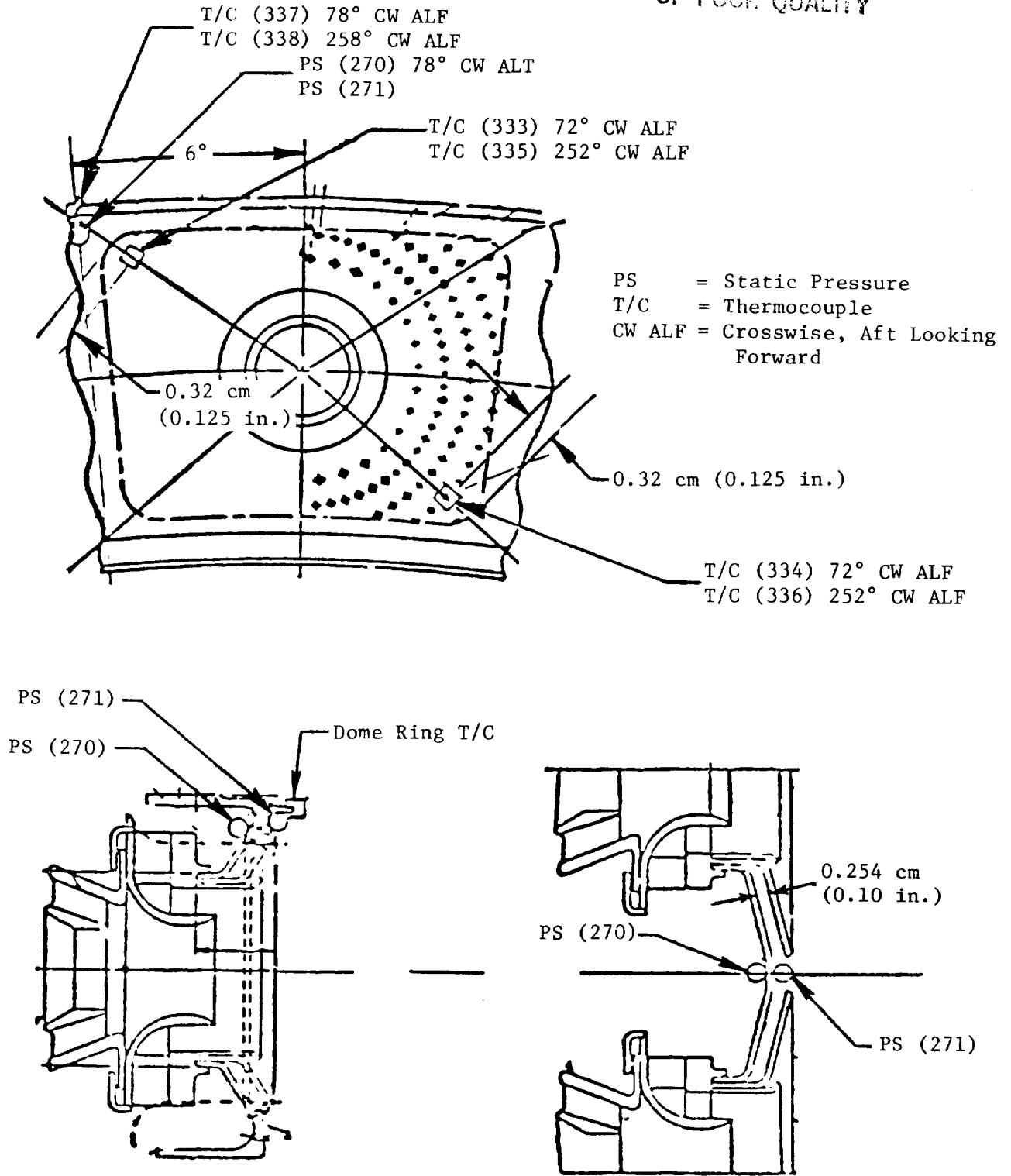
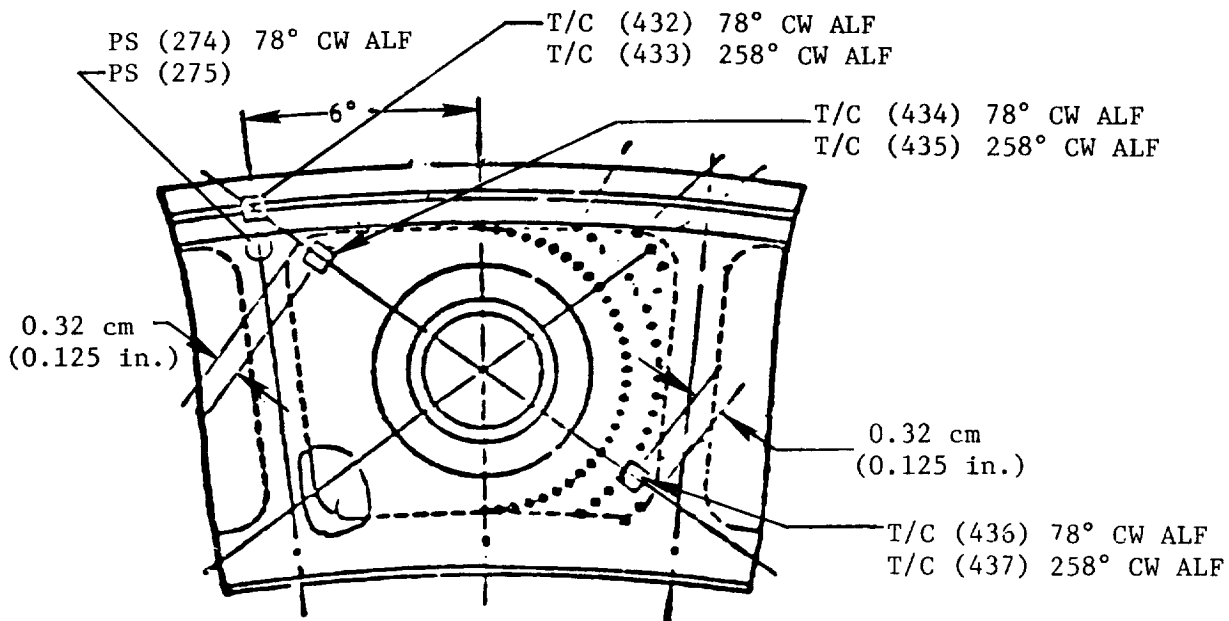


Figure 143. Baseline Combustor Instrumentation Layout.

ORIGINAL PAGE IS
OF POOR QUALITY



PS = Static Pressure
T/C = Thermocouple
CW ALF = Crosswise, Aft Looking Forward

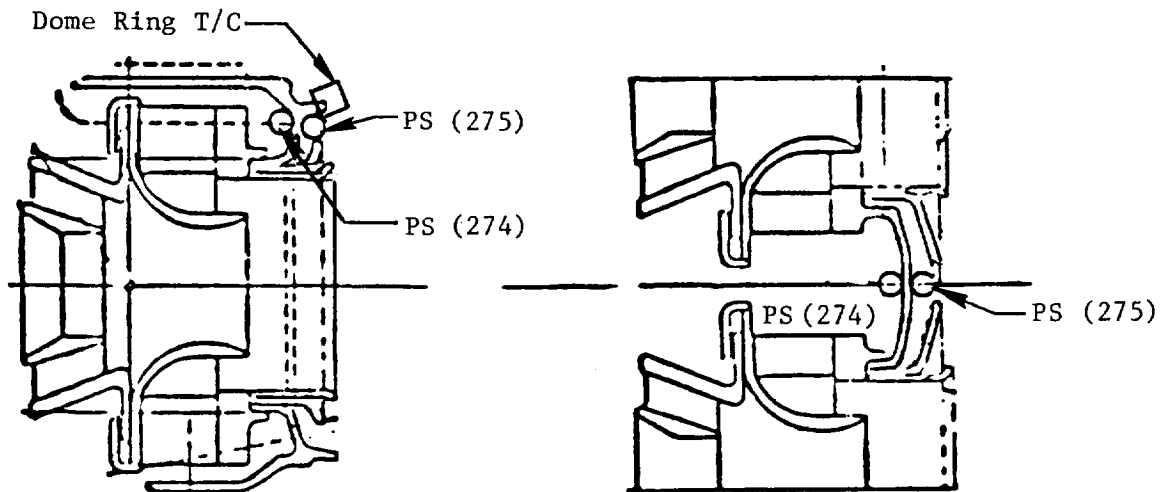


Figure 144. Baseline Combustor Instrumentation Layout.

ORIGINAL PLAN OF
OF PROBABILITY

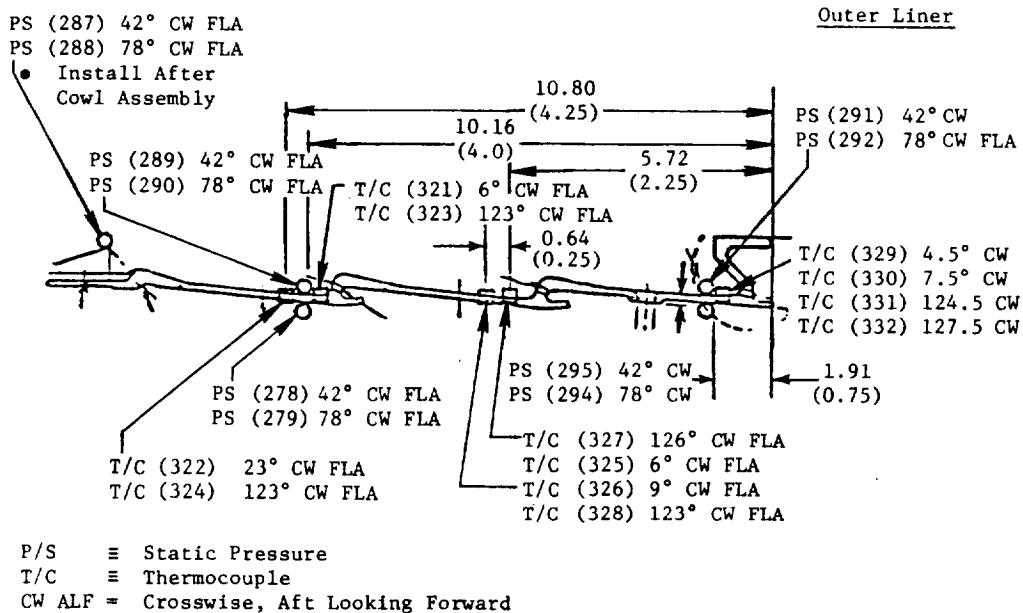
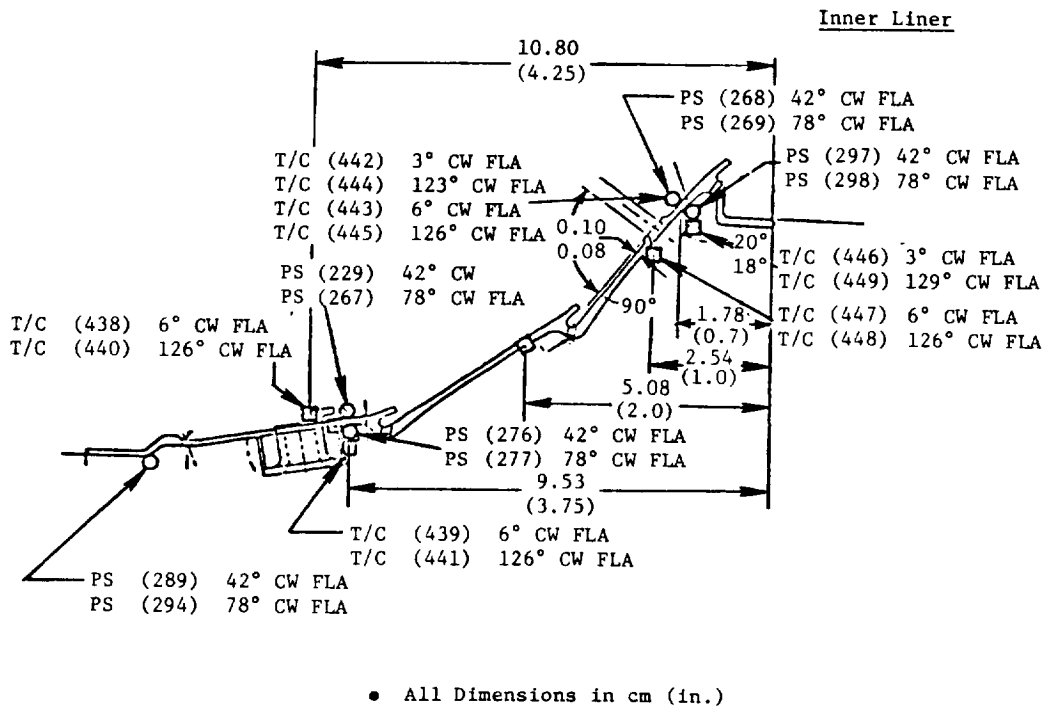
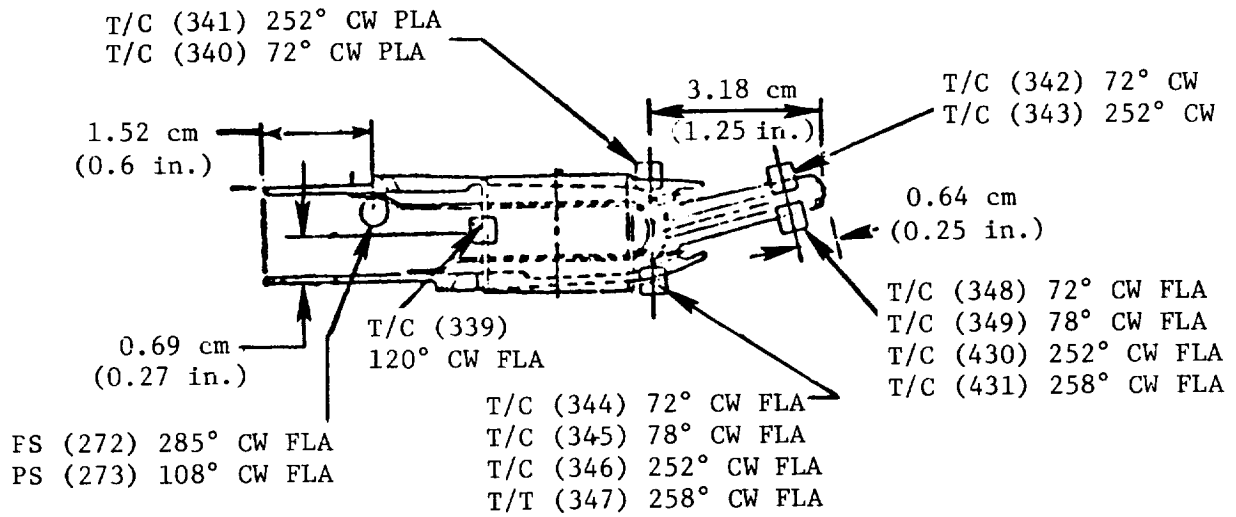
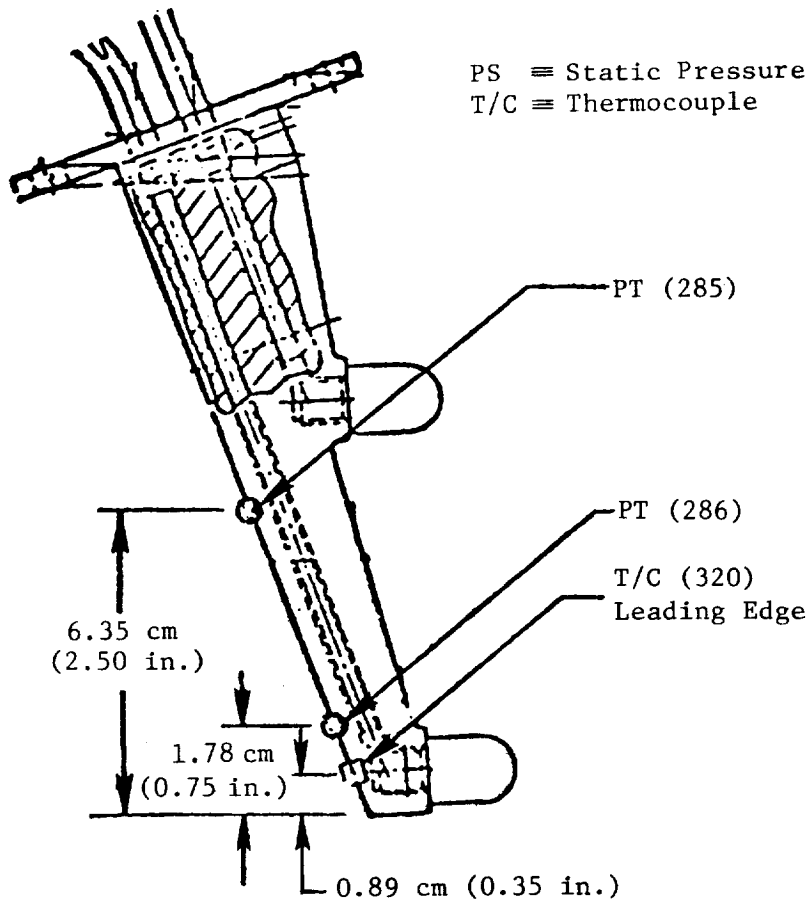


Figure 145. Baseline Combustor Instrumentation Layout.

ORIGINAL PAGE IS
OF POOR QUALITY



Centerbody Instrumentation



Fuel Nozzle Instrumentation (Cup No. 7 Nozzle)

Figure 146. Baseline Combustor Instrumentation Layout.

of heat transfer personnel. Some of the thermocouples were located on the combustor liners at places which had been observed as "hot spots" during the previous exit temperature performance test of this combustor. A dynamic pressure probe was installed through a primary dilution hole in the outer liner of the combustor to monitor combustion frequencies and fluctuations. In addition, numerous pressure and temperature instrumentation was installed on the test rig vehicle. This instrumentation included upstream total pressure and air temperature rakes to measure the combustor inlet total pressure and temperature. Test rig flowpath wall static pressures provided important data concerning diffuser system performance while thermocouples were used to monitor the test rig to ensure the rig mechanical integrity. The location of the more important test rig instrumentation is illustrated in Figure 147.

All CO, HC, and NO_x emissions levels measured were adjusted to reflect emissions levels that would be obtained if measured at the actual E³ FPS design cycle operating conditions.

At the lower power operating conditions (4%, 6%, and 30%), these adjustments provided corrections which accounted for small discrepancies between the test conditions set in the cell, and the cycle conditions represented. At the higher power operating conditions, these adjustments primarily provided corrections for emissions levels measured at reduced inlet pressure and air-flow conditions associated with the facility capacity to simulate the actual high power design cycle operating conditions. The adjustment for the measured NO_x emission levels also includes a correction for inlet air humidity.

The results of the idle emissions testing of this Baseline combustor configuration are presented in Figures 148 and 149. As observed in Figure 148, CO emissions levels of 59.5 g/kg (59.5 lb/1000 lb) of fuel and 57.5 g/kg (57.5 lb/1000 lb) of fuel were obtained, respectively, at the 4% and 6% ground idle design cycle operating conditions. It has been estimated that a CO emissions level of 20.7 g/kg (20.7 lb/1000 lb) of fuel would be required at the 6% ground idle operating condition to satisfy the program CO emissions goal. The small reduction in the measured CO emissions level from the 4% to 6% ground idle test condition is related to the decrease in the design cycle fuel-air ratio which offsets the expected advantages of increased combustor inlet pressure and temperature. At the 6% ground idle condition, a minimum

ORIGINAL PAGE IS
OF POOR QUALITY

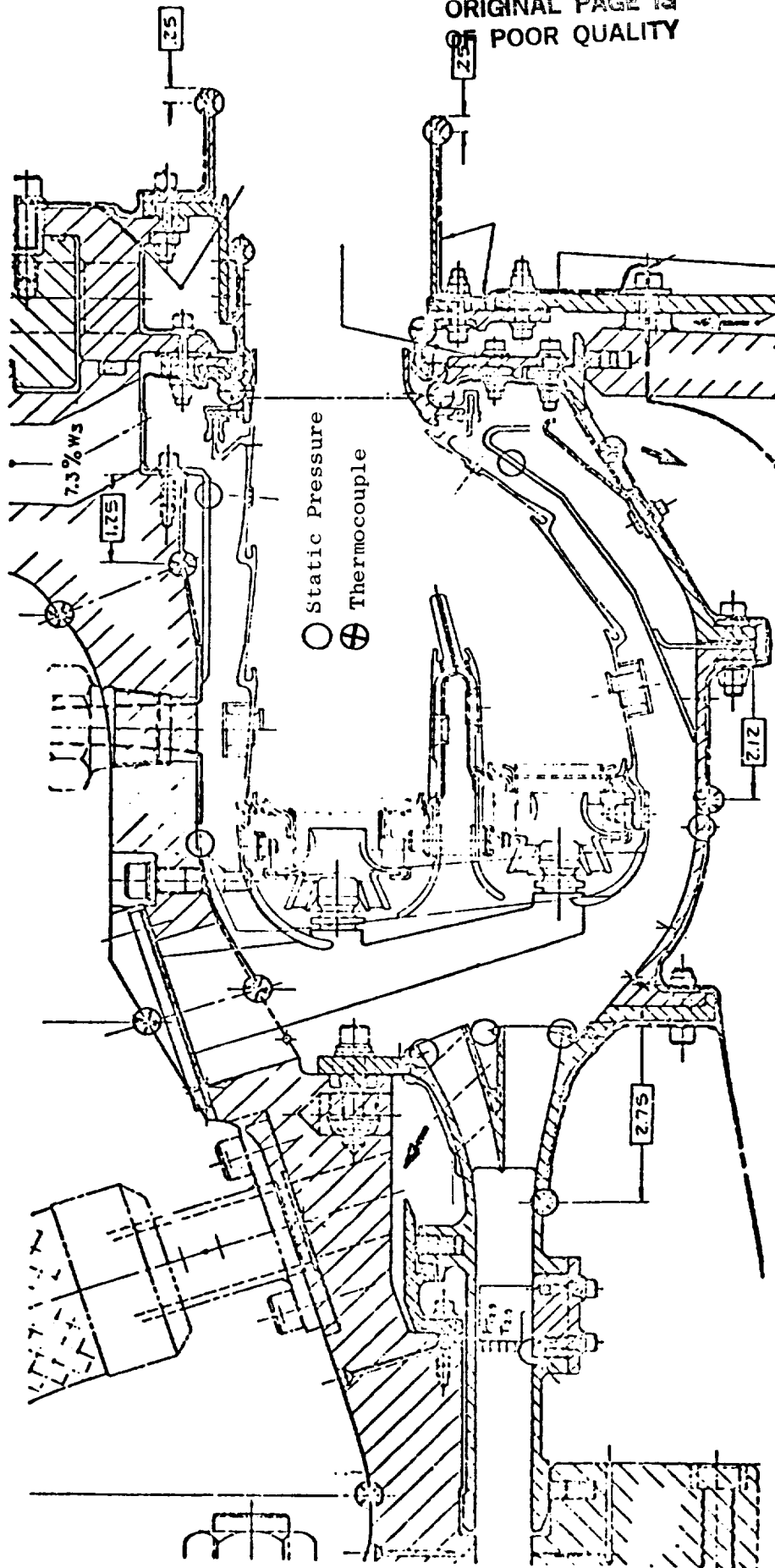


Figure 147. Combustor Test Rig Instrumentation.

ORIGINAL TABLE IS
OF POOR QUALITY

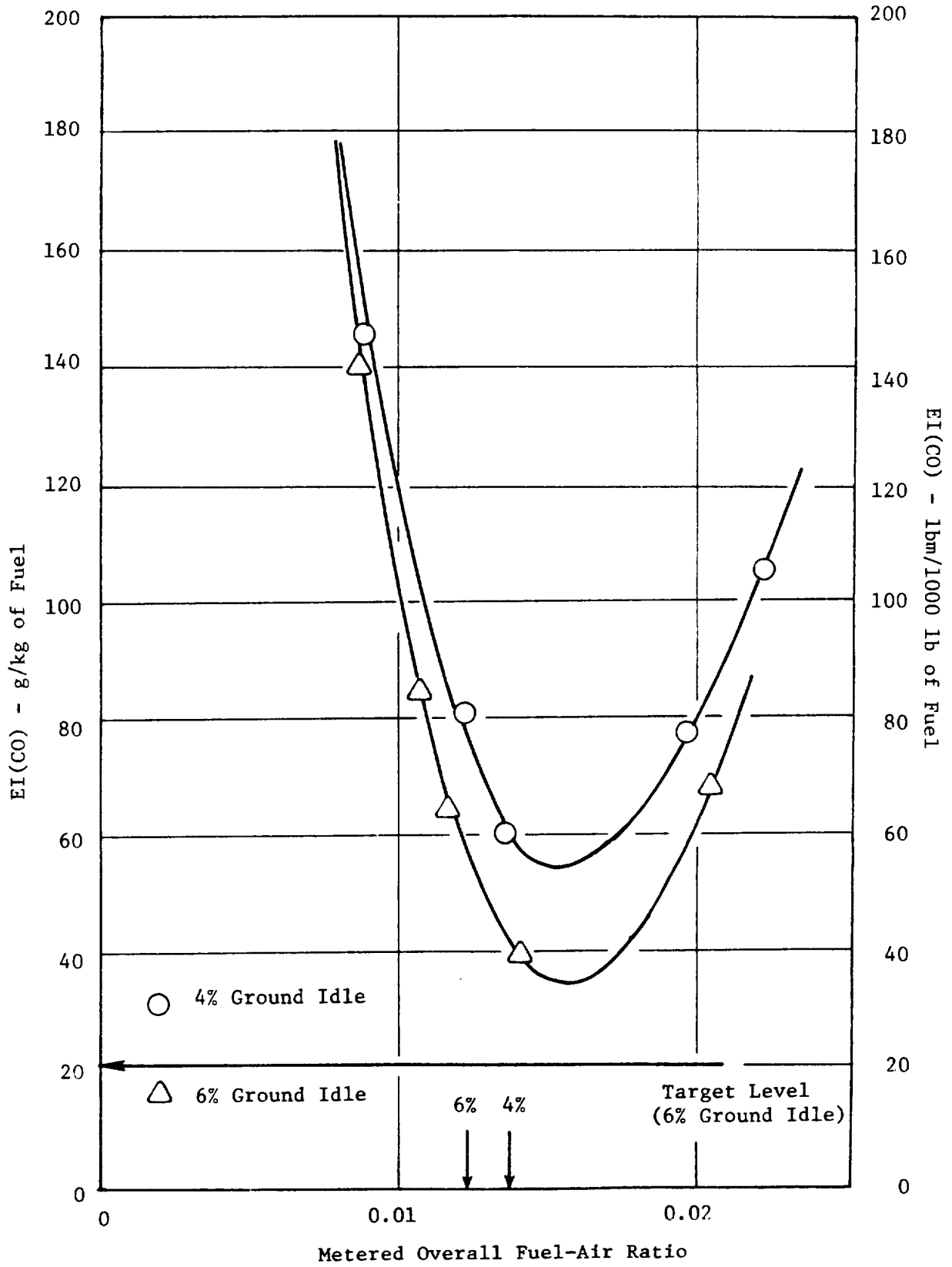


Figure 148. Baseline Combustor Emissions Results.

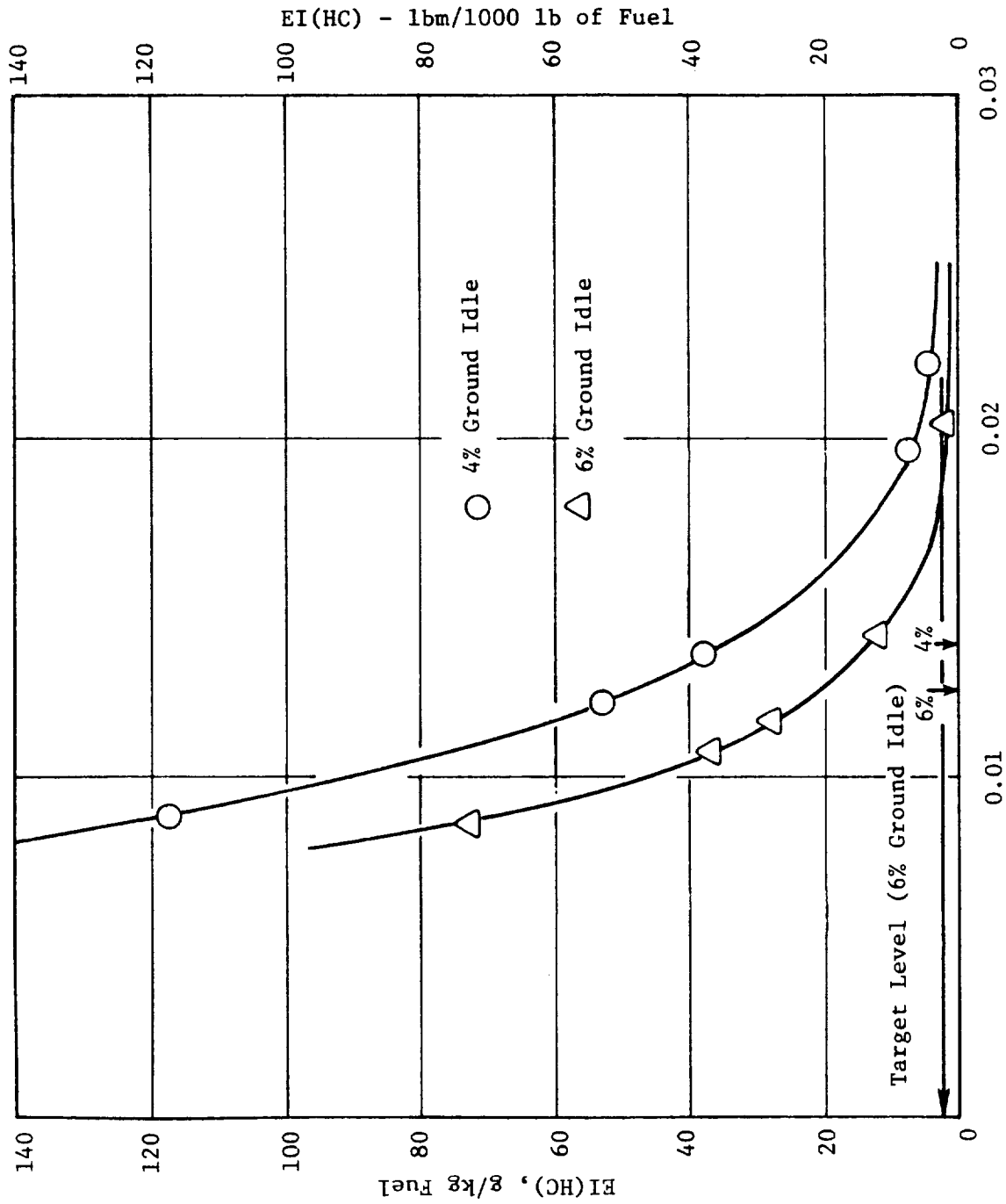


Figure 149. Baseline Combustor Emissions Results.

CO emissions level of 35g/kg (35 lb/1000 lb) of fuel was demonstrated at a metered overall fuel-air ratio of 0.0155. It is also observed from this figure that the CO emissions levels are sensitive to changes in the fuel-air ratio. This characteristic is similar to that observed during earlier test programs conducted on double-annular dome combustor designs such as those developed for NASA/GE ECCP and QCSEE programs. This appears to be related to rapid pilot stage stoichiometry changes under conditions of pilot-only operation in which the addition of fuel occurs in a region containing only a portion of the total combustor dome airflow. HC emissions levels of 36 g/kg (36 lb/1000 lb) of fuel and 22.5 g/kg (22.5 lb/1000 lb) of fuel were obtained, respectively, at the 4% and 6% ground idle design cycle operating conditions. An HC emissions index of 3.0 g/kg (3.0 lb/1000 lb) of fuel had been estimated as the required level at 6% ground idle to satisfy the program HC emission goal. HC emission levels at or below this target level were measured at metered overall fuel-air ratios greater than 0.0180.

Emissions were measured at the 30% power approach operating condition at pilot-only plus pilot-to-total fuel flow splits of 0.50, 0.40, and 0.30. The effects of these fuel staging modes on the measured CO, HC, and NO_x emissions are illustrated in Figure 150. As observed from this figure, the expected trend of low CO emissions levels with accompanying higher NO_x emissions levels at the pilot-only operating mode is evident. However, what was not expected was the very high CO and HC emissions levels obtained with both the pilot and main stages fueled. The apparent cause results from poor combustion efficiency created by excessively lean fuel-air mixtures in both domes when the relatively low overall fuel-air ratio of 0.0140, at the 30% power condition, is divided between the two stages. These lean conditions also contributed to the very favorable NO_x emissions levels obtained.

The adjusted CO, HC, and NO_x emissions levels obtained along the E³ FPS design cycle operating line are presented in Figures 151 and 152. Of particular interest are the NO_x emission levels at the higher power operating conditions. As observed from Figure 152, sea level takeoff NO_x emissions levels from 16.8 g/kg (16.8 lb/1000 lb) of fuel to 17.8 g/kg (17.8 lb/1000 lb) of fuel were obtained. It was unfortunate that at these higher power operating conditions, additional fuel splits, lower than those indicated, could

ORIGINAL PAGE IS
OF POOR QUALITY

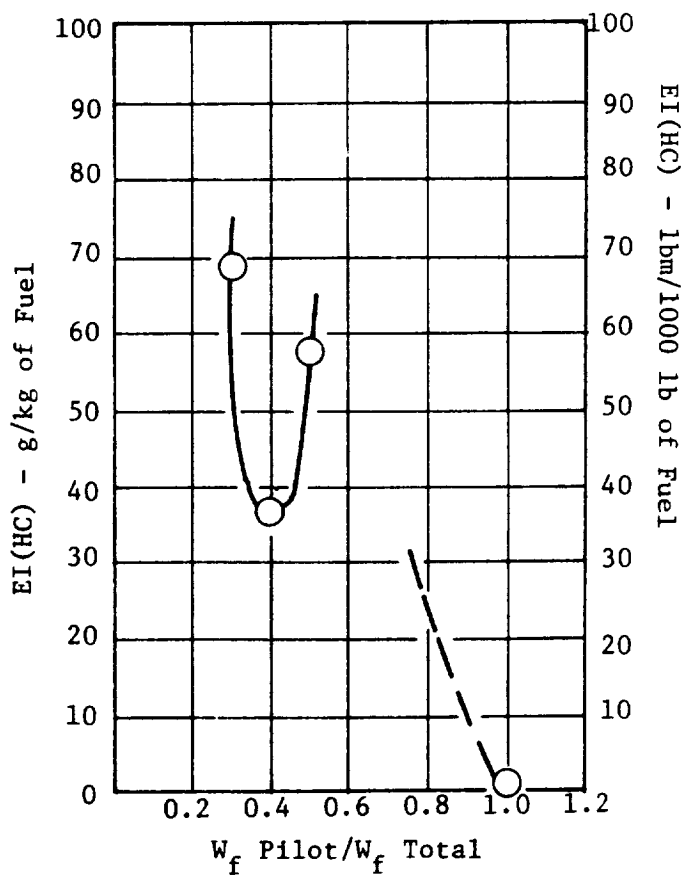
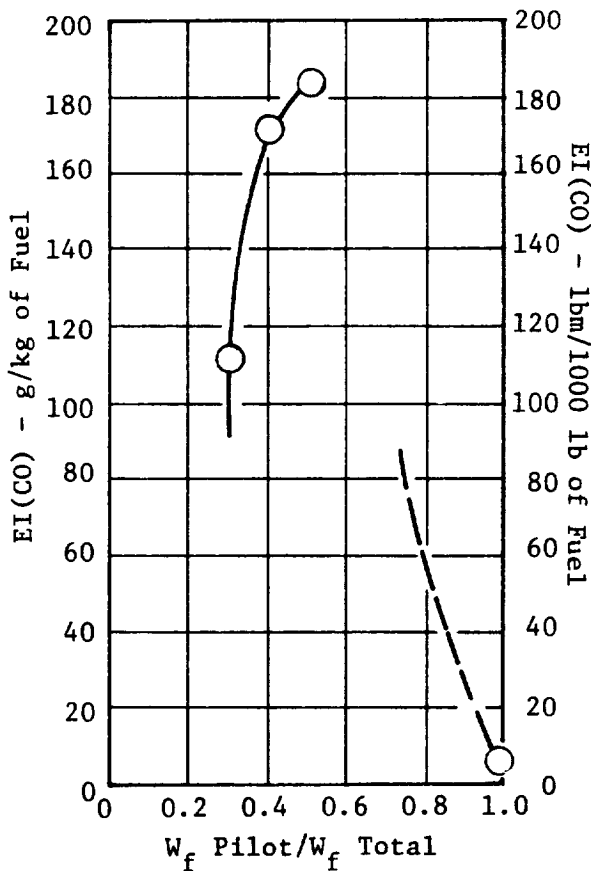
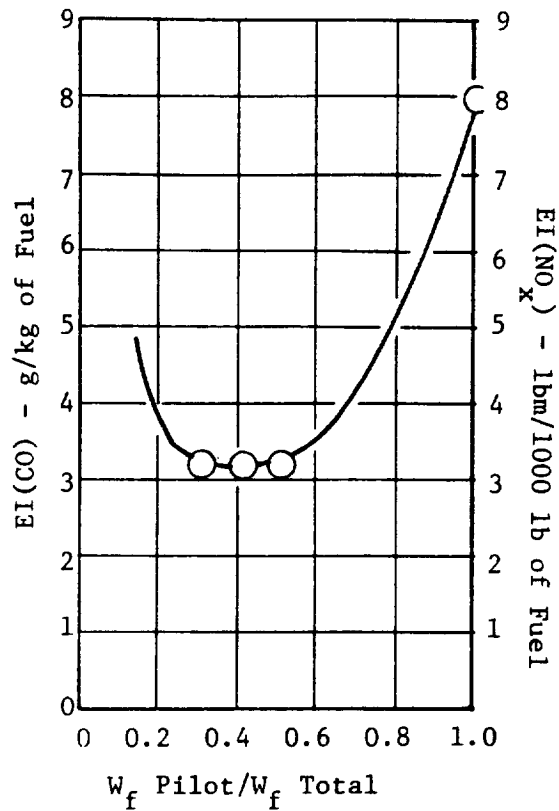


Figure 150. Baseline Combustor Emissions Results, 30% Power Approach Operating Condition.

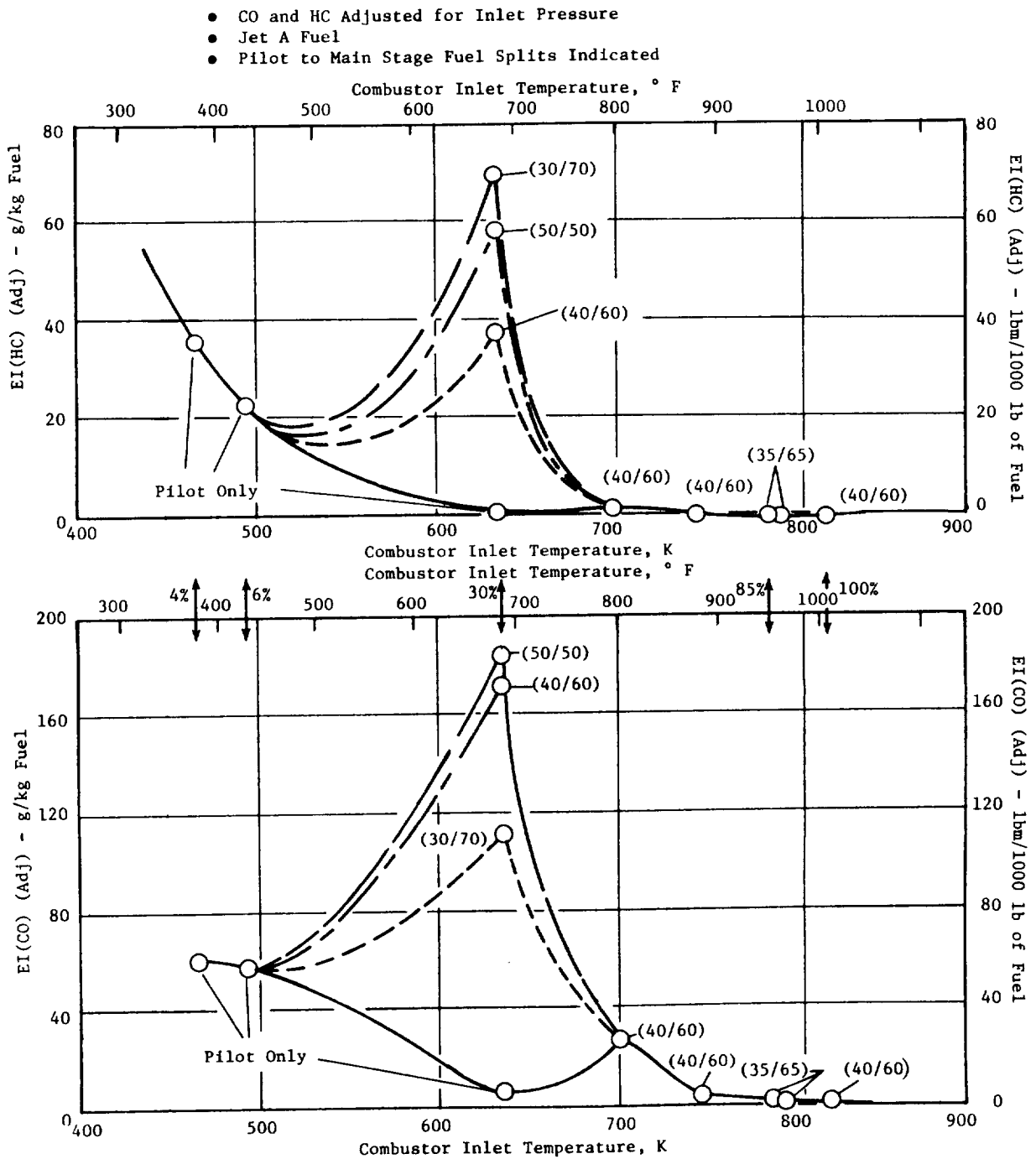


Figure 151. Baseline Combustor Emissions Results.

not be evaluated because of excessively high metal temperatures measured on the inner liner. Thus, insufficient data were obtained at these conditions to determine the fuel split which would produce the lowest NO_x emissions level. At the sea level takeoff condition, a NO_x emission level of 17.5 g/kg (17.5 lb/1000 lb) of fuel had been estimated as necessary to satisfy the program NO_x emissions goal.

Using the emissions results from the Baseline development combustor, EPA Parameter (EPAP) numbers, based on the EPA landing-takeoff cycle for CO, HC, and NO_x, were generated for several cases representing various combustor operating modes at the approach and sea level takeoff conditions. These EPAP results are compared with the E³ program goals in Table XXXIV. The E³ program emissions goals are identical to the EPA 1981 standards for newly certified engines greater than 89 kN (20,000 lb) thrust. As observed from this table, at all of the combustor operating modes investigated, the CO and HC emissions levels were significantly above the E³ program goals. However, the NO_x emissions levels satisfy the goal with at least 7% margin.

Smoke levels obtained are presented along with the combustor operating conditions at which they were measured in Table XXXV. As observed, the smoke levels for this combustor are very low. Although somewhat higher levels would be expected at the actual design cycle conditions at high power, the smoke levels would be expected to be well below the E³ program smoke number goal of 20.

At the simulated sea level takeoff operating condition, data from pressure instrumentation in the diffuser section of the test rig were used to calculate total pressure losses, providing a performance measurement of the split duct diffuser design. Total and static pressures upstream of the diffuser inlet were used to calculate the velocity profile in the test rig passage at the inlet of the diffuser. This profile in the form of the local-to-average Mach number ratio is shown in Figure 153. As observed, the profile is essentially flat, peaked only 2% above average slightly outward from the center of the passage. Calculated diffuser total pressure losses are presented in Table XXXVI. These values are compared with losses measured in the full-annular diffuser model subcomponent tests with center peaked and flat inlet velocity

Table XXXIV. Baseline Combustor EPAP Results.

● Jet A Fuel

<u>Mode of Operation</u>	EPAP		
	<u>lb/1000 CO</u>	<u>lb Thrust-Hour HC</u>	<u>Cycle NO_x</u>
● Pilot Only at Approach 40/60 Split at Climb 45/55 Split at SLTO	8.20	3.03	2.78
● Pilot Only at Approach 40/60 Split at Climb 40/60 Split at SLTO	8.20	3.03	2.82
● 40/60 Split at Approach 40/60 Split at Climb 45/55 Split at SLTO	14.55	7.17	2.49
● 40/60 Split at Approach 40/60 Split at Climb 40/60 Split at SLTO	14.55	7.17	2.53
● 30/70 Split at Approach 40/60 Split at Climb 45/55 Split at SLTO	18.16	5.25	2.49
● Totals (1981 Standards)	3.00	0.40	3.00

Table XXXV. Baseline Combustor Smoke Results.

- Jet A Fuel
- Cell A3 Operating Conditions

<u>P₃</u> <u>atm</u>	<u>T₃</u> <u>K (° F)</u>	<u>W_c</u> <u>kg/s (pps)</u>	<u>f/a</u>	<u>Wf Pilot</u> <u>Wf Total</u>	<u>Combustor</u> <u>SAE Smoke</u> <u>Number</u>	<u>Comments</u>
3.38	466 (839)	7.88 (17.33)	0.0136	1.00	3.45	4% Ground Idle
4.27	493 (887)	10.79 (23.74)	0.0115	1.00	4.38	6% Ground Idle
11.91	634 (1141)	26.34 (57.74)	0.0140	1.00	0.94	30% Approach
16.38	782 (1407)	31.06 (68.33)	0.0223	0.35	2.24	85% Simulated
16.43	814 (1465)	30.67 (67.48)	0.0246	0.40	2.16	100% Simulated

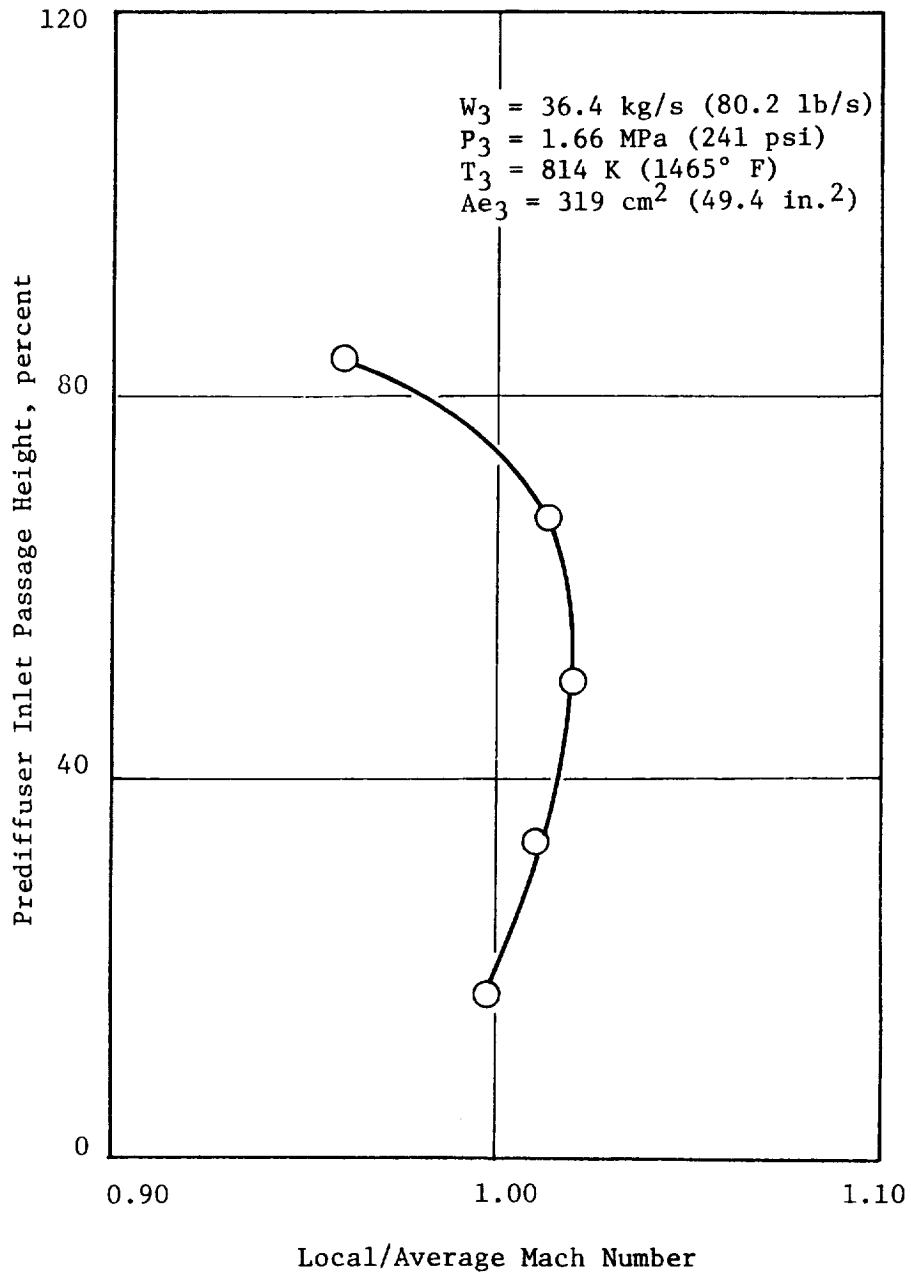


Figure 153. Diffuser Inlet Mach Number Profile (Baseline Test).

profiles. As observed from this comparison, the test rig diffuser performance generally agreed well with the annular diffuser subcomponent test results obtained with a flat velocity profile. The discrepancy in the outer dome loss is most likely related to erroneous outer dome pressure data obtained from the test rig. The comparison also shows that the test rig diffuser performance was considerably below that obtained in the diffuser subcomponent testing with the center peaked velocity profile. It is believed that the level of diffuser performance observed in the test rig is related to the low level of turbulence in the test rig flow upstream of the diffuser, which results from the absence of a velocity profiler. Improvement could be achieved by installing a profiler with a center peaked characteristic into the E³ test rig.

Table XXXVI. Calculated Diffuser Performance for Baseline Test.

● Diffuser Total Pressure Losses

<u>Description</u>	<u>Results from Combustor Emissions Test, %</u>	<u>Diffuser Test Flat Profile</u>	<u>Diffuser Test Center Peaked Profile</u>
Prediffuser Outer Passage	1.86	2.12	1.31
Outer Dump	1.83	1.92	1.66
Total Outer	3.69	4.04	2.97
Prediffuser Inner Passage	1.79	1.93	1.10
Inner Dump	0.99	1.12	0.99
Total Inner	2.78	3.05	2.09
Centerbody	2.30	2.77	1.90
Outer Dome	2.53	1.16	1.19
Inner Dome	1.72	1.47	1.27

Measured overall combustor pressure drops and pilot and main stage dome pressure drops are plotted against the square of the combustor inlet flow function parameter along the E³ FPS design cycle operating line in Figure 154. At sea level takeoff, an overall combustor pressure drop of 5.5% was obtained compared to the engine design value of 5.0%. Prior to the initial testing of this combustor configuration, it had been determined that the total combustor open hole flow area was about 2% less than design. Both the pilot and main stage dome pressure drops appear to be a little low. Pressure drops across the liners were between 2% and 3% while levels of 3% and 3.5% were measured across the centerbody structure.

Dynamic pressures were recorded on tape and later reduced to provide the absolute levels and frequencies. The reduced data indicated that the absolute dynamic pressure levels were below (1.0 psi) peak-to-peak at all operating conditions with no apparent dominant frequencies.

Combustor metal temperatures measured during testing are plotted against the combustor inlet temperature in Figures 155 through 163. To determine the locations of these indicated temperatures, match item numbers on these figures with the item numbers shown on the instrumentation layout shown in Figures 143 through 146. A maximum outer liner temperature of 1232 K (1757° F) was observed on Panel 1 at the simulated sea level takeoff operating condition with a 0.45 pilot-to-total fuel flow split. A maximum inner liner temperature of 1175 K (1655° F) was observed on Panel 1 at the simulated sea level takeoff operating condition with a 0.40 pilot-to-total fuel flow split. These excessively high metal temperatures were experienced within a narrow range of fuel splits and limited the ability to obtain emissions data over a wider range of fuel splits. The thermocouples that indicated these temperatures were located slightly aft and approximately 3° clockwise aft looking forward from the dilution thimble directly in line with the top swirl cup in each dome. Temperature paint applied to two sections of each liner indicated a repetitive pattern of these "hot spots" in the same relative location in the vicinity of each dilution thimble on both the outer and inner liners. Indicated metal temperatures on the centerbody structure were within acceptable limits. A maximum metal temperature of 1160 K (1628° F) was observed on the main stage side of the multijet cooling ring at the simulated sea level takeoff condition with a pilot-to-total stage fuel flow split of 0.40. Peak

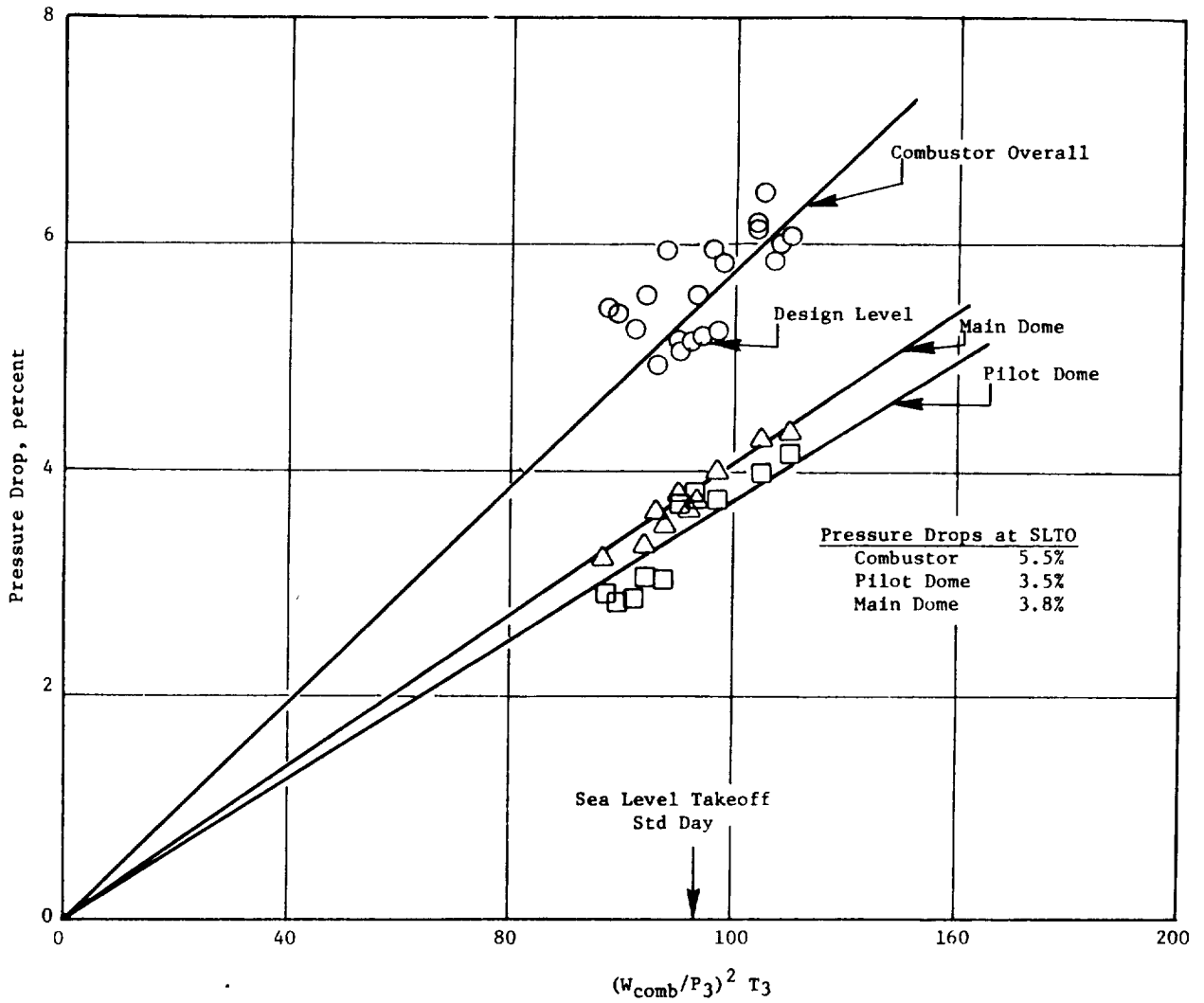


Figure 154. Measured Combusator Pressure Losses for Baseline.

CF

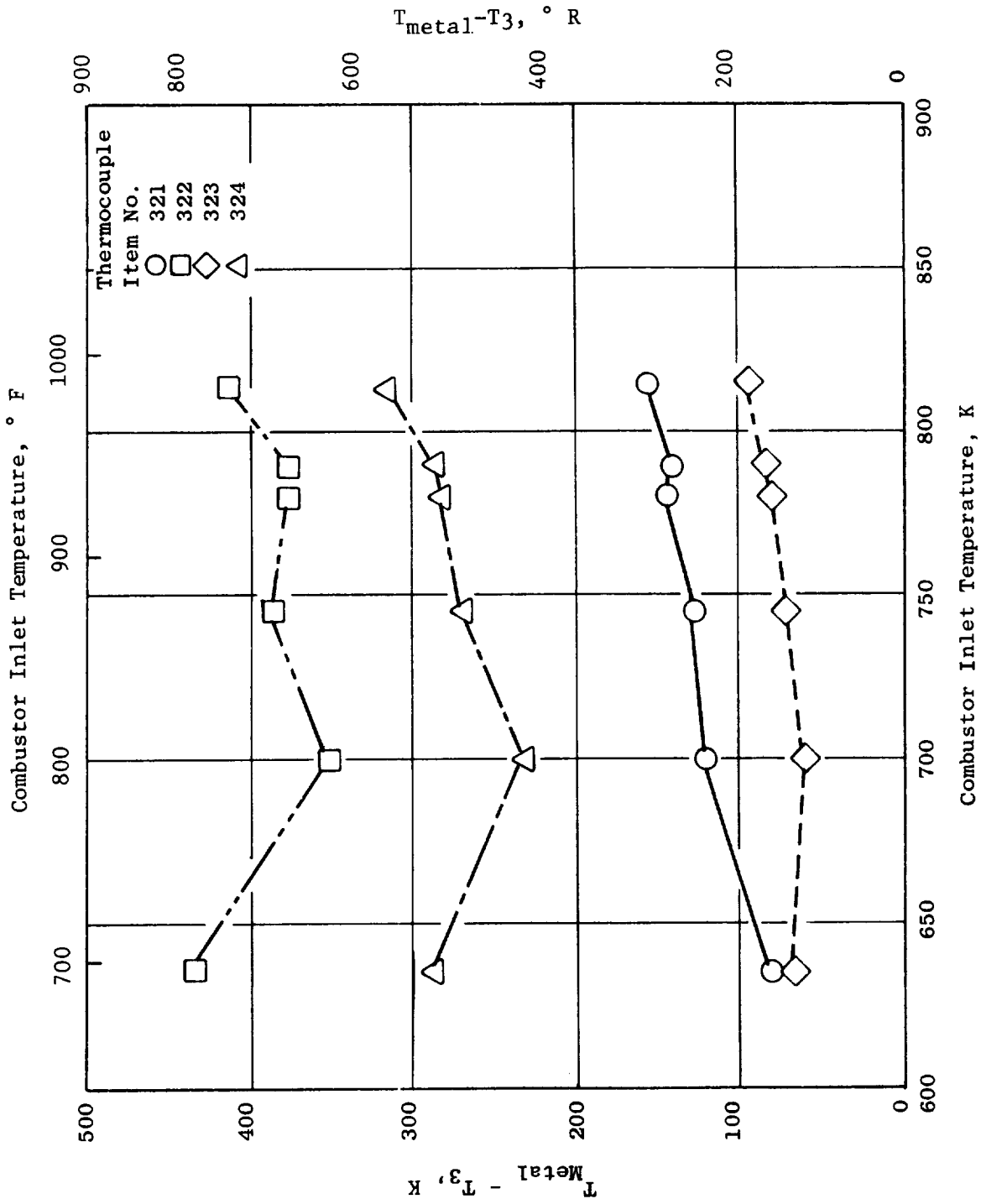


Figure 155. Measured Combustor Metal Temperatures for Baseline Test.

ORIGINAL REVISION
OF POOR QUALITY

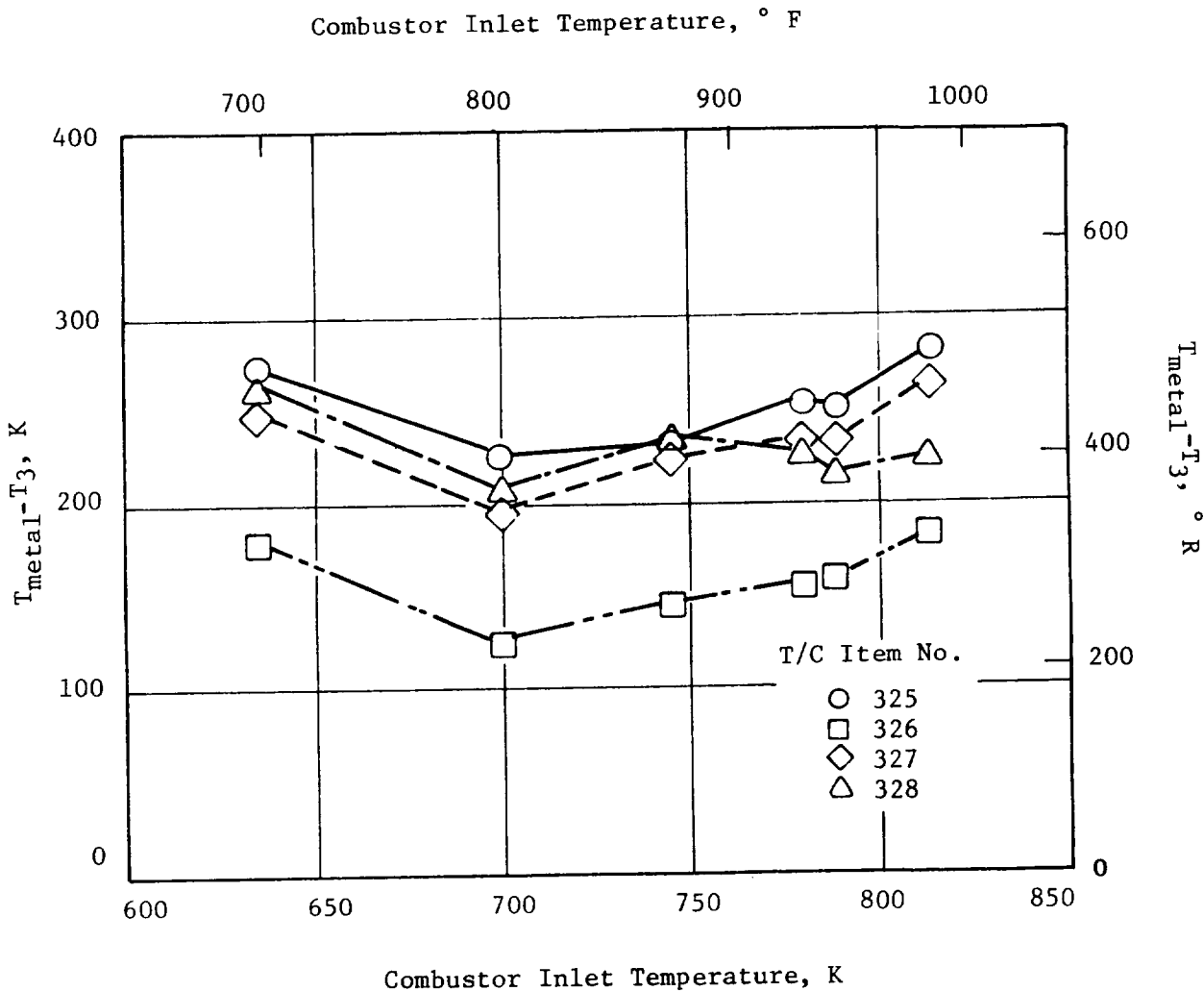


Figure 156. Measured Combustor Metal Temperatures for Baseline Test.

ORIGINAL PAGE IS
OF POOR QUALITY

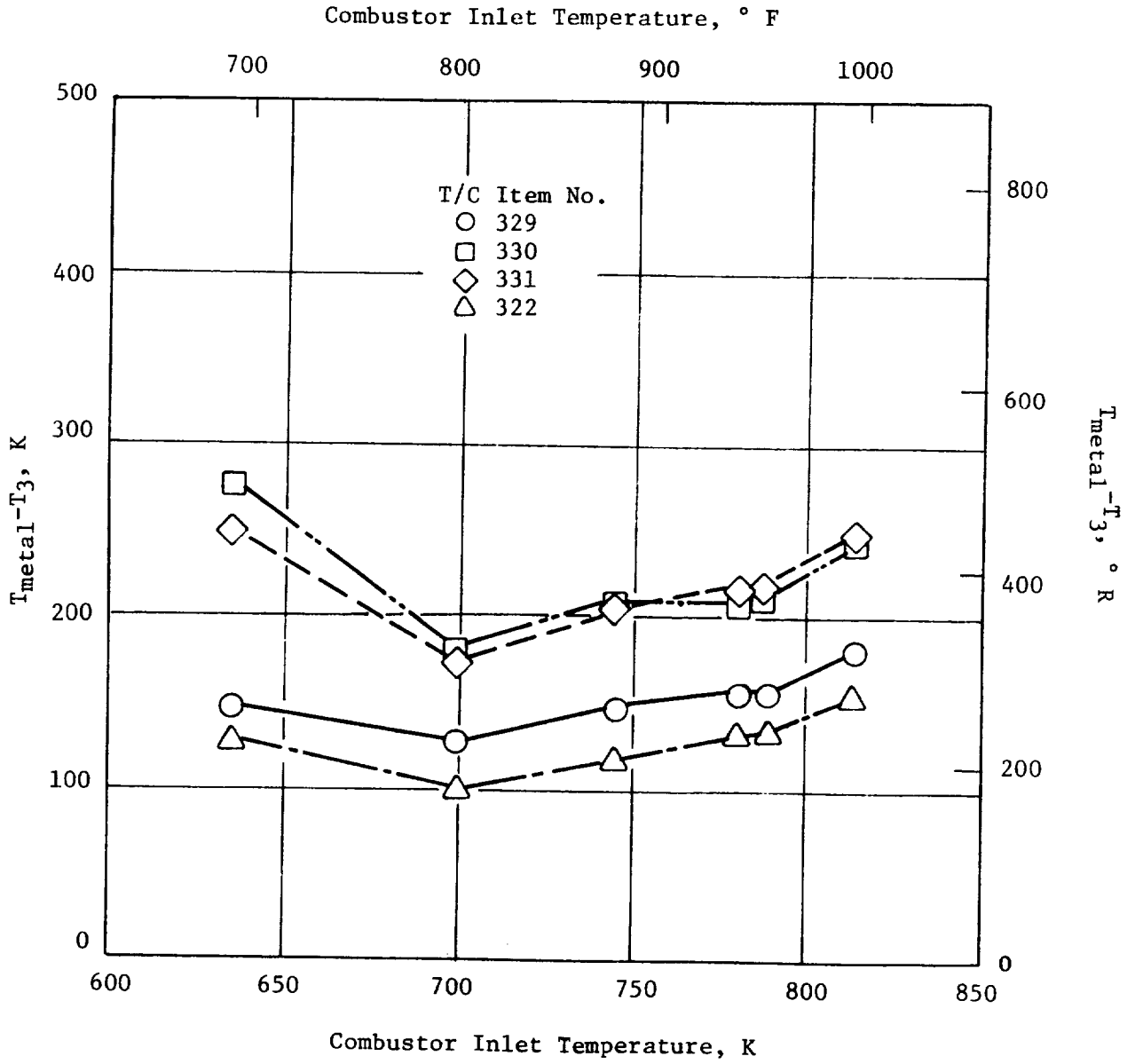


Figure 157. Measured Combustor Metal Temperatures for Baseline Test.

ORIGINAL DOCUMENT
OF POLARON

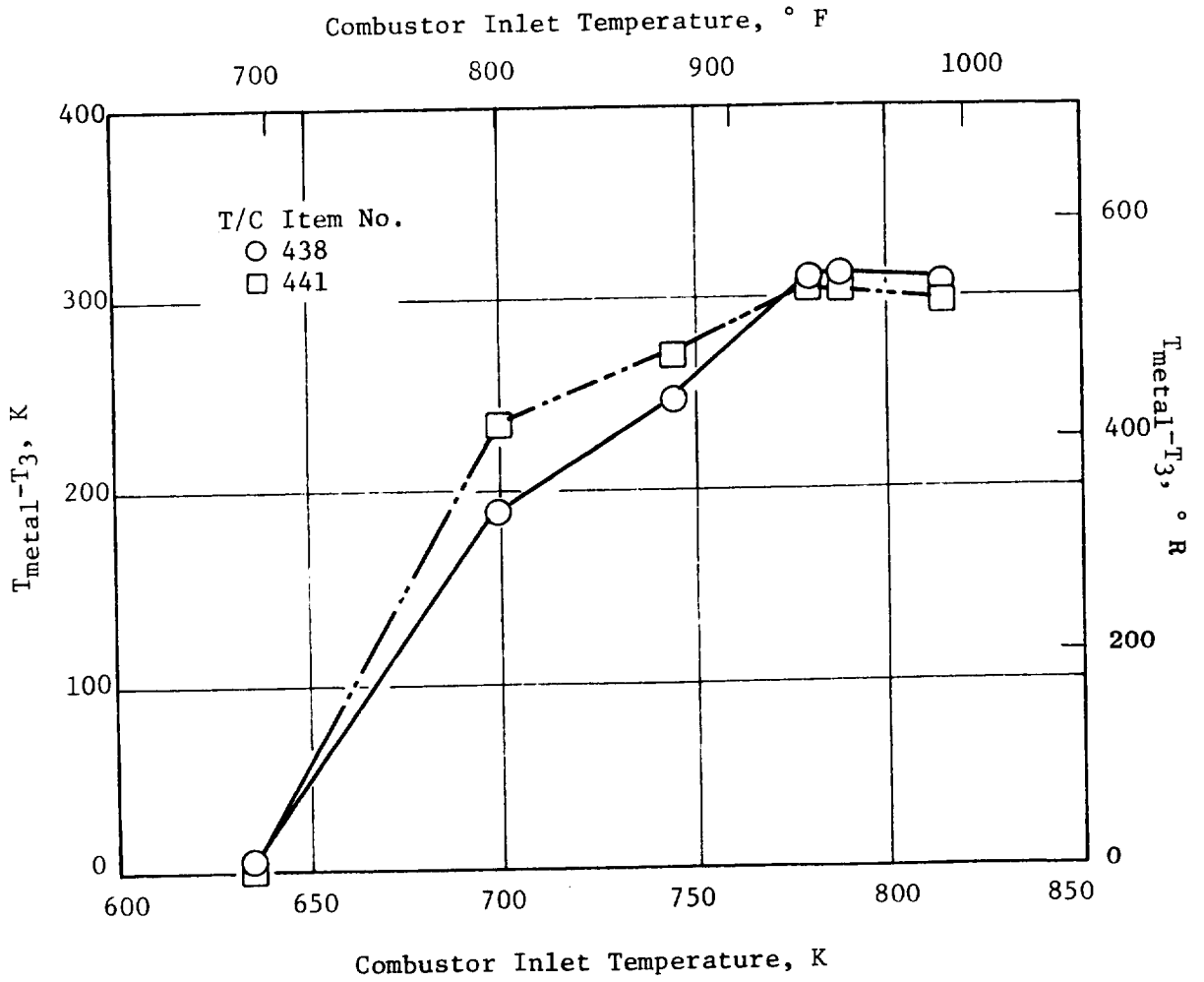


Figure 158. Measured Combustor Metal Temperatures for Baseline Test.

ORIGINAL PAGE IS
OF POOR QUALITY

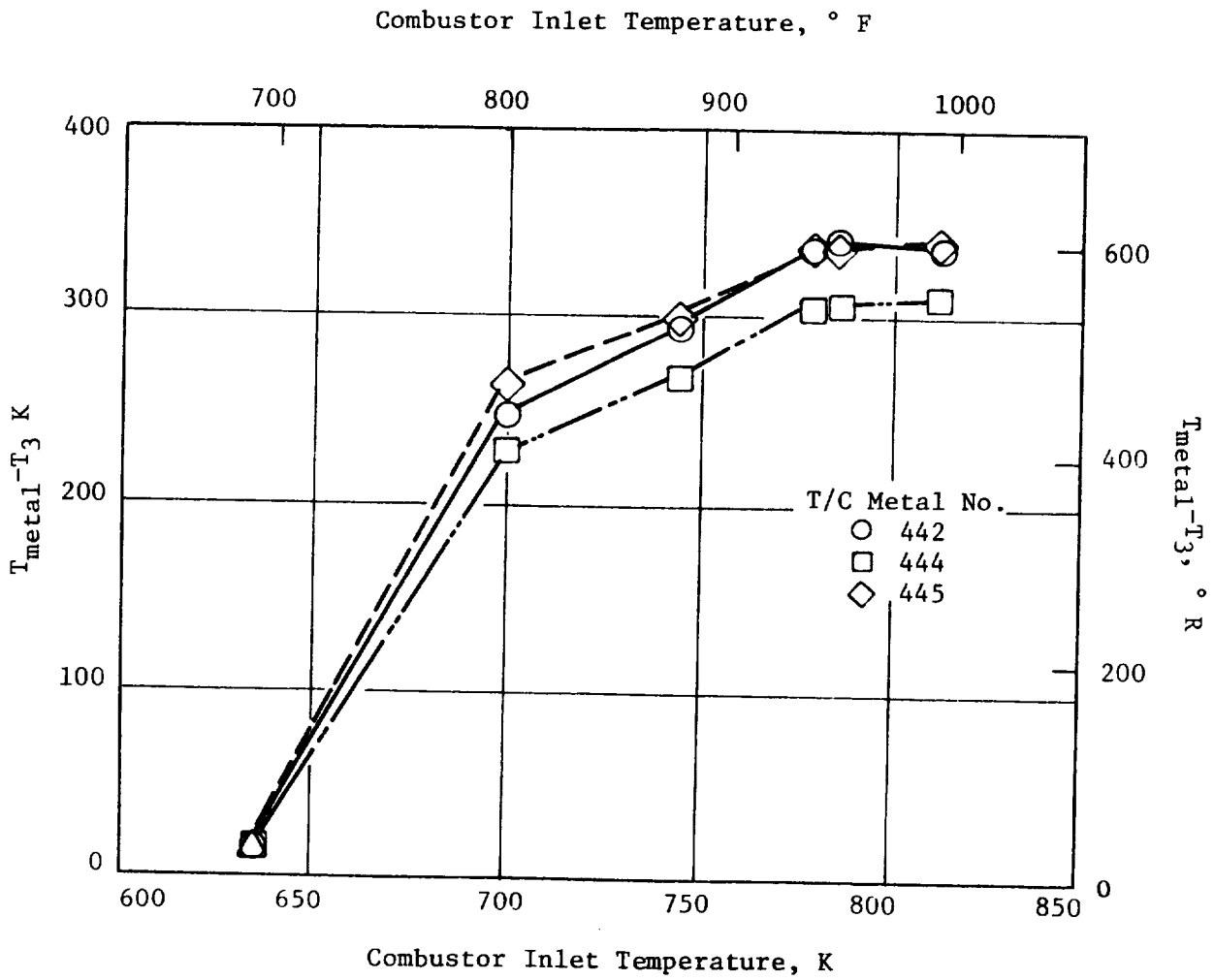


Figure 159. Measured Combustor Metal Temperatures
for Baseline Test.

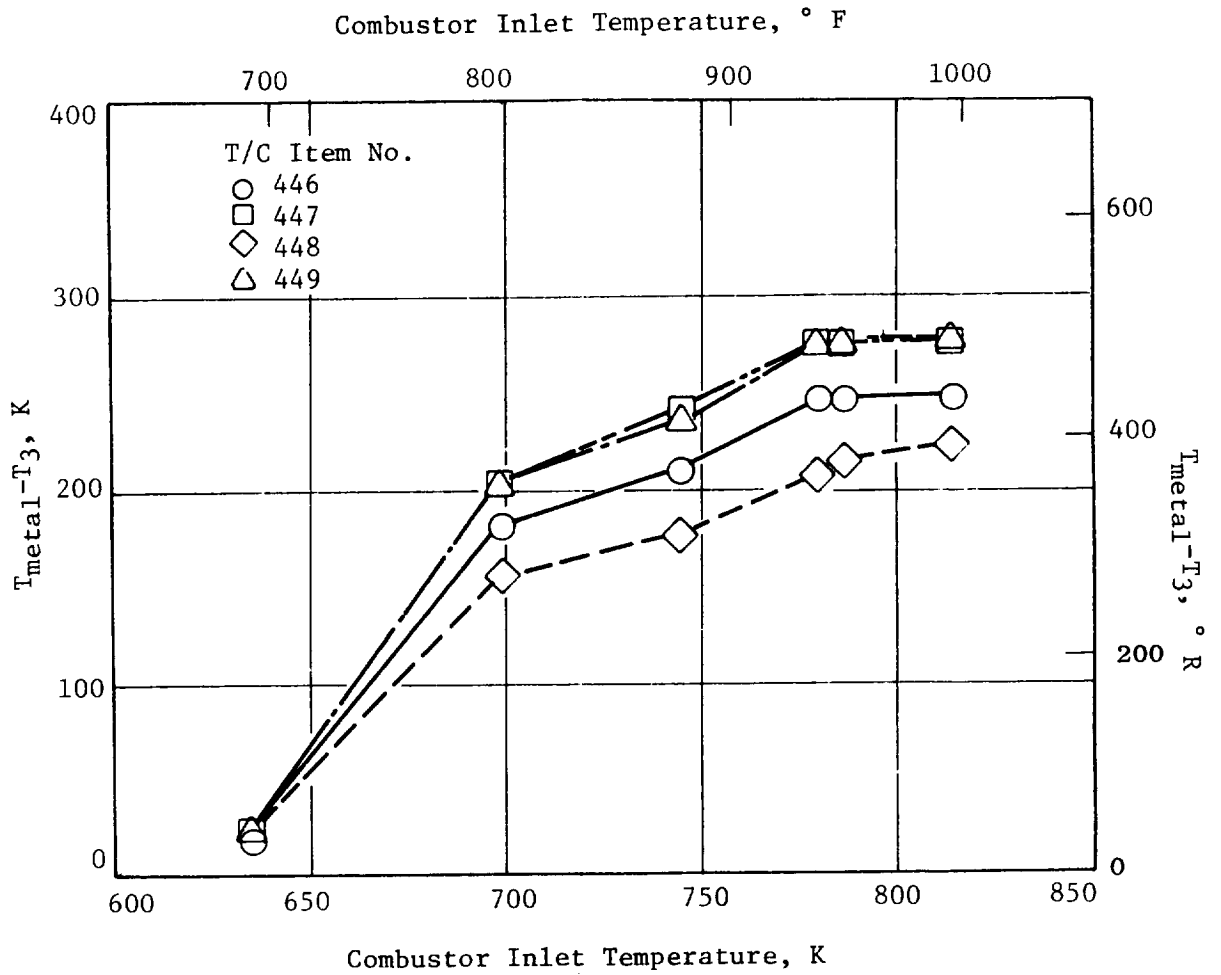


Figure 160. Measured Combustor Metal Temperatures for Baseline Test.

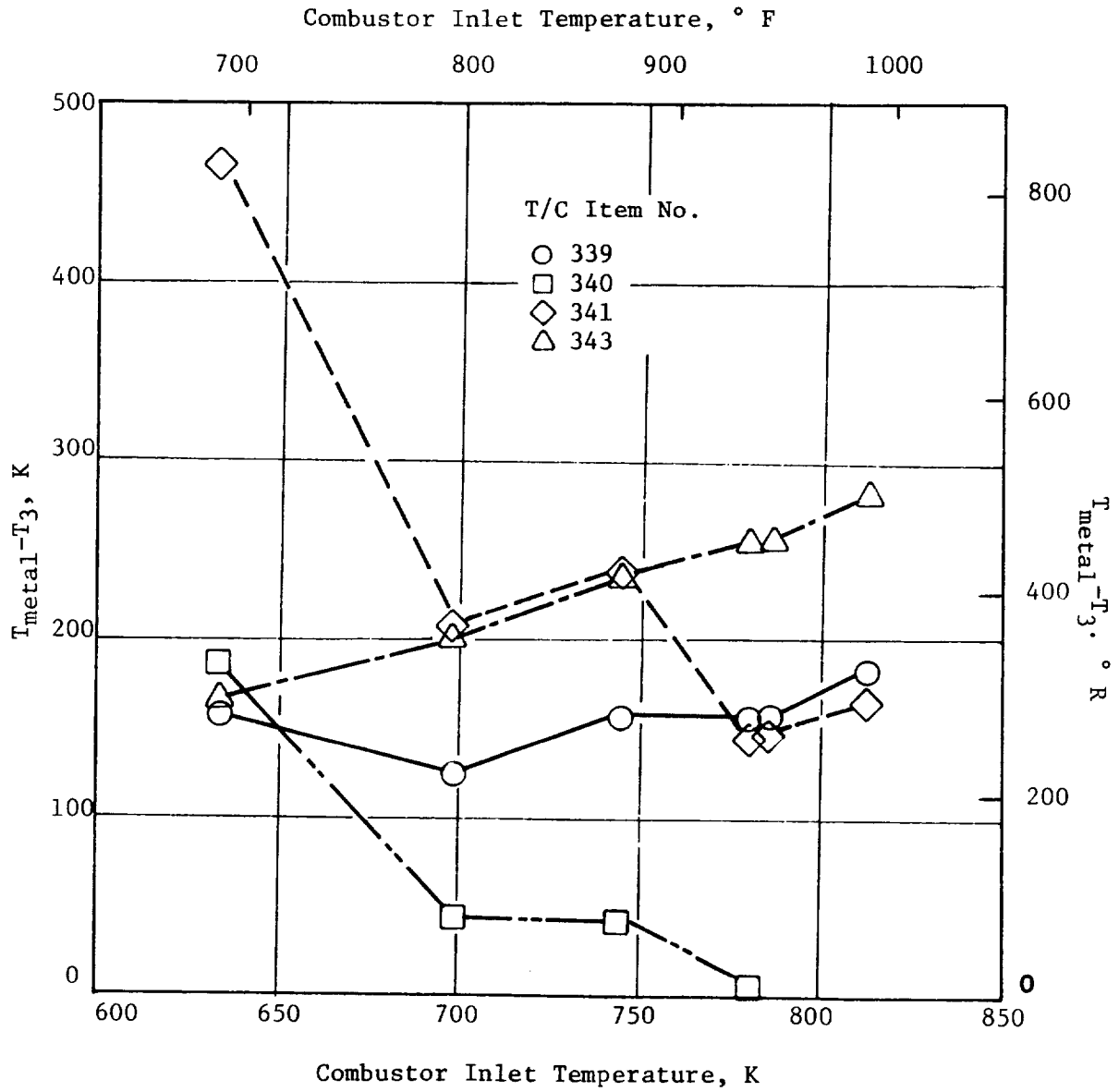
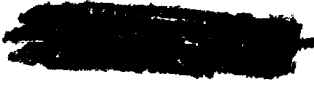


Figure 161. Measured Combustor Metal Temperatures for Baseline Test.

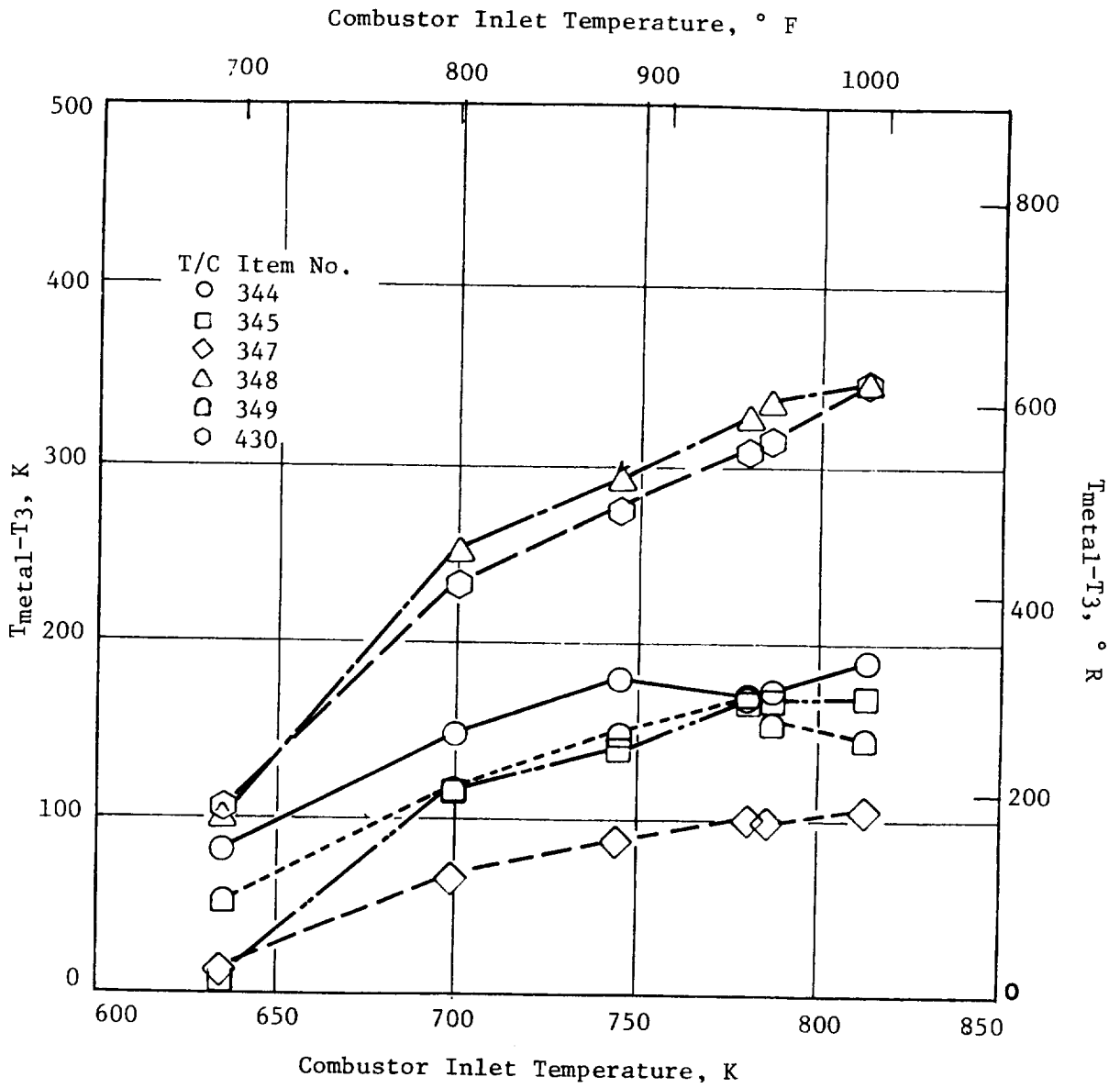


Figure 162. Measured Combustor Metal Temperatures for Baseline Test.

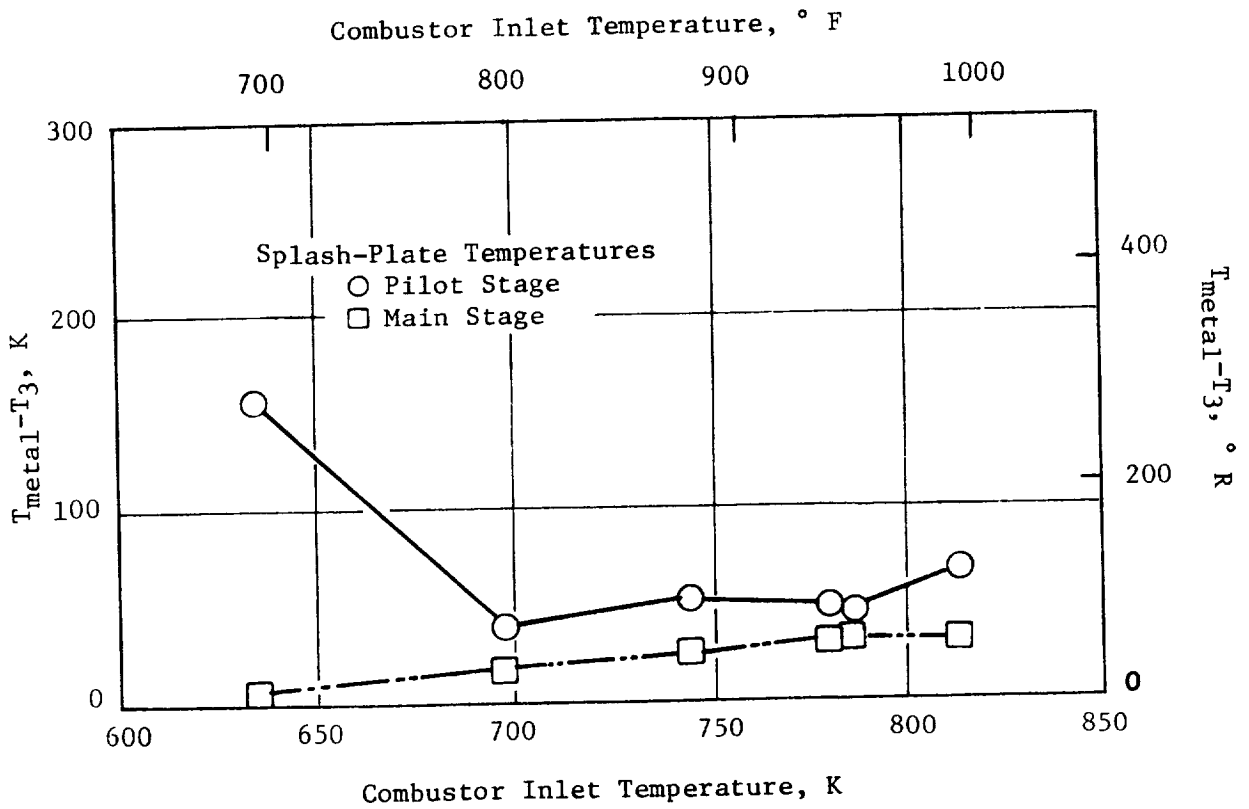


Figure 163. Measured Combustor Metal Temperatures for Baseline Test.

metal temperatures on the crossfire tubes through the centerbody structure between the pilot dome annulus and the main dome annulus remained below 1038 K (1400° F) at all test conditions. There had been some concern that the temperature of these parts might become excessive due to conducting hot gases from the pilot dome to the main dome for ignition of the main stage. Out of a total of six thermocouples located on the pilot dome, only two were reading during testing. One of these thermocouples, located on the splash-plate surface in the lower right corner (aft looking forward), indicated a peak temperature of 894 K (1150° F). The other of these two thermocouples, located on the pilot dome spectacle plate directly between swirl cups, indicated a peak metal temperature of 825 K (1025° F). This was just slightly above the inlet temperature of 814 K (1005° F) at the sea level takeoff condition. Three out of six main dome skin thermocouples were active during testing. Two of these, located on the splash-plate surface in the upper left and lower right corners (aft looking forward), indicated peak metal temperatures only about 28 K (50° F) above the inlet temperature of 814 K (1005° F) at the sea level takeoff condition. The other metal thermocouples, located on the main dome spectacle plate directly between swirl cups, indicated a peak metal temperature of 829 K (1032° F). These pilot and main stage dome temperatures are significantly below the maximum allowable metal temperature and provide strong evidence in support of a significant reduction in the cooling flow levels of each dome.

7.3.4 Concluding Remarks

Testing results obtained from the ground start ignition, exit temperature performance, and emissions evaluations of the E³ double-annular Baseline development combustor were very encouraging, especially considering that this was the first test of this advanced combustor design. However, improvements in all three combustor performance areas were required in order to achieve all of the combustion system goals of the E³. Key problem areas identified from this test series included:

- Improving main stage crossfire and propagation
- Reducing the idle emissions

- Reducing the CO and HC emissions at the 30% power condition in the staged combustor operating mode

Despite obtaining an exit temperature pattern factor which closely approaches the program goal, additional combustor development design optimization would be required to simultaneously satisfy the exit temperature performance and emissions goals.

Immediate attention was directed at identifying combustor design modifications that would provide significant reductions in the ground idle and staged approach emissions levels, plus provide reductions in the outer and inner liner Panel 1 metal temperatures. This would be accomplished by providing added Panel 1 cooling, enriching the pilot stage primary combustion zone to produce more favorable conditions for CO and HC consumption, provide a leaner main stage primary combustion zone to achieve further reductions in the NO_x emissions levels at high power operating conditions, and modify dilution air to provide improvement to the exit temperature performance, and maintain the combustor overall pressure drop.

7.4 MOD I DEVELOPMENT COMBUSTOR TEST RESULTS

The Mod I development combustor featured an enriched pilot stage primary combustion zone. This was accomplished by a reduction in the pilot stage swirl cup flow, the pilot dome splash-plate cooling flow, and the pilot stage primary dilution flow. The pilot dome outer ring cooling flow was increased to provide added film cooling for the forward panel of the outer liner. Outer liner trim dilution was also increased to provide attenuation for the exit temperature radial profile resulting from pilot only operation. This combustor configuration also was redesigned with a leaner main stage primary zone accomplished by an increase in the main stage swirl cup flow. The main dome inner ring cooling flow was increased to provide added film cooling flow for the forward panel of the inner liner. Inner liner trim dilution was also increased to provide improvement in the exit temperature performance at high power operating conditions. In addition, the outer liner, centerbody, and inner liner assemblies were rotated 6° clockwise aft looking forward with respect to the domes relocating the pilot stage and main stage primary dilution holes from in-line to between the swirl cups. With the rotation of

the centerbody, the two pilot-to-main stage crossfire tubes became located between swirl cups. The decision to change to "between cup" primary dilution was based upon sector combustor subcomponent tests. Results from this testing had demonstrated that significant reductions in idle emissions could be obtained by adopting the "between cup" orientation. The design modifications featured in the Mod I combustor configuration are illustrated in Figure 164. The resultant changes in the combustor airflow distribution are presented in Appendix E.

7.4.1 Atmospheric Ground Start Ignition Test

Atmospheric ground start ignition testing of the Mod I development combustor was initiated on 16 July 1980. Test points evaluated simulated combustor inlet conditions along the E³ (9/79) ground start operating line and are presented in Table XXXVII.

Table XXXVII. Development Combustor Mod I Atmospheric Ignition Test Point Schedule.

<u>XNRH,</u> <u>%</u>	<u>T₃</u> <u>K</u>	<u>(° F)</u>	<u>P₃</u> <u>atm</u>	<u>W₃₆</u> <u>kg/s (pps)</u>
21	289	(60)	1.00	1.25 (2.76)
28	289	(60)	1.00	1.69 (3.71)
32	314	(105)	1.00	1.55 (3.40)
46	344	(160)	1.00	1.65 (3.64)
58	383	(230)	1.00	1.86 (4.09)
70	429	(312)	1.00	1.94 (4.26)
77	503	(445)	1.00	2.33 (5.13)

The fuel nozzle assemblies used had the E³ test rig fuel nozzle bodies. The nozzle tips installed in the pilot dome were rated at 12 kg/hr (26.5 pph), while those installed in the main dome were rated at 4.5 kg/hr (10 pph).

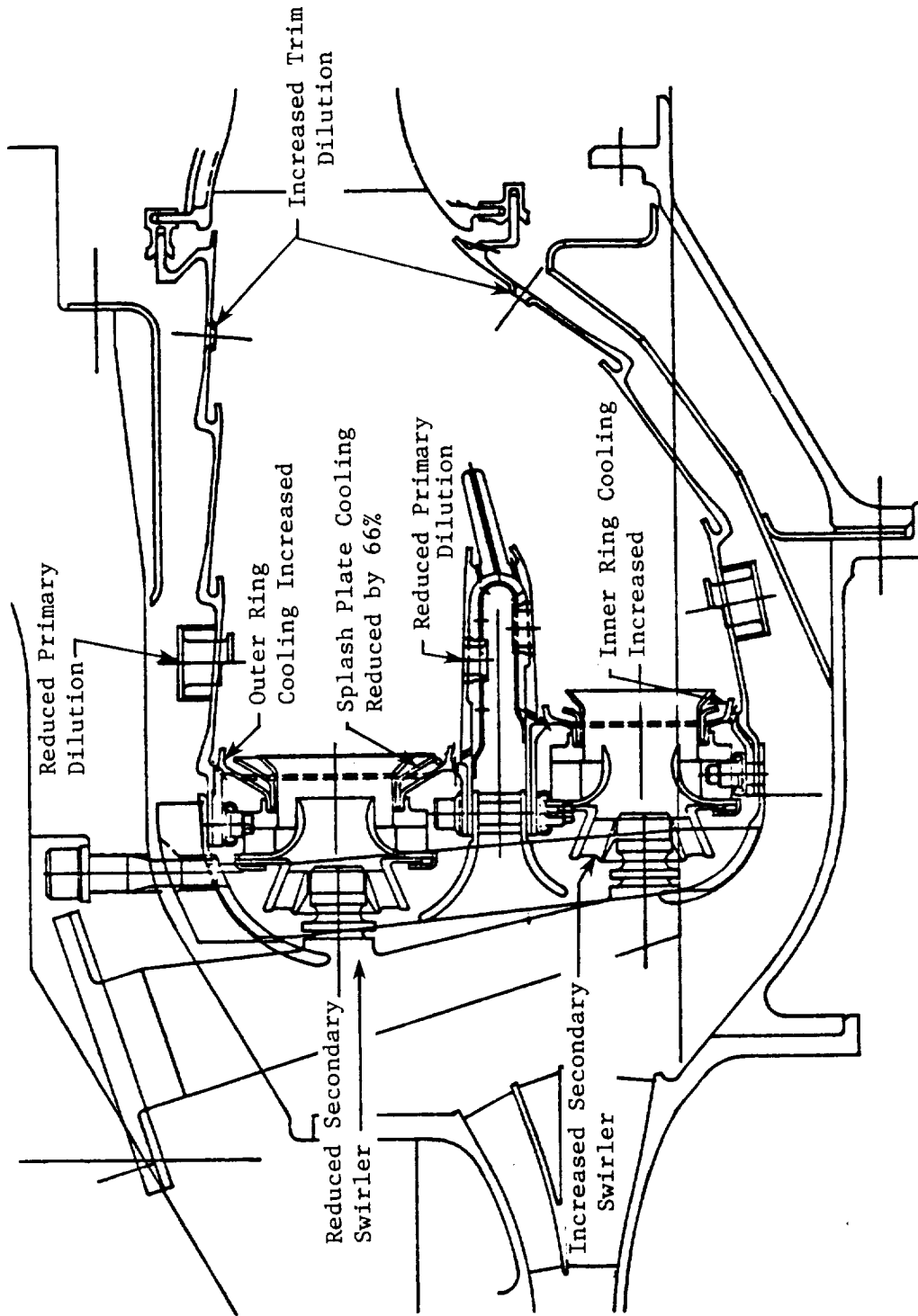


Figure 164. Mod I Combustor Hardware Modifications.

Shutoff-type valves were installed into every other main stage fuel line pigtail to allow evaluating the main stage crossfire and propagation characteristics using a uniform 15 on-15 off fuel nozzle operating mode.

During the initial test run, pilot stage ignition and propagation proceeded without difficulty at all points of the test schedule. However, main stage crossfire was not achieved at any of the test conditions evaluated. Test facility exhaust plenum temperature limitations prevented exceeding a main stage fuel flow level of 600 pph with the pilot stage fueled and burning. From visual observations, it was evident that fire from the pilot stage swirl cups, now between the two crossfire tubes, was not penetrating into the main stage dome annulus through the crossfire tubes. Without conduction of hot pilot stage gases into the main stage dome to provide an ignition source, the ignition of the main stage was unsuccessful. During ground start ignition evaluation of the Baseline combustor configuration, it was observed that main stage ignition was obtained from hot pilot-gas penetrating into the main stage dome annulus through the crossfire tubes located directly in line with Swirl Cups Nos. 6 and 21. The inability to successfully crossfire the main stage in the Mod I configuration was concluded to be the result of the "between cup" location of the existing crossfire tubes. It was decided to remove the combustor from the test rig to incorporate two additional crossfire tubes in the centerbody structure. These additional crossfire tubes were located 180° apart and perpendicular to the alignment of the existing crossfire tubes. Upon reassembly of the combustor, the new crossfire tubes were located directly in line with Cup No. 6 and the igniter Cup No. 21. After completion of the rework, the combustor was installed back into the test rig to resume the ground start ignition evaluation. Through the duration of the atmospheric ground start ignition testing, main stage crossfire was achieved.

Test results obtained from this ground start ignition evaluation of the E³ development combustor Mod I configuration are presented in Figures 165 and 166. As observed from Figure 165, significant improvement in pilot ignition, propagation, and total blowout were achieved compared with the results of the Baseline configuration. It is noted that the Baseline configuration ignition data was obtained with the use of a hydrogen torch ignition system which generally provides better ignition results than would be obtained with

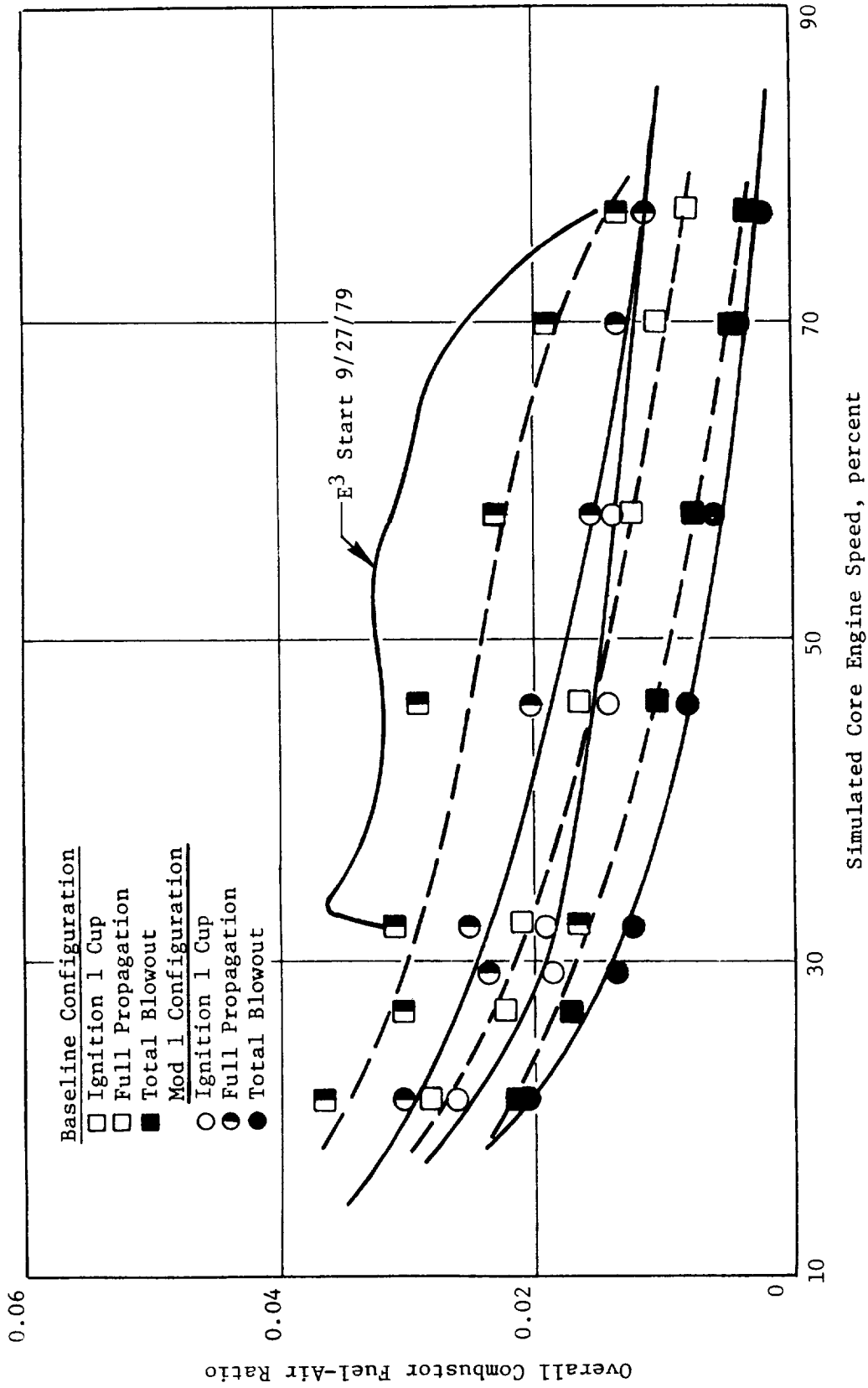


Figure 165. Mod I Atmospheric Ignition Test Results.



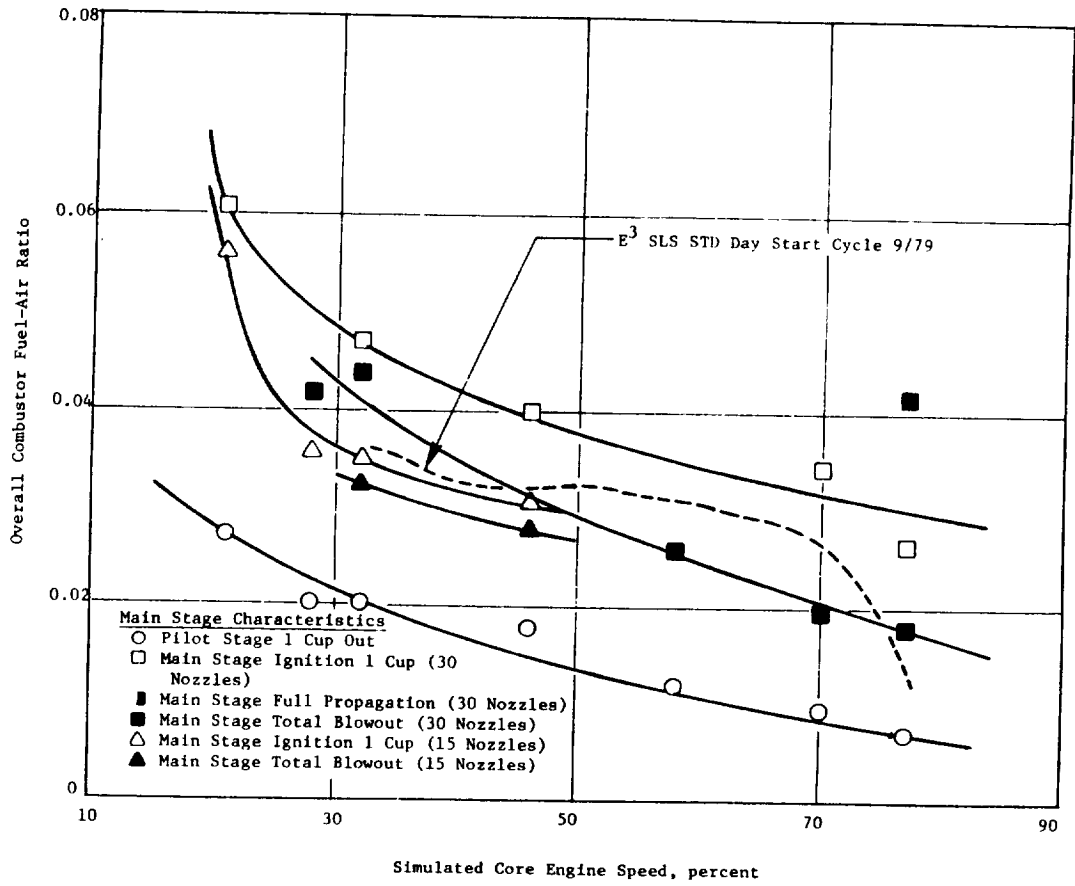


Figure 166. Mod I Atmospheric Ignition Test Results.

the use of an electrical spark discharge ignition system, particularly at the lower speed points. The Mod I configuration demonstrated full propagation of the pilot stage with between 50% and 100% fuel margin compared to the E³ ground start cycle combustor fuel-air ratio operating line, with a minimum of 40% blowout margin. These observed improvements reflected the benefit of the enriched pilot stage stoichiometry of this configuration. Ignition of the main stage was investigated for two fueling modes. In one mode, fuel was supplied to all 30 main stage nozzles. In the second mode, all main stage nozzles in even numbered cups were shut off. The main stage cup in line with the igniter and crossfire tube (Cup No. 21) was fueled. In general, the main stage ignition characteristics of the Mod I configuration were no better than those demonstrated in the Baseline configuration. In the 30 nozzle mode, overall fuel-air ratios exceeding the E³ 9/79 ground start cycle operating line were required to ignite the two main stage swirl cups in line with the crossfire tubes. Full propagation of the main stage demonstrated only at the simulated 77% core engine speed operating condition. However, the propagation fuel-air ratio required was well above the required fuel schedule operating line. Partial propagations were obtained at 48%, 58%, and 70% simulated core engine speed operating conditions. These also occurred at fuel-air ratios well above the requirement. Some benefit in the ignition characteristics of the main stage was obtained using the 15 on-15 off nozzle operating mode. However, full or partial propagations were not obtained in this mode. The adverse effects of the greater effective swirl cup spacing eliminated the benefit of locally richer conditions in the vicinity of the fueled swirl cups. It was observed that the flame in the main stage annulus had difficulty holding position. This flame instability appeared to result from the lean stoichiometry and high dome velocities produced from the increased main stage airflow of this configuration. The main stage swirl cups in the Mod I configuration have approximately 12% increase in airflow. Overall main stage primary zone airflow is up by 14% compared to levels calculated for the baseline combustor configuration.

7.4.2 Atmospheric Exit Temperature Performance Test

Performance testing of the Mod I configuration was conducted on 11-12 August 1980. The purpose of this test was to evaluate the Mod I combustor

configuration for profile and pattern factor at simulated sea level takeoff conditions at various pilot and main dome fuel flow ratios. In addition, data was also obtained at both conditions simulating 46% and 58% core engine speed along the E³ 9/79 ground start operating line, and at simulated 6% ground idle operating conditions with the pilot stage only fueled.

Fuel-air ratios set at both subidle operating conditions were limited to 0.0255 because of the facility fuel pump discharge limitations using the nozzle tips selected for this test. The E³ 9/79 start cycle defines fuel-air ratios of 0.031 and 0.028 respectively for the 46% and 58% core speed operating conditions. Prior to testing, the E³ exit temperature traverse rakes were modified to reduce the rake body height dimension by 0.10 inch. This modification, shown in Figure 133, was made to prevent the interference and rubbing problem experienced during the Baseline combustor performance test. The test point schedule and corresponding combustor operating conditions are presented in Table XXXVIII.

The E³ test rig fuel nozzle assemblies were used featuring nozzle tips rated at 2.3 kg/hr (5 pph) in the pilot stage and nozzle tips rated at 4.5 kg/hr (10 pph) in the main stage.

Indicated exit gas temperatures obtained represented corrected thermocouple readings. A thermocouple radiation loss correction was generated for the E³ combustor using existing corrections for the CF6 and F101 combustor families. This correction characteristic is shown in Figure 167. It was incorporated into the data reduction program used to handle E³ combustor testing.

Test results obtained at the subidle operating conditions and at the 6% ground idle operating condition, are presented in Figure 168. As anticipated, with the pilot stage only fueled, the average and maximum profiles are sharply peaked outward. The anticipated attenuation in these outer peaked profiles did not occur. It was interesting to note that the average and maximum profiles at the 6% ground idle condition were more severe than those obtained at the subidle conditions. This is related to the lower average gas temperature rise, and high maximum gas temperatures associated with the lower fuel-air

Table XXXVIII. Development Combustor Mod I Atmospheric EGT Performance Test Point Schedule.

Test Points	T_3 , k ($^{\circ}$ F)	P_3 Atm	W_3 , kg/s (pps)	W_{Bleed} , kg/s (pps)	W_c , (kg/s)	f/a	Pilot Total	W_{Pilot} kg/hr (pph)	W_{Main} kg/hr (pph)
1	344 (160)	1.00	1.78 (3.92)	0.13 (0.28)	1.65 (3.64)	0.031	1.0	184 (406)	0
2	383 (230)	1.00	2.00 (4.40)	0.14 (0.31)	1.86 (4.09)	0.028	1.0	187 (412)	0
3	495 (432)	1.00	2.55 (5.60)	0.18 (0.40)	2.36 (5.20)	0.0123	1.0	105 (230)	0
4	815 (1007)	1.00	2.41 (5.31)	0.15 (0.34)	2.26 (4.97)	0.0244	0.5	100 (219)	100 (219)
5	815 (1007)	1.00	2.41 (5.31)	0.15 (0.34)	2.26 (4.97)	0.0244	0.4	80 (175)	119 (262)
6	815 (1007)	1.00	2.41 (5.31)	0.15 (0.34)	2.26 (4.97)	0.0244	0.3	60 (131)	139 (306)

ORIGINAL PAGE IS
OF POOR QUALITY

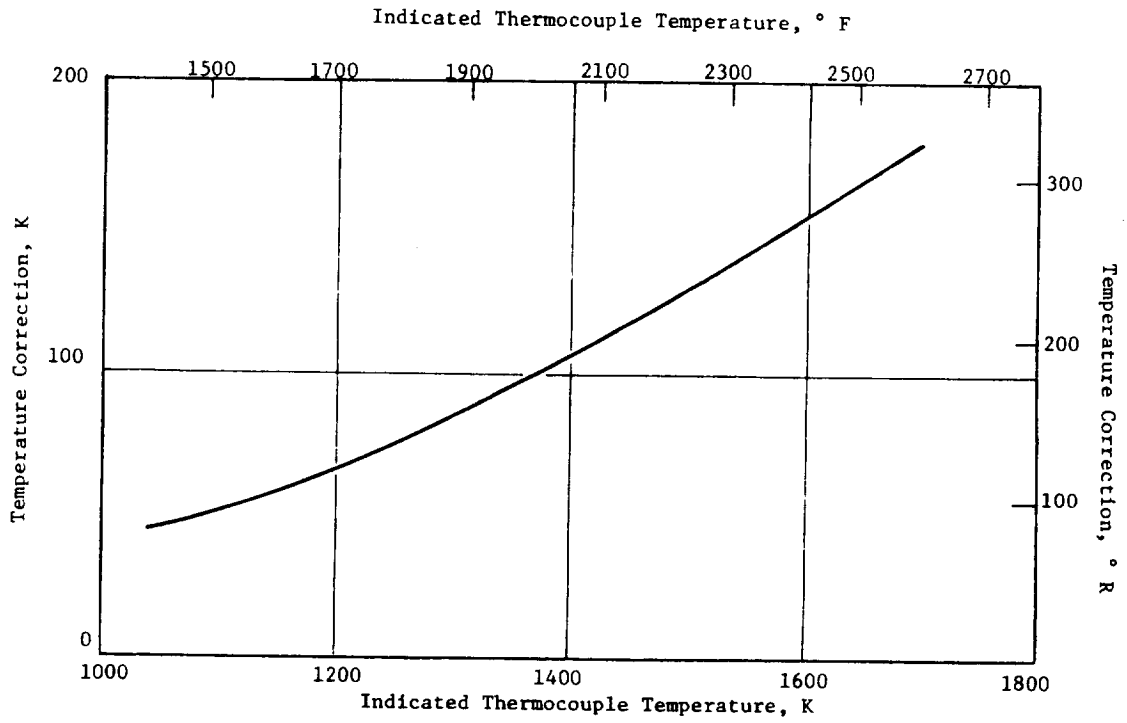


Figure 167. EGT Thermocouple Correction.

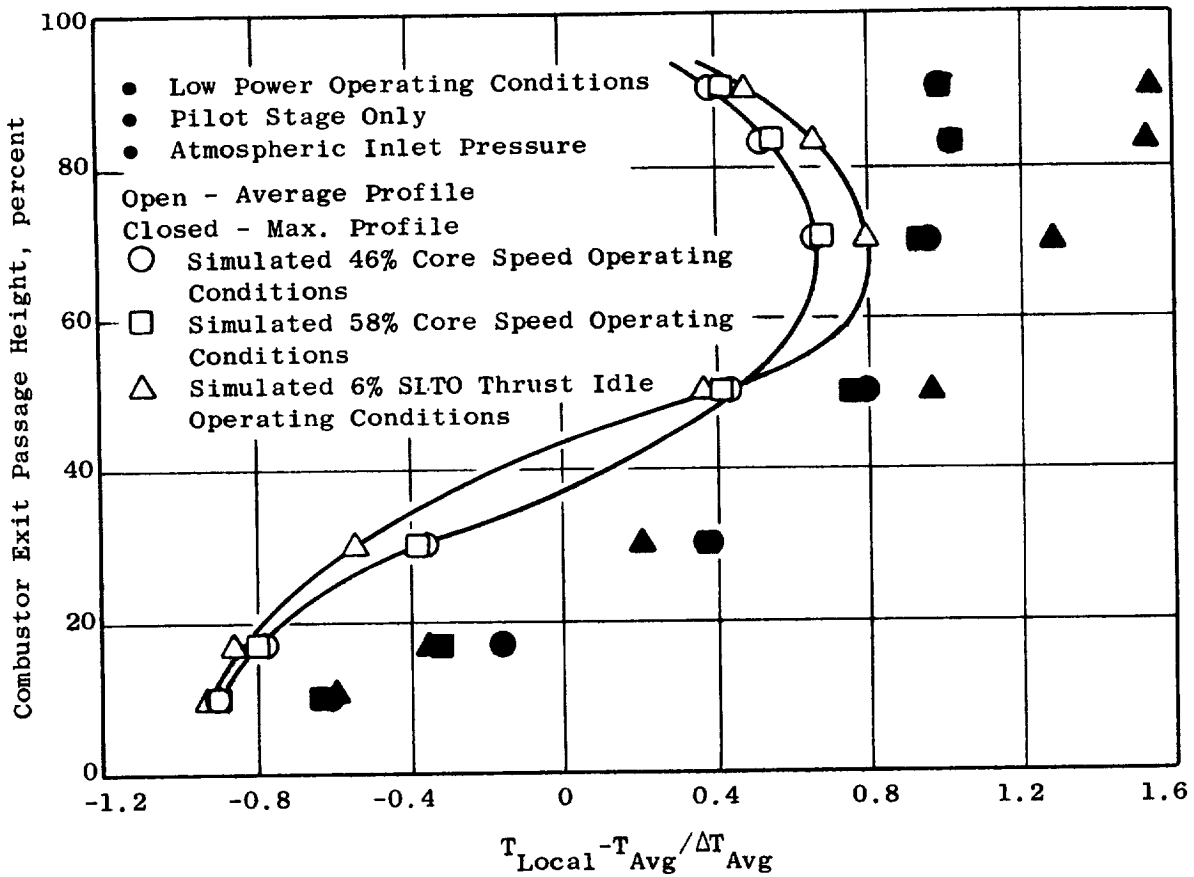


Figure 168. Mod I EGT Performance Test Results.

ratio (0.0123 as compared to 0.0255) and higher combustion efficiency at the 6% ground idle condition. At all three low power conditions, pattern factors in excess of 1.00 were obtained.

At the simulated SLTO operating conditions, exit gas temperature data was obtained at pilot-to-total fuel splits of 0.5, 0.4, and 0.3. At each fuel split evaluated, full propagation of the fire within the main stage could not be achieved. It was observed that several main stage cups were not burning, while others appeared to be unstable. Attempts to achieve full propagation of the main stage by increasing main stage fuel flow were not successful. As a result, temperature traverse data was obtained at the design fuel-air ratio (0.0244) with a partially burning main stage annulus. An analysis was conducted to explain why full propagation of the main stage could not be achieved. The results indicated that equivalence ratios in the main stage swirl cup were near or below the lean stability limit, as determined from the results of the ground start ignition test.

The exit temperature data that was obtained indicated that a 60° section of the combustor between Cups 9 and 14 had stable main stage combustion at all three fuel splits evaluated. The data obtained from this combustor annulus section was used to determine the average and maximum profiles presented in Figures 169 to 171. At a pilot-to-total fuel flow split of 0.5, the average and maximum profiles are within the limits. A pattern factor of 0.243 was obtained at 90% of the passage height, compared to the target value of 0.250. A maximum profile within the required limit was also obtained at a pilot-to-total fuel flow split of 0.4. At this condition, a pattern factor of 0.244 was obtained at 30% of the passage height. However, the average profile exceeded the required limit below 40% of the passage height. At a pilot-to-total fuel flow split of 0.3, both the average and maximum profiles are peaked inward, exceeding the required limits by a considerable amount. At this fuel split, a pattern factor of 0.396 was obtained. The average and maximum profiles obtained from the Mod I combustor configuration show significant improvement in the inner region of the exit passage over the Baseline combustor configuration. This most probably reflects the large increase in the inner liner trim dilution featured in the Mod I combustor.

ORIGINAL PAGE IS
OF POOR QUALITY

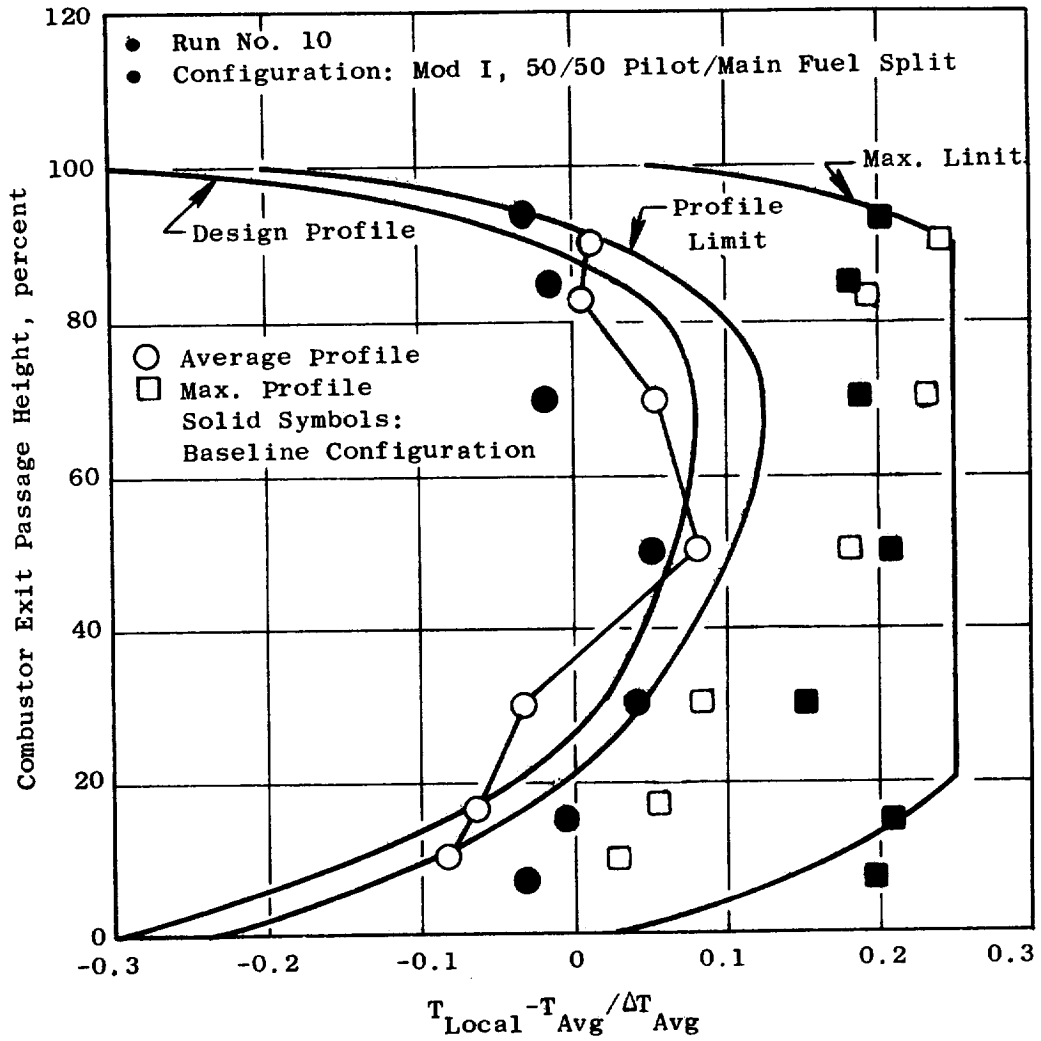


Figure 169. Mod I EGT Performance Test Results.

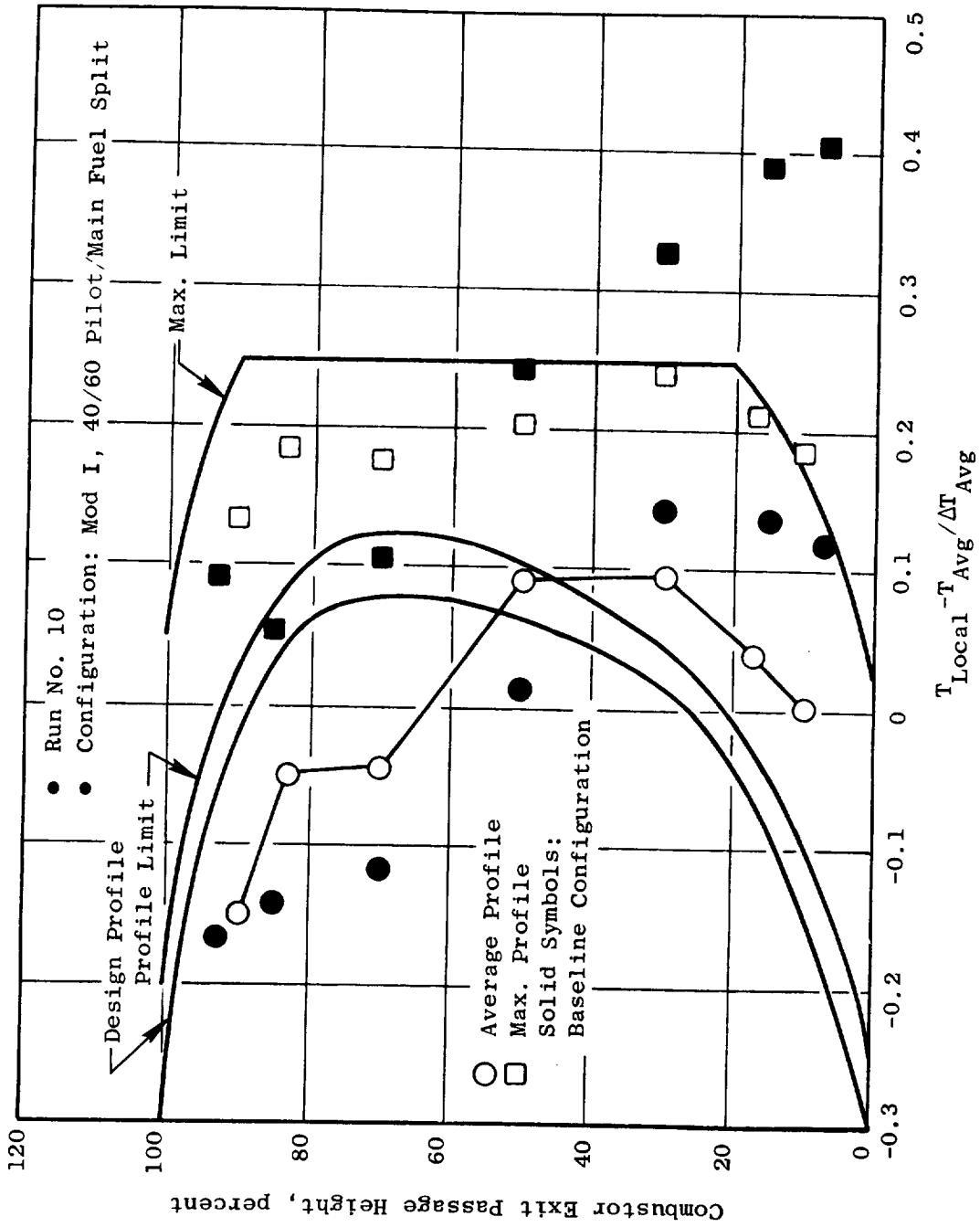


Figure 170. Mod I EGT Performance Test Results.

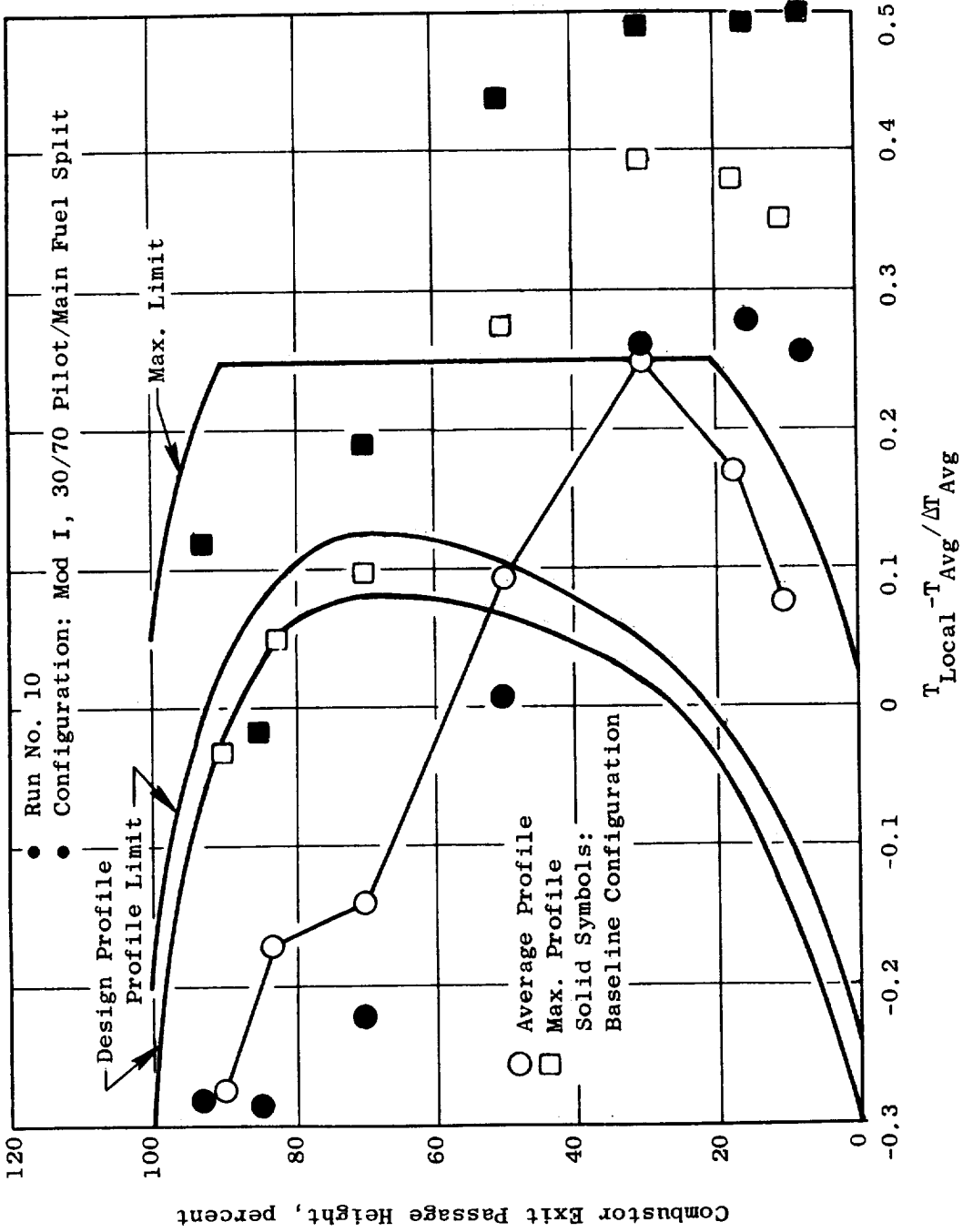


Figure 171. Mod I EGT Performance Test Results.

7.4.3 Emissions Test

As part of the emissions testing of the Mod I combustor configuration, additional ground start ignition testing was conducted at the actual ground start cycle inlet pressures. Ignition, propagation, and blowout of the pilot and main stages were determined from thermocouples mounted onto the five equally spaced gas sampling rakes located in the test rig instrumentation spool. All sampling rake thermocouples plus numerous other combustor hardware skin thermocouples were connected to a thermocouple temperature display (Metrascope) for continuous monitoring.

The E³ test rig fuel nozzle assemblies were used for this test. Nozzle tips rated at 12 kg/hr (26.5 pph) were installed in the pilot stage. Nozzle tips rated at 23 kg/hr (50.0 pph) were installed in the main stage. These nozzle tips were also used for the low power emissions testing.

The pilot and main stage ignition, propagation, and blowout characteristics obtained at actual ground start cycle combustor inlet pressure conditions are shown in Figure 172. Main stage data presented in this figure is based on the pilot stage operating at a fuel flow level at which full pilot stage propagation was achieved. Therefore, this data represents a worst case statement for the overall fuel-air ratios at which the main stage ignition, propagation, and lean blowout were obtained. In reality, the pilot stage would operate at the lowest fuel flow level at which all 30 swirl cups remained burning. However, since it would be difficult to determine this level in the pressure rig, the above approach was selected. It was observed that the ignition and propagation characteristics of the combustor improve substantially when operated at true cycle pressure conditions, as compared to atmospheric operation. However, little if any impact was demonstrated on the blowout characteristics. Even with the pressure performance improvement, the ground start ignition, propagation, and blowout characteristics of the main stage were not adequate to meet the (9/79) engine ground start requirement.

Emissions testing of the Mod I configuration was conducted. The purpose of this test was to evaluate this combustor design for emissions, pressure drop, and metal temperature characteristics at combustor operating conditions

ORIGINAL PAGE IS
OF POOR QUALITY.

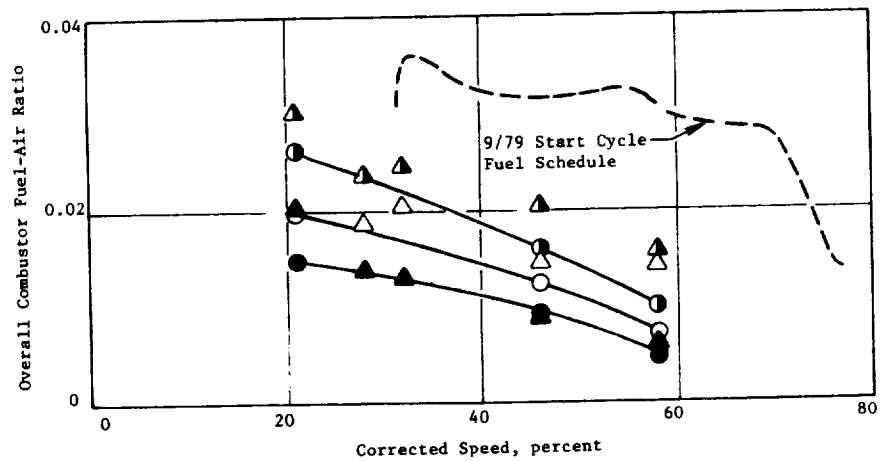
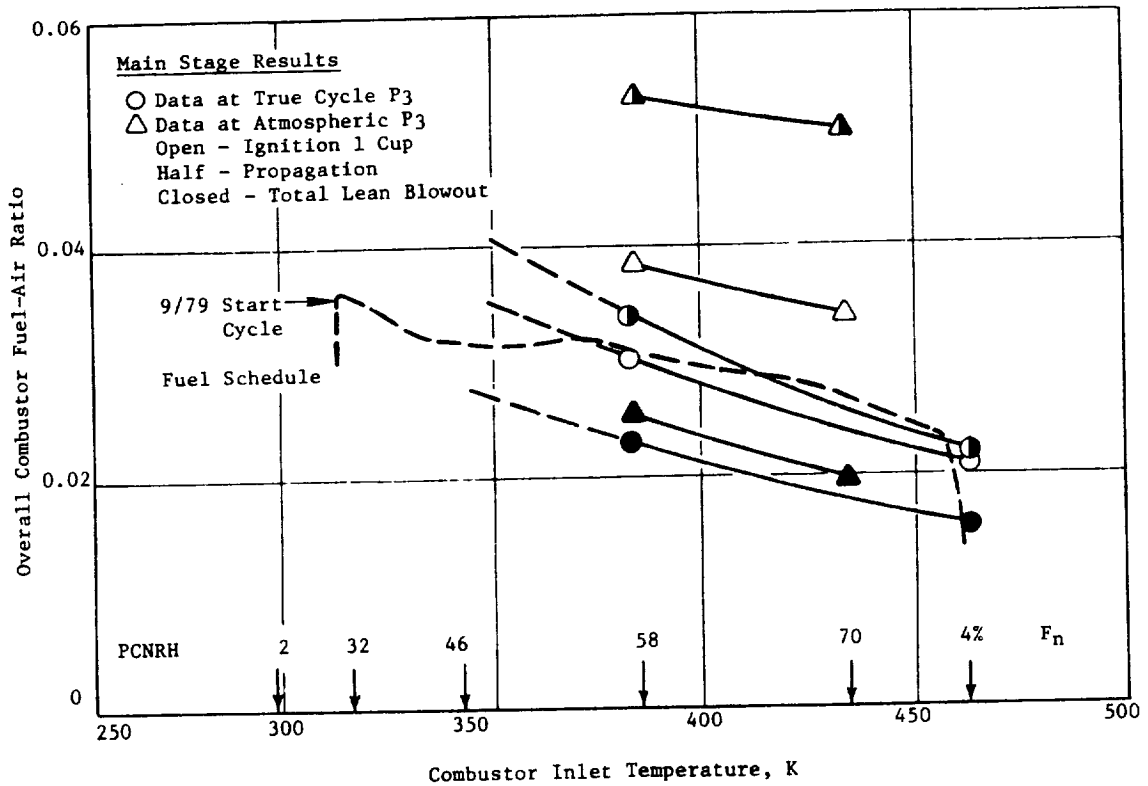


Figure 172. Mod I Ignition Results at True Cycle Conditions.

along the E³ FPS operating line. The test was conducted in two phases. The first phase involved evaluation at 4% and 6% ground idle conditions. The second phase of the test was directed at evaluation at higher power operating conditions. This pause in testing was necessary to allow for a change in the fuel nozzle tip sizes in each dome. In the second phase of the test, nozzle tips rated at 23 kg/hr (50 pph) were installed into the pilot stage, while nozzle tips rated at 55 kg/hr (120 pph) were installed into the main stage. It had been intended to evaluate the combustor at 30% approach conditions, and at simulated SLTO conditions. However, problems with the facility operation resulted in a severe test schedule time restriction. This time problem coupled with indications of excessively high centerbody metal temperatures prevented the acquisition of all of the desired data. As a result, only a limited amount of high power emissions data was obtained at combustor operating conditions that deviated from the E³ FPS design cycle. Test points and corresponding operating conditions evaluated in this test are presented in Table XXXIX.

Combustor instrumentation consisted of 15 static pressures and 27 grounded and capped chromel-alumel thermocouples. The locations of this instrumentation on the combustor hardware is illustrated in Figures 173 to 176. In addition, data from numerous pressure and temperature instrumentation affixed to the test rig vehicle were also obtained. This instrumentation included upstream total pressure and air temperature rakes to measure the combustor inlet total pressure and temperature. Test rig flowpath wall static pressures provided data concerning diffuser system performance, while thermocouples were used to monitor the test rig to assure the rig mechanical integrity.

The results of the idle emissions testing of the Mod I combustor configuration are presented in Figures 177 to 180. As observed from Figure 177, CO emission levels of 48 g/kg (48 lb/1000 lb) of fuel and 30 g/kg (30 lb/1000 lb) of fuel were obtained, respectively, at the 4% and 6% ground idle design cycle operating conditions. These compare to levels of 59.9 g/kg (59.9 lb/1000 lb) of fuel and 57.5 g/kg (57.5 lb/1000 lb) of fuel demonstrated during evaluation of the Baseline configuration. At 6% ground idle, the minimum CO emission level occurred at the design cycle fuel-air ratio. It has been estimated that a CO emission level of 20.7 g/kg (20.7 lb/1000 lb) of fuel at

Table XXXIX. Development Combustor Mod I Emissions Test Point Schedule.

Operating Condition	P3, MPa (psia)	T3, k (° F)	W3, kg/s (pps)	Wbleed Outer, kg/s (pps)	Wbleed Inner, kg/s (pps)	Wbleed Prediff. kg/s (pps)	Wc, kg/s (pps)	f/a, Overall	Pilot Total	Wf pilot kg/hr (pph)	Wf main kg/hr (pph)
4% Idle	0.344 (49.9)	466 (379)	9.55 (21.0)	0.55 (1.2)	0.50 (1.1)	0.59 (1.3)	7.86 (17.3)	0.009	1.0	255 (561)	0
4% Idle	0.344 (49.9)	466 (379)	9.55 (21.0)	0.55 (1.2)	0.50 (1.1)	0.59 (1.3)	7.86 (17.3)	0.0120	1.0	340 (747)	0
4% Idle	0.344 (49.9)	466 (379)	9.55 (21.0)	0.55 (1.2)	0.50 (1.1)	0.59 (1.3)	7.86 (17.3)	0.0138	1.0	390 (858)	0
4% Idle	0.344 (49.9)	466 (379)	9.55 (21.0)	0.55 (1.2)	0.50 (1.1)	0.59 (1.3)	7.86 (17.3)	0.0200	1.0	566 (1246)	0
6% Idle	0.436 (63.3)	495 (432)	12.32 (27.1)	0.73 (1.6)	0.64 (1.4)	0.77 (1.7)	10.18 (22.4)	0.009	1.0	330 (726)	0
6% Idle	0.436 (63.3)	495 (432)	12.32 (27.1)	0.73 (1.6)	0.64 (1.4)	0.77 (1.7)	10.18 (22.4)	0.0110	1.0	403 (887)	0
6% Idle	0.436 (63.3)	495 (432)	12.32 (27.1)	0.73 (1.6)	0.64 (1.4)	0.77 (1.7)	10.18 (22.4)	0.0123	1.0	451 (992)	0
6% Idle	0.436 (63.3)	495 (432)	12.32 (27.1)	0.73 (1.6)	0.64 (1.4)	0.77 (1.7)	10.18 (22.4)	0.0150	1.0	550 (1210)	0
6% Idle	0.436 (63.3)	495 (432)	12.32 (27.1)	0.73 (1.6)	0.64 (1.4)	0.77 (1.7)	10.18 (22.4)	0.0200	1.0	733 (1613)	0
High Power	1.664 (241.3)	702 (804)	34.82 (76.6)	1.64 (3.6)	1.55 (3.4)	3.45 (7.6)	28.14 (61.9)	0.0197	0.4	785 (1728)	1205 (2652)
High Power	1.667 (241.7)	698 (797)	34.77 (76.5)	1.82 (4.0)	1.68 (3.7)	3.05 (6.7)	28.23 (62.1)	0.0226	0.4	873 (1920)	1423 (3130)

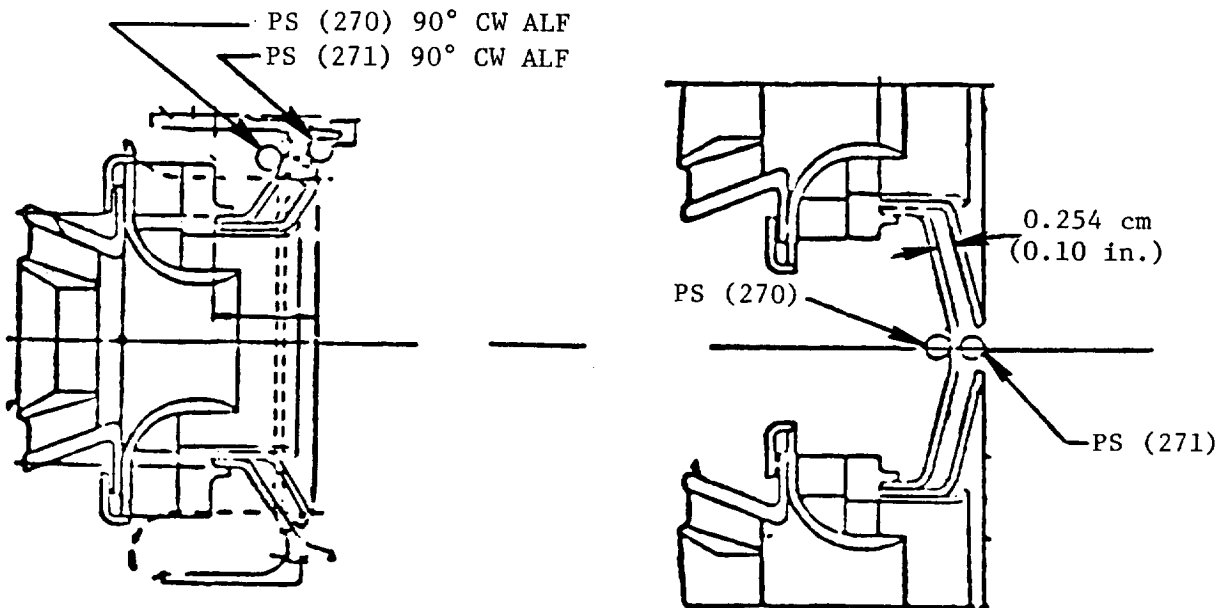
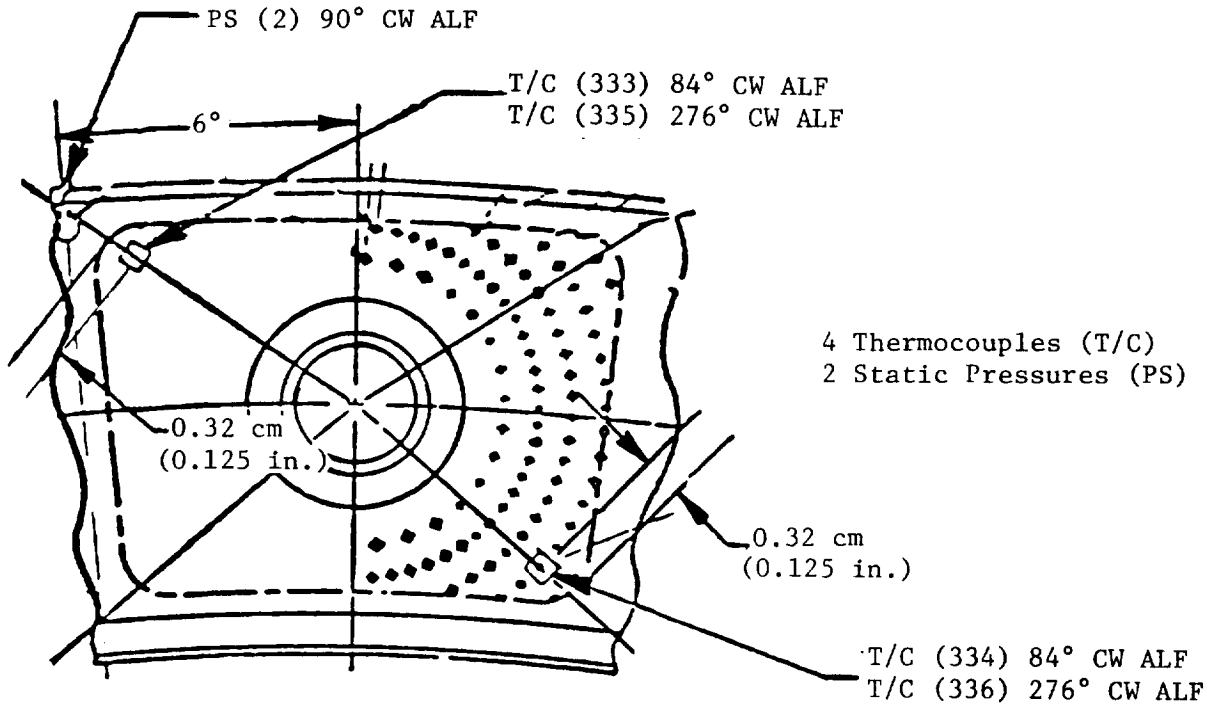
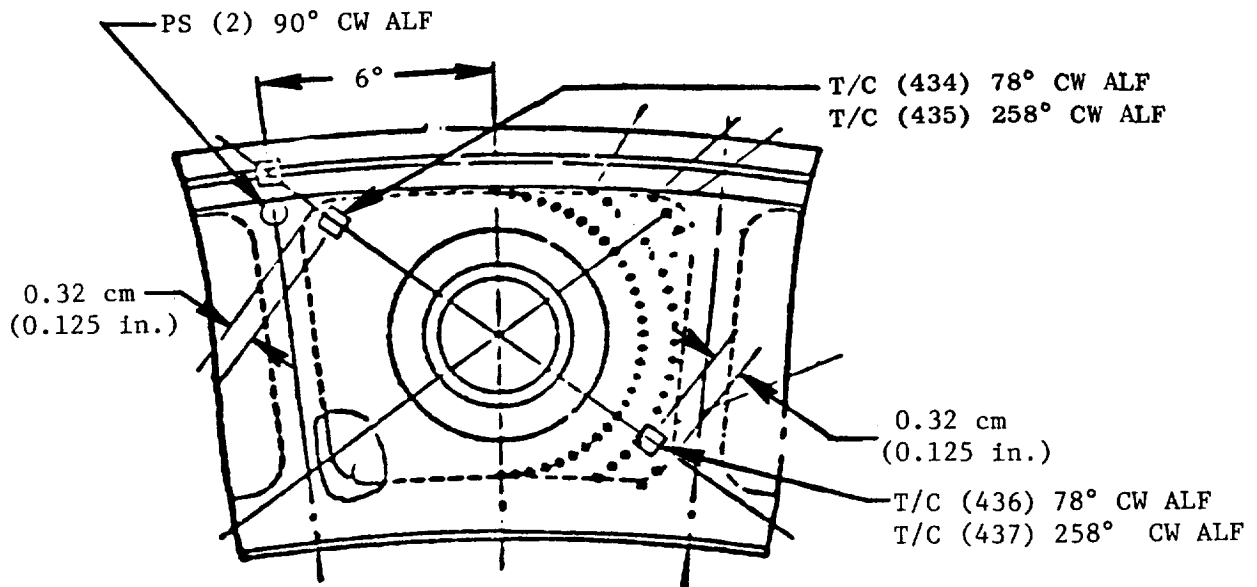


Figure 173. Mod I Combustor Instrumentation Layout.

ORIGINAL PAGE IS
OF POOR QUALITY



4 Thermocouples (T/C)
2 Static Pressures (PS)

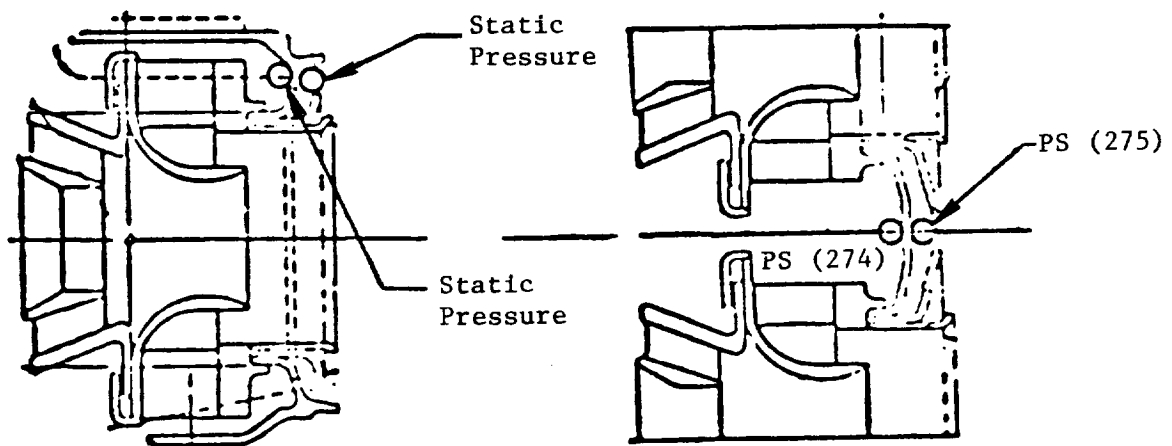


Figure 174. Mod I Combustor Instrumentation Layout.

ORIGINAL
OF FIGURE 175

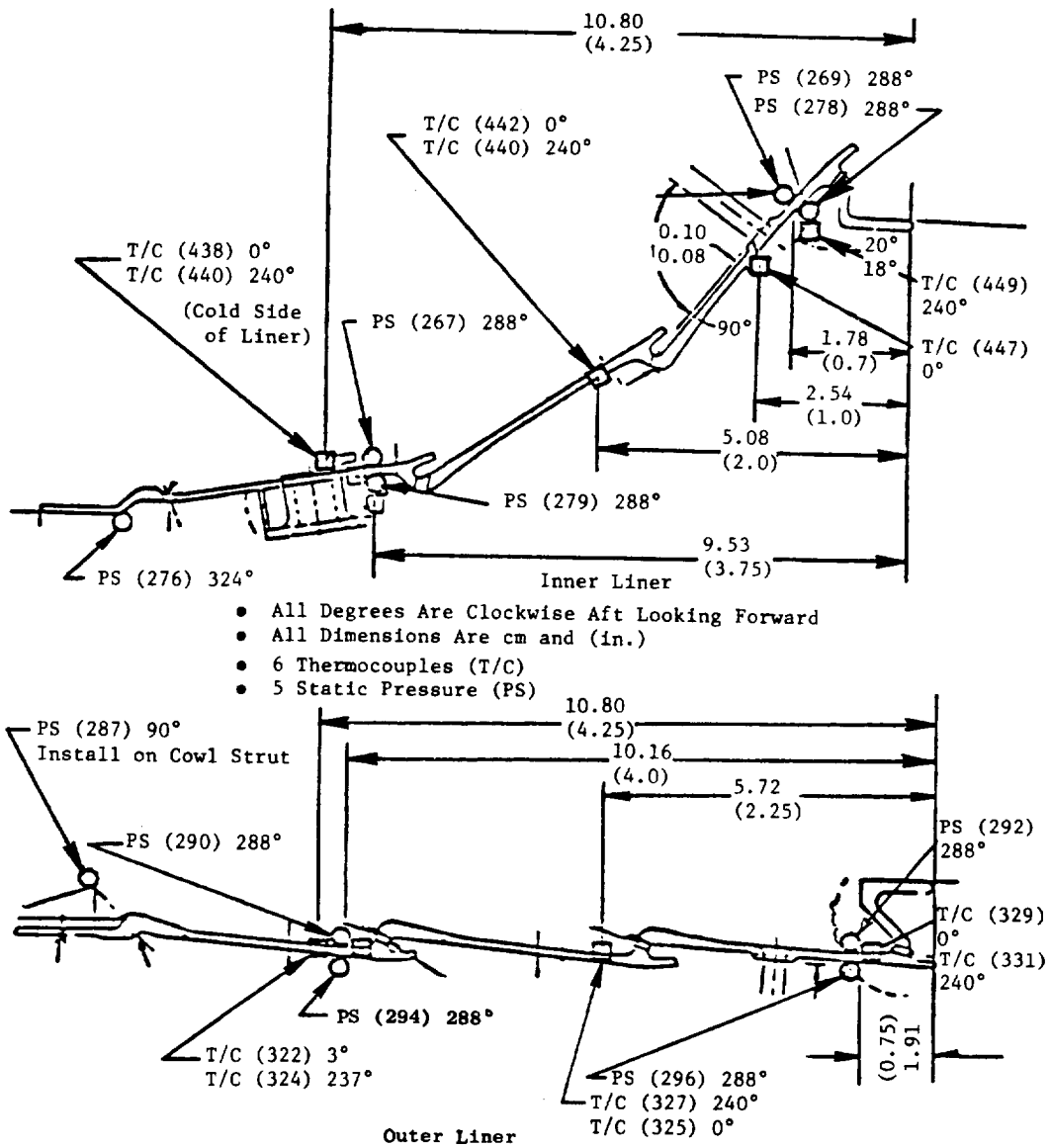


Figure 175. Mod I Combustor Instrumentation Layout.

ORIGINAL PAGE 19
OF POOR QUALITY

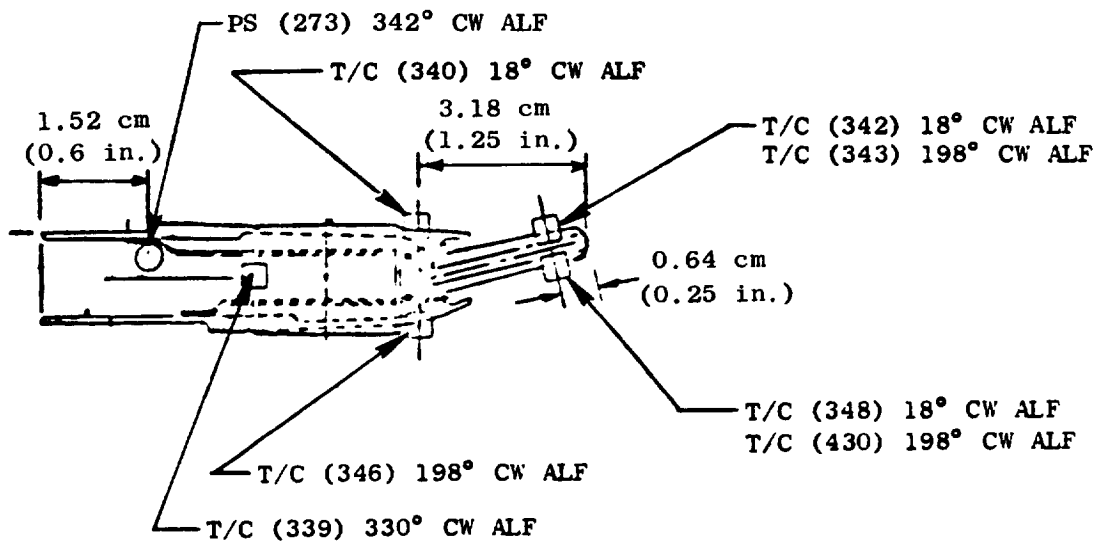


Figure 176. Mod I Combustor Instrumentation Layout.

ORIGINAL PAGE IS
OF POOR QUALITY

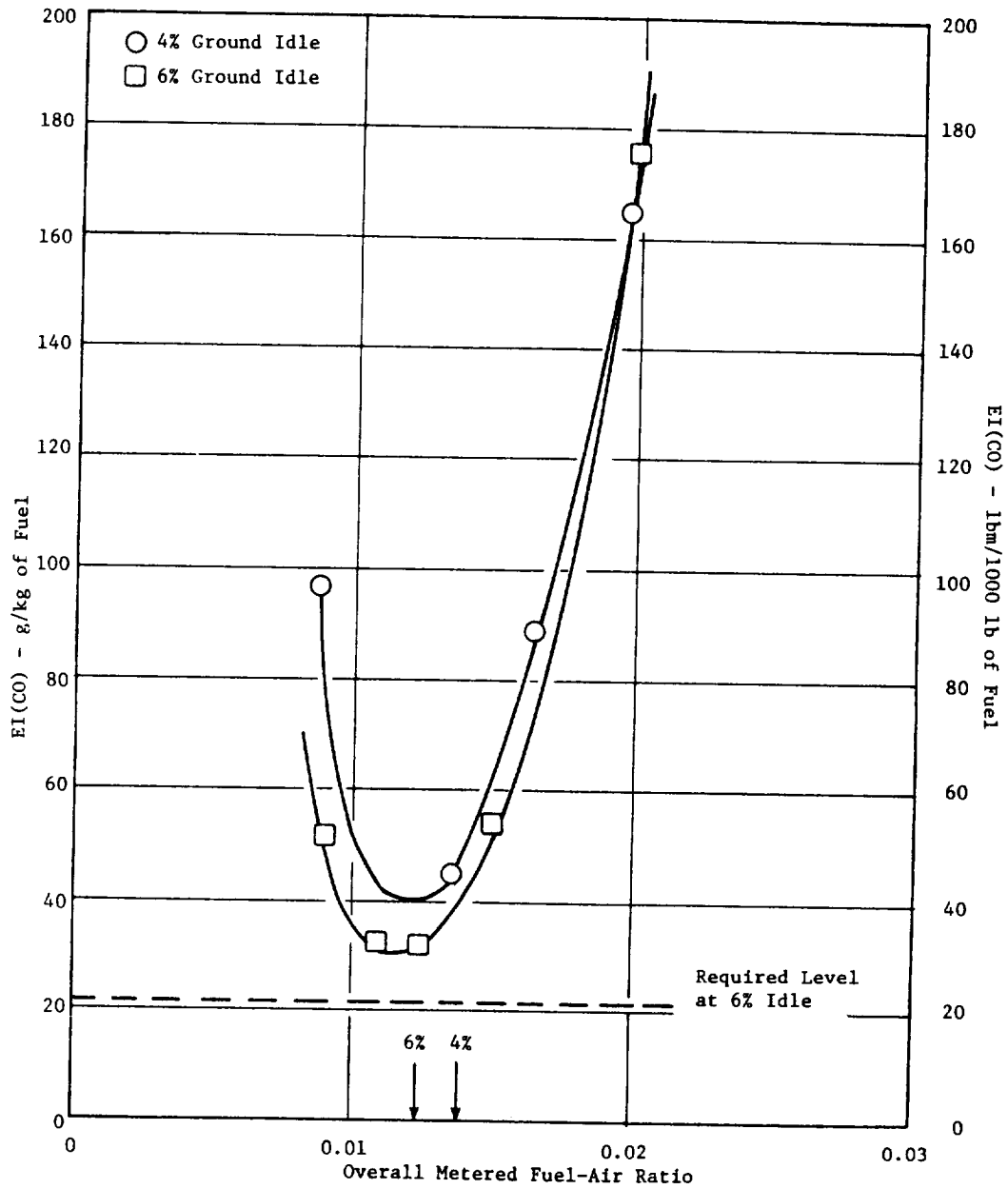


Figure 177. Mod I Emissions Test Results.

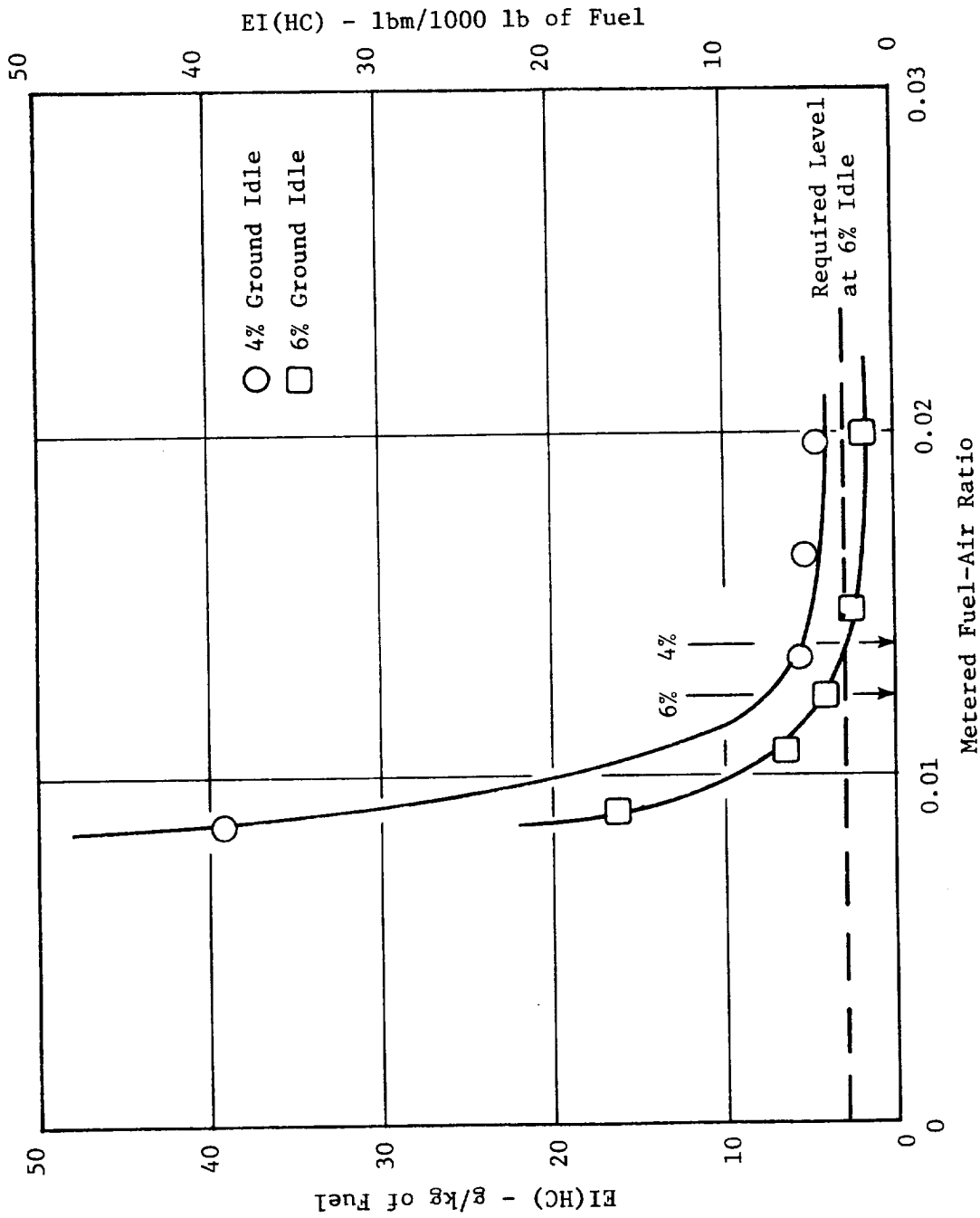


Figure 178. Mod I Emissions Test Results.

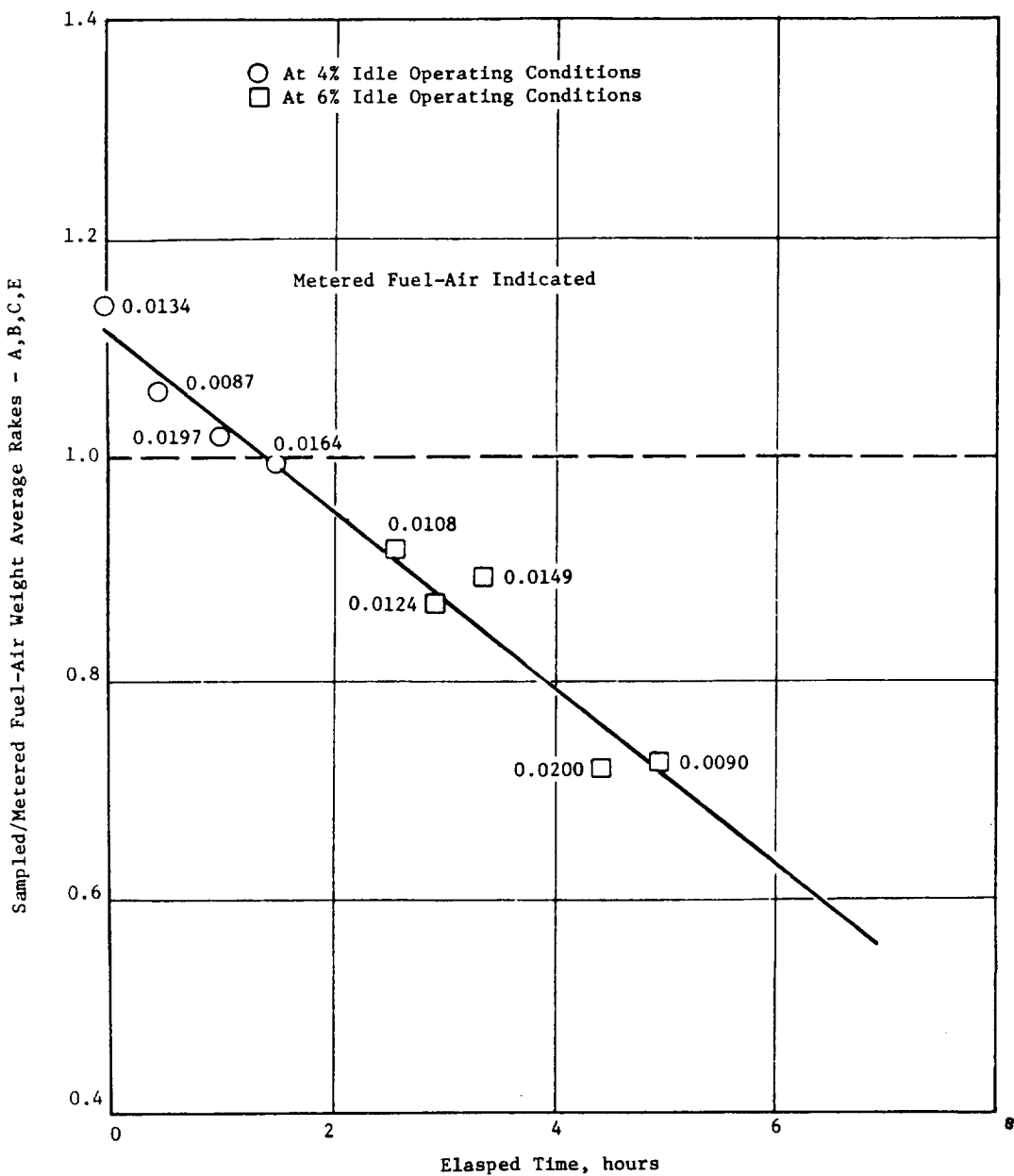


Figure 179. Mod I Emissions Test Results.

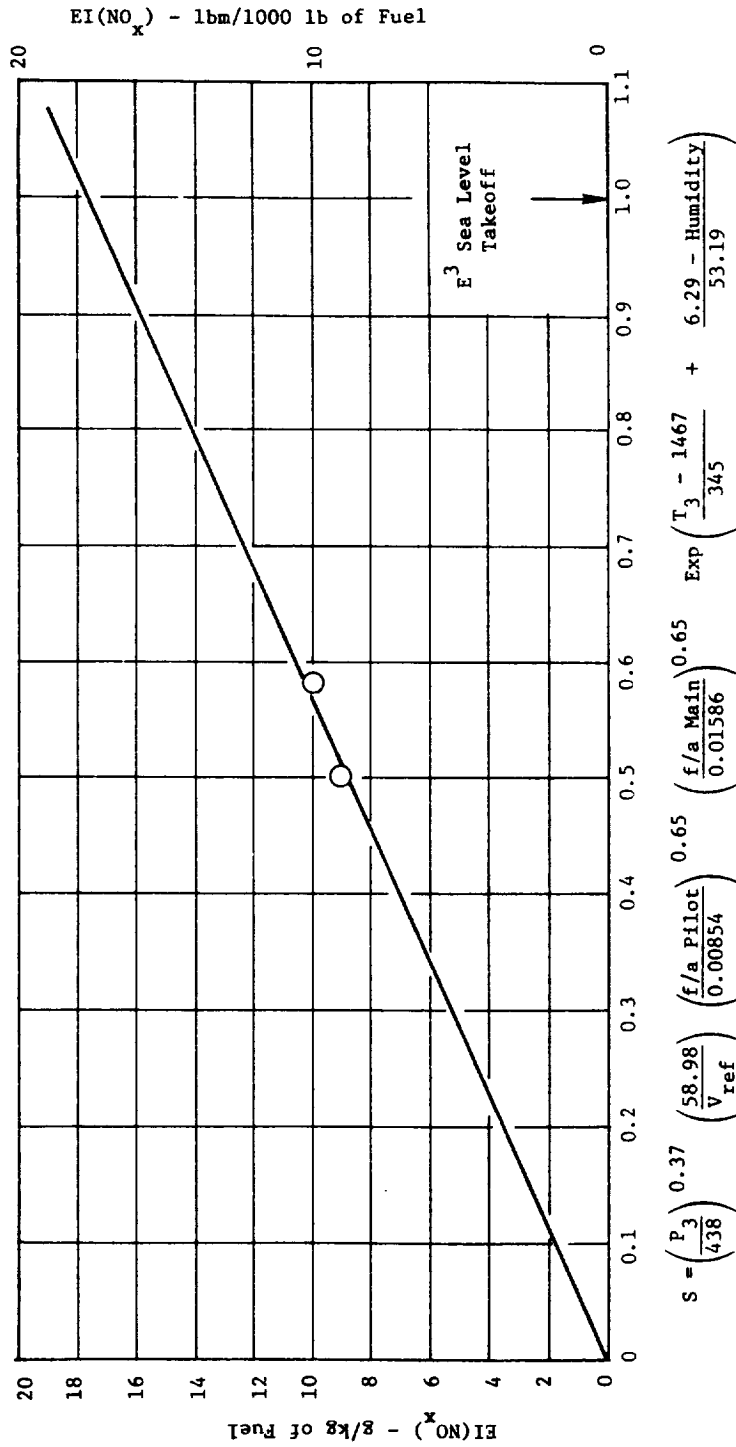


Figure 180. Mod I Emissions Test Results.

the 6% ground idle operating condition would satisfy the E³ Program CO emission goal. Hydrocarbon emission levels of 5.5 g/kg (5.5 lb/1000 lb) of fuel and 4.0 g/kg (4.0 lb/1000 lb) of fuel were obtained, respectively, at the 4% and 6% ground idle design cycle operating conditions. Levels of 36 g/kg (36 lb/1000 lb) of fuel and 22.5 g/kg (22.5 lb/1000 lb) of fuel were demonstrated during evaluation of the Baseline configuration. An HC emission index of 3.0 g/kg (3.0 lb/1000 lb) of fuel has been estimated as the required level at 6% ground idle to satisfy the program HC emission goal. Hydrocarbon levels at or below this target goal were demonstrated at 6% ground idle operating conditions at metered overall fuel-air ratios greater than 0.014.

Prior to testing, each element of the five gas sampling rakes was flowed to determine if all elements of each rake were open and flowing freely. The results of this check indicated that, in general, the flow from the elements of each rake were unbalanced. Elements sampling the inner region of the combustor exit annulus flowed more than those in the outer region. Attempts were made to clear restrictions in the elements and obtain better uniformity. Although these efforts improved the situation, partial restrictions remained in some outer elements of the rakes. During the low power emissions testing, gas sampling problems were experienced. It was evident that as time progressed, the sampling problem became more severe, as illustrated in Figure 179. By the conclusion of the low power emissions testing one rake became almost totally restricted, while the others obtained samples which biased the unfueled inner annulus region. This problem lends suspicion to the quality of the emissions data obtained.

Time restrictions and facility related problems experienced during the high power emissions evaluation prevented the acquisition of data at 30% approach operating conditions. While attempting to establish the simulated SLTO operating conditions, indications of excessively high centerbody metal temperatures were observed. It was decided to obtain emissions and performance data at the combustor operating conditions existing at the time and not continue the test in order to prevent possible damage to the combustor hardware. These combustor operating conditions were not representative of the E³ FPS design cycle. NO_x emission data obtained at these conditions were

plotted against the E³ design cycle severity parameter. This yields a linear relation that can be used for extrapolating to the high-power opportunity conditions. The resulting NO_x emission characteristics shown in Figure 181 yield a NO_x emission index of 17.7 g/kg (17.7 lb/1000 lb) of fuel at the E³ SLTO condition. This is nearly identical to the NO_x emissions levels obtained with the Baseline configuration. At the SLTO condition, a NO_x emission level of 17.5 g/kg (17.5 lb/1000 lb) of fuel had been estimated as required to satisfy the E³ Program NO_x emission goal. Unfortunately, at the high power condition evaluated, additional fuel splits could not be evaluated. Thus, insufficient data was obtained to determine what fuel split would produce the lowest NO_x emission level.

Prior to conducting the high-power emissions test, the gas sampling rakes were flow checked and cleansed out as much as possible. As before, this procedure failed to achieve a satisfactory rake element flow distribution. Thus, emissions data obtained at the high power conditions reflected similar sampling problems as experienced during low power emissions testing. At the conclusion of the high power emissions testing, it was observed that two outer elements of one gas sampling rake and a single outer element of another rake had been burned away. This problem was determined to be related to insufficient water cooling caused by setting water pressure levels too low for the size water hose used in the test rig instrumentation spool.

EPA parameter numbers, based on the EPA landing/takeoff cycle, for CO, HC, and NO_x were generated for combustor operation at 6% ground idle, and pilot only at approach. Because of the lack of data at the approach and climb operating conditions, results obtained with the Baseline combustor configuration at these conditions were used. These EPAP results are compared against those determined for the Baseline configuration and the E³ Program goals in Table XL. This table shows that significant improvements in CO and HC emissions were achieved compared to the Baseline configuration. Carbon monoxide and HC emissions closely approached their respective goals. The NO_x emissions levels demonstrated would meet the goal.

Table XL. Mod I Combustor EPAP Results.

- 6% Ground Idle
- Pilot Only at Approach
- Jet A Fuel
- FPS Design Cycle

<u>CO</u>	EPAP		
	<u>HC</u>	<u>NO_x</u>	
4.55	0.57	2.81	Mod I
8.22	3.10	2.81	Baseline
3.0	0.40	3.0	E ³ Program Goals

At the 6% ground idle design cycle operating condition, data from pressure taps located in the diffuser section of the test rig were used to calculate total pressure losses, thus providing a measurement of the performance of the split duct diffuser. An insufficient amount of usable data was obtained at the high power condition to make an assessment of the diffuser performance at these test conditions. Total and static pressures upstream of the diffuser inlet were used to calculate the velocity profile in the test rig passage at the inlet of the diffuser. This profile in the form of the local-to-average Mach number ratio is shown in Figure 181. The profile is flat, peaked only 1.6% above average and slightly inward from the center of the passage. Calculated diffuser total pressure losses are presented in Table XLI. These values are compared with losses calculated from measured data obtained from evaluation of the Baseline combustor configuration at simulated SLTO operating conditions, and to losses measured in the full-annular diffuser model subcomponent tests with a flat inlet velocity profile and passage flow splits similar to those calculated for the Mod I combustion system. In general, the test rig diffuser performance calculated from the Mod I test data agrees well with the performance calculated for the Baseline combustor test and the diffuser model test. However, the Mod I data shows a sharp increase in the inner dome loss. This was most probably due to instrumentation problems. Due to damaged instrumentation, pressure losses for the centerbody and the outer dome flow streams could not be determined.

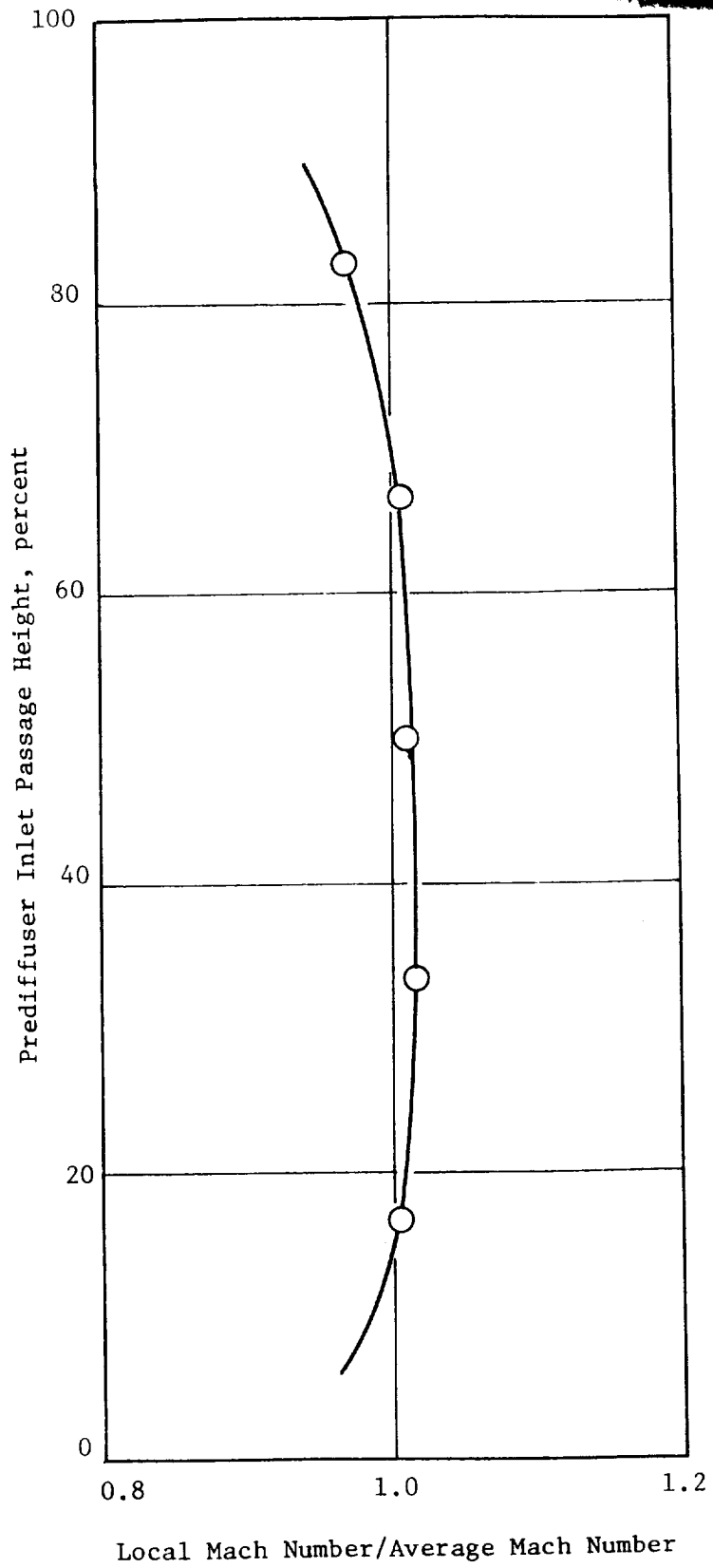


Figure 181. Diffuser Inlet Mach Number Profile (Mod I Test).

Table XLI. Calculated Diffuser Performance for Mod I Test.

	<u>Mod I Configuration</u>	<u>Baseline Configuration</u>	<u>Diffuser Test Flat Profile</u>
Total Outer	3.78	3.69	4.04
Total Inner	3.14	2.78	3.05
Centerbody	No Data	2.30	2.77
Outer Dome	No Data	2.53	1.16
Inner Dome	2.57	1.72	1.47

Measured overall combustor pressure drops and main stage dome pressure drops were plotted against the square of the combustor inlet flow function parameter along the E³ FPS design cycle operating line in Figure 182. The pilot stage dome pressure drop characteristics could not be obtained because of the damaged upstream pressure instrumentation. At SLTO operating conditions, an overall combustor pressure drop of ~6% is estimated. This compared to a value of 5.5% measured in the baseline combustor test and the engine combustor design value of 5.0%. The measured total combustor flow area of the Mod I configuration was nearly identical to the baseline configuration. The higher than anticipated overall total pressure loss was related to difficulty experienced in obtaining good combustor exit total pressures. Some of the difficulty appeared to be associated with facility hookup problems. Since the gas sampling rakes were used to measure exit total pressure, the sample line restrictions evident during testing also contributed. Pressure drops across the liners were between 2% and 3%. Because of damaged instrumentation, pressure drops across the centerbody structure could not be determined.

Combustor metal temperatures measured during emissions testing are plotted against the combustor inlet temperature in Figures 183 through 192. The locations of these temperatures can be obtained by locating the specific thermocouple item number on the combustor instrument layout presented in Figures 173 through 176. As discussed earlier, excessively high metal temperatures indicated on the centerbody structure contributed to the premature termination of high-power emissions testing. It was later determined that

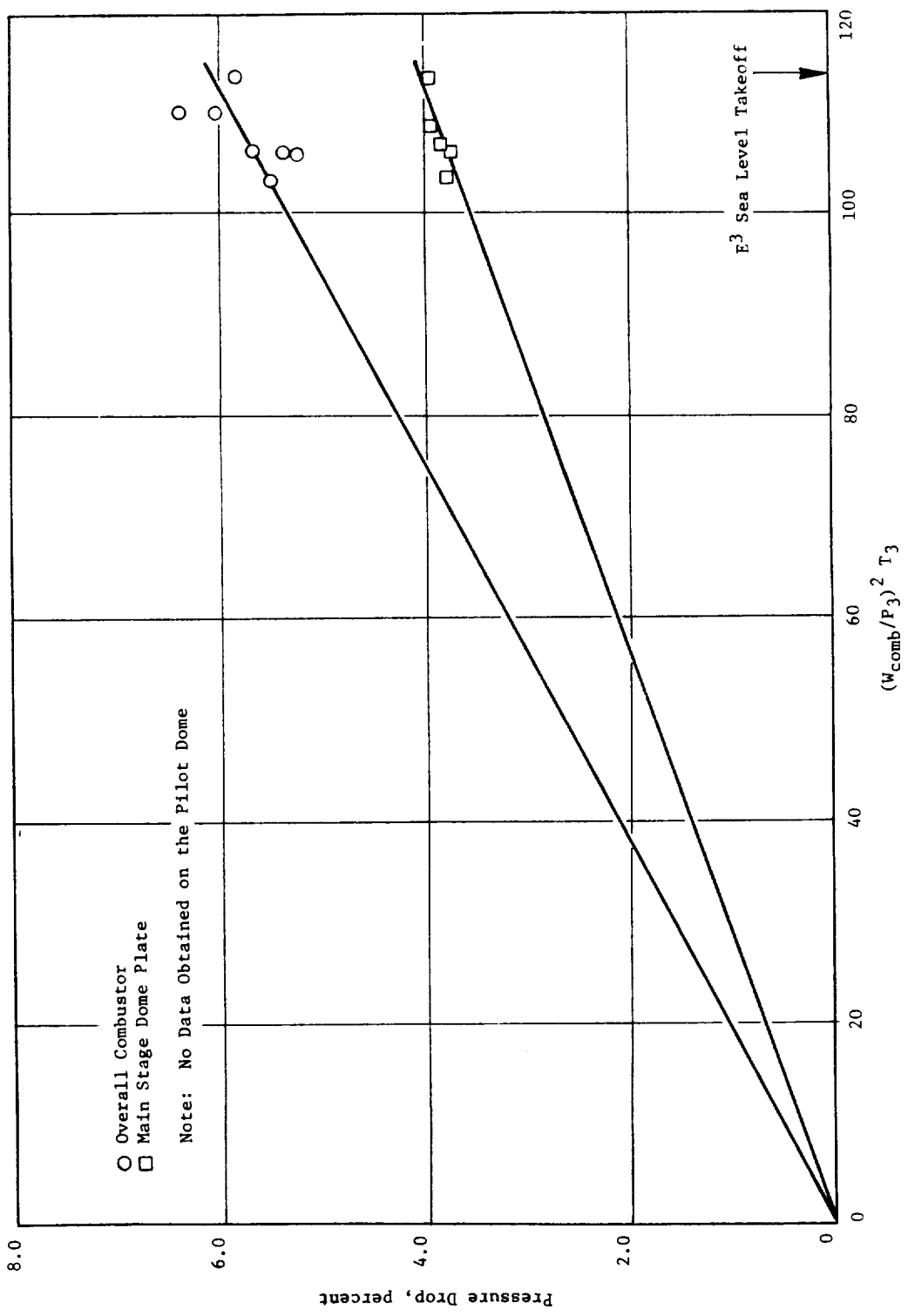


Figure 182. Measured Pressure Losses for Mod I Combustor.

ORIGINAL PAGE IS
OF POOR QUALITY

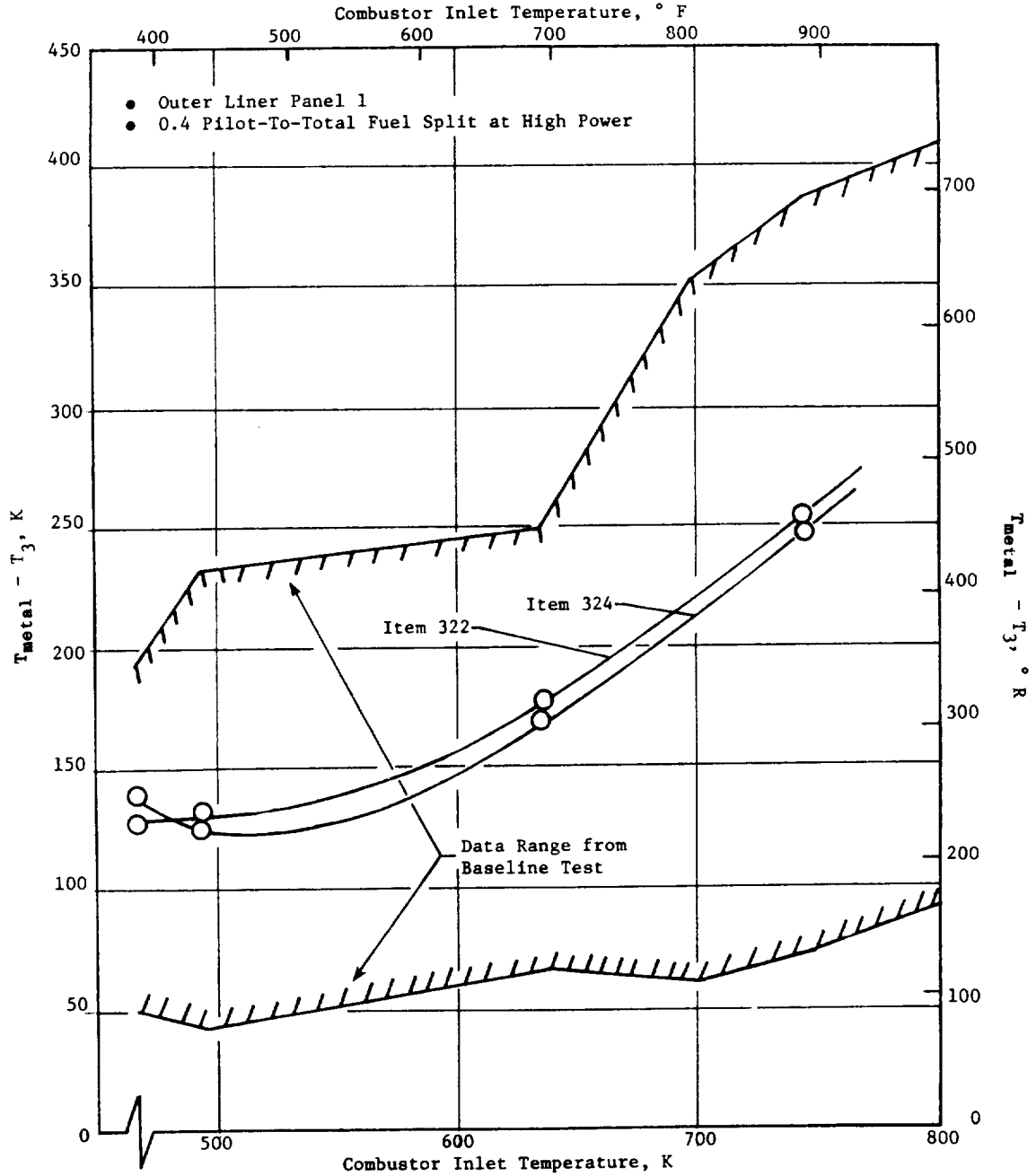


Figure 183. Measured Combustor Metal Temperatures for Mod I Test.

ORIGINAL PAGE IS
OF POOR QUALITY

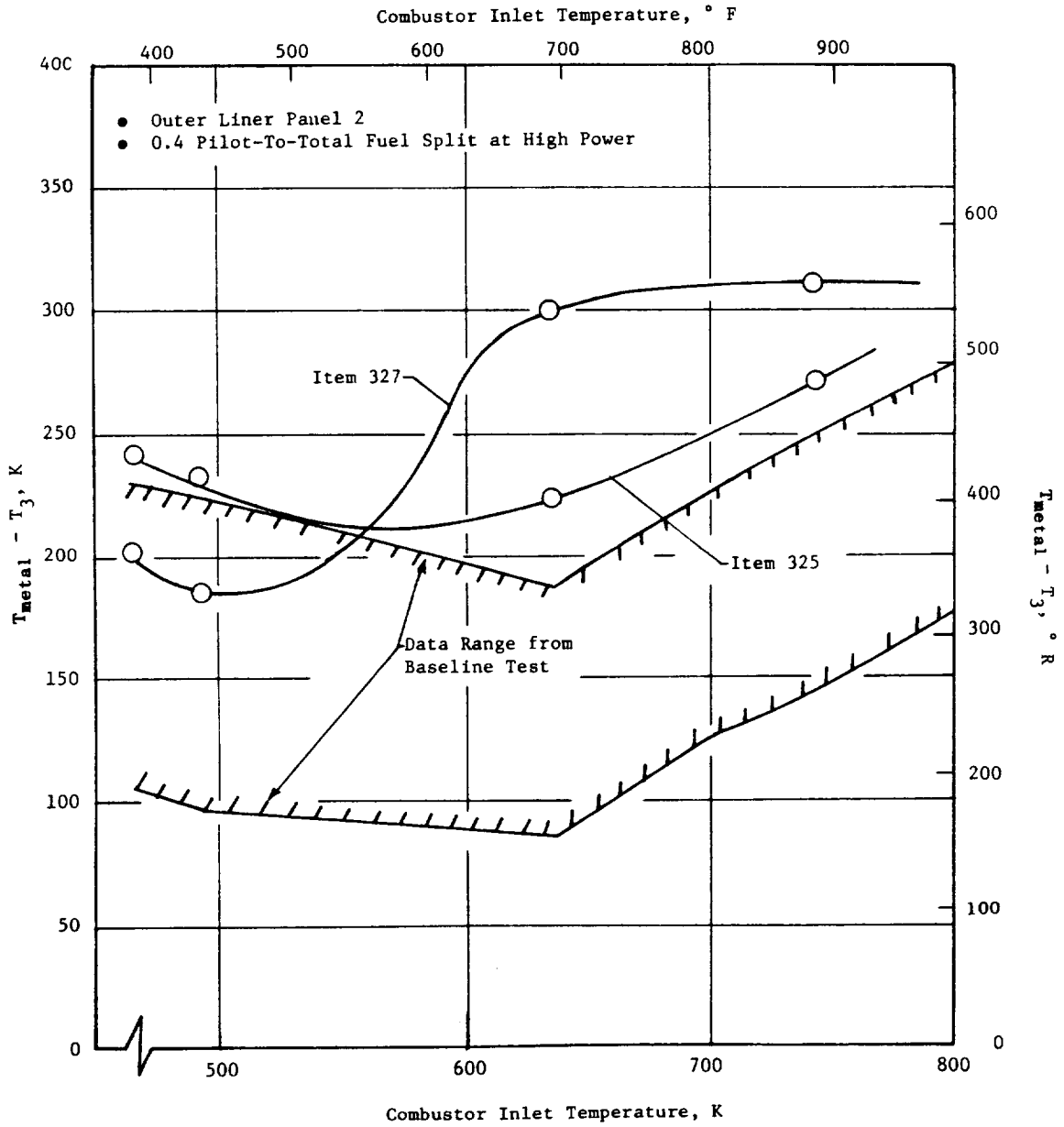


Figure 184. Measured Combustor Metal Temperatures for Mod I Test.

COMBUSTOR METAL TEMPERATURES
 OF LINEAR PANEL 3

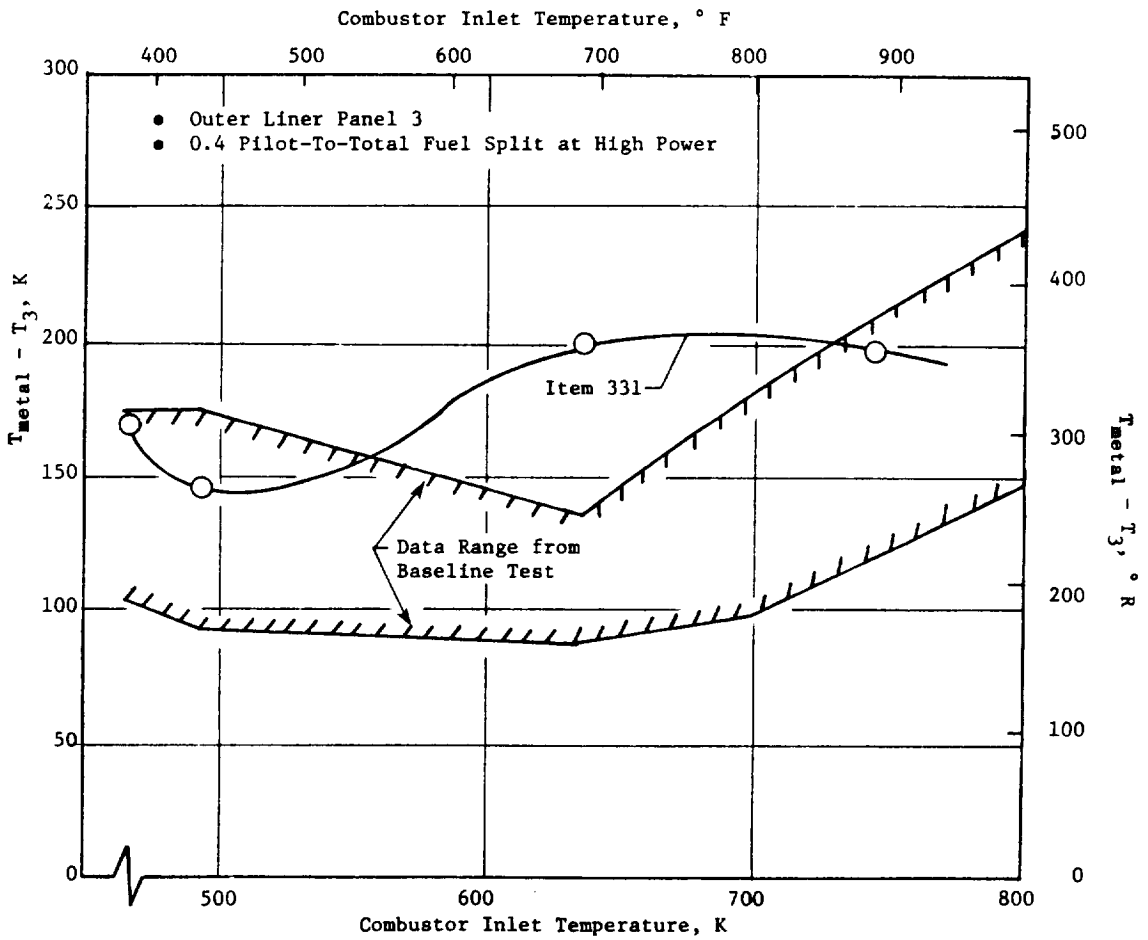


Figure 185. Measured Combustor Metal Temperatures for Mod I Test.

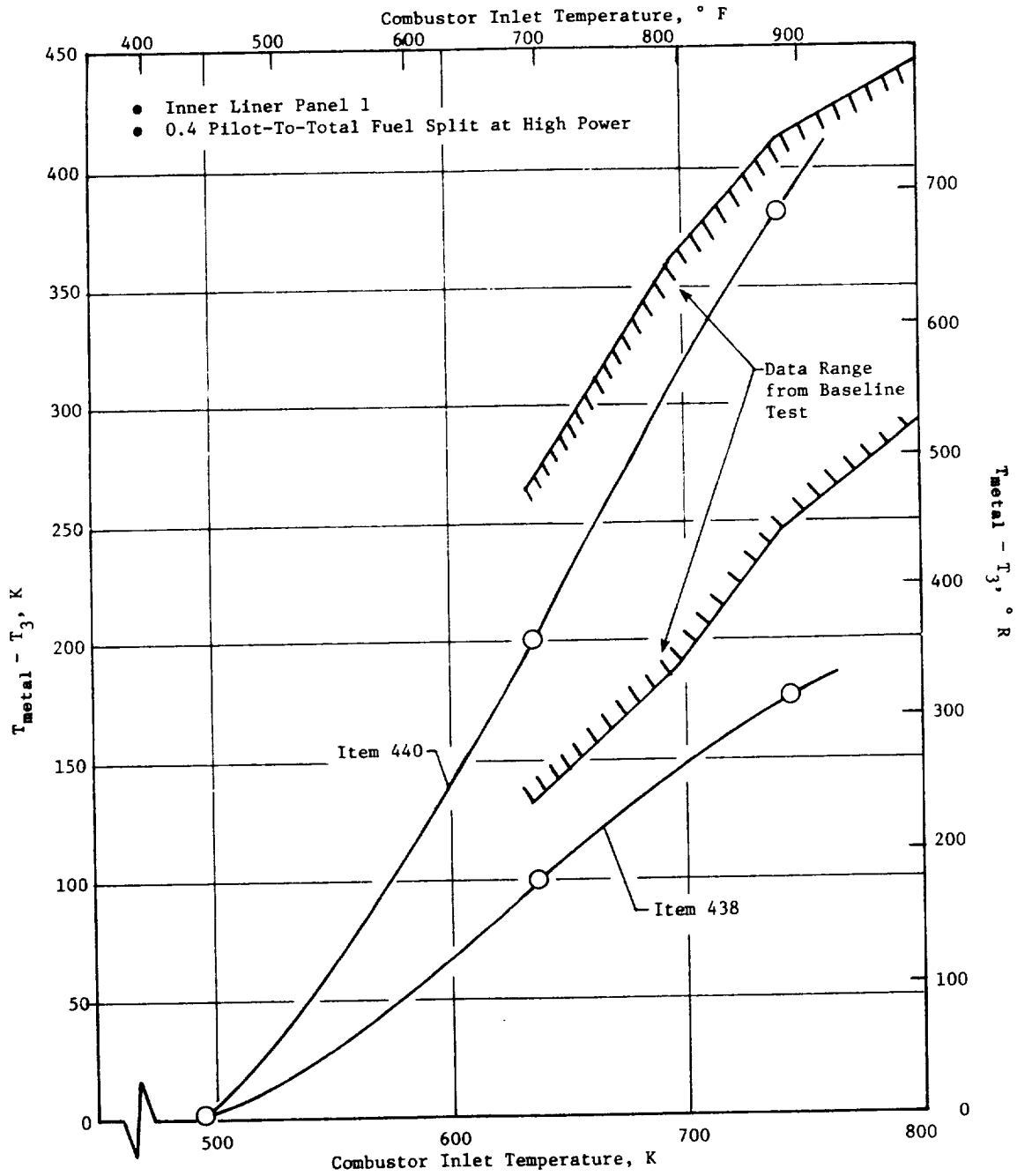


Figure 186. Measured Combustor Metal Temperatures for Mod I Test.

ORIGINAL FIGURE
OF POOR QUALITY

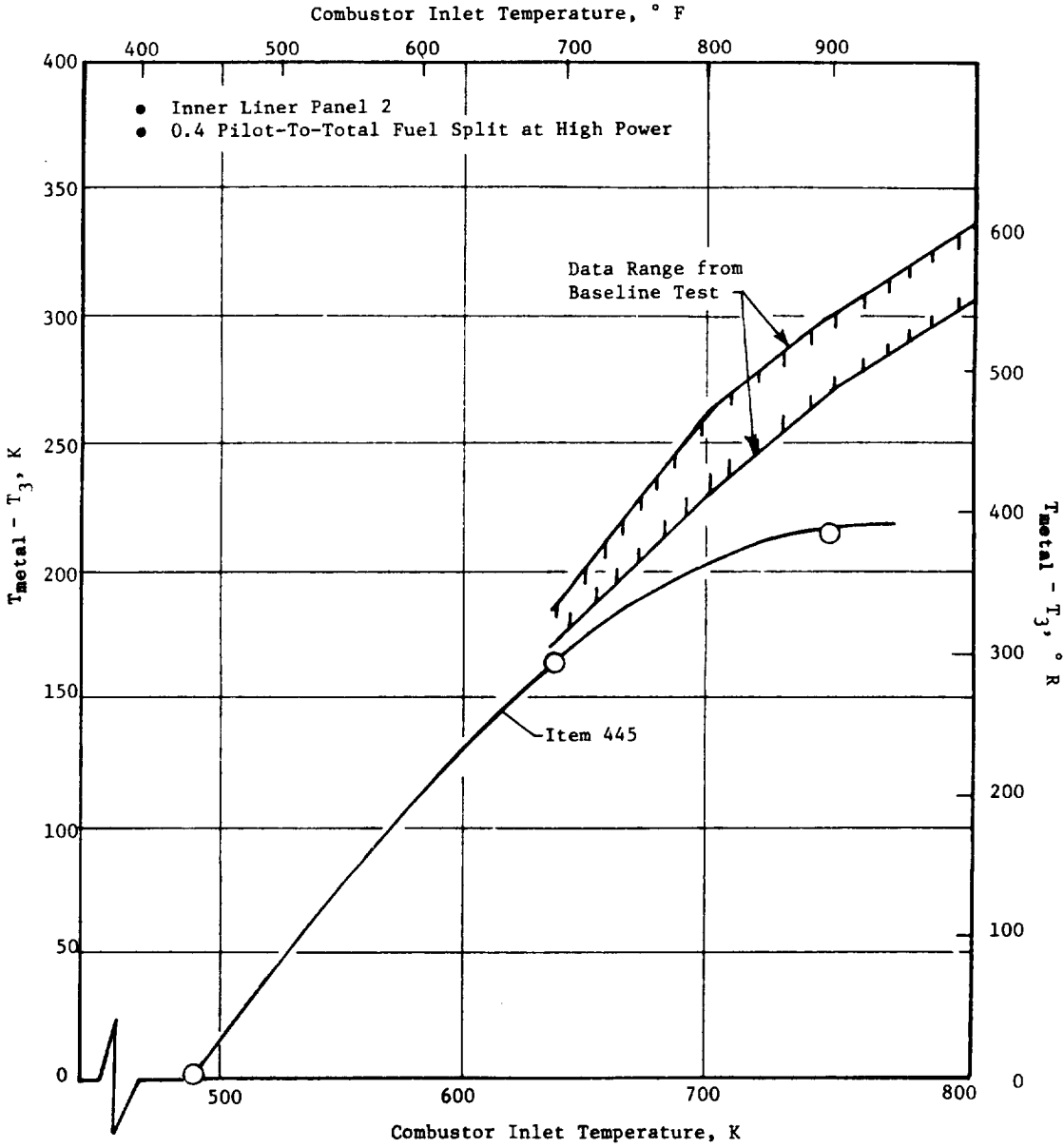


Figure 187. Measured Combustor Metal Temperatures for Mod I Test.

ORIGINAL PAGE IS
OF POOR QUALITY

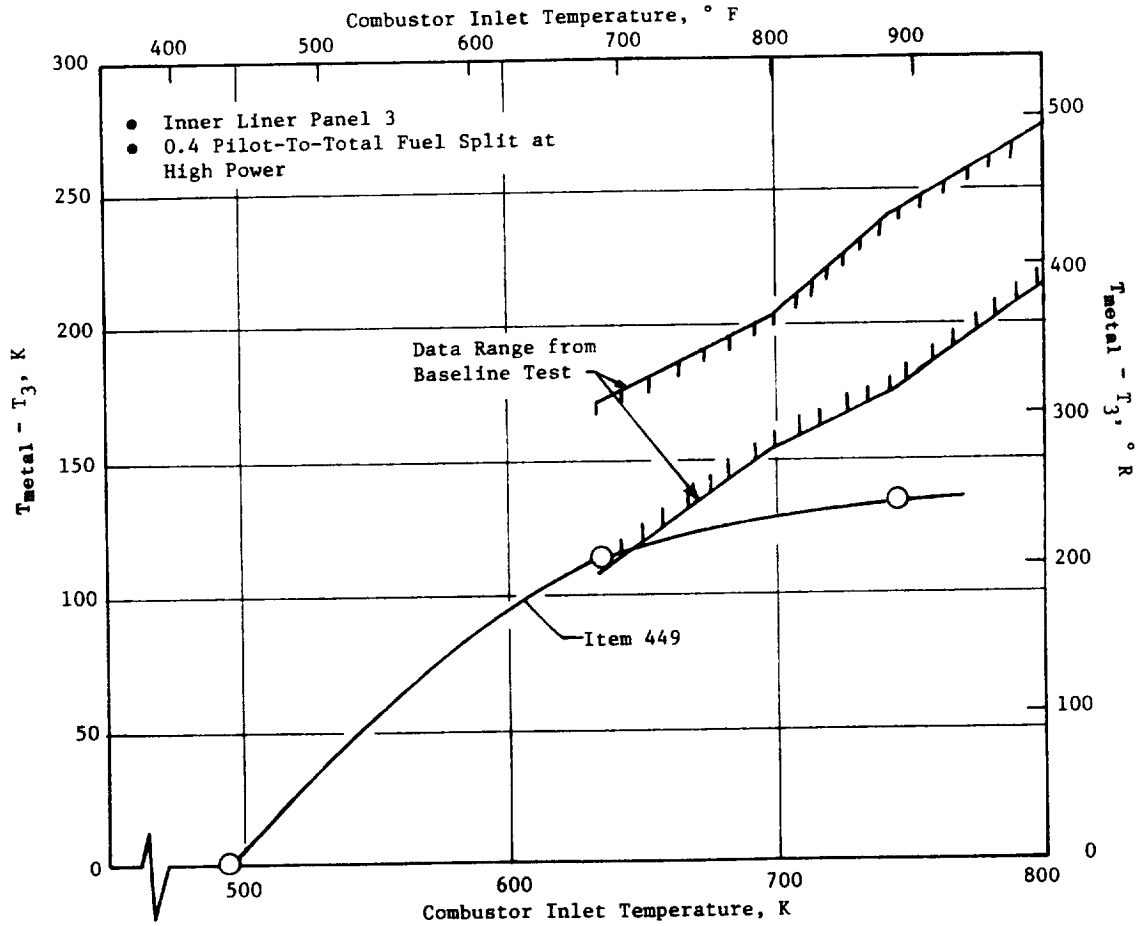


Figure 188. Measured Combustor Metal Temperatures for Mod I Test.

ORIGINAL DOCUMENT
OF POOR QUALITY

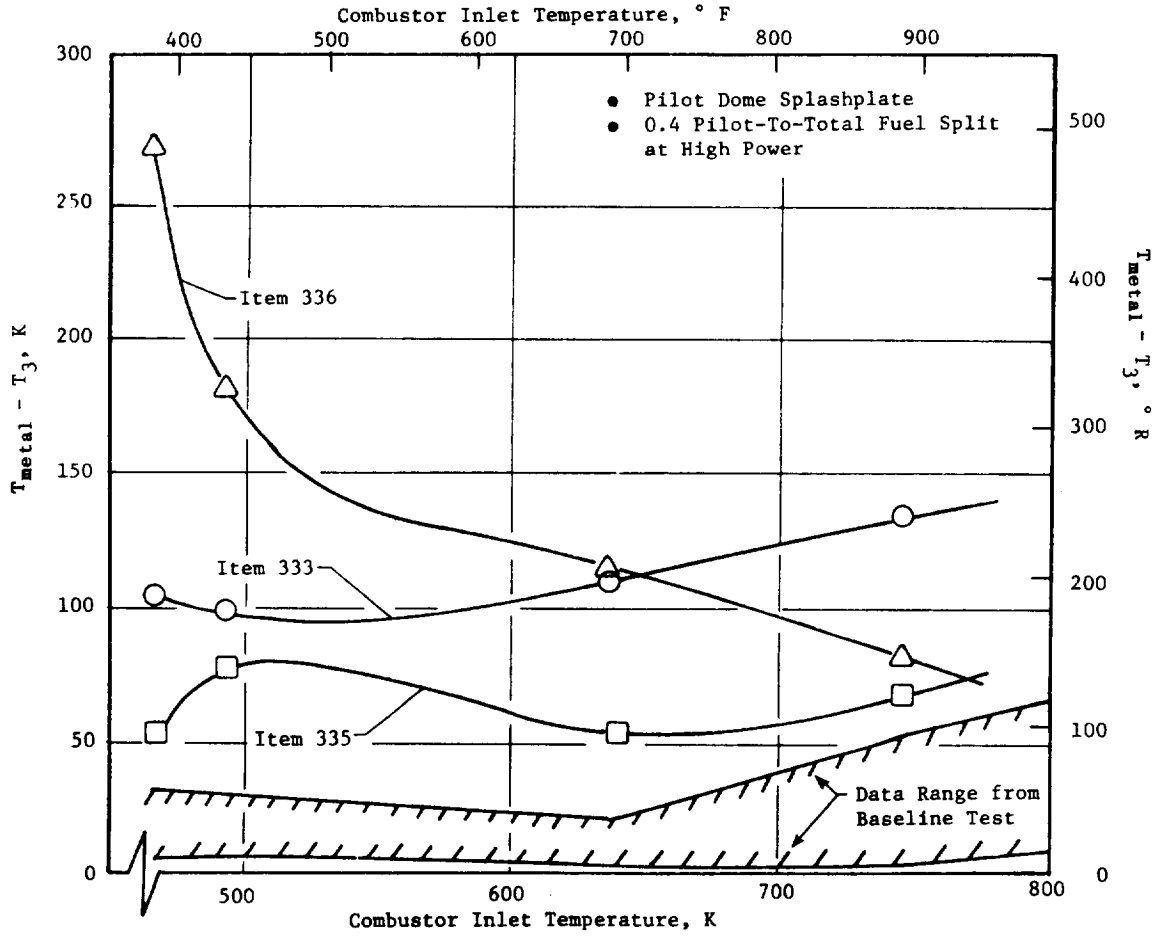


Figure 189. Measured Combustor Metal Temperatures for Mod I Test.

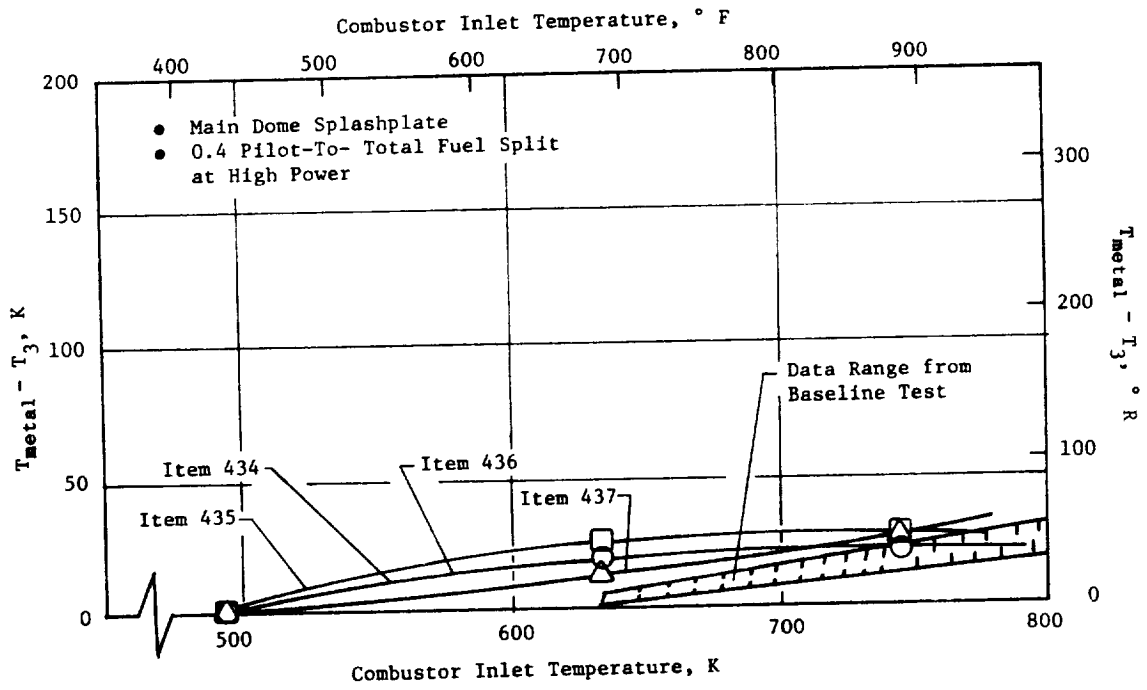


Figure 190. Measured Combustor Metal Temperatures for Mod I Test.

ORIGINAL PAGE IS
OF POOR QUALITY

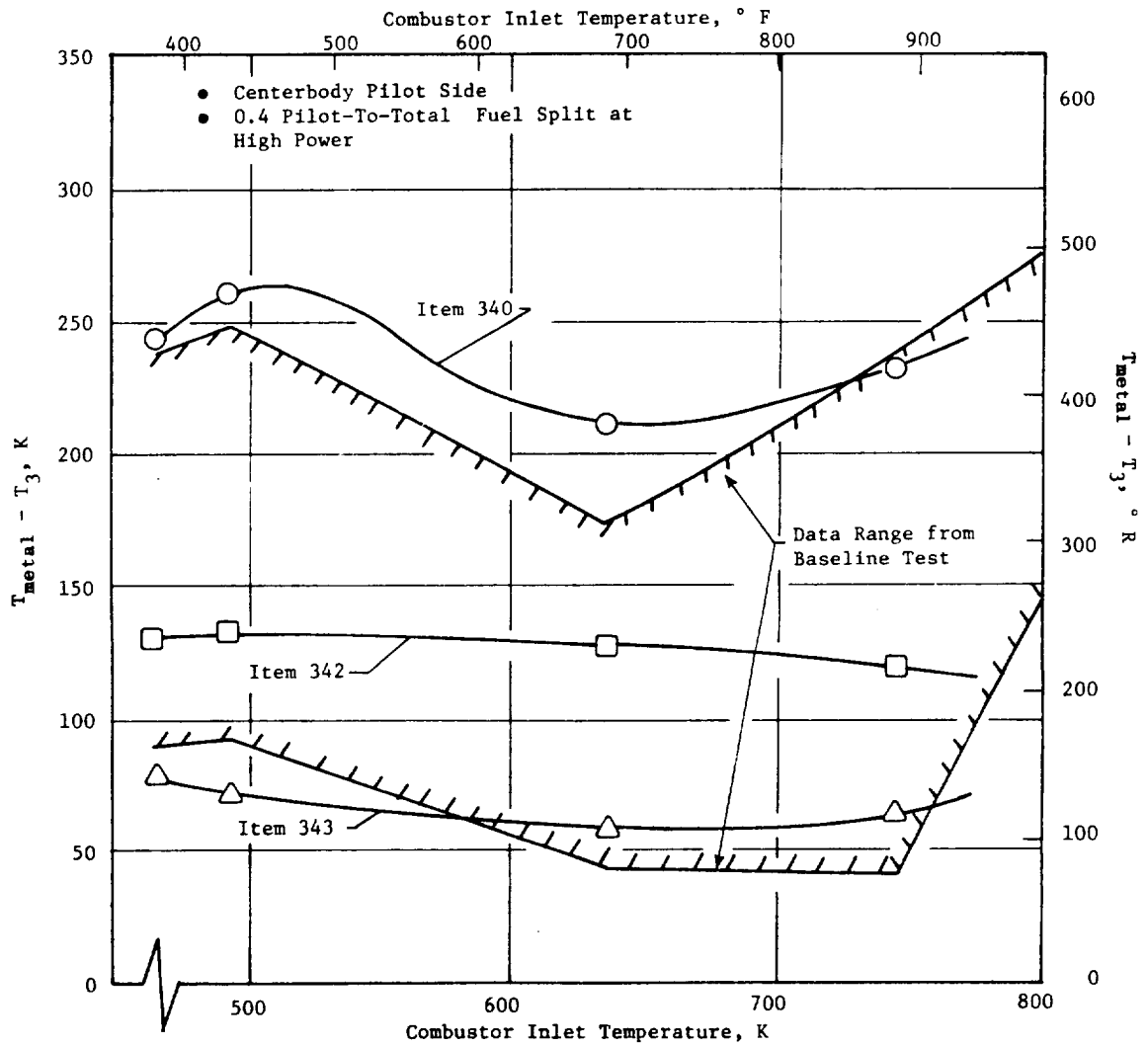


Figure 191. Measured Combustor Metal Temperatures for Mod I Test.

ORIGINAL PAGE IS
OF POOR QUALITY

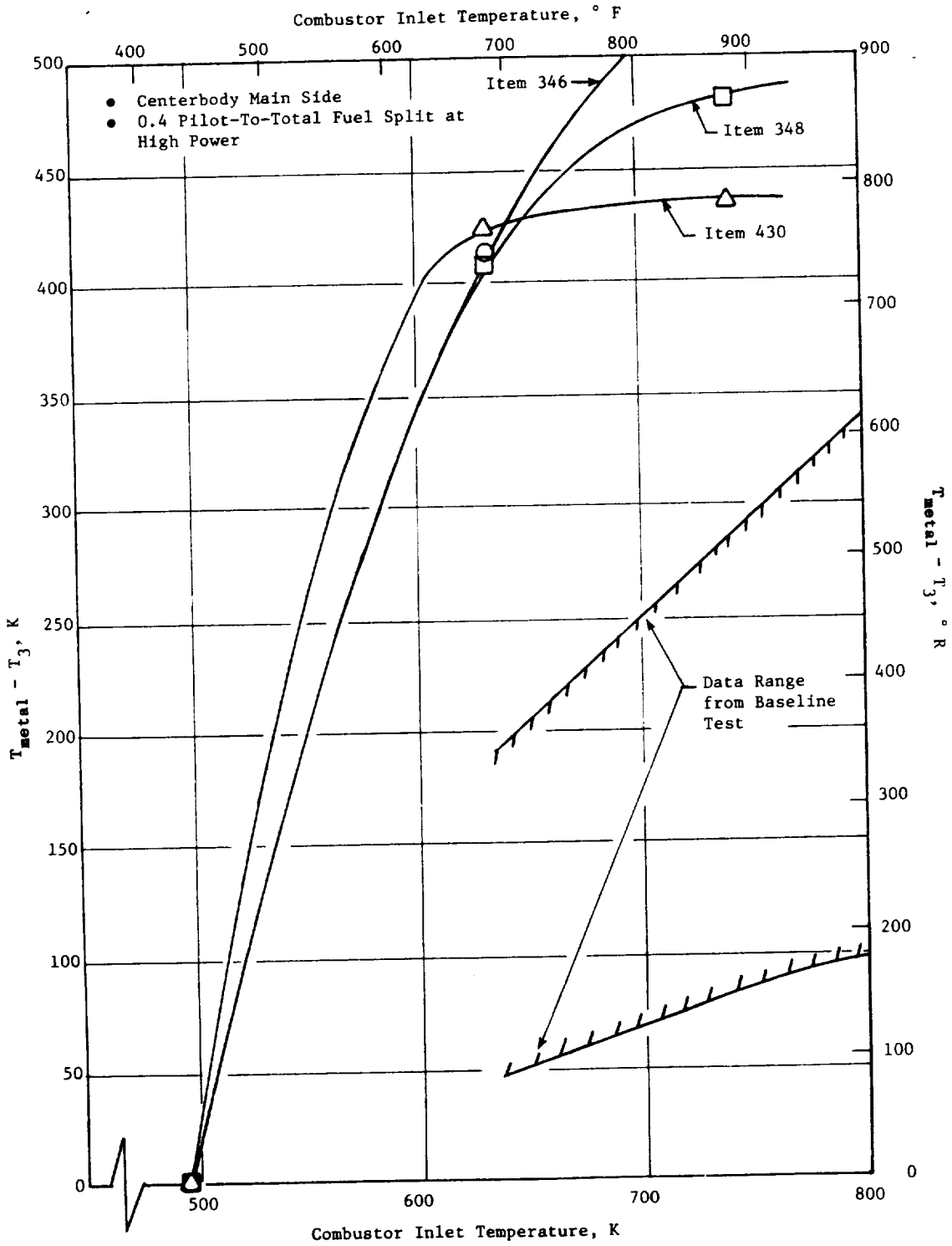


Figure 192. Measured Combustor Metal Temperatures for Mod I Test.

five of the six thermocouples located on the centerbody had secondary junctions exposed to the hot gas stream. Thus, the validity of indicated temperatures from these thermocouples is highly questionable. This is supported by detailed inspection of the centerbody hardware, which revealed no indication of high metal temperatures. Thermocouple Item 340 on the pilot side of the centerbody had no indication of secondary junctions. Pilot dome splash plate temperatures 139 K (250° F) above the combustor inlet temperature were indicated, an increase of approximately 83 K (150° F) over temperatures measured on the Baseline combustor configuration. This change was less than anticipated based on the large reduction in the pilot stage splash plate cooling flow featured in the Mod I combustor configuration. With the exception of outer liner Panel 2, indicated liner metal temperatures generally decreased, compared to the baseline levels. The decrease was more substantial along the inner liner. It is interesting to note that the highest indicated metal temperature along the inner liner was located across from a pilot-to-main stage crossfire tube. This same area on the inner liner was the hottest spot indicated along the inner liner in the Baseline combustor evaluation. No explanation linking the hot-spot location with the crossfire tube was established.

7.4.4 Concluding Remarks

The results of evaluating the Mod I development combustor showed significant reductions in ground idle emissions levels with little effect on the high power NO_x emissions level. Significant improvements in pilot stage ground start ignition characteristics, as well as exit temperature performance, were also demonstrated. However, further improvements in all of these performance areas were necessary to evolve a combustor design capable of demonstrating all of the combustion system goals for the E³. A major problem identified involved the poor ignition and propagation characteristics of the main stage. Substantial improvement would be required to achieve main stage crossfire and propagation during ground start operation, within the fuel schedule defined in the E³ (9/79) ground start cycle.

To address the improvement needs identified, attention was directed to defining further combustor design modifications. These modifications included: redistributing the air in the pilot stage primary zone to provide further

reductions in ground idle emissions; significantly enriching the main stage primary zone to provide better ignition and propagation; and additional main stage trim dilution to further improve the exit temperature performance. In addition, increased cooling flow would be supplied to the centerbody structure as a precaution against exceeding metal temperature limitations.

7.5 MOD II AND MOD III DEVELOPMENT COMBUSTOR TEST RESULTS

Engine starting studies were performed by Systems Engineering using the existing E³ engine cycle model and the E³ 9/79 ground start operating cycle. The fuel schedule generated from these studies along with combustor exit gas temperature profiles measured in the pilot-only mode of operation were used as inputs to conduct a heat transfer analysis of the high pressure and low pressure turbine systems. The results of this analysis indicated that high combustor fuel-air ratios along with sharply outward peaked temperature profiles associated with pilot-only operation along the 9/79 ground start operating line combined to produce excessively high blade metal temperatures in both the high pressure and low pressure turbine systems. To reduce the effects of these high gas temperatures in the subidle region, it was decided to start the E³ engine with both domes of the combustor burning. The original design intent of the combustor main stage dome was to provide a lean primary zone with high velocities and low residence times to reduce high-power pollutant emissions such as NO_x.

However, the high dome velocity, couples with the small dome height of the original main stage configuration, adversely affected the ignition capability, particularly in the very severe ignition environment associated with operation in the subidle region. To enhance the ignition performance of the main stage dome at ground start conditions, various hardware modifications were evaluated in several development combustor configurations.

In the Mod IIA combustor configuration, the pilot stage swirl cup airflow was decreased by reducing the area of the secondary swirler. The pilot stage primary dilution was increased to a level similar to the baseline configuration. Outer liner Ring No. 1 cooling flow was reduced by closing off every fifth cooling hole in both the outer liner cooling Ring No. 1 and the pilot

dome outer cooling ring. Both features feed the first cooling slot. The pilot side centerbody forward cooling flow was increased by enlargement of the cooling holes. Main stage swirl cup airflow was decreased by significantly reducing the secondary swirler area. The main stage primary dilution was increased $\sim 4\% W_c$ by increasing the thimble hole diameter. The main side centerbody forward cooling flow level was increased by enlargement of the cooling holes. Inner liner Panel 2 dilution holes were introduced. The pattern featured 60 holes equally spaced around the circumference directly in-line with and between all swirl cups. In addition to these modifications, the trailing edge of the centerbody structure was shortened by 1.78 cm (0.70 inch). These design modifications were intended to improve idle emissions, improve main stage ignition characteristics, provide better cooling of the centerbody structure, and reduce the trailing edge mass of the centerbody structure. The reduction in the centerbody length was an engine combustor design consideration incorporated into the development combustor.

The Mod IIB combustor configuration modifications involved blocking off all inner liner Panel 2 dilution holes. Observations of the Mod IIA test clearly indicated that the presence of this dilution flow was very detrimental to the main stage ignition.

In the Mod IIIA combustor configuration, the main stage swirl cup airflow was further reduced by blocking off every other primary swirler vane passage. Main stage splash-plate cooling flow was reduced by closing off 46 of 112 holes per splash-plate. The main stage dome outer cooling ring flow was reduced by closing off every other hole in the ring plus six additional holes in line with the crossfire tubes. This provided a sheltered region of 11 consecutive blocked off cooling holes in line with the crossfire tubes. These reductions in main stage dome flow were intended to further enrich the main stage dome, plus reduce the main stage dome velocity to levels similar to those in the pilot stage dome. The outer liner and inner liner aft dilution was increased to maintain the overall combustor pressure drop. The crossfire tubes were replaced with new tubes that featured extended lengths along the upstream surface. The extended length was intended to provide additional shelter for the combustion gases passing through the crossfire tubes allowing them to penetrate deeper into the main stage dome annulus.

In the Mod IIIB configuration, modification involved only blocking off pilot side centerbody forward cooling flow in line with the crossfire tubes. This was to eliminate the film of cooling air that passes over the crossfire tubes, enabling the pilot stage combustion gases to more easily pass through the crossfire tubes onto the main stage annulus. Illustrations of the hardware modifications featured in these four combustor configurations are presented in Figures 193 and 194. Estimated combustor airflow distributions for each configuration can be obtained in Appendix E.

7.5.1 Atmospheric Ground Start Ignition Test

All four combustor configurations were tested for ground start characteristics using nozzle tips rated at 12 kg/hr (26.5 pph) installed in both the pilot and main stage swirl cups. The purpose of this series of tests was to evolve combustor design features that would result in main stage ignition and lean extinction characteristics within the fuel schedule requirements of the E³ 9/79 ground start cycle operating line. To investigate the effect of high combustor airflows on ignition, additional testing was conducted on the Mod IIIB configuration in which combustor airflows were increased 15% and 30% above the cycle level at the 32%, 46%, and 77% corrected core engine speed points. Without heavy bleeding of the compressor, engine combustor airflow levels in the start region could be significantly greater than currently estimated in the ground start cycle. Prediffuser and combustor aft bleed flows were not used in this test series. Test points and corresponding operating conditions are presented in Table XLII.

Test results obtained from ground start ignition evaluation of the Mod IIA combustor configuration are presented in Appendix F. The lightoff characteristics of the pilot stage swirl cup in line with the igniter were similar to the Mod I combustor configuration. Full propagation of the pilot stage was considerably more difficult to achieve. The main stage crossfire and propagation characteristics were very poor. Full main stage propagation was achieved only at the simulated 77% corrected core speed test point. Observations made during the test revealed an unusually strong flow of air passing along the main side of the centerbody trailing edge and penetrating deeply into the

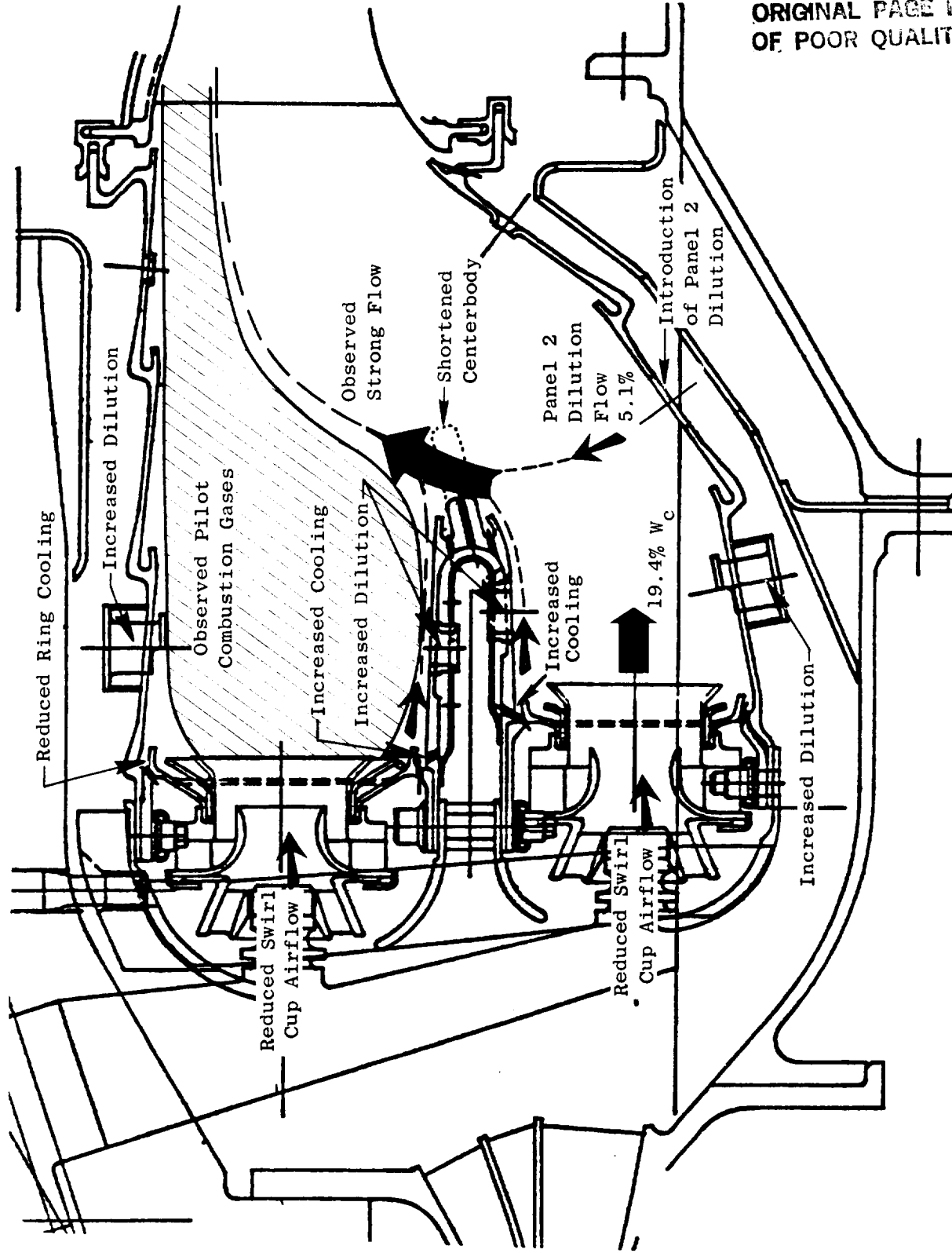


Figure 193. Mod II and Mod III Combustor Hardware Modifications.

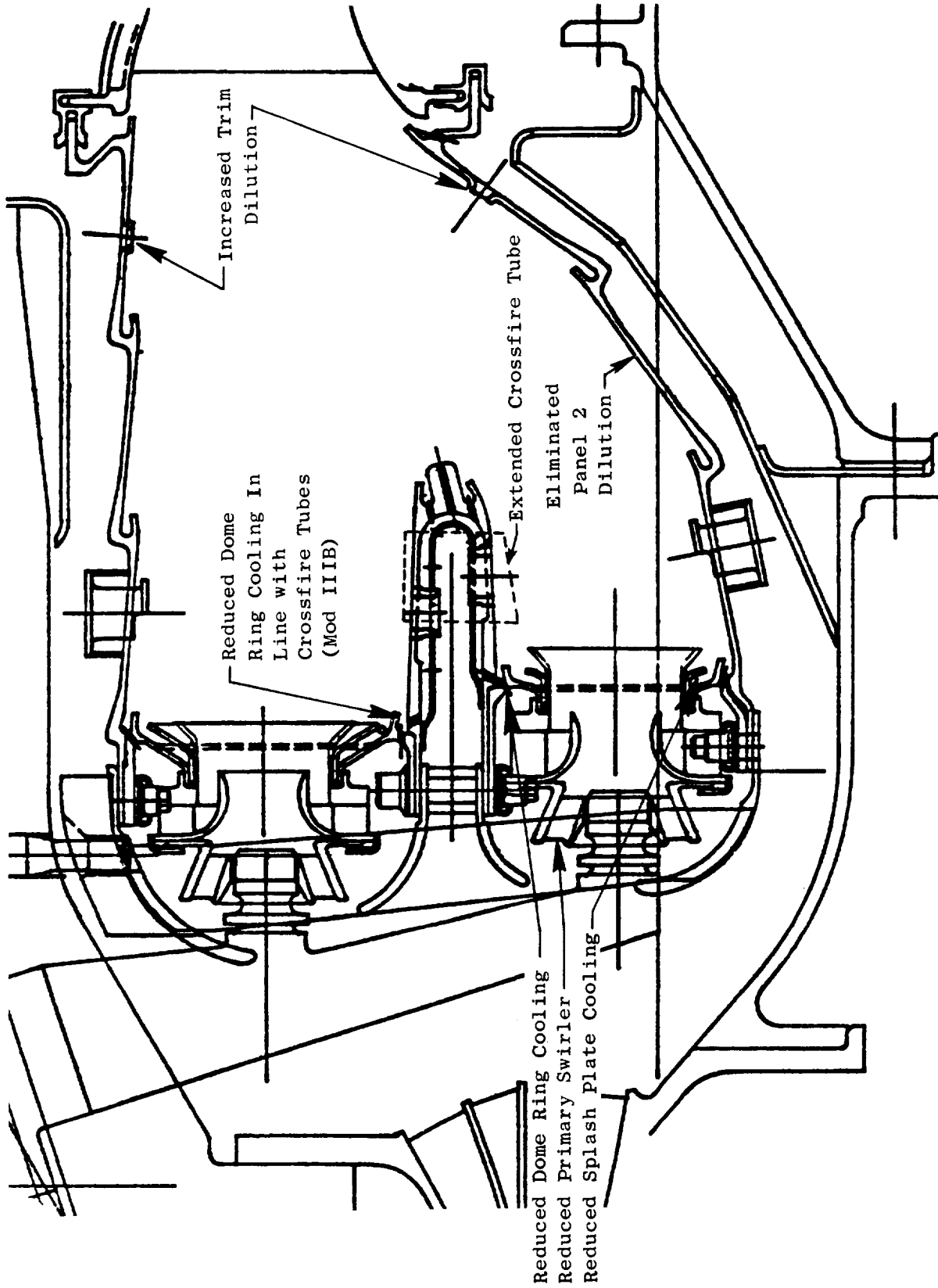


Figure 194. Mod II and Mod III Combustor Hardware Modifications.

Table XLII. Mod II and III Atmospheric Ignition
Test Point Schedule.

- E³ 9/79 SLS Ground Start Operating Cycle
Atmospheric Inlet Pressure

PCNHR, % Test Point	Combustor Inlet Conditions			
	WComb kg/s (pps)	P3, atm	T3, K (° F)	
21	1.25 (2.76)	1.00	289 (60)	Standard Airflow Conditions
28	1.69 (3.71)	1.00	289 (60)	
32	1.55 (3.40)	1.00	314 (105)	
46	1.65 (3.64)	1.00	344 (160)	
58	1.86 (4.09)	1.00	383 (230)	
70	1.94 (4.26)	1.00	429 (312)	
77	2.33 (5.13)	1.00	503 (445)	
32	1.70 (3.75)	1.00	314 (105)	
32	1.94 (4.26)	1.00	314 (105)	
46	1.82 (4.00)	1.00	344 (160)	
46	2.06 (4.34)	1.00	344 (160)	
77	2.54 (5.59)	1.00	503 (445)	
77	2.89 (6.35)	1.00	503 (445)	
Actual Engine Cycle Combustor Inlet Pressures				
PCNHR, %	P3			
	MPa	(psia)		
21	0.103	(15.0)		
28	0.105	(15.2)		
32	0.119	(17.2)		
46	0.144	(20.9)		
58	0.187	(27.1)		
70	0.248	(36.0)		
77	0.428	(62.0)		

pilot combustion gas stream. This strong flow appeared to quench a considerable amount of the pilot combustion gases as they passed downstream beyond the centerbody trailing edge. This sudden quenching appeared to be responsible for the difficulty in obtaining full pilot stage propagation and main stage ignition. Combustion gases passing through the crossfire tubes into the main stage annulus become entrained in this flow along the centerbody, and were swept downstream before penetrating sufficiently into the main stage annulus to provide a good ignition source. The existence of this strong flow of air appeared related to three of the hardware modifications featured in the Mod IIA combustor configuration: the shortening of the centerbody, the introduction of inner line Panel 2 dilution, and the increased centerbody main side cooling flow (see Figure 193). Because of the quantity of the inner liner Panel 2 dilution ($\sim 5.1\% W_{\text{comb}}$), it was suspected that this had the strongest impact of the three.

Test results for the Mod IIB combustor configuration are presented in Appendix F. In comparison to the Mod IIA configuration, no significant improvement in the pilot stage ignition was obtained. Some improvement in the main stage full propagation and lean extinction characteristics was demonstrated, especially at the lower speed operating conditions.

Test results obtained for the Mod IIIA combustor configuration are presented in Appendix F. The implementation of the combustor hardware modifications featured in this configuration proved very effective in achieving significant improvement in the main stage ignition characteristics. Successful ignition and full propagation of the main stage was obtained at simulated corrected core speeds as low as 32%. A partial propagation was obtained at 28% PCNHR. This ignition data was adjusted to true engine cycle combustor inlet pressure conditions using pressure effect characteristics determined from sector subcomponent and Mod I development combustor ignition testing at pressure. As shown in Figure 195, when adjusted for the combustor inlet pressure, the Mod IIIA combustor configuration was estimated to achieve full main stage propagation within the ground start fuel schedule at corrected core speeds at or above 45%. During testing of this configuration, several observations were made. At the lower simulated core speed operating points, hot combustion gases passing through the cross fire tubes were still being swept downstream upon

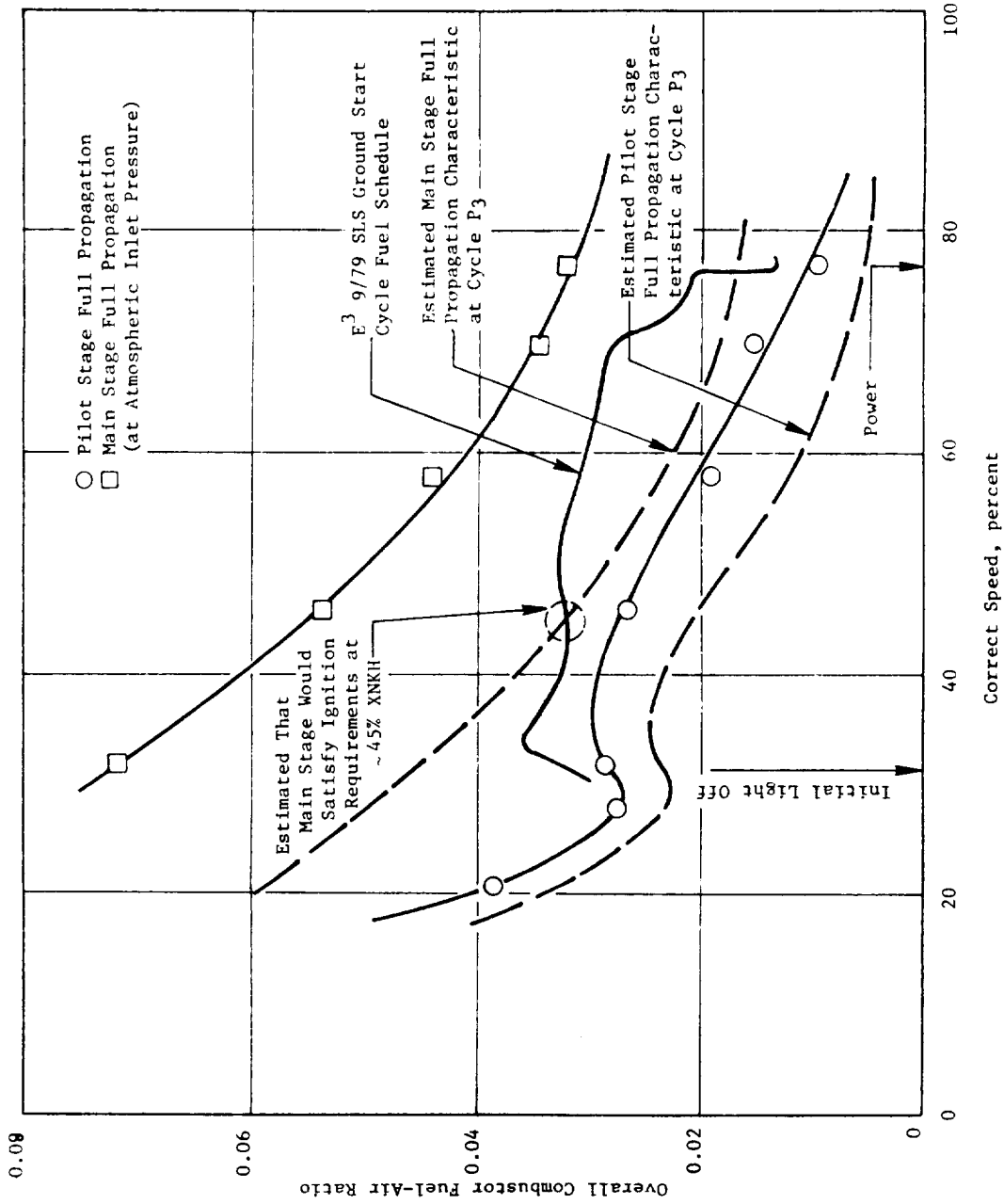


Figure 195. Mod III-A Atmospheric Ignition Test Results.

discharging into the main stage annulus. Main stage ignition and initial flame stabilization appeared to occur in the plane of the main stage liner primary air introduction. As the fuel-air mixture in the main stage leaned out, the flame front propagated upstream into the recirculating zone established by the swirl cup. At test conditions where main stage ignition occurred, the main dome swirl cup equivalence ratios were around 3.0, above the rich stability limit. At the plane of the liner primary dilution, the equivalence ratios were near 1.0, considered ideal for ignition. It appeared that a substantial improvement in the main stage ignition characteristics could be obtained by reducing the equivalence in the main stage dome, and moving the cross fire tubes (ignition source) closer to the main stage swirl cup. Because of the design of the centerbody, moving the cross fire tubes upstream any significant amount was not possible.

Test results obtained for the Mod IIIB combustor configuration was presented in Appendix F. From these results it can be concluded that in general, the hardware modification incorporated into this configuration produced no significant change in the ignition and lean extinction characteristics of the Mod IIIA combustor configuration. However, one significant result did emerge. Substantial improvements were achieved in both the pilot and main stage ignition and lean excitation characteristics at test points where the effect of increased combustor airflow was evaluated. This result may be associated with better fuel atomization and fuel-air mixing created from higher swirl cup airflows and pressure drops offsetting the adverse effects of higher dome velocities. Estimated main stage ignition performance at actual engine combustor inlet pressure is presented for the standard and high flow operating conditions in Figure 196. These results indicate that without compressor bleed during ground start up, the main stage could be successfully crossfired at corrected core engine speeds below 40%.

7.5.2 Concluding Remarks

In summary, the development effort represented in this ignition testing series evolved a promising combustor configuration capable of demonstrating satisfactory pilot and main stage ignition and lean extinction characteristics

ORIGINAL PAGE IS
OF POOR QUALITY

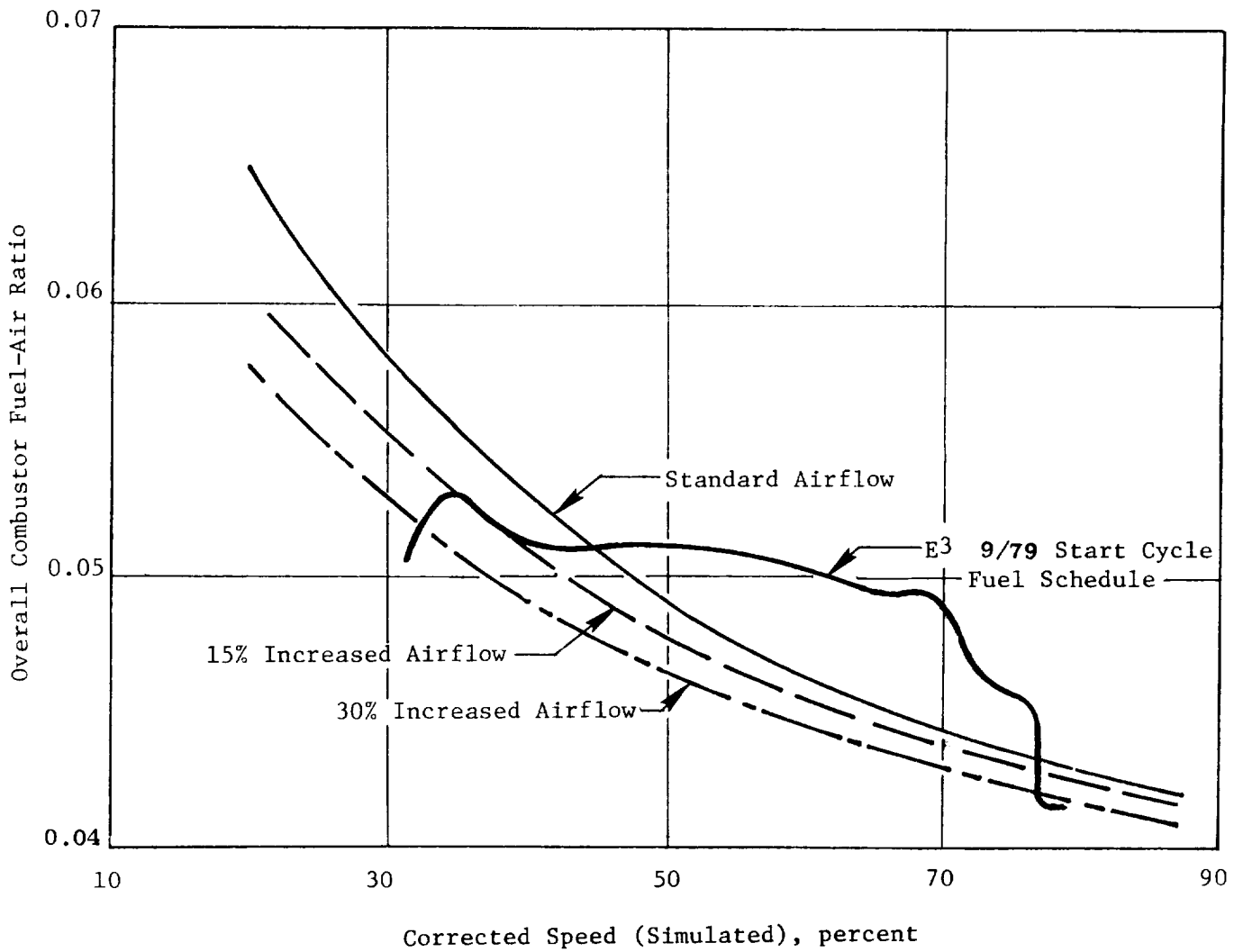


Figure 196. Mod III-B Atmospheric Ignition Test Results.

that would meet the E³ (9/79) ground start cycle requirements. It was further demonstrated that additional improvements in the combustor ignition and lean extinction characteristics would result if the requirement for large amounts of compressor bleed during ground start up were eliminated.

Despite these encouraging results, it was decided to apply additional development effort into the rich main stage design concept to achieve further improvements in ground start ignition characteristics, while demonstrating acceptable exit temperature performance. Modifications in the outer liner and inner liner trim dilution were considered to investigate their impact on these two combustor operating performance characteristics.

7.6 MOD IV AND MOD V DEVELOPMENT COMBUSTOR TEST RESULTS

The Mod IV combustor configuration hardware modifications involved reducing the inner liner panel trim dilution holes while introducing holes in inner liner Panel 2. The dilution hole arrangement in Panel 2 inner was the same pattern featured in the Mod IIA combustor, but the holes were smaller. With this arrangement, the Panel 2 and Panel 3 dilution holes were staggered providing for the introduction of dilution air every 3° around the combustor inner annulus. These dilution modifications had two intentions, to add mixing length by introducing some of the inner liner trim dilution air further upstream and to investigate the impact of a small quantity of Panel 2 dilution on the main stage ignition.

The Mod V combustor configuration hardware modifications involved reducing the size of the main stage inner side and centerbody side primary dilution thimble holes. In addition, 60 equally spaced dilution holes were introduced into Panel 2 of the outer liner. The holes were staggered with respect to the outer liner Panel 3 dilution hole arrangement. These modifications were intended to further enrich the main stage dome to improve the ignition characteristics and attenuate the exit gas temperature profiles, especially in the pilot only mode of operation. Illustrations of the combustor hardware modifications featured in each configuration are presented in Figures 197 and 198. The resultant changes in the combustor airflow distribution for each of these configurations are presented in Appendix E.

ORIGINAL PAGE 15
OF POOR QUALITY

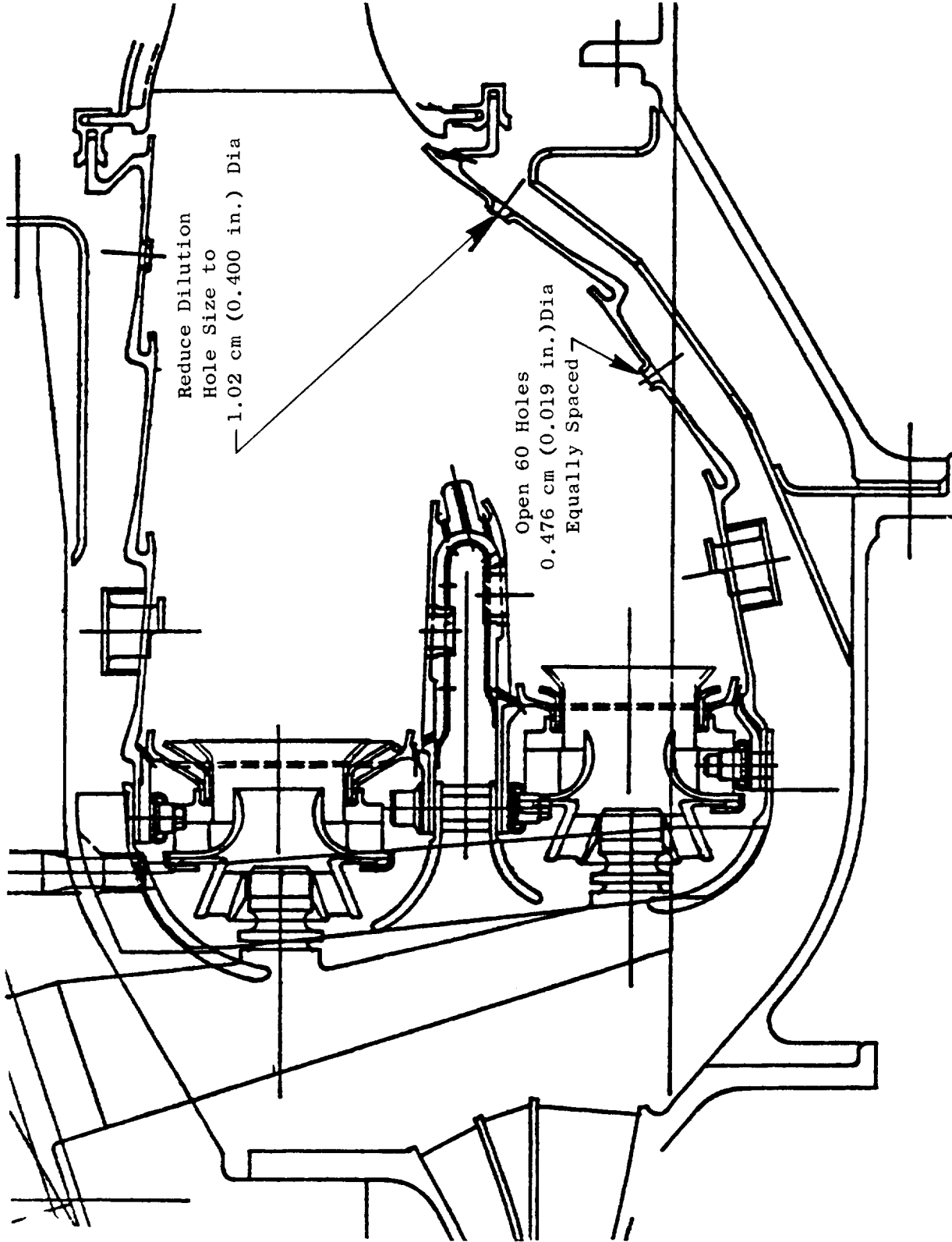


Figure 197. Mod IV Combustor Hardware Modifications.

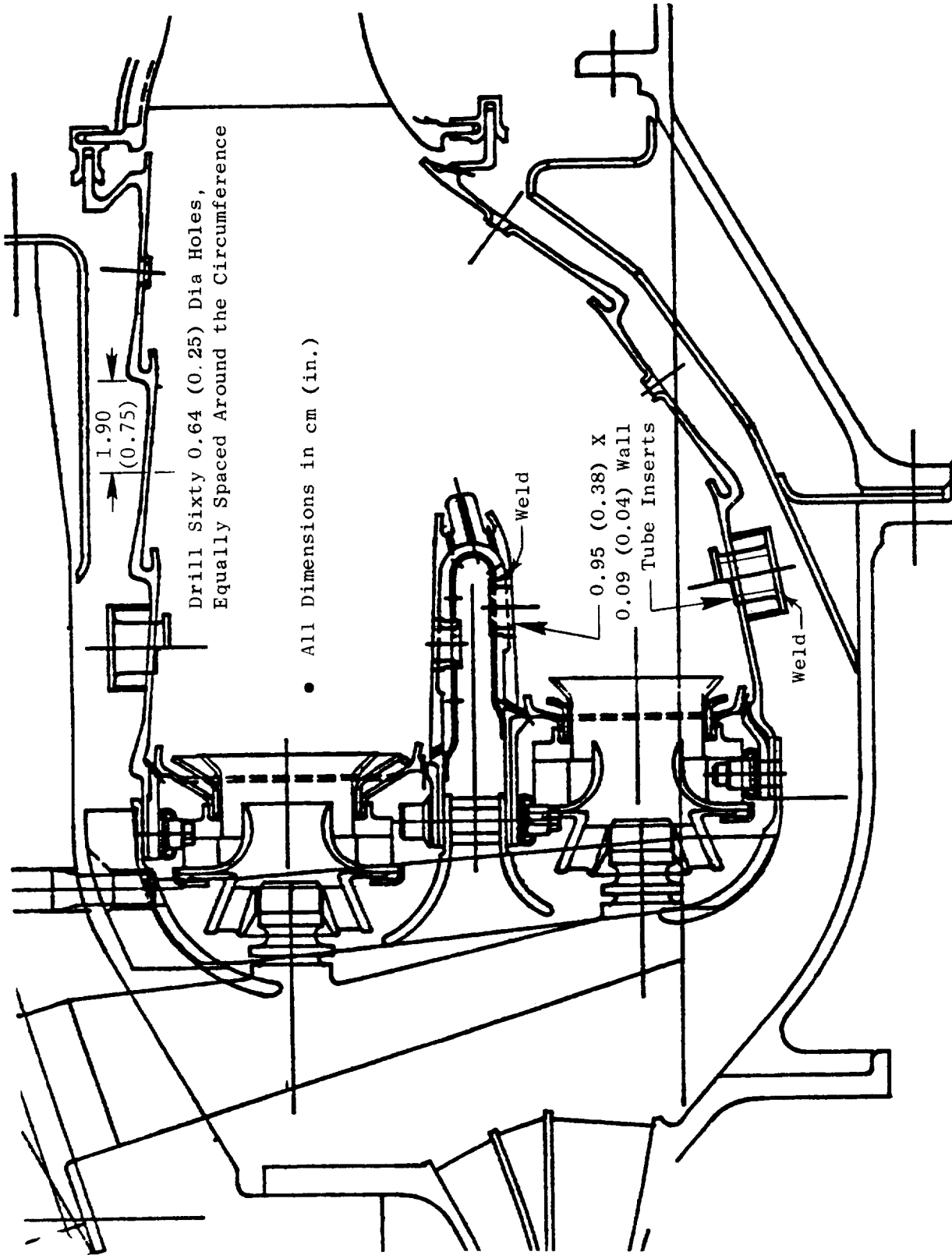


Figure 198. Mod V Combustor Hardware Modifications.

7.6.1 Atmospheric Ground Start Ignition Test

Ground start ignition testing was performed on both the Mod IV and Mod V development combustor configurations. The test points investigated were the same as those investigated with the Mod II and Mod III configurations.

For this ground start ignition test series, the E³ test rig fuel nozzle assemblies were used. Nozzle tips rated at 12 kg/hr (26.5 pph) at 100 psid were installed in both combustor stages.

Ground start ignition test results for the Mod IV combustor configuration are compared with the results obtained from the Mod IIIA configuration in Figure 199. A tabulation of the data is presented in Appendix F. The Mod IIIA configuration had demonstrated marginally acceptable main stage subidle ignition characteristics. As observed from this figure, the pilot stage full propagation and one-cup-out characteristics remained unchanged. This was expected as there were no hardware modifications made to the pilot stage dome. However, some deterioration in main stage full propagation and one-cup-out characteristics did result. Overall combustor fuel-air ratios approximately 10% greater than in the Mod IIIA configuration were required to obtain full propagation of the main stage. Some reduction in the lean stability margin was also observed. Despite the fact that some deterioration in the main stage ignition characteristics did occur, the Mod IV results indicated that small amounts of inner liner Panel 2 dilution did not seriously impact main stage ignition.

Ground start ignition test results for the Mod V combustor configuration are presented as a comparison with the results of the Mod IIIA and Mod IV ignition test results in Figure 200. As observed from the figure, some minor improvements in main stage ignition characteristics over those demonstrated with the Mod IV configuration were obtained. However, the main stage ignition performance is not quite as good as that demonstrated with the Mod IIIA configuration. From these results and estimates of the expected improvements resulting from operation at actual engine cycle combustor inlet pressures, it is estimated that full propagation of the main stage could be achieved at a corrected core engine speed of 50%. This compares to a speed of 45% identified

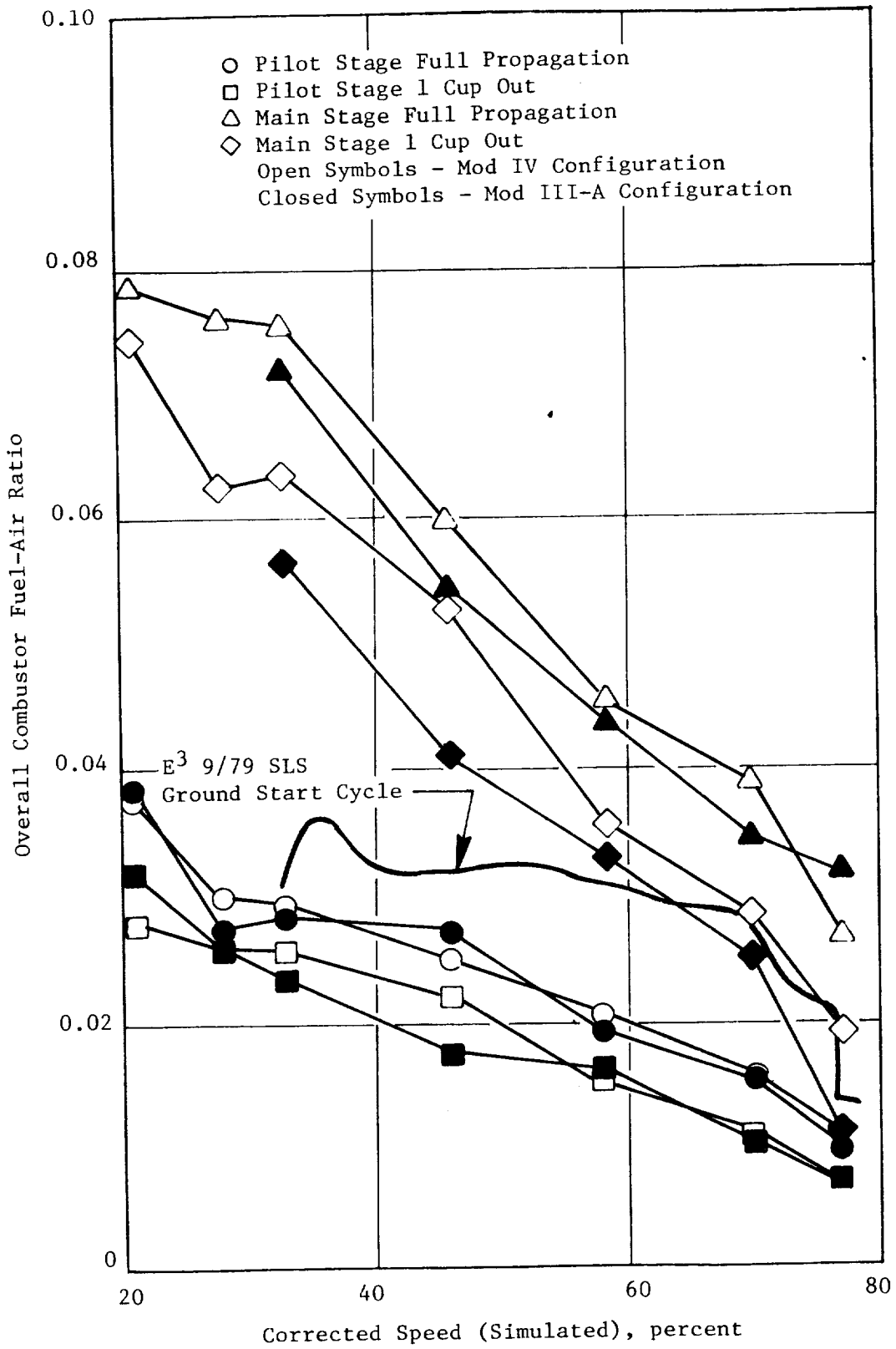


Figure 199. Mod IV Atmospheric Ignition Test Results.

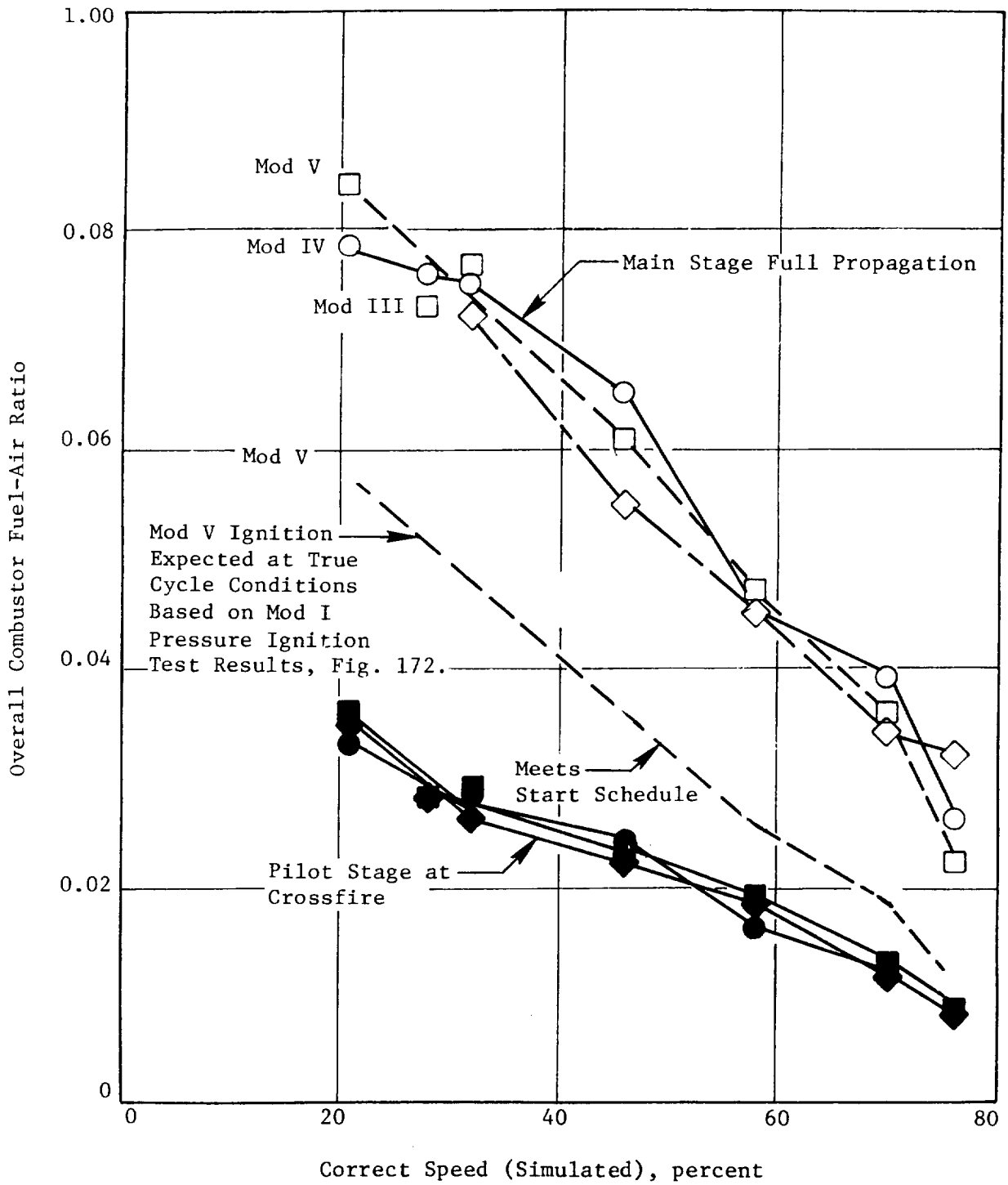


Figure 200. Mod V Atmospheric Ignition Test Results.

for core engine starting. Despite the introduction of some outer liner Panel 2 dilution, the pilot stage ignition characteristics remained unchanged.

7.6.2 Atmospheric Exit Temperature Performance Test

The Mod V development combustor configuration was evaluated for exit temperature performance. Operating conditions simulated sea level takeoff power with pilot-to-total fuel splits of 0.5, 0.4, and 0.3. Data were also taken at operating conditions simulating 77%, 58%, and 46% corrected core engine speeds as defined in the E³ (9/79) ground start cycle. Pilot-to-total fuel splits of 1.0, 0.5, and 0.4 were evaluated at 77 PCNHR, while the pilot only operating mode was evaluated at 58 and 57 PCNHR. At subidle test points, fuel-air ratios 30% lower than cycle conditions were set because of fuel nozzle flow limitations. Test points and corresponding combustor operating conditions are presented in Table XLIII.

Nozzle tips rated at 2.3 kg/hr (5 pph) were installed in the pilot stage. In the main stage, a set of slightly modified nozzle tips were used. These tips originally were rated at 3.2 kg/hr (7 pph). The modifications increased their flow rate to approximately 6.8 kg/hr (15 pph) at the same fuel pressure. Some variance in fuel flow levels (+10%) between these 30 modified nozzle tips was evident from the pretest fuel flow calibration. The variation was attributed to the fact that the modifications were done manually.

Combustor exit gas temperature rakes were positioned with the center element located outward approximately 0.20 cm (0.08 in.) from the center of the exit annulus, and approximately 0.53 cm (0.21 in.) aft of the trailing edge of the test rig aft seals. This "cold" position was selected as a result of an investigation conducted by ACL Test Engineering into the interference problems experienced with the E³ traverse ring. During the performance testing, the only problem encountered with the traverse system involved the extreme elements of each rake occasionally moving out of the combustion gas stream into the film cooling flow behind the test rig aft seals. This was the result of an eccentricity between the combustor exit annulus and the traverse ring, plus the fact that the rakes were positioned downstream of trailing edge of the aft seals. However, none of the thermocouple elements suffered damage from rubbing against the surface of the aft seals.

Table XLIII. Mod V Atmospheric EGT Performance Test Point Schedule.

Test Point	T ₃ , K (° F)	P ₃ , Atm	W ₃ , kg/s (pps)	W _{Bleed} , kg/s (pps)	W _c , kg/s (pps)	f/a	WF (Pilot) WF (Total)	WF (Pilot) kg/h (pph)	WF (Main) kg/h (pph)	Traverse Positions	Traverse Increments, degree
1	815 (1007)	Amb.	2.41 (5.31)	0.15 (0.34)	2.26 (4.97)	0.0244	0.50	99 (218)	99 (218)	120	1.5
2	815 (1007)	Amb.	2.41 (5.31)	0.15 (0.34)	2.26 (4.97)	0.0244	0.40	80 (175)	119 (262)	120	1.5
3	815 (1007)	Amb.	2.41 (5.31)	0.15 (0.34)	2.26 (4.97)	0.0244	0.30	60 (131)	139 (306)	120	1.5
4	314 (105)	Amb.	1.55 (3.40)	0	1.55 (3.40)	*	1.0	*	0	60	1.5
5	344 (160)	Amb.	1.65 (3.64)	0	1.65 (3.64)	*	1.0	*	0	60	1.5
6	344 (160)	Amb.	1.90 (4.19)	0	1.90 (4.19)	*	1.0	**	0	60	1.5
7	383 (230)	Amb.	1.86 (4.09)	0	1.86 (4.09)	*	1.0	*	0	60	1.5
8	495 (432)	Amb.	2.33 (5.13)	0	2.33 (5.13)	*	1.0	*	0	60	1.5
9	495 (432)	Amb.	3.33 (5.13)	0	2.33 (5.13)	*	1.0	*	0	60	1.5
10	495 (432)	Amb.	2.33 (5.13)	0	2.33 (5.13)	*	1.0	*	0	60	1.5

*Set Minimum Pilot Stage Fuel Flow at Which All 309 Cups Are Burning

**Set Same Fuel Flow in Pilot Stage as Was Set in Test Point No. 5

Results from the performance test of the Mod V combustor configuration are presented in Figure 201. The average profile at the 50/50 fuel split is generally within the established limit and reasonably flat. However, as fuel is biased to the main stage, unacceptable profiles result. The maximum profiles are sharply peaked inward and exceed the established limit by a considerable amount. Much of the data obtained from the Mod V performance test suffered from the effects of cold spots caused by blownout swirl cups, bad data from deteriorating thermocouple elements, and the effects of the extreme elements of the rakes measuring the temperature of the inner and outer aft seal film cooling air. These areas were clearly identified through use of combustor exit gas temperature contour plots generated from all of the data obtained. They represented discrete problem areas in the combustor and traverse system and were unrelated to any problem with the aero design of the combustor hardware. Test data obtained in these regions was not considered as representative of the combustor performance. All of the performance data obtained was refined to eliminate the effects of these problem areas. In Figure 202 the performance results for pilot only operation at the simulated subidle conditions are presented. Data obtained at the simulated 77 PCNHR condition with the pilot-to-total fuel splits of 0.5 and 0.4 was of extremely poor quality and not considered worth processing.

It can be seen in Figure 202 that maximum profiles of less than 1.0 were obtained at all of the pilot-only subidle operating conditions investigated. These levels are significantly lower than levels measured during performance testing of the Mod I configuration at the same operating conditions. This improvement is attributed to the outer liner Panel 2 dilution featured in the Mod V configuration. The significance of this result relates to the concern over the effects on turbine hardware survival when subjected to sharply peaked temperature profiles resulting from pilot only operation. Any attenuation in these profiles would be very beneficial to turbine life.

7.6.3 Concluding Remarks

The combustor hardware modifications featured in the Mod IV and Mod V configurations failed to provide any improvement in the ground start ignition characteristics. However, the results did show that small amounts of

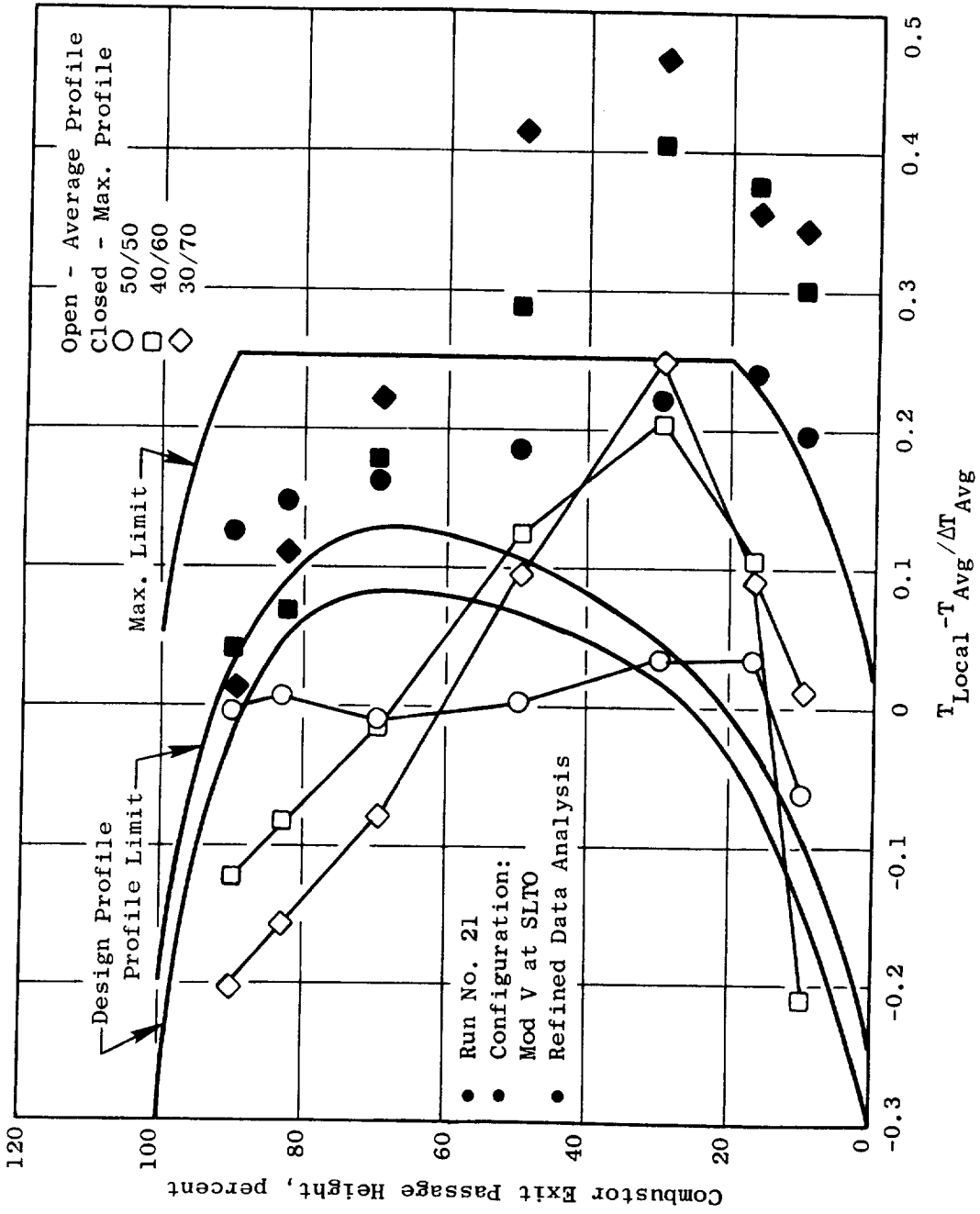


Figure 201. Mod V EGT Performance Test Results.

ORIGINAL PAGE IS
OF POOR QUALITY

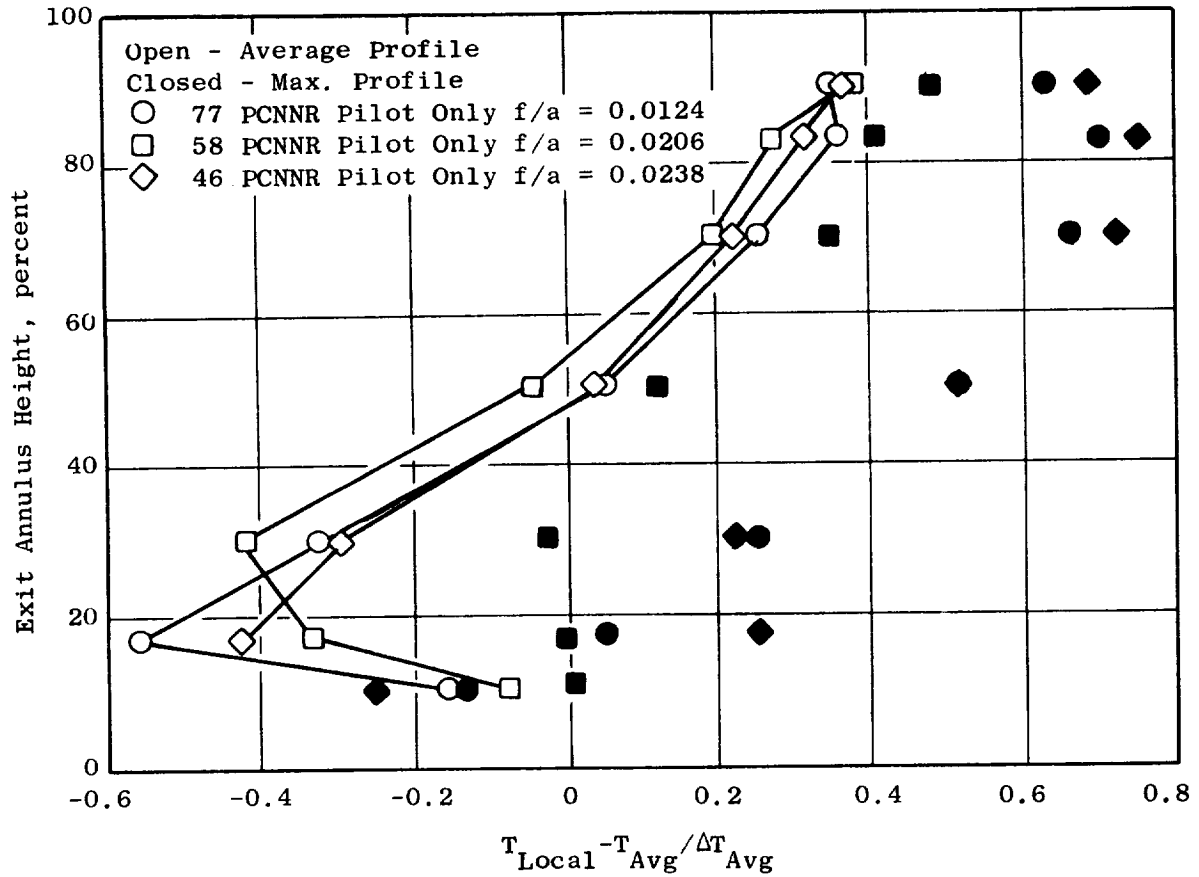


Figure 202. Mod V EGT Performance Test Results.

inner liner Panel 2 dilution could be incorporated into the design without significantly affecting the main stage ignition characteristics.

Exit temperature performance results obtained from the Mod V configuration revealed excessively high pattern factor levels. This despite the large quantities of trim dilution air featured in this rich main stage combustor design. Such results suggest that the short length of the E³ combustor does not provide sufficient length in which to effectively mix large quantities of trim dilution with the combustion gases. A more uniformly mixed combustor could be achieved by introducing most of the combustor air in the primary zones. Here the air and fuel are subjected to intense mixing phenomena and have greater physical length in which to further mix before discharging from the combustor. This design philosophy is supported by making a comparison of the Mod I and Mod V development combustors. In the Mod I combustor, 80% of the combustor air was introduced into the primary zone, while only 5% of the air was introduced as trim dilution. This configuration demonstrated acceptable exit temperature performance levels. In the Mod V combustor, only 64% of the combustor air was introduced into the primary zones, with 21% of the air introduced as trim dilution. This configuration demonstrated poor exit temperature performance levels.

From testing performed on the Mods II, III, IV, and V combustor configurations, design changes involving significant reductions in the main stage primary zone airflow were necessary to evolve the desired main stage ignition characteristics. The large quantities in trim dilution featured in these designs were necessary to compensate for the reduced dome flows in order to maintain the combustor overall total pressure drop. All of this suggests that it will be extremely difficult to evolve a rich main stage design of this short length combustor that will demonstrate the desired main stage ignition characteristics as well as exit temperature performance levels within the E³ goals. Considerably more development effort will be necessary to resolve this problem.

7.7 MOD VI AND MOD VII DEVELOPMENT COMBUSTOR TEST RESULTS

The Mod VI and VII combustor configurations featured hardware modifications intended to revert the combustor design from the rich main stage dome

designs featured in configurations Mod II through Mod V, back to the original lean main stage design concept.

The decision to revert back to the original design intent was based on the results of an updated starting study of the E³ engine system conducted by Systems Engineering. In this study, measured performance data from the major engine components was incorporated into the E³ dynamic start model. Based on this component test data, the measured performance of the compressor and high pressure turbine components was considerably better in the low-speed operating range than had originally been projected. Therefore, it would be possible to start the engine within the specified time requirements with a considerably lower T₄ level, significantly reducing the risk of overtemperaturing the turbine from the high levels of combustor exit temperature pattern factor associated with the pilot only mode of operation.

All of the hardware modifications required to revert back to the original design intent were identified by tracing the development history of the combustor. The combustor hardware modifications featured in the Mod VI configuration are provided below:

- Open all holes currently welded closed in the outer dome outer cooling ring and the outer liner cooling Ring No. 1.
- Open all holes in the outer dome inner cooling ring that are in line with the two crossfire tubes.
- Close off all outer liner Panel 2 dilution holes.
- Reduce the size of all outer liner Panel 3 dilution holes.
- Return the main stage swirl cup primary swirlers to standard configuration by removing the Nichrome patches used in the Mod V combustor to block off every other vane passage. Also, replace the main stage secondary swirlers with larger size swirlers, originally used in the Baseline combustor main stage.
- Restore the main stage splashplate cooling to standard level by opening all holes closed off in the Mod V combustor.
- Reopen all holes closed in the inner dome outer cooling ring.
- Reduce the size of all inner liner Panel 3 dilution holes.

It would have been preferred to incorporate even larger secondary swirlers in the main stage. However, this would have required machining another set of castings leaving an insufficient supply for the core engine combustor.

The Mod VII configuration, like the Mod VI configuration, featured a lean main stage design. The combustor was completely disassembled and refurbished to improve the hardware quality. New dome sleeves were installed in both the pilot stage and main stage swirl cups. The new main stage sleeves featured a shortened overall length with the same trailing edge diameter. In addition, a small amount of inner liner Panel 3 trim dilution was moved upstream into Panel 2. Estimates of airflow distribution of these configurations are presented in Appendix E.

7.7.1 Atmospheric Ground Start Ignition Test

Ground start ignition evaluation of the E³ development combustor Mod VI configuration was conducted in the ACL Cell A3W facility on 6/25/81. The purpose of this test was to evaluate the ignition, crossfire, and lean extinction characteristics of this combustor configuration at selected steady-state operating points along the E³ (6/81), ground start design cycle. For the purposes of main stage crossfire, data was also obtained at simulated steady-state operating conditions representing 4%, 6%, 10%, and 30% of sea level takeoff power along the E³ FPS II design operating cycle. Test points and corresponding operating conditions are presented in Table XLIV.

Ground start ignition test results for the Mod VI combustor configuration are presented in Figure 203. As observed, the pilot stage ignition characteristics satisfy the fuel schedule requirements defined in the revised (6/81) start cycle with and without compressor bleed. Taking into consideration the improvement in ignition characteristics anticipated at actual cycle inlet pressures, the pilot stage would demonstrate considerable ignition margin along the revised start cycle. Also observed from this figure are the main stage crossfire and lean extinction characteristics. Overall combustor fuel-air ratios of 0.030 or higher were required to successfully crossfire and fully propagate the main stage. These levels are well above the fuel schedule in the 4% to 30% power range as defined in the FPS design cycle, and are typical of levels previously demonstrated by other configurations featuring lean

Table XLIV. Mod VI and VII Atmospheric Ignition Test Point Schedule.

- Subidle conditions from 6/81 start cycle
- Higher-power condition from FPS-II cycle
- Standard day
- Atmospheric inlet pressure
- 44.19 cm² (in.²) bleed

Test Point	PCNHR	P ₃ , Atm (psia)	T ₃ , K (°F)	W ₃₆ kg/s (pps)	Comments	
*1	21.0	1.00 (15.0)	304 (87)	2.19 (4.82)	Simulated No Bleed	6/81
*2	21.0	1.00 (15.0)	304 (87)	2.10 (4.61)	Simulated Bleed	6/81
*3	24.5	1.00 (15.0)	310 (98)	2.59 (5.50)	Simulated No Bleed	6/81
*4	24.5	1.00 (15.0)	310 (98)	2.38 (5.24)	Simulated Bleed	6/81
**5	30.0	1.00 (15.0)	322 (120)	2.86 (6.30)	Simulated No Bleed	6/81
**6	30.0	1.00 (15.0)	322 (120)	2.75 (6.00)	Simulated Bleed	6/81
*7	36.9	1.00 (15.0)	339 (150)	3.20 (7.05)	Simulated No Bleed	6/81
*8	36.9	1.00 (15.0)	339 (150)	3.12 (6.87)	Simulated Bleed	6/81
**9	4% F _N	1.00 (15.0)	466 (379)	2.40 (5.29)	FPS II Cycle	
**10	64.3	1.00 (15.0)	483 (410)	2.29 (5.03)	6/81 Cycle	
**11	6% F _N	1.00 (15.0)	495 (432)	2.44 (5.36)	FPS II Cycle	
**12	10% F _N	1.00 (15.0)	539 (510)	2.42 (5.33)	FPS II Cycle	
**13	30% F _N	1.00 (15.0)	637 (687)	2.25 (4.94)	FPS II Cycle	

Note:

* = Core engine motoring combustor inlet conditions (no fuel)

** = Ignition characteristics of main stage to be investigated

ORIGINAL PAGE IS
OF POOR QUALITY

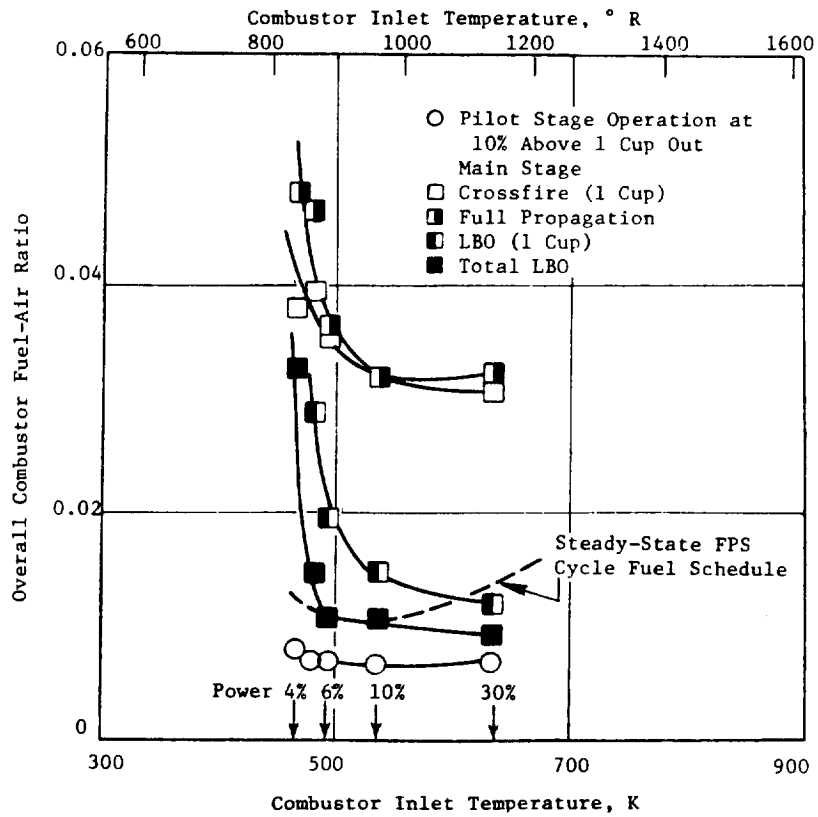
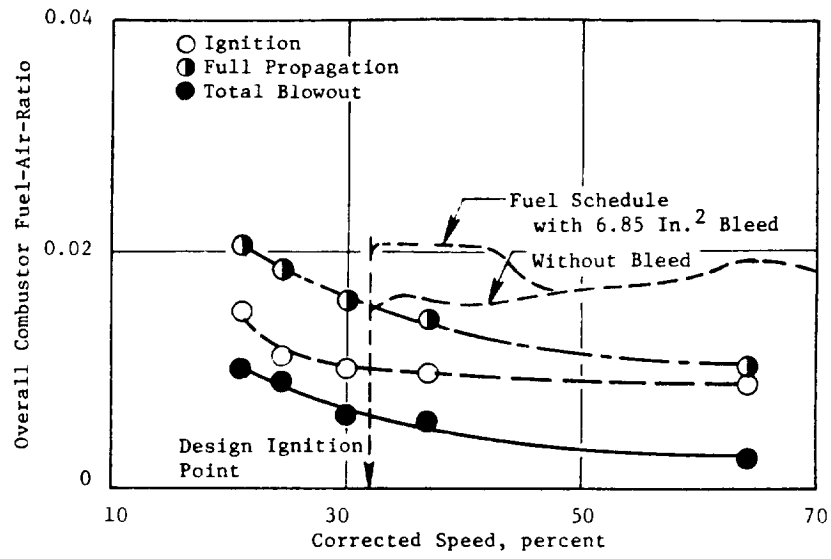


Figure 203. Mod VI Atmospheric Ignition Test Results.

main stage dome designs (Baseline and Mod I configuration). As with the pilot stage, a significant amount of improvement in the main stage crossfire characteristics would be expected at actual engine cycle inlet pressures. However, it is doubted that the amount of improvement would be enough to achieve full main stage propagation below 6% power. The main stage did demonstrate sufficient blowout margin to assure that once fully propagated, it would remain fully propagated at actual cycle operating conditions as low as 4% power.

Since the combustor modifications featured in the Mod VII configuration did not involve aerodynamic changes to the pilot stage, no change in the pilot stage ground start ignition characteristics was anticipated. Some slight change in the main stage ignition characteristics could be anticipated due to the modifications. Because the pilot only operating mode was once again the approach selected for engine ground start, it was felt that no new information of any significance would be obtained by evaluating the Mod VII combustor for ground start ignition characteristics. Thus, this configuration was not tested for this purpose.

7.7.2 Atmospheric Exit Temperature Performance Test

Exit gas temperature performance testing of the E³ double-annular dome development combustor Mod VI configuration was conducted on 6/29/81 in the ACL Cell A3W facility. The purpose of this test was to evaluate this lean main stage dome design for exit gas temperature performance at operating conditions simulating SLTO, 30% thrust, and 6% thrust along the E³ FPS II design cycle. At simulated SLTO operating conditions, performance data was obtained at pilot to total fuel splits of 0.5, 0.4, and 0.3. At the simulated 30% thrust and 4% thrust operating conditions, performance data was obtained in the pilot only mode. All exit temperature rakes were positioned (cold) radially outward 0.127 cm (0.05 in.) from the exit annulus center, and approximately 0.508 cm (0.20 in.) aft of the trailing edge of the aft seals. Test points and corresponding combustor operating conditions are presented in Table XLV.

Table XLV. Mod VI Atmospheric EGT Performance Test Point Schedule.

Test Point	T ₃ , K (° F)	P ₃ , atm	W ₃ , kg/s (pps)	W _{Bleed} , kg/s (pps)	W _{Comb} , kg/s (pps)	f/a	Wf Pilot/ Wf Total	Wf Pilot, kg/hr (pph)	Wf Main, kg/hr (pph)
1	815 (1007)	1.0	2.41 (5.31)	0.15 (0.34)	2.26 (4.97)	0.0245	0.50	99 (218)	99 (218)
2	815 (1007)	1.0	2.41 (5.31)	0.15 (0.34)	2.26 (4.97)	0.0245	0.40	80 (175)	112 (262)
3	815 (1007)	1.0	2.41 (5.31)	0.15 (0.34)	2.26 (4.97)	0.0245	0.30	60 (131)	139 (306)
4	637 (687)	1.0	2.58 (5.68)	0.16 (0.36)	2.42 (5.32)	0.0143	1.00	125 (274)	0
5	495 (432)	1.0	2.55 (5.60)	0.18 (0.40)	2.37 (5.20)	0.0123	1.00	105 (230)	0

E³ test rig nozzle assemblies incorporating nozzle tips rated at 2.3 kg/hr (5 ppm) in the pilot stage, and nozzle tips rated at 6.4 kg/hr (14 pph) in the main stage were used.

Much of the data obtained from the Mod VI performance suffered from the same problems as did data obtained on the Mod V configuration. All of the performance data obtained was refined to eliminate the effects of these problem areas.

The exit temperature performance results for the Mod VI configuration were disappointing. As observed from Figure 204, a pattern factor of 0.36 was obtained at the simulated SLTO operating condition at a pilot-to-total fuel split of 0.4. Even higher pattern factor levels were obtained at the other fuel splits investigated at this operating condition. The pattern factor goal established for this combustor development program is a level of 0.25. At a pilot-to-total fuel split of 0.5, the average profile is center peaked, and generally within the design limit. However, at the 0.4 and 0.3 fuel splits the average profile is inner peaked, and exceeds the design limit in the hub region by a considerable amount. Visual observations of the combustor during testing revealed the existence of streaks in the flame pattern at several positions around the circumference, verifying the poor performance characteristics measured. The most notable streak appeared to originate in the pilot stage in the vicinity of Cup 7. It was later discovered that an undersized pilot stage primary dilution hole existed in the vicinity of this swirl cup lending suspicion to it being the probable cause. Data obtained at the 30% thrust and 6% thrust operating conditions in the pilot only mode are presented in Figure 205. As observed from this figure, the profiles are sharply outward peaked as expected. The pattern factor levels are higher than had been anticipated with a level of 1.35 at simulated 30% thrust conditions, and a level of 1.60 at simulated 6% thrust conditions.

The combustor was removed for a detailed hardware inspection. This inspection revealed numerous hardware quality problems, many of which could be directly linked to the poor performance levels measured. Some of these problems are discussed below.

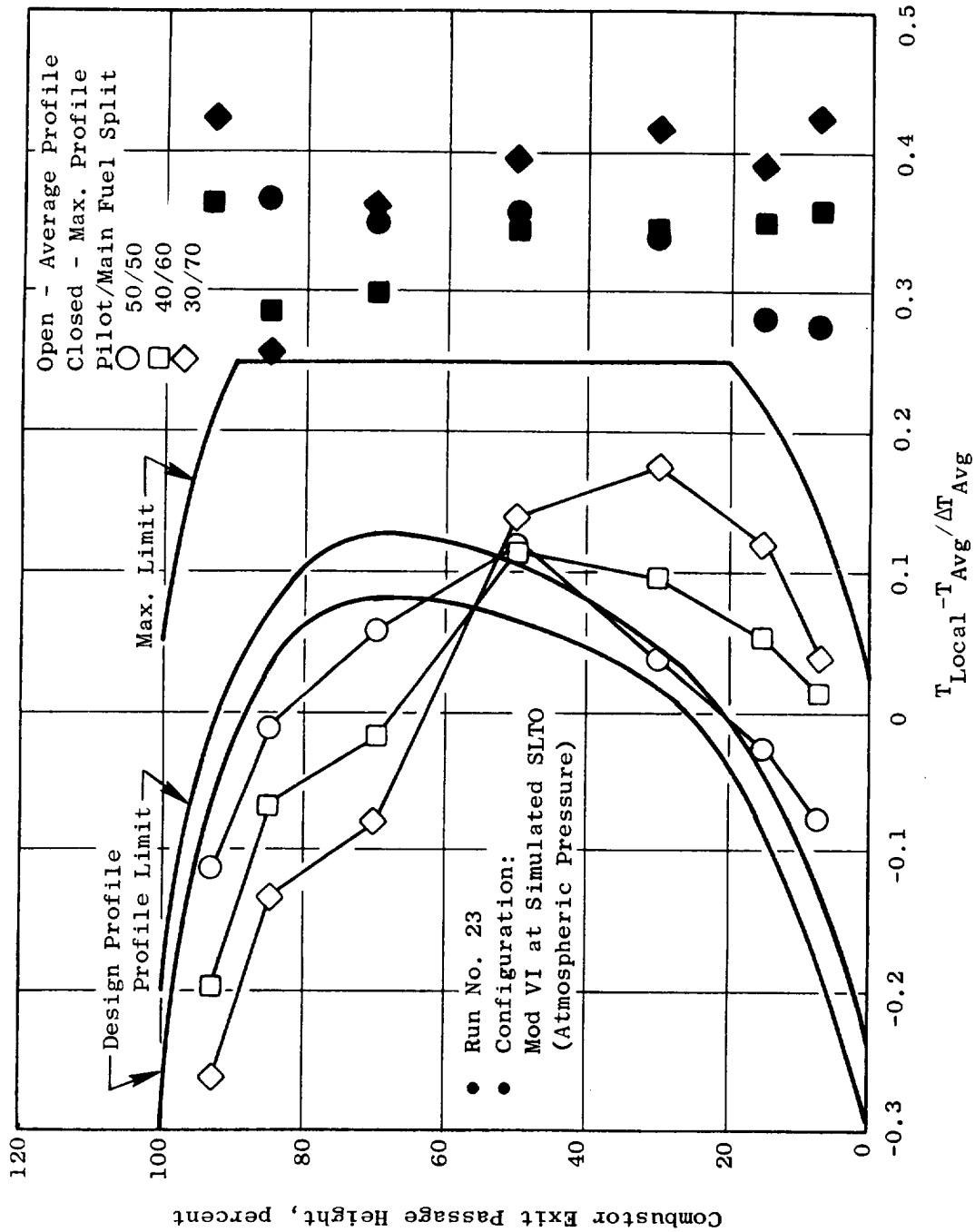


Figure 204. Mod VI EGT Performance Test Results.

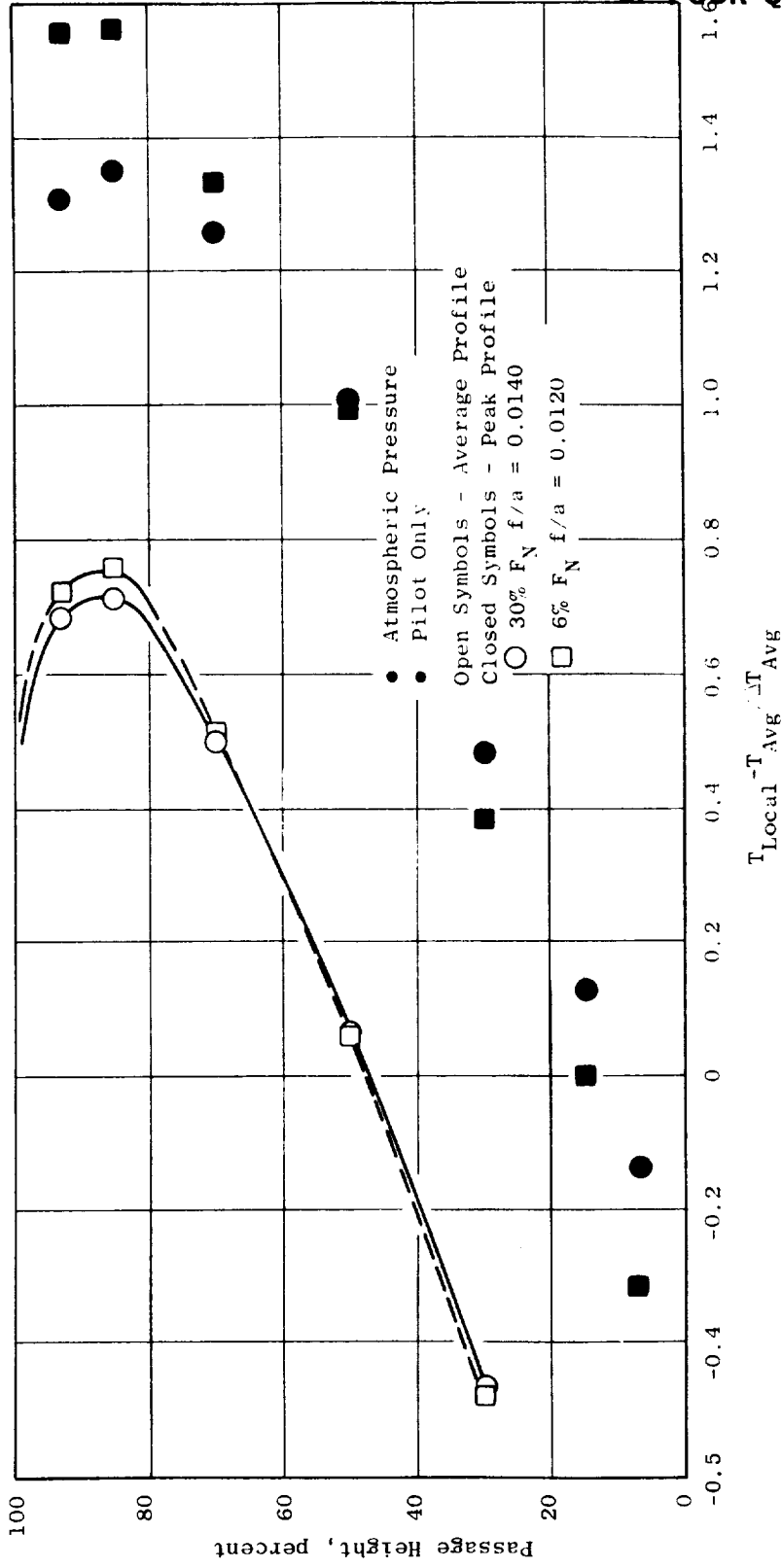


Figure 205. Mod VI EGT Performance Test Results.

Domes - Many of the emissions reduction sleeves were out-of-round or not concentric to the primary venturi. In addition, many sleeves had nicks and dents where they have been impacted during assembly. The emissions sleeves in the main stage also appeared to be too long compared to the design intent.

Liners - Most of the dilution thimbles were cocked such that the coannular gap was closed on one side. Many dilution holes had burrs on the hole trailing edge.

Centerbody - The primary holes on the pilot side had burrs resulting from the use of an installation tool. The primary holes on the main side had weld beads protruding into the hole where an insert was added. The crossfire tubes extended above the centerbody surface 0.051-0.152 cm (0.020-0.060 in.). As was previously mentioned, it was also discovered that the outer liner primary dilution hole between Pilot Cups 7 and 8 was considerably undersized.

This particular set of combustor hardware had been subjected to six major hardware modifications with many extensive design changes implemented. Because of the hardware quality problems, the results from the exit gas temperature performance test of this combustor configuration were not considered representative of the design. The combustor hardware was reworked to improve the quality. It was then retested for exit temperature performance as the Mod VII combustor configuration.

Performance testing of the Mod VII configuration was conducted on 8/21/81. New simplex fuel nozzles rated at 6.4 kg/hr (14 pph) were used in both the pilot stage and main stage. Exit temperature performance evaluation of this combustor was conducted at simulated sea level takeoff operating conditions with pilot-to-total fuel splits of 0.5, 0.4, and 0.3. Data was also taken at operating conditions simulating 30% thrust at pilot-to-total fuel splits of 1.0, 0.5, and 0.4, and at simulated 4% ground idle at pilot-to-total fuel splits of 1.0 and 0.5. Test points and corresponding combustor operating conditions are presented in Table XLVI.

At the simulated SLTO operating conditions, overall combustor fuel-air ratios approximately 10% above design levels were established. At the simulated lower power operating conditions with staged combustion, an overall

Table XLVI. Mod VII Atmospheric EGT Performance Test Point Schedule.

Test Point	T3, K (° F)	P3, atm	W3, kg/s (pps)	W Bleed, kg/s (pps)	W36, kg/s (pps)	f/a	Wf Pilot/ Wf Total	Wf Pilot, kg/hr (pph)	Wf Main, kg/hr (pph)	No. of Traverse Positions	Simulated Condition
1	817 (1011)	1.0	2.27 (5.00)	0.15 (0.34)	2.12 (4.66)	0.0242	0.5	92 (203)	92 (203)	120	SLTO
2	817 (1011)	1.0	2.27 (5.00)	0.15 (0.34)	2.12 (4.66)	0.0242	0.4	74 (162)	111 (244)	120	SLTO
3	817 (1011)	1.0	2.27 (5.00)	0.15 (0.34)	2.12 (4.66)	0.0242	0.3	55 (122)	129 (284)	120	SLTO
4	640 (692)	1.0	2.69 (5.91)	0.17 (0.37)	2.52 (5.54)	0.0140	1.0	127 (279)	0	60	30% FN
5	640 (692)	1.0	2.69 (5.91)	0.17 (0.37)	2.52 (5.54)	0.0140	0.5	63 (139)	63 (140)	60	30% FN
6	640 (692)	1.0	2.69 (5.91)	0.17 (0.37)	2.52 (5.54)	0.0140	0.4	51 (112)	76 (167)	60	30% FN
7	466 (369)	1.0	2.95 (6.48)	0.19 (0.41)	2.76 (6.07)	0.0127	1.0	126 (278)	0	60	4% FN
8	466 (369)	1.0	2.95 (6.48)	0.19 (0.41)	2.76 (6.07)	0.0127	0.5	63 (139)	63 (139)	60	4% FN

combustor fuel-air ratio of 0.024 was established. This compared to the design level of 0.014 at the 30% approach power condition and 0.0125 at the 4% ground idle condition. The higher fuel-air ratios were necessary to achieve and maintain main stage propagation at atmospheric operating conditions. All four thermocouple rakes were positioned radially outward 0.04 inch from the exit annulus center and 0.533 cm (0.21 in.) aft of the trailing edge of the aft seals.

Despite operating the combustor at higher fuel-air ratios, it was observed that several main stage cups failed to light at the simulated SLTO and 30% approach operating conditions. The problem was considerable at the simulated 4% ground idle operating condition where approximately half of the main stage cups failed to light. Throughout the development testing effort, this had been a recurring problem related to the main stage swirl cup dome design as opposed to a problem with the type of fuel nozzles used. Problems were also encountered with the traverse system. The inner most element of two rakes traversed out of the gas stream in a section of the combustor from 220°-270° CW ALF for one rake and 270°-300° CW ALF for the other rake. This also was a recurring problem related to the degree of eccentricity and out-of-roundness of the test rig and traverse ring hardware. Cost and time considerations prohibited obtaining a proper solution to the latter problem.

The exit temperature traverse data obtained required refinement to eliminate the effects of these problem areas. Average and peak profiles determined at the simulated sea level takeoff operating conditions are presented in Figure 206. As observed from this figure, the design average profile was closely approached at a 50/50 fuel split. The minimum peak profile occurred at a 40/60 fuel split with a pattern factor of 0.275. This compared to a minimum pattern factor of 0.36 obtained for the Mod VI configuration demonstrating the degree of improvement achieved by better quality. Despite the improvement, the pattern factor still exceeded the design goal of 0.250 by 10%. At the 40/60 fuel split, the average profile had a center peaked characteristic slightly exceeding the design limit at the hub. Average and peak profiles determined at the simulated lower power operating conditions are presented in Figure 207. It is observed from this figure that pattern factors of 1.25 would be expected from operation of this combustor design in the pilot only mode. A pattern factor

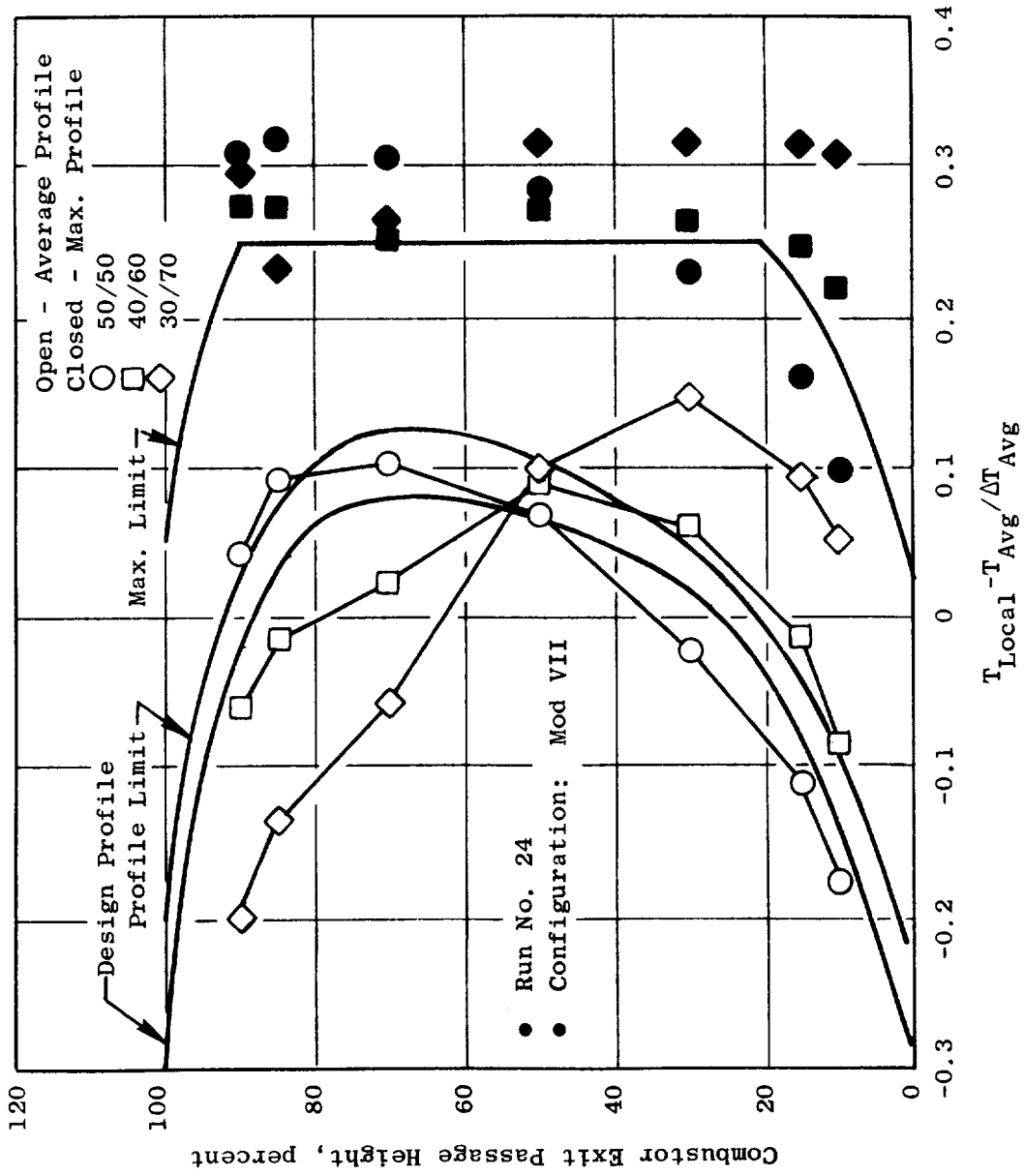


Figure 206. Mod VII EGT Performance Test Results.

level of 1.50 had been previously demonstrated by the Baseline and Mod I combustor configurations at similar operating conditions.

The hardware modifications and refurbishment incorporated into the Mod VII combustor configuration produced significant reductions in pattern factor when compared to results from the Mod VI configuration. Although the results fell slightly short of the design goal, no further hardware modifications intended to provide additional reductions in pattern factor were made. Instead, it was decided to proceed to evaluate this development combustor configuration at true cycle operating conditions for ground start ignition performance and low power emissions at true engine cycle operating conditions.

7.7.3 Emissions Testing

Ignition and emissions testing of the development combustor Mod VII configuration was conducted on 9/15/81 in the AFL Cell A3E test facility. The purpose of this test was to evaluate this combustor design for ground start ignition, crossfire from pilot to main stage domes, and low power emissions characteristics at true engine operating conditions for selected points along the revised (6/81) E³ start cycle operating line and the E³ FPS design cycle operating line. It had been intended to evaluate the combustor for emissions at 30% F_N approach power conditions at slightly derated operating conditions with pilot-to-total fuel splits of 1.0, 0.4, and 0.3. This was required to achieve the desired combustor fuel-air ratio in the pilot only mode of operation using the simplex fuel nozzles selected for use in the outer dome. However, because of problems with the facility operation it was necessary to further derate the approach power test conditions to a maximum inlet total pressure of 0.69 MPa (100 psia) compared to the desired value of 0.90 MPa (130 psia). The engine cycle combustor inlet pressure at this operating condition is 1.21 MPa (175 psia). Test points and corresponding operating conditions are presented in Table XLVII.

Simplex-type fuel nozzles rated at 12 kg/hr (26.5 pph) were used in both the pilot and main stage domes. Because this test was conducted at low power operating conditions, no combustor instrumentation was used.

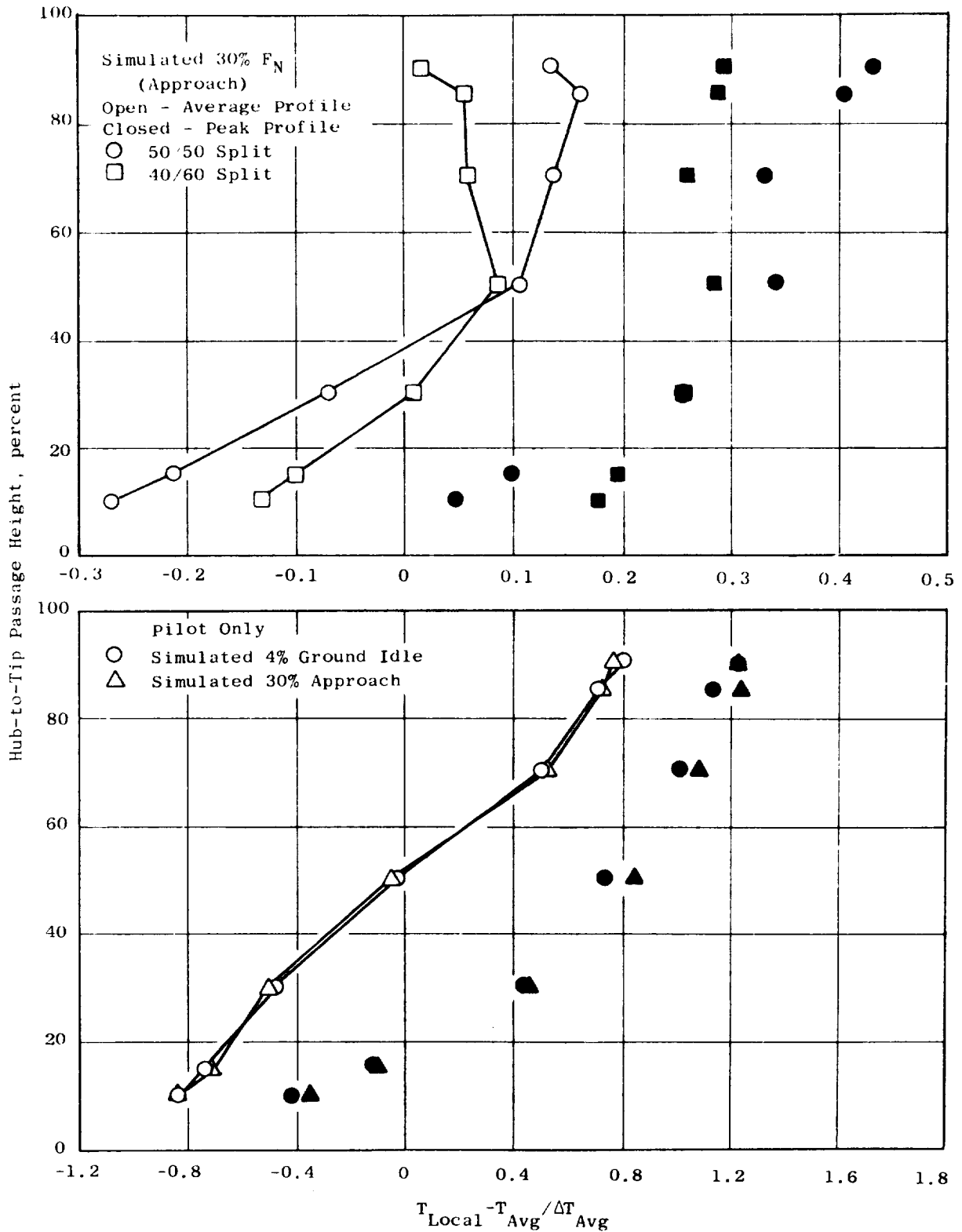


Figure 207. Mod VII EGT Performance Test Results.

ORIGINAL PAGE IS
OF POOR QUALITY

Table XLVII. Mod VII Emissions Test Performance.

Test Point	Operating Condition	T ₃ , K (°F)	P ₃ , MPa (psia)	W ₃ , kg/s (pps)	W _{Blade Outer} , kg/s (pps)	W _{Blade Inner} , kg/s (pps)	W _{Blade Prefir.} , kg/s (pps)	W _{Comb.} , kg/s (pps)	f/a Overall	Wf Total, kg/hr (pph)	Wf Pilot, kg/hr (pph)	Wf Main, kg/hr (pph)	Sampling Mode
1	21 PCNHR	304 (87)	0.112 (16.2)	2.36 (5.2)	0	0	0	2.36 (5.2)					Ignition
2	24.5 PCNHR	310 (98)	0.117 (16.9)	2.81 (6.2)				2.81 (6.2)					Ignition
3	30 PCNHR	322 (120)	0.0125 (18.1)	3.45 (7.6)				3.45 (7.6)					Ignition
4	37 PCNHR	351 (173)	0.161 (23.3)	3.73 (8.2)				3.73 (8.2)					Ignition
5	4% Idle	466 (369)	0.346 (50.2)	8.18 (18.0)				8.18 (18.0)					Ignition
6	6% Idle	492 (426)	0.436 (68.2)	10.41 (22.9)				10.41 (22.9)					Ignition
7	10% Idle	533 (500)	0.396 (86.4)	14.09 (31.0)				14.09 (31.0)					Ignition
8	4% Idle	466 (369)	0.346 (50.2)	9.86 (21.7)	0.57 (1.25)	0.52 (1.15)	0.63 (1.38)	8.19 (17.9)	0.0090	264 (581)	264 (581)	0	G
9	4% Idle	466 (369)	0.346 (50.2)	9.86 (21.7)	0.57 (1.25)	0.52 (1.15)	0.63 (1.38)	8.19 (17.9)	0.0110	323 (710)	323 (710)	0	G
10	4% Idle	466 (369)	0.346 (50.2)	9.86 (21.7)	0.57 (1.25)	0.52 (1.15)	0.63 (1.38)	8.19 (17.9)	0.0127	372 (819)	372 (819)	0	G, I
11	4% Idle	466 (369)	0.346 (50.2)	9.86 (21.7)	0.57 (1.25)	0.52 (1.15)	0.63 (1.38)	8.19 (17.9)	0.0150	440 (968)	440 (968)	0	G
12	4% Idle	466 (369)	0.346 (50.2)	9.86 (21.7)	0.57 (1.25)	0.52 (1.15)	0.63 (1.38)	8.19 (17.9)	0.0200	586 (1290)	586 (1290)	0	G
13	6% Idle	492 (426)	0.436 (63.2)	12.50 (27.5)	0.72 (1.58)	0.66 (1.45)	0.80 (1.75)	10.32 (22.7)	0.0080	297 (654)	297 (654)	0	G
14	6% Idle	492 (426)	0.436 (63.2)	12.50 (27.5)	0.72 (1.58)	0.66 (1.45)	0.80 (1.75)	10.32 (22.7)	0.0100	371 (817)	371 (817)	0	G
15	6% Idle	492 (426)	0.436 (63.2)	12.50 (27.5)	0.72 (1.58)	0.66 (1.45)	0.80 (1.75)	10.32 (22.7)	0.0116	431 (948)	431 (948)	0	G, I
16	6% Idle	492 (426)	0.436 (63.2)	12.50 (27.5)	0.72 (1.58)	0.66 (1.45)	0.80 (1.75)	10.32 (22.7)	0.0150	557 (1226)	557 (1226)	0	G
17	6% Idle	492 (426)	0.436 (63.2)	12.50 (27.5)	0.72 (1.58)	0.66 (1.45)	0.80 (1.75)	10.32 (22.7)	0.0200	743 (1634)	743 (1634)	0	G
18	30% Idle	640 (692)	0.896 (130.0)	23.45 (51.6)	1.37 (2.94)	1.23 (2.71)	1.48 (3.26)	19.41 (42.7)	0.140	978 (2152)	978 (2152)	0	G
19	30% Idle	640 (692)	0.896 (130.0)	23.45 (51.6)	1.37 (2.94)	1.23 (2.71)	1.48 (3.26)	19.41 (42.7)	0.140	978 (2152)	978 (2152)	587 (1291)	G
20	30% Idle	640 (692)	0.896 (130.0)	23.45 (51.6)	1.37 (2.94)	1.23 (2.71)	1.48 (3.26)	19.41 (42.7)	0.140	978 (2152)	978 (2152)	585 (1291)	G

As anticipated, significant improvement in both the pilot stage ignition and main stage crossfire characteristics was demonstrated at true cycle operating pressures as compared to previous atmospheric test results obtained with the Mod VI configuration. As observed from Figure 208, the pilot stage ignition satisfies the E³ (6/81) start cycle fuel schedule with considerable margin at corrected core speeds above 30%. However, it appears unlikely that crossfire and full propagation of the main stage would be accomplished within the start cycle fuel schedule at subidle operating conditions. The main stage did demonstrate sufficient lean blowout margin to assure that once fully propagated, the main stage would remain fully propagated at subidle operating conditions.

The results of the idle emissions testing of the Mod VII combustor configuration are presented in Figure 209. Measured emissions data obtained in the vicinity of Swirl Cup No. 28 (324° CW ALF) showed signs of poor combustion, yielding high levels of CO and HC emissions. A posttest inspection of the fuel nozzles revealed the presence of leaks in both the pilot and main stage nozzle tips that were located at Cup No. 28 position. The leaks appeared related to deteriorated seal rings between the nozzle tips and the mounting stems. Emissions data measured in this vicinity were factored out of the results.

As observed from Figure 209, significant reductions in CO emissions were achieved compared to levels previously demonstrated with the Mod I configuration. At the 6% design idle operating condition, a CO level of 23.3 g/kg (23.3 lb/1000 lb) of fuel was obtained. This closely approached the program target level of 20.7 g/kg (20.7 lb/1000 lb) of fuel. A minimum level of 20 g/kg (20 lb/1000 lb) of fuel was achieved at slightly off-design combustor fuel-air ratio of 0.0129, compared to the design cycle fuel-air ratio of 0.0116. Hydrocarbon emissions were nearly identical to levels previously demonstrated with the Mod I configuration. An HC emissions level of 4.5 g/kg (4.5 lb/1000 lb) of fuel was obtained at the 6% design idle operating condition. The program target level at this operating condition is a level of 2.8 g/kg (2.8 lb/1000 lb) of fuel. HC levels at or below this target level were demonstrated at 6% ground idle operating conditions at overall fuel-air ratios greater than 0.015. CO and HC emissions data obtained at the derated approach power operating condition (30% F_N), were adjusted to correct for the low inlet total

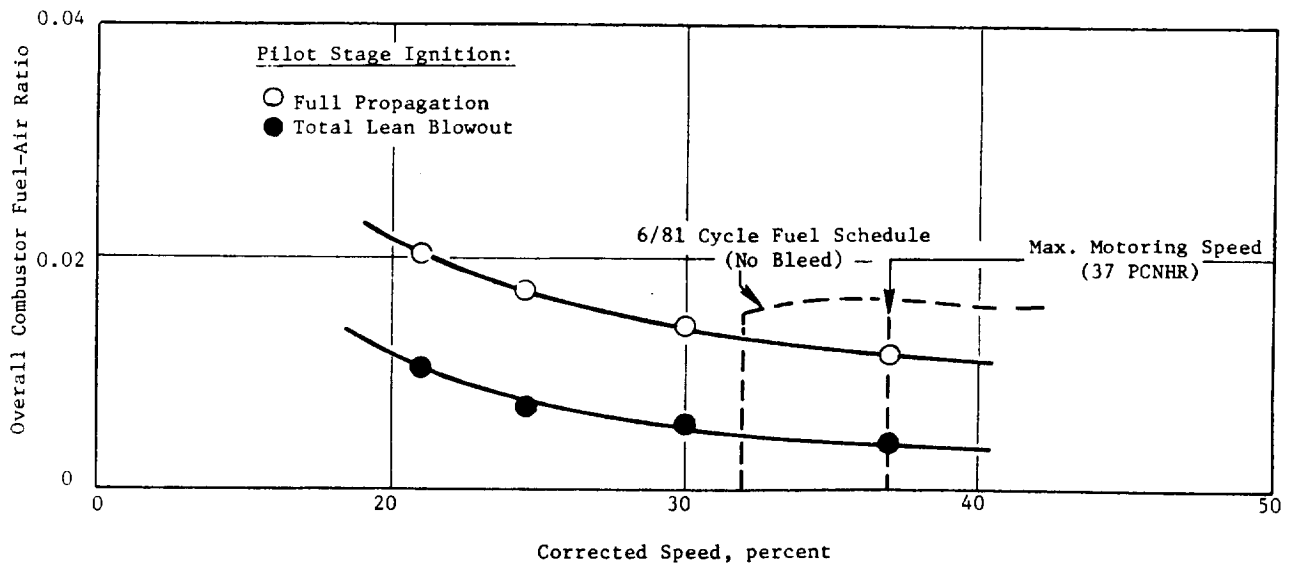
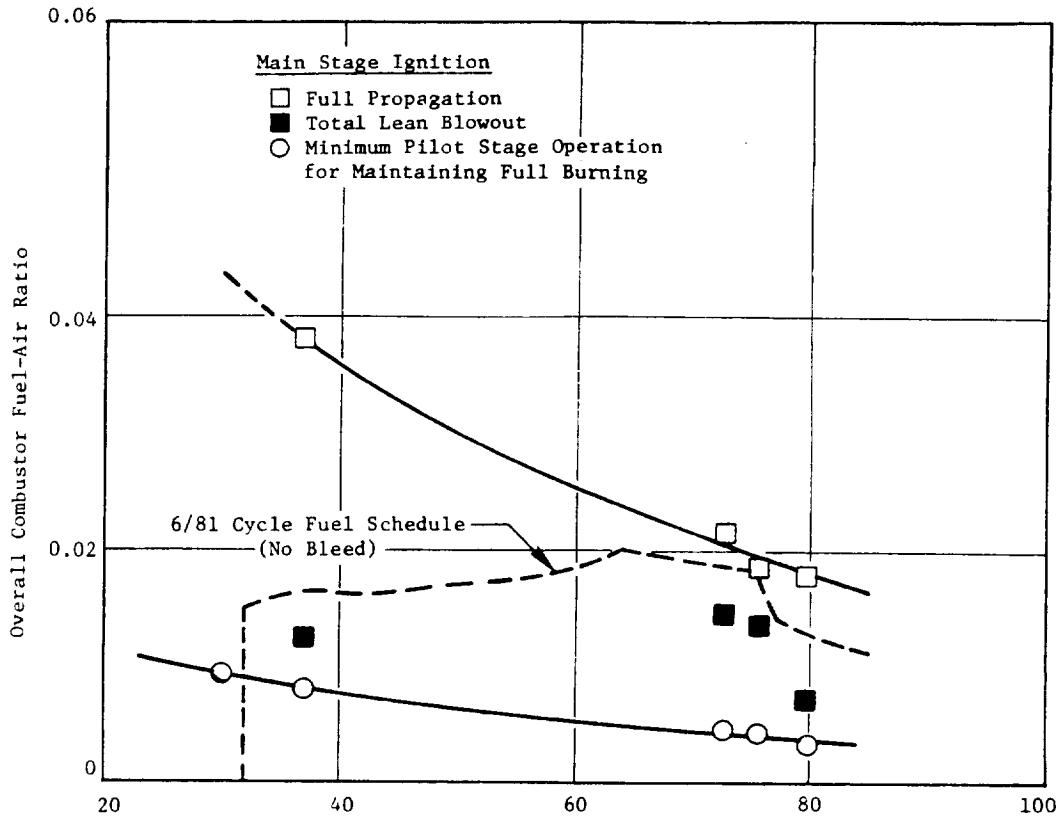


Figure 208. Mod VII Ignition Results at True Cycle Conditions.

ORIGINAL PAGE IS
OF POOR QUALITY

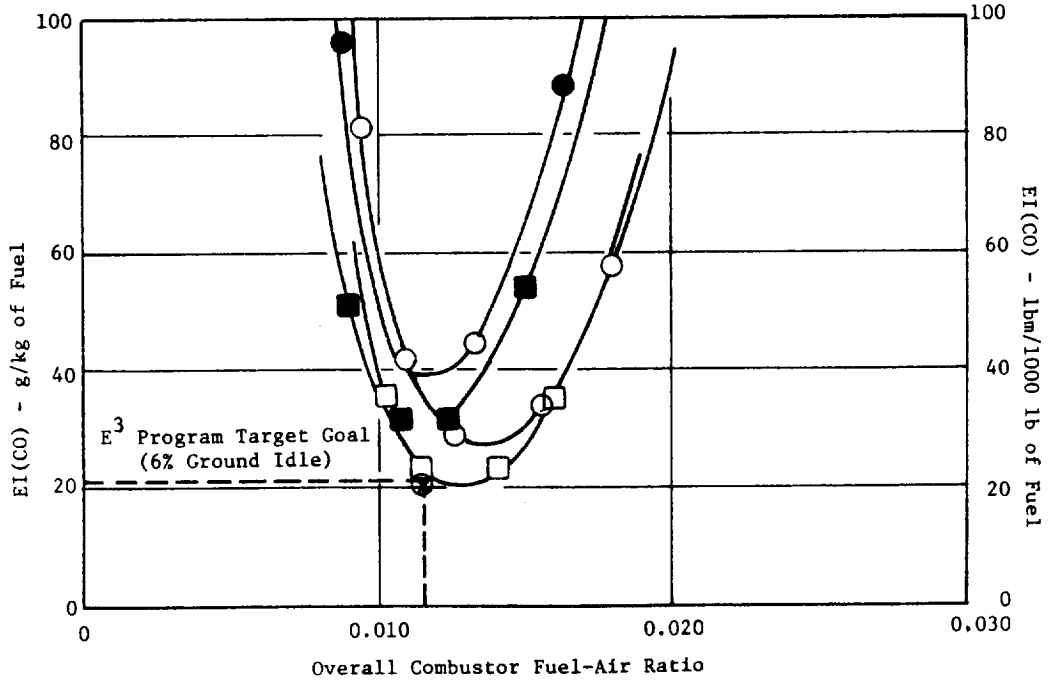
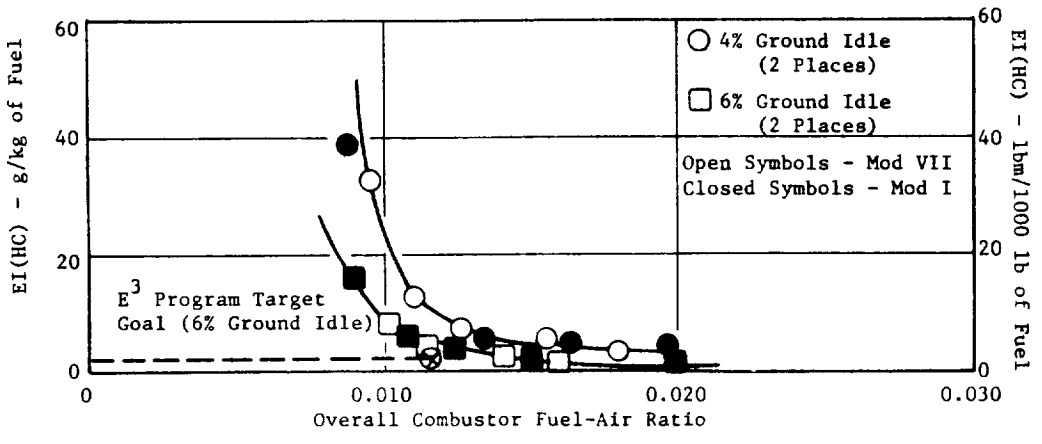


Figure 209. Mod VII Emissions Test Results.



pressures. The results (presented in Table XLVIII) show that very low levels of CO and HC emissions were demonstrated in the pilot only operating mode. However, significantly higher levels resulted for the staged operating modes. These results are similar to those previously obtained for the Baseline and Mod I development combustor configurations evaluated at similar conditions. As previously suggested, the reason for the high CO and HC emissions levels is related to the low design cycle fuel-air ratio of 0.014 at this operating condition which produces two very lean domes in the staged operating mode.

Table XLVIII. Mod VII Emissions Results at Approach Power.

<u>Combustor Operating Mode</u>	<u>Emission Index</u>		
	<u>g/kg (lb/1000 lb) Fuel CO</u>	<u>HC</u>	<u>NO_x</u>
Pilot Only	2.9 (2.9)	0.4 (0.4)	10.7 (10.7)
40/60 Split	54.0 (54.0)	22.9 (22.9)	2.7 (2.7)
30/70 Split	56.0 (56.0)	40.7 (40.7)	2.2 (2.2)

NO_x emission data obtained at the derated approach power operating conditions were also adjusted to the correct operating conditions.

The results for the three pilot-to-total fuel splits are also presented in Table XLVIII. As would be expected, the lean combustion conditions associated with fuel staging yields very low levels of NO_x, while the pilot only operating mode yields levels considerably higher. In Figure 210, the measured NO_x emission levels obtained in the staged operating mode are plotted against the E³ design cycle severity parameter. Also shown in this figure are measured data obtained from the Baseline and Mod I combustor configurations. It is observed from this figure that the NO_x emission characteristic of the

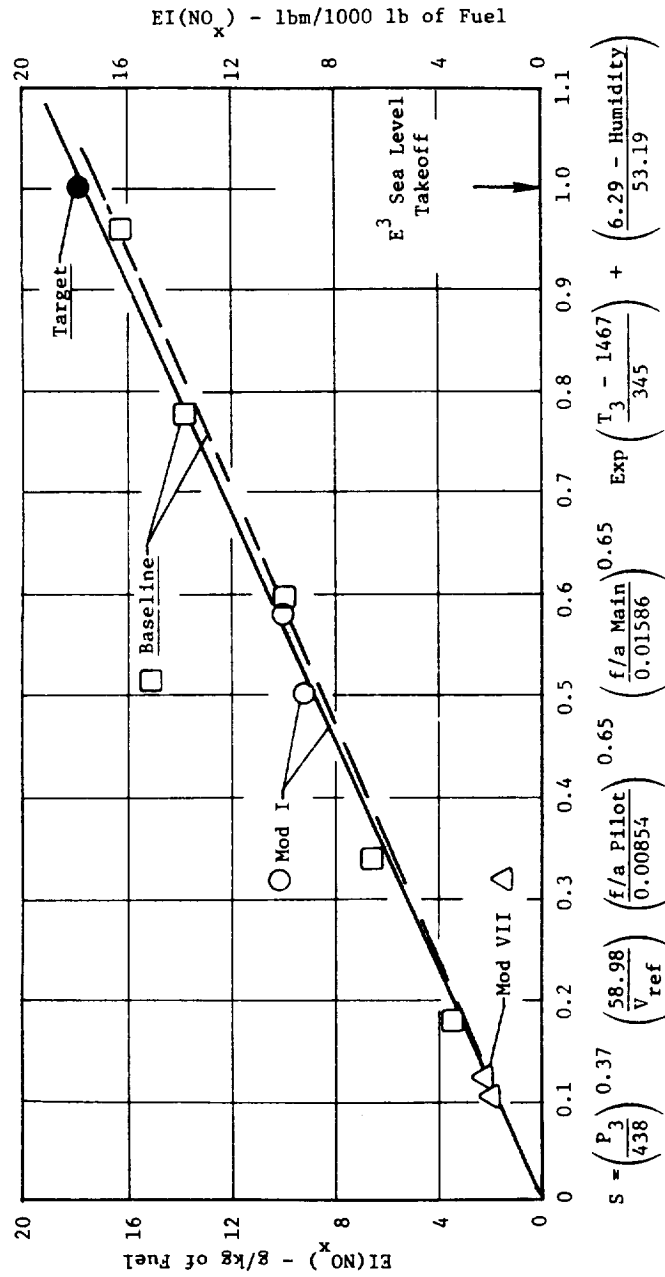


Figure 210. Mod VII Emissions Test Results.

Handwritten mark

Mod VII configuration appears to be very similar to the characteristics demonstrated by the other configurations. Therefore, NO_x emission levels at sea level takeoff operating conditions similar to the other two configurations would be anticipated. Both the Baseline and Mod I combustors demonstrated NO_x levels that satisfied the E³ Program goal.

EPA parameter numbers, based on the EPA landing/takeoff cycle for CO, HC, and NO_x were generated for combustor operation at 6% ground idle and pilot-to-total fuel splits of 1.0 and 0.35 at the approach power operating condition. The results are presented in Table XLIX and are compared to the E³ Program goals for the three emissions categories. As observed from this table, the NO_x emission levels satisfy the program goal with pilot only or staging at the approach power operating condition. However, both the CO and HC emissions levels fail to meet the respective program goals with either operating mode. With the pilot only operating mode, the CO emissions closely approach the goal, while reductions greater than 30% are required for the HC emissions. Significantly greater reductions in both CO and HC emissions are required to satisfy the program target goals for staged combustor operation at approach.

Table XLIX. Mod VII EPAP Results.

	lb-Emission/1000 lb Thrust-Hr-Cycle E ³		
	<u>Pilot Only</u> <u>At Approach</u>	<u>35/65 Split</u> <u>at Approach</u>	<u>Program</u> <u>Goals</u>
Carbon Monoxide	3.27	6.40	3.00
Hydrocarbons	0.58	2.48	0.40
Oxides of Nitrogen	2.96	2.51	3.00

7.7.4 Concluding Remarks

The Mod VII combustor configuration evolved from this test series represented the final E³ development combustor design configuration. This configuration succeeded in demonstrating excellent pilot stage ignition characteristics, acceptable exit temperature performance, and emissions which meet

NO_x or closely approach CO and HC, the combustor development program emissions goals. Like earlier lean main stage designs evaluated in this development program, the main stage ignition characteristics are not good enough to allow staging at subidle operating conditions. However, this should pose no problem in actual engine operation since modifications in the ground start operating cycle permit tolerable starts to idle power with the pilot only staging mode.

Studies conducted on E³ swirl cup hardware have indicated the potential to achieve improvement in the main stage ignition characteristics by adjusting the secondary to primary swirler area ratio. Other studies conducted as part of the E³ sector combustor subcomponent testing have demonstrated a significant impact of fuel nozzle design on emissions performance. Using fuel nozzles with wider spray angles and better atomization (than obtained with the development combustor fuel nozzles) produced significant reductions in CO and HC emissions at idle operating conditions. Thus, improvements in swirl cup design and in fuel nozzle design have the potential to provide improvement in the main stage ignition characteristics, as well as reduce the CO and HC emissions to levels sufficient to satisfy the program goals.

7.8 ENGINE COMBUSTOR TEST RESULTS

The E³ double-annular engine combustor design features a fuel rich pilot stage and a fuel lean main stage with an airflow distribution similar to that evolved in the slave Mod VII development combustor configuration. The engine combustor features the same internal aerodynamic flowpath as the development combustor. The hardware design used in the domes and centerbody assembly is the same as that used in the development combustor. However, the liners are a double-wall film plus impingement-cooled segment shingle design.

7.8.1 Atmospheric Ground Start Ignition Test

Ground start ignition evaluation of the E³ core engine combustor was conducted in the ACL Cell A3W facility on 10/28/81. The purpose of the test was to evaluate the ignition, crossfire, and lean blowout characteristics of this combustor design at selected steady-state operating points along the E³ 6/81 ground start cycle. For the purposes of main stage crossfire, data was

also obtained at simulated steady-state conditions representing 4%, 6%, 10%, and 30% of full rated thrust along the E³ FPS operating line. Test point and corresponding operating conditions are presented in Table L.

Fuel was supplied to the combustor using the E³ test rig fuel nozzle assemblies incorporating simplex nozzle tips rated at 12 kg/hr (26.5 pph) in both the pilot and main stage. The ignition system was the standard GE23 ignition system used in all previous development combustor testing. The igniter was located at 240° CW ALF, immersed flush with the inside shingle wall of the pilot stage.

Test results from this ignition evaluation are presented in Figure 211. From this figure it is observed that the core engine combustor pilot stage ignition and lean blowout characteristics are considerably better than those demonstrated with the Mod VII development combustor configuration. These ignition and blowout characteristics will satisfy the E³ ground start cycle fuel schedule requirements with and without bleed. Even greater margin is expected at actual cycle inlet pressures. The figure also shows that cross-fire and full propagation (staging) of the core engine combustor main stage required overall combustor fuel air ratios well above the fuel schedule defined in the E³ FPS steady-state operating cycle. This is typical of past experience of development combustor configurations featuring lean main stage dome designs. Improvements anticipated at actual cycle inlet pressures would not be sufficient to permit staging at subidle or idle operating conditions. The lean blowout characteristics for the main stage generally fall below the FPS cycle fuel schedule. It is, therefore, possible to achieve staged combustor operation at the low power operating conditions by initially accelerating the engine to a power level where staging can be accomplished within the cycle fuel schedule, then decelerating down to the desired power operating condition.

As part of this test, a dynamic ignition evaluation was conducted on the pilot and main stage. This was an attempt to determine the time required to achieve ignition and full propagation while simulating the engine fuel scheduling as a function of core speed. The pilot stage was evaluated at the simulated 30 PCNHR test condition. A constant fuel flow level of 157 kg/hr (345

Table L. Engine Combustor Atmospheric Ignition Test Point Schedule.

Test Point	PCNHR	P3, atm	T3, K (° F)	W36, kg/s (pps)	Comments
1(a)	21.0	1.00	303 (87)	2.19 (4.82)	Simulated No Bleed, 6/81
2(a)	21.0	1.00	303 (87)	2.10 (4.61)	Simulated Bleed, 6/81
3(a)	24.5	1.00	310 (98)	2.50 (5.50)	Simulated No Bleed, 6/81
4(a)	24.5	1.00	310 (98)	2.38 (5.24)	Simulated Bleed, 6/81
*5(a)	30.0	1.00	322 (120)	2.86 (6.30)	Simulated No Bleed, 6/81
*6(a)	30.0	1.00	322 (120)	2.75 (6.06)	Simulated Bleed, 6/81
7(a)	36.9	1.00	339 (150)	3.20 (7.05)	Simulated No Bleed, 6/81
8(a)	36.9	1.00	339 (150)	3.12 (6.87)	Simulated Bleed, 6/81
*9	4% Fn	1.00	466 (379)	2.40 (5.29)	FPS II Cycle
*10	64.3	1.00	483 (410)	2.29 (5.03)	6/81 Cycle
*11	6% Fn	1.00	495 (432)	2.44 (5.36)	FPS II Cycle
*12	10% Fn	1.00	539 (510)	2.42 (5.33)	FPS II Cycle
*13	30% Fn	1.00	637 (687)	2.25 (4.94)	FPS II Cycle

NOTE:

(a) Core engine motoring combustor inlet conditions (no fuel)

*Ignition characteristics of main stage to be investigated

- Subidle Conditions from 6/81 Start Cycle
- Higher Power Condition from FPS-II Cycle
- Standard Day
- Atmospheric Inlet Pressure
- 44.2 cm² (6.85 in²)

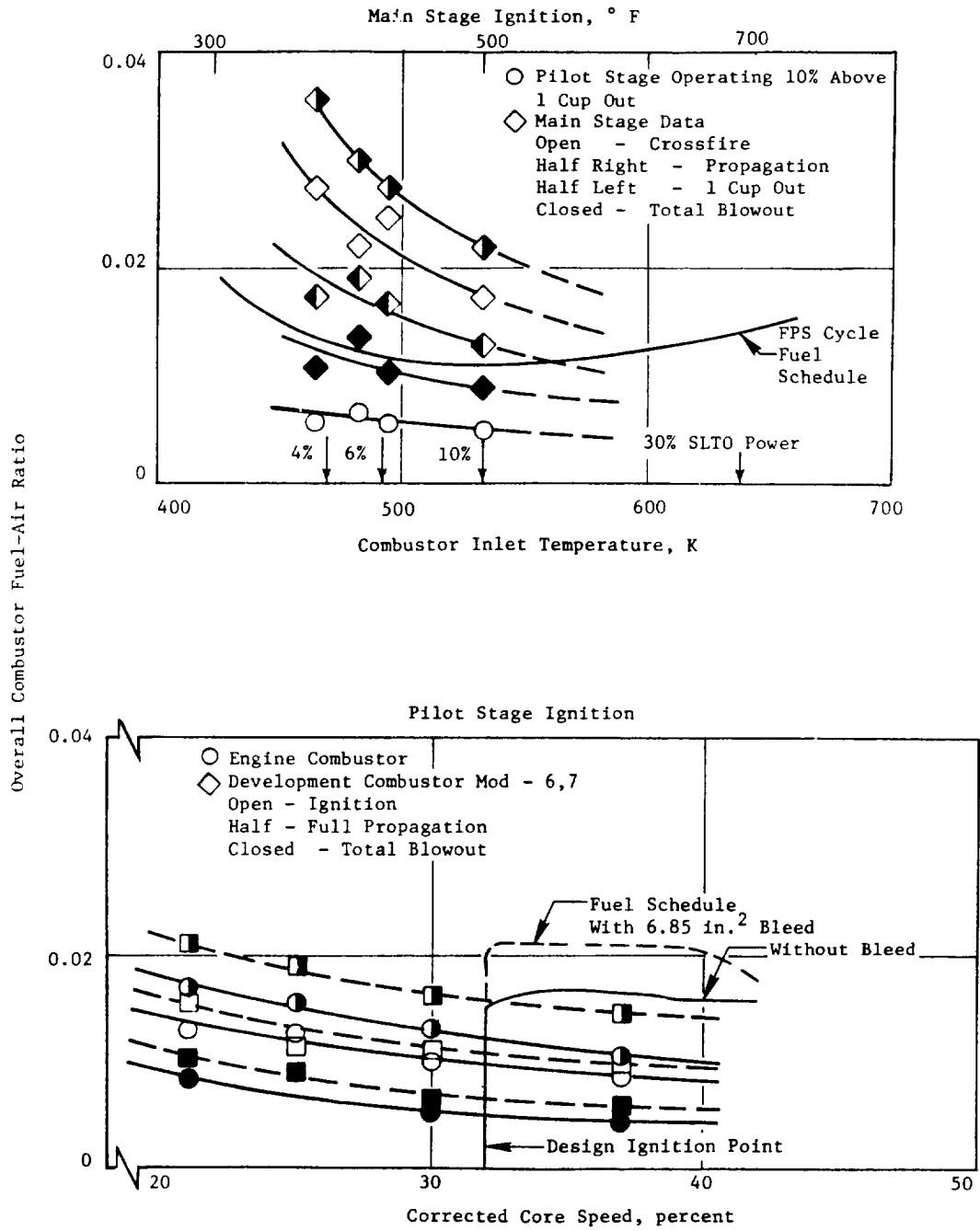


Figure 211. Engine Combustor Atmospheric Ignition Test Results.

dph) was preset in the pilot stage fuel system. The manifold, pigtails, and nozzles were then purged of fuel to simulate a dry start. The igniter was activated, and the pilot stage shutoff valve opened to introduce the surge of fuel. A time of 11 seconds was required to achieve full propagation once the valve was opened. The main stage was evaluated at the simulated 6% and 10% power test conditions. The pilot stage was ignited and set to a fuel flow level of 66 kg/hr (145 pph). Constant fuel flow levels of 168 kg/hr (370 pph) and 145 kg/hr (320 pph) were respectively preset in the main stage at the 6% and 10% power operating conditions. These were sufficient to achieve full propagation as determined from the ignition data. The main stage system was purged of fuel. The shutoff valve was opened sending the surge of fuel to the main stage. This sudden surge caused a slight reduction in the pilot fuel flow level, but did not cause any cups to blow out. At the simulated 6% power operating condition, a time of 10 seconds were required to achieve full main stage propagation. At the simulated 10% power operating condition, 15 seconds were required to achieve full main stage propagation. This delay time of 10-15 seconds could pose a problem during actual engine operation. During an accel and staging maneuver, the majority of the total engine flow is diverted to the main stage for crossfire, causing the pilot stage to lean considerably, reducing the overall energy output of the combustor, possibly resulting in a loss in engine speed. To minimize this crossfire delay time, the engine fuel control system will be set so that the engine main stage fuel system is completely filled with fuel immediately before staging.

7.8.2 Atmospheric Exit Temperature Performance Test

Exit gas temperature performance testing of the engine combustor was conducted in the ACL Cell A3W facility. The purpose of this testing was to evaluate the combustor for pattern factor and average profile characteristics at test conditions simulating sea level takeoff power, 30% approach power, and 6% ground idle. Test points and corresponding operating conditions are presented in Table LI.

Prior to this test, the thermocouple rakes were modified such that the elements were spaced uniformly across the radial annulus. All four rakes were positioned radially outward approximately 0.04 in. from the exit annulus centerline to accommodate rig thermal growth during the tests. The element tips

were axially positioned approximately 12.7 cm (0.50 in.) from the trailing edge of outer liner Panel 3 shingle row, to be in the same plane as the leading edge of the turbine nozzle vanes.

Exit gas temperature performance of the core engine combustor was initiated on 11/5/81. For this test run, simplex nozzle tips rated at 6.4 kg/hr (14 pph) were installed in both the pilot and main stage. Visual observations at the combustor exit revealed that several cups were extinguished in the pilot and main stage domes in the top half of the annulus at simulated sea level takeoff operating conditions. Several attempts at varying fuel splits to the pilot and main stages to achieve cup ignition were unsuccessful. Variations in inlet temperature and airflow were also investigated and found to influence the combustion performance of cups in question. If the inlet temperature was lowered to 589 K (600° F), then all cups would burn. If the airflow and fuel flow were increased by approximately 20%, all cups would burn at the high inlet temperature associated with the sea level takeoff operating condition. Unfortunately, during the investigation period, many of the rake thermocouple elements were lost so no meaningful exit temperature data was obtained.

It was concluded that the problem was related to fuel vaporization within the fuel manifold and nozzle assemblies. Using the fuel nozzle tips selected for the performance testing, the low fuel flows specified at some of the test points resulted in low system fuel pressures. This was especially true in the pilot system where measured fuel pressures were below 0.07 MPa (10 psi) at some test points. These low pressures coupled with the high operating temperatures in the test rig could have caused a vaporization problem with the Jet A fuel used.

Performance testing was resumed on 11/10/81. No changes in fuel nozzle or combustor hardware were made. Insulating material was wrapped around the pilot and main stage fuel manifolds, and around the fuel pigtailed to help shelter the fuel system from exposure to thermal radiation from the hot test rig. Despite the application of the insulation, the same nonburning cup problems were encountered as in the previous test. It was also visually

Table LI. Engine Combustor Atmospheric EGT Performance Test Point Schedule.

Test Point	T3, K (° F)	P3, Atm.	W3, kg/s (pps)	Wbleed, kg/s (pps)	Wcomb, kg/s (pps)	f/a	WF Pilot, WF Total	WF Total, kg/hr(pph)	WF Pilot, kg/hr (pph)	WF Main, kg/hr (pph)	No. of Traverse Positions
1	815 (1007)	1.0	2.41 (5.31)	0.15 (0.34)	2.26 (4.97)	0.0245	0.3	198 (436)	60 (131)	139 (306)	60
2	815 (1007)	1.0	2.41 (5.31)	0.15 (0.34)	2.26 (4.97)	0.0245	0.4	198 (436)	80 (175)	119 (262)	60
3	815 (1007)	1.0	2.41 (5.31)	0.15 (0.34)	2.26 (4.97)	0.0245	0.5	198 (436)	99 (218)	99 (218)	60
4	637 (687)	1.0	2.58 (5.68)	0.16 (0.36)	2.42 (5.32)	0.0143	0.4	125 (274)	50 (110)	75 (164)	60
5	637 (687)	1.0	2.58 (5.68)	0.16 (0.36)	2.42 (5.32)	0.0143	0.5	125 (274)	62 (137)	62 (137)	60
6	637 (687)	1.0	2.58 (5.68)	0.16 (0.36)	2.42 (5.32)	0.0143	1.0	125 (274)	62 (137)	62 (137)	60
7	495 (432)		2.60 (5.72)	0.16 (0.36)	2.44 (5.36)	0.0123	1.0	108 (237)	108 (237)	0	60
8	495 (432)		2.60 (5.72)	0.16 (0.36)	2.44 (5.36)	0.020	0.5	175 (386)	88 (193)	88 (193)	60

observed that several pilot stage swirl cups had very low fuel flow as evidenced by weak flames. The performance test was terminated, and a posttest calibration of the pilot and main stage nozzle tips was conducted. The results of this calibration identified five pilot stages and one main stage nozzle tip which had evidence of flow restrictions, confirming the observations. The restrictions were believed to result from fuel coking within the nozzle body and directly linked to the fuel vaporization problem.

Performance testing of the core engine combustor was continued on 11/19/81. For this test run, fuel nozzle tips in the pilot stage were replaced with higher pressure drop simplex tips. This change was made to increase manifold pressure, eliminating the fuel vaporation and coking problem experienced in the previous two test runs, and to provide improved fuel atomization in the pilot stage to better simulate actual engine operations. The coked-up nozzle tip in the main stage was replaced with another of that type. The higher-pressure nozzle tips were not used in the main stage because the maximum fuel flow rate obtainable with these nozzles and facility pump capacity is lower than flow levels specified for the main stage at several of the test points. With this nozzle change, the fuel vaporization problem was eliminated, and good exit gas temperature data was obtained.

Exit temperature performance results for the E³ core engine combustor at sea level takeoff operating conditions are presented in Figures 212-214. As observed from these figures, a pattern factor of 0.24 was demonstrated at a 40/60 pilot-to-main stage fuel split. This satisfied the E³ combustor development program target goal of 0.25. The maximum profile is relatively flat indicating an acceptable stoichiometric balance between the pilot and main stage at this fuel split. Pattern factors considerably above the target goal were demonstrated at pilot-to-main stage fuel splits of 50/50 and 30/70.

The average profile demonstrated at the 50/50 fuel split is generally within the design limit and has an outboard peaked characteristic. At the 40/60 fuel split, the average profile is center peaked with a profile factor of 0.11 which is within the design limit of 0.125. However, the average profile slightly exceeds the design limit from 30% to 50% of the exit annulus height. Exit temperature traverse data in the form of isothermal contours is

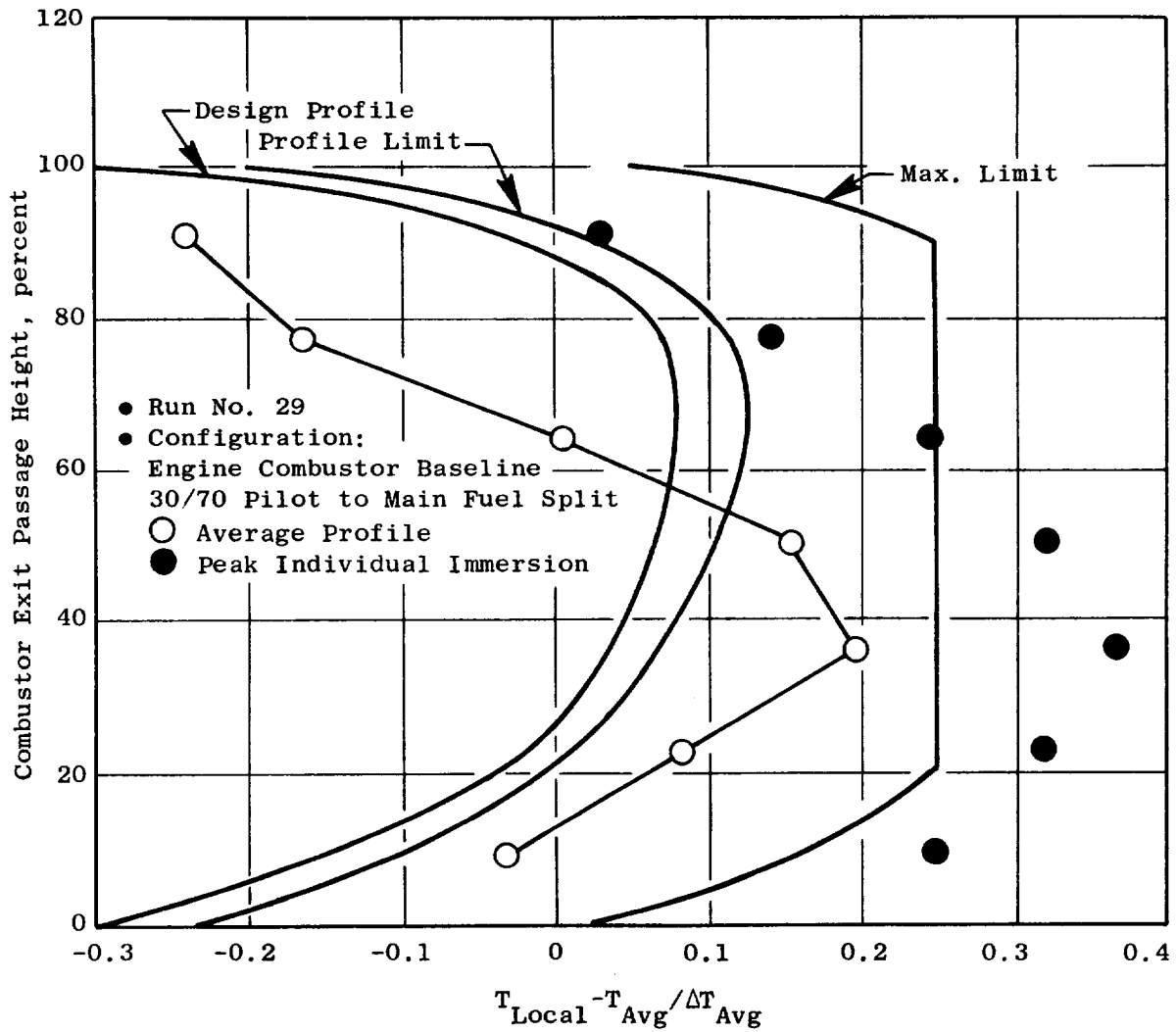


Figure 212. Engine Combustor EGT Performance Test Results.

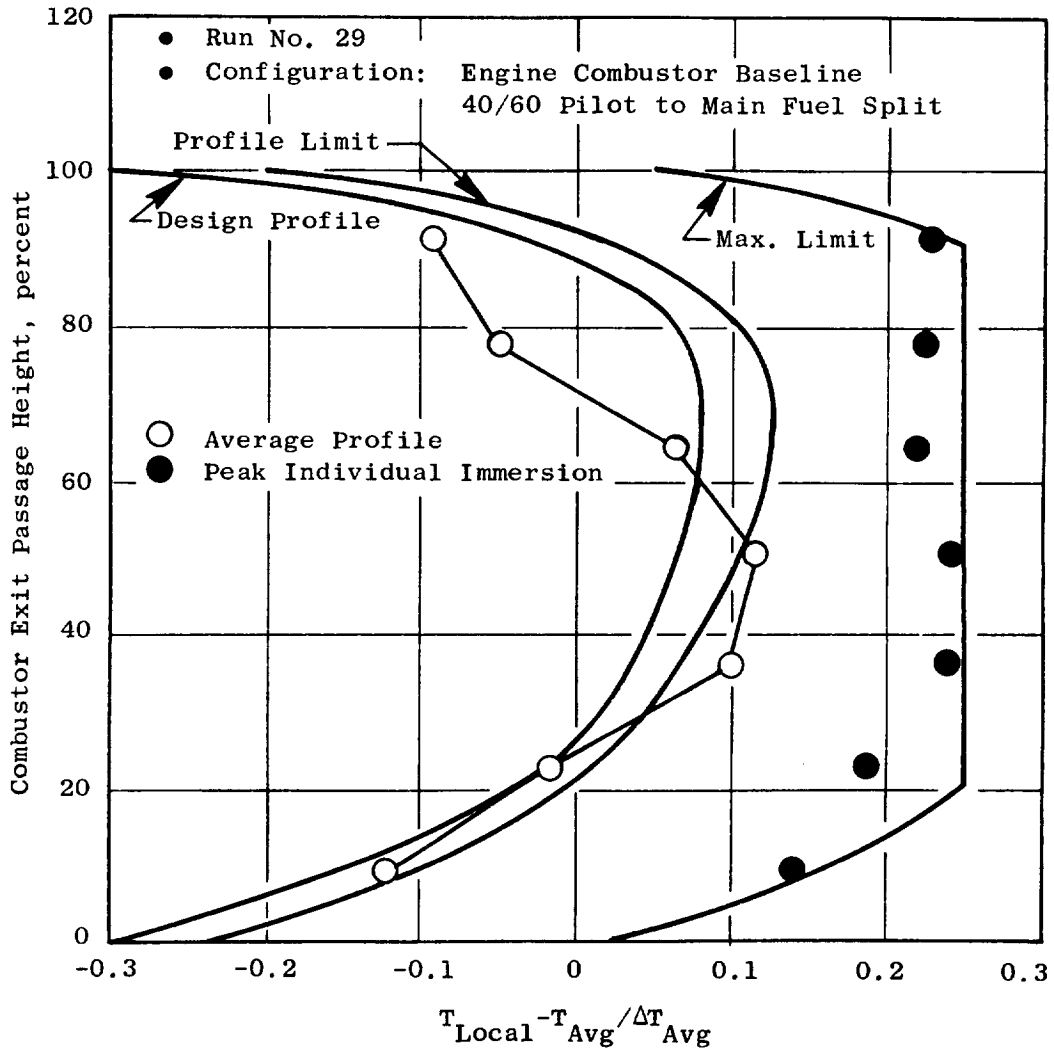


Figure 213. Engine Combustor EGT Performance Test Results.

ORIGINAL PAGE IS
OF POOR QUALITY

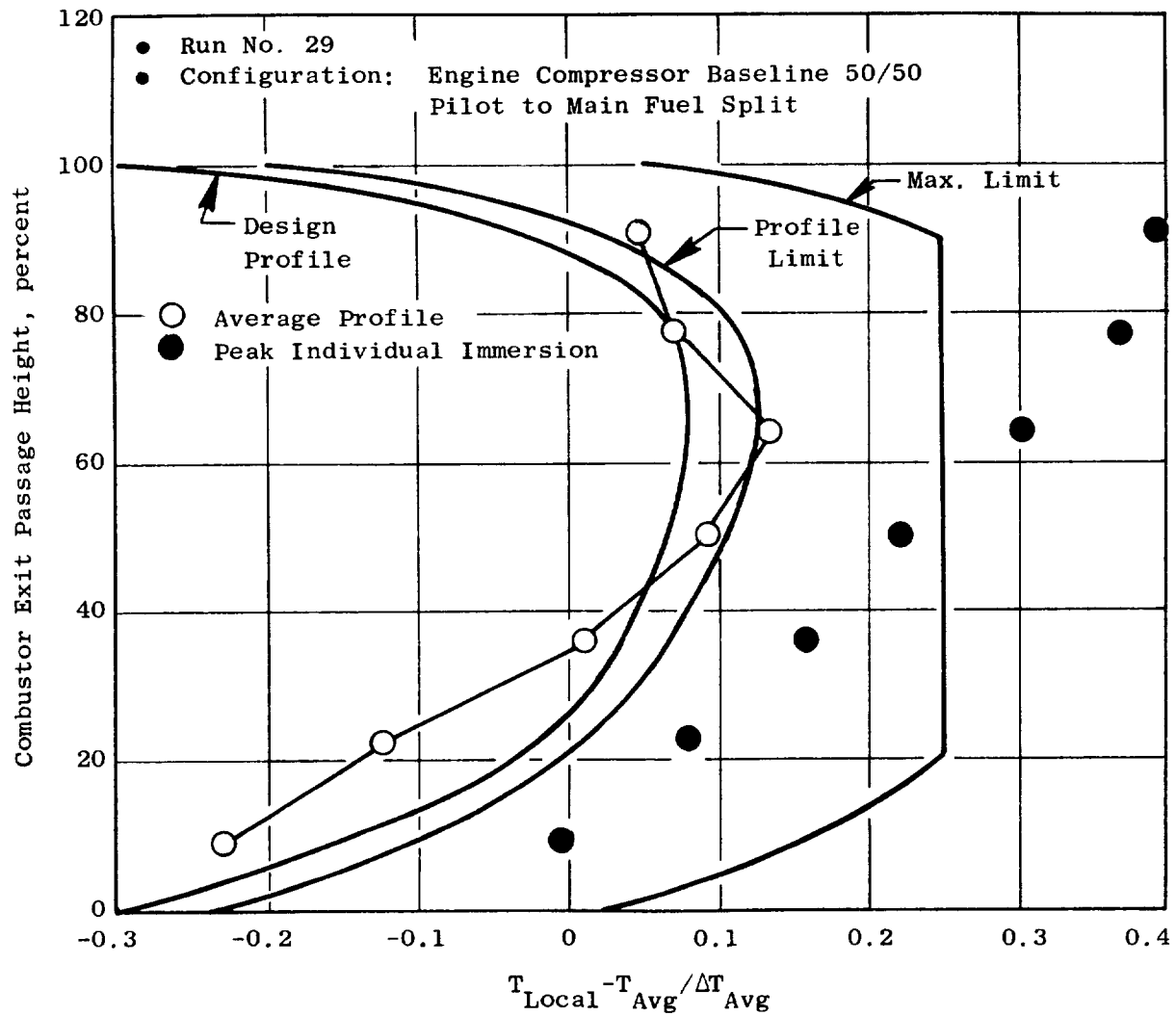


Figure 214. Engine Combustor EGT Performance Test Results.

presented in Figure 215 for the 40/60 pilot to main stage fuel split at simulated sea level takeoff operating conditions.

Average and peak temperature profiles demonstrated at the simulated lower power operating conditions are presented in Figure 216. In the pilot only mode, the combustor demonstrated a pattern factor of 1.23 at the approach power condition and 1.36 at the ground idle condition, 6% of sea level takeoff thrust. As expected, the profiles are sharply outward peaked, and are similar to those demonstrated with the Mod VII development combustor configuration at the same operating conditions. Considerably lower pattern factors were demonstrated in the staged operating mode, illustrating the exit temperature performance advantages of this operating mode. However, as determined from the ground start ignition test results of this combustor, staged operation at idle or subidle conditions may not be possible.

7.8.3 Emissions Test

Emissions testing of the engine combustor was conducted from 2/1/82 through 2/9/82 in the Aero Component Lab (ACL) Cell A3E Testing Facility. As part of this test, the engine combustor was evaluated for ground start ignition, lean extinction, and staging characteristics at true operating conditions for selected points along the revised (6/81) E³ ground start operating line and the E³ FPS design cycle operating line. In addition, this combustor design was evaluated for pressure drop performance, and metal temperature characteristics at selected points from 4% ground idle to simulated sea level takeoff along the E³ FPS design cycle operating line. Additional testing was conducted for the purpose of obtaining a comparison of the CO and HC emissions at ground idle operating conditions obtained between prototype (peanut) fuel nozzles and the standard test rig simplex fuel nozzles. Test points and corresponding operating conditions are presented in Table LII.

Prior to this testing series, several combustor hardware modifications were made to provide increased cooling flow for the centerbody structure. The decision to incorporate these changes into the hardware was based upon visual observations of the combustor made during the open-ended exit temperature performance test. From these observations it was felt that excessively

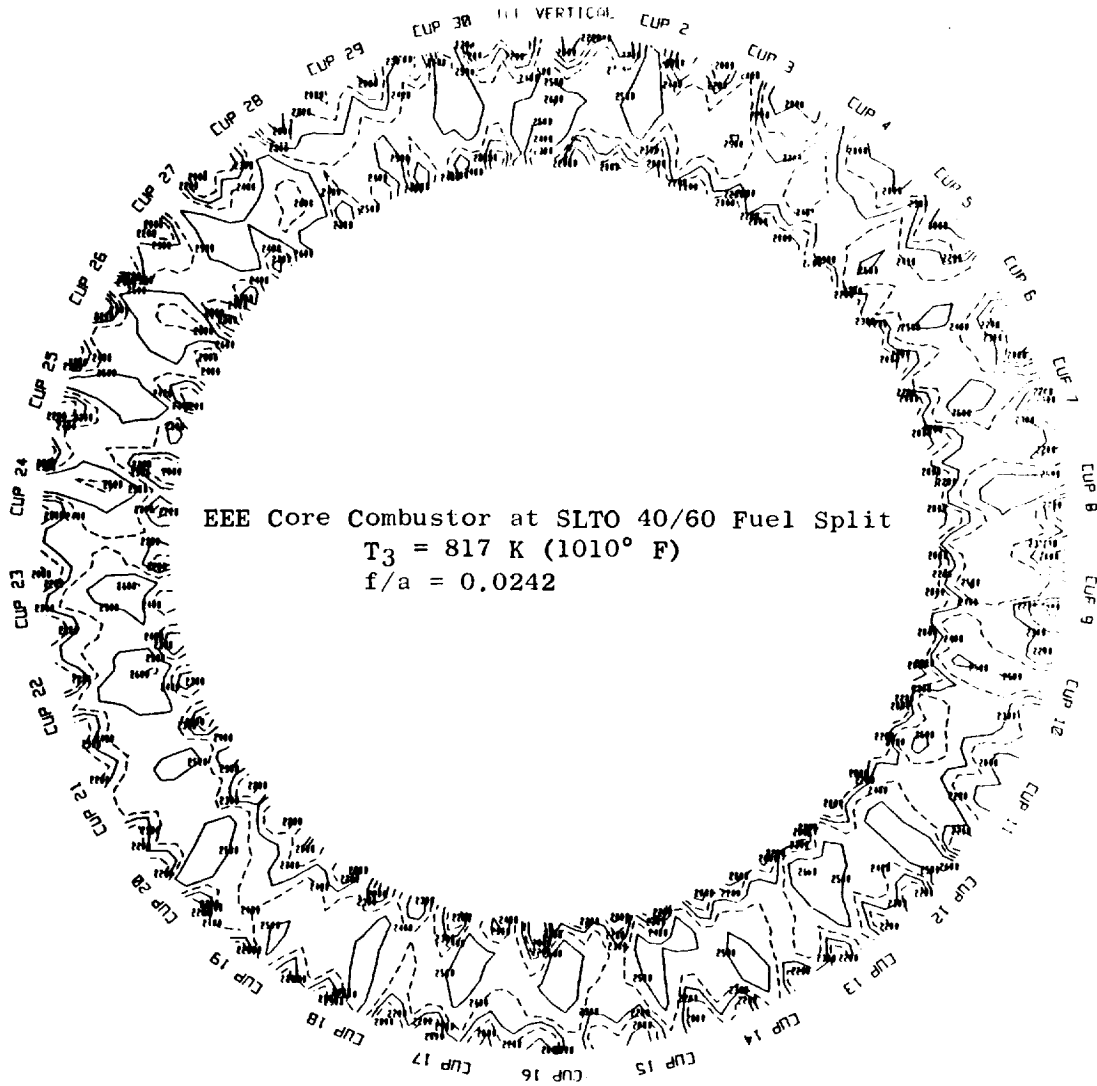


Figure 215. Engine Combustor EGT Performance Test Results.

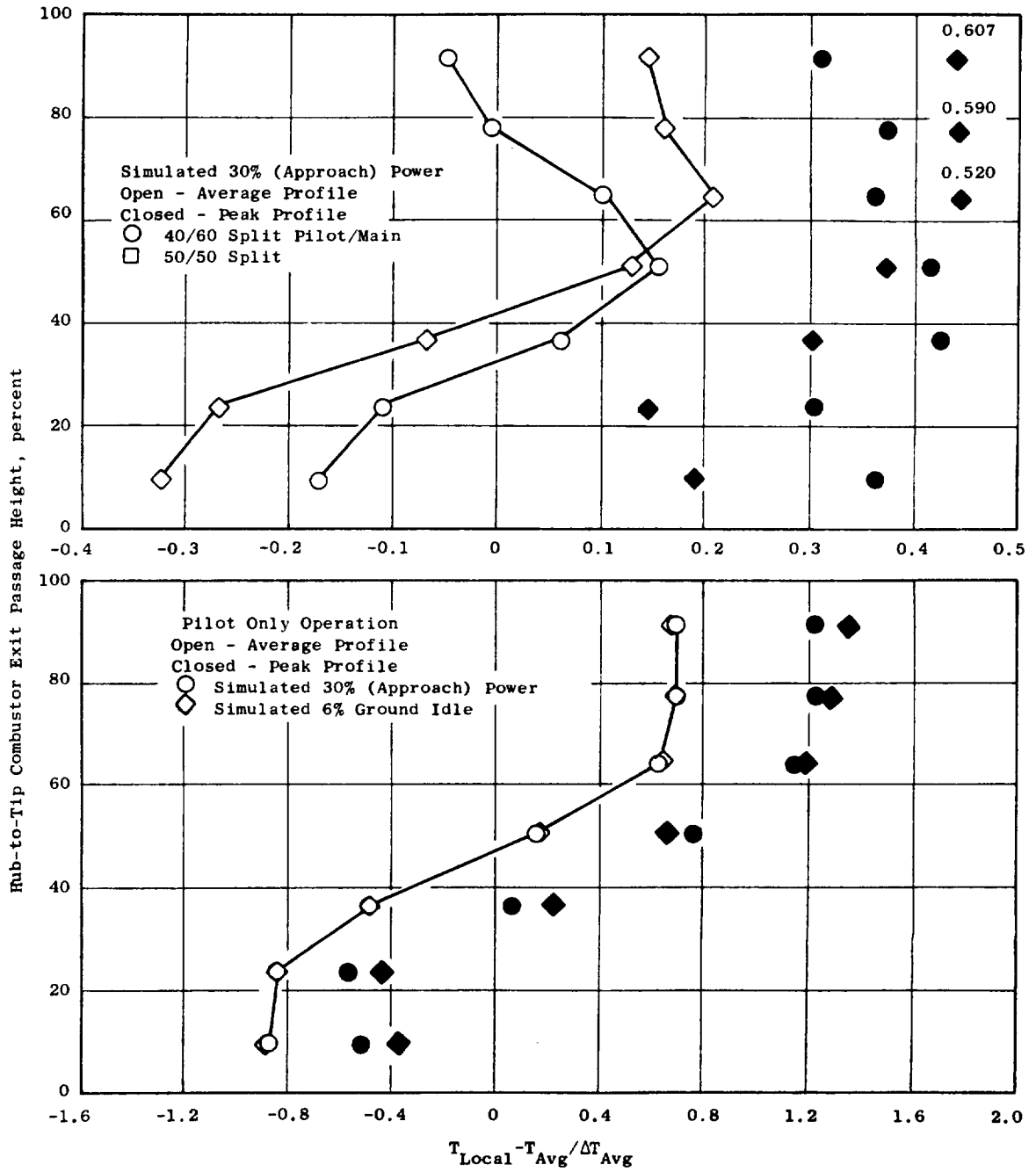


Figure 216. Engine Combustor EGT Performance Test Results.

Table LII. Engine Combustor Emissions Test Point Schedule.

Test Point	Operating Condition	T3, K (°F)	P3, MPa, (psia)	W3, kg/s (pps)	Wblade Outer, kg/s (pps)	Wblade Inner, kg/s (pps)	Wblade Predif, kg/s (pps)	Wc, kg/s (pps)	Overall f/a	WF Total, kg/hr (pph)	Pilot/Total	Wf Pilot, kg/hr (pph)	Wf Main, kg/s (pph)	Sampling Mode
1	21 PCNHR	304 (87)	0.112 (16.2)	2.36 (5.2)	0	0	0	2.36 (5.2)						Ignition
2	24.5 PCNHR	309 (96)	0.117 (16.9)	2.82	0	0	0	2.82 (6.2)						Ignition
3	30 PCNHR	322 (120)	0.125 (18.1)	3.45 (7.6)	0	0	0	3.45 (7.6)						Ignition
4	37 PCNHR	351 (172)	0.161 (23.3)	3.70 (8.2)	0	0	0	3.70 (8.2)						Ignition
5	4X Fn	466 (379)	0.346 (50.2)	8.18 (18.0)	0	0	0	8.18 (18.0)						Ignition
6	6X Fn	492 (426)	0.436 (63.3)	10.41 (23.0)	0	0	0	10.41 (23.0)						Ignition
7	10X Fn	533 (499)	0.596 (86.4)	14.09 (31.1)	0	0	0	14.09 (31.1)						Ignition
8	30X Fn	640 (692)	1.213 (175.9)	25.90 (57.1)	0	0	0	25.90 (57.1)						Ignition
9	4X Fn	466 (379)	0.346 (50.2)	9.86 (21.7)	0.56 (1.24)	0.52 (1.15)	0.60 (1.31)	8.18 (12.0)	0.0090	265 (503)	1.0	265 (503)	0	G, I
10	4X Fn	466 (379)	0.346 (50.2)	9.86 (21.7)	0.56 (1.24)	0.52 (1.15)	0.60 (1.31)	8.18 (12.0)	0.0110	324 (713)	1.0	324 (713)	0	G
11	4X Fn	466 (379)	0.346 (50.2)	9.86 (21.7)	0.56 (1.24)	0.52 (1.15)	0.60 (1.31)	8.18 (12.0)	0.0127	375 (826)	1.0	375 (826)	0	G, S
12	4X Fn	466 (379)	0.346 (50.2)	9.86 (21.7)	0.56 (1.24)	0.52 (1.15)	0.60 (1.31)	8.18 (12.0)	0.0150	444 (976)	1.0	444 (976)	0	G
13	4X Fn	466 (379)	0.346 (50.2)	9.86 (21.7)	0.56 (1.24)	0.52 (1.15)	0.60 (1.31)	8.18 (12.0)	0.0200	591 (1300)	1.0	591 (1300)	0	G
14	6X Fn	492 (426)	0.436 (63.2)	12.50 (27.5)	0.72 (1.58)	0.66 (1.45)	0.71 (1.57)	10.41 (22.9)	0.0080	300 (660)	1.0	300 (660)	0	G
15	6X Fn	492 (426)	0.436 (63.2)	12.50 (27.5)	0.72 (1.58)	0.66 (1.45)	0.71 (1.57)	10.41 (22.9)	0.0100	375 (824)	1.0	375 (824)	0	G
16	6X Fn	492 (426)	0.436 (63.2)	12.50 (27.5)	0.72 (1.58)	0.66 (1.45)	0.71 (1.57)	10.41 (22.9)	0.0116	434 (755)	1.0	434 (755)	0	G, S
17	6X Fn	492 (426)	0.436 (63.2)	12.50 (27.5)	0.72 (1.58)	0.66 (1.45)	0.71 (1.57)	10.41 (22.9)	0.0130	486 (1070)	1.0	486 (1070)	0	G
18	6X Fn	492 (426)	0.436 (63.2)	12.50 (27.5)	0.72 (1.58)	0.66 (1.45)	0.71 (1.57)	10.41 (22.9)	0.0160	599 (1317)	1.0	599 (1317)	0	G
19	30X Fn	640 (692)	1.213 (176.0)	31.54 (69.4)	1.81 (3.98)	1.66 (3.66)	1.80 (3.96)	26.27 (57.8)	0.0140	1328 (2921)	1.0	1328 (2921)	0	G, S
20	30X Fn	640 (692)	1.213 (176.0)	31.54 (69.4)	1.81 (3.98)	1.66 (3.66)	1.80 (3.96)	26.27 (57.8)	0.0140	1328 (2921)	0.5	664 (1460)	664 (1460)	G
21	30X Fn	640 (692)	1.213 (176.0)	31.54 (69.4)	1.81 (3.98)	1.66 (3.66)	1.80 (3.96)	26.27 (57.8)	0.0140	1328 (2921)	0.4	531 (1168)	797 (1760)	G, S
22	30X Fn	640 (692)	1.213 (176.0)	31.54 (69.4)	1.81 (3.98)	1.66 (3.66)	1.80 (3.96)	26.27 (57.8)	0.0140	1328 (2921)	0.3	398 (876)	930 (2045)	G
23	50X Fn	705 (809)	1.655 (241.0)	40.50 (89.1)	2.32 (5.11)	2.14 (4.70)	2.58 (5.67)	33.45 (73.6)	0.0178	244 (4716)	0.4	858 (1807)	1286 (2029)	G
24	70X Fn	755 (900)	1.655 (240.0)	38.64 (85.0)	2.22 (4.88)	2.04 (4.49)	2.46 (5.41)	31.91 (70.2)	0.0208	2389 (5256)	0.4	956 (2103)	1453 (3153)	G
25	85X Fn	785 (954)	1.695 (240.0)	37.45 (82.4)	2.15 (4.73)	1.98 (4.35)	2.38 (5.24)	30.95 (68.1)	0.0221	2464 (6420)	0.5	1232 (2710)	1232 (2710)	G
26	85X Fn	785 (954)	1.695 (240.0)	37.45 (82.4)	2.15 (4.73)	1.98 (4.35)	2.38 (5.24)	30.95 (68.1)	0.0221	2464 (6420)	0.4	985 (2168)	1478 (3352)	G, S
27	85X Fn	785 (954)	1.695 (240.0)	37.45 (82.4)	2.15 (4.73)	1.98 (4.35)	2.38 (5.24)	30.95 (68.1)	0.0221	2464 (6420)	0.3	739 (1626)	1725 (3794)	G
28	90X Fn	802 (984)	1.655 (240.0)	37.09 (81.6)	2.13 (4.68)	1.96 (4.31)	2.36 (5.19)	30.63 (67.4)	0.0238	2625 (5775)	0.4	1050 (2310)	1575 (3465)	G
29	100X Fn	817 (1011)	1.655 (240.0)	36.36 (80.0)	2.09 (4.59)	1.92 (4.22)	2.31 (5.09)	30.05 (66.1)	0.0242	2618 (5760)	0.5	1309 (2880)	1309 (2880)	G
30	100X Fn	817 (1011)	1.655 (240.0)	36.36 (80.0)	2.09 (4.59)	1.92 (4.22)	2.31 (5.09)	30.05 (66.1)	0.0242	2618 (5760)	0.4	1047 (2304)	1571 (2456)	G, S
31	100X Fn	817 (1011)	1.655 (240.0)	36.36 (80.0)	2.09 (4.59)	1.92 (4.22)	2.31 (5.09)	30.05 (66.1)	0.0242	2618 (5760)	0.3	785 (1228)	1833 (4032)	G

G - Ganged Sampling Mode
I - Individual Rate Sampling Mode
S - Smoke Data to Be Obtained

high centerbody temperatures would occur in-line with swirl cups at true operating conditions with the cooling provided. The hardware changes made involved preferentially increasing the pilot dome inner cooling ring flow, and the main dome outer cooling ring flow in-line with the swirl cups. In addition, a circular arc of gill-type cooling holes was incorporated into the pilot stage side of the centerbody structure just downstream of the two cross-fire tubes. These hardware changes are illustrated in Figure 217.

For the ignition and primary emissions test, fuel was supplied to the combustor using the E³ engine fuel nozzle assemblies. This represented the first time that these nozzle assemblies were used. The nozzles were programmed around the combustor to provide the most uniform fuel distribution in the pilot dome for the purpose of demonstrating low idle emissions levels.

For the idle emissions comparison testing, the engine fuel nozzle assemblies were removed from the rig and replaced with the E³ test rig fuel nozzle assemblies. The combustor test rig was configured to feature a 12-cup continuous section of prototype (peanut) nozzles, and an 18-cup continuous section of standard test rig nozzles in the pilot stage dome. Both the peanut and standard nozzles used were rated at approximately 12 kg/hr (26 pph). An illustration of these two nozzle tip designs is presented in Figure 218.

Combustor instrumentation consisted of 28 static pressures, 2 total pressures, and 65 grounded and capped chromel-alumel thermocouples. Of these thermocouples, 19 were embedded into the surface of the centerbody structure at several places around the circumference. This instrumentation provided important performance data concerning combustor pressure drops, airflow distribution, and metal temperatures. The locations of this instrumentation on the combustor hardware are illustrated in Figures 219 through 229. All sampling rake thermocouples plus numerous other combustor skin thermocouples were connected to a temperature display device (Metrascope) for continuous monitoring. A dynamic pressure probe was installed through an available test rig port and immersed into the combustor outer flowpath. This probe was used to monitor the characteristic frequencies and fluctuations of the engine combustor.

ORIGINAL PAGE IS
OF POOR QUALITY

• All Dimensions in cm(in.)

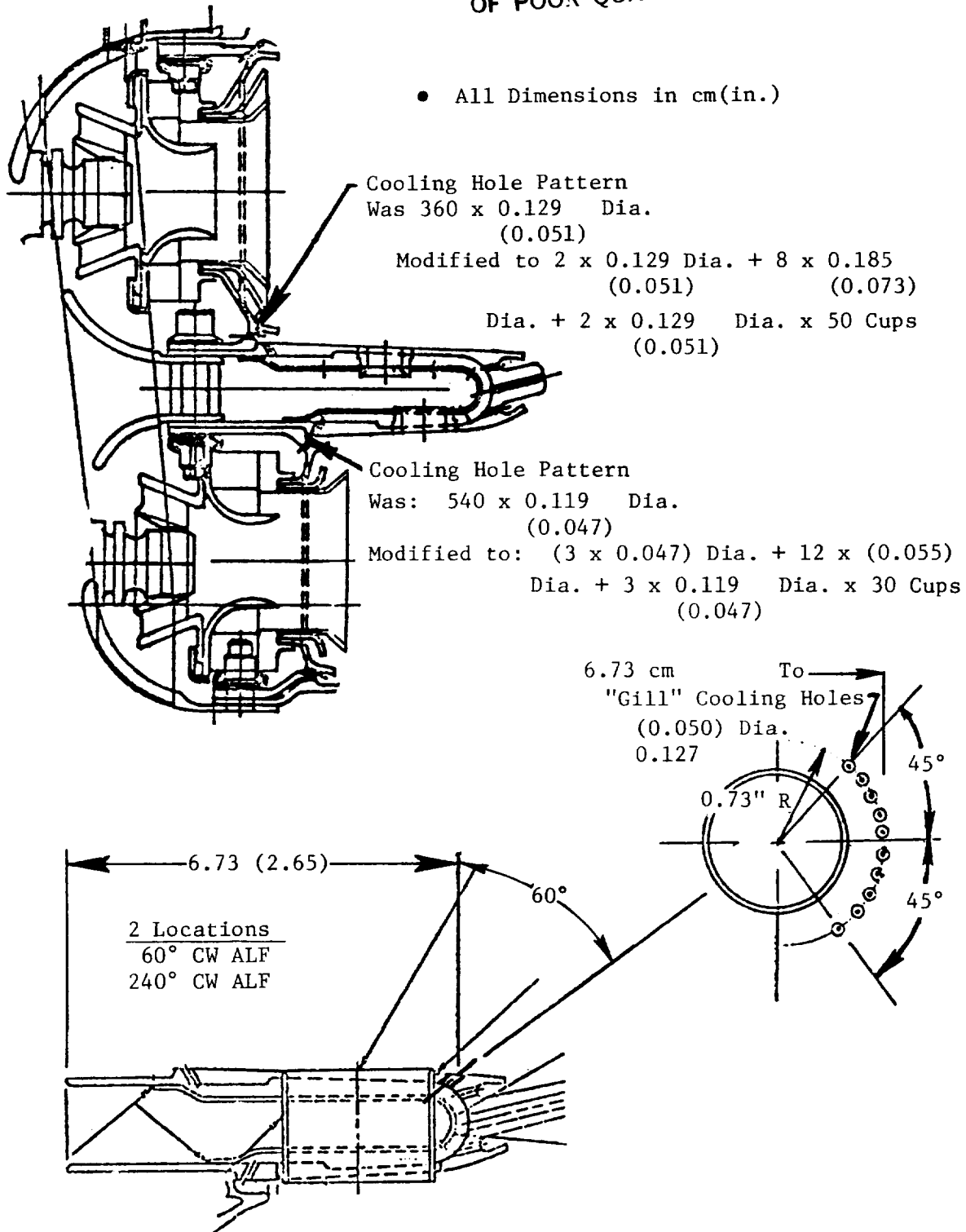
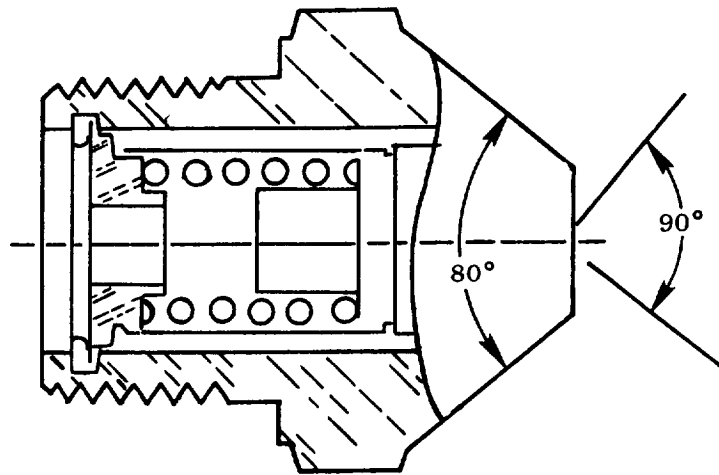


Figure 217. Engine Combustor Hardware Modifications.

Peanut
Simplex



Hago
Development

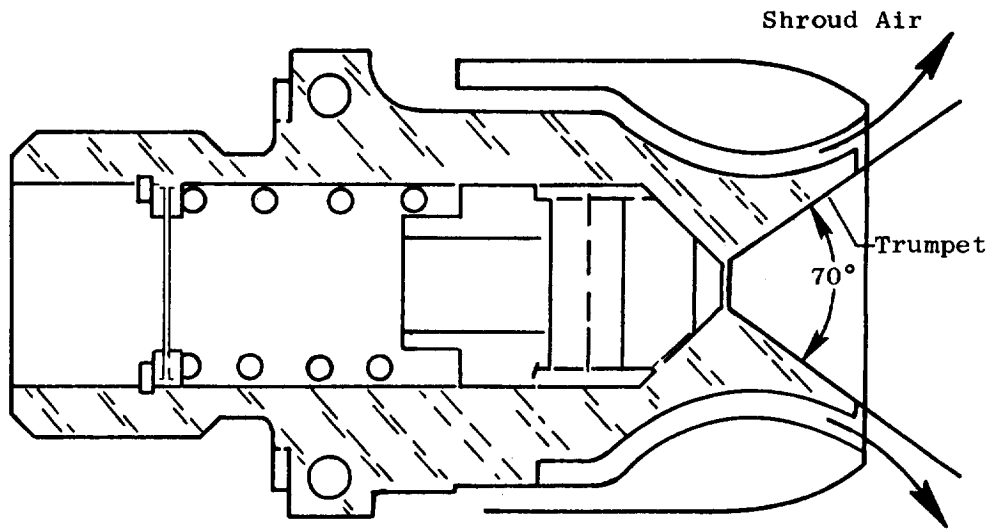
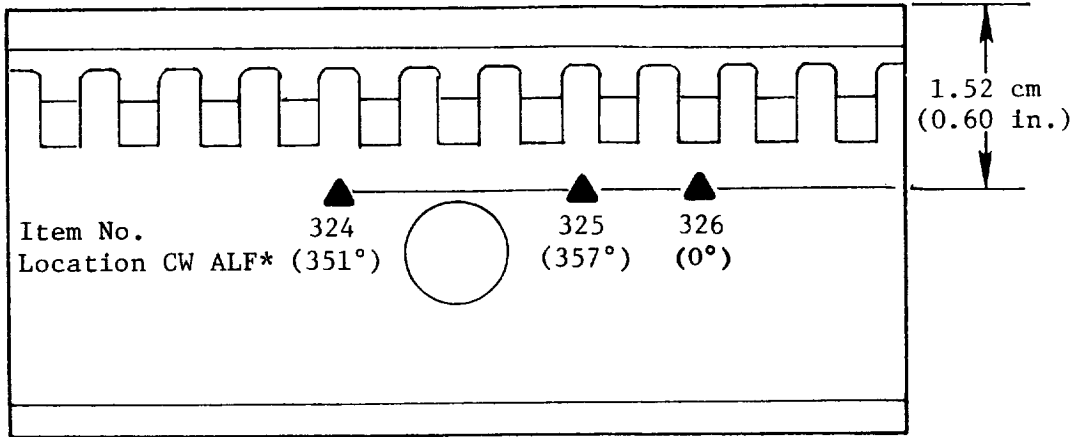


Figure 218. Comparison of Test Rig and Prototype Fuel Nozzle Tips.

Outer Row No. 1 Thermocouples



*Clockwise, Aft Looking Forward

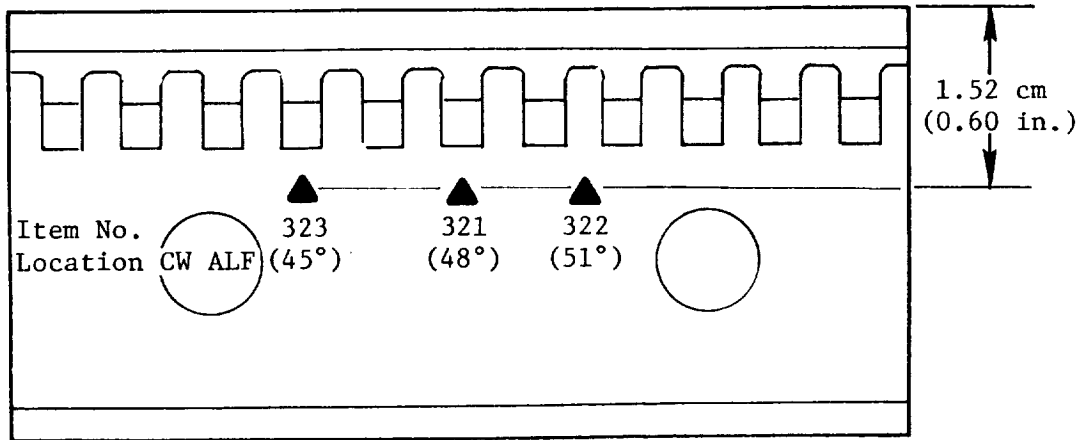


Figure 219. Engine Combustor Instrumentation Layout.

ORIGINAL FILED
OF POOR QUALITY

Outer Row No. 2 Thermocouples

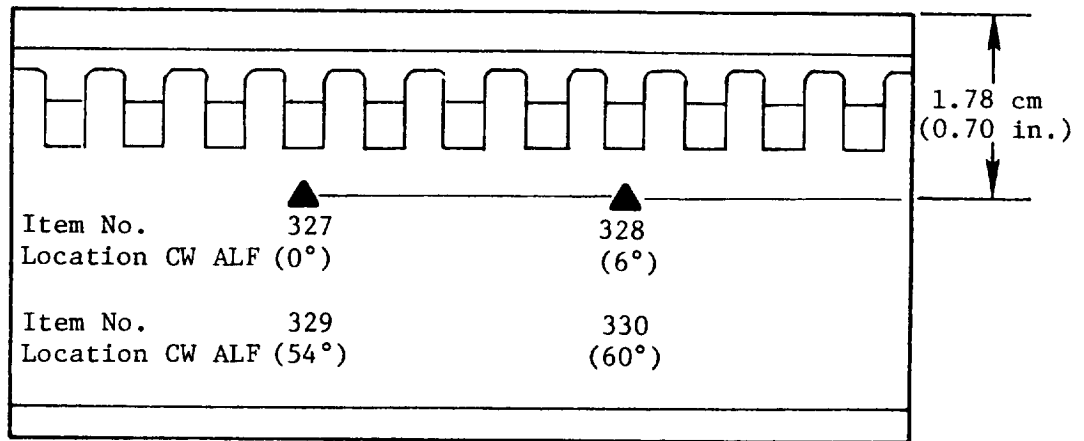


Figure 220. Engine Combustor Instrumentation Layout.

ORIGINAL PAGE IS
OF POOR QUALITY

Outer Row No. 3 Thermocouples

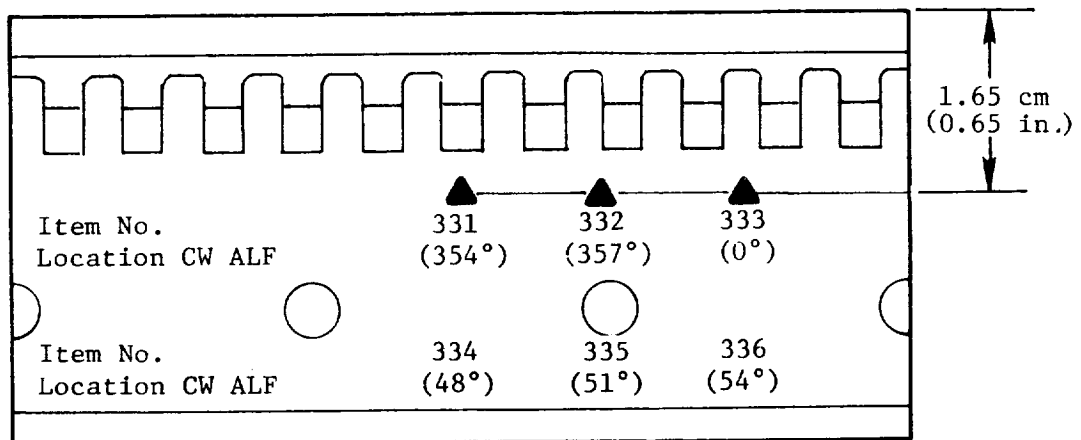


Figure 221. Engine Combustor Instrumentation Layout.

ORIGINAL PAGE IS
OF POOR QUALITY

Inner Row No. 1 Thermocouples

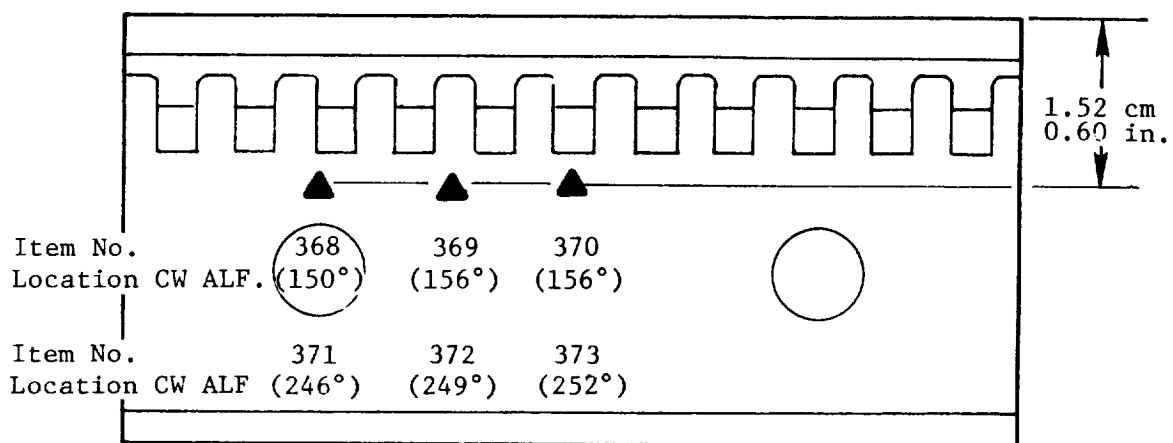
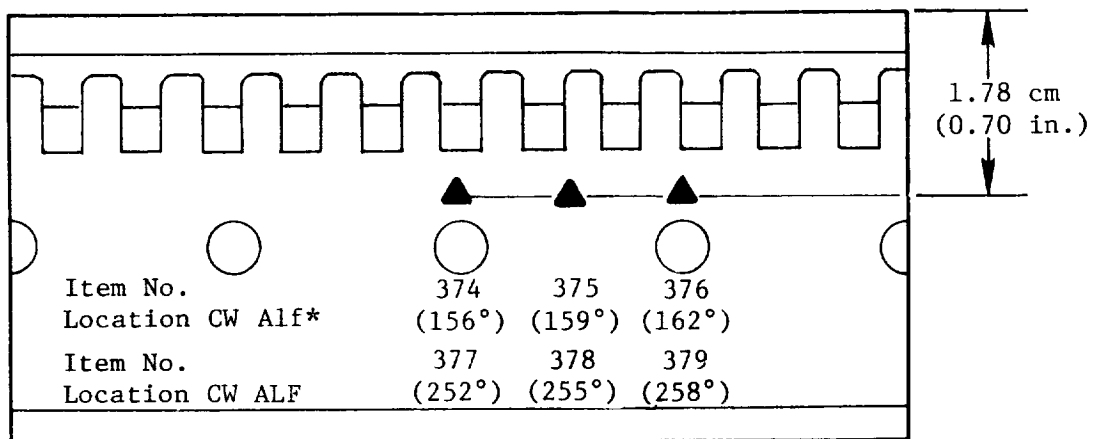


Figure 222. Engine Combustor Instrumentation Layout.

ORIGINAL PAGE IS
OF POOR QUALITY

Inner Row No. 2 Thermocouples



*Clockwise, Aft Looking Forward

Figure 223. Engine Combustor Instrumentation Layout.

ORIGINAL PAGE IS
OF POOR QUALITY

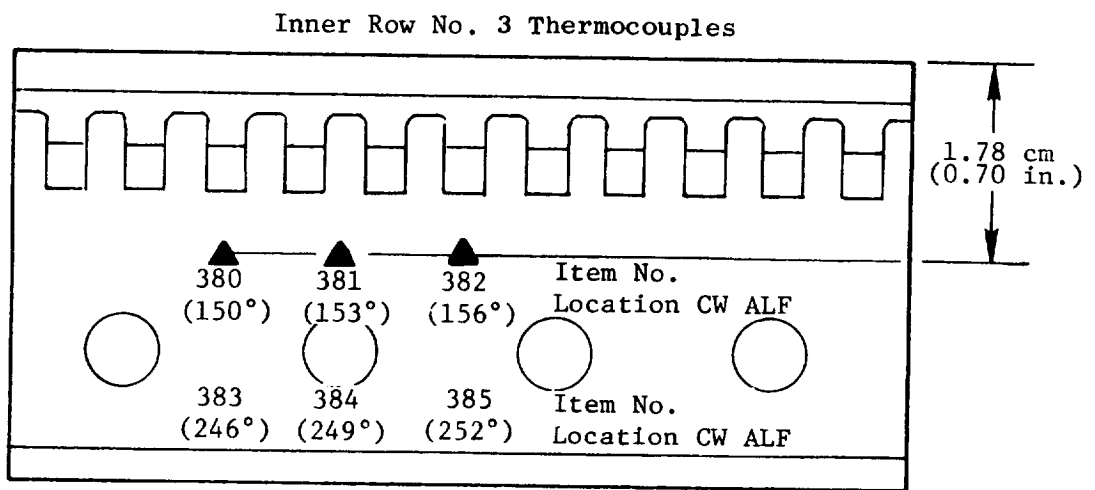


Figure 224. Engine Combustor Instrumentation Layout.

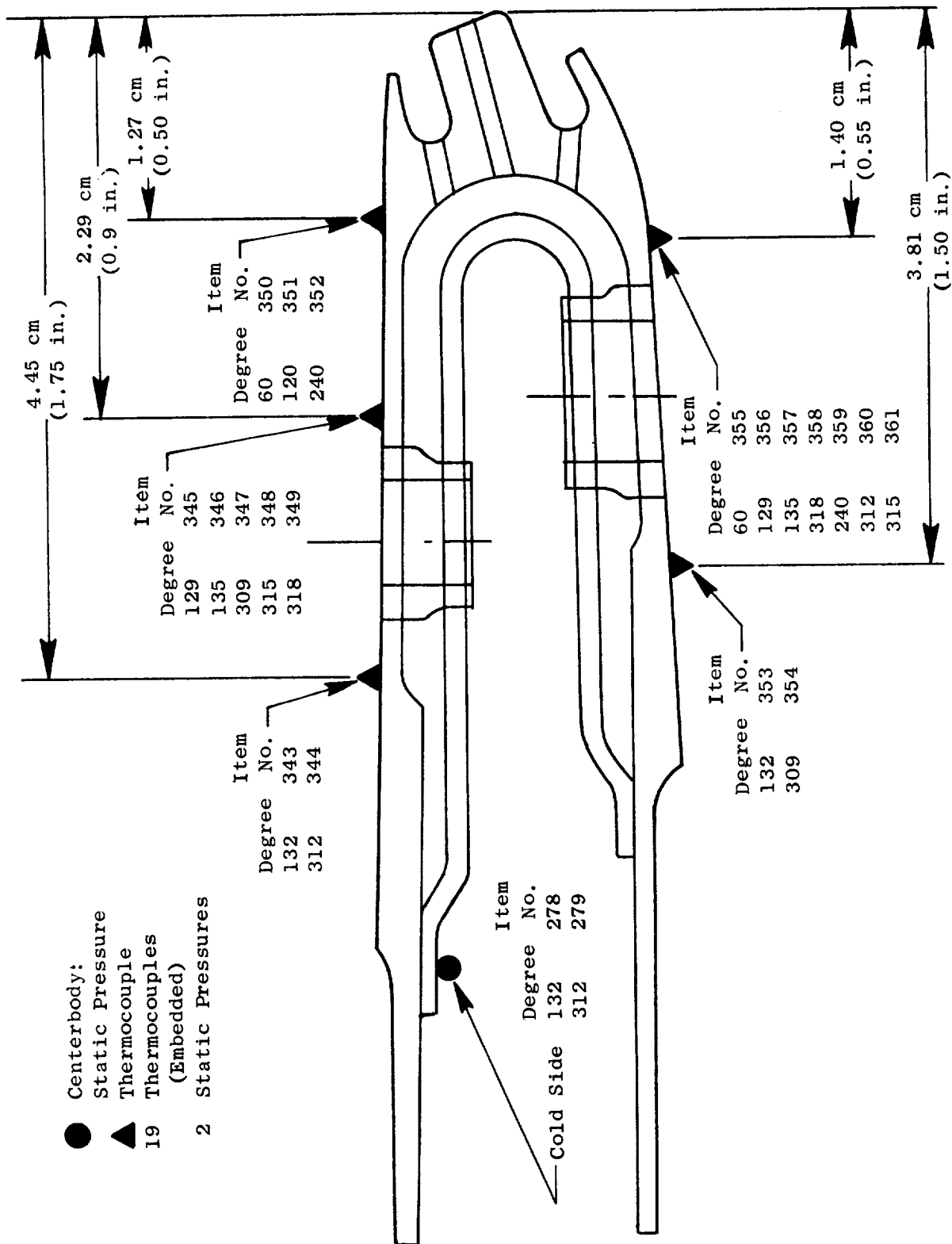
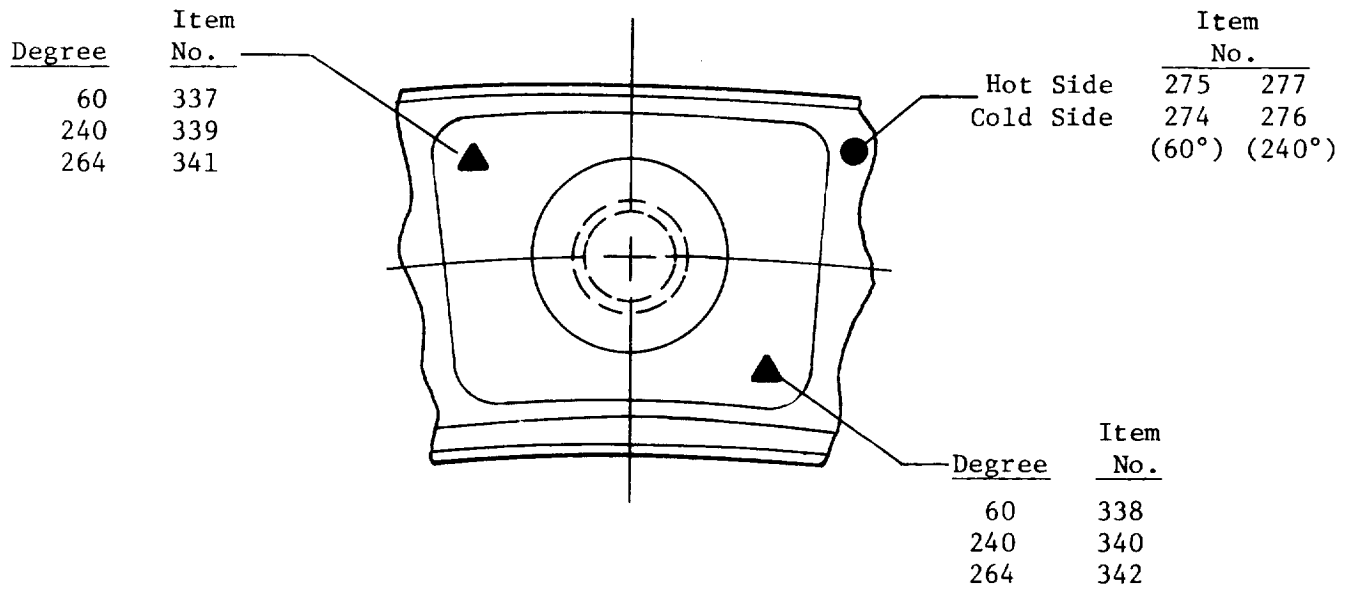


Figure 225. Engine Combustor Instrumentation Layout.

ORIGINAL PAGE IS
OF POOR QUALITY



Outer Dome:

- Static Pressure (4 Total)
- ▲ Thermocouple (6 Total)

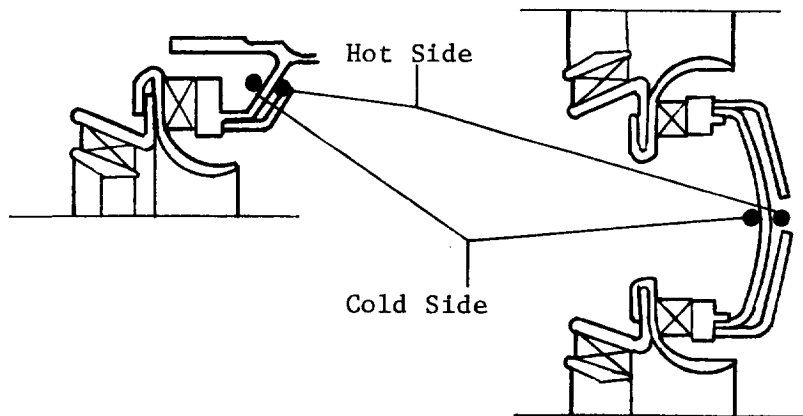


Figure 226. Engine Combustor Instrumentation Layout.

ORIGINAL PAGE IS
OF POOR QUALITY

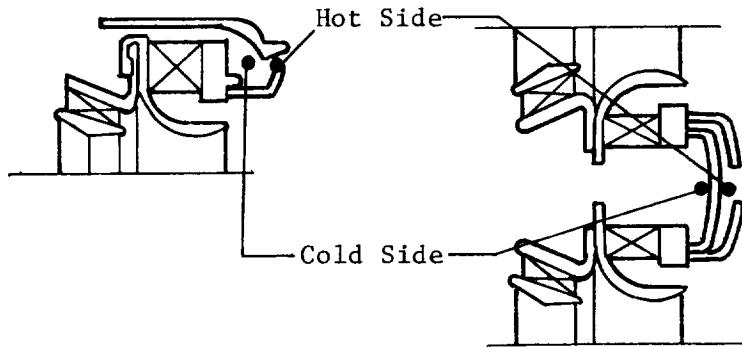
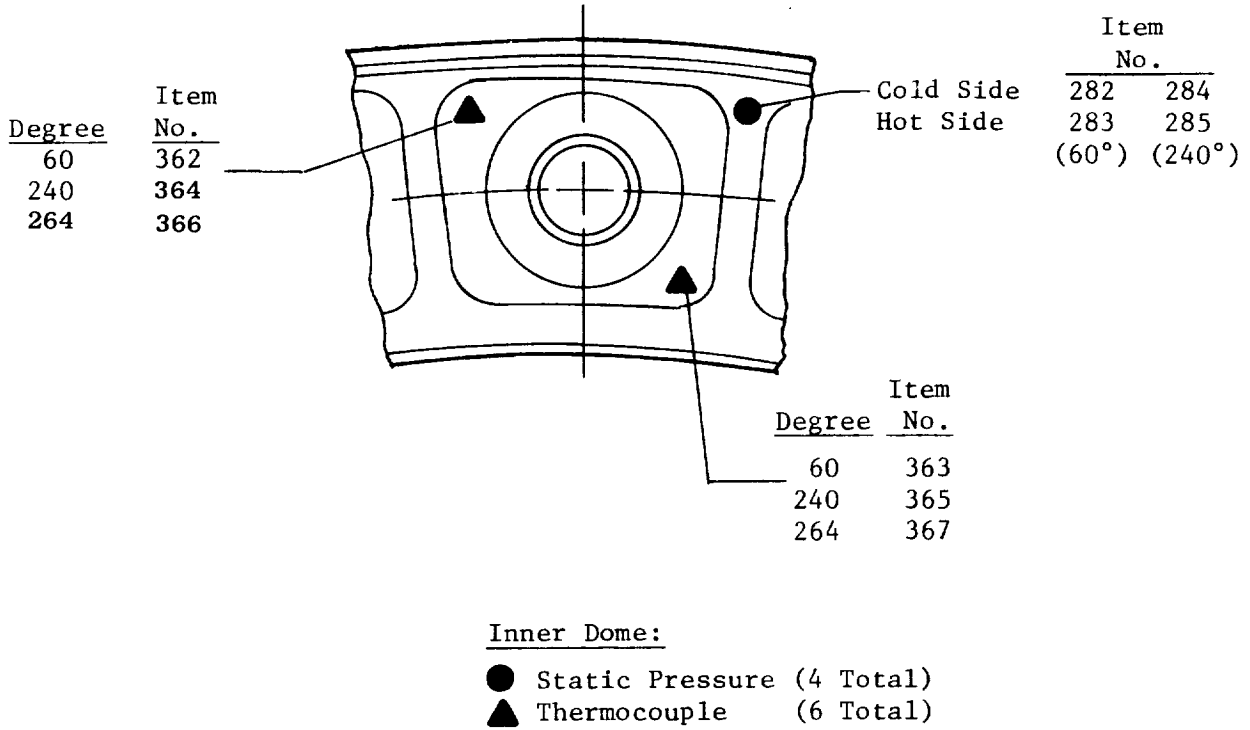
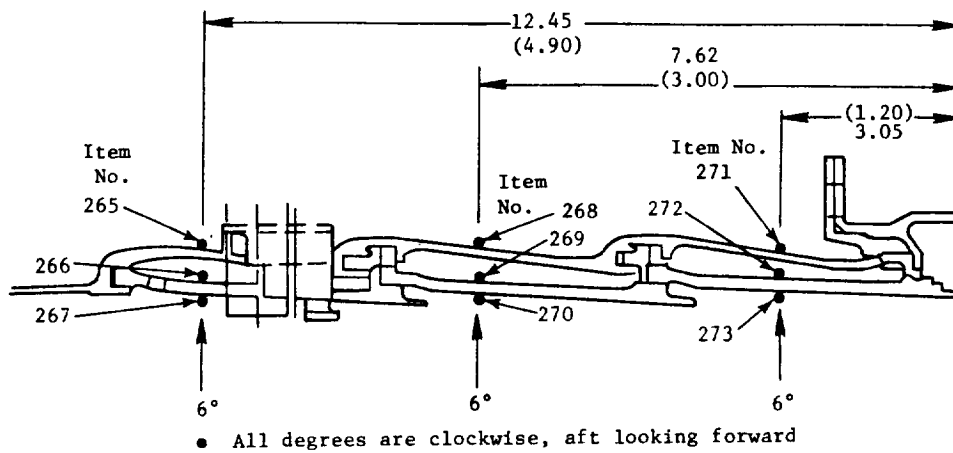


Figure 227. Engine Combustor Instrumentation Layout.

Core Combustor Liners
Outer Liner Assembly (Static Pressures)



Inner Liner Assembly (Static Pressures)

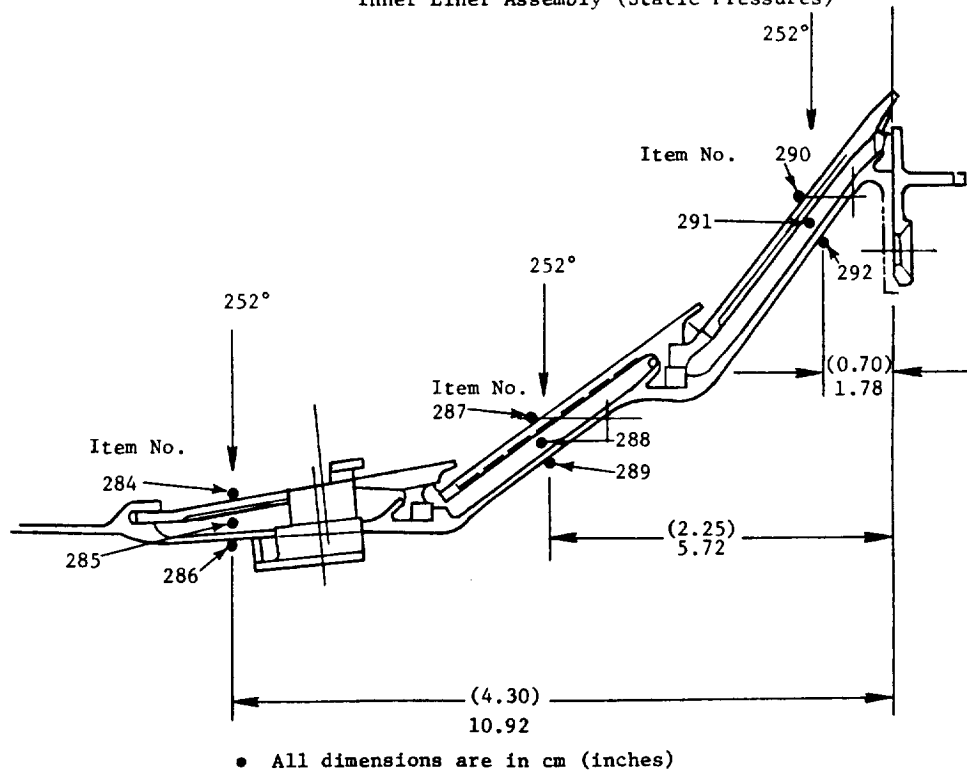


Figure 228. Engine Combustor Instrumentation Layout.

ORIGINAL PAGE IS
OF POOR QUALITY

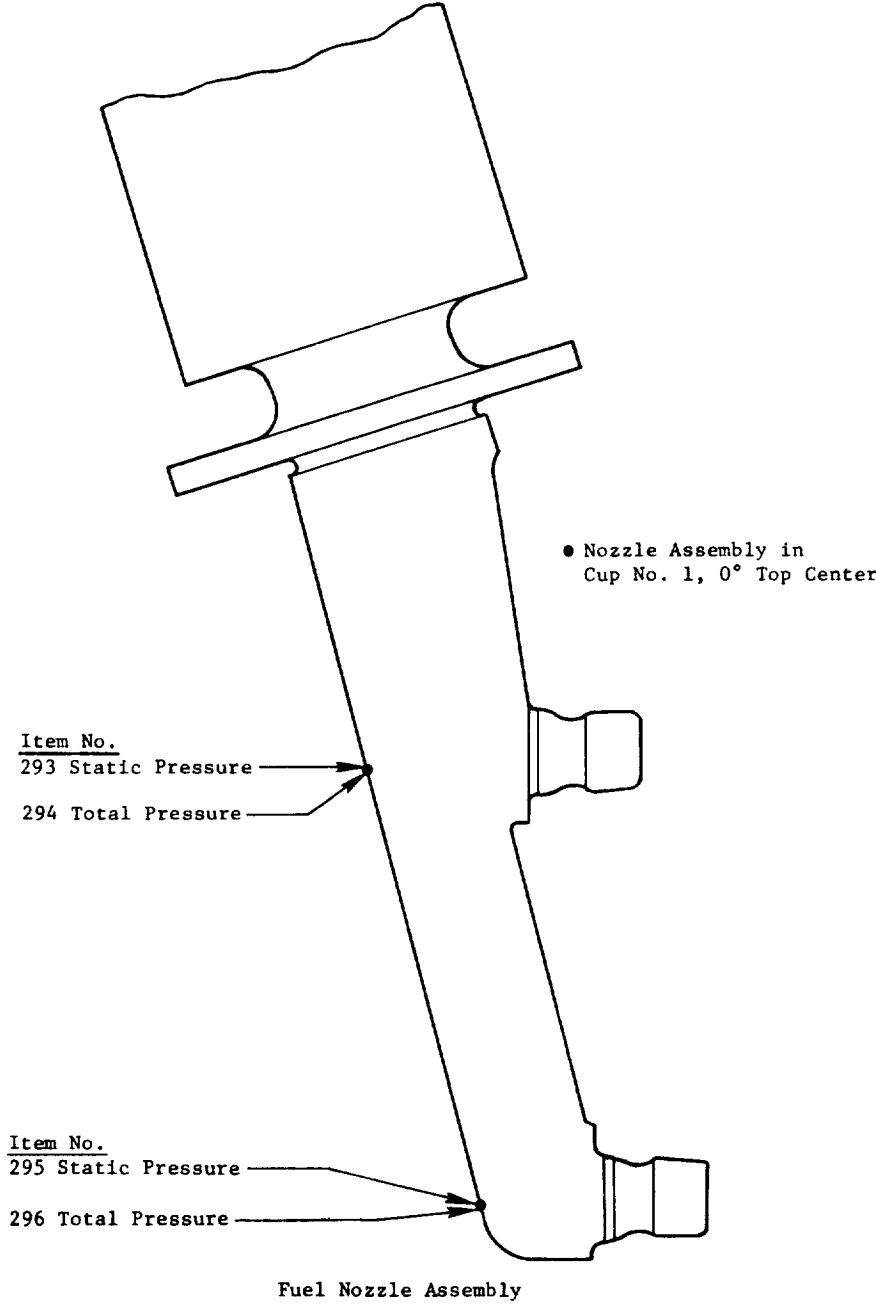


Figure 229. Engine Combustor Instrumentation Layout.

The ground start ignition results obtained on the E³ engine combustor are presented in Figure 230. The pilot stage demonstrated excellent ignition and lean extinction characteristics. Considerable margin was demonstrated against the E³ ground start cycle fuel schedule with or without compressor bleed down to 30% corrected core engine speed. It is interesting to note that these results are very similar to the pilot stage ignition characteristics demonstrated at atmospheric inlet pressure conditions. The anticipated improvement at true cycle inlet pressure was not demonstrated. This is most probably related to the differences in the fuel spray characteristics between the engine fuel nozzle assemblies used in this test and the test rig nozzle assemblies used in the atmospheric test.

As anticipated, test data from the main stage suggests that it will not be possible to achieve main stage ignition within the steady-state FPS cycle fuel schedule at engine power levels up to 10% of sea level takeoff thrust. However, taking into consideration the additional fuel available on the engine accel schedule, staging this combustor while on this accel schedule should be possible at the 10% power operating condition. The lean extinction characteristics of the main stage are sufficiently good to allow staged combustor operation at conditions as low as 4% ground idle presuming that the engine decels to that operating condition from a point where main stage crossfire can occur.

The idle emissions results obtained using the engine fuel nozzle assemblies are presented in Figure 231. As observed from this figure, the engine combustion system achieved exceptionally low levels of CO and HC emissions at both the 4% and 6% ground idle operating conditions. At the 4% ground idle design point ($f/a = 0.0123$), a CO emission level of 18.2 g/kg (18.2 lb/1000 lb) of fuel, and an HC emission level of 1.7 g/kg (1.7 lb/1000 lb) of fuel were demonstrated. At the 6% ground idle design point ($f/a = 0.0113$), the levels demonstrated were 10.8 g/kg (10.8 lb/1000 lb) of fuel, and 0.8 g/kg (0.8 lb/1000 lb) of fuel, respectively for CO and HC emissions. These levels are substantially below CO and HC emissions levels estimated as necessary to satisfy the E³ Program EPAP design goals. Both emissions levels remain at the goal levels or below at combustor fuel-air ratios from 0.009 to 0.0145.

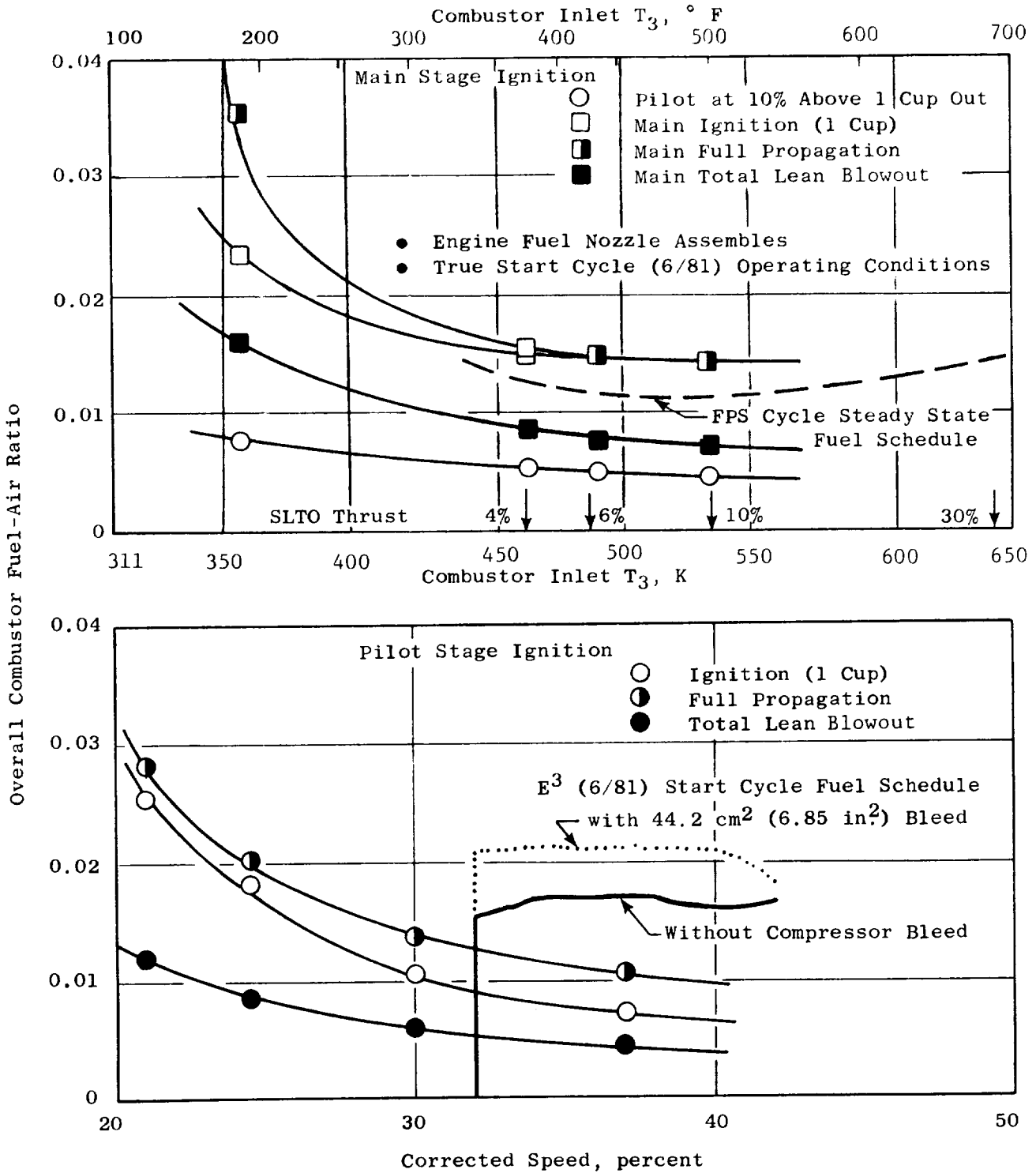


Figure 230. Engine Combustor Ignition Results at True Cycle Conditions.

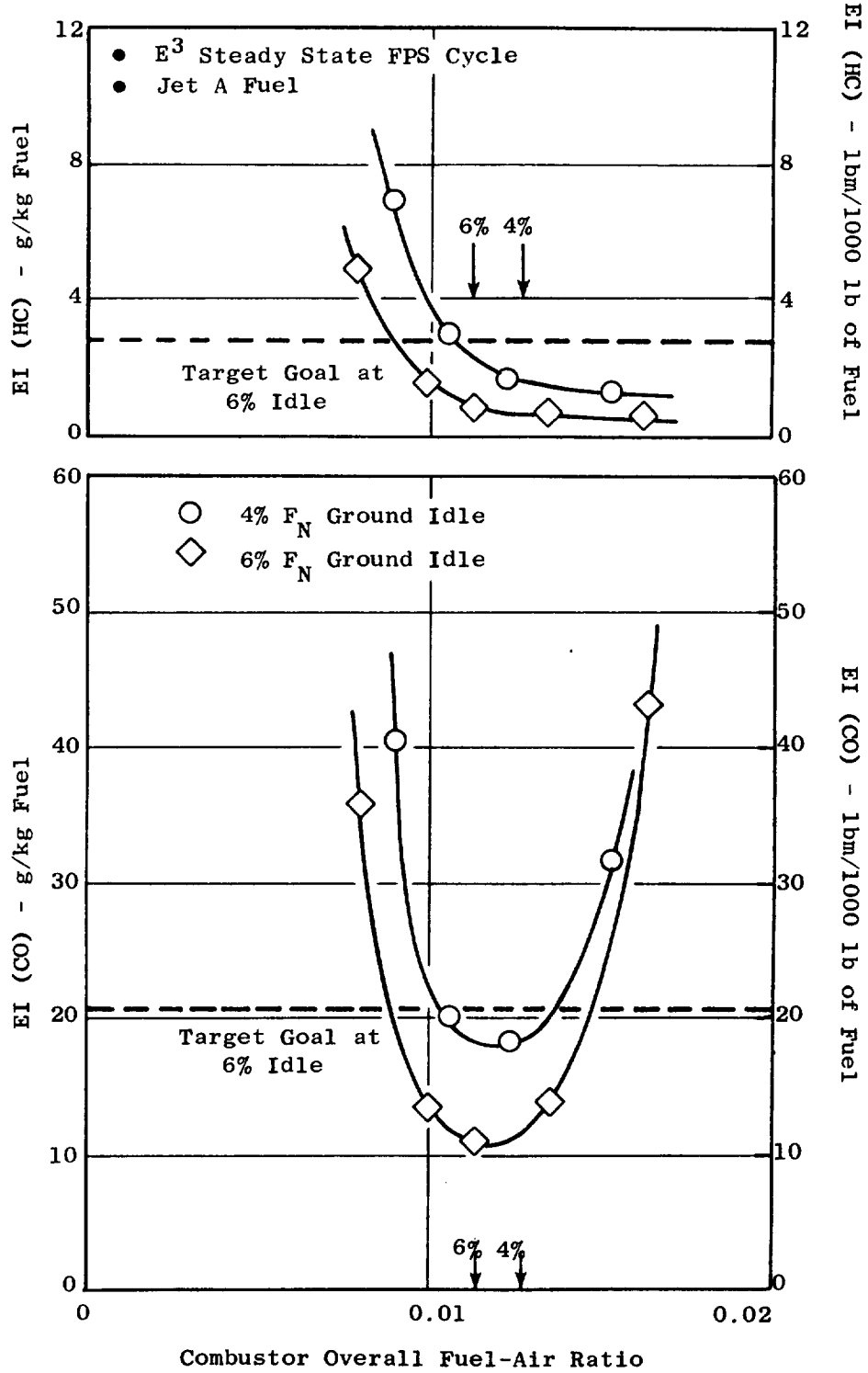


Figure 231. Engine Combustor Emissions Results.

Idle emissions results obtained using the array of peanut and standard test rig fuel nozzles are presented in Figure 232. This testing was prematurely terminated because of a failure in the gas sampling traverse system. Sufficient data was obtained to make the comparison at the 6% ground idle operating condition. The peanut-type fuel nozzles demonstrated CO and HC emissions levels lower than levels obtained from the standard test rig nozzles at fuel-air ratios above 0.0110. This supports results previously obtained from E³ sector combustor subcomponent testing. One of the interesting outcomes of this test involves the difference in fuel-air ratio at which each nozzle type demonstrated the minimum CO emission level. The engine nozzle assemblies achieved a minimum CO level of 10.5 g/kg (10.5 lb/1000 lb) of fuel at a fuel-air ratio of 0.0118; for the peanut nozzles 12.5 g/kg (12.5 lb/1000 lb) of fuel obtained at a fuel-air ratio of 0.0138; and for the standard test rig nozzles, 15.5 g/kg (15.5 lb/1000 lb) of fuel obtained at 0.0129. This could be related to the differences in the fuel spray angle characteristics of each nozzle type. The peanut nozzles and the engine nozzle assemblies are known to have wider fuel spray angles than the standard rig nozzles. An anticipated result of this fact is the observed lesser sensitivity of the CO emissions to fuel-air ratio demonstrated with these two nozzle types.

Emissions were measured at the 30% power (approach), operating condition at pilot-to-total fuel splits of 1.0, 0.5, 0.4, and 0.3. The effects of these fuel staging modes on the measured CO, HC, and NO_x are presented in Table LIII. The expected trend of low CO and HC emissions and high NO_x emissions at the pilot only operating mode is evident. In the staged operating mode, the NO_x levels are reduced, but the CO and HC emission levels increased substantially. This trend has been observed in previous testing of the E³ development combustor. In the staged operating mode at the 30% power operating condition, the low FPS design cycle overall combustor fuel-air ratio of 0.0140 creates very lean fuel-air mixtures in both domes. These lean primary zone conditions cause low combustion efficiencies resulting in the high CO and HC emissions levels. Another contributing factor may involve the fuel spray quality from the engine nozzle assemblies. At fuel flow levels associated with this operating condition and staging mode, the secondary fuel system of the pilot and main stage duplex nozzle tips have just opened. This situation often produces larger fuel droplets mixed in with the nozzle tip fuel spray.

Table LIII. Emissions Results at 30% Approach Power Operation.

Combustor Operating Mode	EI - g/kg (lbm/1000 lb)		
	CO	HC	NO _x
Pilot Only	2.1	0.1	16.0
50/50 Fuel Split	66.9	13.2	6.1
40/60 Fuel Split	71.7	8.8	5.2
30/70 Fuel Split	83.0	8.0	5.4

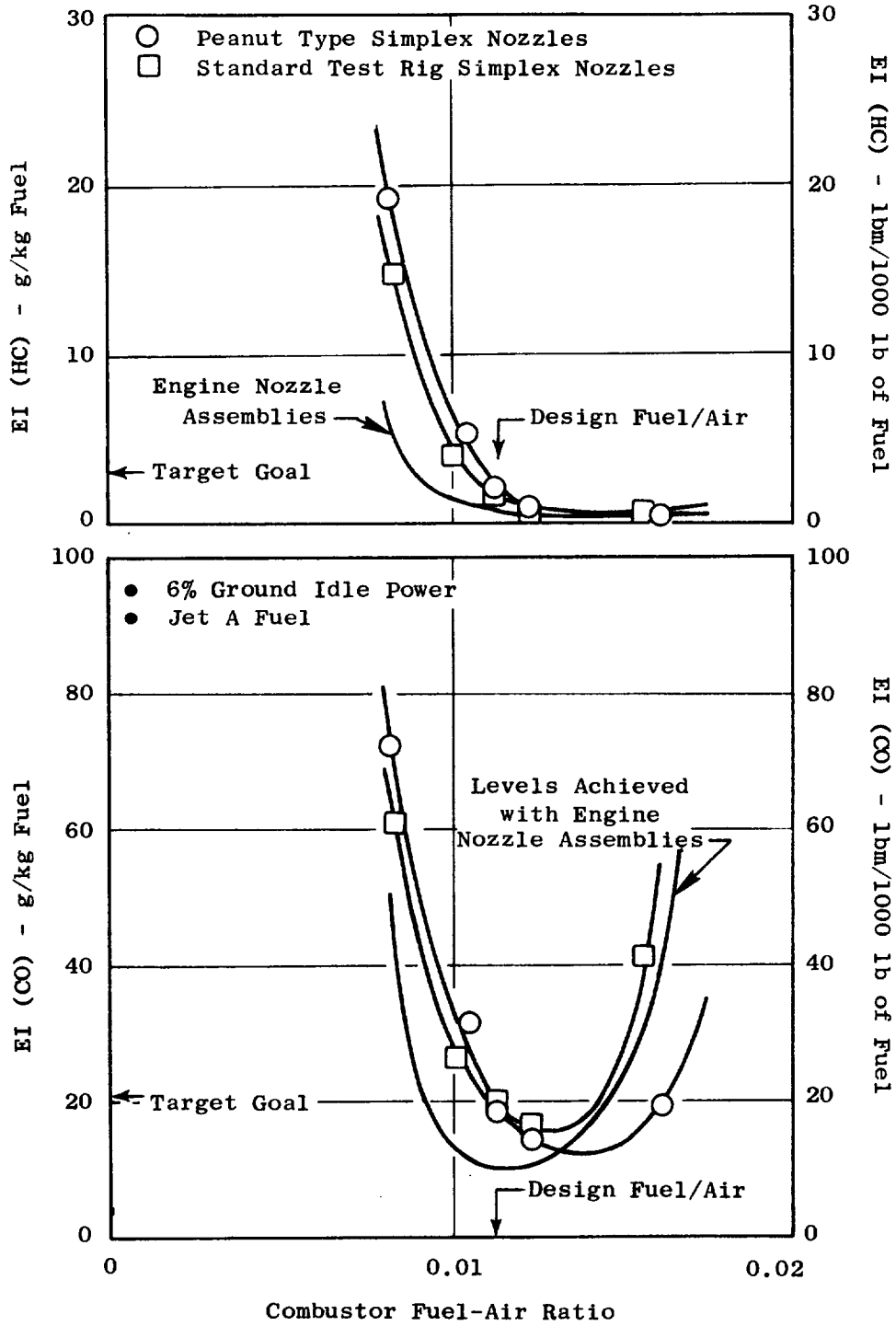


Figure 232. Engine Combustor Emissions Results.

All CO and HC emissions levels measured at the simulated high power operating conditions were adjusted for the scaled down inlet conditions associated with the inability of the facility to provide the actual design cycle inlet conditions. The adjusted CO and HC emissions levels as well as those measured at the lower power operating conditions are plotted against the combustor inlet temperature along the E³ FPS design cycle in Figure 233. In this figure, the design fuel split at the higher power operating condition is considered to be 40/60. The impact of staging is clearly illustrated in this figure.

Measured NO_x emission levels obtained in the staged combustor mode at operating conditions from 30% power up to the simulated sea level takeoff are plotted against the E³ design cycle severity parameter in Figure 234. The resulting correlation yields an NO_x emission index of 27.8 g/kg (27.8 lb/1000 lb) of fuel at the E³ FPS SLTO condition. This level is considerably above the target level of 17.5 g/kg of fuel estimated as being required to satisfy the E³ NO_x EPAP goal, and well above the satisfactory levels previously demonstrated with the Baseline and Mod I development combustor configurations. Slightly lower NO_x levels are obtained by establishing the off-design 30/70 fuel split. A potential explanation involves the main stage primary dilution flow levels and will be addressed in more detail later in the text. The adjusted NO_x emission levels as well as those measured at the lower power operating conditions are plotted against the combustor inlet temperature along the E³ FPS design cycle in Figure 235. The design fuel split at the higher power operating conditions is considered to be 40/60.

The EPA parameter number, based on the EPA landing/takeoff cycle for CO, HC, and NO_x emissions were generated for various combustor operating mode combinations along the E³ FPS design cycle operating line. These EPAP results are compared to the E³ Program goals in Table LIV. In the pilot only operating mode at the 30% power condition, the CO and HC levels satisfy the requirements with margin for both 4% and 6% thrust at ground idle. However, the NO_x levels exceed the requirements by 40% or more depending on the pilot-to-main stage fuel split selected at the higher power operating conditions. Operating the combustor in the staged mode at the 30% power condition provides some reduction in NO_x levels. However, reductions of at least 20% are yet required

ORIGINAL PAGE IS
OF POOR QUALITY

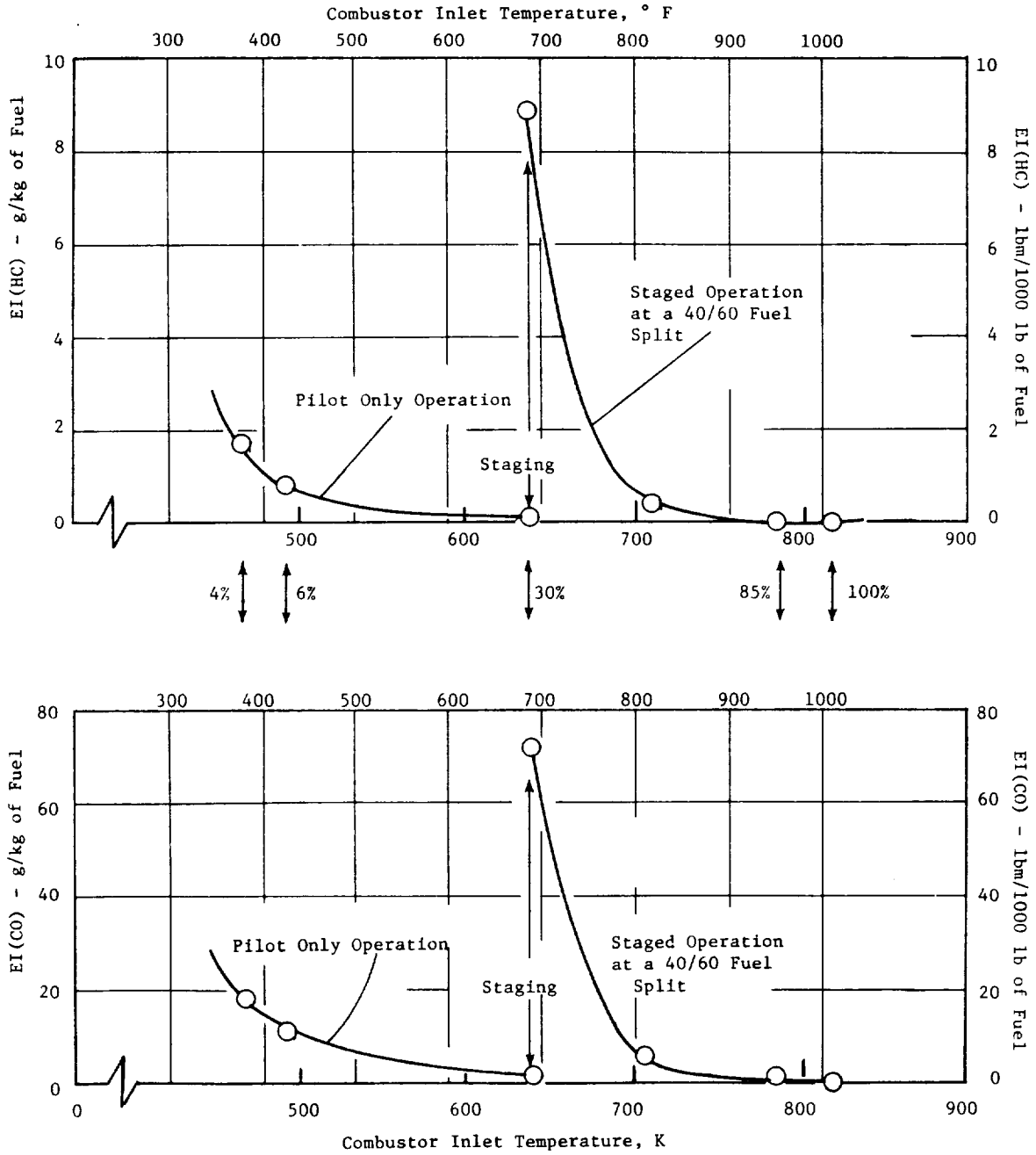


Figure 233. Engine Combustor Emissions Results.

ORIGINAL PAGE IS
OF POOR QUALITY

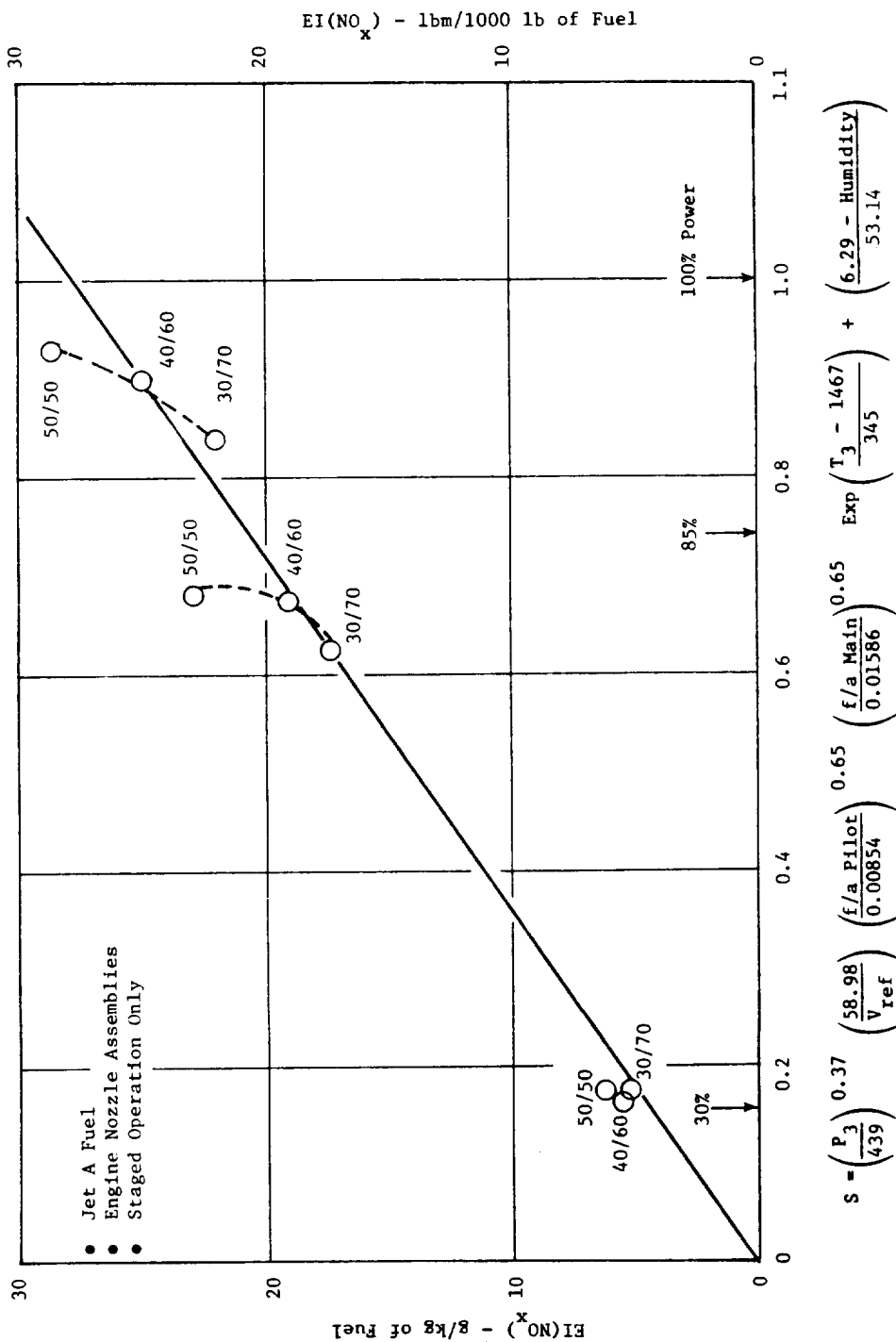


Figure 234. Engine Combustor Emissions Results.

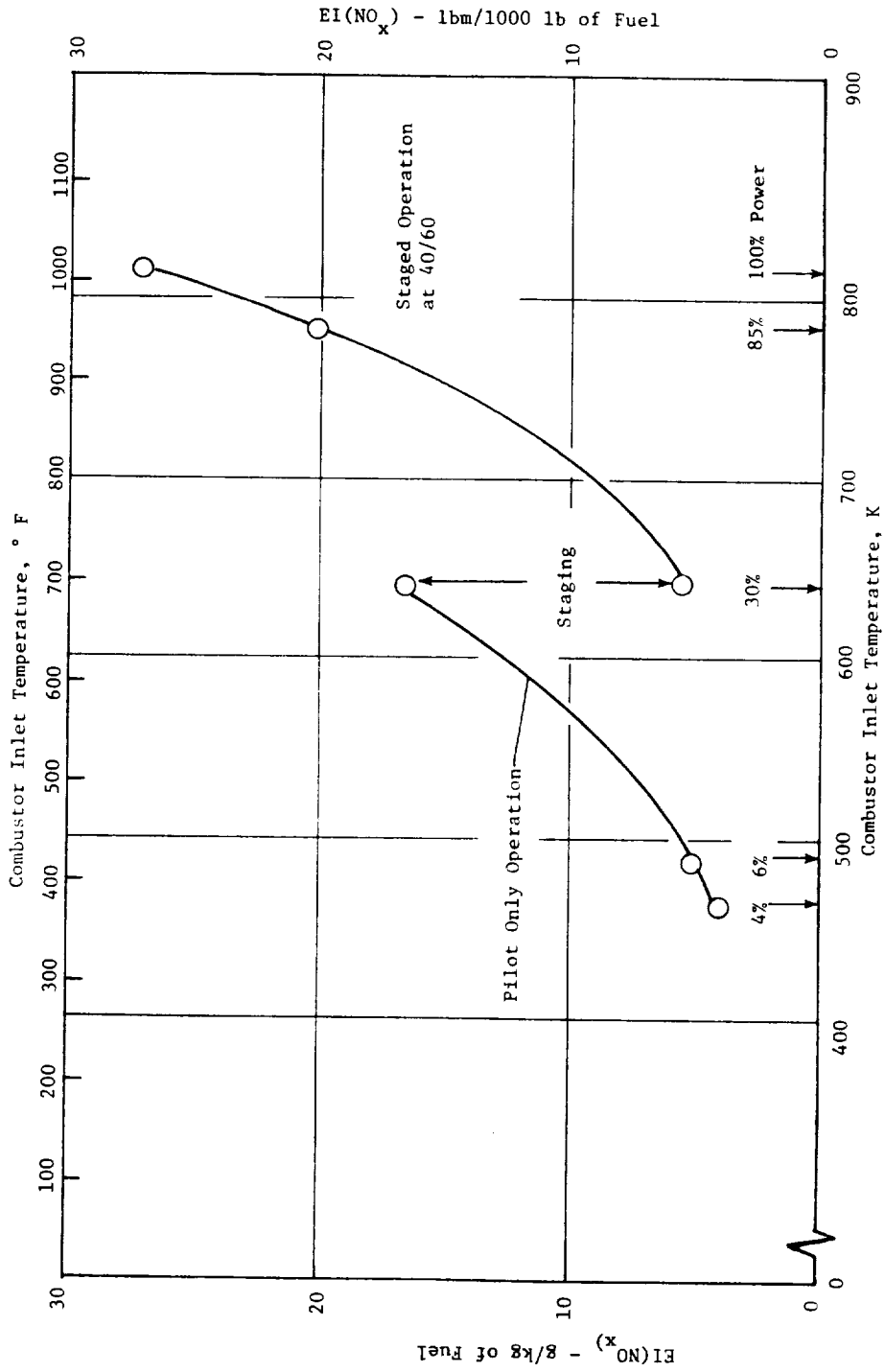


Figure 235. Engine Combustor Emissions Results.

Table LIV. E³ Engine Combustor EPAP Results.

● FPS Design Cycle (Steady-State SLS)

	EPAP - Thrust-hr-Cycle		
	<u>CO</u> g/kg	<u>HC</u> (lbm/1000 lb)	<u>NO_x</u> lb
4% Ground-Idle Pilot Only at Approach 40/60 Split at Climb and SLTO	2.45	0.22	4.97
4% Ground-Idle 40/60 Split at Approach 40/60 Split at Climb and SLTO	7.09	0.80	4.25
4% Ground-Idle Pilot Only at Approach 30/70 Split at Climb and SLTO	2.45	0.22	4.73
4% Ground-Idle 30/70 Split at Approach 30/70 Split at Climb and SLTO	7.84	0.74	4.03
6% Ground-Idle Pilot Only at Approach 40/60 Split at Climb and SLTO	1.58	0.11	4.66
6% Ground-Idle 40/60 Split at Approach 40/60 Split at Climb and SLTO	5.76	0.63	4.02
6% Ground-Idle Pilot Only Approach 30/70 Split at Climb and SLTO	1.58	0.11	4.46
6% Ground-Idle 30/70 Split at Approach 30/70 Split at Climb and SLTO	6.44	0.58	3.82
E ³ Program Goals	3.00	0.40	3.00

to satisfy the requirement. In addition, the CO and HC levels increase significantly, and no longer satisfy or closely approach the requirements.

Smoke levels obtained are presented along with the combustor operating conditions at which they were measured in Table LV. The highest smoke level was measured at the approach operating condition in the pilot only operating mode. Test conditions at this point exactly matched the design cycle operating conditions. Therefore, the measured smoke number of 16.5 would be representative of engine operation at this power setting and combustor operating mode. Slightly lower smoke levels (smoke number of 12.8) were measured at this same operating condition in the staged operating mode. Significantly lower smoke levels were obtained at the simulated high-power operating conditions. Although somewhat higher levels would be expected at the actual design cycle conditions at high power, the levels would be well below the E³ Program smoke number goal of 20.

Measured overall combustion system total pressure drops are plotted against the square of the combustor flow function parameter in Figure 236. A significant amount of data scatter is evident. Throughout this testing, problems were incurred with the facility pressure transducer scanning equipment used to read the combustor exit total pressure. Pretest predictions of the overall loss were approximately 5.3%. This tends to agree with the upper bounds of the measured data obtained. Measured static pressure drops across the domes indicate a drop of 3.3% across the pilot stage dome, and 2.9% across the main stage dome at sea level takeoff operating conditions. Static pressure drops across the liners were between 1.1% and 1.4% for the forward panels, and between 1.5% and 2.8% for the aft panels. Static pressure drops across the centerbody structure were 3.2% on the pilot stage side and 2.3% on the main stage side.

Using the measured combustor static pressures and measured combustor flow areas, an estimate of the combustor airflow distribution was generated and presented in Appendix E. The combustor flow areas were measured on a flow calibration test stand as part of the pretest checkout of the E³ combustor hardware. For comparison purposes, the estimated flow levels are shown with the design levels in Figure 237. Key areas of discrepancy occur in the primary zone of both the pilot stage and main stage. Pilot stage swirl cup and

Table LV. Engine Combustor Smoke Results.

P_3 , MPa (psia)	T_3 , K (° F)	\dot{W}_{Comb} , kg/s (pps)	f/a	$\frac{Wf \text{ Pilot}}{Wf \text{ Total}}$	SAE Smoke Number	Comments
0.345 (50.1)	465 (377)	8.44 (18.57)	0.0123	1.0	8.5	4% Idle
0.436 (63.2)	490 (423)	10.55 (23.20)	0.0114	1.0	13.2	6% Idle
1.214 (176.1)	643 (698)	25.71 (56.57)	0.0143	1.0	1.5	30% Approach
1.216 (176.3)	641 (694)	25.60 (56.33)	0.0144	0.4	12.8	30% Approach
1.517 (220.0)	788 (959)	29.07 (63.95)	0.0215	0.4	5.2	Simulated 85% F_n
1.524 (221.1)	820 (1016)	27.48 (60.45)	0.0242	0.4	6.3	Simulated 100% F_n

ORIGINAL RECORD
OF POOR QUALITY

ORIGINAL PAGE IS
OF POOR QUALITY

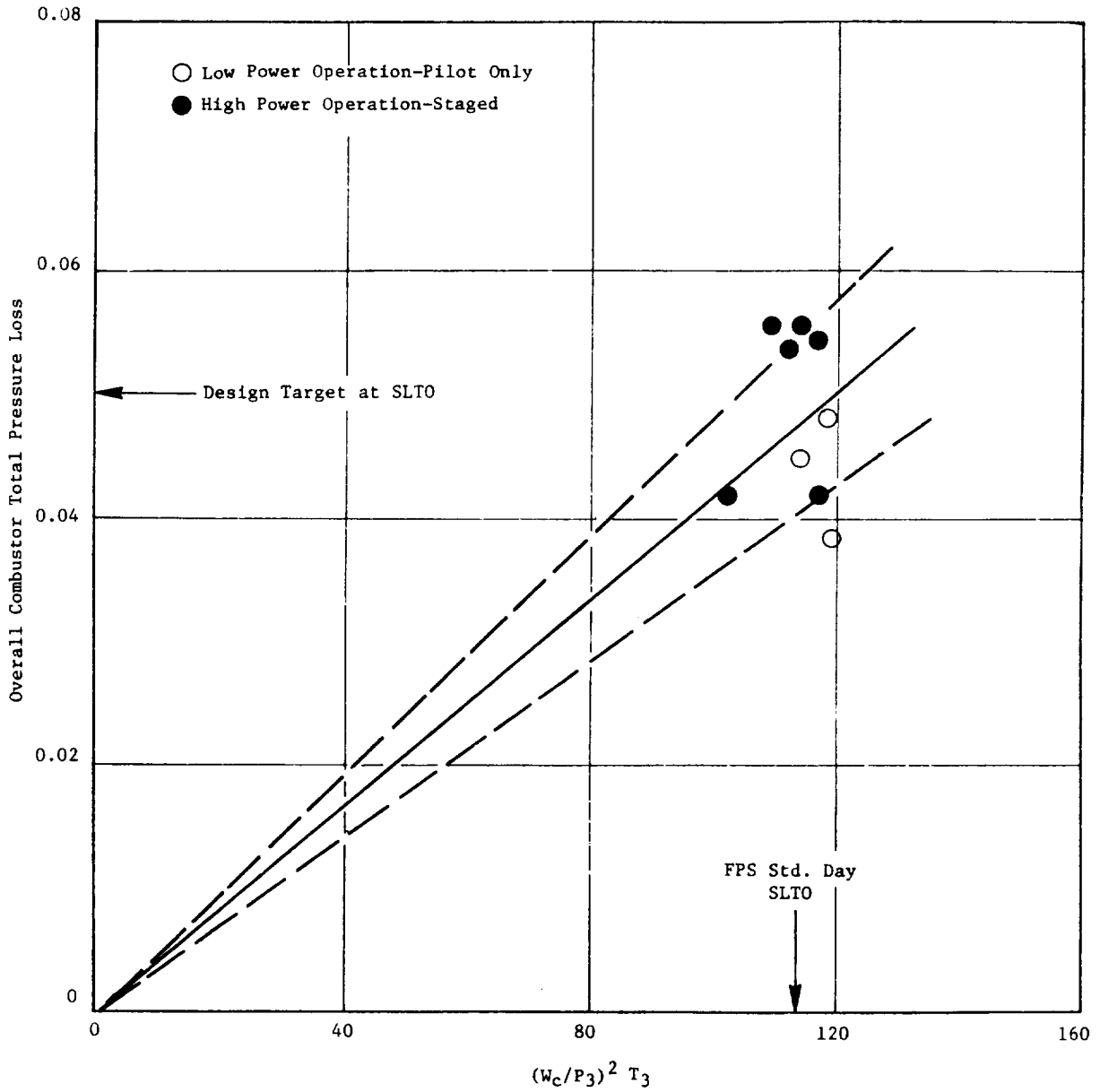


Figure 236. Measured Engine Combustor Pressure Losses.

primary dilution flow levels are considerably above the design intent, while the main stage swirl cup and inner liner primary dilution Panel 1 and Panel 2 cooling flows are below the design intent. The lower swirl cup flow and primary dilution flow in the main stage is most likely responsible for the high NO_x emission levels demonstrated. This redistribution of the airflow reflects the higher pressure drops measured in the pilot dome annulus. One explanation may be higher than expected pressure losses in the diffuser inner flowstream resulting from combustor inner flowpath airflow levels higher than the diffuser design intent. No diffuser performance data was obtained during this test to substantiate this.

Combustor metal temperatures measured during this test are presented in Figures 238 through 247. The locations of these thermocouples can be obtained by identifying the item number and then locating that item number on the instrumentation illustrations presented in Figures 219 through 229. Indicated liner peak metal temperatures at the design point (pilot-to-total fuel split of 0.4) simulated SLTO operating conditions are compared to estimated temperatures based on the design airflow distribution in Figure 248. As observed, the highest liner temperature occurred on the inner liner Row 1 and 2 shingles. These hot spots are located directly in-line with a swirl cup. The calculated estimated airflow distribution indicated that both panels had cooling flow levels considerably below the design intent. However, this condition cannot be applied to explain the higher-than-anticipated temperatures on outer liner Row 1 and 2 shingles. Despite pretest apprehension, the centerbody structure did not exhibit excessively high metal temperatures. This is credited to the increased cooling flow levels incorporated into the design and the application of thermal barrier coating to the exposed surfaces prior to the emissions test.

None of the indicated combustor metal temperatures should pose a problem during upcoming core and fan engine testing. Estimates have been made that suggest that inner liner Panel 1 shingle temperature would increase to 1270 K (1820° F) at full engine cycle operating conditions. The other temperatures would be expected to show similar increases.

7.3.4 Concluding Remarks

The component test results of the E³ engine combustor testing are very satisfactory. The combustor achieved almost all of the design objectives

ORIGINAL PAGE IS
OF POOR QUALITY

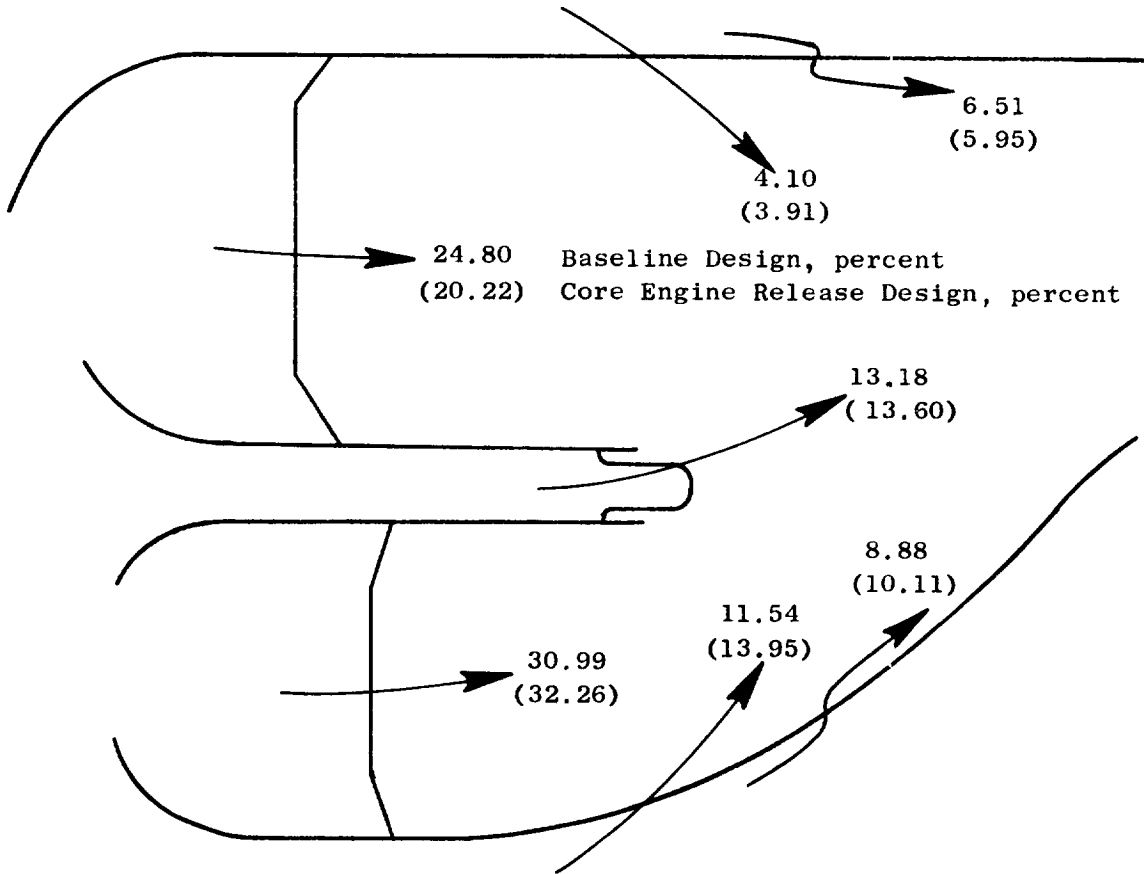


Figure 237. Estimated Versus Design Intent Flow Distribution for Engine Combustor.

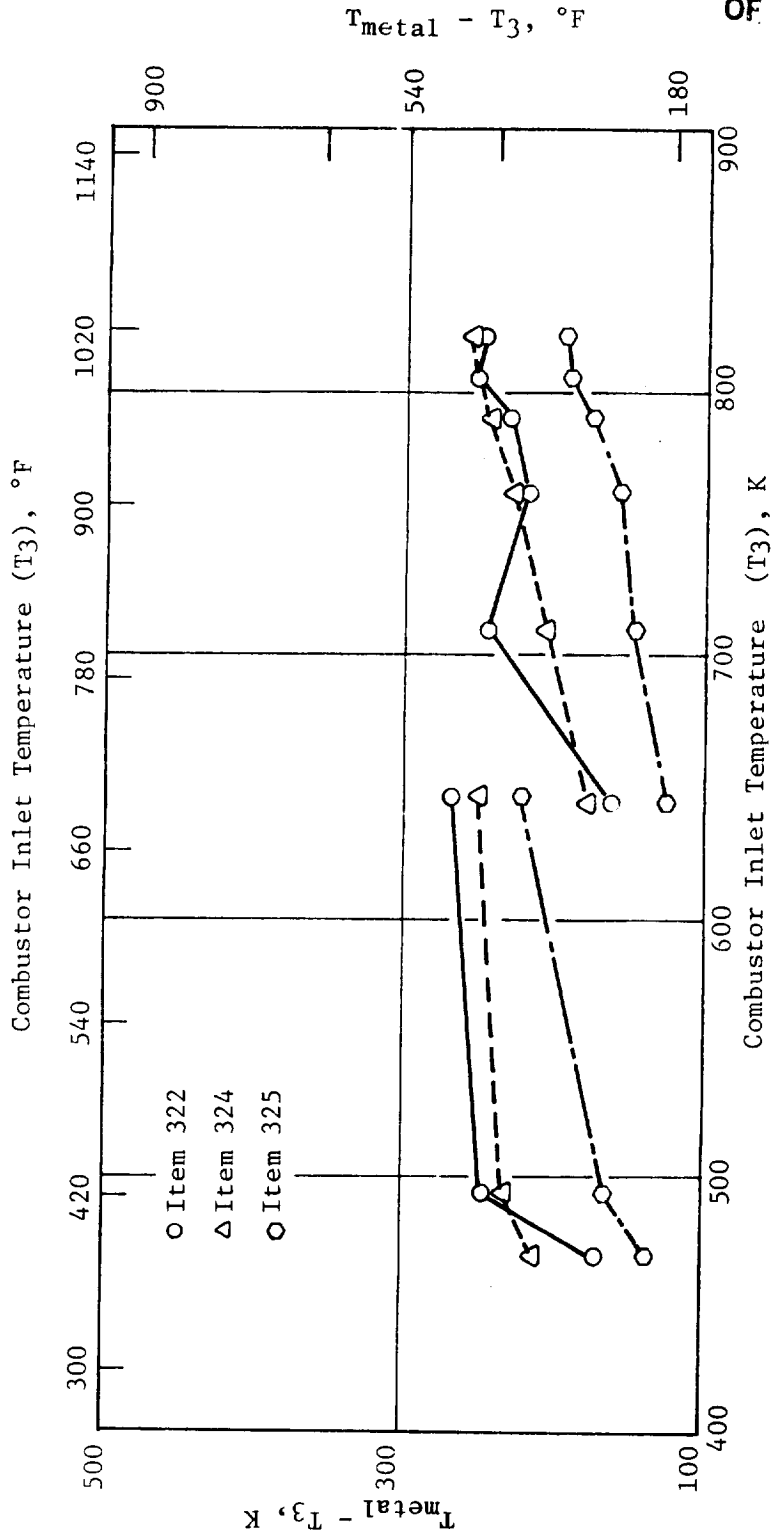


Figure 238. Measured Engine Combustor Metal Temperatures.

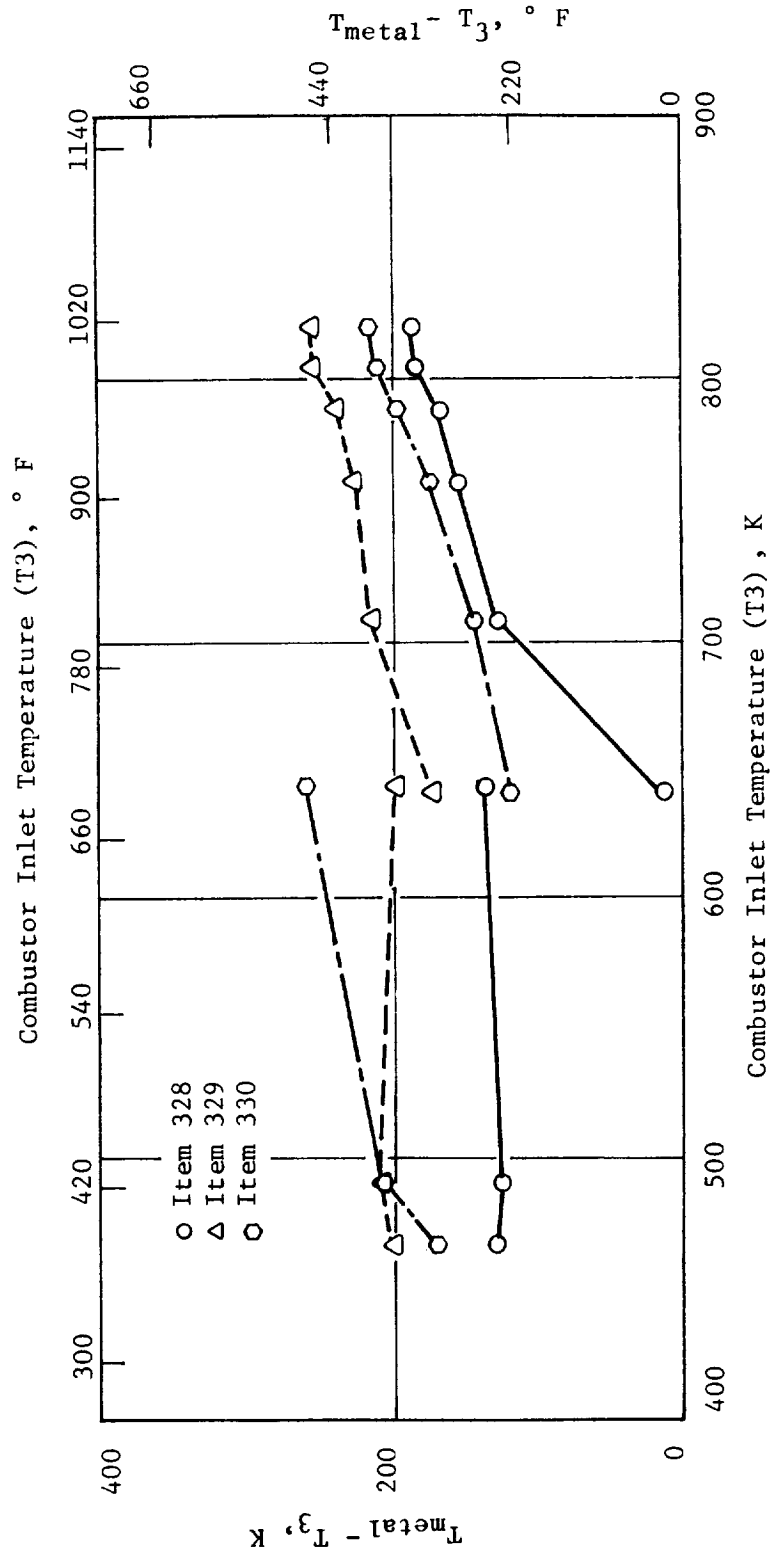


Figure 239. Measured Engine Combusator Metal Temperatures.

ORIGINAL SOURCE OF POOR QUALITY

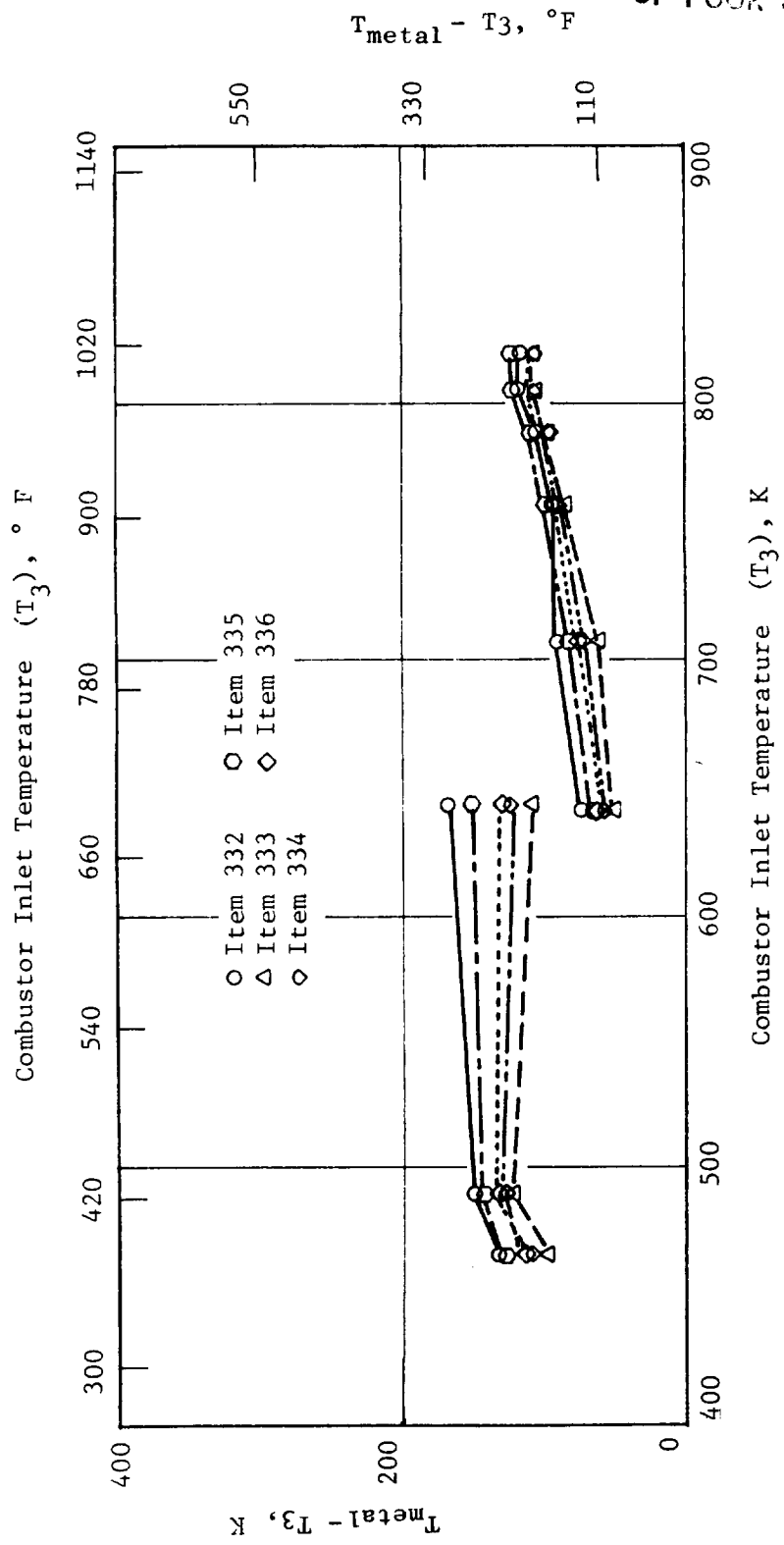


Figure 240. Measured Engine Combustor Metal Temperatures.

ORIGINAL PAGE IS
OF POOR QUALITY

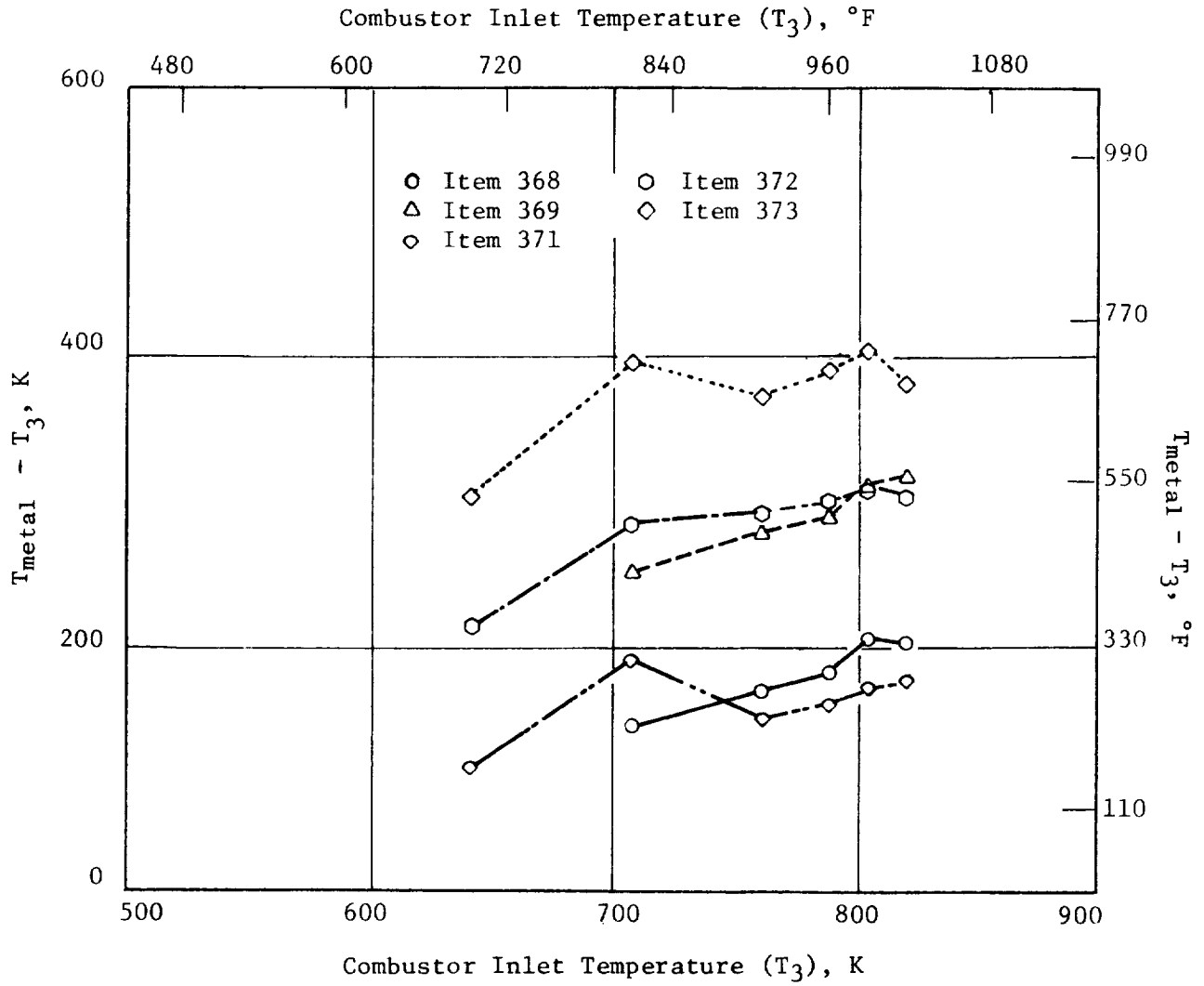


Figure 241. Measured Engine Combustor Metal Temperatures.

ORIGINAL COPY
 OF POOR QUALITY

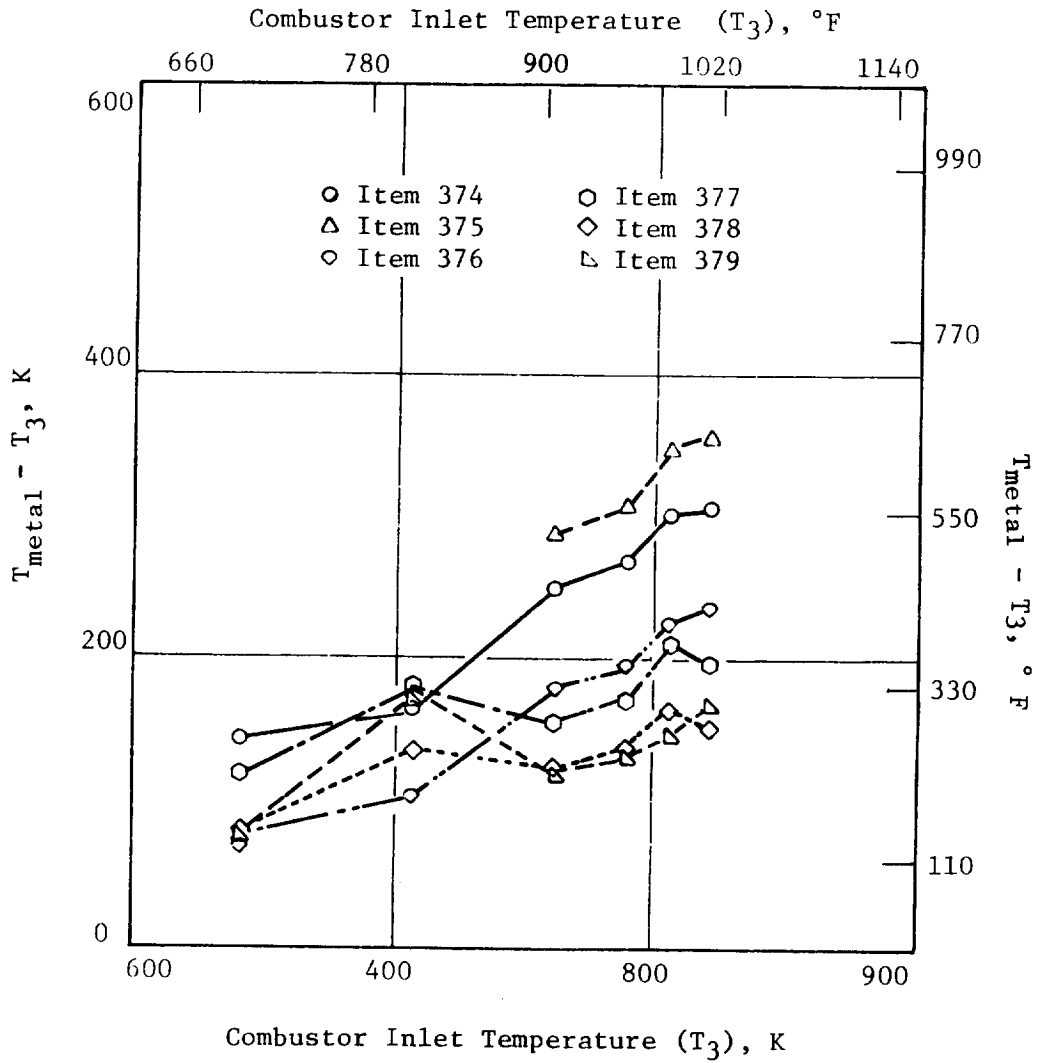


Figure 242. Measured Engine Combustor Metal Temperatures.

ORIGINAL PAGE
OF POOR QUALITY

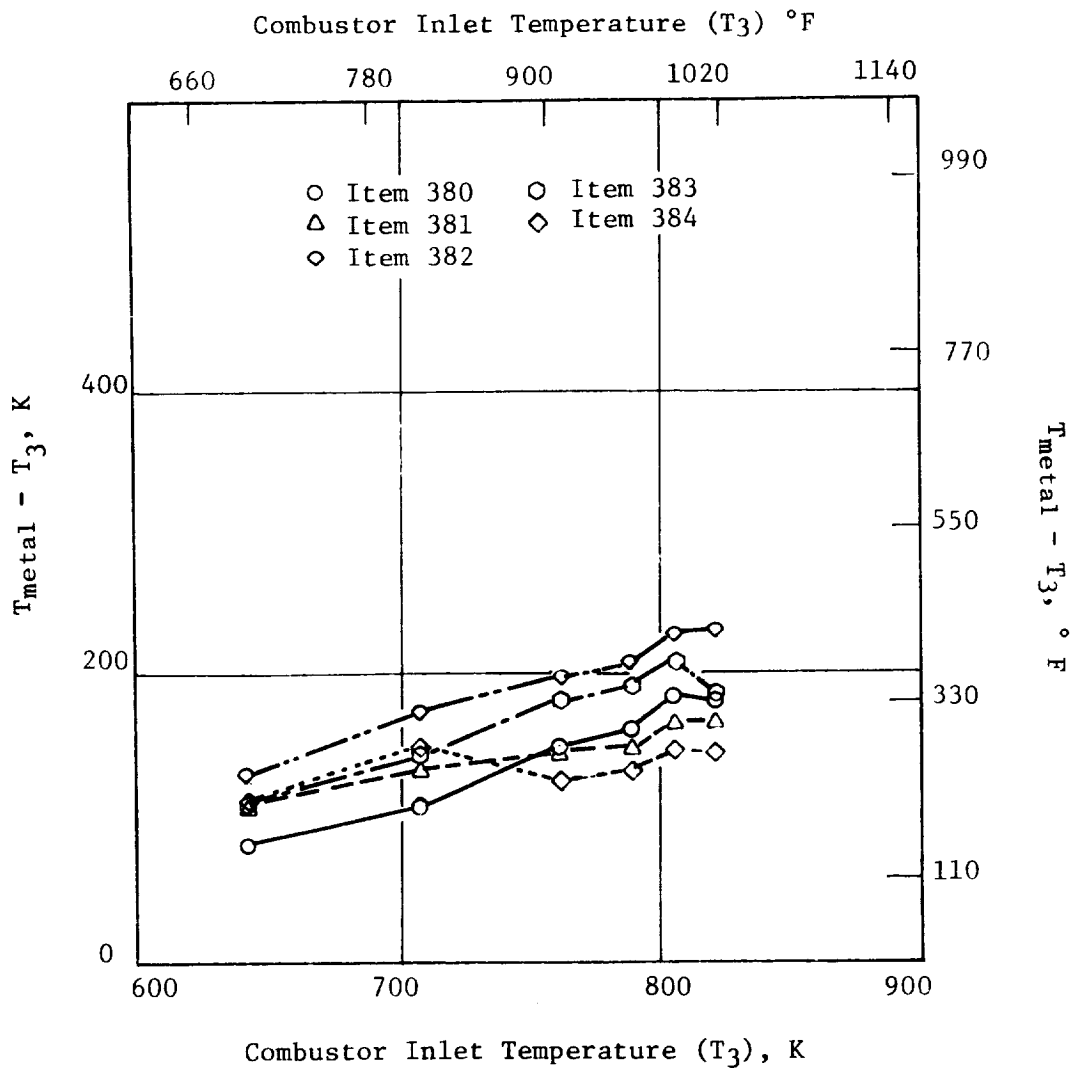


Figure 243. Measured Engine Combustor Metal Temperatures.

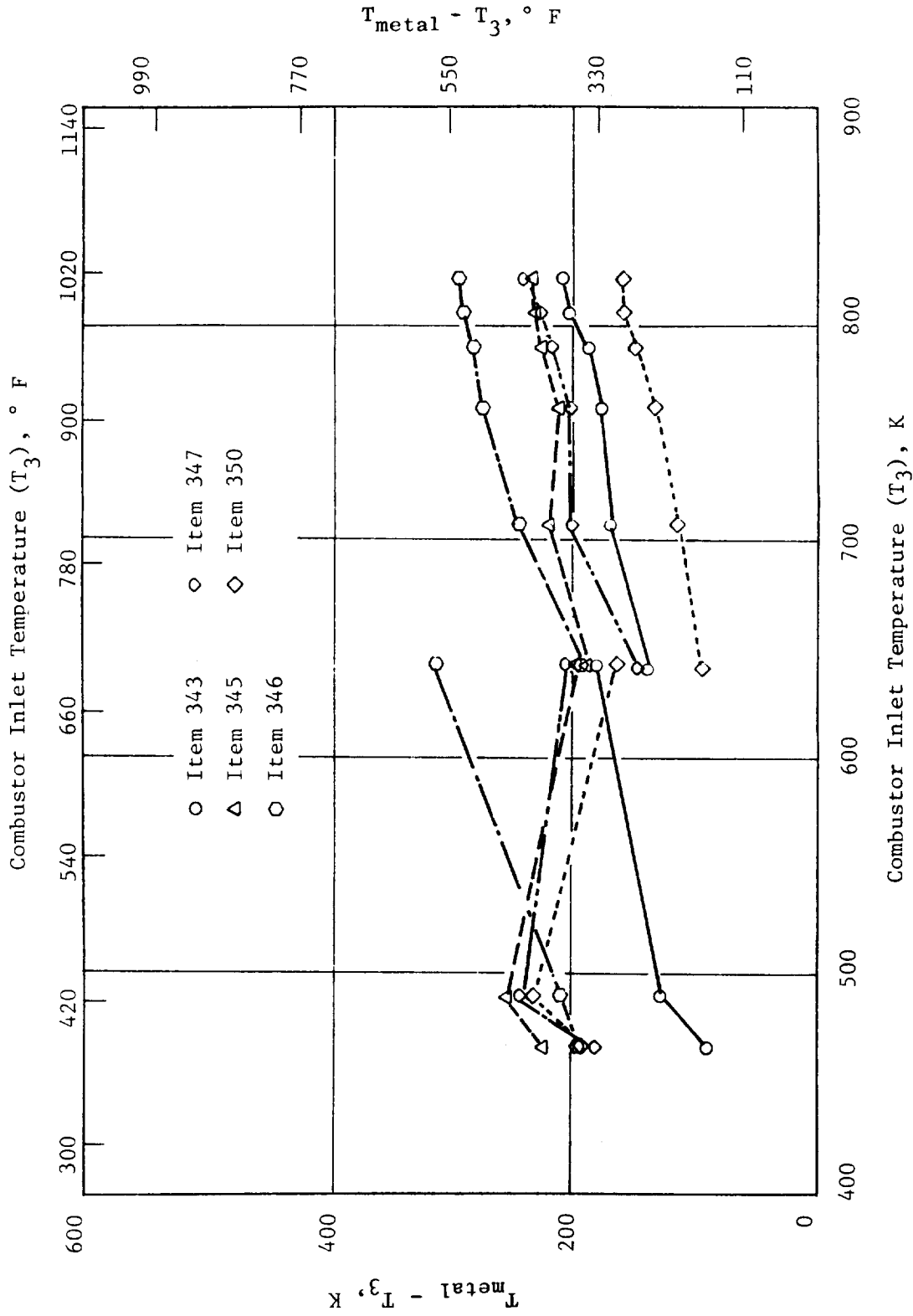


Figure 244. Measured Engine Combustor Metal Temperatures.

ORIGINAL PAGE IS
OF POOR QUALITY

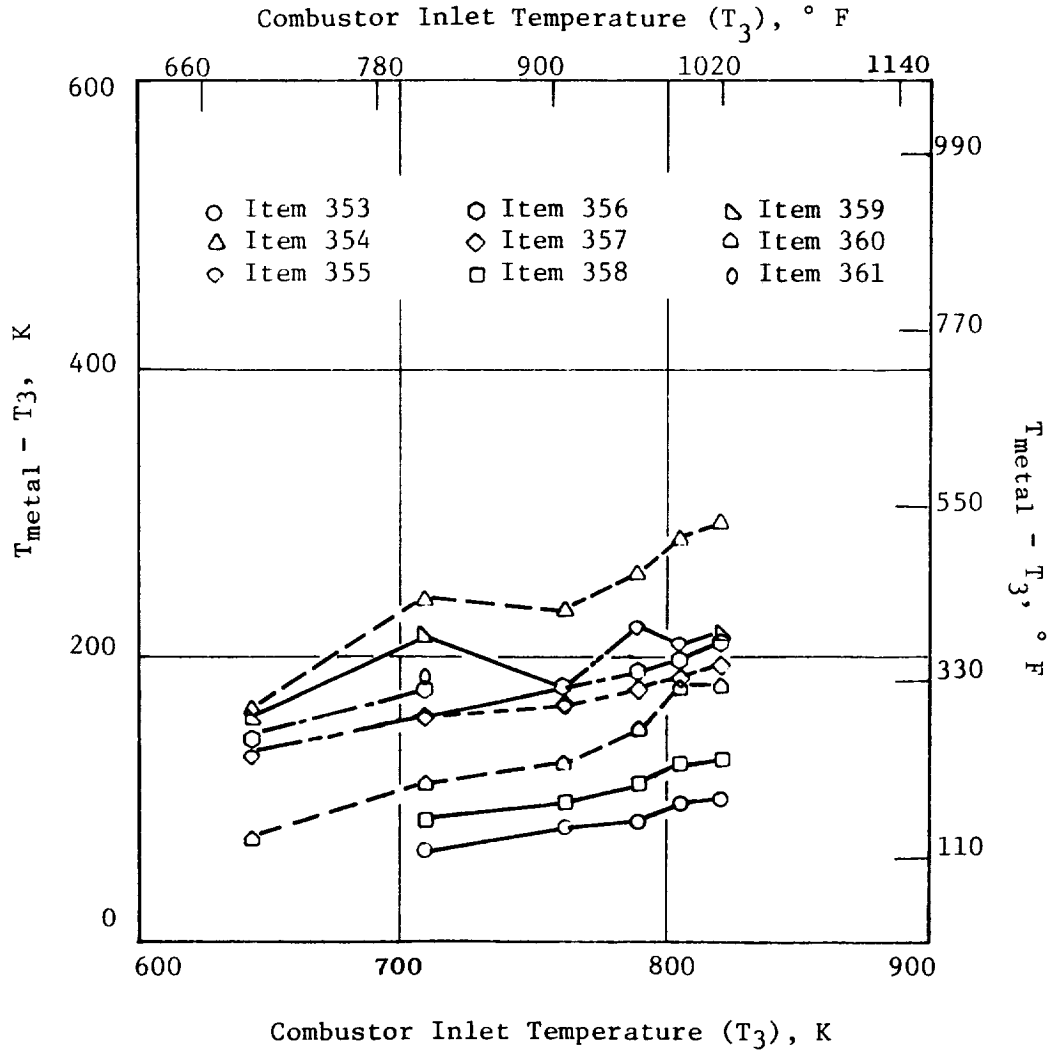


Figure 245. Measured Engine Combusor Metal Temperatures.

ORIGINAL PAGE IS
OF POOR QUALITY

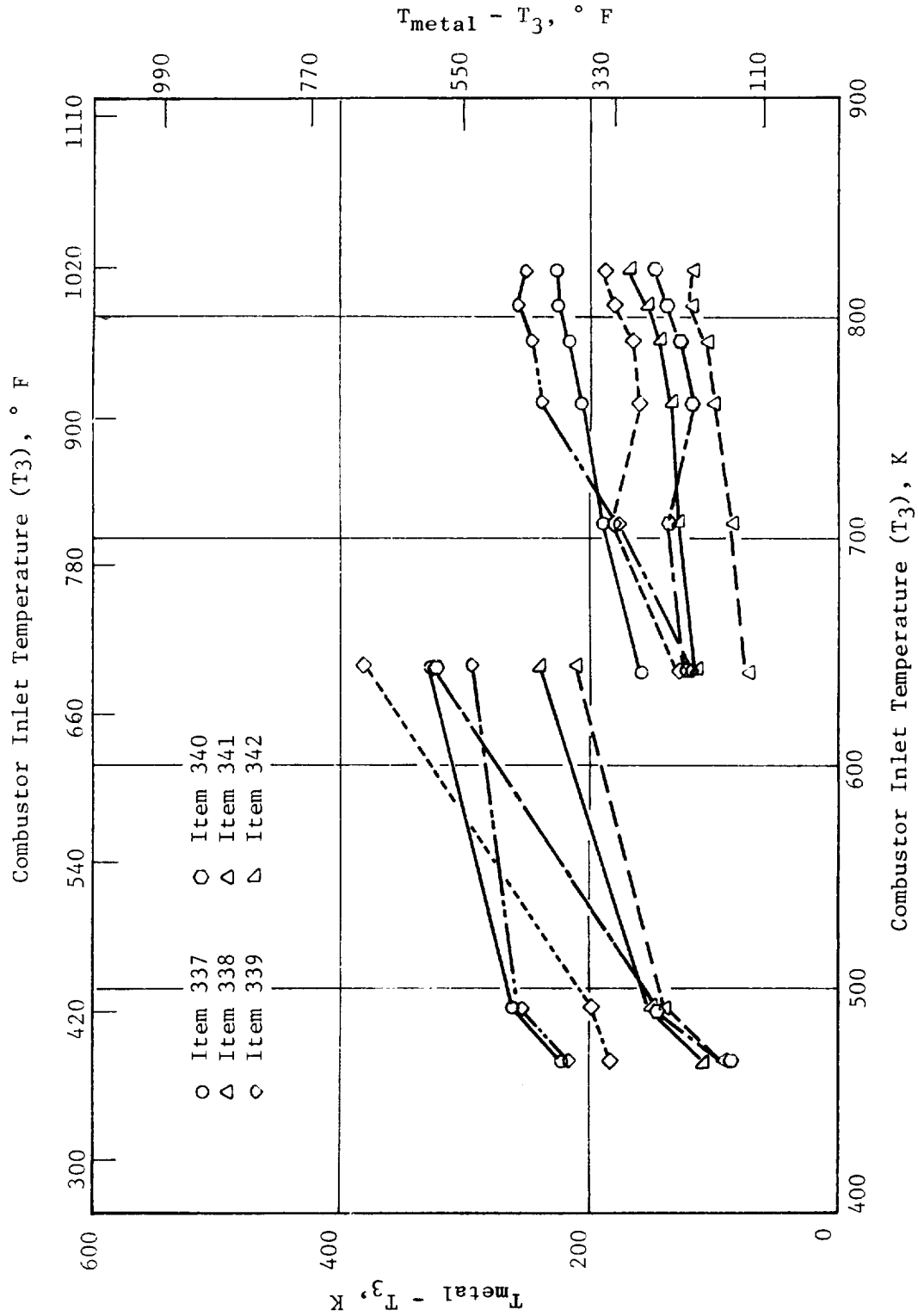


Figure 246. Measured Engine Combustor Metal Temperatures.

ORIGINAL PAGE IS
OF POOR QUALITY

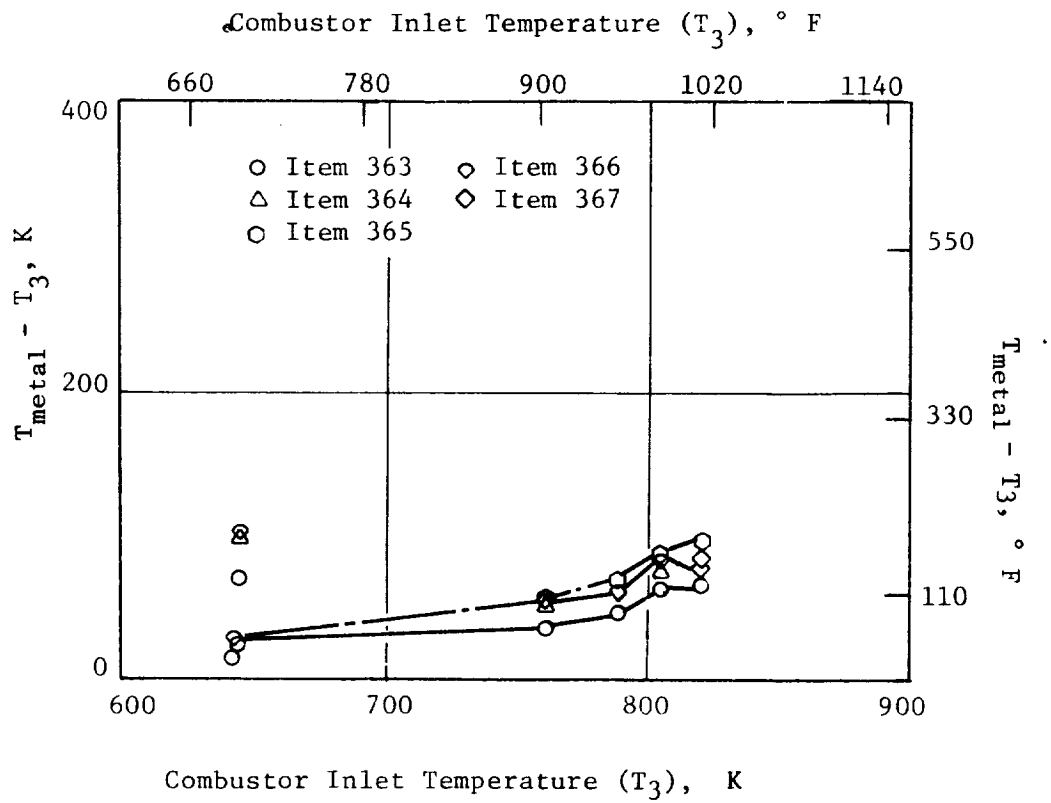


Figure 247. Measured Engine Combustor Metal Temperatures.

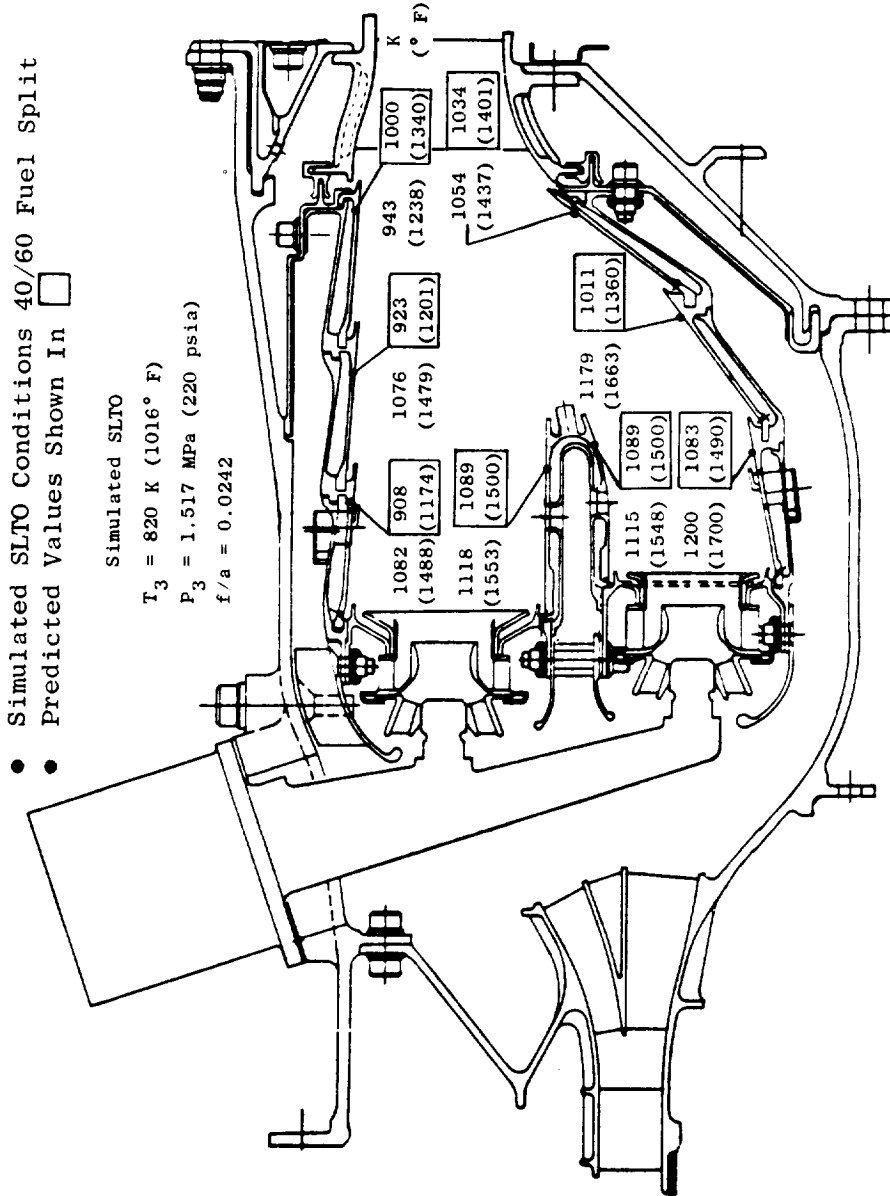


Figure 248. Comparison of Predicted and Measured Peak Metal Temperatures.

established in the combustor development program. The high NO_x levels represent the only shortcoming in what was an excellent overall performance demonstration.

Besides improving the NO_x characteristics, two other areas stand out as requiring further development. One of these areas involves improving the main stage crossfire characteristics to permit staging the combustor at ground idle operating conditions. The other area involves improving the combustion efficiency at 30% approach power in the staged combustor operating mode to get the necessary reductions in the CO and HC emissions.

7.9 CONCLUSION AND SUMMARY

During the E³ full-annular combustor component testing effort, a total of 33 test runs were conducted. These test runs represented ground start ignition, exit temperature performance, and emissions evaluations of ten development combustor configurations (six rich main stage designs; four lean main stage designs), plus the engine combustor configuration. Summaries of these design configurations and their evaluation results are presented in Tables LVI and LVII.

The success of this testing/development effort is evidenced by test results achieved in the component evaluation of the E³ engine combustor evolved from this effort. The test results are as follows:

- Ground start ignition with considerable fuel margin at 30% core speed
- Main stage crossfire at 10% power along the engine accel fuel schedule
- Exit temperature pattern factor of 0.24
- Excellent emissions at 4% and 6% ground idle conditions
- NO_x emissions levels 30% to 40% above the program requirement
- Smoke levels within the program requirement
- Overall total pressure loss near the design goal
- Peak metal temperatures which should pose no problems during engine operation

Table LVI. Summary of Full-Annular Combustor Configurations and Test Results.

Config.	Modifications	Ground Start Ignition Performance	Emissions Performance			Comments
			EGT Performance	CO	HC	
Mod 2a	<ul style="list-style-type: none"> Reduced pilot stage and main stage cup flow Increased pilot stage and main stage primary dilution Increased pilot side and main side C/B cooling flow Introduced inner liner Panel 2 dilution Shortened C/B 	<ul style="list-style-type: none"> Pilot stage ignition characteristics not as good as Mod.-1, but acceptable. Main stage ignition characteristics not as good as Mod 1 	No data obtained	No data obtained	No data obtained	<ul style="list-style-type: none"> Strong airflow current produced from combined effects of inner Panel 2 dilution and C/B cooling flow appears to prevent fire from pilot stage from penetrating into main stage annulus through crossfire tubes for ignition.
Mod 2b	<ul style="list-style-type: none"> Closed off inner liner Panel 2 dilution. 	<ul style="list-style-type: none"> No change in pilot stage ignition characteristics Main stage ignition characteristics improved but still not good enough to permit staging at subidle operating conditions 	No data obtained	No data obtained	No data obtained	<ul style="list-style-type: none"> Combustion gases from pilot stage do not penetrate into main stage annulus thru crossfire tubes.
Mod 3a	<ul style="list-style-type: none"> Reduced main stage dome flow. Blocked off main stage side C/B cooling flow in line with the crossfire tubes. Increased outer liner trim dilution and inner liner trim dilution. 	<ul style="list-style-type: none"> No significant change in pilot stage ignition characteristics Significant improvement in main stage ignition characteristics. At true cycle inlet pressures, staging can occur down to 45% core speed. 	No data obtained	No data obtained	No data obtained	<ul style="list-style-type: none"> Crossfire tube needs to be moved forward to bring ignition source closer to main stage dome.
Mod 3b	<ul style="list-style-type: none"> Blocked off pilot stage side C/B cooling flow in line with the crossfire tubes. 	<ul style="list-style-type: none"> Slight improvement in main stage ignition characteristics. At true cycle inlet pressures, staging can take place at 40% core speed with little or no compressor bleed. 	<ul style="list-style-type: none"> A pattern factor of 0.45 demonstrated at 40/60 fuel split 	No data obtained	No data obtained	<ul style="list-style-type: none"> Too much inner trim dilution. Mixing distance too short to allow that much air to mix with combustion gases to provide better uniformity.
Mod 4	<ul style="list-style-type: none"> Reduced inner liner trim dilution Reintroduced inner liner Panel 2 dilution. 	<ul style="list-style-type: none"> Pilot stage ignition characteristics unchanged Main stage ignition characteristics deteriorated 	No data obtained	No data obtained	No data obtained	<ul style="list-style-type: none"> Introduction of inner liner Panel 2 dilution is detrimental to main stage ignition characteristics.
Mod 5	<ul style="list-style-type: none"> Reduced main stage primary dilution. Introduced outer liner Panel 2 dilution. 	<ul style="list-style-type: none"> Pilot stage ignition characteristics unchanged Main stage ignition improved slightly. At true cycle inlet pressures, staging can take place at 50% core speed. 	<ul style="list-style-type: none"> A pattern factor of 0.50 demonstrated at 40/60 fuel split Average profile inward peaked and exceeds the design limit by a considerable amount 	No data obtained	No data obtained	<ul style="list-style-type: none"> Removing airflow from primary zone of main stage to enrichen for ignition improvements is detrimental to EGT performance of this short length combustor. In conclusion, to evolve a rich dome main stage combustor configuration with acceptable ignition and EGT performance will require substantial additional development.

ORIGINAL PANEL OF POOR QUALITY

Table LVII. Summary of Full-Annular Combustor Configurations and Test Results.

Config.	Modifications	Ground Start Ignition Performance	EGT Performance	Emissions Performance			Comments
				CO	EPAP HC	NOx	
Baseline		<ul style="list-style-type: none"> • Marginal pilot stage ignition characteristics • Poor main stage ignition characteristics in subidle operating range 	<ul style="list-style-type: none"> • Pattern factor of 0.41 at 40/60 fuel split • Pattern factor of 0.26 at 50/50 fuel split 	8.20	3.03	2.78	<ul style="list-style-type: none"> • Main stage not required to ignite at subidle conditions • Minimum CO/HC emissions occurred at f/a above design cycle conditions
Mod 1	<ul style="list-style-type: none"> • Richer pilot stage. • Leaner main stage. • Primary dilution between swirl cups. • Increased outer and inner trim dilution. 	<ul style="list-style-type: none"> • Significantly improved pilot stage ignition characteristics • Satisfies goal with margin. • Main stage ignition characteristics not as good as baseline configuration 	<ul style="list-style-type: none"> • Pattern factor of 0.24 at 40/60 fuel split • Average temperature profile beyond limit in hub region. 	4.55	0.47	2.81	<ul style="list-style-type: none"> • Minimum CO/HC emissions occurred near design cycle f/a.
Mod 6	<ul style="list-style-type: none"> • Increased primary dilution and decreased cup flow in pilot annulus. • Richer main stages. • Panel 2 inner dilution. • Shortened centerbody. 	<ul style="list-style-type: none"> • Pilot stage ignition characteristics satisfy 6/81 start cycle with margin. • Could not achieve main stage full propagation at subidle conditions. 	<ul style="list-style-type: none"> • Pattern factor of 0.36 at 40/60 fuel split. • Average temperature profile beyond limit in hub regions. 	No data obtained			<ul style="list-style-type: none"> • Poor combustor quality believed related to poor EGT performance.
Mod 7	<ul style="list-style-type: none"> • Refurbished combustor hardware to improve the quality. • Reduced inner liner trim dilution. • Increased inner liner Panel 2 dilutions. 	<ul style="list-style-type: none"> • Ignition characteristics of pilot and main stage similar to Mod 6. 	<ul style="list-style-type: none"> • Pattern factor of 0.27 at 40/60 fuel split. • Average profile only slightly beyond limit in hub region. 	3.27	0.58	2.96	<ul style="list-style-type: none"> • Main stage will ignite at operating condition above 10% power.
Core Engine Combustor		<ul style="list-style-type: none"> • Pilot stage ignition characteristics better than Mod 7. • Main stage better but not good enough for subidle staging. 	<ul style="list-style-type: none"> • Pattern factor of 0.24 at 40/60 fuel splits. • Average temperature profile is center peaked and generally within the design limit. 	1.58	0.11	4.66	<ul style="list-style-type: none"> • Additional ignition data to be obtained at actual ground start cycle inlet pressures.

ORIGINAL PAGE IS
OF POOR QUALITY

8.0 CONCLUDING REMARKS

The NASA/GE E³ Combustor Development Program was a very successful component development effort. The technology derived from design studies and development testing efforts evolved into an engine combustion system that demonstrated excellent overall component performance. Despite the successes, several performance areas stand out as requiring further development in order to evolve the design into one which would be totally acceptable for use in advanced aircraft engine applications.

These areas involve improving the main stage crossfire characteristics to permit combustor staging at ground idle operation, improving combustion efficiency at the 30% approach power condition while operating the combustor in the staged mode, and further reducing the high power NO_x emissions.

Significantly better performance levels were predicted for the engine diffuser system than those demonstrated with the combustor component test rig diffuser. Therefore, the high NO_x levels demonstrated in the component (test rig) evaluation of the engine combustion system are not considered representative of the E³ FPS design. From knowledge of the flow characteristics of the combustor and engine diffuser performance predictions, the E³ FPS combustion system will satisfy the E³ Program NO_x emission goal as well as the CO and HC goals. Estimates of the E³ FPS emissions are presented in terms of the EPA parameter in Table LVIII.

The engine combustion system has been released to E³ Evaluation Engineering for incorporation into the core engine CDN assembly buildup. The combustion system will undergo further evaluation as an integral part of the core and ICLS (Integrated Core and Low Pressure Spool) configuration of the E³ later in 1982. It is currently planned to obtain emissions data as part of the overall core engine system evaluations. Some metal temperature and pressure data will also be obtained during the core engine testing effort.

Table LVIII. Estimated EPAP Numbers for E³ FPS Combustion System.

	<u>Program Goal</u>	<u>Ground EPAP</u>	<u>Idle at 4% F_n, Percent Margin</u>	<u>Ground EPAP</u>	<u>Idle at 6% F_n, Percent Margin</u>
CO	3.00	2.45	23	1.58	90
HC	0.40	0.22	82	0.11	364
NO _x	3.00	2.98	1	2.80	7

- EPAP 1bm/1000 lb Thrust-hr Cycle
- E³ FPS Sea Level Static Std Day Operation Cycle
- Pilot Only at Approach Power

APPENDIX A

LOCATION AND NUMBERING OF E³ ANNULAR RIG INSTRUMENTATION

<u>Group No.</u>	<u>Quantity</u>	<u>Axial Location from Start of Diff.</u>	<u>Angular Position(degrees)</u>	<u>Tap No.</u>	<u>Measurement Function</u>
1	4	-2.75	48, 132, 228, 312	101-104	Pressure Recovery
2	2	-0.50	48, 228	105-106	
3	2	0.		107-108	
4	2	0.38		109-110	
5	2	0.76		111-112	
6	2	1.14		113-114	
7	2	1.51		115-116	
8	2	1.89		117-118	
9	2	2.27		119-120	
10	2	0.65		121-122	
11	2	2.50		123-124	
12	2	3.90		125-126	
13	2	4.80		127-128	
14	2	5.90		129-130	
15	4	8.00	48, 132, 228, 312	131-134	Pressure Recovery and Flow Split
16	2	4.25	45, 225	201-202	
17	2	4.97	48, 228	203-204	

ORIGINAL PAGE 19
OF POOR QUALITY

<u>Group No.</u>	<u>Quantity</u>	<u>Axial Location from Start of Diff.</u>	<u>Angular Position(degrees)</u>	<u>Tap No.</u>	<u>Measurement Function</u>
18	2	5.90	48, 228	205-206	
19	4	8.00	48, 132, 228, 312	207-210	Pressure Recovery and Flow Split
20	4	5.60	45, 135, 225, 315	301-304	Pressure Recovery
21	4	8.00		305-308	Flow Split
22	4	5.60	45, 135, 225, 315	401-404	Pressure Recovery
23	4	8.00	48, 132, 228, 312	405-408	Flow Split
24	2	4.80	225	501-502	
25	4	8.00	45, 135, 225, 315	503-506	Pressure Recovery and Flow Split
26	2	4.85	45, 225	601-602	
27	4	8.00	45, 135, 225, 315	603-606	Pressure Recovery and Flow Split
28	4	6.10	45, 135, 225, 315	701-704	Pressure Recovery
29	4	8.00	48, 132, 228, 312	705-708	Flow Split
30	4	6.10	45, 135, 225, 315	801-804	Pressure Recovery
31	4	8.00		805-808	Flow Split
32	2	4.65	45, 225	901-902	
33	2	5.45	45, 225	903-904	
34	4	8.00	48, 132, 228, 312	905-908	Pressure Recovery and Flow Split

<u>Group No</u>	<u>Quantity</u>	<u>Axial Location from Start of Diff.</u>	<u>Angular Position(degrees)</u>	<u>Tap No.</u>	<u>Measurement Function</u>
35	4	-2.75	48, 132, 228, 312	1001-1004	
36	2	-0.50	48, 228	1005-1006	
37	2	0.		1007-1008	
38	2	0.43		1009-1010	
39	2	0.85		1011-1012	
40	2	1.28		1013-1014	
41	2	1.71		1015-1016	
42	2	2.14		1017-1018	
43	2	2.56		1019-1020	
44	2	2.689		1021-1022	
45	2	3.38		1023-1024	
46	2	4.10		1025-1026	
47	2	5.45	48, 228	1027-1028	
48	4	8.00	48, 132, 228, 312	1029-1032	Pressure Recovery and Flow Split
49	2	Prediffuser	48, 228	1101-1102	
50	2	Discharge	48, 228	1103-11-4	

APPENDIX B

COMBUSTOR SPLIT DUCT DIFFUSER PERFORMANCE DATA

This appendix presents static pressure recovery curves for each of the individual passage test runs with the three inlet velocity profiles for the E³ combustor inlet diffuser as shown in Figures 1B through 15B.

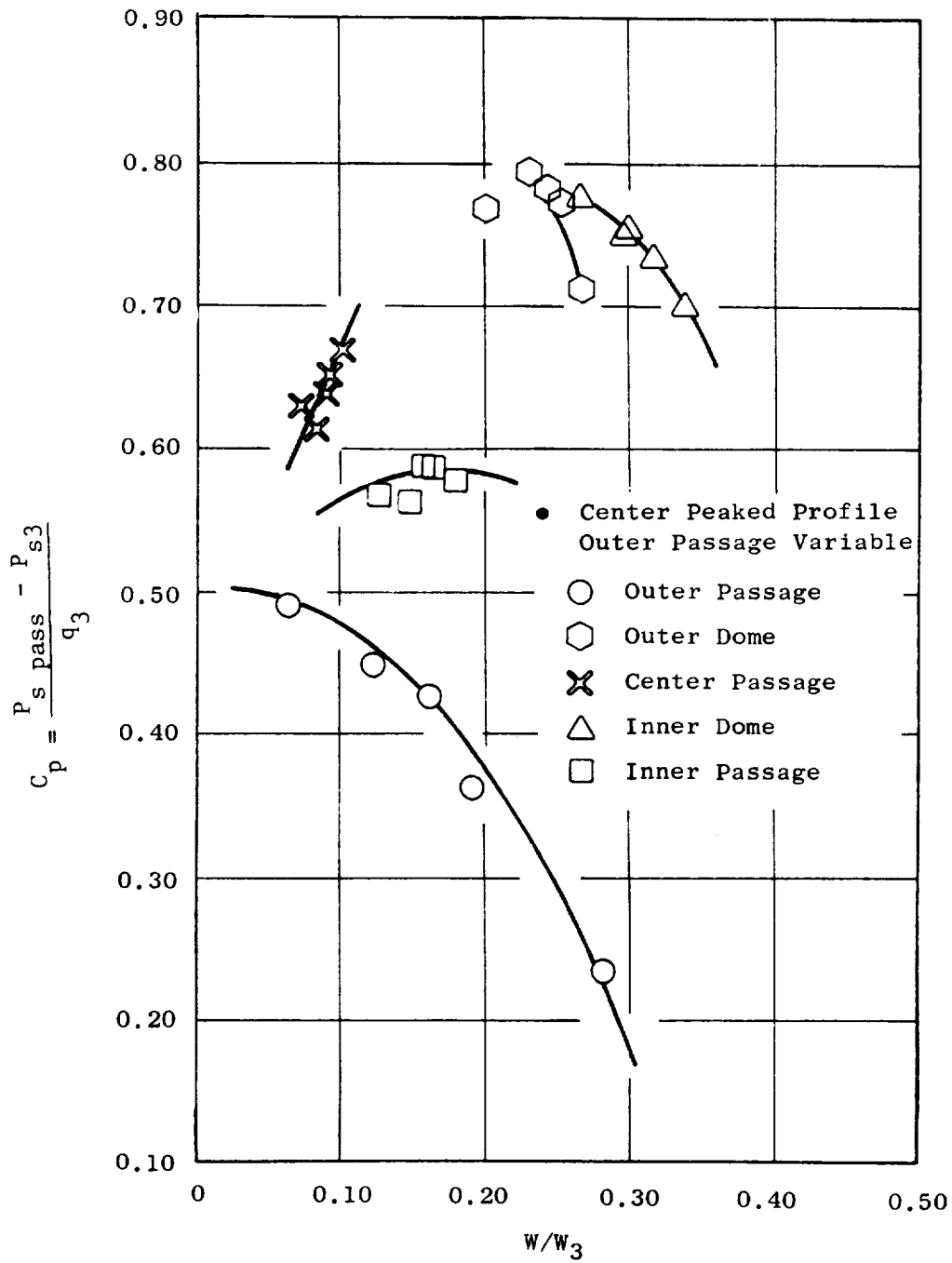


Figure 1B. E³ Combustor Inlet Diffuser CR&D Model Test Data.

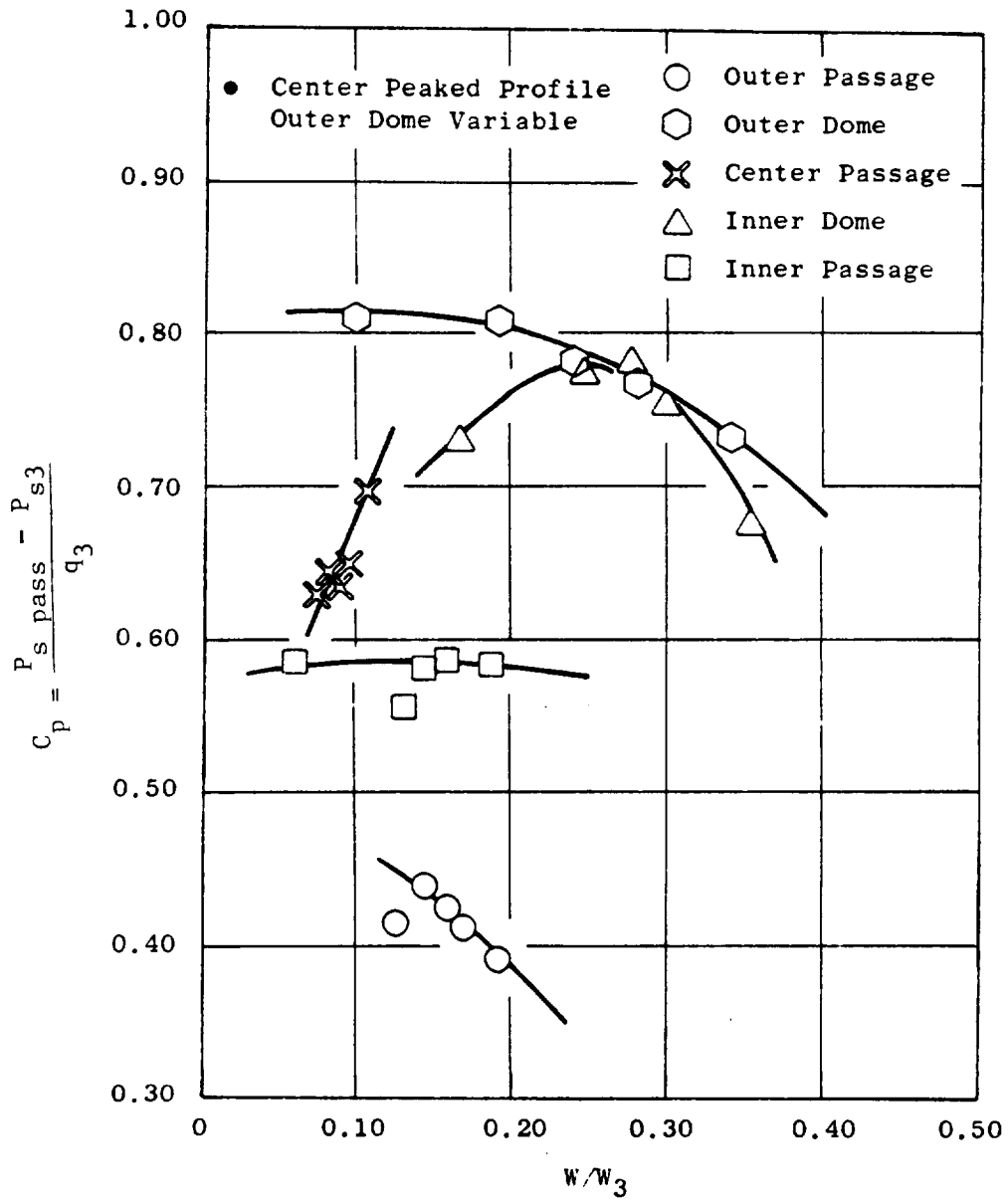


Figure 2B. E³ Combustor Inlet Diffuser CR&D Model Test Data.

ORIGINAL PAGE IS
OF POOR QUALITY

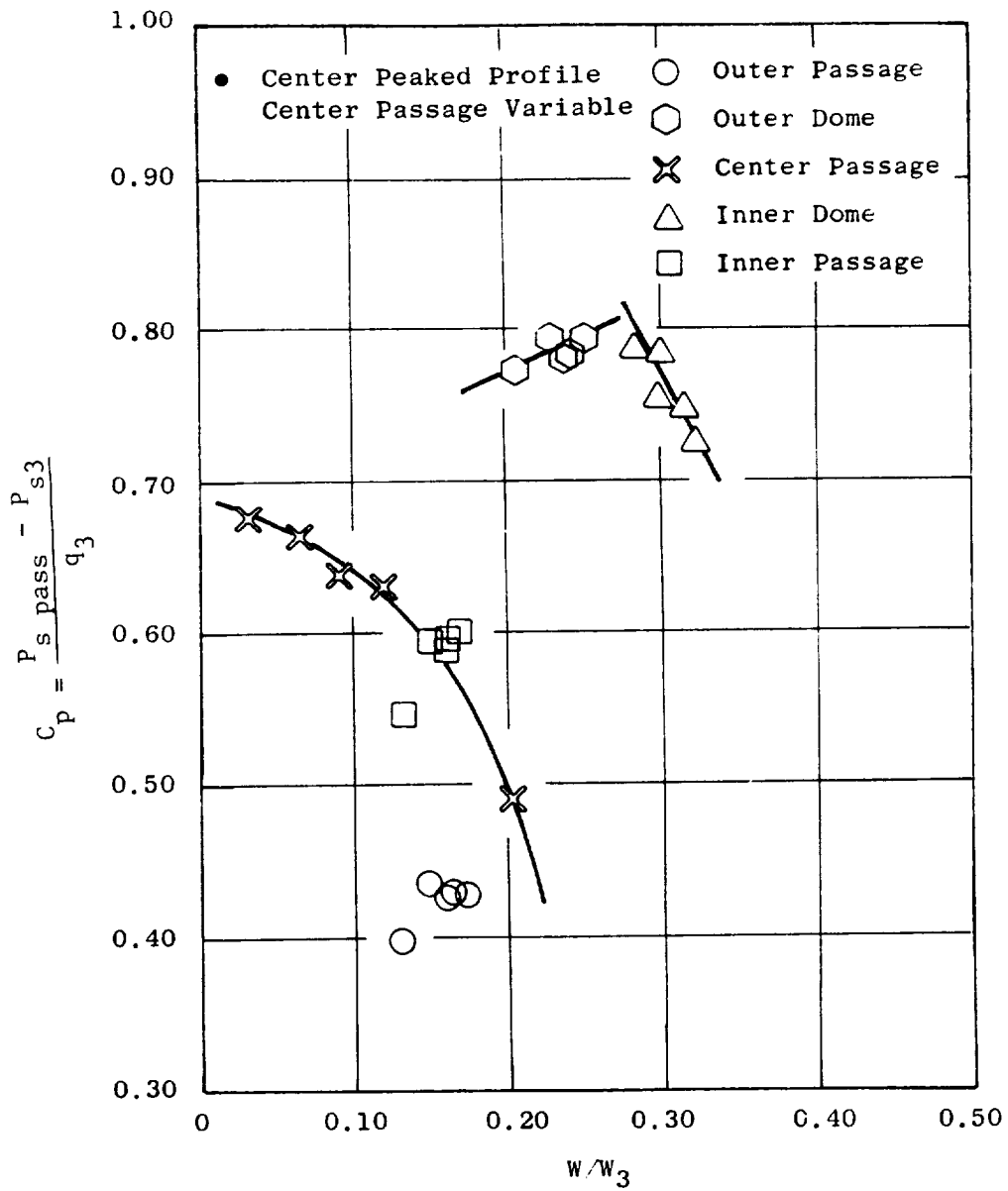


Figure 3B. E^3 Combustor Inlet Diffuser CR&D Model Test Data.

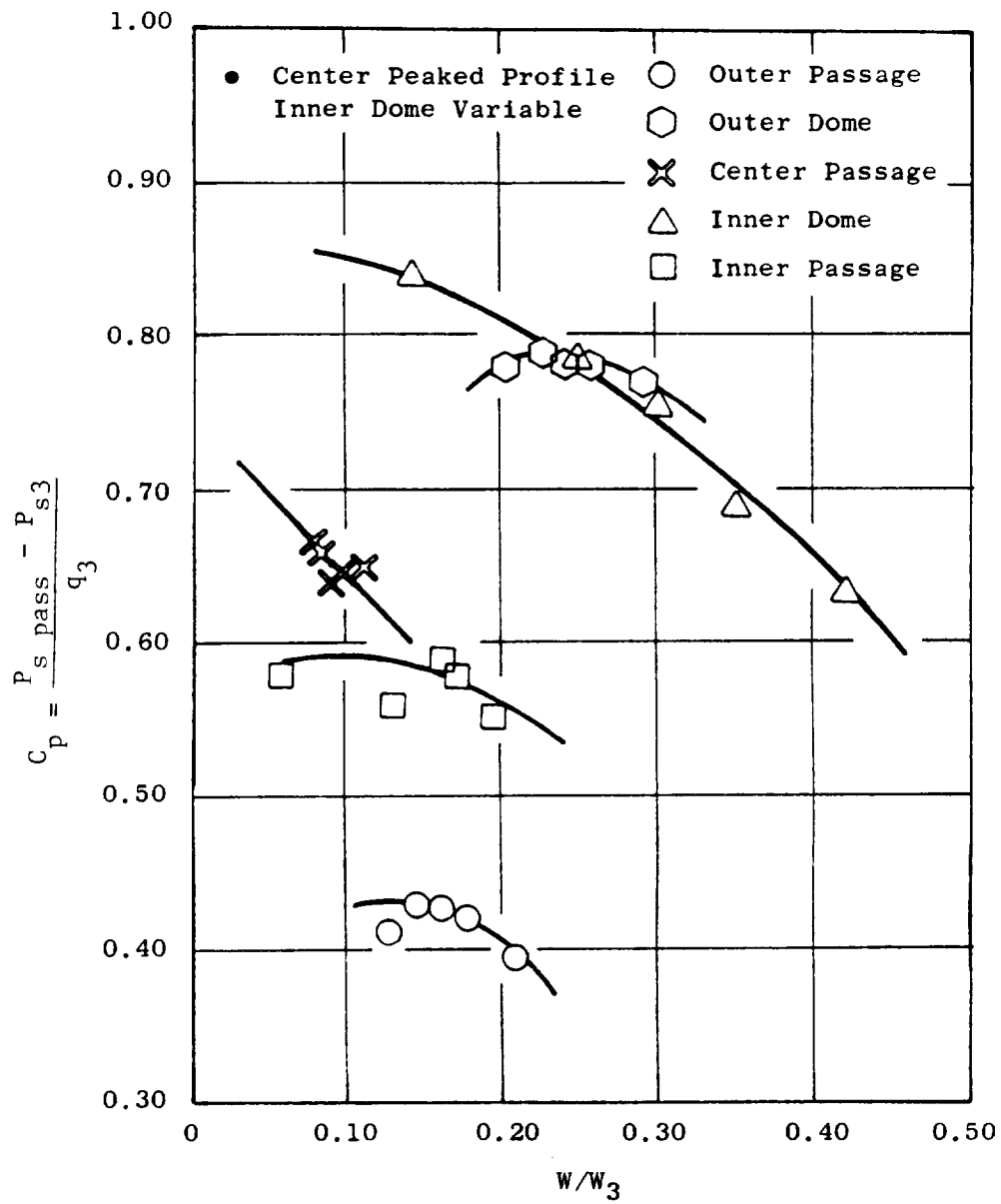


Figure 4B. E³ Combustor Inlet Diffuser CR&D Model Test Data.

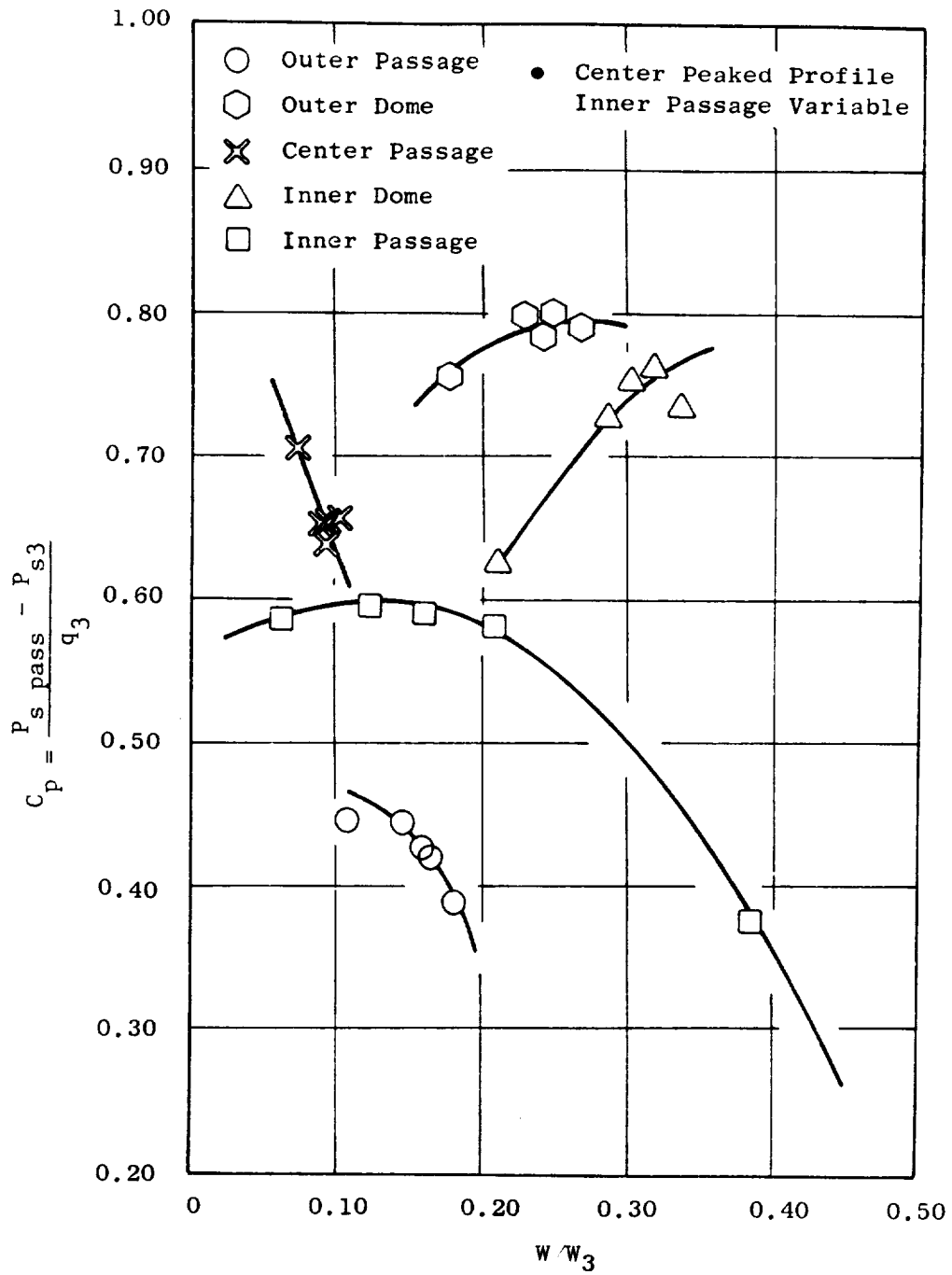


Figure 5B. E³ Combustor Inlet Diffuser CR&D Model Test Data.

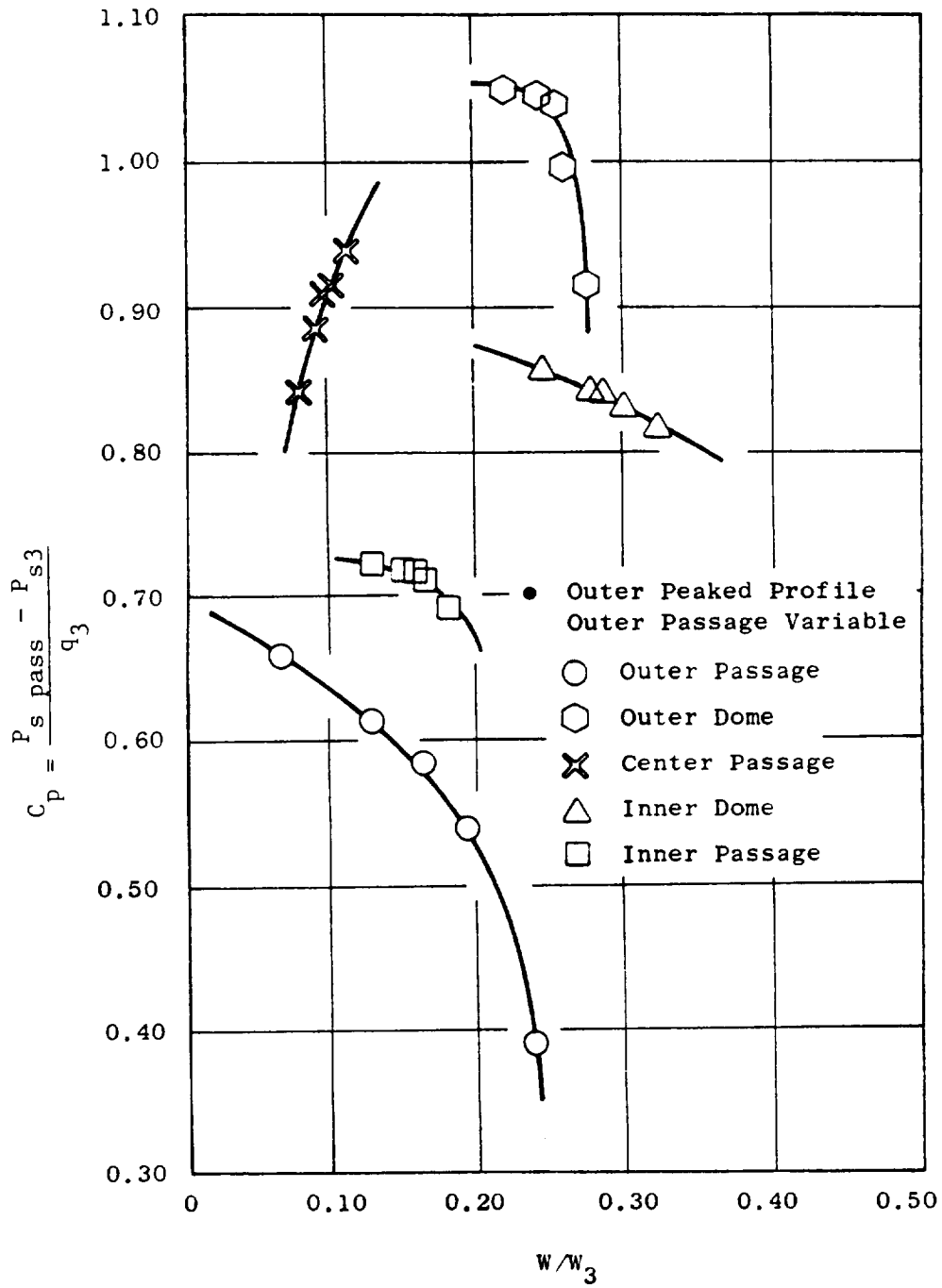


Figure 6B. E^3 Combustor Inlet Diffuser CR&D Model Test Data.

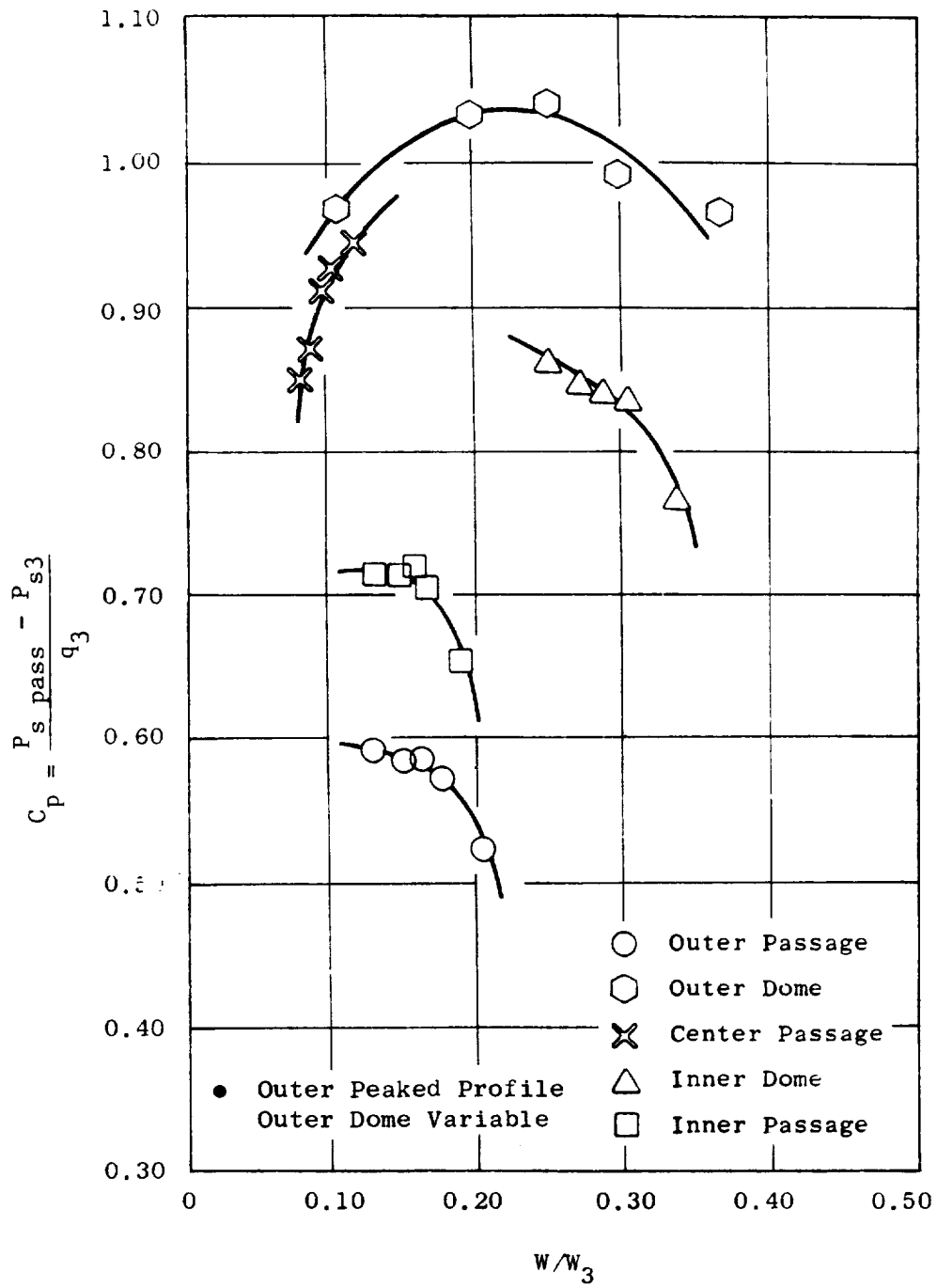


Figure 7B. E³ Combustor Inlet Diffuser CR&D Model Test Data.

Characteristics
OF POOR QUALITY

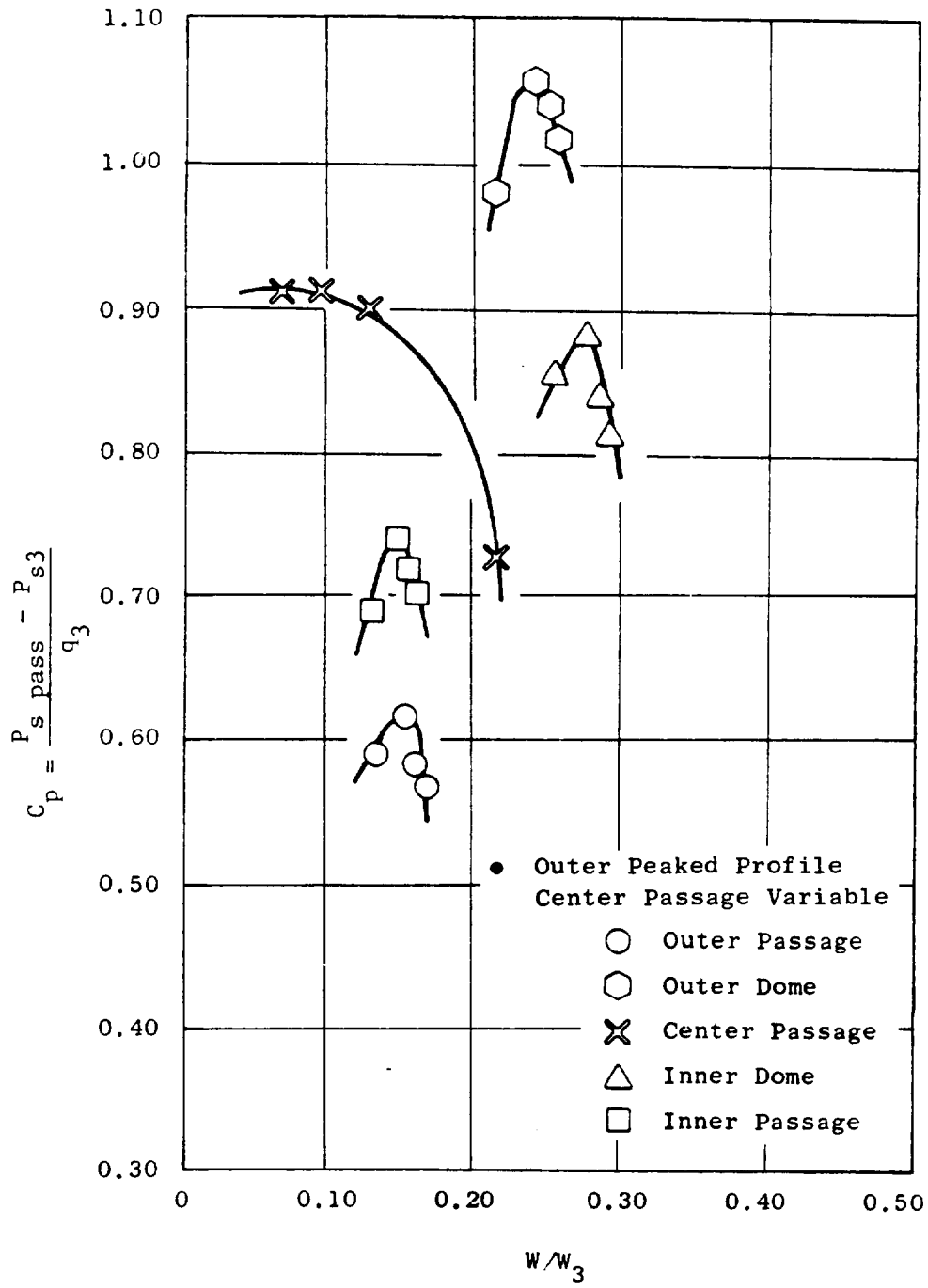


Figure 8B. E³ Combustor Inlet Diffuser CR&D Model Test Data.

ORIGINAL PAGE IS
OF POOR QUALITY

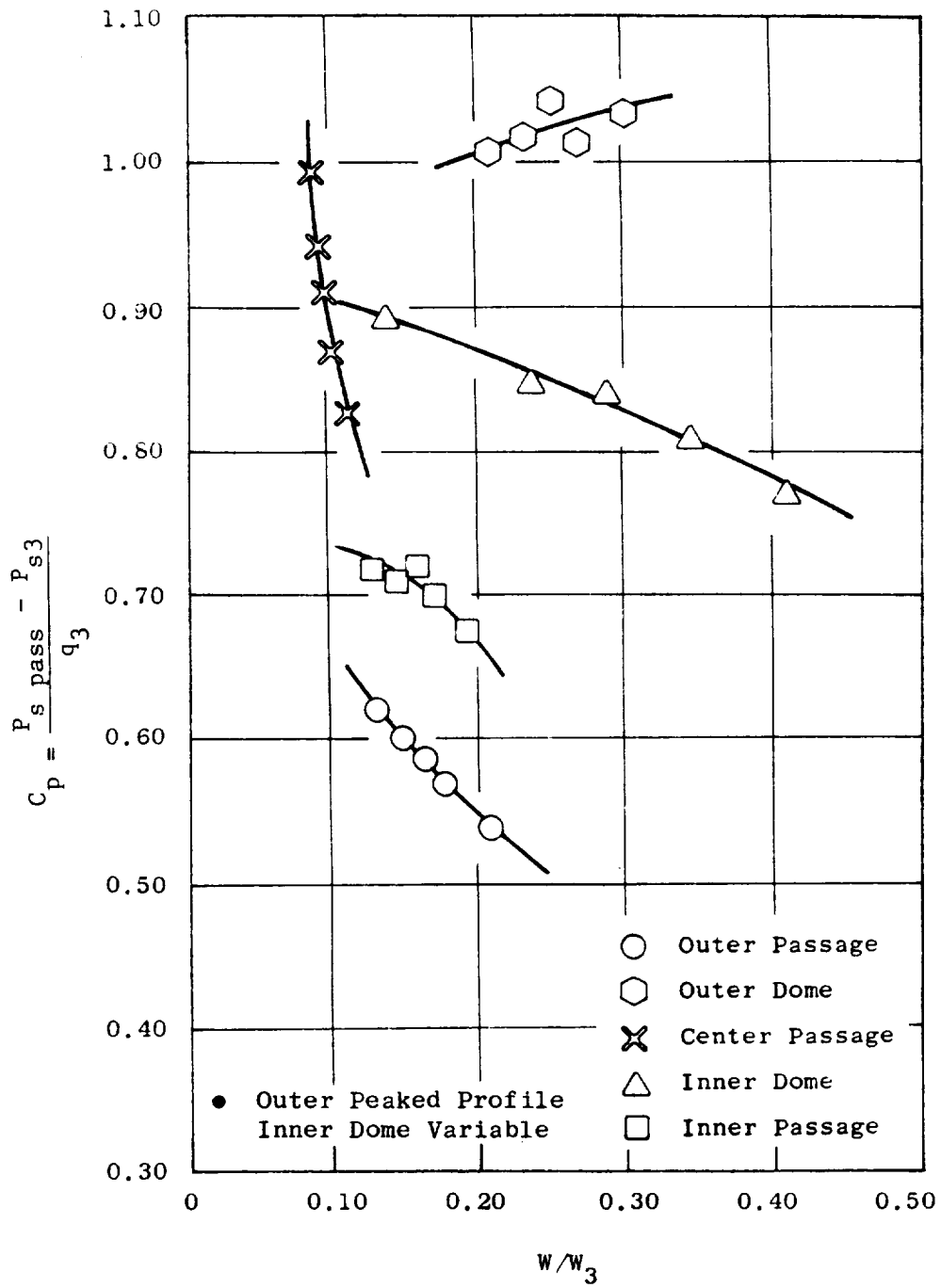


Figure 9B. E³ Combustor Inlet Diffuser CR&D Model Test Data.

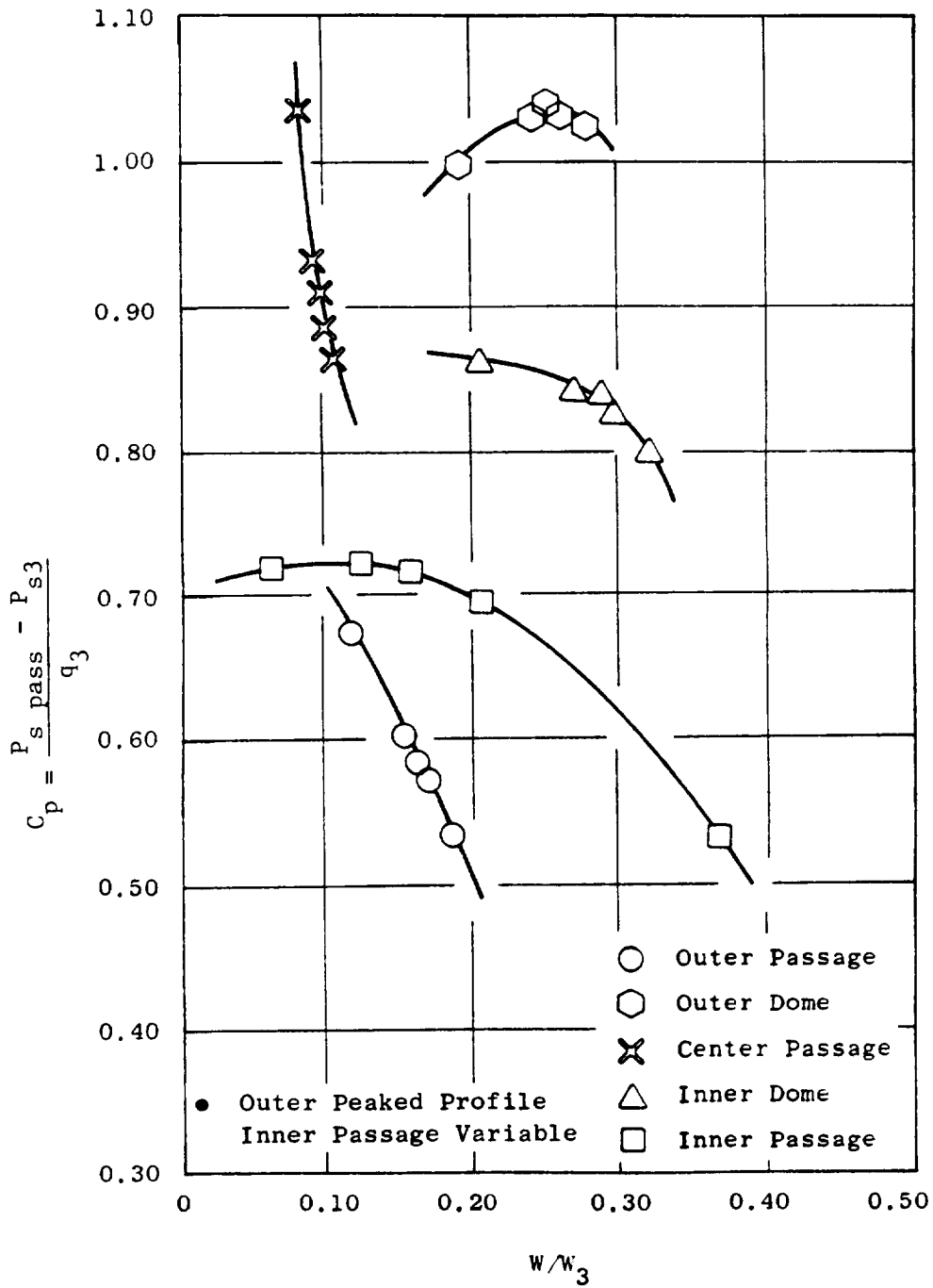


Figure 10B. E³ Combustor Inlet Diffuser CR&D Model Test Data.

ORIGINAL PAGE IS
OF POOR QUALITY

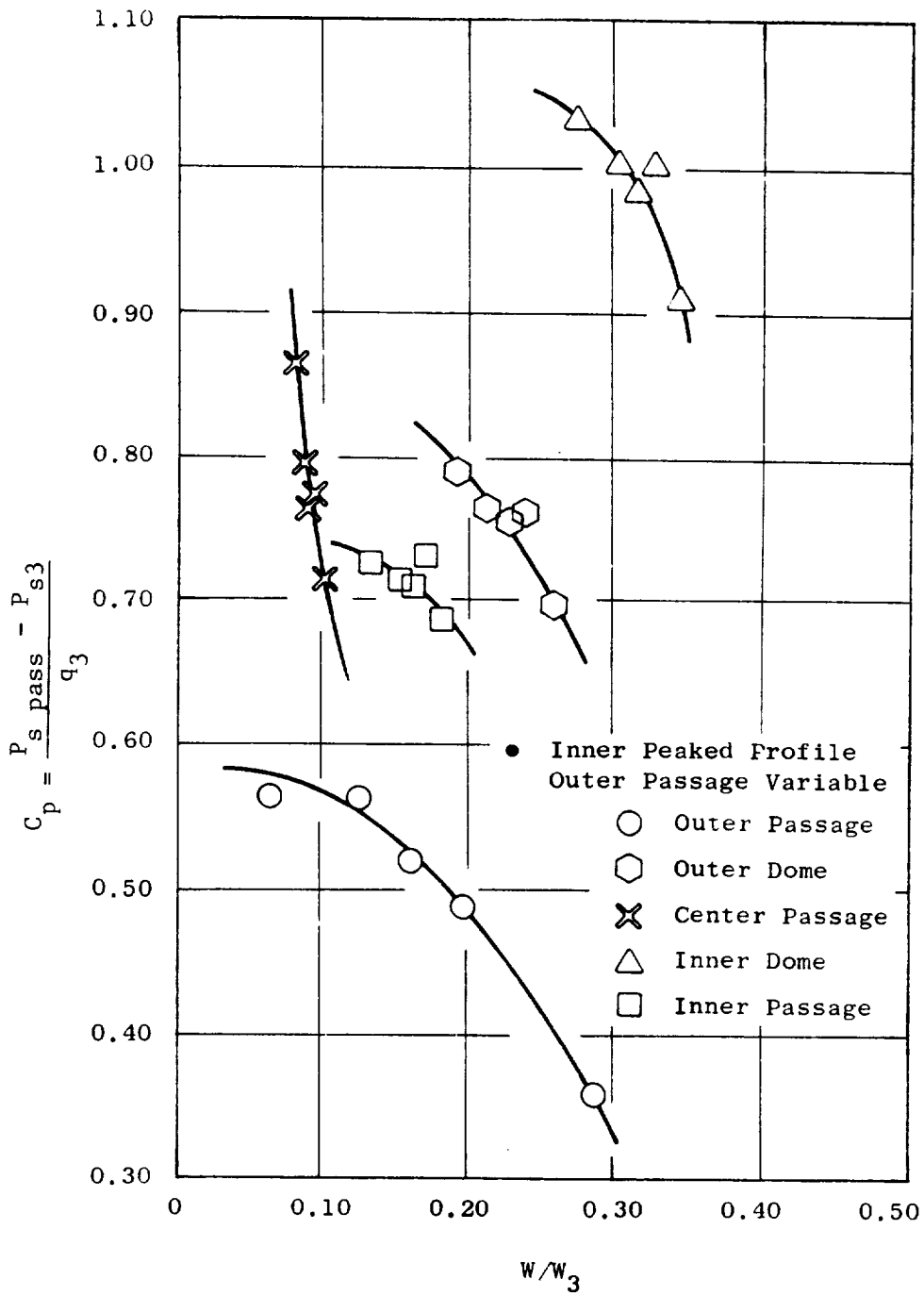


Figure 11B. E^3 Combustor Inlet Diffuser CR&D Model Test Data.

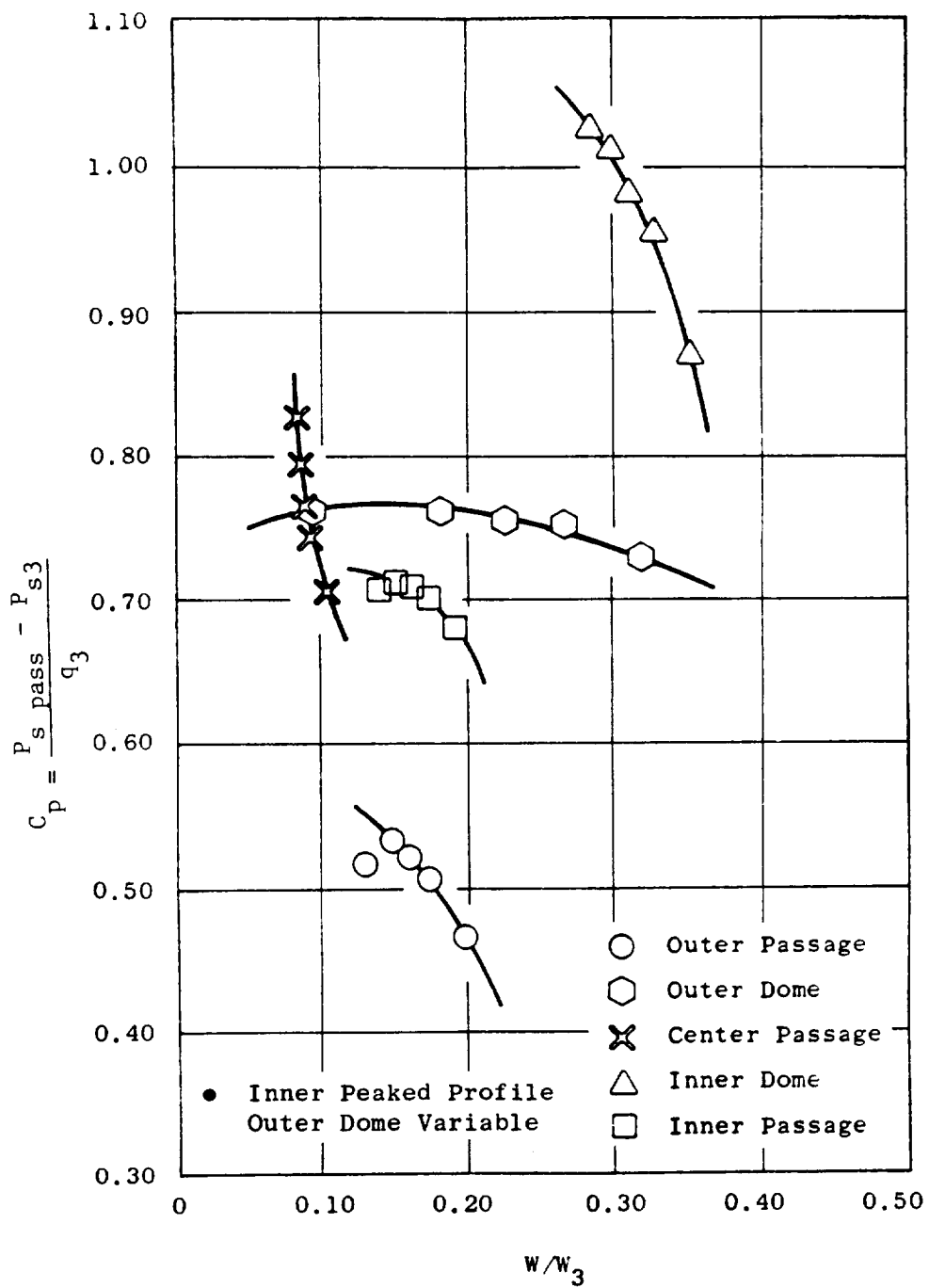


Figure 12B. E^3 Combustor Inlet Diffuser CR&D Model Test Data.

ORIGINAL PAGE IS
OF POOR QUALITY

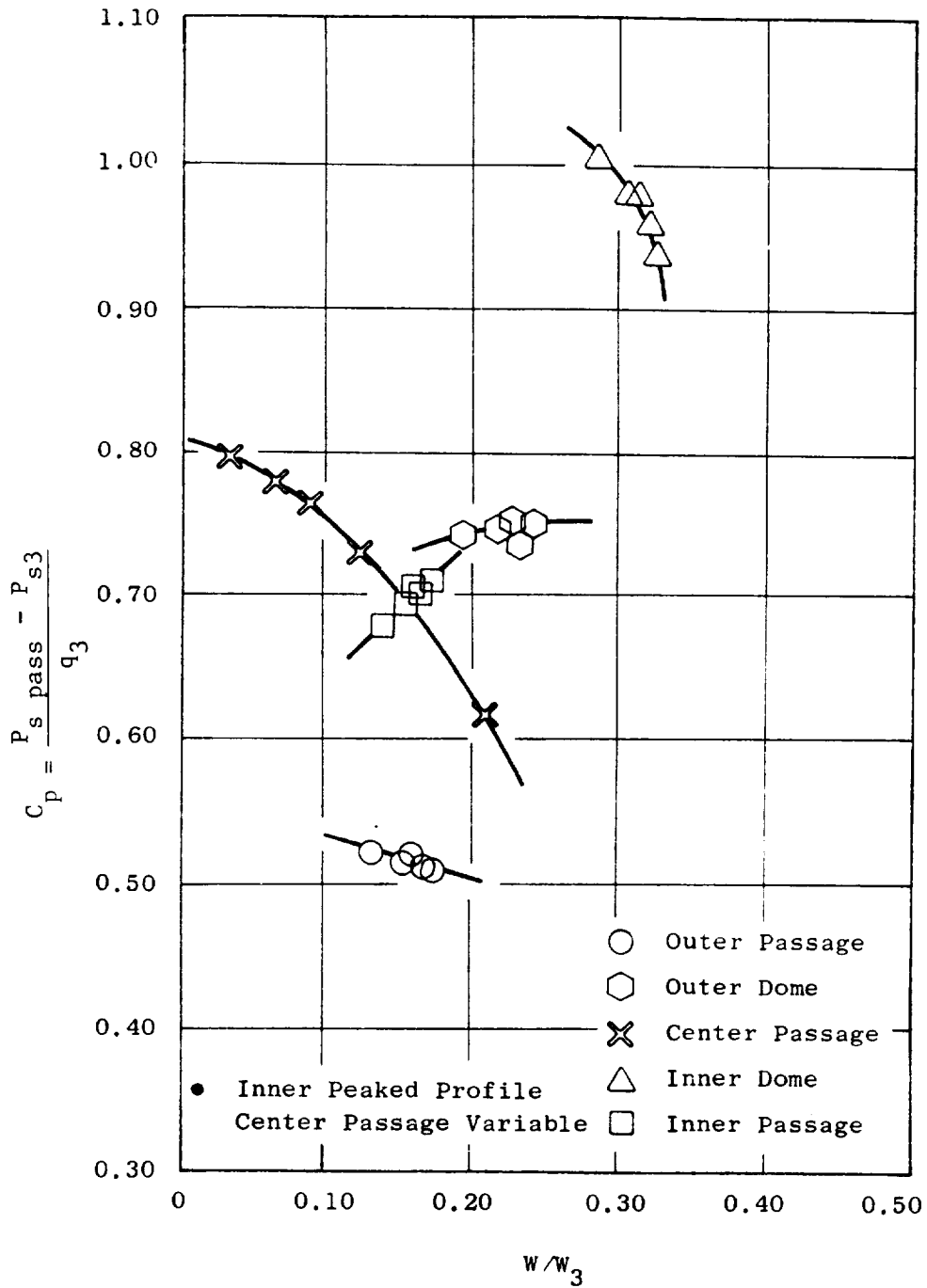


Figure 13B. E^3 Combustor Inlet Diffuser CR&D Model Test Data.

COMPARISON OF
OF FOUR QUALITY

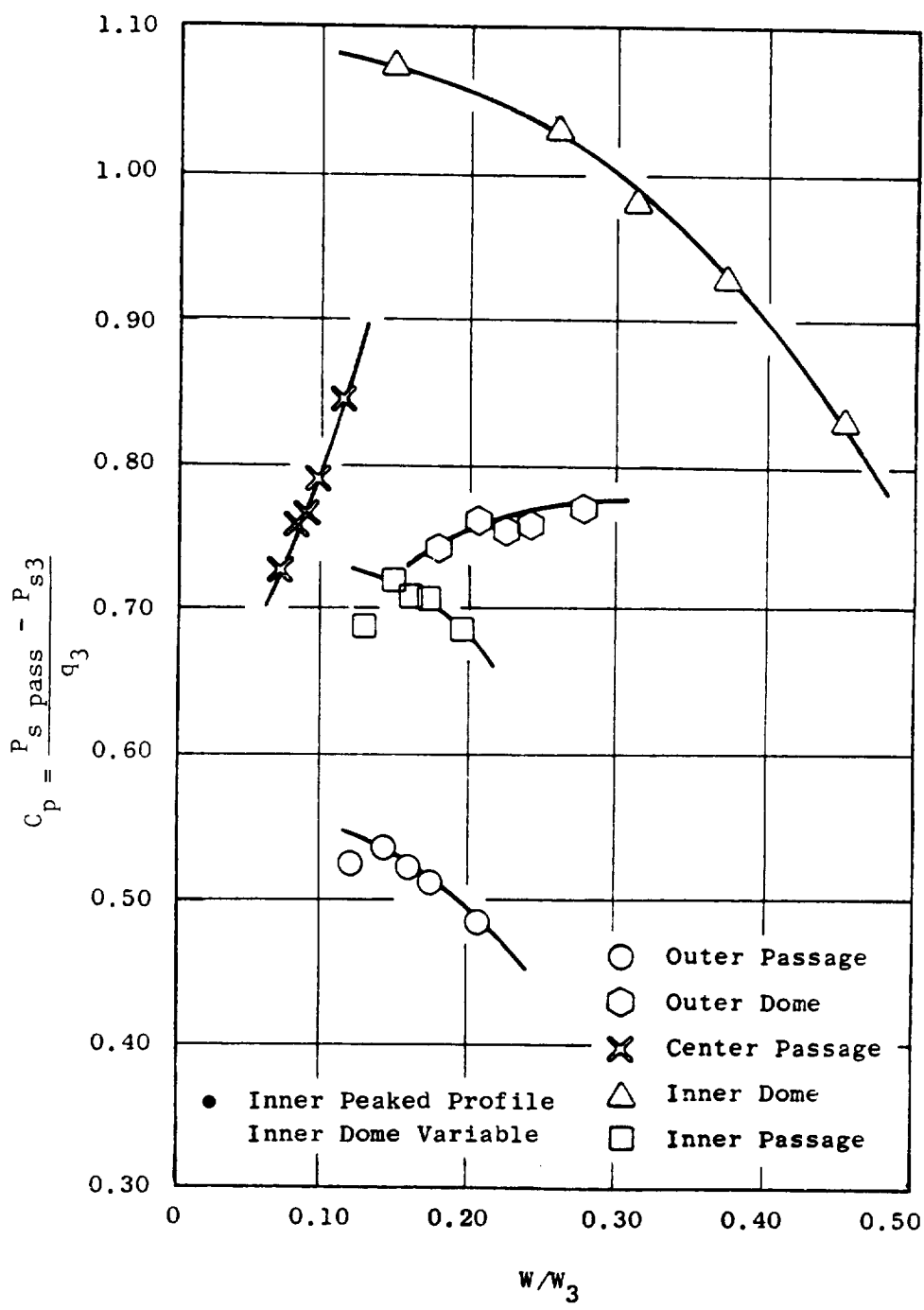


Figure 14B. E³ Combustor Inlet Diffuser CR&D Model Test Data.

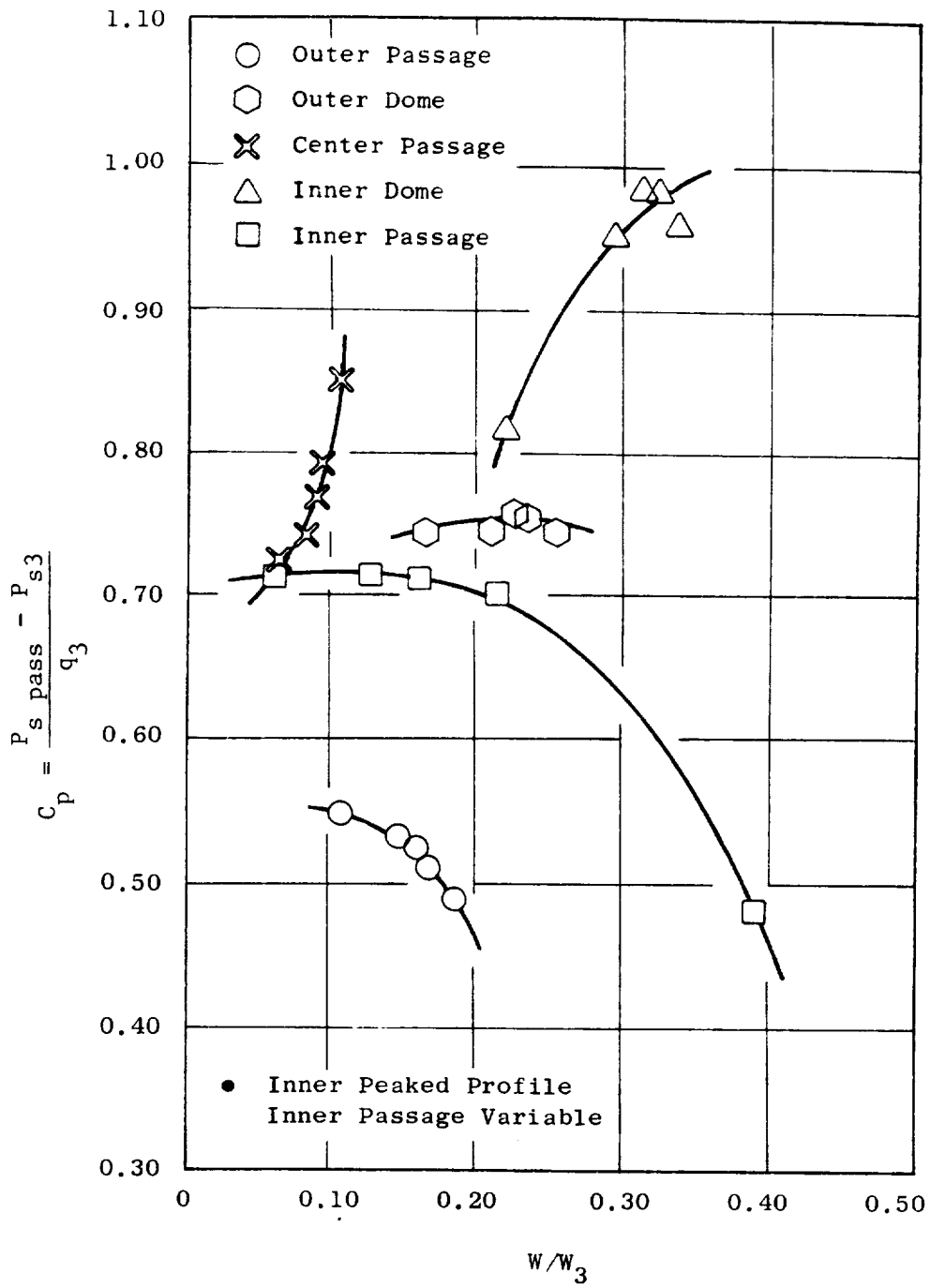


Figure 15B. E³ Combustor Inlet Diffuser CR&D Model Test Data.

APPENDIX C

SUMMARY AND DESCRIPTION OF COMPONENT SECTOR
RIG TEST CONFIGURATIONS AND RESULTS

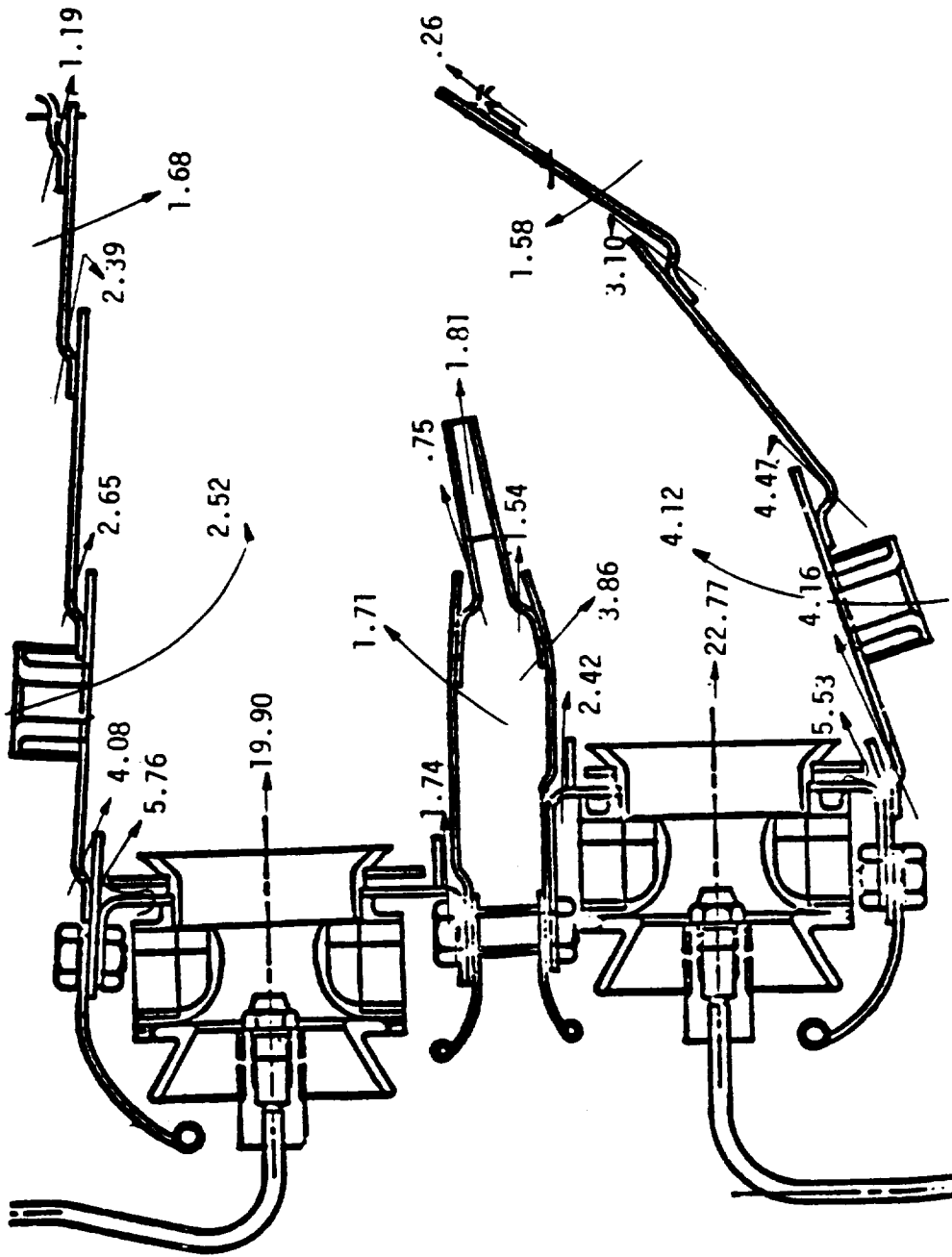


Figure 1C. E³ Sector Combustor Airflow Distribution Mod I Configuration.

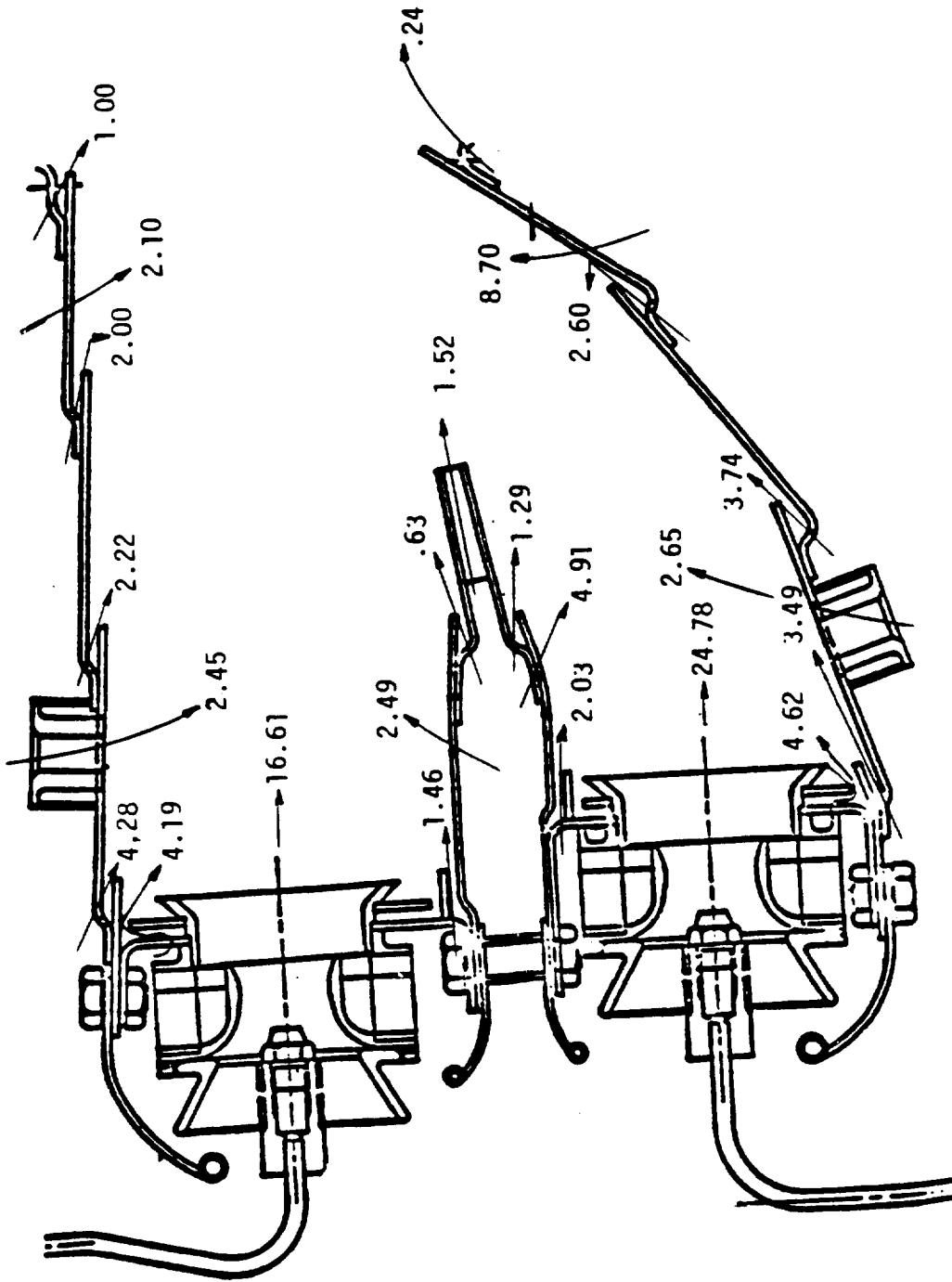


Figure 2C. E³ Combustor Airflow Distribution Mod II Configuration.

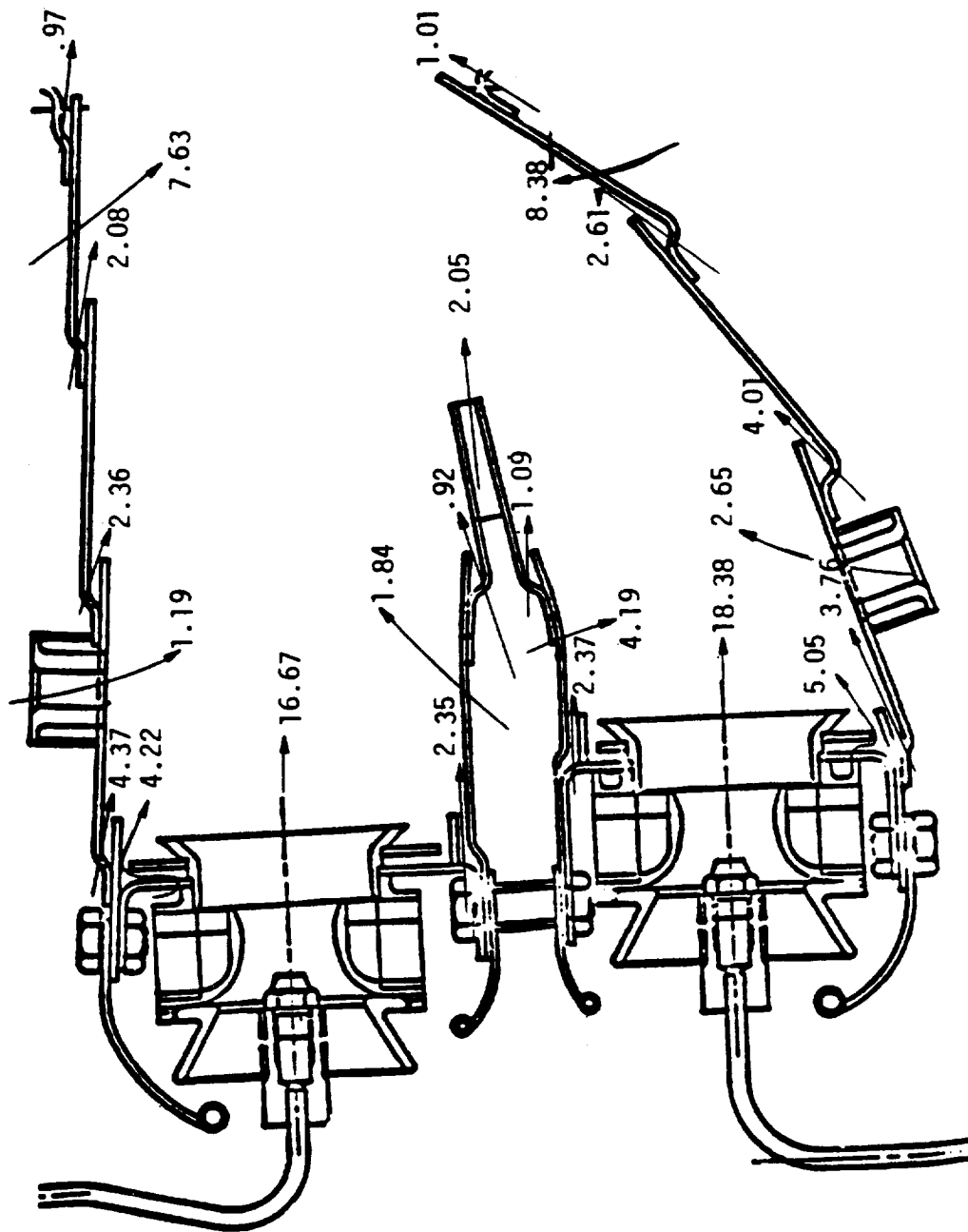


Figure 3C. E3 Sector Combustor Airflow Distribution Mod III Configuration.

ORIGINAL PAGE IS
OF POOR QUALITY

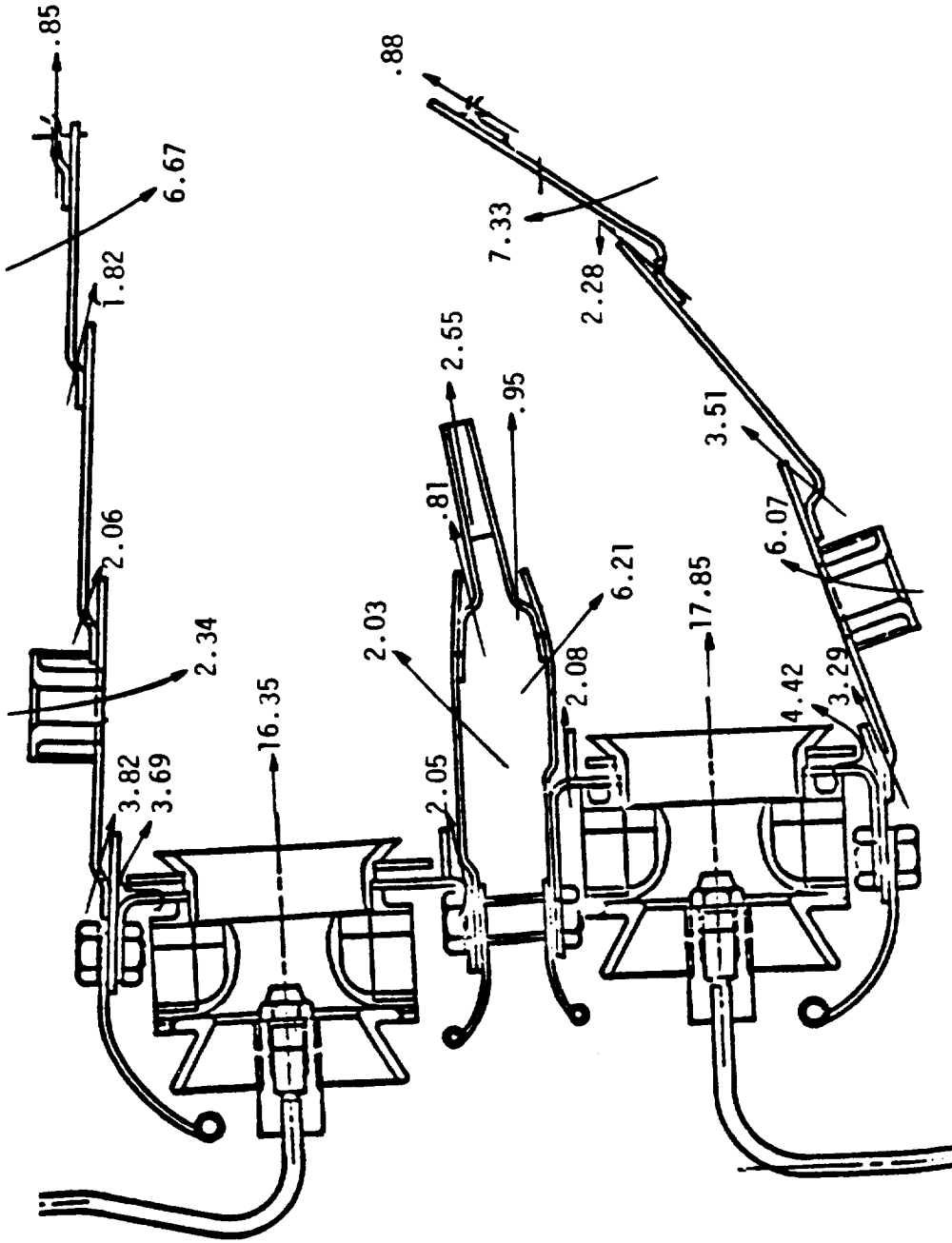


Figure 5C. E³ Sector Combustor Airflow Distribution Mod V Configuration.

ORIGINAL PARTS
OF POOR QUALITY

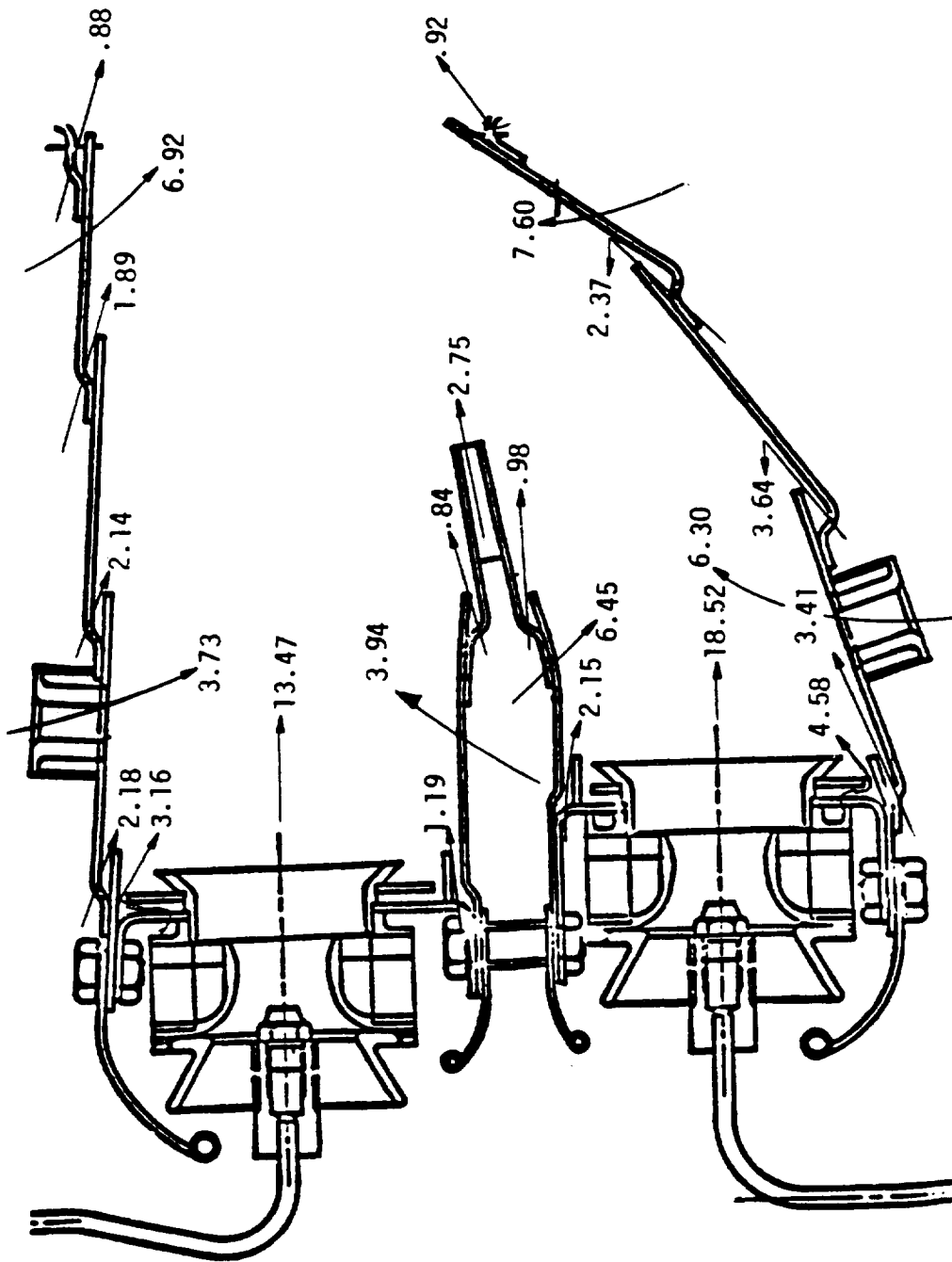


Figure 6C. E³ Sector Combustor Airflow Distribution Mod VI Configuration.

Table IC.

Summary of the E³ Sector Combustor Test Configurations, Features, and Effectiveness

Configuration	Features	Modification Intended for:	Results
Baseline	<ul style="list-style-type: none"> • The primary dilution holes in the outer & inner liners were relocated to between swirl cups from in line with cups. • Forty-five degree sleeves replaced the 90° sleeves. • Pilot dome splashplate cooling reduced by 40%. 	<ul style="list-style-type: none"> • A more uniform fuel-air distribution. • A more dispersed fuel flow. • Lower idle emissions. 	<ul style="list-style-type: none"> • Poor ignition and emissions performance. • Idle emissions reduced. • Ignition slightly improved.
Mod. II	<ul style="list-style-type: none"> • Development type swirl cups replaced the prototype cups. • Reduced pilot stage swirl cup airflow. • Increased main stage aft dilution airflow. 	<ul style="list-style-type: none"> • More closely duplicate the full annular combustor design. • Reduced idle emissions. • Reduce NO_x emissions at high power. 	<ul style="list-style-type: none"> • Idle emissions reduced to meet target levels. • NO_x emissions increased. • Ignition deteriorated.
Mod. III	<ul style="list-style-type: none"> • Reduced main stage swirl cup airflow. • Development type fuel nozzles replaced the prototype nozzles. • Cross fire tube incorporated in the centerbody design. 	<ul style="list-style-type: none"> • Improve main stage cross fire performance. • Duplicate the full annular combustor fuel system. 	<ul style="list-style-type: none"> • Ignition performance improved significantly. • Idle emissions increased.
Mod. III-A Mod. III-B Mod. III-C	<ul style="list-style-type: none"> • Blocked the fuel nozzle shroud air. • Reverted back to prototype fuel nozzles. • Installed larger flow number development type fuel nozzles. 	<ul style="list-style-type: none"> • Reduced idle emissions. • Determine effects of fuel nozzle type on idle emissions. 	<ul style="list-style-type: none"> • See Figure 50.
Mod. IV	<ul style="list-style-type: none"> • Increased pilot stage primary dilution airflow. • Shortened centerbody multijet length. 	<ul style="list-style-type: none"> • Reduced idle emissions. • Mechanical considerations. 	<ul style="list-style-type: none"> • Idle emissions same as Mod. III.
Mod. V	<ul style="list-style-type: none"> • Increased main stage primary dilution airflow. 	<ul style="list-style-type: none"> • Reduce NO_x emissions at high power. 	<ul style="list-style-type: none"> • NO_x emissions increased.
Mod. VI	<ul style="list-style-type: none"> • Reduced pilot stage swirl cup airflow. • Increased pilot stage primary dilution airflow. 	<ul style="list-style-type: none"> • Reduce idle emissions. 	<ul style="list-style-type: none"> • No improvement on idle emissions.
Mod. VI-A	<ul style="list-style-type: none"> • Reduced outer liner Row 1 cooling airflow. • Reduced main stage swirl cup and splashplate cooling airflows. 	<ul style="list-style-type: none"> • Improve cross fire performance. 	<ul style="list-style-type: none"> • No improvement in cross fire performance.
Mod. VI-B	<ul style="list-style-type: none"> • Increased pilot stage swirl cup airflow. 		
Mod. VI-C	<ul style="list-style-type: none"> • Added an extension to the main stage side of cross fire tube. 		
Mod. VI-D	<ul style="list-style-type: none"> • Added an extension to the pilot stage side of cross fire tube. 		
Mod. VI-E	<ul style="list-style-type: none"> • Redesign cross fire tube geometry into a semi-cylindrical shape. 		

ORIGINAL PAGE 12
OF POOR QUALITY

APPENDIX D

EMISSIONS CORRECTION AND CORRELATION EQUATIONS

This appendix contains adjustment relationships which were used to correct the measured emissions data obtained at derated high-power operating conditions to the actual QCSEE double-annular engine design cycle conditions. These relations were developed as part of the EPA/CFM56 and NASA/GE ECCP programs and have generally provided a satisfactory method for adjusting the emissions levels to the correct combustor inlet conditions as specified in an engine cycle.

These relations are defined as follows:

- (1) $EI_{CO}(ADJ) = EI_{CO}(MEA) (P_3/P_3 \text{ Cycle})^{1.5} \text{ ~g/kg fuel}$
- (2) $EI_{HC}(ADJ) = EI_{HC}(MEA) (P_3/P_3 \text{ Cycle})^{2.5} \text{ ~g/kg fuel}$
- (3) $EI_{NO_x}(ADJ) = EI_{NO_x}(MEA) (P_3 \text{ Cycle}/P_3)^{0.37} \text{ Exp } \frac{T_3 \text{ Cycle} - T_3}{345} \text{ ~g/kg fuel}$
- (4) NO_x Severity Parameter -

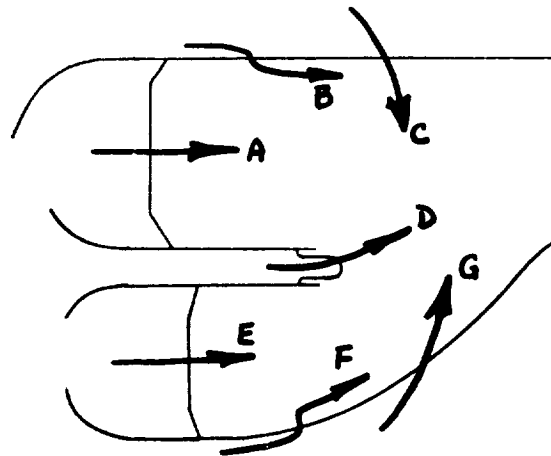
Correlating measured NO_x emissions data with this parameter yields a linear characteristic that allows easy extrapolation of the NO_x levels to high-power operating conditions.

$$\left(\frac{P_3}{P_3^*}\right)^{0.37} \left(\frac{V_{Ref}^*}{V_{Ref}}\right) \left(\frac{f/a \text{ Pilot}}{0.00854}\right)^{0.65} \left(\frac{f/a \text{ Main}}{0.01586}\right)^{0.65} \text{ Exp} \left(\frac{T_3 - T_3^*}{345} + \frac{6.29 - \text{Humidity}}{53.19}\right)$$

Note - The starred values refer to levels at sea level takeoff operating conditions

APPENDIX E

ESTIMATED AIRFLOW DISTRIBUTION FOR FULL-ANNULAR COMBUSTOR CONFIGURATIONS



Configu- ration	A	B	C	D	E	F	G
Baseline	33.61	6.23	4.13	11.55	33.09	6.62	4.77
Mod I	25.44	6.43	3.38	11.58	38.28	6.94	7.95
Mod II	25.80	5.75	4.30	12.98	28.78	7.60	14.79
Mod III	23.78	5.39	9.72	12.79	23.37	9.46	15.59
Mod IV	23.26	6.13	11.92	12.43	22.53	8.40	15.33
Mod V	23.00	6.18	14.69	11.11	22.65	8.47	13.90
Mod VI	23.19	6.13	4.50	11.36	32.42	9.23	13.17
Mod VII	23.20	6.12	4.51	11.41	32.30	9.23	13.23
Engine	24.80	6.51	4.10	13.18	30.99	8.88	11.54

APPENDIX F

DEVELOPMENT ANNULAR COMBUSTOR TEST SUMMARY

This appendix contains test data summaries for all development combustor configurations and the engine combustor tested for component evaluation.

Table 4F. Development Combustor Mod III Test Data.

RING	TEST POINT	INLET TOTAL PRESSURE		INLET TEMPERATURE		COMBUSTOR INLET AIRFLOW		COMBUSTOR INLET FUEL FLOW		COMBUSTOR OVERALL FUEL-AIR RATIO	PILOT STAGE EQUATION (%)		MAIN STAGE EQUIPMENT (%)		EMISSIONS DATA		COMBUSTOR TOTAL FUEL-AIR RATIO		COMMENTS	
		PSIA	MPa	°F	K	PPS	kg/s	PPH	kg/h		1-cup	2-cup	1-cup	2-cup	CO	HC	NOx	%		%
1	1	14.62	0.101	79	299	2.77	1.16	2.77	1.26	—	0.272	0.318	0.202	0.350	—	—	—	—	—	—
2	2	14.71	0.101	86	303	3.79	1.72	3.79	1.72	—	0.282	0.350	0.185	0.255	—	—	—	—	—	—
3	3	14.68	0.101	112	318	3.41	1.55	3.41	1.55	—	0.286	0.350	0.185	0.255	—	—	—	—	—	—
4	4	14.72	0.102	167	354	3.56	1.62	3.56	1.62	—	0.286	0.350	0.185	0.255	—	—	—	—	—	—
5	5	14.73	0.102	167	345	3.63	1.65	3.63	1.65	—	0.286	0.350	0.185	0.255	—	—	—	—	—	—
6	6	14.83	0.102	233	385	4.10	1.86	4.10	1.86	—	0.286	0.350	0.185	0.255	—	—	—	—	—	—
7	7	14.78	0.102	313	429	4.33	1.97	4.33	1.97	—	0.286	0.350	0.185	0.255	—	—	—	—	—	—
8	8	15.13	0.104	444	502	5.08	2.31	5.08	2.31	—	0.286	0.350	0.185	0.255	—	—	—	—	—	—
9	9	14.51	0.100	73	307	2.80	1.27	2.80	1.27	—	0.286	0.350	0.185	0.255	—	—	—	—	—	—
10	10	14.55	0.100	108	315	3.12	1.42	3.12	1.42	—	0.286	0.350	0.185	0.255	—	—	—	—	—	—
11	11	14.62	0.101	106	314	3.78	1.72	3.78	1.72	—	0.286	0.350	0.185	0.255	—	—	—	—	—	—
12	12	14.67	0.101	104	313	4.26	1.94	4.26	1.94	—	0.286	0.350	0.185	0.255	—	—	—	—	—	—
13	13	14.60	0.101	156	342	3.40	1.55	3.40	1.55	—	0.286	0.350	0.185	0.255	—	—	—	—	—	—
14	14	14.66	0.101	153	340	3.86	1.75	3.86	1.75	—	0.286	0.350	0.185	0.255	—	—	—	—	—	—
15	15	14.76	0.102	151	339	4.40	2.09	4.40	2.09	—	0.286	0.350	0.185	0.255	—	—	—	—	—	—
16	16	14.73	0.102	226	381	4.16	1.89	4.16	1.89	—	0.286	0.350	0.185	0.255	—	—	—	—	—	—
17	17	14.78	0.102	307	426	4.33	1.97	4.33	1.97	—	0.286	0.350	0.185	0.255	—	—	—	—	—	—
18	18	15.06	0.104	441	500	5.16	2.35	5.16	2.35	—	0.286	0.350	0.185	0.255	—	—	—	—	—	—
19	19	15.20	0.105	440	500	5.67	2.55	5.67	2.55	—	0.286	0.350	0.185	0.255	—	—	—	—	—	—
20	20	15.40	0.106	440	500	6.36	2.89	6.36	2.89	—	0.286	0.350	0.185	0.255	—	—	—	—	—	—

ORIGINAL PAGE IS OF POOR QUALITY

Table 5F. Development Combustor Mod IV Test Data.

TEST POINT	INLET TOTAL PRESSURE PSIA	INLET TEMPERATURE		COMBUSTOR EXIT AIRFLOW		COMBUSTOR FUEL FLOW		PILOT TO TOTAL FUEL FLOW	COMBUSTOR OVERALL FUEL-AIR RATIO	PILOT STAGE EMISSION (%)						MAIN STAGE EMISSION (%)						EMISSIONS DATA			COMBUSTOR TOTAL PRESSURE LOSS %	COMMENTS											
		°F	K	PPS	kg/s	PPH	kg/h			1-CUP	30-CUP	4/6	1-CUP	30-CUP	4/6	1-CUP	30-CUP	4/6	CO	HC	NOx	3/Kg	N/A	N/A			N/A	%									
1	N/A	78	259	2.87	1.30	2.57	1.30	—	—	0.073	0.315	0.276	0.186	0.328	0.124	0.184	0.272	0.321	0.164	—	0.164	—	—	—	—	—	—	—	—	N/A	N/A	N/A	N/A	I.G. station			
2		74	276	3.71	1.64	3.71	1.64	—	—	0.089	0.388	0.288	0.256	0.418	0.160	0.260	0.360	0.418	0.164	—	0.164	—	—	—	—	—	—	—	—	—	—	—	—	—	—		
3		104	313	3.56	1.62	3.56	1.62	—	—	0.202	0.293	0.254	0.160	0.285	0.235	0.235	0.235	0.235	0.235	0.235	0.235	0.235	0.235	0.235	0.235	0.235	0.235	0.235	0.235	0.235	0.235	0.235	0.235	0.235	0.235	0.235	
4		156	342	3.73	1.70	3.73	1.70	—	—	0.087	0.233	0.224	0.136	0.241	0.178	0.248	0.248	0.248	0.248	0.248	0.248	0.248	0.248	0.248	0.248	0.248	0.248	0.248	0.248	0.248	0.248	0.248	0.248	0.248	0.248	0.248	0.248
5		226	381	4.04	1.84	4.04	1.84	—	—	0.157	0.204	0.144	0.088	0.158	0.253	0.253	0.253	0.253	0.253	0.253	0.253	0.253	0.253	0.253	0.253	0.253	0.253	0.253	0.253	0.253	0.253	0.253	0.253	0.253	0.253	0.253	0.253
6		310	428	4.27	1.94	4.27	1.94	—	—	0.030	0.255	0.109	0.051	0.222	0.318	0.318	0.318	0.318	0.318	0.318	0.318	0.318	0.318	0.318	0.318	0.318	0.318	0.318	0.318	0.318	0.318	0.318	0.318	0.318	0.318	0.318	0.318
7		442	501	5.16	2.35	5.16	2.35	—	—	0.007	0.110	0.071	0	0.081	0.165	0.165	0.165	0.165	0.165	0.165	0.165	0.165	0.165	0.165	0.165	0.165	0.165	0.165	0.165	0.165	0.165	0.165	0.165	0.165	0.165	0.165	0.165
8		160	344	3.66	1.66	3.66	1.66	—	—	0.077	0.247	0.218	0.146	0.246	0.257	0.257	0.257	0.257	0.257	0.257	0.257	0.257	0.257	0.257	0.257	0.257	0.257	0.257	0.257	0.257	0.257	0.257	0.257	0.257	0.257	0.257	0.257

ORIGINAL SOURCE OF POOR QUALITY

Table 6F. Development Combustor Mod V Test Data.

TEST POINT	INLET TOTAL PRESSURE		INLET TEMPERATURE		COMBUSTOR INLET AIR FLOW		COMBUSTOR EXIT AIR FLOW		COMBUSTOR FUEL FLOW		PILOT TO TOTAL FUEL RATIO		PILOT STAGE IGNITION (%)						MAIN STAGE IGNITION (%)						EMISSIONS DATA			COMBUSTOR PRESSURE LOSS		COMMENTS
	PSIA	MPa	°F	K	PPS	kg/s	PPS	kg/s	PPH	kg/h	1-CUP	30-CUP	1-CUP	30-CUP	1-CUP	30-CUP	1-CUP	30-CUP	1-CUP	30-CUP	1-CUP	30-CUP	CO	HC	NOx	%	%			
1	4.77	0.101	78	299	2.77	1.26	2.77	1.26	—	—	0.297	0.366	0.323	0.387	0.356	N/A	—	—	—	—	—	—	N/A	N/A	N/A	N/A	N/A			
2	4.68	0.101	77	298	3.69	1.68	3.69	1.68	—	—	0.304	0.387	0.359	0.407	0.483	0.287	0.349	0.425	0.267	0.361	0.367	0.445	—	—	—	—	—			
3	4.66	0.101	99	310	3.46	1.57	3.46	1.57	—	—	0.189	0.290	0.271	0.286	0.283	N/A	—	—	—	—	—	—	—	—	—	—	—			
4	4.70	0.101	157	343	3.62	1.65	3.62	1.65	—	—	0.210	0.265	0.237	0.116	0.265	0.428	0.473	0.421	0.421	0.421	0.421	0.421	—	—	—	—	—			
5	4.78	0.101	223	379	4.04	1.84	4.04	1.84	—	—	0.184	0.214	0.172	0.038	0.180	0.428	0.473	0.421	0.421	0.421	0.421	0.421	—	—	—	—	—			
6	4.85	0.101	308	426	4.31	1.96	4.31	1.96	—	—	0.125	0.163	0.117	0.035	0.108	0.428	0.473	0.421	0.421	0.421	0.421	0.421	—	—	—	—	—			
7	5.10	0.101	434	496	5.10	2.32	5.10	2.32	—	—	0.110	0.134	0.086	0.028	0.097	0.428	0.473	0.421	0.421	0.421	0.421	0.421	—	—	—	—	—			
8	4.37	0.101	155	341	3.63	1.65	3.63	1.65	—	—	0.208	0.268	0.211	0.109	0.230	0.428	0.473	0.421	0.421	0.421	0.421	0.421	—	—	—	—	—			

ORIGINAL PAGE IS OF POOR QUALITY

Table 7F. Development Combustor Mod VI Test Data.

RUNNING	TEST POINT	INLET TOTAL PRESSURE		INLET TEMPERATURE		COMBUSTOR INLET AIRFLOW		COMBUSTOR EXIT AIRFLOW		COMBUSTOR TOTAL FUEL FLOW	PILOT FUEL TO TOTAL FUEL FLOW	COMBUSTOR OVERALL FUEL-AIR RATIO	PILOT STAGE IGNITION (%)				MAIN STAGE IGNITION (%)				EMISSIONS				COMBUSTOR TOTAL PRESSURE LOSS %	COMMENTS	
		PSIA	MPa	°F	K	PPS	kg/s	PPS	kg/s				PPS	kg/s	%	1-CUP	3-CUP	4-CUP	1-CUP	3-CUP	4-CUP	CO	HC	NOx			%
1	1	14.79	0.102	87	304	4.77	2.17	4.77	2.17	---	---	---	0.153	0.208	0.162	0.102	---	---	---	---	N/A	N/A	N/A	N/A	N/A	N/A	IGNITION
2	2	14.78	0.102	87	304	4.65	2.11	4.65	2.11	---	---	---	0.142	0.211	0.149	0.108	---	---	---	---	---	---	---	---	---	---	---
3	3	14.82	0.103	95	308	5.50	2.50	5.50	2.50	---	---	---	0.115	0.190	0.131	0.091	---	---	---	---	---	---	---	---	---	---	---
4	4	14.89	0.103	96	309	5.32	2.42	5.32	2.42	---	---	---	0.122	0.190	0.132	0.091	---	---	---	---	---	---	---	---	---	---	---
5	5	15.09	0.104	130	328	6.28	2.85	6.28	2.85	---	---	---	0.104	0.162	0.102	0.061	0.124	N/L	---	---	---	---	---	---	---	---	---
6	6	15.04	0.104	138	332	5.98	2.72	5.98	2.72	---	---	---	0.122	0.173	0.076	0.066	0.118	N/L	---	---	---	---	---	---	---	---	---
7	7	15.21	0.106	157	343	7.06	3.21	7.06	3.21	---	---	---	0.103	0.147	0.086	0.060	---	---	---	---	---	---	---	---	---	---	---
8	8	15.28	0.105	167	348	6.90	3.14	6.90	3.14	---	---	---	0.096	0.144	0.084	0.051	---	---	---	---	---	---	---	---	---	---	---
9	9	15.10	0.104	176	344	5.25	2.35	5.25	2.35	---	---	---	0.071	0.113	0.086	0.040	0.082	0.372	0.041	---	---	---	---	---	---	---	---
10	10	15.06	0.104	402	479	5.10	2.32	5.10	2.32	---	---	---	0.084	0.108	0.063	0.032	0.071	0.394	0.165	0.165	0.165	0.165	0.165	0.165	0.165	0.165	---
11	11	15.21	0.105	428	493	5.41	2.46	5.41	2.46	---	---	---	0.075	0.108	0.060	0.031	0.072	0.353	0.162	0.162	0.162	0.162	0.162	0.162	0.162	0.162	---
12	12	15.27	0.105	504	535	5.34	2.43	5.34	2.43	---	---	---	0.068	0.095	0.058	0.034	0.048	0.318	0.149	0.149	0.149	0.149	0.149	0.149	0.149	0.149	---
13	13	15.27	0.105	628	632	4.95	2.25	4.95	2.25	---	---	---	0.062	0.115	0.061	0.017	0.070	0.312	0.121	0.121	0.121	0.121	0.121	0.121	0.121	0.121	---

Table 9F. Engine Combustor Test Data (Concluded).

RUNNING TEST POINT	INLET TOTAL PRESSURE		INLET TEMPERATURE		COMBUSTOR INLET AIRFLOW		COMBUSTOR EXIT AIRFLOW		COMBUSTOR TOTAL FUEL FLOW		PILOT FUEL SPLIT TO TOTAL	COMBUSTOR OVERALL FUEL-AIR RATIO	PILOT STAGE IGNITION (%)				MAIN STAGE IGNITION (%)				EMISSIONS DATA				COMBUSTOR TOTAL FUEL-AIR RATIO	COMMENTS
	PSIA	MPa	° F	K	PPH	kg/s	PPH	kg/s	PPH	kg/h			4/6	1-6/30-6/30	4/6	1-6/30-6/30	4/6	1-6/30-6/30	CO	HC	NOx	%	CO	HC		
19	63.2	0.436	423	490	27.55	12.52	23.19	10.54	9.52	433	1.0	.0114					10.8	0.8	4.5	99.68	4.80				4.80	6% G-IDLE
20	63.2	0.436	424	491	26.52	12.05	21.94	9.97	10.66	485	1.0	.0135				13.8	0.7	5.0	99.61	4.63				4.63		
21	62.7	0.432	429	491	26.85	12.20	22.34	10.15	1312	596	1.0	.0163				43.0	0.7	5.0	99.64	4.55				4.55		
22	106.1	1.214	698	643	68.28	31.26	56.27	25.71	2912	1324	1.0	.0143				2.1	0.1	16.0	99.94	3.82				3.82	30% APPROX	
23	176.9	1.220	702	645	68.49	31.13	56.72	25.78	2940	1336	0.5	.0144				66.4	13.0	16.1	97.82	4.75				4.75		
24	176.3	1.216	694	641	68.36	31.07	56.23	25.60	2920	1327	0.4	.0144				71.6	8.8	5.2	97.86	4.18				4.18		
25	177.1	1.221	697	642	68.62	31.19	56.51	25.65	2950	1341	0.3	.0145				82.2	7.9	5.4	97.89	4.10				4.10		
26	224.1	1.554	813	707	78.02	35.46	64.45	29.60	4316	1962	0.4	.0186				11.2	0.7	7.7	97.68	4.17				4.17	UNADJUSTED	
27	220.8	1.522	812	710	76.87	34.64	63.56	28.87	4942	2246	0.5	.0216				2.3	0.2	23.0	99.93	5.75				5.75		
28	220.0	1.517	809	708	76.88	34.95	63.95	29.07	4950	2250	0.4	.0215				1.4	0.1	19.0	99.96	5.34				5.34	85% FJ	
29	220.3	1.514	808	708	75.67	34.40	63.39	28.81	4724	2240	0.3	.0216				1.3	0.1	17.3	99.96	5.53				5.53		
30	221.2	1.525	816	720	—	—	59.00	27.23	5762	2392	0.5	.0244				1.4	0.1	28.7	99.96	5.62				5.62		
31	221.1	1.524	816	720	—	—	60.45	27.48	5766	2394	0.4	.0242				1.0	0.1	28.9	99.97	5.55				5.55	SLTD	
32	220.3	1.514	814	714	—	—	60.24	27.38	5270	2355	0.3	.0243				1.1	0.1	22.0	99.97	5.30				5.30		

ORIGINAL PAGE IS OF POOR QUALITY

REFERENCES

1. Bahr, D.W., Gleason, L.C., and Rogers, D.W., "Experimental Clean Combustor Program."
2. Bahr, D.W., Burrus, D.L., and Sabla, P.E., "QCSEE Double-Annular Clean Combustor Technology Development Report," NASA CR-159483, May 1979.
3. "Control of Air Pollution from Aircraft and Aircraft Engines," U.S. Environmental Protection Agency, Federal Register Vol. 38, No. 136, July 1973.
4. Reneau, L.R., Johnston, J.P., and Kline, S.J., "Diffuser Design Manual," Dept. of Mechanical Engineering, Stanford University, Report PD-8, September 1964.
5. Waitman, B.A., Reneau, L.R., and Kline, S.J. "Effects of Inlet Conditions on Performance of Two-Dimensional Diffusers," Dept. of Mechanical Engineering, Stanford University, Report PD-5, August 1960.
6. Livesey, J.L. and Turner, J.T., "The Dependence on Diffuser Performance upon Inlet Flow Conditions," Journal of Royal Aeronautical Society, Vol. 69, 1965.

